Modulation de la réactivité astrocytaire par ciblage de la voie JAK2-STAT3 : conséquences dans des modèles murins de la maladie d'Alzheimer

Kelly Ceyzériat

université PARIS-SACLAY

NNT : 2017SACLS556

Thèse de doctorat

UNIVERSITÉ PARIS SUD
Comprendre le monde, construire l'avenir

Modulation de la réactivité astrocytaire par ciblage de la voie JAK2-STAT3 : Conséquences dans des modèles murins de la maladie d'Alzheimer

Thèse de doctorat de l'Université Paris-Saclay
préparée à l'université Paris-Sud
Laboratoire d'accueil : **MIRCen**, CEA

École doctorale n°568
Signalisations et réseaux intégratifs en biologie (Biosigne)

Spécialité de doctorat: Science de la vie et de la santé

Thèse présentée et soutenue à Fontenay-aux-Roses, le 21/12/2017, par

Kelly Ceyzériat

Composition du Jury :

Hervé DANIEL Professeur, Université Paris-Sud (Institut de Neurosciences Paris-Saclay)	Président
Hélène HIRBEC Chargée de Recherche, Université de Montpellier Institut de Génomique Fonctionnelle	Rapporteur
Igor ALLAMAN Chargé de Recherche, Ecole polytechnique fédérale de Lausanne	Rapporteur
Guillaume DOROTHEE Chargé de Recherche, INSERM Centre de recherche Saint-Antoine	Examinateur
Carole ESCARTIN Chargée de Recherche, CNRS – CEA, MIRCen	Directrice de thèse

« Tout obstacle renforce la détermination »

Léonard De Vinci

Remerciements

Je tiens tout d'abord à remercier les membres de mon jury qui ont accepté d'évaluer mon travail et de participer à ma soutenance de thèse. Je remercie particulièrement mes rapporteurs Hélène Hirbec et Igor Allaman.

Je remercie Philippe Hantraye et Emmanuel Brouillet pour m'avoir permis de réaliser mon stage de master 2 puis ma thèse à MIRCen.

Carole, merci de m'avoir choisie pour intégrer ton équipe en M2. Merci de la confiance sans faille que tu m'as accordée alors que j'étais loin sur la liste d'IRTELIS ! Merci de nous laisser le temps de grandir au cours de la thèse, d'être toujours présente dès qu'on en a besoin, de ton encadrement et de ton savoir « manager », en restant toujours positive. Tu n'imagines pas à quel point c'est motivant !! Et merci de nous donner autant l'opportunité de présenter notre travail aux congrès.

Merci Lucile pour ton accueil à mon arrivée dans l'équipe et de m'avoir transmis tant de connaissances sur les différentes techniques et les astrocytes. Merci également pour ton aide lors mes multiples recherches d'anticorps dans les frigos… alors qu'ils étaient généralement devant mon nez.

Maria, merci pour ton aide sur les dizaines de tests d'anticorps à s'en arracher les cheveux, de m'avoir initiée aux joies du robot et des plaques 384 puits, pour tous tes conseils, ton écoute et ta joie de vivre. Toutes mes félicitations pour le petit bout de chou qui ne devrait plus tarder à montrer le bout de son nez !

Je tiens également à remercier Gilles, pour ses questions et conseils avisés en team meeting. Comment ne pas devenir fan des astrocytes en côtoyant un aussi grand passionné ?

Gilles, Alexis et Marc, je vous remercie pour votre soutien avant ma première présentation orale à l'AAIC, les bons repas, vos récits d'aventures et la super ambiance à Toronto. Charlotte, merci pour tes conseils précieux avant cette fameuse grande première. Merci de m'avoir fait profiter de la piscine de l'hôtel ;-) C'était vraiment super que tu restes quelques jours de plus avec nous pour profiter des joies du Canada, en vacances !

Un merci tout particulier à Fanny, pour ton aide précieuse en histo, les longues discussions sur le projet, les différents tests envisageables, l'avenir et même de tout et de rien. Tu as toujours été une oreille attentive, si précieuse pour le moral. Et merci pour cette coloration blonde, avec ta petite touche personnelle que je vais garder un bon moment ! ☺. Merci aussi à toi et Pauline d'avoir toujours répondu présentes pour les manips de dernières minutes, toujours plus efficaces les unes que les autres, en un temps record.

Merci les filles pour votre aide essentielle à chaque injection ! Charlène, pour la production des virus, ta bonne humeur à toute épreuve et ta folie ! Martine, Sueva, Gwen et Mylène pour votre aide pour ces longues journées avec toujours plus de souris : « Martine, HELP !! Je n'arrive pas à la mettre en barres d'oreilles… ». Sueva, merci également pour ton aide précieuse dans la gestion de la colonie APP/PS1. Merci à Clément et Clémence pour leur temps de gestion de la colonie et leur compréhension.

Karine et Julien Mitja, merci de m'avoir initiée au comportement et pour vos nombreux conseils essentiels.

Merci également à tous les membres de l'équipe 1, les Julien, Emmanuel, Géraldine, Gilles, Carole, Jérémy, Edwin, Laurene, Lucie, Marianne, Camille, Ludmila, Mélissa, Francesco, Océane, Pierre-Antoine, et anciennement membres Clémence, Pierrick, Noémie, Brice, Marco, Juliette, Lucile, Laetitia, pour votre intérêt pour mon projet, vos questions et idées. En particulier, merci à Thomas et Océane pour votre aide pour les manips sur les 3xTg. Merci Jérémy, pour ton aide à l'IRM et ces parties de basket pour ne pas piquer du nez au bout de 12h de manip.

Merci à Marie-Claude pour son aide si précieuse en BM. Noëlle, Gwen et Aurélie pour leur bonne humeur et leurs conseils. Merci Caroline pour la formation en histo à mon arrivé et tes conseils. Je remercie aussi Anne-So, pour sa bonne humeur, son franc-parler et les scans de lames à l'axioscan. J'espère que ce filtre Cy3 marchera du tonnerre !

Merci à Romain et Mickael pour ces discussions sur les APP, les anticorps et vos conseils.

Merci à Cécile, Marie-Laure et Marie-Christine pour toutes ces commandes et livraisons au bureau.

Je tiens également à remercier nos collaborateurs. Merci à Nathalie Dechamps et Jan Bayer pour les expériences de FACS. Merci Nathalie d'avoir toujours trié ces petites cellules avec le sourire malgré mes retards réguliers (pour ne pas dire systématiques). Merci à Robert Olaso et son équipe pour leur expertise pour la réalisation de l'analyse transcriptomique sur les astrocytes triés et leur intérêt pour notre projet. Enfin, Merci à Aude Panatier, Stéphane Oliet et leur équipe pour la réalisation de ces belles expériences d'électrophy.

Un petit mot pour tous les M2 passés dans le labo durant ces 3 années, qui nous font prendre conscience à quel point la thèse passe vite…

Une chose que ne peut pas omettre de préciser en parlant de MIRCen, c'est qu'il y a des sportifs ! Merci à la Team piscine de m'avoir motivée à vous accompagner : Maria, Pauline, Gwen, Séverine (deux fois quand même !), Dimitri, Mylène (heureusement que tu avais une obligation ;-)) ; à la Team running de m'avoir intégrée pour de nombreuses courses à pieds entre midi et deux dans la forêt (oui je suis venue tout de même 3 fois !!) et à la Team TBC : Camille, Anastasie, Laurene et Audrey. Enfin, merci à la Team skieurs de l'extrême, Clémence, Camille, Dimitri, Yaël, Ulysse : 4 blessés sur 6 ! J'espère qu'on sera plus doué l'année prochaine !

Tonton Yaël, Tata Lucie et Papa Laurene, merci pour cette soirée à la fête de la musique inoubliable ! Et tous les bons souvenirs qui ont suivi. Je maitrise désormais la danse du micro-ondes et « Pluie violette, pluiiiiie viiiolette !! ».

Noémie, Sev, et Laurene merci pour ces longues discussions dans le bureau sur les joies de la thèse grandissantes au cours des années, sur notre avenir (très prometteur évidemment !) et d'avoir accepté de subir mes choix musicaux, particulièrement inexplicables après 17h ! « Je n'y peux rien, c'est Youtube qui choisit ! ». Laurene, je compte sur toi pour maintenir cette ambiance musicale dans le bureau ! Merci Sev pour tes conseils avisés et ton temps pour m'initier (voire faire) mes macros ImageJ. Sans toi, je serais toujours en train de chercher…

Clémence, merci pour ta compagnie et nos discussions lors des trajets Fontenay-Bagneux. Merci de m'avoir encouragée, motivée (mes captures d'écran de Snapchat me permettront de m'en souvenir longtemps !!) et soutenue tout au long de ces 3 ans et demi passés ensemble ! Laurene, merci pour tous ces délires (entre deux discussions de travail, évidemment !), pour nos soirées « anglais » à essayer désespérément de progresser. Merci également pour ton aide sur tous les petits bouts de manip, surtout au cours de ces derniers mois. Merci pour ton soutien, tes encouragements et d'avoir su maintenir à flot mon magnésium pour lutter contre la fatigue (vive le chocolat !). Merci aussi à Camille, Lucie, Audrey, Anastasie, Séverine et Marianne pour toute cette joie de vivre, les fous rires, les diverses sorties et les discussions sur notre avenir (très prometteur). Oh et merci Lucie de m'avoir avertie des nombreuses précautions à prendre avec Jean-Eudes le robot, et à Marianne pour tous ces délicieux desserts (et merci d'avoir pris le temps de relire mon intro ;-)) ! Je ne pensais pas rencontrer des gens sur qui je puisse autant compter !!
Enfin, merci à mes parents de m'avoir toujours soutenue et de m'avoir donnée l'opportunité de partir à l'autre bout de la France chez les Bretons, puis à Paris pour faire les études qui me tenaient à cœur. Merci à mes amis bretons d'avoir su me changer les idées quand j'en avais besoin. Merci particulièrement à Bérangère d'avoir pris le temps de relire ma thèse (et corriger les fautes !!). Merci à mon cher et tendre de m'avoir encouragée, motivée (voire forcée !) à travailler le weekend, d'avoir été aussi compréhensif et d'avoir supporté mon mauvais carafon accompagnant si facilement la fatigue.

Merci à vous tous MIRCenniens, MIRCenniennes ! Sans vous, cette thèse n'aurait pas été la même !

Sommaire

*Ce manuscrit étant une thèse sur articles, vous trouverez dans le texte des références aux **articles 1 et 2**, articles présentant mon travail de thèse, inclus dans le chapitre « Résultats ». Par ailleurs, j'ai participé à la rédaction de trois revues et d'un article pour lequel je suis second auteur, nommés **Publication 1 à 4** jointes en annexe.*

Liste des abréviations

3xTg-AD	Souris triple transgéniques modèles de la maladie d'Alzheimer
3xTg-GFP/SOCS3/JAK2ca	Souris 3xTg-AD injectées avec l'AAV-GFP ou SOCS3 ou JAK2ca
AAV	Vecteurs adéno-viraux associés
Aβ	Peptide amyloïde beta
ADAM	A desintegrin and metalloproteinase domain-containing protein
ADNc	ADN complémentaire
AICD	APP intracellular domain
AINS	Anti-inflammatoires non stéroïdiens
Aldh1l1	Aldehyde deshydrogenase 1 family member L1
Aph1a	Anterior pharynx-defective 1
ApoE	Apolipoprotéine E
APP	Protéine précurseur de l'amyloïde
APP/PS1dE9	Souris modèles de la MA (APPswe, PS1dE9)
APP/PS1dE9-GFP/SOCS3/JAK2ca	Souris APP/PS1dE9 injectées avec l'AAV-GFP ou SOCS3 ou JAK2ca
BACE1	β-sécrétase
BHE	Barrière hémato-encéphalique
BSA	Bovine serum albumin
C83	83-residue carboxyl-terminal fragment
CAA	Angiopathie amyloide cérébrale
CCL6	C-C chemokine ligand 6
CCR2	Chemokine receptor 2
CD	Cluster of differentiation
CERAD	Consortium to Establish a Registry for Alzheimer's disease
CNTF	Ciliary neurotrophic factor
CtsL	Cathepsine L
DAM	Disease-associated microglia
DNF	Dégénérescences neurofibrillaires
ECE	Endothelin-converting enzyme-1
FACS	Fluorescence-activated cell sorting
FCSRT	Free and cued selective reminding test
[18F]-FDG	[18F]-fluorodeoxyglucose
GABA	Acide gamma aminobutyrique
GFAP	Glial Fibrillary Acidic Protein
GFP	Green fluorescent protein
HBSS	Hanks' Balanced Salt Solution
IDE	Insulin degrading enzyme
IL	Interleukine

i.p	Intra-péritonéale
IRM	Imagerie par résonnance magnétique
JAK2	Janus kinase 2
JAK2ca	Forme constitutivement active de JAK2
KO	Knockout
LB	Lymphocytes B
LC3	Microtubule-associated protein light chain 3
LCR	Liquide céphalo-rachidien
LPS	Lippopolysaccharide
LT	Lymphocytes T
LTP	Potentialisation à long terme
MA	Maladie d'Alzheimer
MAC	Membrane attack complex
MAPK	Mitogen-activated protein kinases
MXO4	Méthoxy-XO4
NEP	Néprylisine
NFAT	Nuclear factor of activated T-cells
NF-κB	Nuclear factor-kappa B
NG2	Neuronal/glial antigen 2
NGS	Normal goat serum
NLRP3	NOD-like receptor protein 3
NMDA	N-méthyl D-aspartate
OMS	Organisation mondiale de la santé
PAP	Prolongements astrocytaires péri-synaptiques
PBS	Phosphate-buffered saline
PBST	PBS avec 0.2% Triton X-100
PCR	Polymerase chain reaction
PIB	11C-labelled Pittsburgh compound B
PS1	Préséniline 1
PSD95	Post synaptic density protein 95
P-STAT3	Forme phosphorylée de STAT3
RMN	Spectroscopie par résonnance magnétique nucléaire
ROS	Espèces réactives de l'oxygène
RT	Température ambiante
Ser	Sérine
SNC	Système Nerveux Central
SOCS3	Suppressors of cytokine signaling 3
STAT3	Signal transducer and activator of transcription 3
TBS	Tris-buffered saline
TBST	TBS avec 0.1% Tween-20
TEP	Tomographie à émission de positrons

TGF-β	Transforming growth factor 1β
Thr	Thréonine
TLR	Tool-like receptor
Tmem119	Transmembrane protein 119 precursor
TNF	Tumor necrosis factor
TNFR1	TNF receptor 1
TREM2	Triggering receptor expressed on myeloid cells 2
Tyrobp	TYRO protein tyrosine kinase-binding protein
UPS	Système ubiquitine/protéasome
VG	Génome viral
WT	Souris sauvages

Liste des figures et tableaux

Introduction

Introduction

1. Les astrocytes : leurs rôles clés dans le système nerveux central

Les neurones ont été les premières cellules du SNC (Système nerveux central) à être décrites et ont monopolisé l'attention de la recherche en Neuroscience pendant un siècle. Cependant, le cerveau est également composé de cellules gliales, longtemps considérées comme de simples cellules de soutien. Ces cellules ont été décrites pour la première fois par Virchow en 1856 et nommées « nervenkitt » ou « colle nerveuse » *(Virchow, 1856)*. Contrairement à ce qui était couramment cité, il a été récemment montré que le ratio neurones/cellules gliales est égal à 1 dans le cerveau humain *(von Bartheld et al., 2016)*. Parmi les cellules gliales, différents types cellulaires ont été identifiés : les astrocytes, la microglie, les oligodendrocytes et les cellules NG2 (Neuronal/glial antigen 2).

1.1. Caractérisation des astrocytes

Les astrocytes sont des cellules caractérisées depuis longtemps par leur **morphologie étoilée** (« astro- » : étoiles, « -cytes » : cellules) *(Figure 1).* Ils ont également une **position stratégique** : 1/ en contact avec les vaisseaux sanguins via leurs pieds astrocytaires, leur permettant de réguler les échanges avec le milieu sanguin à travers la **BHE** (Barrière hémato-encéphalique), 2/ à proximité des **synapses**, participant activement à la transmission synaptique. Ils expriment des **marqueurs spécifiques** comme la GFAP (Glial fibrillary acidic protein), protéine des filaments intermédiaires, « S100 calcium-binding protein β » ou encore Aldh1L1 (Aldehyde deshydrogenase 1 family member L1), qui permettent de les identifier.

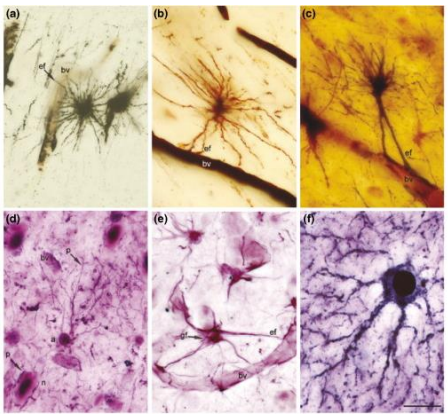

Figure 1 : Morphologie étoilée caractéristique des astrocytes.
Premières études des astrocytes par Ramon y Cajal lui-même, montrant la morphologie d'astrocytes protoplasmiques (**a, c, d, f**) et fibreux (**b, e**). Ces colorations mettent également en évidence le contact des astrocytes avec les capillaires sanguins *(Garcia-Marin et al., 2007)*.

En conditions physiologiques, chaque astrocyte couvre un **domaine tridimensionnel unique**, qui se superpose très peu avec les astrocytes voisins *(Bushong et al., 2002 ; Halassa et al., 2007 ; Figure 2)*. Cependant, ils sont organisés en réseaux fonctionnels permettant une communication intercellulaire à distance, notamment grâce à la formation de jonctions communicantes entre les cellules *(Theis and Giaume, 2012)*. Les astrocytes sont impliqués dans de nombreux rôles vitaux pour le cerveau, allant du soutien énergétique à une participation active dans la communication neuronale *(Cf §1.2).*

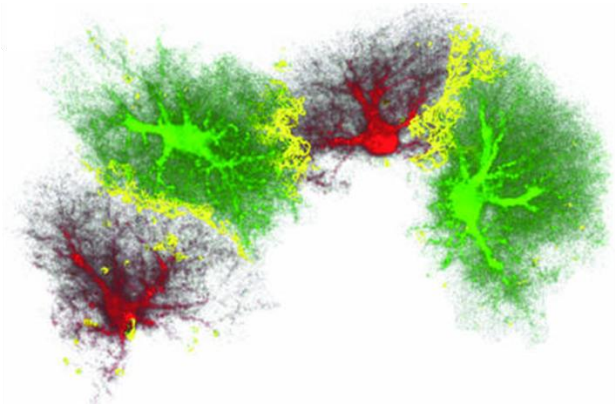

Figure 2 : Domaine tridimensionnel unique de chaque astrocyte.
Reconstruction en 3D des astrocytes dans le gyrus denté montrant l'organisation en domaine unique de chaque astrocyte, avec seulement quelques prolongements en interconnexions (jaune) *(Wilhelmsson et al., 2006).*

Les astrocytes constituent une **population cellulaire très hétérogène**. Ramon y Cajal a été l'un des premiers à décrire cette diversité, il y a plus de 100 ans *(Miller and Raff, 1984)*. Les astrocytes étaient initialement classés en deux grandes catégories. Les astrocytes fibreux sont situés dans la substance blanche et présentent une morphologie allongée, avec des prolongements longs et fins. Les astrocytes protoplasmiques se trouvent dans la substance grise et ont de nombreux prolongements irréguliers *(Andriezen, 1893 ; Figure 1)*.

Depuis, différentes classes d'astrocytes ont été décrites selon la région spécifique du cerveau. On observe par exemple les astrocytes de la glie radiaire, présents essentiellement au cours du développement embryonnaire, qui sont des cellules bipolaires le long desquelles les neurones migrent jusqu'à atteindre leur position finale dans le cortex. La glie de Bergmann désigne un type d'astrocytes présents dans le cervelet et la glie de Muller dans la rétine. D'autres populations d'astrocytes spécialisés ont également été identifiées dans le SNC, comme par exemple les « velate astrocytes » qui forment une gaine autour des neurones granulaires du cervelet, les « interlaminar astrocytes » qui sont observés dans le cortex cérébral des primates *(Fedorff, 2012)*.

Une étude très récente a proposé une classification moléculaire des astrocytes. Cinq populations différentes d'astrocytes ont été identifiées dans le bulbe olfactif, le cortex, le tronc cérébral, le thalamus et le cervelet sur la base du profil d'expression de marqueurs de surface *(John Lin et al., 2017)*. Ces 5 classes expriment différemment marqueurs moléculaires comme CD (Cluster of differentiation) 51, CD63 et CD71, indépendamment de la région étudiée. Ces différentes populations astrocytaires apparaissent à différents stades du développement et ont des propriétés migratoires et prolifératives variées, ainsi qu'un rôle plus ou moins important dans la synaptogenèse *(John Lin et al., 2017)*.

Aux vues de la complexité des astrocytes, il est essentiel de bien comprendre leurs rôles en conditions physiologiques afin d'identifier leurs impacts potentiels en conditions pathologiques, comme dans la MA (Maladie d'Alzheimer). Les astrocytes jouent un rôle central dans le bon fonctionnement du SNC *(Figure 3)*. Ils participent notamment au maintien de l'intégrité de la BHE, au support métabolique pour les neurones, à l'homéostasie du glutamate et à la transmission synaptique via la libération de gliotransmetteurs.

1.2. Rôles des astrocytes en conditions physiologiques

1.2.a. *Essentiels pour les échanges avec le système vasculaire*

Le cerveau est l'organe qui présente la plus forte demande énergétique du corps (environ 20% pour seulement 2% de la masse corporelle). Il requiert donc une vascularisation spécifique afin de répondre à ses besoins en oxygène et en nutriments, tout en restant protégé contre les pathogènes et toxines *(Daneman and Prat, 2015)*. La BHE est composée de cellules endothéliales, de péricytes, des pieds astrocytaires et d'une matrice extracellulaire. Chez l'adulte, les astrocytes libèrent des facteurs de croissance tels que l'angiopoiétine, favorisant la stabilisation des vaisseaux et la diminution de la perméabilité de la BHE via la surexpression de protéines de jonction *(Pfaff et al., 2006)*. Les astrocytes seraient donc impliqués dans le **maintien de l'intégrité de la BHE**. La proximité des astrocytes avec la BHE font d'eux de parfaits candidats pour la moduler *(Alvarez et al., 2013)* et ainsi jouer un rôle essentiel dans les échanges avec le système vasculaire *(Figure 3)*.

1.2.b. *Support métabolique*

Grâce à leur position à proximité de la BHE et de la synapse, les astrocytes assurent l'approvisionnement métabolique nécessaire au bon fonctionnement et à la survie des neurones. Les astrocytes absorbent le glucose présent dans le sang en fonction de l'activité synaptique. En particulier, selon l'hypothèse de la « **lactate shuttle** », en réponse à une augmentation de l'activité synaptique, les astrocytes absorbent le glucose sanguin et l'oxyde en lactate via la glycolyse aérobique. Le lactate est transféré aux neurones via les transporteurs des monocarboxylates pour alimenter leur besoins accrus en énergie *(Magistretti, 2006 ; Figure 3)*. Cependant, les neurones seraient également capables d'utiliser directement le glucose *(Magistretti, 2006)* et ce, de façon majoritaire, comme démontré récemment par microscopie bi-photon en utilisant un analogue du glucose marqué *(Lundgaard et al., 2015)*. De plus, les astrocytes sont les seules cellules du cerveau capables de stocker du **glycogène**. Le glycogène représente la source d'énergie du cerveau la plus importante pendant les périodes de faible apport en glucose, comme lors du sommeil *(Magistretti, 2006)*.

1.2.c. *Maintien de l'homéostasie du glutamate*

Les astrocytes possèdent de nombreux récepteurs et transporteurs aux neurotransmetteurs, qui leur permettent de détecter l'activité neuronale. Ils expriment par exemple des transporteurs au glutamate (Excitatory amino acid transporter gene 1 and 2, nommés respectivement GLAST et GLT-1 chez la souris) sur lesquels se fixe le glutamate libéré par les neurones au niveau de la fente synaptique *(Porter and McCarthy, 1997)*. Ces transporteurs leur permettent de **limiter la concentration du glutamate** dans la fente synaptique, évitant une suractivation des récepteurs post-synaptiques au glutamate, protégeant ainsi les neurones d'une excitotoxicité *(Figure 3).* Le glutamate est ensuite **métabolisé en glutamine** sous l'action de la glutamine-synthase, enzyme uniquement exprimée par les astrocytes. La glutamine est retransmise aux neurones et utilisée comme précurseur du glutamate *(Belanger et al., 2011* ; *Figure 3).*

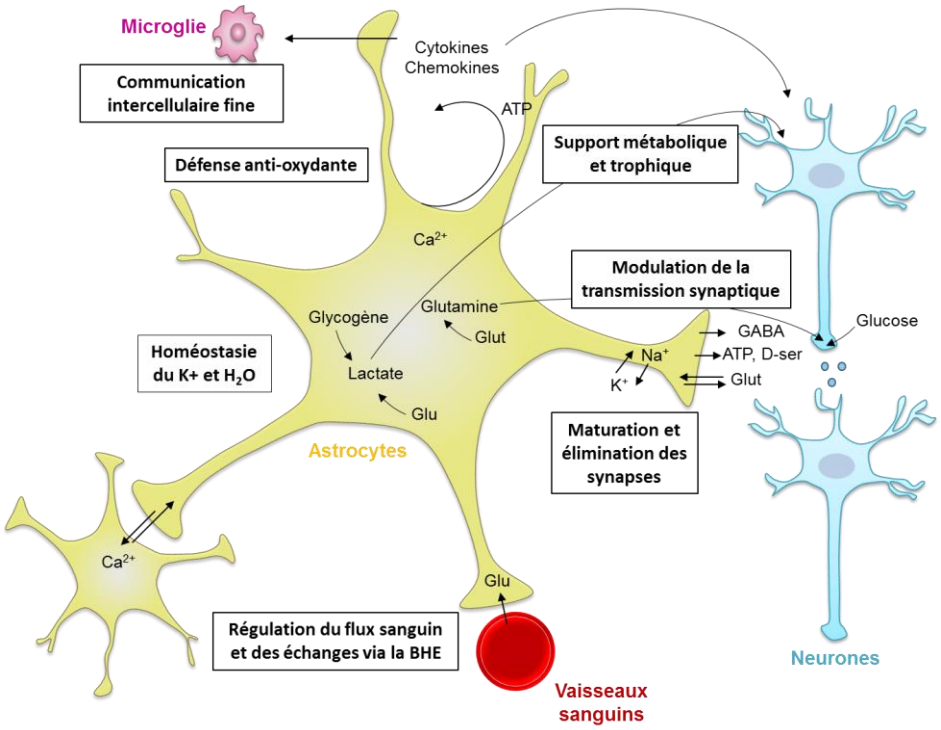

Figure 3 : Rôles centraux des astrocytes en conditions physiologiques.

Les astrocytes jouent de multiples rôles essentiels pour l'activité et la survie neuronale. Ils fournissent un support métabolique et trophique aux neurones. Ils maintiennent également les conditions d'homéostasie nécessaires au bon fonctionnement des synapses en régulant les concentrations extracellulaires d'ions et de neurotransmetteurs, tel que le glutamate. Ils entrent aussi en jeu dans les défenses anti-oxydantes. Au-delà de ces fonctions de support et d'homéostasie, les astrocytes participent activement à la transmission synaptique, notamment via la libération de gliotransmetteurs, ainsi qu'à la maturation et l'élimination des synapses. Glut = Glutamate, Glu = Glucose, D-ser = D-sérine.

1.2.d. *Rôle actif à la synapse*

Depuis une quinzaine d'années, le concept de **synapse tripartite** a été proposé pour intégrer les astrocytes comme un élément à part entière de la synapse *(Araque et al., 1999)*. De multiples études ont montré que les astrocytes jouent un rôle actif dans la transmission synaptique *(Araque et al., 1999 ; Perea et al., 2009)*. Les astrocytes libèrent des **gliotransmetteurs**, comme le glutamate, le GABA (Acide gamma aminobutyrique), l'ATP ou la D-sérine *(Perea et al., 2009 ; Liu et al., 2000)*, suite à l'augmentation de la concentration du Ca^{2+} intracellulaire *(Dani et al., 1992 ; Figure 3).* Ces gliotransmetteurs peuvent réguler directement la transmission synaptique *(Panatier et al., 2011)*, participant ainsi à la LTP (Potentialisation à long terme) ou à la dépression à long terme *(Panatier et al., 2006)*. De plus, les PAP (Prolongements astrocytaires péri-synaptiques) sont dynamiques. La modification de la couverture de la synapse par les PAP peut fortement influencer l'efficacité synaptique en diminuant par exemple l'efficacité de la **recapture du glutamate** par l'éloignement des récepteurs astrocytaires de la fente synaptique *(Oliet et al., 2001).*

1.2.e. *Communication astrocytaire et vague calcique*

Contrairement aux neurones, les astrocytes ne sont **pas électriquement excitables** : ils ne propagent pas de potentiel d'action. Cependant, ces cellules disposent d'une forme d'excitabilité basée sur des variations de concentration calcique. Ces variations sont essentiellement asynchrones et semblent majoritaires dans des microdomaines des prolongements astrocytaires *(Bindocci et al., 2017)*. En condition de stimulation prolongée, des vagues calciques peuvent apparaître et impliquer plusieurs astrocytes connectés. Comme un seul astrocyte est en contact avec plus d'un millier de synapses *(Bushong et al., 2002)*, ils peuvent activer de façon synchronisée des neurones pyramidaux de l'hippocampe suite à une augmentation calcique et à un relargage de glutamate par les astrocytes *(Angulo et al., 2004 ; Fellin et al., 2004)*. Grâce à cette signalisation, les astrocytes peuvent donc avoir une **action à distance** de la synapse active *(Cf Covelo and Araque, 2016 pour une revue complète)*.

1.2.f. *Maturation et élimination des synapses*

Les astrocytes jouent aussi un rôle dans la **maturation et l'élimination des synapses** non seulement au cours du développement mais aussi chez l'adulte *(Chung et al., 2013 ; Figure 3)*. Les astrocytes sécrètent de multiples molécules favorisant la formation et la maturation de nouvelles synapses, comme les thrombospondines *(Christopherson et al., 2005 ; Chung et al., 2015)*. Le rôle des astrocytes dans l'élimination des synapses peut être indirect, via la libération de TGF-β (Transforming growth factor 1β), induisant une surexpression de C1q au niveau de la synapse *(Bialas and Stevens, 2013)*. Cette surexpression agit comme un signal pour guider les cellules microgliales aux synapses à éliminer. Les astrocytes jouent également un rôle direct en phagocytant les synapses via les voies MEGF10 et MERTK *(Chung et al., 2013)*.

1.2.g. *Participation à la défense anti-oxydante*

Le rôle des astrocytes dans la défense anti-oxydante est connu depuis plus de vingt ans. Les astrocytes produisent un grand nombre de **molécules anti-oxydantes** comme la vitamine E, l'acide ascorbique, le glutathion, ainsi que de nombreuses enzymes impliquées dans le métabolisme du glutathion, et ce, de façon bien plus importante que les neurones *(Makar et al., 1994 ; Allaman et al., 2011)*. Ils favorisent ainsi la survie des neurones en condition de stress oxydatif *(Tanaka et al., 1999)*.

Pour plus de détails sur toutes ces fonctions essentielles remplies par les astrocytes, voir *Allaman et al., 2011 ; Belanger et al., 2011 ; Alvarez et al., 2013*.

2. Les astrocytes en conditions pathologiques

Les astrocytes sont capables de répondre à toutes modifications de l'homéostasie du SNC. En conditions pathologiques, aigües ou neurodégénératives, les astrocytes deviennent réactifs. La réactivité astrocytaire est observée chez la plupart des mammifères et des oiseaux. Elle est également conservée dans de nombreuses espèces non mammifères comme chez la grenouille ou la lamproie, qui présentent des cellules de type astrocytaire répondant aux altérations du SNC *(Bloom, 2014)*. Chez la drosophile, les cellules gliales, dont certaines présentent des caractéristiques semblables aux astrocytes, ont une forte activité phagocytaire et changent également de morphologie en présence de dégénérescence neuronale *(Freeman, 2015)*.

Tout au long de ce manuscrit, j'utiliserai uniquement le terme de **réactivité astrocytaire** pour désigner la réponse des astrocytes à toutes conditions pathologiques. Cette réactivité ne doit pas être confondue avec l'**activation astrocytaire** qui est associée à une réponse transitoire suite à leur stimulation par des neurotransmetteurs par exemple. L'activation astrocytaire implique une signalisation calcique et peut s'accompagner de changements morphologiques mineurs, eux-aussi transitoires *(Bernardinelli et al., 2014 ; Cf §1.2)*.

2.1. Qu'est-ce que la réactivité astrocytaire ?

La première description de la réactivité astrocytaire date du 19ème siècle *(Weigert, 1895)*. La réactivité astrocytaire est depuis caractérisée par des **changements morphologiques** comme une hypertrophie du soma et des prolongements astrocytaires *(Wilhelmsson et al., 2006)*. Bien que l'organisation en domaines spécifiques ne semble généralement pas altérée par la réactivité, une augmentation du nombre de prolongements primaires ainsi qu'une polarisation des prolongements vers le site de la lésion ont été décrites *(Bardehle et al., 2013 ; Wilhelmsson et al., 2006)*. La caractérisation de la réactivité astrocytaire s'est précisée avec la découverte de protéines des filaments intermédiaires *(Eng et al., 1971)*. En effet, la réactivité astrocytaire induit une importante surexpression de ces protéines, telle que la GFAP *(Bignami and Dahl, 1976 ; Figure 4)*, la Vimentine, et la Nestine, qui sont depuis utilisées comme marqueurs de la réactivité.

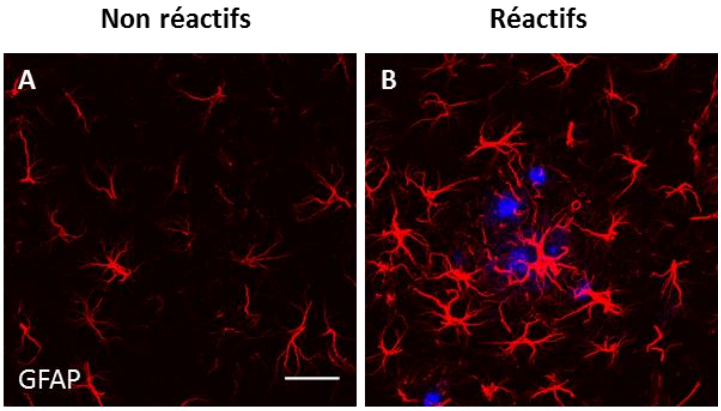

Figure 4 : La réactivité astrocytaire se caractérise par des changements morphologiques et la surexpression de la GFAP.

A) Niveau d'expression basal de la GFAP *(rouge)* par les astrocytes dans l'hippocampe de souris sauvages, **B)** Surexpression de la GFAP, caractéristique de la réactivité astrocytaire, observée notamment à proximité des plaques amyloïdes *(bleu)* dans des souris modèles de la MA (souris APP/PS1dE9). Echelle = 30 µm.

Ces changements morphologiques sont accompagnés de nombreuses **modifications transcriptionnelles** plus récemment identifiées. Celles-ci incluent la surexpression de gènes comme *Lipocaline-2* et *Serpina3n (Zamanian et al., 2012)*. La réactivité astrocytaire est connue comme signature commune à de nombreuses maladies. Mais ce n'est pas pour autant un phénomène de « tout ou rien » homogène. En effet, Zamanian et collaborateurs ont également mis en avant l'hétérogénéité de la réactivité astrocytaire en fonction du contexte pathologique. Bien que de nombreux gènes soient communs entre deux contextes pathologiques donnés (injection de LPS (Lippopolysaccharide) ou ischémie), plus de 50% des gènes modulés par la réactivité sont dépendant de la pathologie *(Zamanian et al., 2012)*. Ces résultats suggèrent donc qu'en fonction du stimulus, les modifications transcriptionnelles et fonctionnelles peuvent être différentes.

La forme la plus sévère de ce phénomène graduel est certainement la formation de la cicatrice gliale induite par une rupture du parenchyme cérébral. La cicatrice gliale est irréversible et induit un remodelage morphologique majeur des astrocytes entourant l'ensemble de la lésion afin de séparer les neurones sains des neurones endommagés. Les effets de cette barrière peuvent être bénéfiques ou délétères *(Anderson et al., 2016)*. Je ne développerai pas la controverse autour de l'impact de cette cicatrice gliale dans ce manuscrit *(Cf Burda et al., 2016 pour une revue complète)*.

La réactivité astrocytaire est donc **non stéréotypique et extrêmement sensible au contexte pathologique**. Une étude très récente propose une classification des astrocytes réactifs selon deux classes majeures : les astrocytes réactifs A1 ou A2 *(Liddelow et al., 2017)*. Cette classification repose sur l'expression de gènes spécifiques à chaque classe. Les **astrocytes A1** expriment par exemple les gènes *Serping1, H2-D1, Gbp2* et *Fbln5*. Ils perdraient leur capacité à promouvoir la croissance axonale, la synaptogenèse, la survie neuronale ainsi que leur fonction de phagocytose. Ils sont donc considérés comme neurotoxiques et sont observés dans de nombreuses maladies neurodégénératives comme la MA, la maladie de Huntington ou encore la sclérose latérale amyotrophique.

A l'inverse, les **astrocytes A2** auraient des fonctions bénéfiques comme la libération de facteurs neurotrophiques. Ils surexpriment par exemple les gènes *Tm4sf1, Cd14, Ptx3, Emp1* et *Tgm1*. Cette classe d'astrocytes A2 est majoritairement observée dans un modèle d'ischémie, favorisant la survie neuronale et la réparation des tissus. De plus, cette étude met en avant l'importance de la communication intercellulaire entre les astrocytes et la microglie. En effet, l'injection de LPS induit majoritairement une réponse astrocytaire de type A1 via une signalisation microgliale. En absence de microglie, aucun astrocyte A1 n'est observé après injection de LPS. Les cytokines telles qu'IL-1α (Interleukine 1α) ou TNF (Tumor necrosis factor), libérées par la microglie activée, favorisent le phénotype A1 des astrocytes réactifs. Ces résultats suggèrent donc que la proportion d'astrocytes A1 (neurotoxiques) et A2 (protecteurs) est dépendante du contexte pathologique et impacte la fonction neuronale.

Aux vues des multiples rôles clés des astrocytes dans le SNC en conditions physiologiques, il est facile d'imaginer que de nombreuses altérations fonctionnelles sont engendrées par les changements transcriptionnels et morphologiques liés à la réactivité. Les altérations fonctionnelles rapportées dans le contexte de la MA seront détaillées dans le chapitre 4.

2.2. Voies de signalisation impliquées dans la réactivité astrocytaire

La réactivité astrocytaire est induite par tout stimulus altérant l'homéostasie du SNC. Les voies de signalisations conduisant à la réactivité sont donc nombreuses. Nous avons écrit en 2015 une revue détaillant **quatre voies majoritaires** impliquées dans cette réactivité *(Figure 5)* : la voie NF-κB (nuclear factor-kappa B), la voie des MAPK (Mitogen-activated protein kinases), la voie NFAT (Nuclear factor of activated T-cells) / Calcineurine et la voie JAK2-STAT3 (Janus kinase 2/ Signal transducer and activator of transcription 3) *(**Publication 1 en annexe**).*

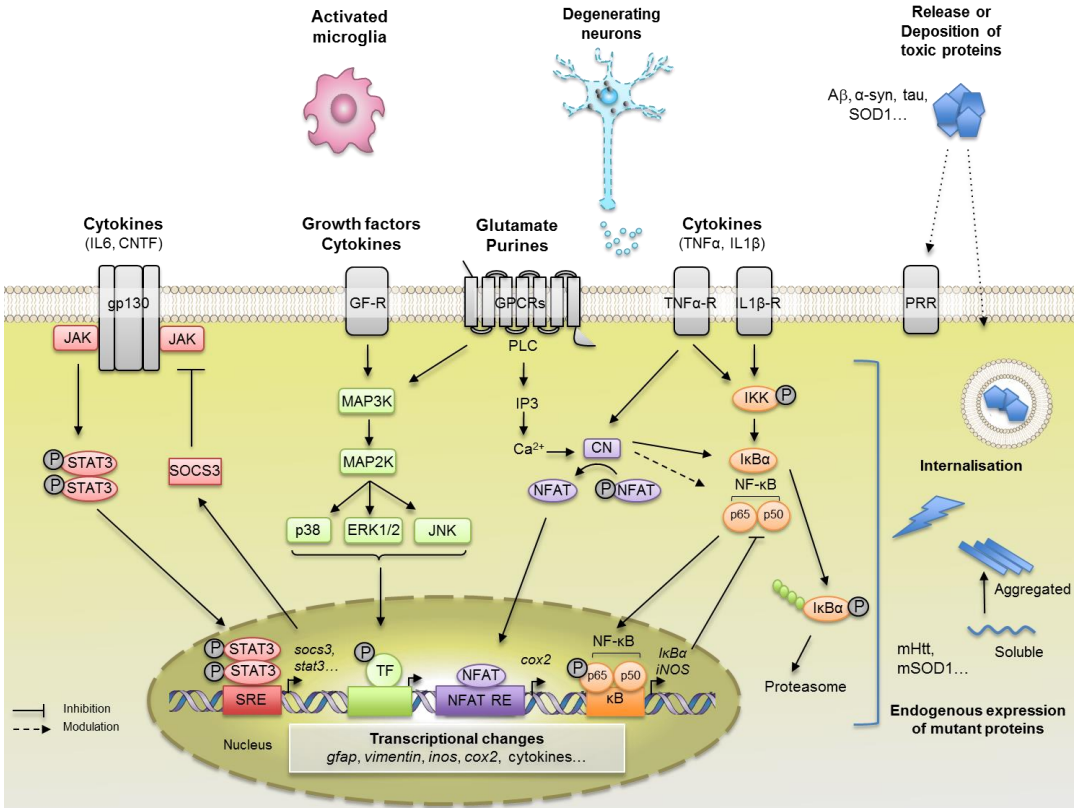

Figure 5 : Voies de signalisations majeures impliquées dans la réactivité astrocytaire.
De nombreuses molécules sont libérées par les neurones en souffrance, la microglie réactive ou les astrocytes eux-mêmes et peuvent se fixer sur des récepteurs spécifiques présents à la membrane astrocytaire. Ces signaux peuvent activer des voies de signalisations impliquées dans la réactivité astrocytaire comme la voie JAK-STAT3 (rouge), des MAPK (vert), Calcineurin/NFAT (violet) ou la voie NF-κB (orange). Abréviations : NFAT RE = NFAT responsive element, GF-R = Growth factor receptor, GPCR = G-protein coupled receptor *(Schéma tiré de la **publication 1 en annexe**).*

Ces voies de signalisation, bien caractérisées dans des modèles aigus, sont aussi activées dans de nombreuses maladies neurodégénératives comme la maladie de Parkinson, la maladie de Huntington, et la MA. Je fais ici le choix de ne pas redévelopper l'ensemble de ces voies ainsi que leurs rôles, qui sont détaillés dans la ***publication 1* en annexe**. La voie JAK2-STAT3, qui est au centre de mon projet de thèse, est détaillée dans le prochain paragraphe.

2.3. La voie JAK2-STAT3 : voie centrale dans la réactivité astrocytaire

L'importance de la **voie JAK2-STAT3** a été amplement détaillée dans la ***publication 2* en annexe**, revue écrite en 2016, dont je suis première auteur. Pour résumer, cette voie ubiquitaire est impliquée dans la modulation de la transcription de gènes responsables de nombreux mécanismes au cours du développement, dans la croissance cellulaire, la prolifération et la différentiation. Cette voie est activée par des polypeptides comme des hormones, des facteurs de croissances et des cytokines de la famille des interleukines (IL-6, CNTF (Ciliary neurotrophic factor) par exemple) suite à leur fixation sur les récepteurs *(Figure 6)*. Les changements conformationels de la partie intracellulaire du récepteur rapprochent les domaines kinases de deux JAKs *(Brooks et al., 2014)*.

Les JAKs sont des tyrosine-kinases associées au récepteur qui peuvent se phosphoryler les unes et les autres mais aussi phosphoryler le récepteur sur plusieurs résidus. Ceci engendre le recrutement au récepteur du facteur de transcription STAT3 et sa phosphorylation par JAK2 sur la tyrosine 705 *(Lim and Cao, 2006)*. Les protéines P-STAT3 se dimérisent et s'accumulent dans le noyau. Ces dimères P-STAT3 se lient à des séquences spécifiques nommées « STAT3-responsive element » sur le promoteur des gènes ciblent et induisent leur transcription *(Darnell, 1997; Shuai et al., 1994)*. Parmi ces gènes ciblent, on retrouve les gènes *GFAP, Vimentine* et *STAT3* lui-même *(Hutchins et al., 2013)*.

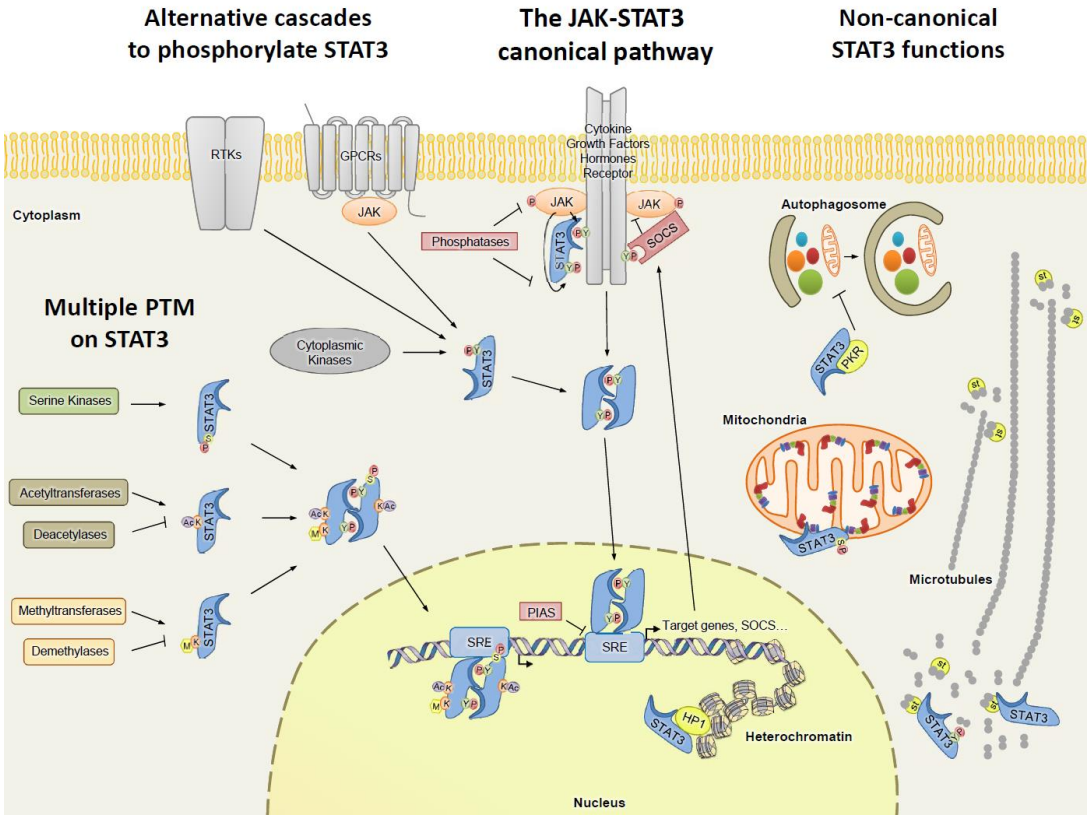

Figure 6 : Représentation de la voie JAK2-STAT3 et sa régulation.

La **voie JAK2-STAT3 canonique** *(centre)* est induite par la liaison de cytokines, hormones ou facteurs de croissance à leurs récepteurs. STAT3 est aussi impliqué dans des **voies de signalisations alternatives** *(gauche)*. Il peut être directement phosphorylé par des récepteurs avec une activité tyrosine kinase ou par les MAP kinases. Les récepteurs couplés aux protéines G (GPCRs) peuvent aussi phosphoryler JAK conduisant à la phosphorylation de STAT3, induisant sa dimérisation et l'activation de la transcription de gènes cibles. STAT3 peut également subir de multiples modifications post-traductionnelles (PTMs). STAT3 est également impliqué dans des **fonctions non canoniques** *(droite)*. STAT3 contribue notamment au maintien des faisceaux de microtubules en prévenant la séquestration de la tubuline par les stathmines (St). Il est également présent à la mitochondrie où il régule la production d'énergie, les défenses anti-oxydantes et l'apoptose. Enfin, STAT3 réprime l'autophagie en inhibant les récepteurs aux protéines kinases (PKR) et en stabilisant la chromatine en liant HP1. La voie JAK2-STAT3 peut être inhibée par au moins trois mécanismes : 1/ déphosphoryraltion des récepteurs, 2/ inhibition directe des JAKs par les protéines SOCSs, 3/ inhibition de la liaison à l'ADN par les PIAS (Protein inhibitors of activated STAT). Abréviations : Ac = Acétylation, M = Méthylation, P = Phosphorylation, K = Lysine, S = Sérine, Y = Tyrosine, SRE = STAT responsive element *(Schéma et légende adaptés de la **publication 2 en annexe**)*.

Plusieurs inhibiteurs de la voie JAK-STAT ont été identifiées comme les SOCSs (Suppressors of cytokine signaling) et les « Protein inhibitors of activated STAT » *(Heinrich et al., 2003)*. Les SOCS inhibent cette voie par deux mécanismes : 1/ en favorisant l'ubiquitination des JAKs et leurs récepteurs associés, permettant leur dégradation par le protéasome, 2/ en inhibant directement l'activité kinase de JAK2 *(Babon et al., 2014)*. SOCS3 est l'inhibiteur le plus efficace et spécifique puisqu'il a la capacité de lier JAK2 et le récepteur phosphorylé simultanément, agissant alors comme un pseudo-substrat de JAK2 *(Kershaw et al., 2013)*. L'expression de SOCS3 est fortement induite par la voie JAK2-STAT3, effectuant un rétrocontrôle sur la voie *(Cf **Publication 2 en annexe** pour une description détaillée des mécanismes de rétrocontrôle)*.

Nous avons montré une accumulation nucléaire de STAT3 dans de plusieurs modèles de maladies neurodégénératives *(**Publication 3 en annexe**)*. Cette activation semble être une caractéristique commune de la réactivité astrocytaire entre différentes maladies, différents régions du cerveau mais également conservés au cours de l'évolution puisqu'elle est observée dans de nombreuses espèces allant de la drosophile au singe *(Doherty et al., 2014 ; **Publication 1 en annexe**)*. La voie JAK2-STAT3 apparaît donc comme une voie conservée et centrale dans l'induction de la réactivité astrocytaire.

3. La maladie d'Alzheimer

La MA est la **maladie neurodégénérative et la cause de démence la plus fréquente**. Elle a été caractérisée pour la première fois par Alois Alzheimer, neurologue allemand, en 1906. Il a examiné une patiente âgée de 51 ans, Auguste D., souffrant de pertes de mémoire, du langage et de troubles psychologiques. A son décès, il a décrit les principales caractéristiques histologiques de cette pathologie telle qu'une atrophie du cerveau, et deux types de dépôts à l'intérieur et à l'extérieur des cellules neuronales, les DNF (dégénérescences neurofibrillaires) et les plaques amyloïdes *(Alzheimer et al., 1995)*.

Une démence est un syndrome dans lequel on observe une perte progressive de mémoire, une dégradation du raisonnement, du comportement et de l'aptitude à réaliser les activités quotidiennes. On compte 47,5 millions de personnes atteintes de démence dans le monde, dont 60 à 70% des cas seraient diagnostiqués comme la MA *(Source : Organisation Mondiale de la Santé ; OMS)*. **En France, 900 000 personnes sont atteintes** de cette maladie. Les études épidémiologiques estiment qu'en 2020, 1 Français sur 4 de plus de 65 ans pourrait être touché par la MA *(Source : Fondation pour la Recherche Médicale)*. Cette maladie représente un enjeu social et économique énorme étant donné que l'OMS estime qu'en 2010, le coût sociétal total lié à la démence dans le monde était de 604 milliards de dollars.

Bien que de nombreux **facteurs de risques** aient été identifiés, comme des facteurs génétiques (ApoEε4, TREM2, etc. ; *Cf §3.3.c*), des facteurs de comorbidité (maladies cardiovasculaires, maladies vasculaires cérébrales, diabètes, dépression, etc. ; *(Jorm, 2001)*), des facteurs environnementaux (aluminium, alimentation riche, manque de sport, etc. ; *(Flaten, 2001)*), ou le sexe (plus forte incidence chez les femmes ; *(Gao et al., 1998)*), le principal facteur de risque pour la MA est l'âge *(Cf **Publication 4 en annexe** pour plus de détails sur ces facteurs de risques)*. **95 % des formes sont**

sporadiques et apparaissent au-delà de 70 ans. Les 5% des cas restants sont dus à des mutations dans des gènes responsables de la production de peptides Aβ (amyloïdes beta), l'un des principaux marqueurs de cette pathologie. Ces **formes familiales**, héréditaires, apparaissent précocement, autour de 50 ans *(Blennow et al., 2006)*.

3.1. Symptômes et physiopathologie

3.1.a. *Symptômes cliniques*

Les symptômes cliniques associés à la MA sont apparentés à la démence. Les patients développent de nombreuses altérations cognitives, dont les plus connues sont les altérations mnésiques.

La mémoire se décompose en mémoire à court terme et mémoire à long terme, cette dernière se formant suite à la consolidation de la mémoire à court terme. On observe trois types majeurs de mémoire à long terme : la mémoire procédurale (liée aux automatismes), la mémoire perceptive (dépendante des modalités sensorielles) et la mémoire déclarative (mémoire des événements et des faits), elle-même subdivisée en mémoire épisodique et sémantique.

La MA se caractérise principalement par une altération de la mémoire épisodique *(Nestor et al., 2006)*. Cette sous-classe de mémoire à long terme nous permet de nous souvenir d'événements vécus avec leur contexte. Chez les patients atteints de la MA, les souvenirs anciens datant de l'adolescence par exemple, sont épargnés plus longtemps que les souvenirs récents. La mémoire épisodique fait appel notamment aux réseaux neuronaux de l'hippocampe et plus généralement à la face interne des lobes temporaux *(Figure 7)*.

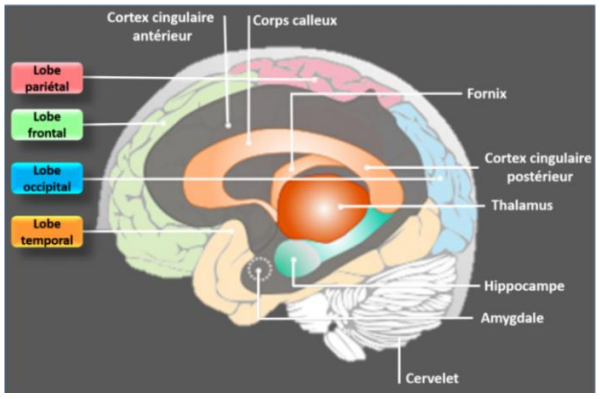

Figure 7: Schéma représentant la face interne de l'hémisphère cérébral droit.
La face interne de l'hémisphère droit est le siège de la mémoire épisodique. L'hippocampe est l'une des régions les plus vulnérables dans la maladie d'Alzheimer (Source : *INSERM*).

Ces pertes de mémoire s'accompagnent généralement de troubles du langage (aphasie), de problèmes moteurs (apraxie) et d'une incapacité à reconnaitre des objets ou des visages pourtant familiers (agnosie). Certains patients développent également des psychoses (hallucinations), et souvent une importante agitation et agressivité. Tous ces symptômes conduisent à une perte d'autonomie du patient *(Masters et al., 2015)*.

3.1.b. *Caractéristiques histologiques*

Chez les patients atteints de la MA, l'hippocampe, le néocortex et le cortex entorhinal sont trois régions particulièrement vulnérables. Elles présentent une **forte atrophie** *(Pini et al., 2016 ; Figure 8)*. L'atrophie de l'hippocampe semble particulièrement corrélée à la sévérité des déficits de mémoire épisodique des patients *(Sarazin et al., 2010)*. De plus, une atrophie des régions subcorticales telles que l'amygdale, le thalamus, le striatum et les ganglions de la base, peut être également observée plus tardivement *(voir Pini et al., 2016 pour plus de détails)*. L'atrophie de ces différentes régions peut être suivie de façon très précise grâce aux différentes techniques d'IRM (Imagerie par résonnance magnétique) et est donc utilisée à des fins diagnostiques *(Cf §3.2)*. Au niveau cellulaire, une importante perte des neurones cholinergiques est observée *(Schliebs and Arendt, 2006)*.

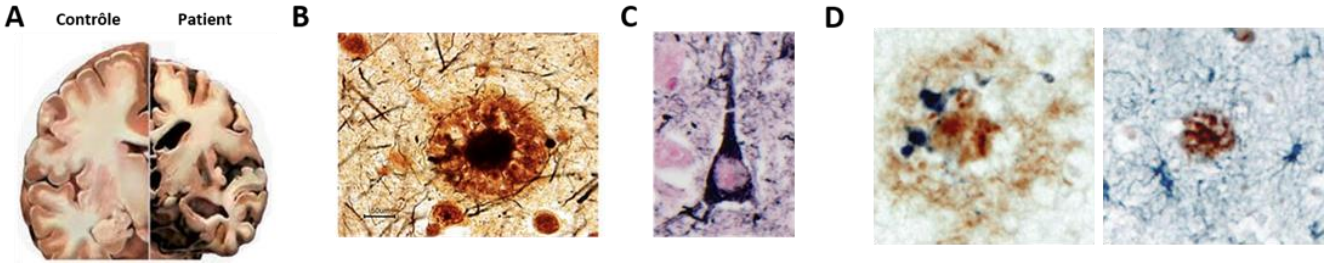

Figure 8 : Caractéristiques histologiques observées chez les patients atteints de la MA.
A) Atrophie cérébrale, **B)** Plaques amyloïdes, **C)** Dégénérescences neurofibrillaires, **D)** Neuroinflammation : Cellules microgliales *(Bleu ; gauche)* et astrocytes réactifs *(Bleu ; droite)* autour d'une plaque amyloïde *(Brun)* dans le cerveau de patients atteints de la MA *(Heneka et al., 2015)*.

Les **plaques amyloïdes** *(Figure 8)* sont une des caractéristiques majeures de la MA. Elles se composent de peptides Aβ de 39 à 43 acides aminés, provenant de la protéolyse de la protéine APP (Glycoprotéine transmembranaire précurseur de l'amyloïde). Les peptides Aβ solubles sont libérés suite au clivage séquentiel de l'APP par l'enzyme BACE1 (β-sécrétase) suivi du clivage intra-membranaire par la γ-sécrétase. Cette voie est nommée **voie amyloïdogénique**. A l'inverse, si le clivage de l'APP est initié par l'α-sécrétase, le fragment P3 est libéré. On appelle cette voie **non amyloïdogénique,** qui est non pathologique *(Figure 9)***.** La γ-sécrétase est constituée de 4 sous-unités dont la PS1 (Préséniline 1), PS2, nicastrine et Aph1a (Anterior pharynx-defective 1). Des mutations dans les gènes de l'*App* (chromosome 21)*, Ps1* ou *Ps2* (chromosome 14 et 1 respectivement) sont responsables des formes familiales de la MA *(Goate et al., 1991 ; Levy-Lahad et al., 1995 ; Schellenberg et al., 1992)*. Ces formes familiales sont à la base de l'hypothèse de la cascade amyloïde, développée dans le paragraphe 3.3.a.

Les **plaques neuritiques** sont des dépôts d'Aβ associés aux neurites dystrophiques. La présence et l'évolution des plaques neuritiques sont évaluées grâce au score CERAD (Consortium to Establish a Registry for Alzheimer's disease). Le score CERAD s'étale de 0 à 3, le score 0 notifiant l'absence de plaque neuritique. Un score égal à 1 correspond à des dépôts épars et le score 3 à une forte présence de plaques neuritiques *(Mirra et al., 1991)*.

De plus, une **CAA** (Angiopathie amyloïde cérébrale) est observée dans 80% des cas de la MA *(Thal et al., 2008)*. Les dépôts vasculaires sont observés dans les artères ou les capillaires et peuvent entrainer une occlusion des capillaires ou des modifications du flux sanguin. Ils sont principalement composés d'Aβ40, contrairement aux plaques amyloïdes dans lesquels le ratio Aβ40/Aβ42 est plus faible *(Roher et al., 1993)*. On distingue 3 stades de CAA, corrélés avec la formation des plaques amyloïdes dans le SNC, en fonction de leur région d'apparition *(Thal et al., 2008)*.

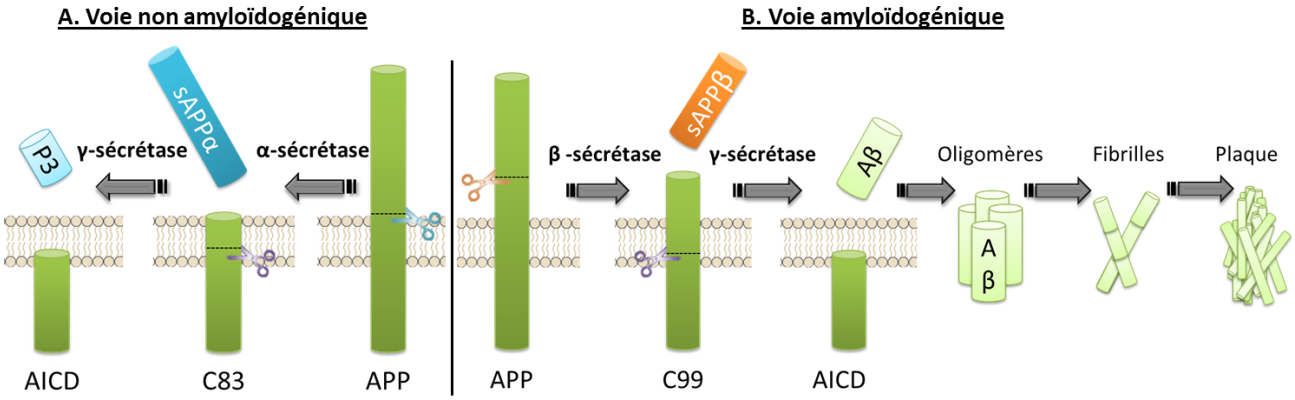

Figure 9 : Métabolisme de l'APP, pouvant conduire à la production de peptides Aβ.
A) L'APP est clivée par l'α-sécrétase libérant deux fragments : C83 (83-residue carboxyl-terminal fragment) et sAPPα ayant des propriétés neurotrophiques. Le fragment C83 est ensuite clivé par la γ-sécrétase libérant les fragments AICD (APP intracellular domain) et P3, **B)** L'APP est anormalement clivée par la β-sécrétase libérant un fragment C99 et sAPPβ. Le fragment C99 est clivé également par la γ-sécrétase produisant le fragment AICD et un fragment pathologique Aβ composé de 39 à 43 acides aminés. L'Aβ soluble peut ensuite s'agréger en oligomères, fibrilles puis plaques amyloïdes.

La présence de **dégénérescences neurofibrillaires** intra-neuronales *(Figure 8)*, composées de formes hyperphosphorylées de la protéine Tau, est également une caractéristique essentielle de la MA. La protéine Tau participe au maintien et à la stabilité du cytosquelette neuronal, ainsi qu'au transport des vésicules le long des axones par sa fixation sur les microtubules en conditions physiologiques. Il existe 6 isoformes de cette protéine, obtenus par épissage alternatif du pré-ARNm issu du gène MAPT, situé sur le chromosome 17q21 *(Neve et al., 1986)*. Ces isoformes se distinguent par les exons présents dans le domaine N-terminal et les séquences répétées dans le domaine de liaison aux microtubules *(Wang and Mandelkow, 2016 ; Figure 10)*. Ces séquences peuvent être présentes sous forme de trois ou quatre répétitions, dénommées formes 3R ou 4R *(Andreadis, 2012)*. Les isoformes de Tau sont anormalement en déséquilibre dans le cerveau des patients. La protéine Tau peut être anormalement phosphorylée sur de nombreux sites Ser (Sérine)/Thr (Thréonine) au niveau des deux domaines riches en proline : Ser-202/Thr-205, Ser-214 et/ou Ser-212, Thr-231 et/ou Ser-235, et Ser-396/Ser-404 *(Figure 10)*. Cette phosphorylation anormale de la protéine Tau diminue son affinité pour les microtubules ce qui conduit à la dissociation de Tau et la désintégration des microtubules *(Figure 10)*. L'évolution et les rôles des DNF dans la pathologie seront développés dans le paragraphe 3.3.b.

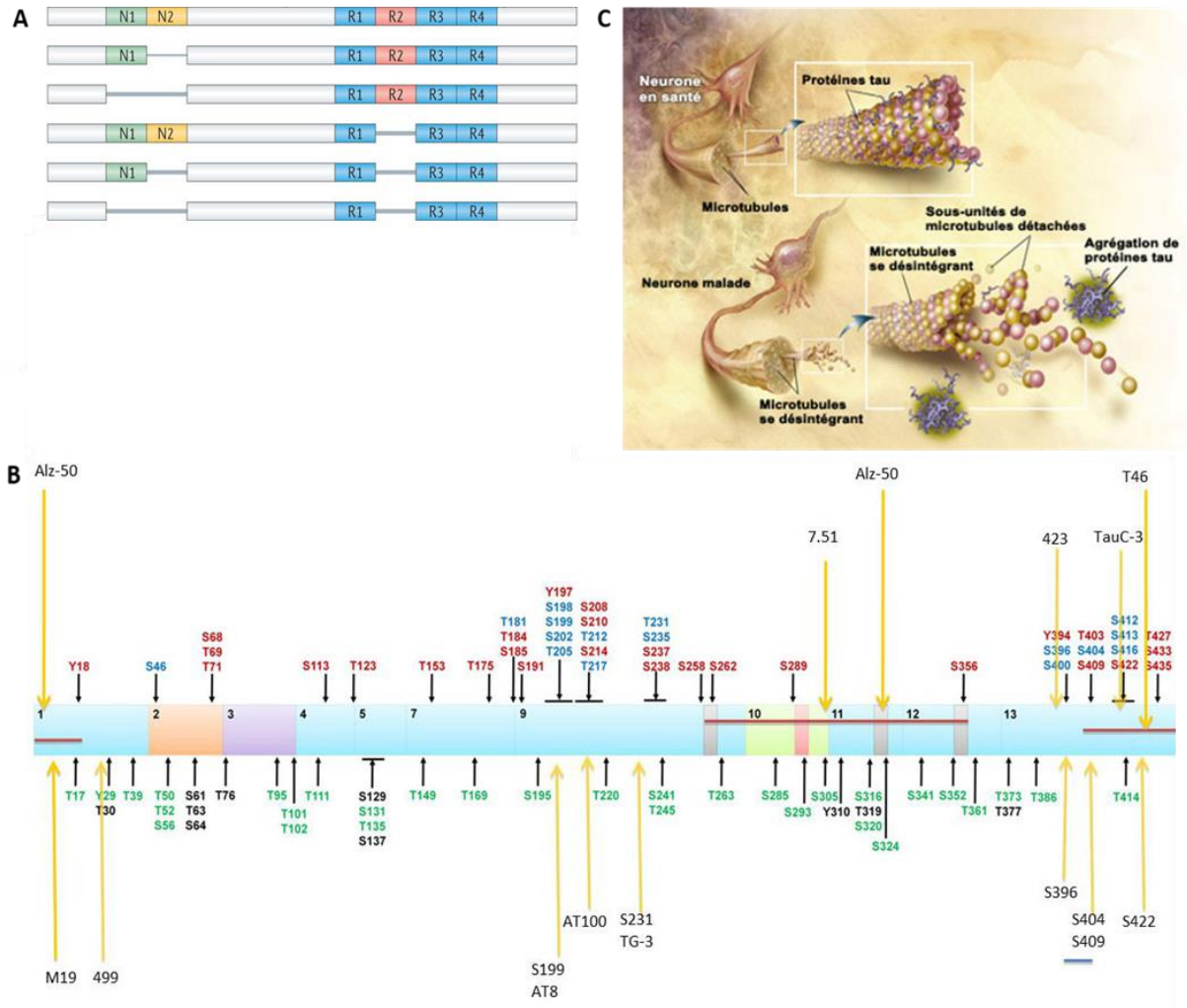

Figure 10 : Formation de dégénérescences neurofibrillaires suite à l'hyperphosphorylation de la protéine Tau.
A) Structure des 6 isoformes la protéine Tau. N1, N2 = inserts dans le domaine N terminal ; R1, R2, R3, R4 = sites de liaisons aux microtubules *(Wang and Mandelkow, 2016)*, **B)** Principaux sites de phosphorylation et sites de reconnaissances des principaux anticorps. Certaines phosphorylations sont observées dans les cerveaux sains (vert), dans les cerveaux sains ou de patients atteints de la MA (bleu), alors que d'autres sont strictement pathologiques (rouge). La localisation des épitopes des anticorps sont indiqués par une flèche jaune. S = Sérine, T = Thréonine *(Luna-Muñoz et al., 2013)*, **C)** La protéine Tau est une protéine associée aux microtubules. Elle interagit avec la tubuline afin de moduler la stabilité des microtubules neuronaux. Lorsque Tau est hyperphosphorylée, elle se dissocie des microtubules induisant leur désintégration. Les protéines Tau hyperphosphorylées peuvent alors s'agréger et former des dépôts intra-neuronaux : les dégénérescences neurofibrillaires *(Source : National Institute on Aging/U.S. National Institutes of Health)*.

La MA est loin d'être une maladie neurodégénérative homogène. En effet, en plus des dépôts amyloïdes et DNF, marqueurs classiques de la MA, certains patients présentent des **dépôts d'α-synucléine**. Cette protéine pré-synaptique est observée sous forme agrégée dans les plaques amyloïdes et dans les terminaux synaptiques des neurones en dégénérescence *(Brookes and St Clair, 1994)*. Une forte augmentation de la concentration en α-synucléine est également mesurable dans le **LCR** (liquide céphalorachidien) des patients atteints de la MA *(Tateno et al., 2012)*. Son rôle ne sera pas développé dans ce manuscrit *(Cf Wirths and Bayer, 2003 pour plus de détails)*.

Ces trois protéines anormalement conformées sont à la base de l'**hypothèse« prion-like »** de la MA *(Goedert, 2015)* qui propose que les protéines mal conformées peuvent induire une mauvaise conformation des protéines physiologiques, permettant leur propagation au sein du SNC. Ceci suggère également une certaine transmissibilité de la MA *(Jaunmuktane et al., 2015)*. Cette dernière affirmation reste controversée et ne sera pas développée dans ce manuscrit *(Cf Eisele and Duyckaerts, 2016 pour une revue détaillée)*.

Enfin, une forte **neuroinflammation** est observée dans le cerveau des patients, notamment autour des plaques amyloïdes *(Figure 8)*. La neuroinflammation joue un rôle important dans de nombreuses maladies neurodégénératives. Elle est caractérisée par une réactivité astrocytaire, une réactivité microgliale, voire par le recrutement de cellules immunitaires du système périphérique *(Cf §3.3.c).*

3.2. Diagnostic de la maladie d'Alzheimer

La première étape du diagnostic de la MA est la **caractérisation du déclin cognitif**, notamment les déficits de mémoire épisodique. De multiples tests sont aujourd'hui disponibles en clinique pour caractériser la démence. Deux tests sont majoritairement utilisés : l'échelle de mémoire de Wechsler et le FCSRT (Free and cued selective reminding test). Le premier consiste au rappel immédiat de la mémoire. Il permet d'évaluer la mémoire épisodique en quatre épreuves : 1/ évaluation de la « mémoire logique », la personne doit restituer deux textes lus par le testeur ; 2/ évaluation de la capacité de « reproduction visuelle » où la restitution concerne des figures géométriques ; 3/ épreuve des « mots couplés » où il y a apprentissage de 10 couples de mots en trois essais ; 4/ évaluation de la « mémoire de travail visuo-spatiale » où le patient doit restituer des symboles. Le FCRST est divisé en deux grandes phases. La première phase consiste également au rappel immédiat de la mémoire, la seconde fait appel à la mémoire à long terme. Pour chaque phase, le sujet dispose de 2 minutes pour se souvenir librement des images ou mots présentés auparavant, puis des indices lui sont donnés. Vingt minutes après cette première phase, le patient est confronté à une nouvelle phase de rappels libres puis indicés. Le FCSRT semble être le plus adapté pour diagnostiquer des altérations de la mémoire épisodique *(Derby et al., 2013)* et corrèlent avec l'atrophie de l'hippocampe des patients *(Sarazin et al., 2010)*. Ce sont ces déficits de mémoire qui poussent généralement les patients à consulter, ne permettant qu'un diagnostic tardif de la MA.

Une **atrophie du cortex et de l'hippocampe** est ensuite recherchée. Parmi les principaux biomarqueurs de la MA visibles en IRM, l'atrophie de l'hippocampe est la mieux documentée *(Figure 11 A)*. Son suivi est utilisé pour déterminer la progression de la pathologie *(Jack et al., 2011)*. Les différentes techniques d'IRM disponibles aujourd'hui permettent également d'obtenir des images à haute résolution et de quantifier *in vivo* l'atrophie de régions corticales spécifiques (en termes de perte de volume, de changements morphologiques et d'épaisseur corticale). Néanmoins, ces atrophies ne sont pas spécifiques de la MA et ne permettent donc pas de poser un diagnostic absolu.

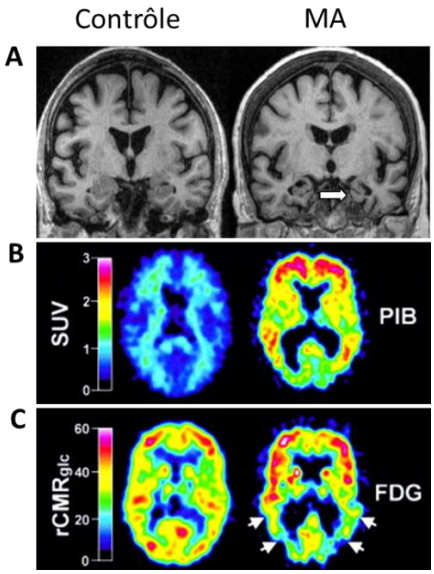

Figure 11 : L'imagerie pour le diagnostic de la MA.

A) Atrophie de l'hippocampe visible par IRM chez les patients atteints de la MA (droite) par rapport aux contrôles (gauche) *(Xu et al., 2013)*, **B)** Imagerie TEP de plaques PIB^+ *(Klunk et al., 2004)*, **C)** Hypométabolisme visible en imagerie TEP du [18F]-FDG *(Klunk et al., 2004)*.

Par imagerie TEP (Tomographie à émission de positrons), il est également possible de visualiser chez les patients la présence de **plaques amyloïdes** *(Figure 11 B)*. Le traceur PIB (^{11}C-labelled Pittsburgh compound B) est l'un des plus utilisés pour le diagnostic puisqu'il corrèle bien avec les dépôts amyloïdes observés dans le cerveau des patients *post mortem (Ikonomovic et al., 2008)*. Le développement de ces techniques d'imagerie ont permis de mettre en évidence un stade préclinique, au cours duquel les patients présentent des plaques amyloïdes PIB^+, sans aucune altération cognitive *(Mintun et al., 2006)*. Cependant, le pourcentage d'individus présentant des plaques amyloïdes PIB^+ qui progresseront vers une phase symptomatique n'est pas établi *(Dubois et al., 2014)*, compliquant les possibilités de diagnostic précoce. Des traceurs reconnaissant **Tau** sont essentiels pour favoriser le diagnostic de la MA et améliorer l'évaluation des thérapies. Des traceurs sont actuellement en développement et commencent à être utilisés en clinique pour le diagnostic de différentes tauopathies, y compris la MA (traceurs THK5317, THK5351, AV-1451, et PBB3) *(Saint-Aubert et al., 2017)*. Néanmoins, de plus amples études sont nécessaires afin de mieux caractériser leurs propriétés de liaison à la protéine Tau. La validation de ces traceurs permettra de distinguer les sujets Alzheimer pré-symptomatiques ($A\beta^+$, Tau^+) des sujets asymptomatiques à hauts risques pour la MA ($A\beta^+$, Tau^-) et d'affiner la détermination de l'avancement de la pathologie selon les stades de Braak *(Schöll et al., 2016 ; Cf §3.3.b)*. Le [18F]-FDG ([18F]-fluorodeoxyglucose *; Figure 11 C*), un analogue du glucose marqué au Fluor 18, permet également de mettre en évidence un **hypométabolisme** cortical par imagerie TEP chez les patients atteints de la MA *(Fukuyama et al., 1994)*.

Un dernier aspect du diagnostic de la MA est la mesure de la **concentration des peptides Aβ** (Aβ40 et Aβ42 essentiellement ; anormalement basse car inversement corrélée à la quantité d'Aβ dans le cerveau) et de la **protéine Tau** totale et de formes phosphorylées (concentrations anormalement hautes) dans le LCR *(Dubois et al., 2014)*.

La **validation** du diagnostic ne peut se faire que ***post mortem***. Cette validation se fait grâce au score ABC, basé sur les stades de Thal (A = Amyloïde ; *§3.3.a*), les stades de Braak (B ; pathologie Tau ; *§3.3.b*) et l'étendue des plaques neuritiques (C = CERAD). Cette échelle de diagnostic permet de classer les changements neuro-pathologiques liés à la MA en 4 classes (nuls, faibles, modérés et forts). Les changements modérés et forts sont considérés comme étant suffisants pour expliquer la démence *(Montine et al., 2012)*.

3.3. Quels sont les mécanismes pathologiques de la maladie d'Alzheimer ?

Basées sur les observations histologiques, deux grandes hypothèses cherchent à expliquer la cause de la MA : l'hypothèse de la cascade amyloïde et la pathologie Tau. Plus récemment, un troisième mécanisme a été proposé comme étant au centre de cette pathologie : la neuroinflammation.

3.3.a. *L'hypothèse de la cascade amyloïde*

L'hypothèse de la cascade amyloïde a été proposée pour la première fois il y a plus de 20 ans. Elle suggère que **les dépôts d'Aβ sont la première cause de la neurodégénérescence** observée dans la MA *(Hardy and Higgins, 1992).*

Comme expliqué par la figure 9, les peptides Aβ sont produits suite au clivage successif de l'APP par la β-sécrétase et la γ-sécrétase. Ces peptides solubles, hautement toxiques *(Walsh and Selkoe, 2007)*, peuvent s'agréger et former des plaques amyloïdes. La cascade amyloïde est une hypothèse neuro-centrique, linéaire, qui suppose que les peptides Aβ initient la cascade lorsqu'ils s'agrègent puis induisent par la suite la pathologie Tau, les altérations synaptiques, la perte neuronale et inévitablement les déficits cognitifs *(Figure 12)*. Cette hypothèse est soutenue par la présence de formes familiales de la maladie, liées uniquement à des mutations sur des gènes impliqués dans le métabolisme de l'APP et la production de l'Aβ.

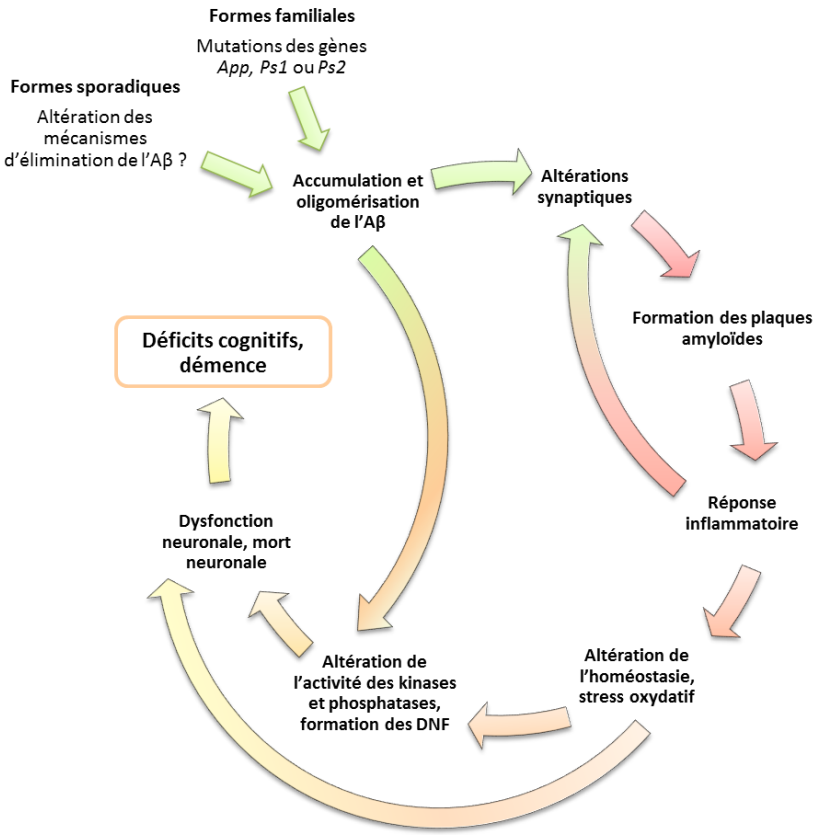

Figure 12 : Hypothèse de la cascade amyloïde.

Chez les patients atteints de la MA, une accumulation anormale d'Aβ40 et Aβ42 est observée. Celle-ci peut être due à des mutations génétiques dans les gènes directement liés à la production de l'Aβ (formes familiales), ou à une altération des mécanismes d'élimination de l'Aβ pour la majorité des formes sporadiques *(De Strooper and Karran, 2016)*. L'accumulation anormale d'Aβ, hautement toxique, peut directement altérer la transmission synaptique. Les peptides peuvent s'agréger et former des plaques amyloïdes. Ceci engendre une réponse inflammatoire (impliquant la microglie et les astrocytes, voire le système immunitaire périphérique) notamment autour des plaques. Cette neuroinflammation module l'homéostasie cellulaire, altère également les synapses, et engendre un stress oxydatif pouvant altérer le fonctionnement neuronal. La formation des DNF cause également une souffrance neuronale. L'ensemble de ces mécanismes conduisent à un dysfonctionnement des neurones et à leur mort, causant les déficits cognitifs observés chez les patients *(Hardy and Higgins, 1992)*.

La majorité des techniques de diagnostic et des essais cliniques ayant eu lieu ou étant encore en cours aujourd'hui est basée sur cette hypothèse *(Cf §3.2 et §3.4)*. Cependant, les études et connaissances acquises à partir de cette théorie sont aussi à la base de sa remise en question. En effet, la présence de plaques PIB^+ chez des personnes ne présentant pas d'atteinte cognitive suggère bien que les plaques amyloïdes ne sont pas, en tout cas pas seules, à l'origine des déficits cognitifs associés à la MA.

De plus, la pathologie amyloïde est **stéréotypique**. Elle s'initie dans le néocortex et diffuse dans un second temps dans l'hippocampe puis dans les régions subcorticales et enfin dans le cervelet *(*évolution décrite selon les **5 stades de Thal** ; *Thal et al., 2002 ; Figure 13)*. Néanmoins, la progression de la pathologie amyloïde dans le SNC ne corrèle pas parfaitement avec l'apparition des symptômes chez les patients atteints de la MA *(Masters et al., 2015 ; Figure 13)*.

3.3.b. *Le rôle émergeant de Tau*

Bien que la pathologie amyloïde soit clairement impliquée dans les formes familiales, la forme pathologique de la protéine Tau **corrèle mieux avec les déficits cognitifs** associés à la MA. La progression de la pathologie Tau dans les différentes régions du cerveau au cours de la maladie a été décrite par Braak et Braak en 1991 *(Braak and Braak, 1991)*. On **observe 6 stades de Braak** dans la MA. Au cours des stades les plus précoces (stades I et II) des DNF sont observées dans le cortex transentorhinal. Les deux stades suivants correspondent à l'atteinte du système limbique, incluant l'hippocampe et le cortex entorhinal (stades III et IV). Enfin, les stades les plus sévères (stades V et VI) atteignent l'ensemble de l'isocortex *(Figure 13)*. Ces stades progressifs corrèlent parfaitement avec le déclin cognitif observé au cours de la MA, contrairement à la pathologie amyloïde *(Masters et al., 2015 ; Figure 13)*.

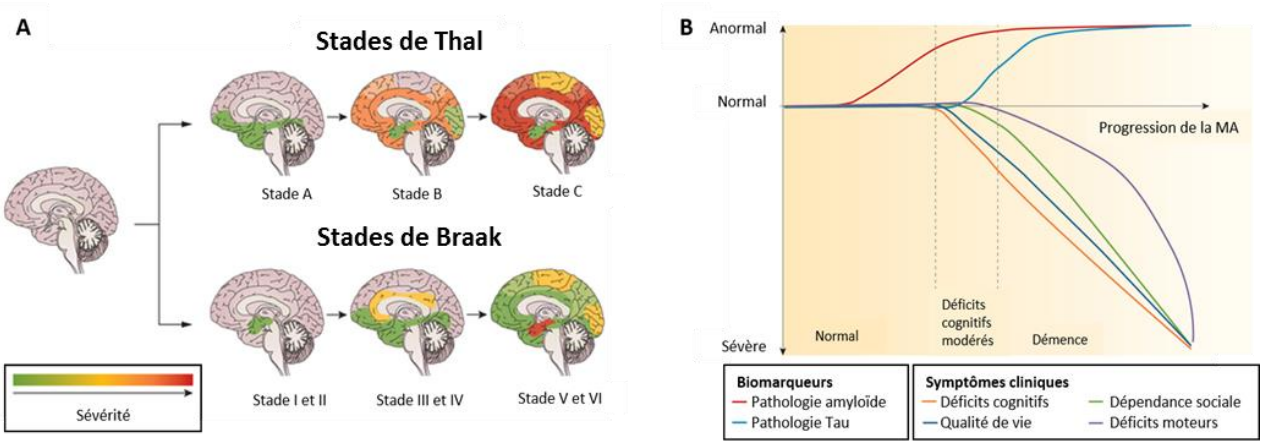

Figure 13 : Propagation des plaques amyloïdes et de la pathologie Tau au cours de la MA et corrélation avec les symptômes cliniques.

A) Propagation de la pathologie amyloïde au cours de la MA selon les stades de Thal et propagation de la pathologie Tau selon les stades de Braak, **B)** Meilleure corrélation entre l'apparition et la progression de la pathologie Tau et les symptômes cliniques *(Figure adaptée de Masters et al., 2015)*.

Comme mentionné précédemment, la protéine Tau favorise, en conditions physiologiques, l'assemblage et le maintien des microtubules. Dans la MA, les protéines Tau hyperphosphorylées se polymérisent et forment des dégénérescences neurofibrillaires qui ne peuvent plus se lier à la tubuline et inhibent l'assemblage des microtubules *(Alonso et al., 1994; Li et al., 2007)*. Cette propriété toxique de la protéine Tau hyperphosphorylée implique également la séquestration de protéines Tau normales *(Alonso et al., 1994, 1996)*, mais également de deux autres protéines neuronales associées aux microtubules, MAP1 et MAP2 *(Alonso et al., 1997)*. Ce gain de fonction toxique altère donc le cytosquelette et conduit à la neurodégénérescence axonale et dentrique des neurones affectés. Des hypothèses récentes suggèrent une propagation trans-synaptique des agrégats de protéines Tau, induisant ainsi la progression de la pathologie *(Liu et al., 2012; Wang et al., 2017)*. Inhiber les formes pathologiques hyperphosphorylées de Tau apparait donc comme une stratégie thérapeutique prometteuse *(Cf §3.4.b)*.

Aucune mutation génétique liée à la protéine Tau engendrant une pathologie amyloïde n'a été identifiée à ce jour. En effet, les mutations génétiques liées à cette protéine sont responsables de tauopathies, comme la démence fronto-temporale par exemple. Or, les plaques amyloïdes et les DNF doivent être présentes pour parler de MA, et non de tauopathie. La présence de la protéine Tau anormale n'est donc pas suffisante pour expliquer la MA. En effet, ces deux mécanismes majeurs (cascade amyloïde et pathologie Tau) sont centrés sur les neurones. Ils ne prennent pas en compte l'ensemble des types cellulaires impliqués directement dans la MA.

3.3.c. *Importance de la neuroinflammation*

La neuroinflammation est une caractéristique commune à de nombreuses conditions pathologiques aigües comme neurodégénératives. Elle implique les astrocytes, la microglie et les cellules immunitaires du système périphérique, qui peuvent agir soit à distance, soit en infiltrant le SNC.

Les différents partenaires de la neuroinflammation

Les astrocytes réactifs

Bien que certains astrocytes réactifs soient observés autour des DNF formant ainsi une couronne *(Bouvier et al., 2016)*, ils sont essentiellement observés autour des plaques amyloïdes chez l'Homme et les modèles animaux de la MA *(Figure 4)*. Cependant, les plaques amyloïdes ne sont pas systématiquement entourées par des astrocytes *(Simpson et al., 2010)*.

Des astrocytes atrophiés peuvent aussi être observés à distance des plaques dans certains modèles murins de la MA *(Olabarria et al., 2010)*. De plus, des études montrent que la réactivité astrocytaire peut être observée avant la formation des plaques dans des modèles murins de la MA *(Heneka et al., 2005)*. Grâce à des études par TEP avec des traceurs spécifiques des astrocytes réactifs, il a été montré que les astrocytes deviennent réactifs à des stades très précoces de la maladie, voire même avant l'apparition des symptômes *(Carter et al., 2012 ; Rodriguez-Vieitez et al., 2016)*. Les astrocytes réactifs pourraient donc jouer un rôle dans l'initiation et la progression de la MA.

La microglie réactive

Décrites pour la première fois en 1920 par Del Rio Hortegua, les cellules microgliales sont les **cellules immunitaires du SNC**, présentant d'importantes capacités migratoires et phagocytaires *(Heneka et al., 2014)*. L'origine de ces cellules est déterminée depuis peu. Elles proviennent de progéniteurs erythromyéloïdes du sac vitellin, qui entrent dans le cerveau où ils se différencient en cellules microgliales *(Ginhoux et al., 2010)*. Elles constituent une **population dynamique** qui **scanne l'environnement** en continu grâce à leurs nombreux prolongements ramifiés et qui interagit finement avec les neurones *(Li et al., 2012)*.

La réactivité microgliale peut être induite par des « Pathogen associated molecular patterns » (virus, bactéries, champignons, parasites) et des « Danger associated molecular patterns », dont l'Aβ, induisant de multiples cascades pro-inflammatoires et conduisant à la formation de l'inflammasome et à la production de cytokines *(Venegas and Heneka, 2017 ; **Publication 4 en annexe**)*. Cette réactivité se traduit par des **changements morphologiques** : elle passe d'une morphologie très ramifiée à une morphologie dite amiboïde, présentant de très courts et fins prolongements *(Figure 14)*. Une fois sous forme amiboïde, la capacité migratoire de la microglie est réduite *(Lively and Schlichter, 2013)*, contrairement à son activité phagocytaire qui est augmentée *(Hickman et al., 2008)*.

Dans la MA, la microglie réactive est essentiellement positionnée autour des plaques amyloïdes *(McGeer et al., 1988)* mais ne semble pas s'organiser spécifiquement autour des DNF *(Bouvier et al., 2016)*. La microglie est donc positionnée en première ligne pour dégrader les plaques amyloïdes *(Cf §4.4)*.

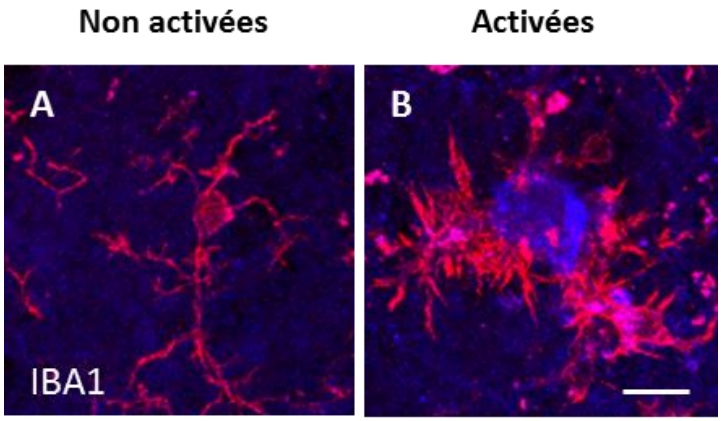

Figure 14 : Les changements morphologiques de la microglie reflètent son activation.
A) Morphologie classique d'une cellule microgliale IBA1^{+} *(rouge)* homéostatique dans l'hippocampe de souris sauvage, **B)** Morphologie amiboïde caractéristique de l'activation de la microglie, observée notamment à proximité des plaques amyloïdes *(bleu)* dans le modèle 3xTg-AD, modèle de la MA. Echelle = 10 µm.

La microglie réactive est couramment classée en deux catégories : **M1, pro-inflammatoire** et **M2, anti-inflammatoir**e *(Varnum and Ikezu, 2012)*. Bien qu'une transition du phénotype M2 vers le phénotype M1 au cours de la maladie soit souvent proposée, cette classification fait l'objet de forts débats puisque l'activation microgliale apparait plutôt sous de multiples états qui dépendent du contexte pathologique précis *(Lire Ransohoff, 2016 pour une discussion complète)*.

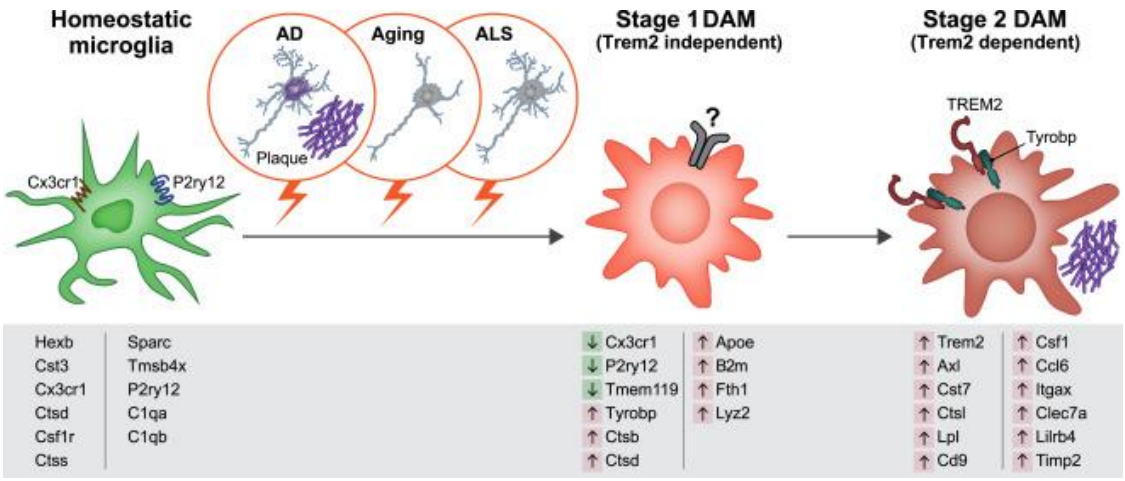

Figure 15 : L'activation des DAM se produit en deux étapes.

Illustration schématique des stades d'activation des DAM, observées notamment autour des plaques amyloïdes. Chaque stade se caractérise par une modulation de l'expression de multiples gènes dont les gènes clés sont présentés ici. Les flèches vertes représentent une diminution de l'expression, les flèches rouge symbolisent une augmentation *(Keren-Shaul et al., 2017)*. Abréviations : AD = Alzheimer's disease, ALS = Amyotrophic lateral sclerosis, DAM = Disease-associated microglia.

Une étude très récente a mis en évidence une nouvelle catégorie de microglie, dynamique au cours de la MA, basée sur leur profil d'expression génique : les **DAM** (Disease-associated microglia) *(Keren-Shaul et al., 2017)*. Elles sont retrouvées essentiellement autour des plaques amyloïdes dans un modèle murin transgénique de la MA, mais elles ont également été observées chez les patients et dans d'autres pathologies, comme la sclérose latérale amyotrophique. Les DAM apparaissent via deux stades d'activation *(Figure 15)*. Le premier stade est indépendant de Trem2 (Triggering receptor expressed on myeloid cells 2), récepteur majoritairement microglial, impliqué dans l'inflammation et la phagocytose *(Ulrich et al., 2017)*. A ce stade, on observe une diminution de certains gènes comme « *C-X3-C motif chemokine receptor 1* » ou *Tmem119* (Transmembrane protein 119 precursor) mais aussi la surexpression de gènes liés à la MA comme *Apoe (*Apolipoprotéine) et *Tyrobp* (TYRO protein tyrosine kinase-binding protein). Le second stade d'activation des DAM est Trem2-dépendant et se caractérise par une surexpression de gènes liés à l'inflammation comme *Ccl6* (C-C chemokine ligand 6) ou à la phagocytose tels que *Ctsl* (Cathepsine l). Cette nouvelle classe a été complétée par une seconde étude transcriptomique qui a mis en évidence deux autres classes de cellules microgliales en fonction du stade (précoce ou tardif) de la MA. La microglie étudiée à un stade précoce présente un profil transcriptionnel différent des DAM de stade 1, et pourrait correspondre à un stade plus « naïf ». Par contre, la microglie étudiée à un stade tardif a un grand nombre de gènes communs avec les DAM2 *(Mathys et al., 2017)*. Ces données suggèrent donc la présence de différents types de cellules microgliales, évoluant au cours de la pathologie et appuient le fait que la classification M1/M2 n'est pas suffisante.

Les cellules immunitaires du système périphérique

Il existe deux types de réponses immunitaires : innée et adaptative. Dans le cerveau, la **réponse innée** est médiée par la microglie. Le SNC possède également des cellules myéloïdes non

microgliales, dont les macrophages méningiaux et les macrophages des plexus choroïdes, qui ne sont pas présents dans le parenchyme cérébral en conditions physiologiques *(Figure 16)*. La **réponse immunitaire adaptative** se caractérise principalement par la participation des LT (lymphocytes T) et des LB (lymphocytes B). Les LT sont responsables de la réponse cellulaire (reconnaissance de l'antigène) alors que les LB sont responsables de la réponse humorale (production des anticorps suite à la reconnaissance d'un antigène). Des lymphocytes sont observés dans les méninges *(Figure 16)* et pourraient influencer les fonctions de cerveau sans même entrer dans le parenchyme cérébral.

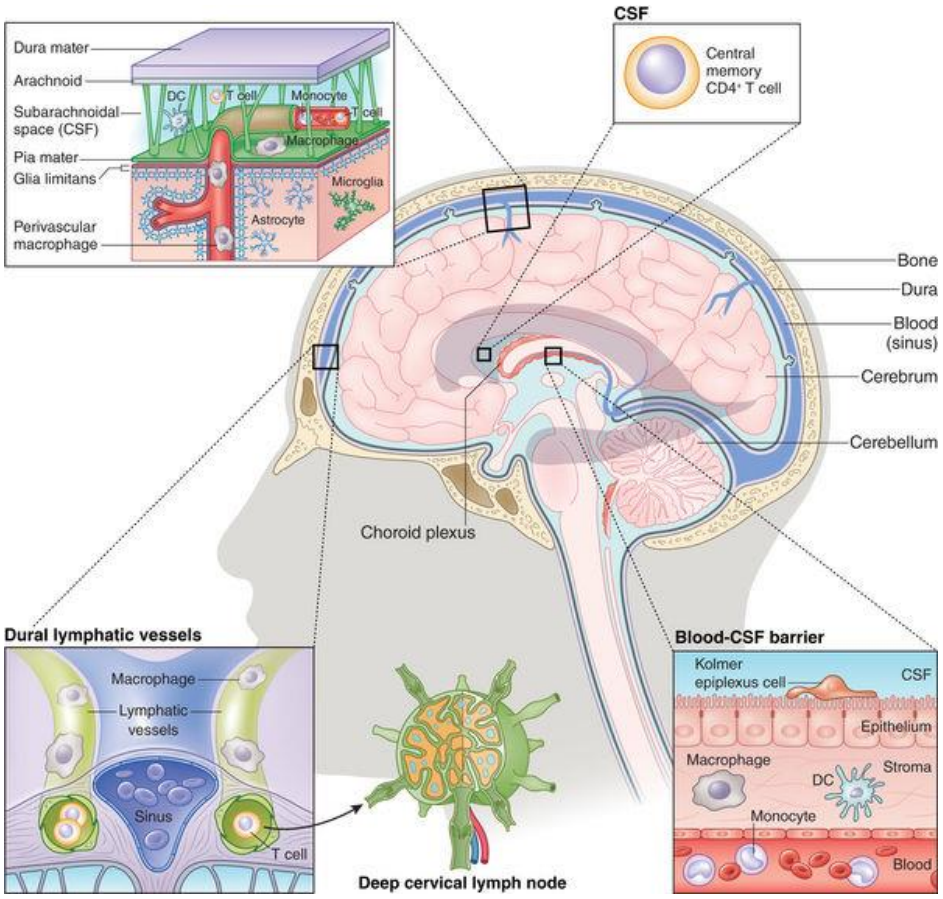

Figure 16 : Localisation des cellules immunitaires au niveau du SNC en conditions physiologiques.
Les leucocytes (granulocytes, lymphocytes T et B) restent dans les vaisseaux sanguins et n'entrent pas dans le parenchyme cérébral en conditions physiologiques. Les cellules immunitaires dans le SNC incluent la microglie, présente dans le parenchyme, et les macrophages non parenchymateux (macrophages périvasculaires, méningiaux et des plexus choroïdes) *(Prinz and Priller, 2017)*. Abréviations : CSF = Liquide céphalo-rachidien, $CD4^+$ T cell = Lymphocytes T $CD4^+$, DC = Cellules dendritiques.

Au cours de la progression de la MA, la BHE subit de nombreuses modifications dont une augmentation de sa perméabilité *(Bowman et al., 2007)*, notamment due à l'altération des cellules endothéliales par l'Aβ ou par certaines cytokines *(Desai et al., 2002)*. Cette altération de la BHE permet l'entrée de multiples substances neurotoxiques comme des cytokines pro-inflammatoires libérées par les cellules immunitaires périphériques *(Persidsky et al., 2006)*, voire l'entrée des cellules elles-mêmes dans le SNC *(Cf §4.3)*.

Inflammation et MA : apport des études génétiques

Des études épidémiologiques suggèrent un rôle prépondérant de l'inflammation dans la MA et sont à la base des essais cliniques ciblant la neuroinflammation *(Pour plus de détails, voir §3.4.b).*

Néanmoins, la recherche sur la réponse inflammatoire dans la MA s'est intensifiée récemment depuis l'avancée des études génétiques. En effet, de nombreux **facteurs de risques génétiques** identifiés par les études d'associations génétiques (GWAS) sont liés au système immunitaire. Ces gènes incluent : *Clusterine*, *« Complement component 3b/4b receptor 1 »* tous deux impliqués dans la cascade du complément*, « Major histocompatibility complex, class II - DR 5β* » impliqué dans la présentation d'antigènes, *Il-6, Il-1β, Il-10, Ccl2, Ccl3,* codant pour des cytokines et chemokines, etc. *(López González et al., 2016)*.

D'autres facteurs de risques pour la MA pointent vers les cellules gliales comme **ApoEε4** et **TREM2**. L'allèle ε4 du gène *Apoe (ApoEε4)* est le plus grand facteur de risque pour la MA, contrairement à l'allèle ε2 qui est protecteur. L'allèle ε4 augmente de 3 à 4 fois le risque de développer cette pathologie *(Corder et al., 1993)*. Les astrocytes expriment fortement ApoE, qui transporte le cholestérol des astrocytes aux neurones *(Bu, 2009)*. Ceci suggère donc un rôle important des astrocytes dans la MA. La découverte récente d'une mutation rare sur le gène *TREM2* (mutation R47H), qui augmente de 3 à 5 fois le risque de développer tardivement la MA, a renforcé le rôle de la microglie dans la MA *(Guerreiro et al., 2013; Jonsson et al., 2013)*. TREM2 est l'un des récepteurs transmembranaires les plus exprimés par la microglie (jusqu'à 300 fois plus que dans les astrocytes) *(Hickman and El Khoury, 2014)*. L'hypothèse la plus évidente est donc que la mutation R47H entraine une diminution de la phagocytose microgliale, induisant une augmentation de la charge amyloïde. Un partenaire de TREM2, nommé TYROBP ou DAP12, est également au cœur des recherches actuelles. Une analyse d'expression génique sur le génome entier de patients atteints de la MA a mis en avant un module, groupant essentiellement des gènes de l'immunité innée, qui corrèle avec la maladie *(Zhang et al., 2013)*. TYROBP apparaît comme le meilleur régulateur de ce module. Une étude récente suggère que de rares variants de *Tyrobp* pourraient augmenter le risque de développer une forme précoce de la MA *(Pottier et al., 2016 ; Cf Ulrich et al., 2017 pour une revue détaillée sur le rôle de TREM2 dans la MA)*.

De plus, le sexe est un facteur de risque majeur dans la MA (Incidence plus forte chez les femmes *; Gao et al., 1998*). Plusieurs études mettent en avant des différences morphologiques et fonctionelles des cellules impliquées dans l'inflammation, dont les astrocytes et la microglie, au cours du développement mais également chez l'adulte *(Cf Schwarz and Bilbo, 2012 ; Nelson and Lenz, 2017 pour revues)*. Une plus forte inflammation est d'ailleurs observée chez la femme après la ménopause, probablement due aux modifications hormonales *(Uchoa et al., 2016)*. Ces données suggèrent donc également un rôle de l'inflammation dans la susceptibilité des femmes à développer la MA.

Enfin, d'autres études basées sur la modulation de l'inflammation dans les modèles animaux de la MA mettent en avant son rôle dans la MA. Ces études, directement en lien avec mon projet de thèse, seront discutées dans le chapitre 5.

La pathologie amyloïde, la pathologie Tau et la neuroinflammation, tous les trois centraux dans la MA sont donc ciblés par les nombreux essais cliniques en cours.

3.4. *Traitements et essais cliniques*

Il n'y a à l'heure actuelle aucun traitement curatif de la MA. L'enjeu social et économique que représente la MA a conduit à plus de 200 essais thérapeutiques. La moitié de ces essais ont déjà été arrêtés pour cause d'inefficacité ou d'effets secondaires trop importants *(Source : Alzforum.org)*. Pour qu'un médicament soit mis sur le marché, au moins une amélioration sur un test de mémoire doit être observée ainsi qu'une amélioration de la vie quotidienne du patient. Seuls cinq essais cliniques ont été à ce jour approuvés, procurant seulement des traitements symptomatiques pour les patients présentant des altérations cognitives modérées.

3.4.a. *Traitements symptomatiques disponibles*

Les quatre molécules (Donepezil, Galantamine, Rivastigmine et Tacrine) actuellement disponibles visent le système cholinergique, dont les efférences arrivent dans le néocortex et l'hippocampe. Ce système est fortement impliqué dans les processus de mémoire et subit une importante dégénérescence chez les patients atteints de la MA *(Schliebs and Arendt, 2006)*. L'objectif de nombreux essais est de favoriser la neurotransmission cholinergique limitant la dégradation de l'acétylcholine, neurotransmetteur produit par les neurones cholinergiques et donc déficitaire dans la MA. La Tacrine est le premier **inhibiteur de l'acétylcholinestérase** mis sur le marché. Il est depuis majoritairement retiré à cause de ses effets secondaires trop importants sur le foie. Le Donepezil, la Galantamine, la Rivastigmine et la Tacrine améliorent modestement et temporairement la cognition des patients *(Blennow et al., 2006)*.

La cinquième molécule, la Mémantine, est un **antagoniste** non compétitif, avec une affinité faible à modérée des **récepteurs au glutamate de type NMDA** (N-méthyl D-aspartate). Elle bloque ainsi l'hyperactivité des récepteurs NMDA observée chez les patients *(Cf §4.1.a)*, sans bloquer leur activité normale, évitant l'excitotoxicité du glutamate *(Nyakas et al., 2011)*. Ce médicament présente de nombreux intérêts cliniques puisqu'il permet de diminuer les hallucinations, l'agitation, l'agressivité et l'irritabilité des patients présentant ces symptômes ou de retarder leur apparition *(Reisberg et al., 2003 ; Gauthier et al., 2008)*.

Ces médicaments sont généralement bien tolérés par les patients et induisent des effets secondaires majoritairement limités à des troubles gastro-intestinaux (nausées, vomissements et diarrhées). Ces effets secondaires sont souvent réduits en commençant le traitement avec de faibles doses, progressivement augmentées *(Blennow et al., 2006)*. Mais bien que leur efficacité et leurs bienfaits sur la cognition et l'état global soient établis, les effets de la Mémantine et des inhibiteurs de l'acétylcholinestérase sur le déclin cognitif des patients restent modérés *(Raina et al., 2008)*.

3.4.b. *Essais cliniques en cours*

Les essais cliniques ciblant la pathologie amyloïde ont été les premiers à être mis en place et sont toujours très nombreux, alimentés par l'hypothèse de la cascade amyloïde *(Tableau 1)*.

Principaux essais cliniques	Résultats sur modèles animaux	Premiers résultats chez les patients	Phase des essais actuels	Références principales
Immunothérapie active *	Diminution des plaques amyloïdes, de la réactivité astrocytaire et des neurites dystrophiques	Diminution des plaques amyloïdes mais encéphalopathie chez 6% des patients : essai stoppé	6 essais cliniques en phases I, II ou III	*(Gilman et al., 2005)*
Immunothérapie passive **	Diminution de la charge amyloïde	Diminution de la charge amyloïde	3 essais cliniques en phase III	*(Bard et al., 2000)*
Inhibiteurs de BACE1	Absence de production d'Aβ	Aucun effet concret	Essais en cours en phases I, II et III	*(Luo et al., 2001)*
Inhibiteurs de la γ-sécrétase	Non spécifique de la voie amyloïde : essais rapidement stoppés		Modulateurs en phase I	*(Yan, 2016)*
Modulateurs de l'α-sécrétase	Favorise la voie non amyloïdogénique	Premiers résultats encourageants	Bryostatine en phase II	*(Etcheberrigaray et al., 2004; Nelson et al., 2017)*

Tableau 1 : Principaux essais cliniques ciblant la pathologie amyloïde.

* L'immunothérapie active consiste à stimuler le système immunitaire pour induire la fabrication de lymphocytes mémoires dirigés contre les peptides Aβ, permettant une réponse plus efficace. ** L'immunothérapie passive à l'inverse ne fait pas appel à la mémoire immunitaire. Elle est basée sur l'injection d'anticorps au patient (ex : injection d'anticorps dirigés contre le peptide Aβ) *(Sources : Alzforum.org ; clinicaltrials.gov).*

Les essais cliniques ciblant la pathologie Tau sont plus récents. Seulement dix essais cliniques sur Tau sont en cours, dont 4 sont déjà arrêtés *(Source : Alzforum.org ; Tableau 2)*.

Principaux essais cliniques	Résultats sur modèles animaux	Premiers résultats chez les patients	Phase des essais actuels	Références principales
Immunothérapie active	Diminution des formes phosphorylées ou des formes oligomériques de Tau, des DNF et amélioration des fonctions sensorimotrices	Essais en cours	2 essais cliniques (ACI-35 et AADvac1) en phase I, II respectivement	*(Theunis et al., 2013 ; Kontsekova et al., 2014)*
Immunothérapie passive	Diminution des formes solubles et insolubles de Tau, de l'activation microgliale, de l'atrophie et amélioration des déficits comportementaux	Essais en cours	2 essais cliniques (RO 7105705 et C2N 8E12) en phase I et II respectivement	*(Yanamandra et al., 2013, 2015)*
Agents stabilisateurs des microtubules	Stabilisation des microtubules efficace	Essais en cours	1 essai (TPI 287) en phase I	*(Panza et al., 2016)*
Inhibiteurs de kinases	Inhibition de la glycogen synthase-3	Premiers résultats positifs mais non confirmés par une seconde étude à plus grande échelle	Essais stoppés	*(del Ser et al., 2013 ; Lovestone et al., 2015)*
Molécules anti-agrégantes	Interfère avec la liaison des protéines Tau, diminue la charge amyloïde et restaure les déficits cognitifs	Amélioration des fonctions cognitives	1 essai en phase III (TRx0237, Bleu de méthylène)	*(Crowe et al., 2013 ; Medina et al., 2011 ; Panza et al., 2016)*

Tableau 2 : Principaux essais cliniques ciblant la pathologie Tau.
(Sources : Alzforum.org ; clinicaltrials.gov)

Comme dit précédemment, de nombreux essais cliniques sont également basés sur des observations épidémiologiques et mettent en avant le rôle de la neuroinflammation dans la MA. En effet, un traitement de longue durée avec des **AINS** (Anti-inflammatoires non stéroïdiens) diminuerait le risque de développer la MA *(Aisen, 2002)*. Certains AINS diminuent la charge amyloïde dans des modèles transgéniques, soit via l'inhibition de la cyclo-oxygénase, soit en modulant l'activité de la γ-sécrétase *(Eriksen et al., 2003)*. Cependant, différents anti-inflammatoires testés en clinique n'ont montré aucun effet bénéfique sur les déficits cognitifs des patients *(Aisen, 2002 ; Cf Table 1 de la **publication 4 en annexe** pour une table détaillée des principaux essais cliniques avec des AINS)*. L'absence d'effet de ces anti-inflammatoires pourrait s'expliquer par un traitement trop tardif des patients, alors que la pathologie est déjà trop avancée. Les AINS pourraient plutôt prévenir le déclenchement de la maladie et non la réverser.

Comme ApoEε4 est le plus important facteur de risque pour la MA, des études rétrospectives ont également soulevé un intérêt thérapeutique pour les médicaments diminuant le **cholestérol**, tels que les statines. En effet, la prise de statines diminuerait l'incidence de la MA *(Wolozin et al., 2000)*. Il a également été montré sur des modèles animaux que ce traitement diminue la charge amyloïde *(Refolo et al., 2001)*. Cependant, les premiers essais cliniques n'ont pas été concluants *(Hoglund et al., 2005)*.

Les essais cliniques pour la MA sont donc extrêmement nombreux. Mais comment expliquer qu'ils ont, jusqu'à présent, tous échoués ? Le principal problème soulevé est généralement le manque de diagnostic précoce, ce qui engendre un traitement trop tardif. En effet, les premiers symptômes apparaissent alors que la pathologie progresse depuis des années. Même si le traitement arrive à stopper la progression de la MA, les atteintes sont probablement trop importantes pour être restaurées. Enfin, la grande majorité des essais est neuro-centrique et basée sur l'hypothèse de la cascade amyloïde. Les molécules ou vaccins montrent donc un intérêt clinique uniquement si les plaques amyloïdes sont effectivement responsables du déclin cognitif. D'importants espoirs se placent sur les essais cliniques novateurs concernant la pathologie Tau puisqu'elle corrèle mieux avec l'apparition et la progression des symptômes.

3.5. Les modèles murins utilisés en recherche préclinique

Il existe de nombreux modèles animaux de la MA. La plupart sont des modèles rongeurs transgéniques. Néanmoins, certaines espèces développent naturellement des lésions associées à la MA, comme certains primates non humains *(Malm et al., 2011)*. L'avantage de ces modèles, en plus de leur système nerveux plus complexe et donc plus proche de celui de l'homme que celui des rongeurs, est évidemment qu'ils peuvent déclencher naturellement la maladie en vieillissant, ce qui est plus proche de la pathologie humaine. Cependant, des études sur de telles espèces nécessitent non seulement des temps d'étude plus longs (jusqu'à 20 ans chez le macaque avant l'apparition des plaques), mais également un dispositif d'hébergement plus complexe, coûteux, et avec des considérations éthiques significatives.

Les modèles murins transgéniques, développés grâce à des constructions génétiques, sont les plus couramment utilisés car ils présentent des avantages non négligeables : modèles variés permettant le développement d'une pathologie plus ou moins rapide et sévère, pathologie amyloïde seule ou combinée avec la pathologie Tau, facilité de mise en œuvre des expériences ainsi que la facilité et le moindre coût d'hébergement.

Il existe aujourd'hui 124 modèles murins de la MA et tauopathies *(Source : Alzforum.org)*. Ces modèles murins transgéniques sont basés sur les mutations génétiques identifiées dans les formes familiales de la MA telles que les mutations sur les gènes *App, Ps1* ou *Ps2*. Afin de combiner la pathologie amyloïde et la pathologie Tau, des modèles présentant une mutation sur le gène *Mapt* (codant pour la protéine Tau) ont également été développés. Ces mutations liées à Tau ne sont pas observées chez les patients atteints de la MA mais dans les tauopathies. L'ensemble de ces mutations présentent donc plusieurs limites : 1/ les mutations liées à la pathologie amyloïde ne représentent que 5% des formes de la MA, 2/ on ne peut pas exclure que la pathologie Tau soit différente entre la MA et les tauopathies. De plus, ces modèles murins demeurent éloignés de la pathologie humaine *(Duyckaerts et al., 2008)*. En effet, selon le modèle, la pathologie peut se développer très rapidement et les protéines pathologiques telles que l'APP ou Tau sont souvent surexprimées. La majorité d'entre eux ne développent pas de perte neuronale ou d'atrophie cérébrale et la progression des plaques ou des DNF, stéréotypique chez l'homme, n'est pas reproduite dans les modèles transgéniques *(Duyckaerts et al., 2008)*. Néanmoins, ces modèles murins transgéniques présentent les avantages de développer une ou les deux pathologies (amyloïde et tau), permettant des études dans un contexte spécifique. Ils développent également de la neuroinflammation, des altérations synaptiques et des déficits comportementaux plus ou moins marqués, pouvant s'apparenter aux symptômes observés chez les patients. En conséquence, chaque modèle doit être choisi spécifiquement en fonction de la question étudiée. Leur utilisation est essentielle pour mieux comprendre la mise en place de la pathologie au cours du temps, et ainsi identifier de nouvelles cibles thérapeutiques.

Nous nous focaliserons dans ce paragraphe sur les caractéristiques des modèles souris APP/PS1dE9 et 3xTg-AD, qui sont utilisés dans ce projet.

3.5.a. *Le modèle APP/PS1dE9*

Le modèle APP/PS1dE9 *(Jankowsky et al., 2004)* présente la mutation swedish sur le gène humanisé de l'APP (APP_{swe}) correspondant à une mutation KM670/671NL et une délétion de l'exon 9 sur le gène humain de la PS1. Ces deux gènes sont sous le contrôle du promoteur prion PrP *(Figure 17)*. Ce modèle est donc exclusivement amyloïde et présente l'avantage d'être très bien caractérisé.

Ce modèle APP/PS1dE9, comme l'ensemble des modèles APP, présente une augmentation de la concentration d'Aβ avec l'âge dans le SNC. La pathologie amyloïde se met relativement rapidement en place avec l'apparition des premières **plaques amyloïdes** à l'âge de 6 mois. Des plaques abondantes dans le cortex et l'hippocampe sont observables à 9 mois *(Jankowsky et al., 2004 ; Végh et al., 2014)*. Le nombre de plaques continue d'augmenter jusqu'à 12 mois (Garcia-Alloza et al.,

2006). Certains dépôts diffus sont également observés à partir de 9 mois dans le thalamus et le cervelet *(van Groen et al., 2006)*. De plus, ce modèle développe une légère CAA puisque la présence d'Aβ dans quelques vaisseaux sanguins a été observée autour de 9 mois. Comme chez les patients, la concentration d'Aβ40 dans le sang est supérieure à celle de l'Aβ42 à 6 et 12 mois (ratio 2,31 : 1). Ce ratio est inversé dans le cerveau (ratio 1 : 2,17) *(Xiong et al., 2011)*.

Ce modèle présente également l'avantage de développer une importante **neuroinflammation** accompagnant l'apparition des plaques amyloïdes *(Garcia-Alloza et al., 2006 ; Végh et al., 2014)*.

Tout comme chez les patients, des **altérations synaptiques** sont observées. Une diminution de la colocalisation entre des marqueurs pré (synaptophysine) et post-synaptique (PSD95 ; Post-synpatic density protein 95) est observée dès 3 mois *(Hong et al., 2016)*. Un déficit de la LTP au niveau des cellules pyramidales de CA3, est observé à 6 mois *(Viana da Silva et al., 2016),* mais les déficits à la synapse collatérale de Schaffer/CA1, plus couramment étudiée, sont décrits plus tardivement *(Volianskis et al., 2010; Métais et al., 2014)*. La présence de **neurites dystrophiques** est aussi rapportée, essentiellement au niveau des plaques *(Blazquez-Llorca et al., 2017)*.

Une **altération de la neurogenèse** dans la zone sub-granulaire de l'hippocampe a été observée autour de 6 mois. Le nombre de neurones nouvellement générés est inchangé par rapport aux souris contrôles mais leur survie à long terme est altérée *(Verret et al., 2007)*.

Des **déficits comportementaux**, comme des déficits de la mémoire contextuelle (test du conditionnement par la peur) ont été décrits dès 6 mois *(Kilgore et al., 2010).* L'apprentissage spatial et la mémoire à long terme (observés grâce au test de la piscine de Morris) sont affectés à partir de 10 mois *(Ma et al., 2012 ; Volianskis et al., 2010).* Des altérations du comportement spontané chez ces souris, notamment pour la construction du nid, sont observées plus tardivement, à 12 mois *(Janus et al., 2015)*.

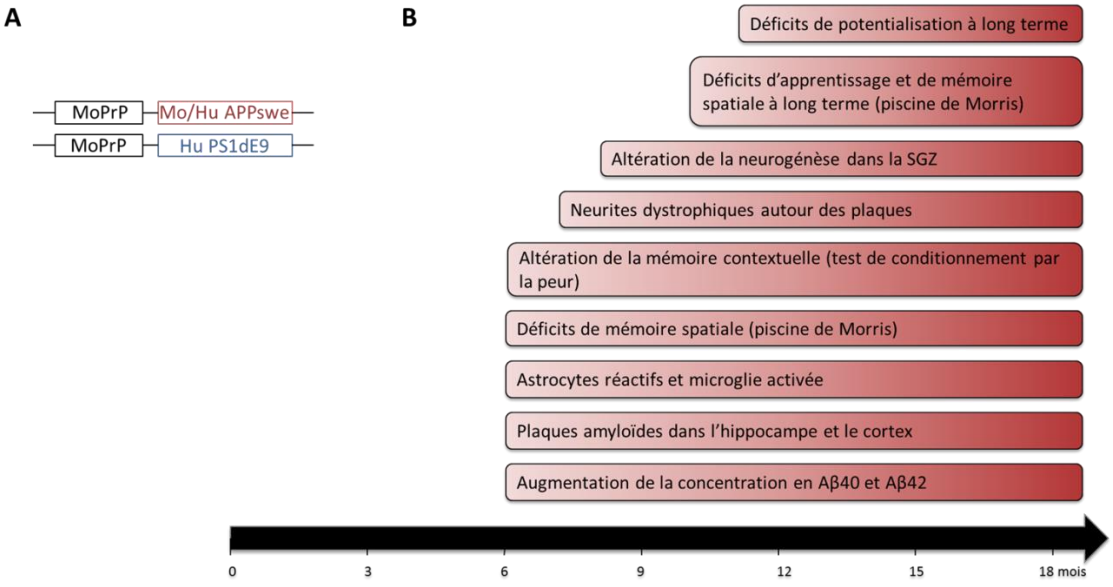

Figure 17 : Le modèle APP/PS1dE9 : construction génétique et caractéristiques pathologiques.
A) Construction du modèle transgénique *(Jankowsky et al., 2004)*, **B)** Apparitions des différentes altérations modélisant la MA. SGZ = Zone sub-granulaire. MoPrP = Promoteur prion murin. Mo/Hu = Séquence chimérique murine et humaine.

Le principal inconvénient de ce modèle est évidemment l'absence de formation de DNF. De plus, comme la majorité des modèles murins, aucune perte neuronale ou d'atrophie cérébrale n'est observée.

3.5.b. *Le modèle 3xTg-AD*

Le modèle triple transgénique *(3xTg-AD ; Oddo et al., 2003a)* présente la mutation M146V dans le gène murin de la PS1 (knock-in). Les gènes mutés App_{swe} (KM670/671NL) et Tau_{P301L} sont eux sous le contrôle du promoteur Thy-1, exclusivement neuronal *(Figure 18)*. Ce modèle présente donc l'avantage de développer une pathologie amyloïde et une pathologie Tau, comme la pathologie humaine.

Une **accumulation intra-neuronale d'Aβ** est observée dès 6 mois dans les neurones pyramidaux de la couche CA1 *(Oddo et al., 2003a)*. Néanmoins, les **plaques amyloïdes** apparaissent plus tardivement dans l'hippocampe (autour de 12 mois) que dans le modèle APP/PS1dE9, bien que quelques plaques aient été décrites dans le néocortex à 6 mois *(Oddo et al., 2003a)*. La présence d'Aβ42 est également détecté par test ELISA dès 3 mois et ces taux augmentent avec l'âge *(Clark et al., 2015)*.

L'expression de la forme humaine de Tau dans l'hippocampe a été vérifiée à 6 mois et augmente au cours du vieillissement *(Oddo et al., 2003a)*. Les formes hyperphosphorylées de Tau sur différents sites (Ser199/202, Thr231, et Ser396) ont été observées à 8 mois dans les neurones pyramidaux de la couche CA1 *(Clark et al., 2015)*.Les **DNF** $AT8^+$ (annticorps reconnaissant les sites de phosphorylation Ser202 et Thr205) sont clairement présentes à 15 mois dans cette région et dans le cortex *(Oddo et al., 2003b)*. La pathologie amyloïde apparait donc avant la pathologie Tau, comme chez les patients.

Une étude a mis en évidence, dès l'âge de 3 mois, des changements morphologiques des astrocytes (légère diminution du nombre de prolongements primaires et de l'arborisation), et cela avant même l'apparition des plaques amyloïdes *(Rodriguez et al., 2009)*. Néanmoins, une très claire **neuroinflammation** (astrocytes réactifs et microglie amiboïde) est observée plus tardivement à 12 mois, autour des plaques principalement *(Rodriguez et al., 2009)*.

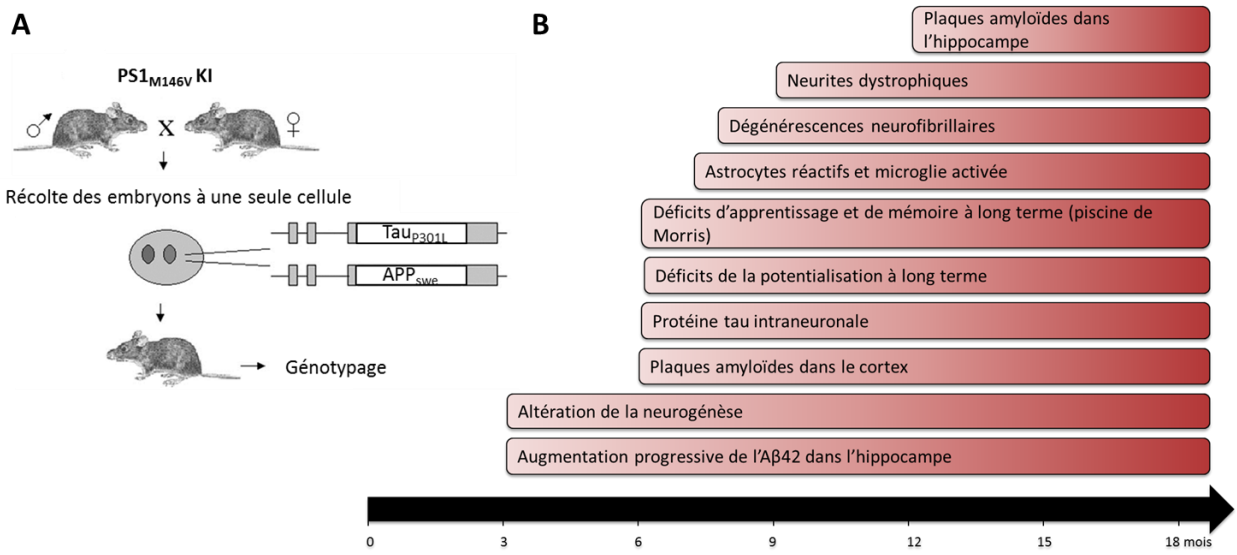

Figure 18 : Le modèle 3xTg-AD : construction et caractéristiques pathologiques.

A) Développement du modèle transgénique *(Adapté de Oddo et al., 2003a)*, **B)** Apparitions des différentes altérations modélisant la MA.

Les souris 3xTg-AD présentent une forte altération de la transmission synaptique basale et de la LTP dès 6 mois, avant l'apparition des plaques et des DNF *(Oddo et al., 2003a)*. Ces **déficits synaptiques** précoces pourraient s'expliquer par la présence d'Aβ intra-neuronal à cet âge *(Oddo et al., 2003a ; Billings et al., 2005)*. Des **neurites dystrophiques** sont observées à 9 mois *(Oh et al., 2010)*.

Une **altération de la neurogenèse** dans le gyrus denté est également observée dans ce modèle dès 3 mois chez les femelles et à partir de 9 mois chez les mâles *(Rodríguez et al., 2008)*.

Les **déficits d'apprentissage et de mémoire** apparaissent autour de 6 mois *(Clinton et al., 2007)*. Ces déficits ont été observés dans de nombreuses études *(Cf Webster et al., 2013 pour un tableau récapitulatif)*.

Il est également important de noter que les femelles 3xTg-AD développent plus précocement les différentes altérations de la MA *(Clinton et al., 2007)*. Tout comme les souris APP/PS1dE9, les souris 3xTg-AD ne présentent aucune perte neuronale.

	Modèle APP/PS1dE9	Modèle 3xTg-AD
Transgènes	APP_{swe} (KM670/671NL)	
	Délétion de l'exon 9 sur le gène humain de la PS1	Mutation M146V dans le gène de la PS1 (KI : expression endogène)
	Aucune	Mutation P301L dans le gène de Tau
Promoteurs	PrP	Thy-1
Caractérisation du modèle	Très bien caractérisés	
Pathologie amyloïde	Précoce et étendue Etude de son effet propre	2 pathologies présentes comme chez les patients
Pathologie Tau	Absente	
Neuroinflammation	Réactivité astrocytaire plus précoce	Réactivité astrocytaire plus tardive
Neurogenèse	Altération précoce	
Transmission synaptique	Altération plus tardive	Altération précoce
Cognition	Déficits mesurables	

Tableau 3 : Avantages des deux modèles de souris transgéniques utilisés.
Les deux modèles développent des caractéristiques complémentaires et une forte inflammation dont une importante réactivité astrocytaire, bien que le modèle APP/PS1dE9 développe cette caractéristique essentielle à notre étude plus rapidement. Abréviations : PS1 = Préséniline 1, KI = Knock-In, PrP = promoteur prion.

La présence ou non de DNF, le décours de la pathologie amyloïde, les symptômes et leur sévérité diffèrent entre le modèle 3xTg-AD et le modèle APP/PS1dE9. L'utilisation de ces deux modèles est donc complémentaire *(Tableau 3)* et permet l'étude de multiples aspects de la MA, afin de mieux comprendre la pathologie observée chez l'homme.

4. Les astrocytes réactifs dans la maladie d'Alzheimer

Comme présenté précédemment, la neuroinflammation fait intervenir les astrocytes, la microglie et parfois les cellules du système immunitaire périphérique. Nous nous focaliserons essentiellement dans ce chapitre sur les altérations fonctionnelles des astrocytes liées à la réactivité, qui pourraient contribuer au dysfonctionnement et à la souffrance neuronale dans la MA : altérations de l'homéostasie du glutamate, du métabolisme du glucose et du cholestérol, et altération de leur « sécrétome ». La communication astrocyte/microglie ainsi que leur importance pour la dégradation de l'Aβ et le recrutement des cellules immunitaires périphériques seront également développées.

4.1. Altération des fonctions de support des astrocytes

Nous avons décrit en 2015 les multiples altérations liées à la réactivité astrocytaire dans différentes pathologies neurodégénératives, y compris dans la MA ***(Publication 1 en annexe)***. En fonction de la sévérité et du type de perturbation dans le SNC, les astrocytes réactifs peuvent démontrer soit une perte de fonction (par exemple une altération de l'homéostasie du glutamate, du métabolisme énergétique ou du métabolisme du cholestérol) soit un gain de fonction (production d'un grand nombre de molécules dont les cytokines). Je fais ici le choix de ne développer que les altérations non spécifiées dans la revue, ou celles essentielles à la compréhension du projet.

4.1.a. *Altération de l'homéostasie du glutamate*

Une altération de l'homéostasie du glutamate est observée dans la MA. Les astrocytes contribuent fortement à cette altération. En effet, une modulation de l'expression des transporteurs astrocytaires au glutamate en présence d'Aβ est décrite dans les modèles de la MA et chez les patients ***(Publication 1 en annexe)***. De façon intéressante, la diminution de l'expression des transporteurs au glutamate est également observée dans un modèle murin exprimant la protéine Tau humaine spécifiquement dans les astrocytes *(Dabir et al., 2006)*. En plus de cette diminution de sa recapture par les astrocytes, une libération accrue de glutamate par les astrocytes et les neurones est observée *(Rudy et al., 2015)*. L'augmentation de la concentration du glutamate au niveau de la fente synaptique qui en découle conduit à une suractivation des récepteurs neuronaux post-synaptiques, favorisant la mort des neurones par **excitotoxicité** *(Maragakis and Rothstein, 2004)*.

Les altérations du cycle glutamate-glutamine sont également observées et peuvent directement contribuer au dysfonctionnement neuronal ***(Publication 1 en annexe)***. De plus, la recapture du glutamate est couplée à l'entrée de glucose. Toute altération de l'homéostasie du glutamate est donc susceptible d'altérer le métabolisme énergétique cérébral.

4.1.b. *Altération du métabolisme énergétique*

Comme mentionné dans le §3.2, un **hypo-métabolisme du glucose** est observé par imagerie TEP chez les patients atteints de la MA. Une diminution de l'expression des transporteurs du glucose comme GLUT-1, une rétraction des pieds astrocytaires ainsi qu'une altération de la morphologie des péricytes ont été observées au niveau de la BHE dans des souris modèles de la MA *(Merlini et al., 2011)*.

Certaines voies métaboliques présentées précédemment en conditions physiologiques (comme la « lactate shuttle » par exemple) sont compartimentées entre les neurones et les astrocytes. Ceci confère un rôle régulateur fondamental aux astrocytes. Les déficits énergétiques observés communément dans les maladies neurodégénératives *(Lin and Beal, 2006)* suggèrent que certaines interactions métaboliques sont altérées lorsque les astrocytes deviennent réactifs. Cependant, l'implication des astrocytes réactifs dans ces déficits énergétiques n'a pas clairement été démontrée. Pour de plus amples détails, voir la ***publication 1*** **en annexe**.

4.1.c. *Altération du métabolisme du cholestérol*

L'allèle ApoEε4 étant le facteur de risque majeur pour la MA, il suggère une implication du métabolisme du cholestérol, produit par les astrocytes. En réalité, ApoE influence le développement de la MA à plusieurs niveaux : via la régulation du métabolisme du cholestérol, du métabolisme de l'APP et la dégradation de l'Aβ *(Bu, 2009)*. Dans le cerveau de patients, une **accumulation d'ApoE** est observée au niveau des plaques amyloïdes *(Namba et al., 1991)*. ApoE stimule fortement la transcription d'APP et la **production d'Aβ** dans des neurones humains. La forme ε4 stimule d'ailleurs plus fortement cette production qu'ApoEε2 *(Huang et al., 2017)*. De plus, l'agrégation d'Aβ sous forme de plaques est plus abondante dans les patients porteurs de l'allèle ε4 *(Schmechel et al., 1993)*. Ces résultats suggèrent qu'ApoE affecte l'**agrégation de l'Aβ**. ApoE est également une **protéine chaperonne liant l'Aβ** au récepteur des lipoprotéines de faible densité dans les astrocytes *(Koistinaho et al., 2004)*. Une diminution de l'expression des enzymes et des transporteurs liés au métabolisme du cholestérol dont ApoE, est observée dans des astrocytes de souris APP/PS1dE9 *(Orre et al., 2014)*, suggérant une diminution de la capacité de clairance de l'Aβ par cette voie.

4.2. Sécrétome des astrocytes réactifs et dysfonction neuronale

La réactivité astrocytaire modifie donc de nombreuses fonctions liées à l'homéostasie cellulaire. Elle altère également le « sécrétome » des astrocytes puisque ceux-ci libèrent de nombreuses molécules actives, pouvant agir directement ou indirectement sur les autres types cellulaires du SNC *(Figure 19)*.En effet, le milieu de culture d'astrocytes mis en présence d'Aβ suffit à induire une forte mort neuronale *(Allaman et al., 2010)*, suggérant la libération de facteurs neurotoxiques par les astrocytes.

4.2.a. *Participation au stress oxydatif*

Les astrocytes jouent un rôle clé dans la défense contre le stress oxydatif *(Allaman et al., 2011)*. Cependant, ils peuvent également libérer des **facteurs pro-oxydants** *(Figure 19).* Les études et mécanismes mettant en évidence ce phénomène sont explicités dans la ***publication 1*** **en annexe**.

La production d'espèces réactives de l'oxygène (ROS) peut également activer l'expression de la β-sécrétase dans les astrocytes, alors qu'elle est exprimée uniquement par les neurones en conditions physiologiques *(Rossner et al., 2005)*. Ceci implique donc que les astrocytes sont également capables de produire de l'Aβ.

Le stress oxydatif est une caractéristique commune aux maladies neurodégénératives et suggère l'implication des astrocytes réactifs dans la dysfonction neuronale.

4.2.b. *Libération de gliotransmetteurs et impact sur la LTP*

Dans des modèles de la MA, des altérations du relargage de gliotransmetteurs ***(Publication 1 en annexe)***, tel que le glutamate *(Cf §4.1.a)* et le GABA sont observés. En particulier, deux études ont mis en évidence une libération anormale de GABA par les astrocytes réactifs dans deux modèles murins de la MA *(Jo et al., 2014 ; Wu et al., 2014)*. Cette libération abondante de GABA conduit à une **inhibition tonique** des cellules granulaires du gyrus denté de l'hippocampe. L'inhibition de la synthèse du GABA ou un blocage pharmacologique des transporteurs du GABA restaurent la plasticité synaptique et les déficits comportementaux observés chez ces souris *(Jo et al., 2014 ; Wu et al., 2014)*.

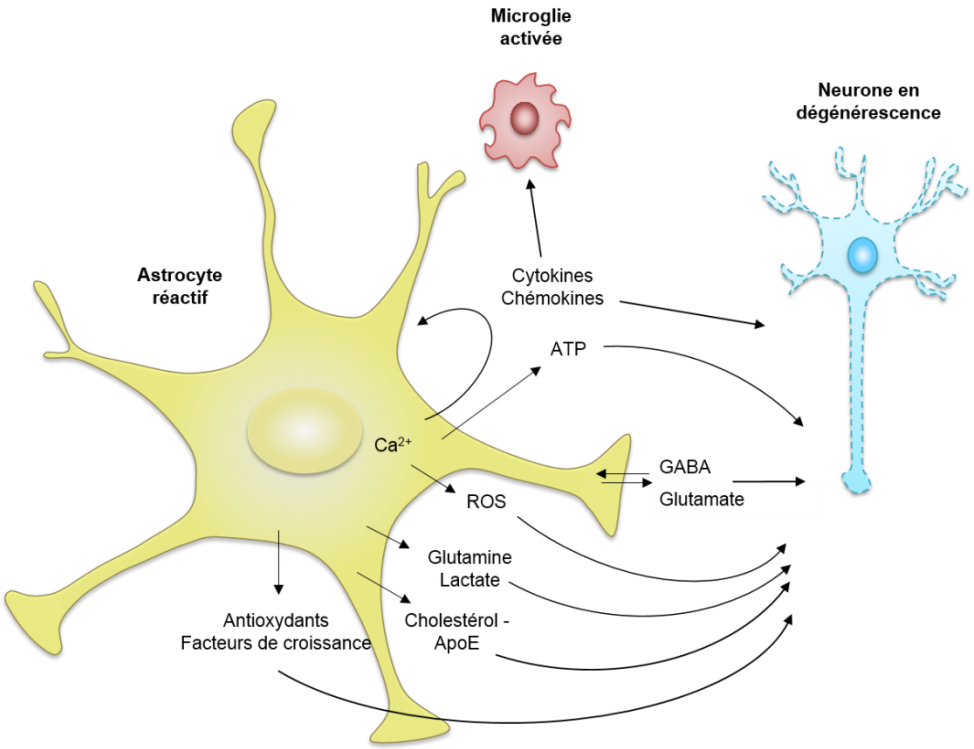

Figure 19 : Les astrocytes réactifs libèrent de nombreuses molécules actives modulant les communications intercellulaires.

Les astrocytes interagissent avec les autres types cellulaires en libérant de nombreuses molécules actives. Lorsqu'ils deviennent réactifs, cette signalisation intercellulaire est modifiée, notamment à cause de changements de production de gliotransmetteurs, de facteurs de croissance, d'antioxydants et ROS ou encore de cytokines et chemokines *(Schéma adapté de la **publication 1 en annexe**).*

Globalement, des études complémentaires, essentiellement *in vivo*, sont nécessaires pour déterminer précisément comment la libération de gliotransmetteurs par les astrocytes réactifs est modulée par les pathologies amyloïdes et Tau et comment ceci impacte la transmission synaptique.

4.2.c. *Cascade du complément et souffrance neuronale*

Une accumulation de molécules du complément est observée dans les régions présentant de nombreuses plaques amyloïdes, comme le cortex entorhinal et l'hippocampe chez les patients atteints de la MA *(Yasojima et al., 1999)*. Cette accumulation est essentiellement visible au niveau des plaques, des DNF et dans les neurites dystrophiques *(Emmerling et al., 2000)*. L'Aβ et Tau peuvent activer cette cascade, en se liant à des molécules du complément comme C1q ou C3 *(Shen et al., 2001, 2013 ; Figure 20)*. L'interaction des peptides Aβ avec C1q favorise leur agrégation *(Webster and Rogers, 1996)*, ce qui peut activer à nouveau la cascade du complément.

Une fois activée, cette cascade conduit à la formation de structures poreuses à la membrane des cellules (complexe MAC ; Membrane attack complex), conduisant à leur lyse. Cette cascade induit également la production d'opsonines, qui marquent les cellules qui seront phagocytées *(Shen et al., 2013 ; Figure 20)*, et de molécules pro-inflammatoires telles que C3a, C5a.

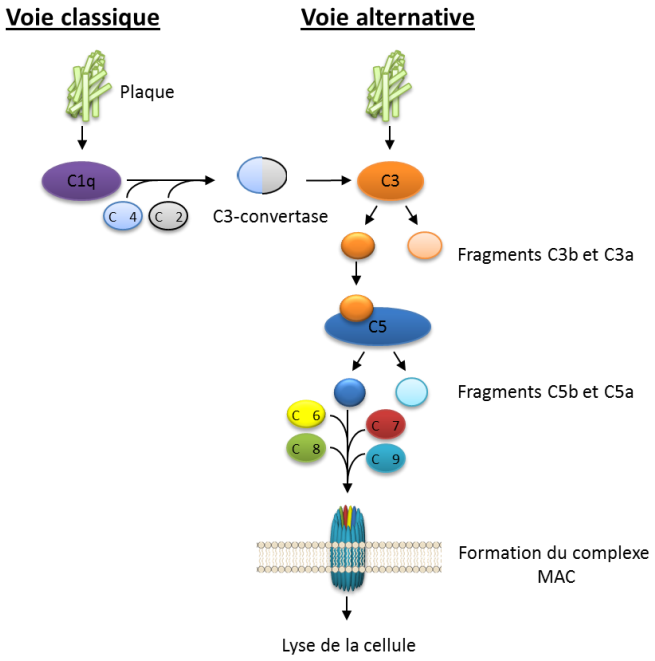

Figure 20 : Activation de la cascade du complément dans la maladie d'Alzheimer.
L'Aβ et Tau peuvent activer cette cascade en se liant à des molécules du complément telles que C1q ou C3. Cette activation induit l'hydrolyse de C3 en C3b et C3a. C3b clive C5 en deux fragments : C5a et C5b. C5b se lient à différentes molécules du complément pour former le complexe MAC (composé de C5b, C6, C7, C8 et C9). Ce dernier complexe forme une structure poreuse dans la membrane, conduisant à la lyse des neurones *(Figure adaptée de Shen et al., 2013)*.

Les astrocytes expriment des récepteurs aux fragments C5a et C3a *(Emmerling et al., 2000)*. La microglie exprime également ces deux récepteurs mais aussi les récepteurs CR3, CR1, CR4 et C1qR *(Emmerling et al., 2000)*. CR1 et C5aR sont également exprimés par les neurones.

De plus, l'implication des astrocytes et de la microglie, tout comme les neurones, dans la **synthèse de molécules du complément** est connue depuis plus de 20 ans *(Barnum, 1995)*. L'analyse transcriptomique d'astrocytes réactifs isolés à partir du modèle APP/PS1dE9, a confirmé que les astrocytes réactifs surexpriment des gènes liés au système du complément comme C1q et C4b *(Orre et al., 2014)*. L'activation de la voie NF-κB par l'Aβ induit une surproduction de C3 par les astrocytes. Ceci altère la morphologie des dendrites, l'homéostasie calcique dans les neurones et les réponses à la synapse excitatrice via sa fixation sur les récepteurs C3a neuronaux *(Lian et al., 2015)*. Les molécules C3 libérées par les astrocytes réactifs peuvent également se fixer sur les récepteurs C3a microgliaux, altérant leur capacité de phagocytose de l'Aβ, *in vitro* et *in vivo (Lian et al., 2016 ; Cf §4.4.b)*.

Récemment, Hong et collaborateurs ont mis en évidence le rôle de la microglie dans la **perte précoce des synapses** dans des modèles murins de la MA, via la cascade du complément *(Hong et al., 2016)*.

Le système du complément joue donc un rôle primordial dans la phagocytose précoce des synapses et la souffrance neuronale, mettant à nouveau en évidence l'implication des astrocytes réactifs et de la microglie réactive dans la MA.

4.2.d. *Libération de cytokines et communication intercellulaire*

L'augmentation de la production de cytokines et chemokines est une des caractéristiques principales de la neuroinflammation, observée dans les régions vulnérables du cerveau ou dans le LCR des patients *(Heneka et al., 2014)*. La microglie et les astrocytes sont les **principaux producteurs de cytokines anti- et pro-inflammatoires** dans le SNC. Bien que les cellules microgliales soient les cellules productrices majeures, les astrocytes voient leur production augmenter lorsqu'ils deviennent réactifs. En effet, une étude transcriptomique a récemment mis en évidence que les astrocytes réactifs expriment en grande quantité plusieurs cytokines dans le modèle APP/PS1dE9 *(Orre et al., 2014)*. Le nombre de gènes induits et leur niveau d'induction sont plus élevés dans les astrocytes réactifs que dans la microglie. Ces résultats suggèrent donc que les astrocytes réactifs participent significativement à la production de molécules inflammatoires, bien que les niveaux absolus d'expression restent plus élevés dans la microglie. La littérature concernant la libération de ces cytokines par les astrocytes et la microglie étant extrêmement dense, je développerai ici seulement le rôle de quatre cytokines (IL-10, IL-1β, IL-6 et TNF-α), centrales dans la MA. Pour une revue plus exhaustive des cytokines libérées par la microglie et les astrocytes, consulter *Bagyinszky et al., 2017*.

Un polymorphisme dans le gène codant pour IL-10, cytokine anti-inflammatoire, représente un facteur de risque pour la MA *(Vargas-Alarcon et al., 2016)*. La surexpression d'IL-10 dans un modèle murin de la MA n'affecte pas la réactivité astrocytaire mais **impacte la phagocytose** de l'Aβ par la microglie *(Chakrabarty et al., 2015)*. Elle induit également une diminution de l'expression de la synaptophysine et PSD-95, suggérant une altération de l'intégrité synaptique.

De plus, la maturation de cytokines comme IL-1β par l'inflammasome dans le cytosol des cellules microgliales est bien décrite dans la MA. Il existe différents inflammasomes mais les peptides Aβ activent particulièrement l'inflammasome NLRP3 (NOD-like receptor protein) *(Halle et al., 2008)*. Ce dernier est composé de la protéine senseur NLRP3, d'une protéine adaptatrice « Apoptosis associated Speck-like protein containing a caspase activating and recruitment domain » et de la pro-caspase I. L'activation de cette caspase conduit au clivage et à l'activation de cytokines pro-inflammatoires de la famille d'IL-1β, modulant ainsi la synthèse de cytokines pro-inflammatoires et de facteurs neurotrophiques par la microglie *(Shaftel et al., 2008)*. Une expression d'IL-1β et d'IL-6 dans les astrocytes à proximité des plaques amyloïdes a été mise en évidence récemment *(Bouvier et al., 2016)*. De plus, la caspase 1 colocalise avec IL-1β dans ces cellules. L'expression des deux cytokines pro-inflammatoires augmente avec la progression de la MA dans des modèles murins. Ces niveaux d'expression variables en fonction du type cellulaire sont également observés chez l'Homme *(Bouvier et al., 2016)*. Ces résultats suggèrent donc aussi une activation de l'inflammasome dans les astrocytes. Seules deux autres études avaient déjà suggéré que la stimulation de l'inflammasome conduit à la production d'IL-1β par les astrocytes (Minkiewicz et al., 2013 ; Zeis et al., 2015). Il est important de noter que l'expression d'IL-1β, IL-6 ou TNF-α **stimule la synthèse de peptides Aβ40 et Aβ42** *(Blasko et al., 2000)*. Ceci conduirait à un cercle vicieux où l'Aβ active sa propre synthèse via les cytokines. Enfin, des amas d'IL-1β^{+} sont observés dans les astrocytes autour des agrégats de protéines tau hyperphosphorylées *(Bouvier et al., 2016)*.

Les cytokines de la grande famille des TNF peuvent conduire à l'**apoptose** en se liant à leur récepteur *(Combs et al., 2001)*. Les neurones surexpriment ces récepteurs pro-apoptotiques (Fas, TNFR1 (TNF receptor-1), « TNF-related apoptosis-inducing ligand », « Death receptor 4 » et « Death receptor 5 »). Les cytokines de la famille de TNF-α, sont surexprimées par les astrocytes réactifs et la microglie réactive *(Orre et al., 2014)*. La présence de Tau, tout comme l'Aβ, stimule la production de TNF *(Wang et al., 2015a)*. De plus, TNF-α peut induire une **excitotoxicité** en diminuant la recapture du glutamate par les astrocytes, en augmentant leur production de glutamate via TNFR1, tout en modulant les récepteurs glutamatergiques et GABAergiques neuronaux *(Olmos and Lladó, 2014)*. La mort neuronale dans la MA peut donc être médiée par l'apoptose, ou par une excitotoxicité, suite à la libération de facteurs comme les cytokines par la microglie et les astrocytes réactifs.

Par conséquent, l'activation des cellules gliales conduit à la libération de cytokines et chemokines, leur permettant de communiquer finement, et à la libération de molécules anti-oxydantes afin de limiter le stress oxydatif. Cette communication pourrait ensuite engendrer un engrenage pro-inflammatoire, conduisant à la libération majoritaire de ROS et d'oxyde nitrique par exemple, induisant un fort stress oxydatif et participant ainsi à la souffrance neuronale. Le système du complément joue également un rôle important dans la dysfonction neuronale observée dans la MA. En effet, cette cascade protéolytique conduit à la lyse des cellules. Le complément agit également comme facteur chemo-attractant favorisant la phagocytose des synapses dans la MA. Une surexpression neuronale de récepteurs liés à l'apoptose conduit à leur mort en réponse aux cytokines de la famille des TNF libérées par les astrocytes ou la microglie. La libération majoritaire de toutes ces molécules par les astrocytes et la microglie, lie directement la neuroinflammation à la souffrance et à la mort neuronale.

4.3. Dialogue avec les cellules du système immunitaire périphérique et recrutement dans le SNC

En condition physiologique, les cellules du système immunitaire périphérique ne passent pas la BHE. La microglie et les astrocytes veillent sur l'homéostasie cellulaire et sont les acteurs de l'immunité innée du SNC. Dans la MA, les cellules immunitaires périphériques peuvent **agir depuis la périphérie** sur la pathologie. Par exemple, les monocytes, acteurs périphériques de l'immunité innée, peuvent dégrader les dépôts d'Aβ présents dans les micro-vaisseaux du cerveau, notamment en les internalisant et transportant dans la circulation sanguine *(Michaud et al., 2013)*. De plus, les cytokines, libérées par les astrocytes réactifs et la microglie activée, peuvent altérer l'intégrité de la BHE *(Desai et al., 2002)*, laissant passer des facteurs inflammatoires libérés par les cellules immunitaires périphériques.

Certaines cytokines et chemokines pourraient agir comme des facteurs chemotactiques, favorisant le **recrutement des cellules** elles-mêmes dans le SNC *(Figure 21)*. En effet, une étude *in vitro* a montré que l'expression de TNF-α par la microglie suite à une exposition à des peptides Aβ, favorise la migration des LT au travers des cellules endothéliales via l'expression du complexe majeur d'histocompatibilité de classe I *(Yang et al., 2013)*.

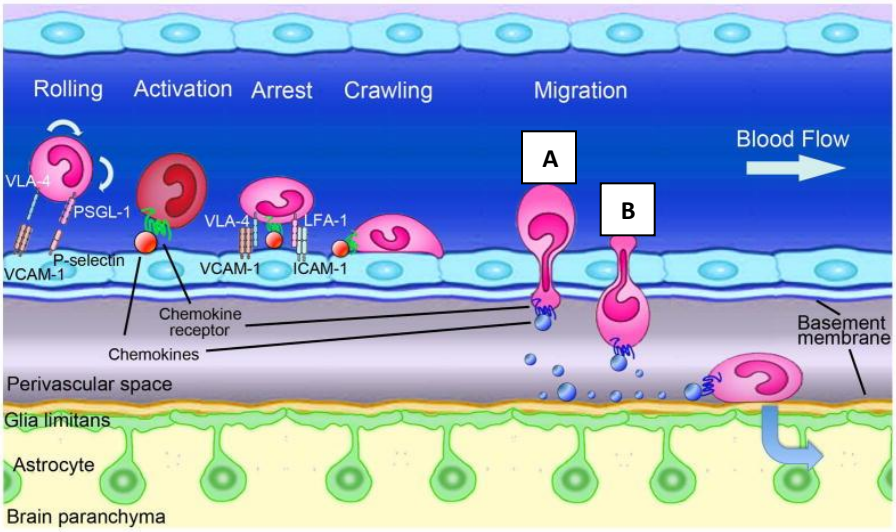

Figure 21 : Recrutement des cellules immunitaires périphériques à travers la BHE.
L'infiltration des cellules immunitaires périphériques se déroule en 5 étapes : 1) Le roulement via la formation de liaisons faibles et transitoires avec les cellules endothéliales, 2) L'activation des intégrines sur les leucocytes permettant leur interaction avec des cytokines sur les cellules endothéliales, 3) L'arrêt du roulement grâce à l'expression de molécules d'adhésion par les leucocytes se fixant sur les récepteurs endothéliaux, 4) « Crawling », les cellules rampent le long des cellules endothéliales jusqu'au site d'inflammation, 5) La transmigration via les voies paracellulaire ou transcellulaire. Les cellules du système périphérique telles que les macrophages ou les lymphocytes adhèrent aux cellules endothéliales et peuvent migrer jusqu'au site d'inflammation. Elles peuvent ensuite passer la BHE soit par la voie paracellulaire **(A)**, soit par la voie transcellulaire **(B)**. A) Les cellules immunitaires périphériques rampent (« Crawling ») le long des cellules endothéliales, rompent les jonctions intercellulaires, puis passent entre deux cellules endothéliales jusqu'au cerveau. B) Les cellules immunitaires périphériques passent au travers des cellules endothéliales *(adaptée de Takeshita and Ransohoff, 2012)*.

Une des voies de recrutement des cellules immunitaires les plus étudiées dans le contexte de la MA est la **voie CCL2 / CCR2** (C-C chemokine receptor 2). CCL2, initialement nommé « Monocyte chemoattractant protein-1 » est l'un des ligands de CCR2 et est majoritairement produit par les astrocytes. Une étude a suggéré que les microglies préférentiellement recrutées au niveau des plaques ont un profil génique spécifique dont notamment la surexpression de CCR2 *(Mildner et al., 2011)*. L'absence d'expression de CCR2 uniquement dans les cellules péri-vasculaires diminue drastiquement l'élimination de l'Aβ dans des modèles murins de la MA *(Mildner et al., 2011)*. Ceci suggère que les cellules immunitaires périphériques sont attirées au niveau des plaques suite à la libération locale de chemokines et qu'elles sont responsables de leur dégradation. Une surexpression de CCL2 est observée dans les formes intermédiaires de la MA mais pas chez les patients atteints d'une forme sévère *(Galimberti et al., 2006)*. Ces résultats suggèrent que la libération de CCL2 par les astrocytes fait partie de la phase précoce de la pathogenèse de la MA et pourrait être impliquée dans le recrutement des cellules périphériques.

De plus, CXCR3 est détecté dans les neurones et son ligand CXCL10 est surexprimé par les astrocytes réactifs dans des cerveaux de patients atteints de la MA (Xia et al., 2000). Ce récepteur serait majoritairement impliqué dans le recrutement des lymphocytes *(Savarin-Vuaillat and Ransohoff, 2007)*. De multiples **autres chemokines**, comme CCL4, CCL5 et CCL6 par exemple, sont surexprimées

par les astrocytes réactifs et la microglie réactive *(Orre et al., 2014)*. Ces chemokines sont impliquées dans l'infiltration des LT dans l'hippocampe dans un modèle de tauopathie *(Laurent et al., 2017)*. De plus, une surexpression de CCR5 par la microglie réactive a été décrite dans le contexte de la MA. Ses ligands CCL3 et CCL4 sont détectés dans les neurones et les astrocytes réactifs dans le cerveau de patients *(Xia et al., 1998)*. Ces chemokines pourraient donc également entrer en jeu dans le recrutement des cellules immunitaires périphériques dans la MA.

Cependant, l'origine (résidente ou périphérique) des cellules myéloïdes autour des plaques amyloïdes reste très débattue. Certaines études suggèrent la prolifération de la microglie résidente au site de lésion, comme autour des plaques amyloïdes *(Wang et al., 2016)* alors que d'autres favorisent l'hypothèse du recrutement périphérique *(Jay et al., 2015)*.

Ces cellules périphériques sont une source importante de cytokines et chemokines, pouvant favoriser la neuroinflammation, mais sont également des cellules capables de phagocytose, pouvant entrer en jeu dans la dégradation de l'Aβ. De plus amples études sont donc nécessaires pour mieux comprendre leur implication dans la MA.

4.4. Alliance des astrocytes et de la microglie pour dégrader l'Aβ

Il est très bien décrit dans la littérature que la microglie et les astrocytes sont capables de dégrader l'Aβ soluble et l'Aβ fibrillaire via de multiples mécanismes *(Figure 22)*. Nous détaillerons ici les mécanismes majeurs impliqués dans cette dégradation par ces cellules, qui collaborent finement.

4.4.a. *Les systèmes de dégradation extracellulaire*

L'Aβ soluble peut être dégradé via la libération d'enzymes permettant une dégradation extracellulaire. Les **métalloendopeptidases** sont produites majoritairement par les neurones et la microglie, bien que leur production ait aussi été démontrée dans les astrocytes *(Yamamoto et al., 2014)*. Elles incluent IDE (Insulin degrading enzyme), NEP (Néprylisine), ECE1 (Endothelin-converting enzyme-1) et ECE2 qui dégradent essentiellement les formes monomériques d'Aβ *(Eckman et al., 2001 ; Hickman et al., 2008)*. Ces enzymes ont beau être surexprimées au cours de la pathologie *(Miners et al., 2009)*, ceci n'est pas suffisant pour répondre à l'augmentation d'Aβ. Les **matrix métalloprotéinases** sont principalement produites par les astrocytes et la microglie et permettent la dégradation des formes monomériques et fibrillaires de l'Aβ *(Yan et al., 2006)*.

De plus, **ApoE**, produit par les astrocytes, est une protéine chaperonne liant l'Aβ au récepteur des lipoprotéines de faible densité, permettant de favoriser son élimination via le système sanguin *(Castellano et al., 2012)* ou via les astrocytes *(Koistinaho et al., 2004)*. Néanmoins, les astrocytes issus de cerveau de patients ne répondent pas aux complexes Aβ-ApoE par une augmentation de NEP ou « Scavenger receptor class B member 1 » comme le font les astrocytes issus de cerveau de sujets

sains *(Mulder et al., 2012)*. Par conséquent, même si les astrocytes participent à l'élimination de l'Aβ, cette capacité n'est pas optimale et semble être impactée par la pathologie elle-même.

4.4.b. *La phagocytose et les systèmes de dégradation intracellulaire*

Il a également été montré *in vitro* que les astrocytes sont capables de phagocyter l'Aβ *(Shaffer et al., 1995 ; Wyss-Coray et al., 2003 ; Nielsen et al., 2009)*. Cependant, les données *in vivo* sont peu nombreuses *(Wyss-Coray et al., 2003 ; Koistinaho et al., 2004 ; Iram et al., 2016)*. Au contraire, la dégradation des plaques amyloïdes par phagocytose microgliale est bien établie.

La microglie exprime de nombreux récepteurs notamment des **« scavenger receptors »** tel que CD36, CD14, CD47, ou encore plusieurs TLRs (Toll-likereceptors), dont TLR2 et TLR4, impliqués dans les mécanismes d'endocytose de l'Aβ *(Li et al., 2012 ; Liu et al., 2005)*. L'Aβ peut être ensuite dégradé par des **peptidases lysosomales** telles que les cathepsines *(Nakanishi, 2003)*. Cependant, une accumulation persistante d'Aβ intracellulaire induit également la libération de multiples cytokines et molécules pro-inflammatoires telles qu'IL-1β et TNF-α, par la microglie elle-même ou par les astrocytes réactifs. Cette surexpression de cytokines peut impacter leur capacité de phagocytose *in vitro* en diminuant l'expression de certains de ces récepteurs *(Hickman et al., 2008)*. A l'inverse, la surexpression de TGF-β peut favoriser la phagocytose de l'Aβ par la microglie *(Wyss-Coray et al., 2001)*.

Comme présenté précédemment, le **récepteur TREM2**, spécifiquement microglial et facteur de risque pour la MA, est également impliqué dans les mécanismes de phagocytose de l'Aβ. Une altération de la phagocytose par les cellules exprimant la forme mutée de TREM2 est observée *in vitro (Kleinberger et al., 2014)*. Deux études utilisant des souris transgéniques modèles de la MA et KO (Knockout) de TREM2 mettent en évidence des résultats opposés *(Ulrich et al., 2014 ; Wang et al., 2015b)*. Dans la première étude, aucun effet du KO de TREM2 sur la charge amyloïde, sur l'expression de cytokines ni même sur l'activation microgliale n'a été mis en évidence *(Ulrich et al., 2014)*. A l'inverse, Wang et collaborateurs ont observé une augmentation du nombre de plaques, de marqueurs d'activation microgliale ainsi qu'une augmentation de la production de cytokines *(Wang et al., 2015b)*. De plus, les enzymes de la famille des ADAM (A desintegrin and metalloproteinase domain-containing protein), comme ADAM10, sont responsables de la protéolyse intra-membranaire de TREM2. La génération de la forme soluble de TREM2 via une surexpression d'ADAM10 est réduite en présence de la mutation R47H *(Kleinberger et al., 2014)*. Ceci induit une diminution de la maturation de TREM2 ainsi que de son transport à la surface de la membrane et donc une diminution de la phagocytose par la microglie.

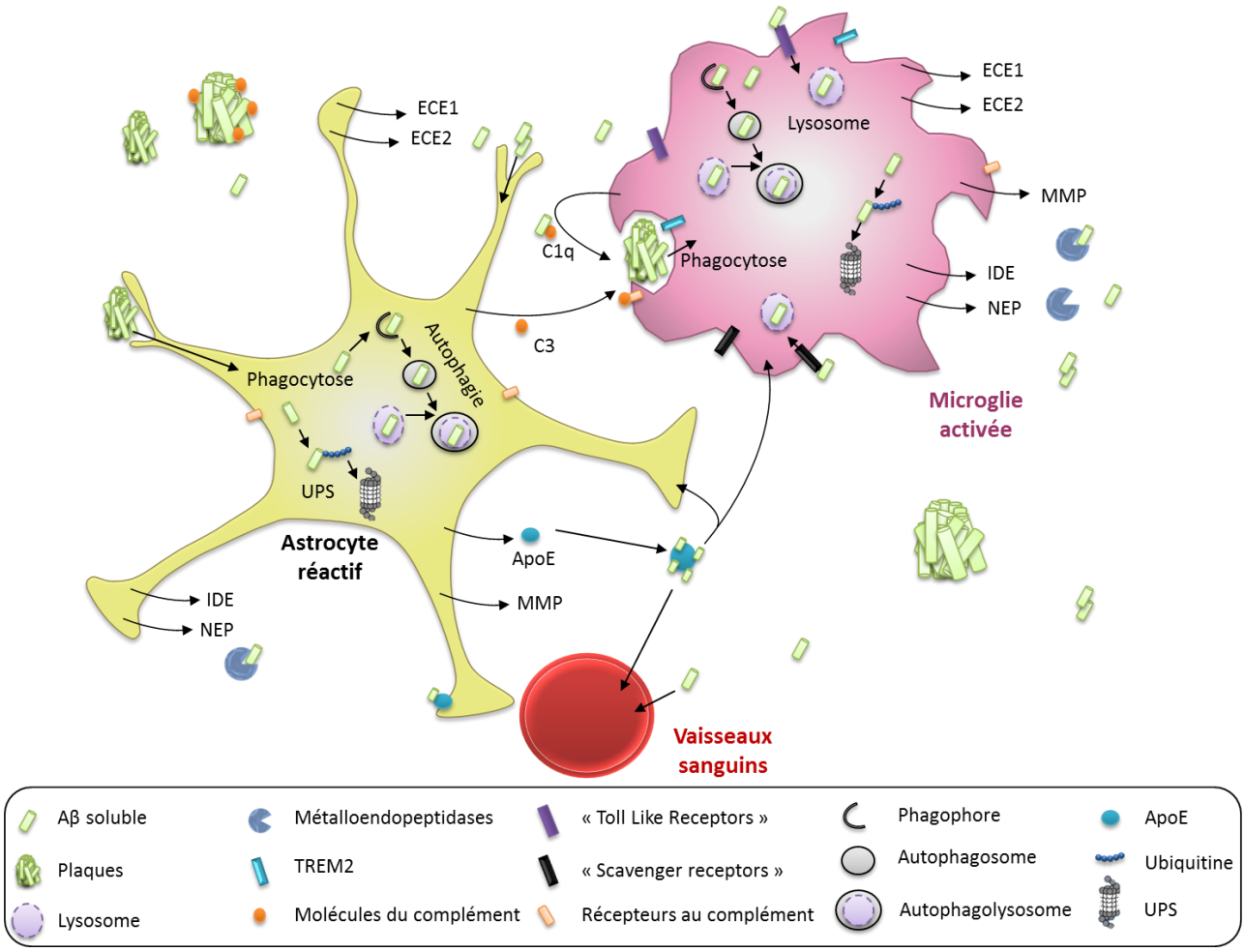

Figure 22 : Multiples voies de dégradation de l'Aβ par les astrocytes et la microglie.

Dans la MA, de nombreux mécanismes entrent en jeu dans la dégradation des oligomères et des plaques Aβ par les astrocytes et la microglie. Leur dégradation est extracellulaire (libération d'endo ou métallopeptidases), intracellulaire (phagocytose puis autophagie ou système ubiquitine protéasome) ou ils sont éliminés dans la circulation sanguine. Abréviations : ApoE = Apolipoprotéine, ECE1/2 = Endothelin-converting enzyme, IDE = Insulin degrading enzyme, MMP = Matrix metalloprotéinase, NEP = Néprylisine, UPS = Ubiquitin proteasome system.

Le **système du complément** apparait aussi impliqué dans les mécanismes de dégradation de l'Aβ fibrillaires. En effet, une accumulation de molécules du complément est observée sur les plaques amyloïdes *(Emmerling et al., 2000)*. Ces molécules agissent comme des facteurs chemotactiques, participant au recrutement des cellules microgliales au niveau des plaques. L'Aβ stimule lui-même la cascade du complément soit via sa liaison à C1q, soit via sa liaison à C3b, induisant une phagocytose bien plus agressive *(Lee and Landreth, 2010)*. A l'inverse, l'Aβ active la voie NF-κB dans les astrocytes, conduisant à une forte libération de C3, qui altère la phagocytose microgliale via sa liaison sur le récepteur C3a *(Lian et al., 2016)*.

L'UPS (Système ubiquitine/protéasome) est un mécanisme dégradant sélectivement les protéines à courte durée de vie, endommagées ou mal conformées. Avant d'être dégradée par le protéasome, les protéines sont identifiées par poly-ubiquitination via l'activité consécutive de trois enzymes (E1, E2 puis E3). Il est intéressant de noter que le système ubiquitine/protéasome est plus efficace dans

les cellules gliales que dans les neurones *(Jansen et al., 2014)*. L'UPS peut directement dégrader l'Aβ mais également BACE1, ce qui diminue le clivage de l'APP et donc la production d'Aβ *(Hong et al., 2014)*. Néanmoins, bien que l'activité de l'UPS soit augmentée lorsque les cellules gliales sont activées *(Orre et al., 2013)*, son fonctionnement semble être altéré dans la MA. En effet, une accumulation d'ubiquitine est observée au niveau des plaques amyloïdes et des DNF *(Perry et al., 1987)*. Ces structures contiennent une protéine ubiquitine mutée (contenant une extension C-terminale de 19 acides aminés), qui bloque la protéolyse ubiquitine-dépendante dans les neurones *(Lindsten et al., 2002)* et qui pourrait être associé à la toxicité de l'Aβ *(Song et al., 2003)*.

L'**autophagie** entre en jeu pour la dégradation de protéines à longue durée de vie, de protéines agrégées ou des organelles. Des protéines importantes pour l'autophagie tels qu'Atg5, Atg12 et LC3 (microtubule-associated protein light chain 3) sont observées au niveau des plaques et des DNF dans le cerveau de patients atteints de la MA *(Ma et al., 2010)*. Le rôle de l'autophagie par les cellules gliales n'est étudié que depuis peu. L'autophagie par la microglie joue un rôle important dans l'élimination des fibrilles d'Aβ extracellulaires et dans la régulation de l'inflammasome *in vitro* et *in vivo (Cho et al., 2014)*. Une diminution de l'expression de Beclin1, impliquée dans l'initiation de l'autophagie, est observée dans les cellules microgliales isolées de cerveaux de patients *(Pickford et al., 2008 ; Lucin et al., 2013)*, suggérant une altération de l'autophagie dans ces cellules. Il a également été montré récemment que l'autophagie entre en jeu dans l'internalisation de l'Aβ par les astrocytes. En effet, une forte expression de LC3 a été observé dans les astrocytes d'un modèle murin de la MA et l'internalisation des fibrilles d'Aβ est dépendante de l'autophagie *in vitro (Pomilio et al., 2016)*. Il est également intéressant de noter que l'altération de l'autophagie pourrait être impliquée dans la production d'Aβ. En effet, une accumulation de vacuoles autophagiques a été décrite dans le cerveau de patients et des modèles murins de la MA, certainement due d'un déficit de leur maturation en lysosomes *(Nixon et al., 2005)*. Ces vacuoles apparaissent comme des réservoirs majeurs d'Aβ dans le cerveau et présentent également une accumulation d'APP, PS1 et BACE, qui sont nécessaires et suffisants à la génération de peptides Aβ *(Yu et al., 2004, 2005)*. Ceci suggère que les astrocytes et la microglie peuvent produire de l'Aβ par ce biais.

Les mécanismes de dégradation de l'Aβ par la microglie et par les astrocytes sont donc très nombreux *(Cf Ries and Sastre, 2016 pour une revue plus détaillée de ces mécanismes de dégradation)*. Ces deux types cellulaires sont finement organisés autour des plaques amyloïdes et communiquent notamment via la libération de cytokines et chemokines. Néanmoins, leur activation peut altérer leurs capacités de dégradation de l'Aβ soluble et fibrillaire, suggérant un rôle prépondérant de la neuroinflammation dans la progression de la MA.

La réactivité induit donc de multiples changements fonctionnels astrocytaires, mettant en avant leur rôle complexe dans la MA. En effet, ils pouvent impacter positivement ou négativement, à plusieurs niveaux, le développement et la progression de la MA (altération du soutien des neurones, participation au stress oxydatif, sécrétion de molécules pro-inflamamtoires pouvant impacter les

neurones, la microglie, les cellules immunitaires périphériques ou les astrocytes eux-mêmes, ou encore participation à la dégradation de l'Aβ). Il est donc très difficile de déterminer avec certitude quel est l'impact des astrocytes réactifs dans la MA.

5. Rôles bénéfiques ou délétères de la réactivité astrocytaire dans la maladie d'Alzheimer ?

5.1. Les controverses de la littérature

Comme les astrocytes réactifs polarisent leurs prolongements en direction des plaques et qu'ils sont capables de dégrader les plaques amyloïdes, nous pourrions d'abord penser à un rôle bénéfique des astrocytes réactifs dans la MA. Cependant, comme présenté dans la partie 4.1, la réactivité astrocytaire engendre de nombreux changements morphologiques, transcriptionnels et fonctionnels, induisant aussi bien des pertes de fonctions que des gains de fonctions toxiques. Afin d'évaluer si les astrocytes réactifs jouent un rôle bénéfique ou délétère dans la MA, différentes stratégies ont été utilisées pour **moduler (inhiber ou induire) globalement** la réactivité astrocytaire. Pour mieux comprendre les effets controversés qui découlent de ces études, il est important de préciser les différentes méthodes utilisées pour moduler la réactivité astrocytaire *(Tableau 4).* Pour une même molécule, plusieurs stratégies peuvent être employées. Par exemple, des cytokines peuvent être surexprimées ou inhibées par vectorisation virale, transgénèse, ou via des molécules pharmacologiques (inhibiteurs ou anticorps dirigés contre la cytokine notamment). Cependant, ces stratégies vont impacter les astrocytes réactifs mais aussi la microglie. La littérature modulant la neuroinflammation et donc les astrocytes réactifs est très dense. Je fais ici une synthèse des principaux articles ayant étudié la réactivité astrocytaire dans la MA *(Tableau 4)*. Les stratégies ciblant plus spécifiquement les astrocytes sont indiquées par un astérisque. Les études modulant l'inflammation, sans étudier la réactivité astrocytaire, ne sont pas présentées.

Stratégie	Effets sur				CCL globale sur la MA	Principales références
	la RA	la microglie	la charge amyloïde	les autres index de la MA		
Surexpression de cytokines						
AAV-IL-4 Souris APP + PS1 (Sexe ?, 8mo)	↘	Activation x ↘recrutement	↘	↘ déficits cognitifs	-	*(Kiyota et al., 2010)*
AAV-IL-10 Souris APP + PS1 (Sexe ?, 8mo)	↘	Activation x ↘recrutement	=	déficits cognitifs	-	*(Kiyota et al., 2012)*
Cxcr3$^{-/-}$ Souris APP$_{swe}$/PS1dE9 (M, 8mo)	↘	↘ activation	↘	↘ déficits cognitifs	-	*(Krauthausen et al., 2015)*
AAV-IL-6 Souris TgCRND8 (Sexe ?, 3mo)	↗	↗ activation	↘	X	+	*(Chakrabarty et al., 2010a)*
AAV-IFNγ Souris TgCRND8 (Sexe ?, 4-5mo)	↗	↗activation	↘	X	+	*(Chakrabarty et al., 2010b)*
AAV-TNFα Souris TgCRND8 (Sexe ?, 5,5mo)	↗	↗ activation ↗recrutement	↘	X	+	*(Chakrabarty et al., 2011)*
Cassette IL-1β^{XAT} Souris 3xTg-AD (F + M, 16-18 mo)	↗	↗ activation ↗recrutement	↘amyloïde + ↗ de Tau	X	?	*(Ghosh et al., 2013)*
Délétion de cytokines						
Inhibiteur de TNFα (3,6'-dithiothalidomide) Souris 3xTg-AD (M, 10 et 17mo)	↘	↘ activation	↘amyloïde + ↘ de Tau	↘ altérations synaptiques	-	*(Tweedie et al., 2012)*
IL-12$^{-/-}$ Souris APPPS1$^{+/-}$ (F + M, 6mo)	↘	Activation x ↘Recrutement	↘	X	-	*(Vom Berg et al., 2012)*
IL-10$^{-/-}$ Souris APP$_{swe}$/PS1dE9 (M + F, 12-13mo)	↗	↗ activation	↘	↘ déficits cognitifs et altérations synaptiques	+	*(Guillot-Sestier et al., 2015)*
KO de molécules du complément						
C3$^{-/-}$ Souris APP$_{swe}$/PS1dE9 (M, 16mo)	↘	↘ activation ↘ recrutement	↗	↘ déficits cognitifs et altérations synaptiques	-	*(Shi et al., 2017)*
C1q$^{-/-}$ Souris Tg2576 (Sexe ?, 16mo)	↘	↘ activation	=	↘ altérations synaptiques	-	*(Fonseca et al., 2004)*

Stratégie	Effets sur				CCL globale sur la MA	Principales références
	la RA	la microglie	la charge amyloïde	les autres index de la MA		
KO de protéines des filaments intermédiaires *						
GFAP$^{-/-}$, Vimentin$^{-/-}$ Souris APP$_{swe}$/PS1dE9 (Sexe ?, 12mo)	↘	↗ activation ↗ recrutement	↗	↗ neurites dystrophiques	+	*(Kraft et al., 2013)*
GFAP$^{-/-}$, Vimentin$^{-/-}$ Souris APP$_{swe}$/PS1dE9 (Sexe ?, 6, 9 et 15mo)	↘	X activation = prolifération	=	X	=	*(Kamphuis et al., 2015)*
Activation de voies de signalisation dans les astrocytes *						
Forme constitutivement active de la Calcineurine Souris APP/PS1 (Sexe ?, 8mo)	↘	↘ activation	↘	↘ déficits cognitifs	-	*(Fernandez et al., 2012)*
Inhibition de voies de signalisation dans les astrocytes *						
AAV-VIVIT, inhibiteur sélectif de NFAT Souris APP$_{swe}$/PS1dE9 (M, 16-17mo) ; 5xFAD (Sexe ?, 8mo)	↘	↘ activation	↘	↘ déficits cognitifs, altérations synaptiques et hyperactivité neuronale	-	*(Furman et al., 2012; Sompol et al., 2017)*

Tableau 4 : Principales études modulant la réactivité astrocytaire dans la MA.
Sélection d'articles clés qui ont évalué l'effet de la modulation de la neuroinflammation, incluant les astrocytes réactifs, sur différents index de la MA. * Stratégies ciblant plus spécifiquement les astrocytes. L'effet de la modulation de l'inflammation sur le recrutement microgliale au niveau des plaques amyloïdes est précisé uniquement s'il a été étudié dans les articles cités. Abréviations : RA = Réactivité astrocytaire (évaluée généralement grâce à des critères morphologiques ou l'expression de marqueurs tels que la surexpression de la GFAP), M = males, F = femelles, mo = mois (age auquel le modèle a été étudié), « ↘ » = diminution, « ↗ » = augmentation, « = » = pas d'effet, « - » = délétère, « + » = bénéfique, « X » = aucune donnée, CCL = conclusion sur l'effet global de la neuroinflammation/réactivité astrocytaire sur la MA.

Une forte controverse sur le rôle de la neuroinflammation et des astrocytes réactifs dans la MA apparait donc dans la littérature. L'expression ou la délétion de cytokines ou de molécules du complément agissent sur tous les acteurs de la neuroinflammation (astrocytes et cellules microgliales) et parfois les cellules immunitaires périphériques. Ce ne sont donc pas des méthodes assez sélectives pour pouvoir conclure sur le rôle des astrocytes réactifs dans la MA. Des techniques plus spécifiques des astrocytes ont été développées pour moduler leur réactivité (stratégies annotées avec une *, *Tableau 4*). Néanmoins, que ce soit via des KO des protéines des filaments intermédiaires telles que la GFAP et la Vimentine ou via la modulation de voie de signalisation dans les astrocytes, les résultats ne sont pas concordants.

Il est important de noter que l'ablation de protéines des filaments intermédiaires induit de multiples changements transcriptionnels *(Kamphuis et al., 2015)* et impacte bien évidemment de nombreuses fonctions normales des astrocytes *(Shibuki et al., 1996)*. De plus, la surexpression des protéines de filaments intermédiaires est une caractéristique classique des astrocytes réactifs mais la bloquer ne signifie pas forcément que les astrocytes ne sont plus réactifs.

L'ensemble des études visant la voie NFAT/Calcineurine, impliquée dans la réactivité astrocytaire *(Cf §2.2),* suggère un rôle délétère de la réactivité astrocytaire. Cependant, le peptide VIVIT utilisé dans ces études ne réduit que partiellement la réactivité (30% de diminution du marqueur GFAP) et il peut être sécrété par les astrocytes. On ne peut donc pas exclure un effet direct du peptide sur les cellules avoisinantes en particulier les neurones, dans lesquels la voie calcineurine a de nombreuses fonctions *(Baumgärtel and Mansuy, 2012)*. De plus, la séquence du peptide VIVIT a été identifiée sur d'autres substrats de la calcineurine *(Li et al., 2011)*, suggérant que les effets observés ne sont pas forcément spécifique de la voie calcineurine/NFAT. Enfin, il est intéressant de noter que les deux études ciblant cette voie de signalisation *(Fernandez et al., 2012 ; Furman et al., 2012)* décrivent des effets différents sur la voie, bien que les deux stratégies induisent une inhibition de la réactivité astrocytaire. En effet, Fernandez et al., utilisent une forme constitutivement active de la calcineurine alors que le peptide VIVIT bloque spécifiquement l'interaction entre la calcineurine et NFAT *(Aramburu et al., 1999)*, inhibant ainsi la voie. Le mécanisme par lequel cette de voie de signalisation impacte la réactivité astrocytaire n'est donc pas encore bien établi.

Il est également important de noter que dans la majorité de ces études, la réactivité astrocytaire est caractérisée uniquement à l'aide de critères morphologiques ou de la surexpression de la GFAP. Ces index ne permettent donc pas d'identifier les modifications fonctionnelles des astrocytes engendrées par les stratégies de modulation.

En fonction de la stratégie expérimentale et du modèle utilisé, les résultats concernant le rôle de la réactivité astrocytaire dans la MA sont donc **contradictoires.** Afin de mieux comprendre le rôle des astrocytes réactifs dans la MA, le ciblage d'une voie de signalisation contrôlant la réactivité astrocytaire apparait donc comme la stratégie la plus spécifique. Néanmoins, **il est important de cibler une voie de signalisation centrale et spécifique de cette réactivité**.

5.2. Problématique, objectifs de la thèse et stratégie

Quel est l'impact global de la réactivité astrocytaire sur la MA ? Comme démontré dans le paragraphe précédent, la réponse à cette question est toujours controversée. Il est important d'identifier les cascades de signalisation contrôlant la réactivité astrocytaire puisque ceci permettra de manipuler les astrocytes afin de contrôler leur statut et ainsi de favoriser leurs fonctions bénéfiques au cours des maladies neurodégénératives. Dans ce but, nous nous sommes intéressés à la voie JAK2-STAT3, qui apparait comme centrale dans la réactivité astrocytaire au cours de maladies neurodégénératives *(**Publication 3 en annexe** et §2.3)*.

Ce projet présente deux objectifs majeurs :

1/ Etablir l'importance de la voie JAK2-STAT3 pour la réactivité astrocytaire.

Nous avions déjà mis en évidence l'activation de la voie JAK-STAT3 dans des modèles murins de la maladie de Huntington et de la MA grâce à l'accumulation nucléaire de STAT3 dans les astrocytes. La surexpression de SOCS3, inhibiteur endogène de la voie JAK-STAT3, inhibe efficacement la réactivité astrocytaire (diminution de l'expression de la GFAP) dans ces modèles ***(Publication 3 en annexe)***. Pour répondre au premier objectif de la thèse, nous avons tout d'abord complété nos précédents résultats en étudiant l'activation de la voie JAK-STAT3 dans d'autres modèles de la maladie de Parkinson et de tauopathies. De plus, nous avons été plus loin que l'analyse morphologique et la surexpression des protéines des filaments intermédiaires pour caractériser la réactivité. En effet, nous avons amplement étudié l'effet de la réactivité sur le profil transcriptionnel des astrocytes ainsi que sa restauration par SOCS3 dans un modèle de la MA. A l'inverse, l'injection de vecteur codant pour une forme constitutivement active de la kinase JAK2 (JAK2ca) dans les astrocytes de souris WT (Sauvages) révèle que la voie JAK2-STAT3 est nécessaire et suffisante pour induire la réactivité astrocytaire. Moduler la voie JAK2-STAT3 par transfert de gène est donc un bon outil pour manipuler les astrocytes au cours de maladies neurodégénératives comme la MA.

2/ Evaluer l'effet global de la réactivité astrocytaire sur différents index de la MA.

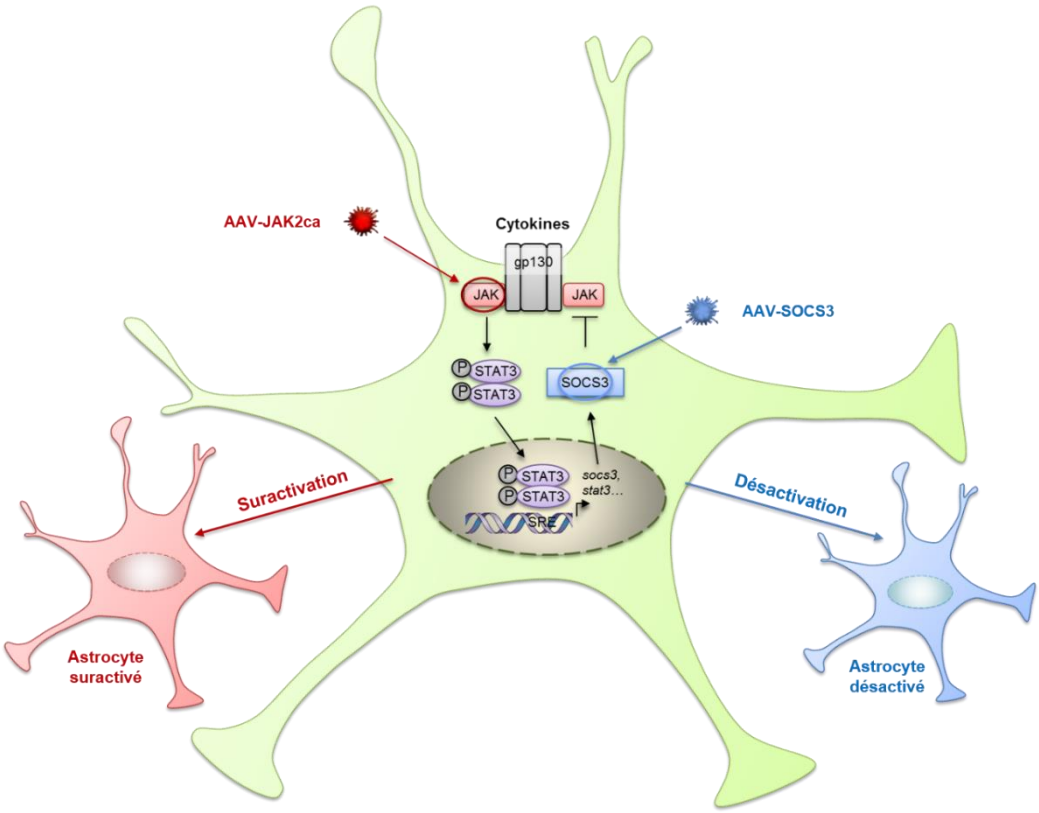

Figure 23 : Modulation de la voie JAK2-STAT3 pour étudier l'effet la réactivité astrocytaire dans la MA.
Grâce à des vecteurs viraux adéno-associés (AAV), nous modulons la voie JAK2-STAT3 spécifiquement dans les astrocytes. Les astrocytes sont suractivés par l'expression constitutivement active de JAK2. A l'inverse, ils sont désactivés par la surexpression de SOCS3.

Afin d'atteindre ce second objectif, nous avons utilisé deux modèles murins complémentaires de la MA : les souris APP/PS1dE9 et 3xTg-AD, pour mieux comprendre l'effet de la réactivité astrocytaire sur la pathologie amyloïde d'une part et son effet dans un second contexte, alliant pathologie Tau et amyloïde d'autre part. Les vecteurs viraux surexprimant SOCS3 ou JAK2ca ont été utilisés dans ces modèles *(Figure 23)*, afin de définir si la réactivité astrocytaire a un effet global bénéfique ou délétère. Ces études révèlent des effets complexes et contexte-dépendants de la réactivité astrocytaire dans la MA.

« Tout obstacle renforce la détermination »

Léonard De Vinci

Matériel et méthodes

Matériel et Méthodes

Les méthodes sont décrites dans chacun des manuscrits intégrés dans la partie résultats. J'ai choisi de reprendre ici les méthodes principales que j'ai utilisées au cours de ma thèse et de compléter celles qui n'étaient que succinctement décrites.

1. Modèles murins de la maladie d'Alzheimer

Tous les protocoles expérimentaux ont été approuvés par un comité d'éthique local indépendant et soumis au Ministère français de l'Education et de la Recherche (Autorisation 15-081). Ils ont été réalisés en accord avec les réglementations de l'Union Européenne (Directive 2010-63/UE) pour la protection des animaux utilisés à des fins scientifiques

Le modèle APP/PS1dE9

Des souris transgéniques APP/PS1dE9 (mâles) co-exprimant une protéine APP chimérique souris/humaine contenant les mutations suédoises K595N et M596L (APPswe) et la PS1 humaine délétée de l'exon 9 (PS1dE9), sous le contrôle d'un promoteur de la protéine prion de souris sur un fond génétique C57BL/6J ont été utilisés *(Jankowsky et al., 2004)*. Un génotypage des souris APP/PS1dE9 a été réalisé par PCR (Polymerase chain reaction) à 4-6 semaines. L'ADN a été extrait à partir d'échantillons d'oreilles en utilisant le kit « Kappa protease » et amplifié par PCR. Un gel à 2% d'agarose a été utilisé pour faire migrer les échantillons et vérifier la taille de l'amplicon. Les oligonucléotides suivants ont été utilisés : **APP-F** AGGACTGACCACTCGACCAG ; **APP-R** CGGGGGTCTAGTTCTGCAT. Les souris WT « littermates » ont été utilisées comme souris contrôles.

Le modèle 3xTg-AD

Des souris femelles triples transgéniques (3xTg-AD) co-exprimant la protéine mutée APPswe humaine et les protéines PS1 mutée (PS1M146V) et Tau humaine mutée (tauP301L) sur un fond mixte C57Bl6 x 129S ont également été utilisées *(Oddo et al., 2003a)*. Les souris 3xTg-AD sont élevées en croisant des souris homozygotes, un génotypage n'est donc pas nécessaire. Les souris WT du même fond génétique (C57Bl6 x 129S) ont été utilisées comme souris contrôles.

2. Vecteurs viraux

Construction des vecteurs viraux adéno-associés

Des vecteurs adéno-viraux associés de sérotype 9 (AAV2/9) codant pour l'ADNc (ADN complémentaire) murin de SOCS3 (AAV-SOCS3) ou pour une forme constitutivement active de JAK2 (JAK2T875N ; AAV-JAK2ca) ont été utilisés respectivement pour désactiver ou lsuractiver les astrocytes *(Haan et al., 2009)*. Un AAV codant pour la GFP (Green fluorescente protein ; AAV-GFP) a été utilisé comme vecteur contrôle.

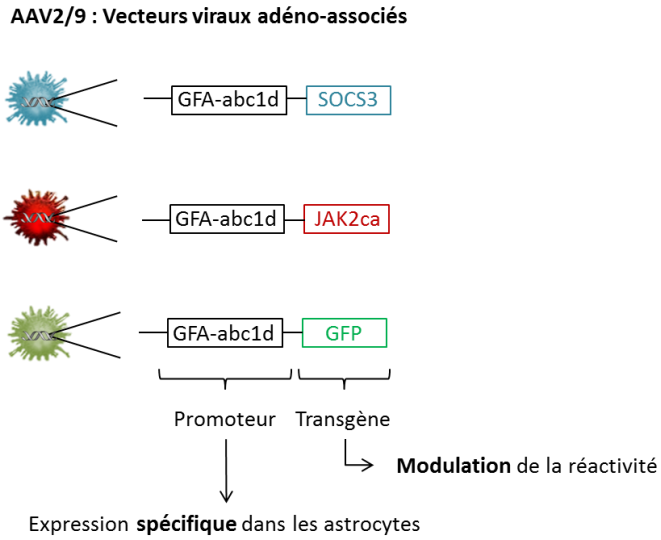

Figure 24 : Construction des vecteurs viraux utilisés.

Tous les transgènes étaient sous le contrôle du promoteur GFA-abc1d, promoteur synthétique de la GFAP *(Lee et al., 2008)*, permettant une expression des transgènes spécifiquement astrocytaire. Les AAV-SOCS3 et JAK2ca ont été co-injectés avec l'AAV-GFP afin de visualiser les cellules infectées (plus de 99 % de co-expression des deux transgènes dans ces cellules ; données obtenues au laboratoire). Les AAV ont été produits et stockés sur la plateforme de production virale de MIRCen.

Chirurgie stéréotaxique

Avant la chirurgie, les souris APP/PS1dE9 ont été anesthésiées par injection *i.p* (Intra-péritonéale) de Kétamine (100 mg/kg)/Médetomidine (0.25 mg/kg) suivi d'une injection d'atipamezole (0.25 mg/kg) 45 min post-induction. Les souris 3xTg-AD ont été anesthésiées par injection *i.p* de Kétamine (100 mg/kg)/Xylasine (10 mg/kg). Pour les deux lignées, une injection sous cutanée de Lidocaïne (7 mg/kg) a également été réalisée au site d'incision, 10 min avant l'injection stéréotaxique.

Tous les groupes ont été injectés bilatéralement dans l'hippocampe avec 2 µl de solution de vecteurs viraux par hémisphère ($2{,}5x10^9$ génome viral (VG)/µL soit $5x10^9$ VG/site). Les solutions utilisées étaient les suivantes : AAV-GFP ($2{,}5.10^9$ VG/µL) ou AAV-SOCS3 + AAV-GFP ($2{,}10^9$ VG/µL + $5{,}10^8$ VG/µL respectivement ; simplifié par la suite par AAV-SOCS3) ou AAV-JAK2ca + AAV-GFP ($2{,}10^9$ VG/µL + $5{,}10^8$ VG/µL respectivement ; simplifié par la suite par AAV-JAK2ca), à une vitesse de 0,2 µL/min à l'aide d'une pompe. Le titre viral a été choisi afin éviter l'induction d'inflammation par le vecteur viral lui-même. Les canules d'injections ont été laissées en place pendant 5 min avant d'être remontées doucement pour éviter tout reflux du vecteur pendant la remontée de la canule. La peau a ensuite été agrafée et désinfectée. Les souris APP/PS1dE9 et 3xTg-AD ont été injectées à l'âge de 2-4 mois avec un AAV-SOCS3, un AAV-JAK2ca, ou un AAV-GFP seul, avant que les astrocytes ne soient réactifs. Les souris WT du même fond génétique ont été injectées avec un AAV-SOCS3 ou un AAV-GFP seul. Pour des raisons de faibles disponibilités de souris transgéniques, le premier lot de souris 3xTg-SOCS3 et contrôles correspondants ont été injectés à 5-6 mois. Afin d'étudier la capacité de SOCS3 à inhiber la réactivité déjà mise en place, des souris APP/PS1dE9 ont été injectées à 15 mois et sacrifiées un mois post-injection.

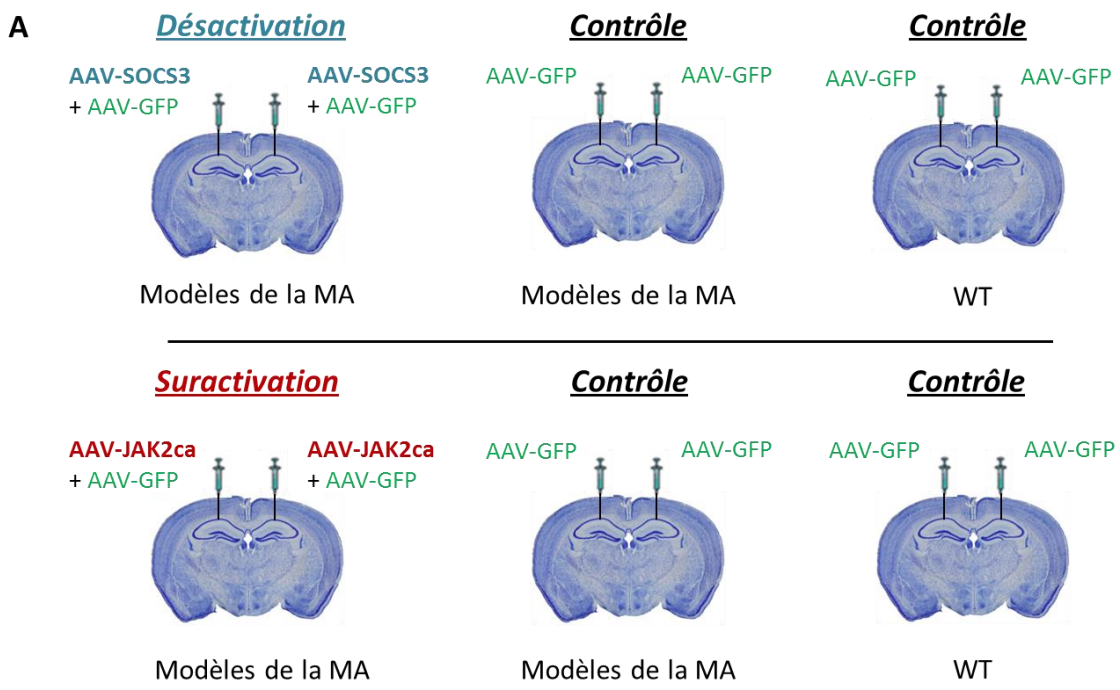

B

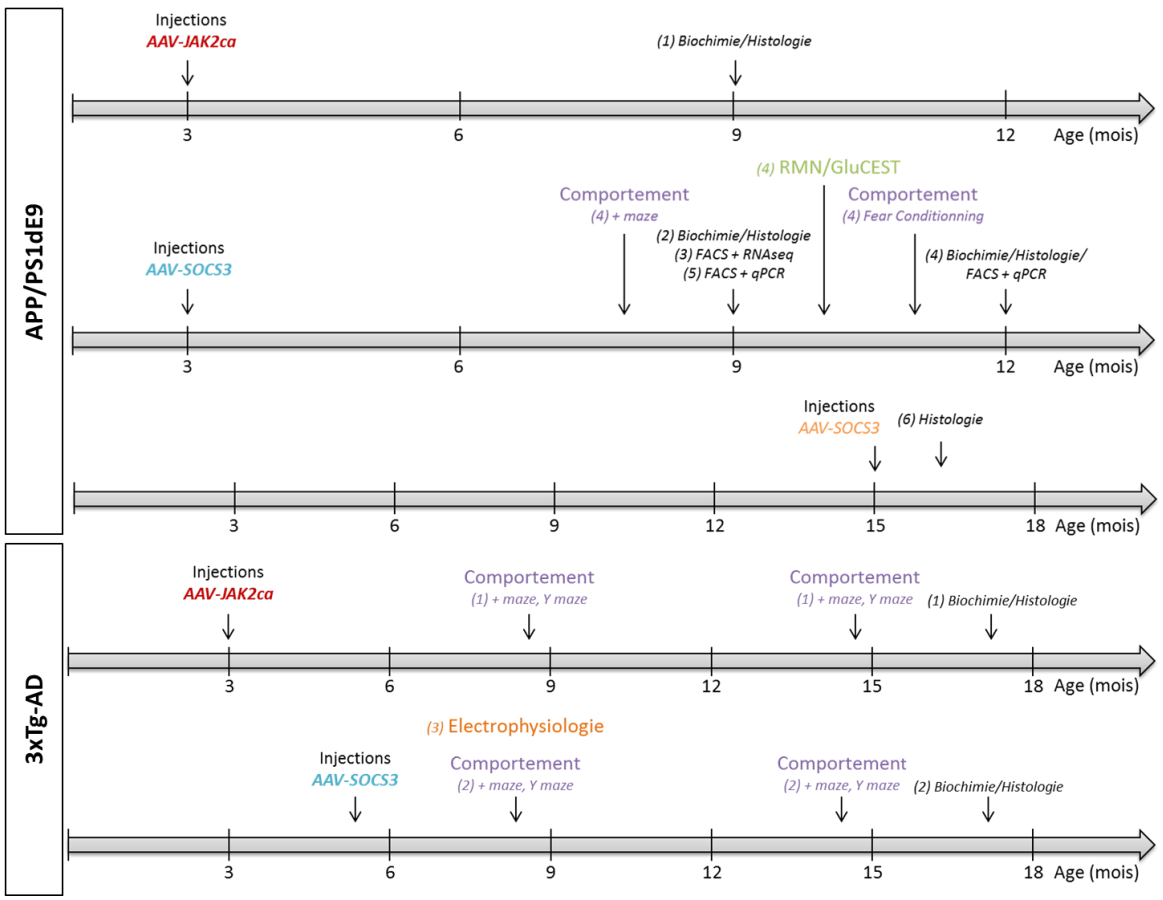

C

	n / groupe		
Cohorte	**WT-GFP**	**APP/PS1dE9-GFP**	**APP/PS1dE9-SOCS3 ou JAK2ca**
1	7	6	6
2	5	10	8
3	7	4	5
4	16	9	11
5	11	6	8
6	x	4	4
Cohorte	**WT-GFP**	**3xTg-GFP**	**3xTg-SOCS3 ou JAK2ca**
1	9	8	8
2	7	9	10
3	9	8	8

Figure 25 : Schéma expérimental.

A) Schéma expérimental représentant les différents groupes injectés. Chaque cohorte d'intérêt (désactivation ou suractivation de la réactivité astrocytaire) inclus deux groupes contrôles : souris modèles de la MA injectées avec un AAV-GFP et souris WT injectées avec un AAV-GFP, **B)** Chronologie des expériences effectuées sur les deux modèles. Les différentes cohortes de chaque modèle sont identifiées par le chiffre entre parenthèse, **C)** Nombre d'animaux par groupe au sein de chaque cohorte. Abréviations : + maze = Labyrinthe en croix surélevé.

Dans un premier temps, pour cibler l'hippocampe, les coordonnées suivantes ont été utilisées (par rapport au bregma) : antéro-postérieur -2 mm, latéral +/-2 mm, ventral -1.2 mm à partir de la dure-mère. Ces coordonnées ont ensuite été modifiées pour les coordonnées suivantes (par rapport au bregma) : antéro-postérieur -3 mm, latéral +/-3 mm, ventral -1.5 mm à partir de la dure-mère, permettant une meilleure diffusion du virus. Seules les deux premières cohortes de souris APP/PS1dE9 analysés par la suite à 9 mois (cohortes 1 et 2) ont été injectés avec les premières coordonnées visant la région CA1 antérieur.

3. Etudes comportementales

Toutes les souris ont d'abord été habituées à être manipulées 2 min par jour, pendant une semaine, avant le début des tests. Le change des cages a également été effectué par l'expérimentateur pendant toute la durée des tests de comportement.

Analyse comportementale sur les souris 3xTg-AD

Test du labyrinthe en croix surélevé

Ce test a été réalisé à 8-9 mois et 14-15 mois sur des souris 3xTg-AD et WT injectées avec des AAV-SOCS3 (3xTg-SOCS3), AAV-JAK2ca (3xTg-JAK2ca) ou AAV-GFP (3xTg- ou WT-GFP). Il permet d'évaluer l'anxiété. L'appareil est fait de plexiglas noir et éclairé à 100 lux en son centre. Il est composé de 4 bras élevés à 50 cm du sol. Deux bras sont fermés (bras non anxiogènes ; extrémités éclairées à 15 lux) et les deux autres sont ouverts (bras anxiogènes ; extrémités éclairées à 150 lux). Chaque souris a été placée au centre face à un bras ouvert et filmée pendant une seule session d'exploration de 6 min, avec l'expérimentateur hors la pièce. Après chaque acquisition, le sol et les bords ont été lavés à l'éthanol 10% et séchés. Les paramètres suivants ont été mesurés et analysés avec le système de vidéo tracking EthoVision (Noldus) : distance parcourue et temps passé dans chaque bras, fréquence d'entrée dans les bras ouverts ou fermés, durée et nombre de fois où la souris se penche au niveau des bras ouverts (manuellement mesurés pendant l'expérience). Les souris étant restées immobiles, ayant une fréquence d'entrée <4 (la moyenne de l'ensemble des animaux étant de 12 bras visités) lors du test ont été exclues de l'analyse (n=3/26 (cohorte SOCS3), 5/25 (cohorte JAK2ca) animaux exclus/total).

Test du labyrinthe en Y

Le test du labyrinthe en Y a été réalisé à 8-9 mois et 14-15 mois sur des souris 3xTg-AD et WT injectées avec des AAV-SOCS3, AAV-JAK2ca ou AAV-GFP. Il permet d'évaluer la mémoire spatiale de travail. L'appareil est composé de trois bras en plexiglas noir et éclairé à 110 lux en son centre. Chaque souris a été placée à l'extrémité du bras « start », et laissée pour une session d'entrainement de 15 min, avec l'un des deux autres bras fermés à l'aide d'une porte en plexiglas noir. Après l'acquisition, le sol et les bords ont été lavés à l'éthanol 10% et séchés, la porte enlevée (le bras précédemment fermé correspond donc au nouveau bras). La souris est ensuite replacée à l'extrémité du bras « start » et laissée pour une session test de 5 min. Le test repose sur la curiosité naturelle de la souris qui va l'amener à explorer davantage le nouveau bras. La position de la porte a été alternée entre le bras droit et le bras gauche. La distance parcourue et le temps passé dans chaque bras ont été mesurés par vidéo-caméra et analysées avec le système de vidéo tracking EthoVision. Les animaux ayant visités un seul bras lors de l'entrainement ou moins de 4 bras lors du test ont été exclus (la moyenne pour l'ensemble des animaux étant de 12 bras visités ; n=10/26 (cohorte SOCS3), 7/25 (cohorte JAK2ca) animaux exclus/total).

Analyse comportementale sur les souris APP/PS1dE9

Test du labyrinthe en croix surélevé

Le test du labyrinthe en croix surélevé a été réalisé à 9 mois sur des APP/PS1dE9 et WT injectées avec des AAV-SOCS3 (APP-SOCS3) ou AAV-GFP (APP- ou WT-GFP). Le même protocole que décrit précédemment pour les souris 3xTg-AD a été suivi. Critères d'exclusions : distance parcourue <850 cm (la moyenne pour l'ensemble des animaux étant de 1300 cm ; n=4/36 animaux exclus/total).

Test de conditionnement par la peur

Le test de conditionnement par la peur a été réalisé à 11 mois sur des souris APP/PS1dE9 et WT injectées avec des AAV-SOCS3 ou AAV-GFP. La souris a été placée au centre du dispositif pour une première phase d'entrainement. Après 3 min d'exploration, la souris a reçu un choc électrique de 0.35 mA pendant 1 sec. Après 1 min, un second choc a été appliqué (0.35 mA, 1 sec). Après 30 sec, la souris a été sortie du dispositif et placée dans une nouvelle cage. 24h, 7 jours et 14 jours après le test, la souris a été replacée dans le dispositif pendant 5 min. Le dispositif a été nettoyé avec de l'éthanol 70% et séché entre chaque animal. La durée du « freezing » pendant la phase de test a été mesurée grâce à au logiciel LE118-8. Critères d'exclusions : temps de freezing > 20% avant le choc (n=7/36 animaux exclus/total).

4. Cytométrie en flux

Analyse de la recapture de l'Aβ in vivo

Les souris APP/PS1dE9 ont été injectées 3h avant le sacrifice avec du méthoxy-XO4 (MXO4), un dérivé du rouge congo passant la BHE, permettant de marquer l'Aβ (Tocris #4920 ; 10 mg/kg), préparé à 2.5 mg/ml dans une solution 50% DMSO/50% NaCl [0.9%], pH 12. Elles ont été sacrifiées par overdose de pentobarbital sodique (180 mg/kg) puis une perfusion intracardiaque avec une solution saline phosphate (dPBS ; Life Technologies, Gibco, #14190-094) froide a été réalisée afin d'éliminer au maximum les macrophages circulants. Le cerveau a été disséqué, les deux hémisphères ont soient été séparés et utilisés pour des expériences de tri cellulaire et d'histologie ou de biochimie (Cohorte n°4 : Tri cellulaire : n=6-12/groupe ; Histologie : n=5-7/groupe ; Biochimie : n=4-9/groupe), soient poolés afin de collecter un plus grand nombre de cellules par échantillons (Cohorte n°5).

Dissociation des cellules

Le ou les hippocampes ont entièrement été disséqués sur glace et immédiatement placés dans une solution froide d'HBSS (Hanks' Balanced Salt Solution) sans Mg^{2+} ni Ca^{2+} (Sigma, #55021C). Les cellules ont ensuite été dissociées mécaniquement et enzymatiquement en utilisant des pipettes Pasteur polies et un kit de dissociation tissulaire à la papaïne (Miltenyi, #130-092-628) respectivement. La myéline a été extraite des échantillons en utilisant des billes magnétiques couplées à un anticorps fixant la myéline (Myelin removal beads II, Miltenyi, #130-096-731) et des colonnes MS (Miltenyi, #130-042-201) placées sur un aimant comme décrit dans le protocole du fournisseur. Après centrifugation, soit un marquage de la microglie a été réalisé, soit les cellules été directement resuspendues dans 400 µl d'HBSS avec Mg^{2+} et Ca^{2+} (Sigma, #55037C) et analysées par cytométrie en flux (FACS ; Fluorescence-activated cell sorting).

Marquage de la microglie

Après dissociation, les cellules ont été centrifugées à 300 g, 5 min, à 4°C et resuspendues dans du Fc block 1/100 (TruStainFcX™ (anti-mouse CD16/32), Biolegend, #101319) dilué dans de l'HBSS avec Mg^{2+} et Ca^{2+}, 10 min sur glace, pour prévenir la fixation des anticorps sur les récepteurs Fc. Les échantillons ont de nouveau été centrifugés et resuspendus dans la solution d'anticorps suivante : anti-CD11b-PE 1/100 (eBioscience, #12-0112) et anti-CD45-PE-Cy5 1/300 (eBioscience, #15-0451) dilués dans la solution « cell staining buffer » (Biolegend, #420201) et incubés 30 min sur glace, sous faible agitation. Après un rinçage à l'HBSS, les cellules ont été resuspendues dans 400 µl d'HBSS avec Mg^{2+} et Ca^{2+} (Sigma, #55037C) et analysées par cytométrie en flux.

Tri cellulaire

L'expression du MXO4 a été mesurée dans les différentes populations cellulaires (astrocytes GFP$^+$, microglie CD11b$^+$/CD45$^+$ et dans la population « Other », comprenant des astrocytes non infectés, des neurones, des cellules NG2, des cellules endothéliales et des oligodendrocytes majoritairement éliminés au cours de la déplétion de la myéline). Les cellules ont été triées grâce au trieur BD influx, équipé de lasers 408 nm, 488 nm et 561 nm et de détecteurs 450/30 (MXO4), 530/40 (GFP), 594/26 (CD11b-PE), et 670/30 (CD45-PE-Cy5) (Collab. J. Baijer, N. Dechamps, IRCM).

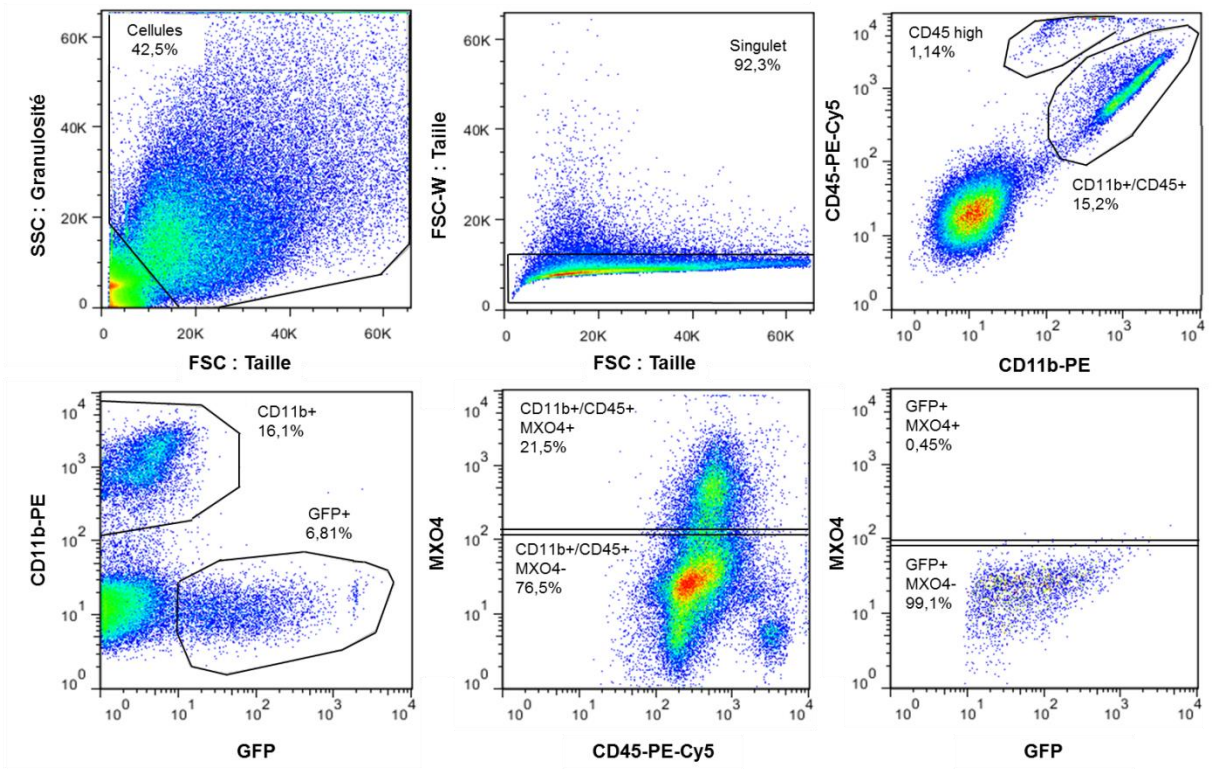

Figure 26 : Sélection des différentes populations cellulaires triées par FACS.

La population de cellules a été déterminée en fonction de leur taille et de leur granulosité. Parmi cette population cellulaire, nous nous sommes assurés de compter une seule cellule à la fois (Singulets). Au sein des singulets, l'émission de fluorescence de la GFP, CD11b-PE, CD45-PE-Cy5 est mesurée pour chaque cellule. L'expression du MXO4 a été mesurée au sein de la population CD11b$^+$ (microglie) ou GFP$^+$ (astrocytes).

Une suspension de cellules non marquées ou marquées avec un seul fluorophore ont été utilisées pour régler le gain des détecteurs et la position des fenêtres *(Figure 26).* Ces réglages ont été conservés au cours de l'expérience. Les populations cellulaires suivantes ont été collectées séparément : GFP$^+$ (astrocytes), CD11b$^+$/CD45$^+$/MXO4$^-$ (microglie n'ayant pas phagocyté de l'Aβ), CD11b$^+$/CD45$^+$/MXO4$^+$ (microglie ayant phagocyté de l'Aβ) ainsi que les quadruples négatives (« Other »). Les cellules ont ensuite été lysées dans 400µl TRIzol avant l'extraction de l'ARN.

5. Analyses transcriptomiques

Extraction d'ARN

Les cellules ont été placées 5 min à RT (Température ambiante) puis 400 µl de chloroforme ont été ajoutés au TRIzol pendant 3 min. Les échantillons ont été vortexés et centrifugés à 12000 g, 15 min à RT. La phase aqueuse a été collectée et 1 volume d'éthanol 70% a été ajouté. Les échantillons ont ensuite été transférés dans des colonnes *RNeasyMin* (Qiagen, RNeasy micro kit, #74004) et le protocole du fabricant a été suivi. Un traitement à la DNase I a été réalisé sur colonne. L'ARN a été élué dans 14 µl d'eau dé-ionisée sans RNAse, déposée au préalable au centre de la colonne pendant 5 min. Après centrifugation, les échantillons ont ensuite été stockés à -80°C avant les analyses transcriptomiques.

Analyse par qPCR

La transcription inverse a été réalisé avec le kit VILO™ selon le protocole du fabriquant (Life Technologies, SuperScript® VILO™ cDNAsynthesis kit, #11733-038). Les échantillons provenant de cellules triées ont été dilués dans une solution H2O/BSA (Bovine serum albumin) (100 µg/ml) au 1/20. Les qPCR ont été réalisées en utilisant des oligonucléotides à 10 µM et du 2X SYBR-Green® (Bio-Rad, iTaq™ Universal SYBR® Green Supermix, #1725124). L'expression des gènes d'intérêt a été normalisée par un couple de gènes de *ménages (Actine* et *Eef1a1) avec* la méthode du ΔCt. Les meilleurs gènes de ménages ont été sélectionnés suite à une analyse Genorm comme décrit dans *Vandesompele et al., 2002*. Les séquences d'oligonucléotides utilisées ont été construites comme décrit dans le Tableau 5.

Gène	Amorce Sens	Amorce Anti-sens
Aif1 (Iba1)	CCAGCCTAAGACAACCAGCGTC	GCTGTATTTGGGATCATCGAGGAA
Aldh1l1	TTCGCTGGCTGGTGTGATAAGA	GGTCAAGGTCAGGTTGCGGTT
Actine	AGAGGGAAATCGTGCGTGAC	CGATAGTGATGACCTGACCGT
ApoE	CTGAACCGCTTCTGGGATTACCTG	CATAGTGTCCTCCATCAGTGCCGTC
C1qb	CCACGCAACGGCAAGTTCAC	CGGCCACGAACGAGATTCAC
Cspg4 (Ng2)	AGGGAGCAGGCAAACGAAGA	TGAAGCTGCCACGGATAGGA
Ctss	GGCATGAACGATATGGGAG	TCAGGCAATGTCCGATTAGA
Eef1a1	CTACCCTCCACTTGGTCGCTT	GCAACTGTCTGCCTCATGTCAC
Gfp	TGCAGCTCGCCGACCACTACCA	GCAGGACCATGTGATCGCGCTTC
Gfap	ACGACTATCGCCGCCAACT	GCCGCTCTAGGGACTCGTTC
Mal2	GGCCACCTCCCTGCATGACC	AAGCCAGACCCAAACTGCAACCA
Mbp	CTTCAAAGACAGGCCCTCAG	CCTGTCACCGCTAAAGAAGC
Serpina3n	CAACCTTACAGGCCAACCCAT	GGGCACCAAGTAGTCCTAGATGCT
SOCS3	CGAGAAGATTCCGCTGGTACTGA	TGATCCAGGAACTCCCGAATG
Tmem119	GTGTCTAACAGGCCCCAGAA	AGCCACGTGGTATCAAGGAG
Trem2	AATGGGAGCACAGTCATCGCAGA	ACTGGTAGAGGCCCGCGTCAC

Tableau 5 : Séquences des oligonucléotides utilisés pour l'analyse par qPCR.

RNAseq sur astrocytes triés

Afin d'optimiser les nombres d'astrocytes triés, les souris APP/PS1dE9 et WT ont été injectées avec 2,5 µL de solution de vecteurs viraux par hémisphère ($7x10^9$ VG/site ; AAV-SOCS3 ou AAV-GFP seul). Les souris ont été sacrifiées par dislocation cervicale à 9 mois, les deux hippocampes ont été disséquées et regroupés. Les échantillons ont ensuite été dissociés et la myéline a été extraite comme décrit précédemment. Les astrocytes GFP^+ et la population « Other » (comprenant des astrocytes non infectés, des cellules microgliales, des neurones, des cellules NG2, des cellules endothéliales et des oligodendrocytes majoritairement éliminés au cours de la déplétion de la myéline) ont été triés et l'ARN extrait. Le séquençage a été réalisé par l'équipe du Dr. R. Olaso à l'Institut de génomique d'Evry. Chaque échantillon provenant d'une souris a été dissocié, trié et séquencé individuellement. L'intégrité et la concentration des échantillons ont été vérifiées au BioAnalyser (Kit RNA 6000 pico assay, Agilent technologies). Les librairies d'ADNc ont ensuite été construites avec le kit « smarter ultra low V4 » et Nextera XT (Takara-Clontech) et utilisées pour l'analyse RNAseq sur la plateforme Hiseq 2000 Illumina (séquencage en 2x100 bp).

Analyse des données de RNAseq

Le contrôle qualité et l'analyse des séquences a été réalisé par GenoSplice technology® (*www.genosplice.com*) à l'aide des logiciels FastQC, Picard-Tools, Samtools et rseqc. Les séquences (« reads ») ont été identifiées en utilisant STARv2.4.0 *(Dobin et al., 2013)* sur l'assemblage du génome murin mm10. La comparaison de l'expression génique entre les groupes a été réalisée comme décrit dans *Noli et al., 2015*. Brièvement, pour chaque gène présent dans la version « mouse FAST DB v2016-1-full » du génome murin, les séquences s'alignant sur des régions constitutives (qui ne subissent pas d'épissage alternatif par exemple) ont été comptées. La normalisation du nombre de séquences comptées par gène et l'analyse de l'expression différentielle entre groupes ont ensuite été réalisées en utilisant DESeq2 *(Love et al., 2014)* du logiciel R (v.3.2.5). Seuls les gènes exprimés dans au moins une des deux conditions expérimentales comparées ont été analysés. Les gènes ont été considérés comme exprimés si leur valeur de rpkm (« reads per kilobase million ») était supérieure à 97.5% de la valeur rpkm du bruit de fond, mesurée dans les régions inter-géniques. Les gènes ont été considérés comme différentiellement exprimés lorsque la valeur-$p \leq 0.05$ et le ratio d'expression entre les deux groupes est ≥ 1.5 (« fold-change »).

Trois analyses ont été réalisées : 1/ n=7 échantillons GFP^+ (nommés ASTRO) ont été comparés à n=3 échantillons « Other » pour valider le tri cellulaire ; 2/ n=4 ASTRO de souris APP/PS1-GFP comparés à n=7 ASTRO de souris WT-GFP pour identifier les changements transcriptionnels liés à la MA dans les astrocytes réactifs; 3/ n=5 ASTRO de souris APP/PS1-SOCS3 comparés à n=4 ASTRO de souris APP-GFP pour identifier les gènes astrocytaires normalisés par SOCS3 dans des souris modèles de la MA.

Les fonctions « dist » et « hclust » de R ont été utilisées pour réaliser les analyses non supervisées, en utilisant la distance Euclidienne et la méthode d'agglomération de Ward. L'analyse d'ontologie des gènes (« GO term analysis ») a été réalisée avec le logiciel DAVID (v6.8) *(Huang et al., 2009)*. L'analyse « WGCNA » (en anglais *« weighted correlation network analysis »*) a été réalisée en utilisant le package WGCNA du logiciel R.

6. Immunohistologie

Excepté pour les échantillons ayant été utilisés pour le RNAseq, l'ensemble des souris ont été sacrifiées par overdose de pentobarbital sodique (180 mg/kg). Les deux hémisphères des cerveaux ont été séparés permettant d'obtenir des échantillons pour deux techniques d'analyses post-mortem différentes à partir du même animal.

Préparation des coupes

Les hémi-cerveaux ont été post-fixés pendant 24h dans une solution 4% paraformaldéhyde. Les cerveaux ont ensuite été cryo-protégés par incubation dans une solution de sucrose à 30% et des coupes coronales de 30 µm ont été réalisées au microtome. Les coupes ont été conservées dans une solution de stockage (glycogène, glycérol, PB 1M, H_2Od) à -20°C avant utilisation.

Immunofluorescence

Les coupes ont été rincées dans du PBS 0.1M, 3 x 10 min. Les coupes ont ensuite été bloquées avec une solution de 4.5% NGS (Normal goat serum)/PBS 0.1M/0.2% Triton X-100 (PBST), 1h à RT. Les coupes ont été incubées sur la nuit à 4°C avec les solutions d'anticorps primaires diluées dans une solution 3% NGS/PBST *(Tableau 6)*. Les coupes ont été rincées dans du PBS 0.1M, 3x10 min et incubées avec les anticorps secondaires fluorescents appropriés (anticorps conjugués Alexa Fluor, Invitrogen) dans 3% NGS/PBST, 1h à RT. Pour le marquage STAT3α, les coupes ont été prétraitées avec une solution 100% méthanol, 10 min à -20°C, rincées et bloquées 1h dans une solution 4,5% NGS/PBS 0.1M/0.3% Triton X-100. Elles ont ensuite été incubées avec l'anticorps primaire anti-STAT3α dans la solution « Signal Stain® antibody diluent » (Cell signaling, #8112L) 72h à 4°C. Après rinçage, elles ont été incubées avec l'anticorps secondaire approprié dilué au 1/500 dans 1% BSA/PBS 0.1M/0.3% Triton X-100, 1h à RT.

Anticorps	Références	Espèces	Dilution		
			IHC	IF	WB
6E10	Covance	Souris			1/500
Aβ42	Life technologies	Lapin	1/500		
Actine	Sigma	Souris			1/5000
ApoE	Abcam	Lapin			1/1000
AT8	Thermofisher	Souris	1/400		
Bace1	Cell signaling	Lapin		1/500	1/1000
CD14	BD	Rat		1/500	
GAPDH	Cell signaling	Lapin			1/5000
GFAP	Dako	Lapin		1/1000	1/5000
GFAP-Cy3	Sigma			1/1000	
GFP biotinylé	Vector			1/500	
HT7	Innogenetics	Souris	1/1000		
IBA1	Wako	Lapin		1/500	
IDE	Abcam	Lapin			1/400
MBP	Sigma	Lapin		1/500	
NeuN	Chemicon	Souris		1/500	
P-TauS422	Abcam	Lapin	1/400		
PSD95	BD	Souris			1/500
STAT3α	Cell signaling	Lapin		1/200	
Synaptophysine	Stressgen	Souris			1/1000
Tubuline α	Sigma	Souris			1/1000
Tm4sf1	R&D system	Mouton		1/200	
Vimentine	Abcam	Poulet		1/1000	

Tableau 6 : Liste d'anticorps utilisés et dilutions selon leurs applications.

Abréviations : IHC : immunohistochimie, IF : Immunofluorescence, WB : Western Blot

Pour le marquage MXO4 sur coupe, la solution a été diluée à 33 µg/ml (Tocris, #4920) dans du PBS 0.1M et incubée 30 min à RT. Après 3 rinçages au PBS 0.1M, les coupes ont été systématiquement incubées avec un anticorps anti-GFP biotinylé dans 3% NGS/PBST, sur la nuit à 4°C, rincées et incubées avec un anticorps Streptavidine-FITC 1/1000 (ThermoFisher Scientific, #SA100-02) dans 3% NGS/PBST, 1h à RT. Pour le marquage CD14, les coupes ont été pré-traitées avec une solution de citrate de sodium 1X, 20 min à 80°C. Après rinçage, elles ont été bloquées dans une solution 3% BSA/PBST 1h à RT. Après 3 rinçages, elles ont été incubées dans une solution 3% BSA/ PBST sur la nuit à RT, puis rincées et incubées avec l'anticorps secondaire approprié, 1h à RT. Pour le marquage Tm4sf1, les coupes ont été bloquées 1h dans une solution 5% BSA/PBST puis incubées 72h à 4°C avec l'anticorps primaire anti-Tm4sf1 dilué dans une solution 3% BSA/PBST. Après rinçage, elles ont été incubées avec l'anticorps secondaire approprié biotynilé (1/500 ; Vector, #BA-6000) dilué dans 3%

BSA/PBST, 1h à RT. Les coupes ont été rincées puis incubées avec une solution streptavidine-Cy3 (1/500 ; Sigma, #S6402) dilué dans 3% BSA/PBST, 1h à RT.
Pour finir, les coupes n'ayant pas été marquées au MXO4 ont été rincées et marquées avec du DAPI 1/2000 (Invitrogen, #D21490) dans du PBST, 10 min à RT. Elles ont ensuite été montées sur des lames SuperFrost® Plus (ThermoFisherScientifc, #J1800AMNZ) avec du milieu de montage Fluorsave™ (Calbiochem, #345789) ou Fluormount™ (Sigma, #F4680). Pour le marquage BAM10 1/1000 (Mouse, Sigma, #A3981), le kit « Mouse-On-Mouse » (Vector Laboratories, #BMK-2202) a été utilisé selon le protocole du fabriquant pour diminuer le marquage non spécifique.

Immunohistochimie

Les coupes ont été rincées dans du PSB 0.1M, 3x10 min. Pour le marquage HT7, les coupes ont d'abord été démasquées avec une solution citrate de sodium 1X, 20 min à 90°C. Les coupes ont été laissées 20 min à RT avant les rinçages pour éviter un choc thermique. Puis elles ont été traitées avec une solution d'H_2O_2 1/100, 20 min à RT pour inhiber les péroxydases. Elles ont ensuite été bloquées pendant 1h à RT dans 4,5% NGS/PBST pour l'anticorps anti-Aβ42, anti-AT8 et anti-HT7 ou dans 3% BSA/PBST pour l'anticorps P-TauS422. Les coupes ont été incubées sur la nuit ou 48h à 4°C avec les anticorps primaires dilués dans 3% NGS/PBST *(Tableau 6).* Les coupes ont été rincées et incubées avec l'anticorps secondaires biotinylés appropriés (Vector Laboratories) dans 3% NGS/PBST, 1h à RT, rincées et incubées avec le complexe avidine/biotine, 1/250 chacun dans du PBST, 1h à RT. Pour finir, après avoir été rincées, les coupes ont été révélées en utilisant une solution de VIP (Vector Laboratories, #SK-4600), montées sur des lames SuperFrost® Plus et séchées sur la nuit à RT. Enfin, les coupes ont été déshydratées comme suivant : 2x1 min dans un bain d'acétone, 2x3 min dans un bain de xylène et montées avec du milieu de montage Eukitt (Chem-Lab, #UN1307).

Microscopie et quantification des immunomarquages

Mesure de volumes, d'intensité de marquage et comptage des plaques amyloïdes.

Les coupes marquées avec l'anticorps anti-CD14 ont été acquises avec un Axio scanZ.1 (Zeiss), avec un grossissement x40. Un seuillage a été appliqué et le pourcentage d'aire $CD14^+$ a été mesurée en utilisant le logiciel ImageJ. Les coupes marquées avec l'anticorps anti-Aβ42 ont été acquises avec l'Axio scanZ.1 (Zeiss), avec un grossissement x10. Un seuillage a été appliqué et une sélection semi-automatique des plaques de l'hippocampe a été effectuée sur le logiciel Morphostrider. Pour les marquages GFAP, BAM10, MXO4, AT8, HT7 et P-TauS422, des reconstructions en mosaïques ont été acquises avec un microscope à épifluorescence (Leica, BM6000B) au 10x. Le niveau de gris moyen du marquage GFAP a été automatiquement mesurée grâce au logiciel ImageJ dans la zone infectée (GFP^+), manuellement délimitée sur 10 coupes environ par animal (espace inter-coupes de 240 µm).

Le bruit de fond a été mesuré dans une zone hors marquage et soustrait. Le nombre de plaques BAM10$^+$ et MXO4$^+$ ainsi que l'aire AT8$^+$ et P-TauS422$^+$ ont été mesurées de façon semi-automatique à l'aide d'un seuillage dans l'hippocampe entier, manuellement délimité, avec le logiciel ImageJ. L'aire HT7$^+$ a été manuellement délimitée dans l'hippocampe.
Des images de l'hippocampe (3 images/coupes sur 3 coupes/souris) ont été acquises par microscopie confocale (Leica TCS SPE) à l'objectif 40X avec un pas de 1 µm et un zoom de 1,5. Pour le marquage STAT3α, les corps cellulaires ont été manuellement délimités et l'intensité du marquage mesuré. Le niveau de gris moyen du marquage MAP2 a été mesuré sur l'intégralité de l'image. L'épaisseur de la couche CA1 a été manuellement mesurée à partir du marquage NeuN.

Comptages cellulaires

Des images de l'hippocampe (3 images/coupes sur 3 coupes/souris) ont été acquises par microscopie confocale (Leica TCS SPE) à l'objectif 40X avec un pas de 1 µm et un zoom de 1,5. Pour les marquages Vimentine et Tm4sf1, les cellules ont été manuellement comptées en utilisant le logiciel Image J.

Mesure de l'accumulation de l'Aβ dans les cellules microgliales.

Pour la quantification de la recapture de l'Aβ par la microglie, des images confocales ont été acquises au 63x, zoom 2. L'intégralité de la plaque a été acquise avec un pas de 0,4 µm. Les cellules IBA1$^+$ ont été classées manuellement en 3 catégories : MXO4$^+$ au niveau de la membrane, MXO4$^+$ dans le soma et MXO4$^-$. La présence de MXO4 dans la cellule a été vérifiée grâce à des projections orthogonales. L'ensemble des cellules IBA1$^+$ a été, par la même occasion, compté pour mesurer leur accumulation autout des plaques amyloïdes.

7. Biochimie

Extraction des protéines

Les hémi-cerveaux ont été sectionnés en tranches de 1 mm et la zone GFP$^+$ de l'hippocampe a été disséquée à l'aide de poinçons (« punches » ; Ted Pella, Redding, CA) sous un macroscope à fluorescence (Leica Macrofluo, Leica). Les « punches » ont été immédiatement congelés dans de l'azote liquide et stockés à -80°C jusqu'à l'extraction protéique. Le tampon de lyse composé de 50 mM Tris HCl pH7.4, 150 mM NaCl, 1% Triton X-100 avec inhibiteurs de phosphatases 1/100 (Sigma, cocktail 2, #P5726) et inhibiteurs de protéases 1X (Roche, #04693124001) (25 µl/punch). Les échantillons ont ensuite été lysés mécaniquement par sonication et centrifugés à 20000 g, 20 min à 4°C. Le surnageant récolté correspond aux protéines solubles dans le Triton X-100. La concentration protéique a été mesurée grâce à un test BCA (Pierce). Les échantillons protéiques ont été stockés à -80°C jusqu'à leur utilisation pour des western blot ou tests ELISA MSD®.

Western blot

Les échantillons ont été équi-chargés dans du LB1X (Nu PAGE® LDS sample buffer, Invitrogen, #NP0007) + DTT1X (Nu PAGE® sample reducing agent, Invitrogen, #NP0009). Après dénaturation à 90°C pendant 5 min, 10 µg de protéines ont été déposées pour chaque échantillon sur un gel NuPAGE™ 4-12% Bis-Tris (Life Technologies). La migration a été réalisée à 200 V dans un tampon de migration NuPAGE™ (Invitrogen, #NP0002-02). Les protéines ont ensuite été transférées sur une membrane de nitrocellulose avec l'appareil de transfert iBlot (Invitrogen, #NR22056-01). La migration des protéines et leur transfert sur membrane ont été systématiquement vérifiés en utilisant du rouge Ponceau. Les membranes ont été rincées avec une solution de TBS 1X/0.1% Tween 20 (Tris-buffered saline ; TBS-T) 3x10 min et bloquées avec 5% lait/TBS-T ou 5% BSA/TBS-T (pour P-TauS422) pendant 1h à RT. Les membranes ont ensuite été incubées 2h à RT, sur la nuit ou 48h à 4°C avec les anticorps primaires dilués dans 5% lait/TBS-T ou 5% BSA/TBS-T *(Tableau 6).* Après rinçage, les membranes ont été incubées 1h à RT avec les anticorps secondaires conjugués-HRP dilués dans 5% lait/TBS-T ou 5% BSA/TBS-T et à nouveau rincées. Les membranes ont été révélées utilisant les substrats ECL Clarity (Bio-Rad) appliqué 2 min et le signal a été détecté avec une caméra Fusion FX7 (ThermoFisher Scientific). L'intensité des bandes a été quantifiée sur le logiciel ImageJ et normalisée par l'expression de l'actine, de la tubuline α ou de la GAPDH.

Test ELISA MSD®

Pour le test permettant de mesurer différentes formes d'Aβ (Aβ38, Aβ40 et Aβ42), les concentrations des fractions solubles dans le Triton X-100 ont été soit normalisées en utilisant les tampons d'extractions d'origine soit normalisées à postériori au cours de l'analyse. Les échantillons ont été diluées au 1/10 et 1/25 respectivement dans le diluent fourni par le kit (V-PLEX Aβ Peptide Panel 1 (6E10) kit, K15200E, MSD®).

Pour le test permettant de mesurer la concentration totale de Tau et la forme phosphorylée sur la thréonine 231 (P-TauTh231 ; kit K15121D, MSD®), les échantillons ont été dilués au 1/500 dans 20 mM Tris HCl pH7.4, 150 mM NaCl, 1 mM EDTA, 1 mM EGTA, 1% Triton X-100, inhibiteurs de phosphatases et protéases. Les concentrations ont été normalisées à postériori lors de l'analyse. Pour tous les tests MSD®, les échantillons ont été déposés en duplicatas et le protocole du fabricant a été suivi. Les concentrations protéiques ont été calculées grâce à une courbe standard, en utilisant le logiciel Discovery Workbench4.0, MSD®.

8. Statistiques

Les résultats sont exprimés en moyenne ± SEM. Les analyses statistiques ont été réalisées en utilisant le logiciel STATISTICA. Pour chaque analyse, la normalité des résidus et le test de Levene pour vérifier l'homogénéité des variances ont été effectués. Lorsque les deux conditions étaient respectées, des

tests paramétriques ont été appliqués. Le test *t* de Student (pour des échantillons indépendants) ou un *t* test apparié (pour des échantillons dépendants) a été réalisé pour comparer deux groupes. Une ANOVA à un facteur suivi d'un test post hoc de Tukey ont été appliqués pour comparer 3. Si l'une ou les deux conditions (homogénéité des variances ou normalité des résidus) n'étaient pas respectées, un test de Kruskal-Wallis a été réalisé pour comparer de multiples échantillons indépendants (groupe) et/ou un test de Mann-Whitney a été effectué pour comparer deux à deux des échantillons indépendants (groupe). Le test du Chi-2 d'indépendance a été appliqué pour comparer, entre deux groupes, les distributions des plaques amyloïdes en fonction de leur aire. La différence a été considérée comme significative pour $p\text{-}value \leq 0.05$.

La puissance statistique a été évaluée posteriori pour chaque analyse, en utilisant le logiciel STATISTICA. Tous les résultats présentés dans les deux articles scientifiques inclus dans la partie « Résultats » ont une puissance statistique supérieure à 80%. Par contre, les données de comportements présentées dans la partie « Données complémentaires » ont une faible puissance statistique (~20% pour les souris APP/PS1dE9 et les souris 3xTg-JAK2 et ~60% pour les souris 3xTg-SOCS3), rendant leur interprétation délicate.

Résultats

Résultats

1. La voie JAK2-STAT3 est une voie de régulation majeure de la réactivité astrocytaire dans les maladies neurodégénératives

Contexte, objectifs et synthèse de l'article 1

Les astrocytes deviennent réactifs en réponse à toute altération de l'homéostasie cellulaire, comme dans les maladies neurodégénératives. Cependant, les signaux responsables de la mise en place de la réactivité ne sont pas strictement établis. De multiples cascades de signalisation ont été associées à cette réactivité comme les voies des MAPK, NF-κB, NFAT/Calcineurine ou la voie JAK-STAT3, présentées en introduction. Mais souvent, ces études se basent uniquement sur des aspects morphologiques et quelques marqueurs comme la GFAP. Or la réactivité astrocytaire implique des changements transcriptionnels importants *(Cf §2.1)* qu'il est important d'évaluer. De plus, les astrocytes forment une population hétérogène, y compris en conditions pathologiques comme mis en évidence récemment par l'identification de classes moléculaires disctinctes d'astrocytes réactifs *(Astrocytes A1 (délétères) et A2 (protecteurs) ; Liddelow et al., 2017)*. Néanmoins, les voies de signalisations impliquées dans l'induction et le maintien de ces classes ne sont pas connues. Identifier ces voies est crucial afin de, par la suite, pouvoir favoriser les fonctions bénéfiques de ces cellules dans un contexte pathologique donné.

Notre équipe a développé des vecteurs viraux afin de moduler spécifiquement la voie JAK2-STAT3 dans les astrocytes *in vivo (Figure 23).* La surexpression de SOCS3, inhibiteur endogène de la voie JAK-STAT3, diminue des marqueurs de la réactivité tels que l'expression de la GFAP et de la Vimentine dans un modèle murin de la maladie de Huntington et dans le modèle 3xTg-AD ***(Publication 3 en annexe)***. Nous avons également développé des vecteurs viraux qui surexpriment une forme constitutivement active de JAK2 (JAK2ca), afin d'amplifier la réactivité astrocytaire. Ici, nous complétons notre compréhension du rôle de la voie JAK-STAT3 dans la réactivité astrocytaire en mettant en évidence son activation dans d'autres modèles de la maladie de Parkinson et de tauopathie. Nous montrons également que le blocage de la voie JAK-STAT3 dans des modèles de la MA restaure non seulement les changements morphologiques liées à la réactivité mais également leur profil transcriptionnel. A l'inverse, la surexpression de JAK2ca dans des souris WT induit une réactivité astrocytaire dans l'hippocampe et dans le striatum, en absence de tout contexte pathologique. Elle suffit également à induire des altérations neuronales semblables à celles observées dans la MA, comme une altération de la LTP. Il est également intéressant de noter que SOCS3 diminue l'expression de marqueurs d'astrocytes A1 et A2 alors que l'expression de JAK2ca les augmentent. L'ensemble de ces données met donc en évidence que la voie JAK2-STAT3 est nécessaire et suffisante pour induire et contrôler à long terme la réactivité astrocytaire, au-delà des classes d'astrocytes A1 et A2.

Article 1

The JAK2-STAT3 pathway is a master regulator of astrocyte reactivity in neurodegenerative diseases

Ben Haim L.[1*#], Ceyzériat K.[1#], Carrillo-de Sauvage M.A.[1§], Denizot A.[4§], Abjean L.[1], Gipstein P.[1], Derbois C.[2], Palomares M.A.[2], Pommier D.[4,5], Matos M.[4], Guillemaud O.[1], Petit F.[1], Jan C.[1], Veran J.[4,5], Guillermier M.[1], Auregan G.[1], Dufour N.[1], Joséphine C.[1], Hérard A.S.[1], Juricek L.[1], Aron-Badin R.[1], Cambon K.[1], d'Orange M.[1], Gaillard M.C.[1], Bémelmans A.[1], Dhenain M.[1], Robil N.[3], Oliet S.H.R.[4], De la Grange P.[3], Deleuze J.F.[2], Hantraye P.[1], Brouillet E.[1], Panatier A.[4,5], Olaso R.[2], Escartin C.[1]

[1] Commissariat à l'Energie Atomique et aux Energies Alternatives, Département de la Recherche Fondamentale, Institut de Biologie François Jacob, MIRCen, F-92260 Fontenay-aux-Roses, France
and
Centre National de la Recherche Scientifique, Université Paris-Sud, UMR 9199, Neurodegenerative Diseases Laboratory, F-92260 Fontenay-aux-Roses, France

[2] Commissariat à l'Energie Atomique et aux Energies Alternatives, Département de la Recherche Fondamentale, Institut de Biologie François Jacob, Centre National de Recherche en Génomique Humaine, 91000 Evry, France

[3] GenoSplice Technology, 75013 Paris, France

[4] Neurocentre Magendie, INSERM U1215, 33077 Bordeaux, France

[5] Université de Bordeaux, 33077 Bordeaux, France

# or § equal contribution

Key words: Reactive astrocytes – Signaling cascades – Viral vectors – Neuroinflammation – Cell-specific transcriptomics – Mouse models

Corresponding author:
Carole Escartin Ph.D.
18, route du Panorama
92260 Fontenay-aux-roses
carole.escartin@cea.fr

Number of pages: 43
Number of figures: 10
Number of words in Abstract: 198
Introduction: 706
Discussion: 2060

Conflict of interest
The authors declare no competing financial interests.

ABBREVIATION LIST

AAV	Adeno-associated vectors
ACSF	Artificial cerebrospinal fluid
AD	Alzheimer's disease
ALS	Amyotrophic lateral sclerosis
BSA	Bovine serum albumin
CN	Calcineurin
CNS	Central nervous system
CNTF	Ciliary neurotrophic factor
FACS	Fluorescence-activated cell sorting
FC	Fold-change
fEPSP	Field excitatory post-synaptic potentials
GFAP	Glial fibrillary acidic protein
GO	Gene ontology
HBSS	Hank's balanced salt solution
HD	Huntington's disease
HFS	High-frequency stimulation
JAK2	Janus kinase 2
JAK2ca	Constitutively active JAK2
LPS	Lipopolysaccharide
LTP	Long term potentiation
LV	Lentiviral vectors
MAPK	Mitogen-activated protein kinase
Mpi	Months post infection
ND	Neurodegenerative diseases
NFAT	Nuclear factor of activated T-cells
NF-κB	Nuclear Factor of κ light polypeptide gene enhancer in B-cells
NGS	Normal goat serum
NI	Non injected
OPC	Oligodendrocyte precursor cells
PBS	Phosphate buffer saline
PBST	0.2% Triton X-100 in PBS
PD	Parkinson's disease
P-ERK	Phosphorylated form of ERK
PFA	Paraformaldehyde
RNAseq	RNA sequencing
RT	Room temperature
SRE	STAT3 responsive element
STAT3	Signal transducer and activator of transcription 3
SOCS3	Suppressor of cytokine signaling 3
VG	Viral genome
VSV	Vesicular stomatitis virus
WGCNA	Weighted gene correlation network analysis
WT	Wild type

ABSTRACT

Astrocyte reactivity is a well-described hallmark of neurodegenerative diseases (ND). However, its functional consequences are debated, especially after the recent report of distinct molecular classes of reactive astrocytes with specific functional properties. Importantly, the signaling cascades controlling the emergence and maintenance of sub-populations of reactive astrocytes are totally unknown.

We used selective viral vector gene transfer to manipulate astrocyte signaling cascades, cell-specific transcriptomics, electrophysiology, histology and animal models of neurodegenerative diseases to explore the role of the JAK2-STAT3 pathway in the control of astrocyte reactivity *in vivo*. STAT3 was activated in reactive astrocytes of mouse, rat and primate models of ND. Viral gene transfer of SOCS3, the pathway inhibitor, blocked and even reversed morphological and molecular features of astrocyte reactivity, including molecular markers of the different reactive astrocyte classes. Conversely, expression of a constitutively active mutant of JAK2 in astrocytes of wildtype mice, activated STAT3, induced the morphological and molecular hallmarks of reactivity and triggered significant synaptic plasticity deficits.

The JAK2-STAT3 pathway is a master regulator of astrocyte reactivity, prevailing over specific classes. It is necessary and sufficient to switch astrocyte reactivity on. It is a potent molecular target to establish the role of reactive astrocytes in ND.

INTRODUCTION

Astrocytes become reactive in virtually all pathological conditions affecting the central nervous system (CNS). This widespread response has been known for over a century and is defined by two classic hallmarks: cellular hypertrophy and overexpression of intermediate filament proteins such as Glial Fibrillary Acidic Protein (GFAP) and vimentin (Hol and Pekny, 2015). Despite these well-identified morphological changes, the functional consequences of astrocyte reactivity are still currently debated (Burda and Sofroniew, 2014, Ben Haim et al., 2015a, Liddelow and Barres, 2017). In particular, it is still unclear how the reactive state of astrocytes impacts their role at the synapse, where they influence synaptic transmission and plasticity (Araque et al., 2014). Alterations in astrocyte recycling of neurotransmitters or release of gliotransmitters could underlie the synaptic deficits consistently observed in ND patients and animal models (Oddo et al., 2003, Wojtowicz et al., 2013, Viana da Silva et al., 2016, and see Ben Haim et al., 2015a for review).

The signaling cascades inducing or controlling astrocyte reactivity in progressive ND are still not firmly established. Several cascades have been associated with reactivity including the Nuclear Factor of κ light polypeptide gene enhancer in B-cells (NF-κB) pathway, the Mitogen-Activated Protein Kinase (MAPK) pathways, the calcineurin/Nuclear Factor of Activated T-cells (CN/NFAT) pathway or the Janus Kinase (JAK) - Signal Transducer and Activator of Transcription 3 (STAT3) pathway (Kang and Hebert, 2011, Ben Haim et al., 2015a). Activation of other pathways like Sonic Hedgehog, N-cadherin and Notch pathways was described in acute models of brain diseases (Sirko et al., 2013, LeComte et al., 2015, Hara et al., 2017) such as spinal cord injury or trauma. However, their involvement in chronic ND, in which there is no overt opening of the blood brain barrier or immune cell recruitment is not clear. Importantly, the direct control of these pathways on astrocyte reactivity in ND, is usually not demonstrated and the characterization of reactive astrocyte phenotype is often limited (Ben Haim et al., 2015a).

Thus, identifying the signaling cascades regulating astrocyte reactivity is a crucial step towards manipulating these cells to promote beneficial outcomes in ND. Especially since recent studies have underlined the heterogeneity of astrocytes in physiological and pathological conditions (Matyash and Kettenmann, 2010, Zhang and Barres, 2010, Anderson et al., 2014). Reactive astrocytes may form different molecular and functional sub-populations, with A1 neurotoxic and A2 neuroprotective reactive astrocytes as extreme classes (Liddelow et al., 2017).

With advances in cell-type specific molecular techniques like viral gene transfer and transcriptomics, it becomes possible to re-explore the signaling cascades involved in the regulation of reactivity *in situ*. In a previous publication, we showed that STAT3, the downstream effector of the JAK2-STAT3 pathway, accumulates in the nucleus of reactive astrocytes in different brain regions of several murine and primate models of Alzheimer's disease (AD) and Huntington's disease (HD) (Ben Haim et al., 2015b). The JAK2-STAT3 is activated by multiple cytokines and growth factors. Activation of the kinase JAK2 leads to STAT3 phosphorylation and nuclear accumulation. In astrocytes, STAT3 induces the expression of multiple target genes including GFAP and suppressor of cytokine signaling 3 (SOCS3), the endogenous inhibitor of the pathway (Mertens and Darnell, 2007, Ceyzeriat et al., 2016).

Here, we extend our previous findings by reporting STAT3 activation in reactive astrocytes in additional animal models of Parkinson's disease (PD) and tauopathy. Viral gene transfer of SOCS3

blocked and even reversed astrocyte reactivity in the APP/PS1dE9 mouse model of AD. RNAseq analysis showed that SOCS3 normalized the transcriptional profile of reactive astrocytes, reduced neuroinflammatory genes and restored the levels of A1 and A2- reactive markers. Mirror experiments were performed by expressing a constitutively active mutant of JAK2 (JAK2ca) in astrocytes of WT mice to activate the JAK2-STAT3 pathway in the absence of any pathological environment. JAK2ca expression in striatal and hippocampal astrocytes activated STAT3. JAK2ca-expressing astrocytes displayed morphological changes and overexpressed GFAP along with many transcripts characteristics of reactive astrocytes. Importantly, JAK2ca-mediated activation of astrocytes altered synaptic plasticity in the hippocampus.

Overall, our results show that the JAK2-STAT3 pathway is necessary and sufficient for astrocyte reactivity in progressive ND models. This core cascade regulates the induction and maintenance of different classes of reactive astrocytes, controlling key morphological and molecular features, as well as important functional outcomes for neighboring neurons.

MATERIEL and METHODS

Animals.

Animal cohorts included in this study are listed in **Table 1**. APP/PS1dE9 transgenic mice (APP; http://jaxmice.jax.org/strain/005864.html) harbor a chimeric mouse/human *App* gene with the Swedish mutations K594N and M595L (APPswe) and the human *Psen1* variant lacking exon 9 on a C57BL/6J background (Jankowsky et al., 2004). Non-transgenic littermates were used as controls. Breeding pairs were obtained from the Mutant Mouse Regional Resource Centers. Mouse Thy-Tau-22 on the C57bl6 background were used as a model of tauopathy (Schindowski et al., 2006). C57bl6 mice were used as controls.

Parkinsonism was induced in *Macaca fascicularis* by 7-day cycles of intramuscular injections of 0.2 mg/kg of 1-methyl-4-phenyl-1,2,3,6-tetrahydropyridine (MPTP) (Sigma, Saint-Louis, MO) until a significant reduction (≥80%) in spontaneous locomotor activity was measured in reference to baseline activity, as previously described (Aron Badin et al., 2013).

All experimental protocols were reviewed and approved by the local ethics committee (CETEA N°44) and submitted to the French Ministry of Education and Research (Approvals # APAFIS#4565-20 16031711426915 v3, APAFIS#4503-2016031409023019 and 12_074). They were performed in a facility authorized by local authorities (authorization #B92-032-02), in strict accordance with recommendations of the European Union (2010-63/EEC) and Standards for Humane Care and Use of Laboratory Animals of the Office of Laboratory Animal Welfare (OLAW – n°#A5826-01). All efforts were made to minimize animal suffering and animal care was supervised by veterinarians and animal technicians skilled in the healthcare and housing of non-human primates and rodents. Animals were housed under standard environmental conditions (12-hour light-dark cycle, temperature: 22 ± 1°C and humidity: 50%) with ad libitum access to food and water.

Viral vectors.

We alternatively used lentiviral vectors (LV) or adeno-associated virus (AAV, serotype 9) to drive specific expression in astrocytes (**Supplemental Fig. 1)**. LVs are pseudotyped with the Mokola envelope and contain four repeats of the Mir124 target to repress transgene expression in neurons (Colin et al., 2009). AAV2/9 vectors bear a synthetic promoter derived from the GFAP promoter (Lee et al., 2008).

To modulate the JAK2-STAT3 pathway in mouse astrocytes, viral vectors encoding murine SOCS3 or murine $JAK2^{T875N}$ (JAK2ca, Haan et al., 2009) were used. Supplemental experiments were also performed with LV encoding for other mutants of the cascade [$JAK2^{Y317F,\ Y570F}$ (Robertson et al., 2009), wildtype JAK2 and a mutant of STAT3 (STAT3-C, Bromberg et al., 1999)]. Control viral vectors encoded GFP or LacZ. Viral vectors encoding SOCS3 or JAK2ca were co-injected with a viral vector encoding GFP to visualize infected cells (same total viral titer, see **Table 1**).

We generated a reporter construct for STAT transcriptional activity, by placing GFP cDNA under the control of a minimal thymidine kinase promoter and 6 repeats of a consensus STAT responsive element (SRE, Ehret et al., 2001) in a LV backbone. A LV encoding the cytokine ciliary neurotrophic factor (CNTF) was used as a positive control for astrocyte reactivity, it was injected in the mouse striatum. This vector (LV-CNTF) is described in details in (Escartin et al., 2006). An AAV2/8 vector encoding human Tau with the P301L mutation under the CBA promoter was used to model Tauopathy in the rat hippocampus. An untranslated mutant of GFP was used as control. This viral-based rat model of Tauopathy is described in details in (d'Orange et al., in revision), including surgical procedures.

Stereotactic injections.

Mice were anesthetized with an *i.p.* injection of ketamine (100 mg/kg) and xylazine (10 mg/kg). For APP mice, xylazine was replaced by medetomidine (0.25 mg/kg) and anesthesia was reversed by an i.p. injection of atipamezole (0.25 mg/kg) at the end of the surgical procedure. Lidocaine (7 mg/kg) was injected subcutaneously at the incision site, 10 min before injection. The full description of the injections (including viral vector type, titer and stereotactic coordinates) is shown in **Table 1**.

AAV were diluted in 0.1M phosphate buffer saline (PBS) with 0.001% pluronic acid, at a final total concentration of 2.5 10^9 viral genome (VG)/µl. LV were diluted in PBS with 1% bovine serum albumin (BSA), at a total final concentration of 100 ng p24/µl. Between 2 to 3.5 µl of viral suspensions were injected at a rate of 0.2 µl/min.

In addition, 2 months old C57BL/6 mice received unilateral intrastriatal injections of lipopolysaccharide (LPS) [1 µl at 5 mg/ml in PBS (*E. Coli*, serotype 055:B5; Sigma)]. These mice were used as positive controls and were processed for histology after 7 days.

Immunohistology.

Some mice were killed by an overdose of sodium pentobarbital (180 mg/kg) and perfused with 4 % paraformaldehyde (PFA). Alternatively, mice were killed by cervical dislocation and one brain hemisphere was rapidly dissected and drop-fixed in 4% PFA. Brains were post-fixed for 24h in 4% PFA, cryoprotected in 30% sucrose solution and cut on a freezing microtome into 30 µm-thick coronal sections. Slices were rinsed in PBS for 3x10 min and were blocked in 4.5% normal goat serum (NGS), 0.2% Triton X-100 in PBS (PBST) for 1h at room temperature (RT). Slices were incubated overnight at 4°C with the following primary antibodies diluted in 3% NGS/PBST: anti-GFAP-Cy3 (1:1,000; Sigma,

#C9205), anti-GFAP (1:1,000, Rabbit; Dako, Troy, MI, #Z0334), anti-IBA1 (1:500, Rabbit; Wako, Richmond, VA, #019-19741), anti-MBP (1:500, Rabbit; Sigma, #M3821), anti-S100β (1:500, Mouse; Sigma #S2532) or anti-Vimentin (1:1,000, Chicken; Abcam, Cambridge, UK, #ab24525).

Slices were rinsed 3x10 min in PBS and incubated with secondary Alexa Fluor-conjugated antibodies (Invitrogen, Carlsbad, CA) in 3% NGS/PBST for 1h at RT. After 3 washes in PBS, slices were incubated overnight at 4°C with an anti-GFP biotinylated antibody (1:500; Vector Laboratories, Burlingame, CA, #BA-0702) in 3% NGS/PBST. After 3 rinses with PBS, sections were incubated for 1h at RT with Streptavidine-FITC (1:1,000; ThermoFisher Scientific, Waltham, MA, #SA100-02) in 3% NGS/PBST. Slices were rinsed 3 times with PBS before being mounted on SuperFrost® Plus (ThermoFisher Scientifc) slides and coverslipped with Fluorsave™ (Calbiochem, Darmstadt, Germany) or Fluormount™ (Sigma) medium.

For STAT3α, STAT1 and P-ERK stainings, slices were pretreated with 100% methanol for 10 min at -20°C and incubated with primary antibodies (STAT3α, 1:200, Rabbit #8768P; STAT1, 1:400, Rabbit #14994; P-ERK 1:250, Rabbit #9101, Cell signaling, Danvers, MA) in SignalStain® antibody diluent (Cell signaling, #8112L) for 72h at 4°C. For CD14 staining, slices were pretreated in citrate buffer at 80°C for 20 min and NGS was replaced by BSA in blocking solution and antibody diluent. Primary antibody (1:500, Rat; BD bioscience, San Jose, CA, #553738) was incubated O/N at RT. For Tm4sf1 staining, slices were blocked in 5% BSA/PBST for 1h at RT and incubated with the primary antibody (1:200, sheep; R&D system, Minneapolis, MN, #AF7514) in 3% BSA/PBST for 72h at 4°C. Slices were rinsed and incubated with anti-sheep biotinylated secondary antibody (1:500; Vector Laboratories) for 1h30 in 3% BSA/PBST. Slices were rinsed in PBS and incubated with a streptavidine-Cy3 antibody (1:500; Sigma) in 3% BSA/PBST for 1h at RT. For NeuN (1:500, Mouse; Chemicon, Billerica, MA, #MAB377) staining, the mouse on mouse kit (MOM, Vector Laboratories) was used, according to the manufacturer's instructions to reduce non-specific background. Double or triple immunofluorescent stainings were performed successively, with each antibody incubated alone.

Microscopy and immunostaining quantification.

Images were acquired on a Leica (Nussloch, Germany, BM6000B) TCS SP8 confocal microscope. Stacked confocal images (10 to 18 z-steps of 1 µm, kept constant within a cohort, maximum intensity stack) were acquired on 3 slices per animal and 3 fields on each slice with a 40x objective. For STAT3α quantification, cell bodies were manually segmented and the mean grey value was measured for each cell. $Tm4sf1^+$ cells were manually counted. GFAP immunoreactivity was quantified on 10x-tiled images acquired with an epifluorescence microscope (Leica). Virally transduced GFP^+ area was manually segmented and the corresponding GFAP mean signal was measured with Image J. Background signal was measured on unstained areas and subtracted to the GFAP total signal. Serial sections stained for CD14 were scanned with an Axio scanZ.1 (Zeiss, Oberkochen, Germany) and immunopositive pixels were automatically detected with an intensity threshold applied with ImageJ on the GFP^+ area.

A Sholl analysis was performed on $GFAP^+$ hippocampal astrocytes to quantify morphological parameters, with an Image J plugin described in (Ferreira et al., 2014). GFAP immunofluorescent staining was detected using Image J threshold function on maximum projection confocal z-stack images (40x, average 12 steps, 1 mm step, zoom 1). A Sholl analysis was run with defined radius parameters (starting: 5 µm; ending: 100 µm; step radius: 5 µm). This analysis was only possible on hippocampal astrocytes that express detectable GFAP levels in control conditions. This was not

possible for the study of JAK2ca effects on striatal astrocytes because they express very little GFAP in control conditions. Only the area of GFP^+ astrocyte cell bodies was manually segmented and measured with ImageJ. Similarly, de-activated astrocytes in APP-SOCS3 mice could not be analyzed due to their very low GFAP immunoreactivity.

Cell sorting of GFP+ astrocytes.

Mice were killed and their striatum or hippocampus rapidly collected in Hank's Balanced Salt Solution (HBSS; Sigma). Cells were mechanically and enzymatically dissociated with fire-polished Pasteur pipettes and the neural tissue dissociation kit with papaïn (Miltenyi Biotec, Bergisch Gladbach, Germany), following manufacturer's instructions. After filtration through a 50 µm-filter, cells were centrifuged 10 min at 300 g, and diluted in 500 µl of HBSS before sorting. A myelin-removal step was included for hippocampal samples. Myelin removal beads II and MS columns (Miltenyi Biotec) were used to deplete myelin from cell suspensions, as described by the manufacturer's protocol.

Cell sorting was performed on a BD Influx cell sorter, equipped with a 488 nm laser and a 530/40 detector. Non-fluorescent brain cells were used to set up the detector gain and position the gates, which were kept constant throughout the sorting procedure. Cells were gated on a forward scatter/side scatter plot, then singlets were selected and finally cells were collected based on their GFP expression. GFP^+ cells correspond to infected astrocytes, they are called "*ASTRO"* and GFP^- cells correspond to all other cells: uninfected astrocytes, neurons, microglial cells and oligodendrocyte precursor cells, oligodendrocytes being mostly eliminated with myelin removal; these cells are called "*OTHER*". Cells were centrifuged at 300 g for 5 min at RT, lyzed in 400 µl TRIzol (Invitrogen) and stored at -80°C before RNA extraction. For microarray analysis of striatal astrocytes, the two striata of 4 mice were pooled before processing and sorting. For RNAseq analysis of hippocampal astrocytes, each mouse was processed and sorted independently. Typically, 6,500 to 20,000 GFP^+ astrocytes and 100,000 GFP^- were collected for each sample within 15-25 min.

RNA extraction.

Sorted cells were placed 5 min at RT and chloroform was added to TRIzol for 3 min. Samples were centrifuged at 12,000 g for 15 min at RT. Aqueous phase was collected and 1 volume of 70% ethanol was added. Samples were transferred onto an RNeasyMin Elute spin column and RNA was purified according to manufacturer's instructions, with on-column DNAse treatment (RNeasy micro kit, Qiagen, Hilden, Germany). RNA was eluted with 14 µl of RNAse-free deionized water and stored at -80°C before transcriptomic analysis.

Microarray analysis.

A total of 10 sorted cell samples were processed for microarray analysis (4 ASTRO of the control WT-GFP group, 4 ASTRO of the WT-JAK2ca group and 2 OTHER from the WT-GFP group to assess sorting efficiency). RNA quality and integrity was evaluated with an Agilent RNA 6000 Pico assay and the Agilent 2100 Bioanalyzer (Agilent technologies, Santa Clara, CA). RNA was amplified with the Ovation PicoSL VTA system V2 kit (NuGen technologies, San Carlos, CA). Single strand DNA and SPIA cDNA were purified with Agencourt RNAClean XP (NuGen technologies). cDNA concentration was measured with a Nanodrop-1000 spectrophotometer (Labtech France). The Encore biotiNL kit (NuGen technologies) was used for the fragmentation and labeling of the purified SPIA cDNA prior to hybridization on the

Illumina BeadChip mouse WG-6v2, which contains more than 45,000 unique 50-mer oligonucleotides (Illumina, San Diego, CA). BeadChips were scanned on the Illumina Iscan. A control summary report was generated by the GenomeStudio software (Illumina) to evaluate the performance of built-in controls (variation in hybridization and background signals and background/noise ratio). When the signal for a probe had a *p* value below 0.01, this probe was considered undetectable. Two sets of analysis were performed: (1) 4 ASTRO samples were compared to 2 OTHER samples from the GFP group, to validate sorting efficiency; (2) 4 ASTRO-GFP samples were compared to 4 ASTRO-JAK2ca samples to identify transcriptional changes in reactive astrocytes.

GenomeStudio software was used to apply quantile normalization without background subtraction to all samples within an analysis. The normalized hybridization value for each probe and sample was then analyzed with Microscoft Excel. Only probes that were detected in all samples of at least one group were considered (see details below). To obtain the most comprehensive list of differentially expressed genes, we compared the average signal between the two groups with a *t* test. First, we generated a list of 708 differentially expressed probes between ASTRO and OTHER cells from the GFP group, which was used to control the cell-type identity of sorted populations. Then we identified a list of 409 differentially expressed probes between ASTRO cells from the GFP and JAK2ca groups. In addition, we manually included probes for which no statistical test could be applied because probe signal was undetectable in 3 or 4 samples of a given group. To exclude false positives from the list of probes down-regulated to undetectable levels in the ASTRO-JAK2ca group, we only selected probes i/ that were expressed at a sufficient level above background (fluorescent signal threshold set at >170) and with a CV <50% in the ASTRO-GFP group and, when applicable, ii/ for which the only sample of the ASTRO-JAK2ca group expressed it at low level (<170) and at less than 80% of the ASTRO-GFP group (N=158 probes). Eleven probes undetectable in the ASTRO-GFP group, were also included, based on similar criteria. These probe lists were combined (N=578 differentially expressed probes, corresponding to 539 unique genes) and used for pathway analysis.

RNAseq analysis.

RNA quality and integrity were evaluated with an Agilent RNA 6000 Pico assay and the Agilent 2100 Bioanalyzer (Agilent technologies, Santa Clara, CA). As the number of sorted cells was limited, especially in the ASTRO fraction, we quantified total RNA with Agilent RNA 6000 Pico assay and used 0.8 to 1 ng of total RNA per sample. Full length double strand cDNA librairies were constructed with the Smarter Ultra Low Input RNA kit v4 (Takara-Clontech, Mountain View, CA) using 11 to 14 LD-PCR cycles. Purification was done with Ampure XP (Beckman Coulter Genomics, Brea, CA). The full length ds cDNA libraries were qualified with an Agilent High Sensitivity DNA kit and quantified with the Qubit dsDNA HS Assay Kit (Invitrogen). All libraries were normalized to 750 pg in 5µl as starting materiel to Nextera XT sample preparation kit (Illumina Incorporated, San Diego, CA). Ligation products were amplified with 12 PCR cycles. A stringent purification was done (0.6X of AMPure XP) to remove small inserts that would be sequenced preferentially. mRNAseq libraries were qualified and quantified with Agilent High Sensitivity DNA kit and Qubit dsDNA HS Assay Kit respectively, before sequencing on a HiSeq 2000 Illumina platform (2x100bp). Quality controls and data analysis was performed by GenoSplice technology® (www.genosplice.com). Sequencing data quality, read repartition and insert size estimation were performed with FastQC, Picard-Tools, Samtools and rseqc. Reads were mapped on the mm10 Mouse genome assembly with STARv2.4.0 (Dobin et al., 2013). Gene expression analysis

was performed as described in (Noli et al., 2015). Briefly, for each gene present in the Mouse FAST DB v2016_1_full annotations, reads aligning on constitutive regions (i.e. that are not prone to alternative splicing) were counted. Normalization of read counts and differential gene expression were performed using DESeq2 (Love et al., 2014) on R (v.3.2.5). Only genes expressed in at least one of the two compared experimental conditions were analyzed. Genes were considered as expressed if their rpkm value was greater than 97.5% of the background rpkm value measured in intergenic regions. Results were considered statistically significant for *p* values ≤ 0.05 and fold-changes ≥ 1.5.
Three sets of analysis were performed: (1) 7 ASTRO samples were compared to 3 OTHER samples from the WT-GFP group, to validate sorting efficiency; (2) 4 ASTRO-APP-GFP samples were compared to 7 ASTRO-WT-GFP samples to identify transcriptional changes in reactive astrocytes due to AD; and (3) 5 ASTRO-APP-SOCS3 samples were compared to 4 ASTRO-APP-GFP samples to identify astrocyte genes that are normalized by SOCS3 in AD mice. Hierarchical clustering between ASTRO and OTHER samples was generated using MeV software, using Euclidean distance and average agglomeration method.

Gene Ontology analysis.

Analysis for enriched Gene ontology (GO) terms were performed with Database for Annotation, Visualization and Integrated Discovery (DAVID) Functional annotation Tool (v6.8) (Huang da et al., 2009). GO terms and pathways were considered as enriched for fold enrichment ≥ 2.0, uncorrected *p* value ≤ 0.05 and minimum number of regulated genes in pathway/term ≥ 2.0.

Weighted correlation network analysis (WGCNA).

WGCNA was performed using WGCNA R package (Langfelder and Horvath, 2008). For RNASeq, genes expressed in at least 20% of samples (14 029) were used. Modules with at least 30 genes and a kME>0.7 were defined, with split = 2. For microarray analysis, 75% of most variant probesets (33 960) were used, with the same parameters for module definition. ANOVA was performed on the Eigengene calculated in each sample, as defined in (Langfelder and Horvath, 2008). Modules with a $p < 0.05$ were further analyzed.

RT-qPCR on brain homogenates.

Mice were euthanized with an overdose of sodium pentobarbital. Brains were rapidly collected and sliced into 1 mm-thick coronal sections using a brain matrix. The GFP^+ area was dissected on each slice using 1 mm- diameter punches under a fluorescence macroscope (Leica). Punches were stored in RNA later (Sigma) at -80°C until further processing. Total RNA was isolated from punches with TRIzol (Life sciences) according to the manufacturer's instructions. RNA concentration was determined with a Nanodrop-1000 spectrophotometer (ThermoFisher Scientific). Reverse transcription was performed with the VILO™ kit according to the manufacturer's protocol (SuperScript® VILO™ cDNA synthesis kit; Life Technologies, Carlsbag, CA). Samples were diluted in H_2O with 100 µg/ml BSA at 0.2 ng/µl and mixed with 250 nM of primers and Platinum SYBR-Green® (Platinum® SYBR® Green qPCR SuperMix-UDG; Life Technologies) for qPCR. PCR efficiency was between 85 and 110% for each set of primers (sequences shown in **Supplementary table 1**). Nuclease-free water and samples without reverse transcription were used as negative controls. Expression levels of genes of interest were normalized to the abundance of actin with the ΔCt method.

Electrophysiological recordings.

Transverse hippocampal slices were prepared as described previously (Panatier et al., 2011), from adult (3-5 months) non-injected male mice (NI), WT-GFP and WT-JAK2ca mice. Briefly, mice were anesthetized with 5% isoflurane and decapitated. The brain was rapidly removed and placed in ice-cold artificial cerebrospinal fluid (ACSF) saturated with 95% O_2 and 5% CO_2, containing (in mM): 125 NaCl, 2.5 KCl, 1.25 NaH_2PO_4, 1.3 $MgCl_2$, 2 $CaCl_2$, 26 $NaHCO_3$ and 10 glucose (pH = 7.3; 300-305 mOsmol/kg). A block of tissue containing the hippocampus was prepared and 350 µm transversal hippocampal slices were cut on a vibratome (Leica). Slices were incubated 30 min at 32°C and allowed to recover for at least 1h at RT.

Slices were transferred to a recording immersion chamber and were perfused with ACSF (3 ml/min) at RT during the whole experiment. An incision between CA3 and CA1 regions was made to avoid epileptiform activity caused by the addition of 50 µM picrotoxin in the perfusion bath before recording. CA3 and CA1 areas were identified with differential interference contrast microscopy and the region of interest (GFP^+) was visualized with the epifluorescent mode of the microscope (Olympus BX50, Tokyo, Japan). Field excitatory postsynaptic potentials (fEPSPs) were evoked by orthodromic stimulations (100 µs, 0.033 Hz) of Schaffer collaterals using a glass pipette filled with ACSF and placed in the *stratum radiatum,* more than 200 µm away from the recording electrode. Then, fEPSPs were recorded with a glass pipette filled with ACSF (2-3 MΩ) and placed in the GFP^+ region, in the *stratum radiatum* of CA1 area. Data were acquired using a Multiclamp 700B amplifier (Molecular Devices, Sunnyvale, CA), digitized with a Digidata 1320A digitizer (Axon Instruments Inc., Sunnyvale, CA), recorded and analysed off line with pClamp and Clampfit 10.3 respectively (Molecular Devices). Recordings were low-pass filtered at 2 kHz and digitized at 10 kHz.

A stable baseline was recorded for at least 20 min before starting the input/output experiment. The same amplitude of stimulation was applied 3 times (0.033 Hz), before being increased up to 50V. Paired-pulse stimulation experiments were performed with two pulses of stimulation induced at 100 ms interval. The paired pulse ratio was calculated as the slope of the second fEPSP over the slope of the first fEPSP. In another set of experiments, long-term potentiation (LTP) was induced after 20 min of baseline recording, by applying a high-frequency stimulation (HFS) protocol (100 Hz train of stimuli for 1 s, repeated 3 times at 20 s interval) in current clamp mode.

Statistical analysis.

Results are expressed as mean ± SEM. Statistical analysis were performed with STATISTICA software (StatSoft, Tulsa, OK). For each analysis, normality of variables or residues and homoscedasticity were assessed. We used paired or unpaired Student's t test to compare two groups or one-way ANOVA and Tukey's post hoc test to compare 3 groups. If any or both conditions of application were not fulfilled, we used non-parametric tests. Two groups were compared by the Mann-Whitney test and 3 independent groups were compared by a Kruskal-Wallis test followed by Mann-Whitney test. The significance level was set at p value < 0.05.

RESULTS

STAT3 activation is a conserved hallmark of astrocyte reactivity in ND animal models

We previously showed that STAT3 is activated in reactive astrocytes in 3xTg-AD and APP/PS1dE9 mice (later called APP mice), as well as in a mouse and primate lentiviral vector-based model of HD (Ben Haim et al., 2015b). Here, we extended these results by studying STAT3 activation in models of tauopathy and PD in mice, rats or primates. STAT3 phosphorylation is difficult to detect *in situ*, especially in progressive models of ND (O'Callaghan and Sriram, 2004, Ceyzeriat et al., 2016). Therefore, the nuclear accumulation of STAT3, caused by nuclear translocation upon activation and increase of its own transcription, was used as surrogate index of STAT3 activation, as previously described (Tyzack et al., 2014, Ben Haim et al., 2015b). Astrocytes were reactive, as they overexpressed GFAP and were hypertrophic in a virus-based model of tauopathy in rats (d'Orange et al., in revision), in a transgenic mouse model of tauopathy (Schindowski et al., 2006), and a toxin-based primate model of PD (**Fig. 1**). STAT3 accumulated in the nucleus of reactive astrocytes, revealing an activation of the JAK-STAT3 pathway. Of note, STAT3 induction was observed in different brain regions where reactive astrocytes are present in these models (CA1 region of the hippocampus for tauopathy and *substantia nigra* for PD, **Fig. 1**).

SOCS3 suppresses morphological features of astrocyte reactivity

To better understand the regulatory effects of the JAK-STAT3 pathway on astrocyte reactivity, we performed astrocyte-specific gene transfer of SOCS3, an endogenous inhibitor of the JAK-STAT3 pathway (Shuai and Liu, 2003, Linossi et al., 2013). We studied SOCS3 effects in APP mice that display strong astrocyte reactivity in the hippocampus and cortex, where amyloid plaques accumulate (Jankowsky et al., 2004, Ben Haim et al., 2015b). Serotype 9 adeno-associated vectors (AAV) with a GFA_{ABC1D} promoter were used to target hippocampal astrocytes in APP mice (**Supplemental Fig. 1**). Three month-old APP mice were injected with AAV-GFP or AAV-SOCS3 + AAV-GFP in the hippocampus (same viral titer) and analyzed 9 months later (APP-GFP and APP-SOCS3 mice respectively). Wildtype (WT) littermates injected with AAV-GFP (WT-GFP mice) were used as controls. *Socs3* mRNA levels were 12 to 16 times higher in astrocytes of the APP-SOCS3 group than in the APP-GFP and WT-GFP groups respectively (see **Fig. 4c**), demonstrating the efficiency of the AAV-SOCS3 vector. SOCS3 expression in astrocytes efficiently reduced STAT3 nuclear accumulation, even in reactive astrocytes in contact with plaques (**Fig. 2a, b**). SOCS3 also prevented the induction of GFAP observed in APP mice (**Fig. 2a, b**) and normalized astrocyte morphology. Interestingly, SOCS3 was still efficient in aged APP mice that already display strong astrocyte reactivity around amyloid plaques. Injection of AAV-SOCS3 in the hippocampus of 15 month-old APP mice efficiently reversed astrocyte reactivity, as seen by a significant decrease in GFAP levels (**Fig. 2c**).

Of the 7 members of the STAT family, STAT3 is expressed at highest levels in the brain and is enriched in hippocampal astrocytes (Sharma et al., 2015, and our own RNAseq data), but STAT1 may play important roles in brain inflammatory processes as well (Rothhammer et al., 2016). In the hippocampus of WT-GFP mice, STAT1 immunoreactivity was very low compared to positive controls (brains with strong neuroinflammation induced by lipopolysaccharide injection (LPS) or brains with strong astrocyte reactivity induced by CNTF, see methods, **Fig. 3a**). In the positive controls, STAT1 was

mainly observed in the nucleus of S100β negative cells, most probably neurons. In APP mice, there was no evidence of nuclear accumulation of STAT1 in any cell type, confirming that STAT3 is the main effector STAT in astrocytes (**Fig. 3a**). We also studied the active, phosphorylated form of extracellular signal-regulated kinase (P-ERK), a downstream effector of the MAPK pathways, as it was reported to be activated in reactive astrocytes in some ND models, and it can be activated by JAKs, at least in cell lines (Chung et al., 2005, Eulenfeld et al., 2012, Kuipers et al., 2017). In the LPS positive control, numerous P-ERK^{+} cells were found with a morphology typical of astrocytes (**Fig. 3b**). Similarly to STAT1, only a faint P-ERK staining was observed in the hippocampus of WT-GFP and APP mice (**Fig. 3b**), suggesting that P-ERK is not activated in AD astrocytes.

We previously showed that viral gene transfer of SOCS3 in astrocytes prevents reactivity in HD mouse models and 3xTg-AD mice (Ben Haim et al., 2015b, and data not shown). SOCS3 thus efficiently blocks the JAK-STAT3 pathway, thereby inhibiting and even reversing the basic morphological hallmarks of reactivity (intermediate filament overexpression and hypertrophy), in multiple mouse models of ND.

SOCS3 restores the transcriptional profile of astrocytes in APP mice

Besides these two morphological features, astrocyte reactivity is characterized by the induction of transcriptional programs resulting in significant changes in gene expression (Zamanian et al., 2012, Orre et al., 2014, Liddelow et al., 2017). To determine whether SOCS3 restores a non-reactive transcriptomic profile in astrocytes, we performed RNA sequencing (RNAseq) on astrocytes acutely isolated from WT-GFP, APP-GFP and APP-SOCS3 hippocampi. Astrocytes from 9 month-old WT and APP mice were collected by fluorescence-activated cell sorting (FACS), based on their GFP expression (ASTRO fraction). Non-fluorescent cells (including neurons, microglial cells and non-infected astrocytes) were collected as a single fraction called "OTHER". Genome-wide RNAseq analysis of OTHER and ASTRO cells taken from WT-GFP mice identified 6949 genes differentially-expressed with a fold-change (FC) > 1.5 and $p < 0.05$. Hierarchical clustering based on these genes clearly separated ASTRO from OTHER samples (**Fig. 4a**). Among differentially expressed genes, astrocyte-specific genes such as *Aldh1l1, Gjb6 (Cx30)* and *Slc1a2* were enriched in the ASTRO fraction (**Fig. 4b**). On the contrary, genes specific for microglial cells, neurons and oligodendrocyte precursor cells (OPC) were enriched in the OTHER fraction (**Fig. 4b**). Oligodendrocyte genes were nearly undetectable due to the myelin removal step during cell dissociation (**Fig. 4b**). The sorting procedure being validated, we then studied gene expression in astrocytes from the 3 groups.

There were 234 genes differentially expressed between astrocytes of the APP-GFP and WT-GFP groups and 472 genes between the APP-SOCS3 and APP-GFP groups (FC > 1.5, $p < 0.05$, **Fig. 4d**). Interestingly, a majority of genes were down-regulated by SOCS3, consistent with its inhibitory action on the JAK2-STAT3 pathway (**Fig. 4d**). Differentially-expressed genes between WT-GFP and APP-GFP included genes (e.g. *Cst7, Ctss, Tyrobp*) that were previously described as up regulated in astrocytes sorted from the same AD mice but at an older age (15 month-old, Orre et al., 2014). By comparing the two lists of 234 and 472 genes, 53 genes were identified, whose expression was dysregulated in APP-GFP mice relatively to WT-GFP mice and restored by SOCS3. A Gene Ontology (GO) enrichment analysis was performed on this list, with DAVID (Huang da et al., 2009). It was significantly enriched in GO terms (biological process) linked to inflammation/immunity and signaling ($p < 0.05$, **Fig. 4e**). Interestingly, in the list of 472 genes mainly downregulated by SOCS3 in APP mice, there was an even

larger number of significantly enriched GO terms ($p < 1.10^{-3}$) linked to signaling (13 GO terms including *signal transduction* and *LPS-mediated signaling pathway*) and inflammation/immunity (14 GO terms including *innate immune response* and *inflammatory response*, data not shown). This analysis confirms that SOCS3 efficiently normalizes inflammatory processes in APP astrocytes. For example, SOCS3 was able to abrogate the induction of the cytokines and chemokines *Il1ß, Ccl2, Ccl4* and *Ccl6* observed in astrocytes of APP-GFP mice (**Fig. 5a**). Interestingly, SOCS3 also regulated several genes of the complement system (**Fig. 5b**), which is a key component of neuroinflammatory responses and is involved in synaptic pruning in different diseases, including AD (Hong et al., 2016). The expression of *C1qa, C1qb, C1qc* and *C4b* was higher in APP-GFP astrocytes than in WT-GFP astrocytes and normalized in APP-SOCS3 astrocytes (**Fig. 5b**).

We then studied genes specific of reactive astrocytes, including the recently described markers for the A1 and A2 classes of reactive astrocytes (Zamanian et al., 2012, Liddelow et al., 2017). The mRNA levels of *Gfap,* the classic, pan reactive marker tended to be higher in astrocytes isolated from the APP-GFP group than in the WT-GFP group (**Fig. 5c**). SOCS3 significantly reduced *Gfap* expression, as well as *Serpina3n* and *Hspb1*, two other pan reactive astrocyte genes. The same profile of expression was found for A1-specific genes (*Gbp2, H2-D1 and Serping1)* and for A2-specific genes (*Cd14, Tm4sf1)*, suggesting that SOCS3 normalizes the transcriptional profile of all classes of reactive astrocytes (**Fig. 5c, and data not shown**). The presence of A1 reactive astrocytes was reported in the brain of patients with AD and other brain diseases (Liddelow et al., 2017), but less is known about A2 reactive astrocytes. In APP-GFP mice, there was a 3-fold increase in the number of astrocytes expressing the A2 marker Tm4sf1. The number of $Tm4sf1^+$ astrocytes was significantly reduced by SOCS3 (**Fig. 5d**), confirming that SOCS3 also prevents the A2 type of astrocyte reactivity.

To gain more insight into the transcriptional networks regulated by the JAK-STAT3 pathway and identify modules of co-expressed genes across the 3 groups, a weighted gene correlation network analysis (WGCNA) was performed. One module among 19 was identified as differentially expressed between the 3 groups (p = 0.018, **Fig. 5e**). This module was formed by 567 genes mainly down-regulated by SOCS3 (**Fig. 5e**). Interestingly, the 8^{th} most connected gene (i.e. hub gene) in this module was *Serping1*, a marker of A1 reactive astrocytes (**Table 2**). In fact, this module contained several pan *(Gfap, Vimentin)*, A1 (*Serping1*, *H2-D1, Srgn)* and A2 (*Tm4sf1, CD14*) genes, as well as genes related to inflammation (e.g. *C1qa, C1qb, C1qc, Ccl3*). These results confirm that SOCS3 operates as a master regulator on transcriptional programs of reactivity, inhibiting different classes of reactive astrocytes.

Overall, our RNAseq data points to a significant involvement of inflammatory processes in AD and their normalization with SOCS3 expression in astrocytes. SOCS3 is thus able to produce a global and efficient inhibition of astrocyte reactivity, restoring a basal transcriptional profile in APP astrocytes.

Expression of constitutively active JAK2 in astrocytes is sufficient to induce reactivity

We next performed mirror experiments to activate the JAK2-STAT3 pathway in WT astrocytes with a constitutively active mutant of JAK2 (JAK2ca).

JAK2 levels were increased by a factor 4 after AAV-gene transfer of JAK2ca in striatal astrocytes (see **Fig. 8a**). JAK2ca-expressing astrocytes displayed STAT3 nuclear accumulation, demonstrating an activation of the JAK2-STAT3 pathway (**Fig. 6a, b**). To further demonstrate that JAK2ca activates this cascade, we implemented a lentiviral-based reporter system to detect STAT3-mediated transcriptional activity in astrocytes. In this reporter, GFP expression is under the control of six STAT3 consensus

binding sites coupled to a minimal promoter (**Fig. 6c**). This lentiviral reporter was co-injected with LV-JAK2ca or a non-fluorescent control vector encoding β-galactosidase (LV-LacZ) in the striatum of WT mice. In the JAK2ca group, there were more GFP^+ cells than in the control LacZ group. GFP^+ cells were reactive astrocytes, as they co-expressed GFAP (**Fig. 6c**). JAK2ca-mediated activation of the STAT3 promoter was also visible by FACS as a fourfold increase in GFP levels (**Fig. 6d**). In contrast to the significant increase in STAT3 expression (**Fig. 6b**), STAT1 immunoreactivity remained low in the striatum injected with AAV-JAK2ca, as in the control side injected with AAV-GFP (**Fig. 6e**). Similar results were found with P-ERK, suggesting that STAT3 is the main effector transcription factor activated by JAK2ca (**Fig. 6f**).

JAK2ca expression in astrocytes was sufficient to induce reactivity in the striatum in naïve adult WT mice. JAK2ca-astrocytes overexpressed GFAP and vimentin (**Fig. 7a, b, c**). They had an enlarged soma with tortuous processes (**Fig. 7b, d**). Other elements of the cascade were overexpressed in striatal astrocytes: murine JAK2, mutant $JAK2^{Y317F,\ Y570F}$ that lacks two epitopes for inhibitory phosphorylation (Robertson et al., 2009) or an active mutant of STAT3 (STAT3-C, Bromberg et al., 1999). All of them also increased GFAP and vimentin expression in the mouse striatum, further demonstrating the importance of the JAK2-STAT3 pathway for astrocyte reactivity (**Supplemental Fig. 2**).

JAK2ca was also able to efficiently trigger astrocyte reactivity in the hippocampus (**Supplemental Figure 3**), indicating a universal role of the JAK2-STAT3 pathway for astrocyte reactivity across brain regions.

JAK2ca induces transcriptional changes characteristic of reactive astrocytes

To determine whether JAK2ca induces a transcriptional profile typical of reactive astrocytes, we performed microarray analysis on sorted striatal astrocytes infected with AAV-GFP or with AAV-JAK2ca + AAV-GFP. The purity of sorted cells was controlled with the expression of cell-type specific markers in the ASTRO and OTHER fractions. Astrocyte-specific genes (*Gjb6, Slc1a1*) were enriched by a factor 5 to 7 in the ASTRO fraction. Other astrocyte genes like *Aldh1L1* were undetectable in the OTHER fraction, which was enriched with microglial, neuronal and oligodendrocyte genes (**data not shown**).

We then compared the expression profile of the 4 ASTRO samples in the WT-GFP group with the 4 ASTRO samples in the WT-JAK2ca group. To have stringent analysis criteria, we only considered probes that had good signal quality and were detected in all samples of at least one group (see methods). We found 578 probes differentially expressed between JAK2ca-astrocytes and control GFP-astrocytes, which correspond to 539 unique genes (**Fig. 8b**). DAVID analysis of this list revealed a specific enrichment in 69 GO terms. Among them, several GO terms related to signaling as well as antigen presentation were present (**Fig. 8c**). Interestingly, two GO terms linked to memory were also found enriched in the list of genes regulated by JAK2ca. In addition, four GO terms associated with ion homeostasis, a key astrocyte function allowing proper synaptic transmission, were also found enriched, suggesting a link between induction of reactivity with JAK2ca and changes in synaptic transmission and plasticity (**Fig. 8c**).

JAK2ca had opposite transcriptional effects on WT striatal astrocytes from those triggered by SOCS3 in APP astrocytes. It increased the expression of several cytokines and chemokines such as *Il1b*, *Ccl3, Ccl4* and *Ccl7* (**Fig. 9a**). Interestingly, the same members of the complement cascade that were down regulated by SOCS3 (*C1qa, C1qb* and *C4b*) were induced in JAK2ca-astrocytes relatively to control GFP-astrocytes, as well as *C4a* (**Fig. 9b**). In addition, JAK2ca induced the expression of pan (*Gfap* and

Serpina3n) and A1 (*H2-D1, H2-T23* and *Srgn)* reactive astrocyte markers (**Fig. 9c, and data not shown**). However, no A2 markers were found in the list of genes modulated by JAK2ca. In fact, all A2 markers described in Liddelow *et al.* were undetectable at least in 6 of the 8 samples of the two groups, suggesting that these transcripts are expressed at very low levels in the mouse striatum and remain undetectable upon astrocyte activation. We thus used immunohistochemistry to detect the expression of CD14, an A2 marker gene on brain sections from WT-GFP and WT-JAK2ca mice. CD14 was not detected in the striatum of WT-GFP mice. There was a striking increase in CD14 expression in $GFAP^+$ reactive astrocytes in WT-JAK2ca mice, visible a small vesicles in the soma of $GFAP^+$ reactive astrocytes (**Fig. 9d**). These results show the JAK2ca is also able to induce A2 markers in astrocytes.

Some of the transcriptional changes induced by JAK2ca were validated in an independent mouse cohort injected in the striatum with LV-GFP or LV-JAK2ca. Whole striatum RT-qPCR was performed, so only genes known to be enriched in astrocytes were studied. *Jak2* mRNA levels was increased by a factor 2 in WT-JAK2ca mice compared with WT-GFP mice. *Socs3* mRNA levels were also increased by a factor 6, an indication of JAK2-STAT3 pathway activation. Reactive astrocyte markers *Gfap, Vimentin* and *Serpina3n* mRNA levels were all increased in the WT-JAK2ca group whereas the glutamate transporter S*cl1a2* (*Glt-1*) was not differentially expressed between the two groups, suggesting a specific effect of JAK2ca on reactive astrocyte transcripts (**Supplemental Fig. 4)**.

WGCNA was also performed on microarray data. Eighty modules of co-expressed genes were identified, among which 8 were differentially expressed between WT-GFP and WT-JAK2ca samples ($p < 0.05$, **Fig. 9e**). We further explored the module n°51 and the module n°63, which are the two most differentially expressed modules between the two groups ($p = 1.86\ 10^{-3}$ and $9.99\ 10^{-4}$ respectively). The *Jak2* gene itself was part of each of these modules, further demonstrating that they gather genes co-regulated by JAK2ca. Module n°51 was formed by 2171 genes mainly up-regulated by JAK2ca (**Fig. 9e**). Strikingly, the second top hub gene for this module was the universal marker of reactivity *Gfap* (**Table 3a**), and *Cxcl10*, another pan reactive gene was also part of this module. The 20 hub genes of this module included several genes linked to neuroinflammation and signaling and a cathepsin *(Ctsc),* similarly to the module identified by WGCNA on APP-SOCS3 mice (**Table 2**). Interestingly, *Nfkbia* (i.e. IκBα, the main inhibitor of the canonical NF-κB pathway), was also one of these highly connected genes and was found up-regulated by more than 4-fold in JAK2ca-expressing astrocytes ($p < 0.05$), suggesting that JAK2ca induces NF-κB pathway inhibition in astrocytes. In accordance, module n°63, which was formed by 2850 genes mainly down-regulated by JAK2ca was enriched in genes linked to signaling cascades (*Map4k5, Ppp2r5d,* **Table 3b***).* Overall, our transcriptomic analyses underline the central action of the JAK2-STAT3 pathway in regulating core genes for astrocyte reactivity. They also suggest that activation of this cascade has an inhibitory action of alternative signaling pathways.

We next wanted to determine the functional consequences of JAK2ca-induced astrocyte reactivity on neurons. We focused on synaptic transmission and long term potentiation (LTP) at the Schaffer collateral-CA1 synapse in the hippocampus, because i) astrocytes are known to play a key role in this process (Araque et al., 2014), ii) there are consistent reports of LTP alterations in mouse models of ND (in particular AD models, (Oddo et al., 2003, Volianskis et al., 2010, Viana da Silva et al., 2016) and iii) our transcriptomic analysis identified significant changes in functions related to synaptic transmission and memory in JAK2ca-expressing astrocytes.

Induction of astrocyte reactivity by JAK2ca alters LTP at the CA1-Schaffer collateral synapse

WT mice were injected in the CA1 region with AAV-GFP or AAV-JAK2ca +AAV-GFP (at the same total viral load). Non injected WT mice (NI) were also analysed to control for any effect of viral infection or transgenic protein expression. We studied basal glutamatergic synaptic transmission, short-term and long-term synaptic plasticity in acute hippocampal slices prepared from the 3 groups. Field excitatory post-synaptic potentials (fEPSPs) were recorded in the infected GFP^+ CA1 region (**Fig. 10a**).

Induction of astrocyte reactivity by JAK2ca did not impact basal glutamatergic synaptic transmission, as the input/output relationship for evoked fEPSPs at CA3-CA1 synapses was similar in the 3 groups (**Fig. 10b**). In addition, the paired-pulse ratio, a measure of short term plasticity dependent on presynaptic mechanisms, was also not impacted by JAK2ca (**Fig. 10c, d**). LTP was induced by stimulation of Schaffer collaterals with 3 high frequency stimulations trains (100 Hz during 1s, 20s interval). This protocol induced LTP in NI and WT-GFP groups (45 to 60% increase in fEPSP after 45 min) but it failed to do so in the JAK2ca group (**Fig. 10e**). These results show that induction of astrocyte reactivity by JAK2ca causes significant deficits in long-term synaptic plasticity.

DISCUSSION

Activation of the JAK-STAT3 pathway is a common feature of astrocyte reactivity

We previously reported that the JAK-STAT3 pathway is activated in reactive astrocytes in two mouse models of AD, as well as in a mouse and primate lentiviral vector-based model of HD (Ben Haim et al., 2015b). In this study, we extended these observations by showing STAT3 activation in models of tauopathy and PD in 3 different species. As previously discussed by us and others, STAT3 upregulation and nuclear accumulation were used as surrogates for STAT3 activation, as phospho-STAT3 remains undetectable in these slowly progressing ND models (Tyzack et al., 2014, Ben Haim et al., 2015a, Ceyzeriat et al., 2016). These ND involve diverse etiology, with aggregation of different misfolded proteins (Huntingtin, Tau or extracellular Aβ) in distinct vulnerable brain regions (hippocampus, cortex, striatum). Therefore, diverse pathological stimuli present in these ND appear to converge -either directly or indirectly- on the JAK-STAT3 pathway to trigger astrocyte reactivity. The JAK-STAT3 pathway is also activated in reactive astrocytes following acute brain diseases like ischemia or trauma (see, Ceyzeriat et al., 2016, for review). Altogether, these results show that the activation of the JAK-STAT3 pathway is a universal feature of astrocyte reactivity.

Activation of the JAK2-STAT3 pathway mediates astrocyte reactivity in ND models

We used viral-based strategies to inhibit or activate the JAK2-STAT3 pathway in astrocytes and found that this cascade is both necessary and sufficient to mediate astrocyte reactivity. Indeed, the JAK-STAT3 is responsible for mediating astrocyte reactivity in AD mice, as overexpression of SOCS3 abolished reactive astrocyte phenotype both at the morphological and molecular level. Interestingly, SOCS3 was not only able to prevent astrocyte reactivity but also to reverse it in the hippocampus aged APP mice. This important result suggests that the JAK-STAT3 pathway is necessary both for the induction and the long-term maintenance of astrocyte reactivity in AD mice. These results, in addition

to our data showing that SOCS3 inhibits astrocyte reactivity in other mouse models of AD and HD (Ben Haim et al., 2015a), demonstrate that SOCS3 is a universal and potent tool to block astrocyte reactivity *in situ*.

As further evidence that the JAK-STAT3 pathway is a key cascade for astrocyte reactivity, we show that overexpression of a constitutively active form of JAK2 (or other WT or active mutants of the JAK2-STAT3 pathway) in naive WT mice is sufficient to trigger robust and stable STAT3 activation, as shown with the SRE-GFP reporter construct. JAK2ca induces astrocyte reactivity in the absence of any pathological stimulus or neuroinflammation, and is also able to over-activate astrocytes that are already reactive in ND models (unpublished data). JAK2ca expression in astrocytes recapitulates key features of reactivity including morphological changes, up-regulation of intermediate filament proteins and induction of complex transcriptional programs. In this study, we used a variety of viral vectors (LV and AAV) in different brain regions (hippocampus and striatum) and observed reproducible effects of either the blockade or induction of the JAK2-STAT3 pathway in astrocytes.

In addition of controlling the expression of reactive astrocyte markers, we showed that the JAK2-STAT3 pathway regulates the expression of many genes linked to neuroinflammation. Global analysis with DAVID and WGCNA of gene expression changes mediated by SOCS3 and JAK2ca consistently identified key genes or functions linked to inflammation and immunity. In particular, SOCS3 was sufficient to abolish the induction of a wide array of cytokines and complement factors induced in APP astrocytes. Conversely, the same genes were upregulated by JAK2ca, demonstrating that the JAK2-STAT3 pathway is a key regulator for the neuroinflammatory signals released by reactive astrocytes. Cytokines and complement factors are induced in astrocytes (and microglia) in AD mice (Orre et al., 2014, Lian et al., 2015, Srinivasan et al., 2016). They are now clearly associated with some of the synaptic alterations and molecular defects characteristics of AD and other ND (Stephan et al., 2012, Heneka et al., 2014, Heneka et al., 2015, Lian et al., 2015, Hong et al., 2016). Identifying a signaling cascade that coordinate their production by astrocytes is thus of high therapeutic value for these diseases (see last §).

Besides the JAK2-STAT3 pathway, other cascades were reported to be activated during ND (Kang and Hebert, 2011, Ben Haim et al., 2015a). However their role in mediating astrocyte reactivity is either unclear or transient. JAK2 can phosphorylate other STATs beside STAT3, such as STAT1 (Murray, 2007) and may activate the MAPK pathways, at least *in vitro* (Eulenfeld et al., 2012). However, we did not find evidence for STAT1 activation in JAK2ca-expressing astrocytes or in APP mice, suggesting that STAT3 is the downstream transcription factor mediating JAK2ca effects. Other cascades linked to astrocyte reactivity in ND include the CN/NFAT and NF-κB pathways. Constitutive activation of CN in AD mice decreases astrocyte reactivity (Fernandez et al., 2012). Surprisingly, the opposite manipulation of CN through expression of a blocking peptide, also attenuates astrocyte reactivity in the same mouse model, but only by 30% (Furman et al., 2012), questioning the regulatory action of CN over astrocyte reactivity. Activation of NF-κB is also reported in reactive astrocytes in models of AD, HD and amyotrophic lateral sclerosis (ALS) (Carrero et al., 2012, Hsiao et al., 2013, Medeiros and LaFerla, 2013, Frakes et al., 2014). Astrocyte NF-κB activation, triggered by a conditional knock-out of its inhibitor IκBα or by expression of a constitutively active upstream kinase IKK, increases glial reactivity in the cortex and hippocampus (Oeckl et al., 2012, Lian et al., 2015). However, in the $SOD1^{G93A}$ mouse model of ALS, overexpression of a constitutively active mutant of IκBα in astrocytes is

only able to slightly decrease astrocyte reactivity in the spinal cord at disease onset, but not at later symptomatic stages (Crosio et al., 2011). Together, these results suggest that the modulation of the CN or NF-κB pathways have inconsistent, transient or moderate effects on astrocyte reactivity in ND models, compared with those obtained with the JAK2-STAT3 pathway. Interestingly, the effects of JAK2-STAT3 modulation on astrocyte reactivity were remarkably stable over time (JAK2ca: 4 mpi; SOCS3: 9 mpi). Overall, the JAK2-STAT3 cascade appears to regulate astrocyte reactivity in a universal and robust manner across ND models.

A core JAK2-STAT3 pathway versus heterogeneity of reactive astrocytes

The concept of reactive astrocyte heterogeneity is timely and exciting but it remains elusive (Anderson et al., 2014, Liddelow and Barres, 2017). Recent work based on the comparison of reactive astrocyte transcriptome after ischemic injury (A1) or neuroinflammation (A2) identified subsets of differentially expressed genes depending on the stimulus (Zamanian et al., 2012). More recently, A1 reactive astrocytes were shown to have neurotoxic effects *in vitro* and *in vivo* (Liddelow et al., 2017), while A2 reactive astrocytes are expected to have neuroprotective effects as they overexpress synaptogenic and trophic genes (Zamanian et al., 2012). These landmark studies provide a new framework to understand astrocyte reactivity. It opens the possibility that reactive astrocytes display alternative molecular and functional profiles, forming multiple subpopulations distinct from these two extreme classes, depending on disease context. But the precise signaling pathways controlling these states are not known.

Strikingly, we found that manipulation of the JAK2-STAT3 cascade impacted the expression of pan, A1 and A2 specific genes. In fact, the core modules of genes regulated by SOCS3 identified by WGCNA contained both A1 and A2 markers as well as pan reactive markers. These results suggest that the JAK2-STAT3 pathway is able to trigger a global switch on astrocyte reactivity. This cascade can be viewed as a master regulator of reactivity, which operates beyond specific classes of reactive astrocytes. We found that Tm4sf1 and CD14, two A2 reactive markers, were almost totally co-expressed with the pan reactive marker GFAP in reactive astrocytes. However, it remains to be determined whether A1 and A2 genes are co-regulated by the JAK2-STAT3 cascade within the same individual astrocytes or they are expressed in distinct astrocytes. If the JAK2-STAT3 cascade is able to control different types of reactivity, then, how the observed heterogeneity is generated? Normal astrocytes are quite heterogeneous already in physiological conditions (Ben Haim et al., 2015a), as further demonstrated recently by an elegant molecular study (John Lin et al., 2017). Distinct subpopulations of astrocytes could engage in different transcriptional programs of reactivity upon JAK2-STAT3 pathway activation in diseases. Alternatively, disease-specific pathologic signals could activate specific signaling networks around the core JAK2-STAT3 pathway and induce different classes of reactive astrocytes, with distinct molecular and functional features. More experiments with refined molecular analysis are needed to tease out this important question.

Interactions between the JAK2-STAT3 pathway and other signaling cascades

There are multiple levels of crosstalk between the JAK2-STAT3 and other signaling cascades including the NF-κB pathway and the MAPK pathways (Yang et al., 2007, Fan et al., 2013, Ben Haim et al., 2015a, Ceyzeriat et al., 2016). These cascades can inhibit or stimulate one another or have

synergetic effects. Our pathway analysis of transcriptomic data shows that JAK-STAT3 pathway modulation by SOCS3 or JAK2ca significantly affects astrocyte signaling. We found multiple changes in the expression of signaling intermediates in several canonical pathways for signal transduction, including the NF-κB and the MAPK pathways. For example, several members of the IκB family such as *Nfkbia* or *Nfkbiz* were significantly induced by JAK2ca and/or reduced by SOCS3, suggesting that the JAK2-STAT3 pathway inhibits NF-κB signaling. This would explain why we failed to detected NF-κB activation in reactive astrocytes of AD and HD mouse models (Ben Haim et al., 2015b). These results are also in line with previous studies showing that SOCS3-deficient astrocytes have increased NF-κB activation (Ma et al., 2010, Rothhammer et al., 2016).

Additional experiments are needed to decipher the functional relevance of such reciprocal interactions, especially in astrocytes and *in vivo.* However, it is tempting to speculate that in reactive astrocytes, the core JAK2-STAT3 cascade regulates the expression of several signaling intermediates belonging to parallel intracellular signaling pathways, resulting in their modulation or inhibition.

Reactive astrocytes at the synapse

The contribution of reactive astrocytes to pathological processes in ND is still a matter of debate. In particular, it is unclear how reactive astrocytes participate to synaptic deficits observed in many ND (Ben Haim et al., 2015a, Kim et al., 2017, Singh and Abraham, 2017).

In the present study, we showed that activation of the JAK2-STAT3 pathway in astrocytes alters LTP at the CA3-CA1 synapse in naive WT mice. Such LTP alteration with JAK2ca is reminiscent of what is observed in mouse models of AD (Oddo et al., 2003, Volianskis et al., 2010, Viana da Silva et al., 2016), and these results are particularly important for AD, where LTP deficits correlate with cognitive impairment. Recent studies showed that abnormal release of GABA by reactive astrocytes contributes to cognitive impairment in two AD models (Jo et al., 2014, Wu et al., 2014). Inhibition of GABA synthesis or pharmacological blockade of GABA transporters restored synaptic plasticity and memory deficits in AD mice (Jo et al., 2014, Wu et al., 2014). Alternatively, it was proposed that the release of C3 by reactive astrocytes was responsible for alterations in the morphology and function of synapses (Lian et al., 2015). However, in these studies, it is sometimes difficult to isolate the unique contribution of astrocyte reactivity from all other pathological processes (i.e. microglial activation, amyloid deposition). Similarly, a previous study reported that astrocyte reactivity induced by high titers of AAV-GFP leads to LTP deficits, by decreasing GABAergic inhibitory transmission in the CA1 region (Ortinski et al., 2010). But again, this strategy could have side effects on multiple cell types including neurons and microglial cells. Our model of astrocyte reactivity induced by JAK2ca expression in astrocytes replicates the signaling involved in ND and allows the dissection of astrocyte-specific mechanisms of synaptic impairment. More experiments are needed to identify the molecular mechanisms involved. They may include change in the release of gliotransmitters but also alterations in ion homeostasis, as suggested by transcriptomic data. Indeed, it is interesting to note that pathway analysis on JAK2ca-genes also identified several GO terms linked to memory. Therefore, JAK2ca-mediated transcriptional changes could be responsible for the observed synaptic deficits. Interestingly, the JAK2-STAT3 pathway was already shown to mediate NMDAR-dependent long term depression in hippocampal neurons (Nicolas et al., 2012), suggesting that this cascade is connected to synaptic plasticity in different cell types. Altogether, our study identifies an upstream signaling cascade triggering astrocyte reactivity that is potentially implicated in synaptic plasticity deficits, with therapeutic implications for AD.

CONCLUSIONS

Overall, we show that the JAK2-STAT3 pathway is a core signaling cascade for the induction and maintenance of astrocyte reactivity in ND. It controls key morphological features and coordinates gene expression changes in reactive astrocytes, regardless of the recently described classes of reactive astrocytes. We developed versatile viral-based tools to manipulate this pathway in astrocytes *in situ*. They could be used in any disease models, stages, brain regions and even species, to decipher the contribution of reactive astrocytes to pathogenesis.

The JAK2-STAT3 pathway, as a master regulator of reactivity, is an appealing molecular target to better understand the roles of reactive astrocytes in CNS diseases and develop new astrocyte-centered therapeutic strategies.

FIGURES

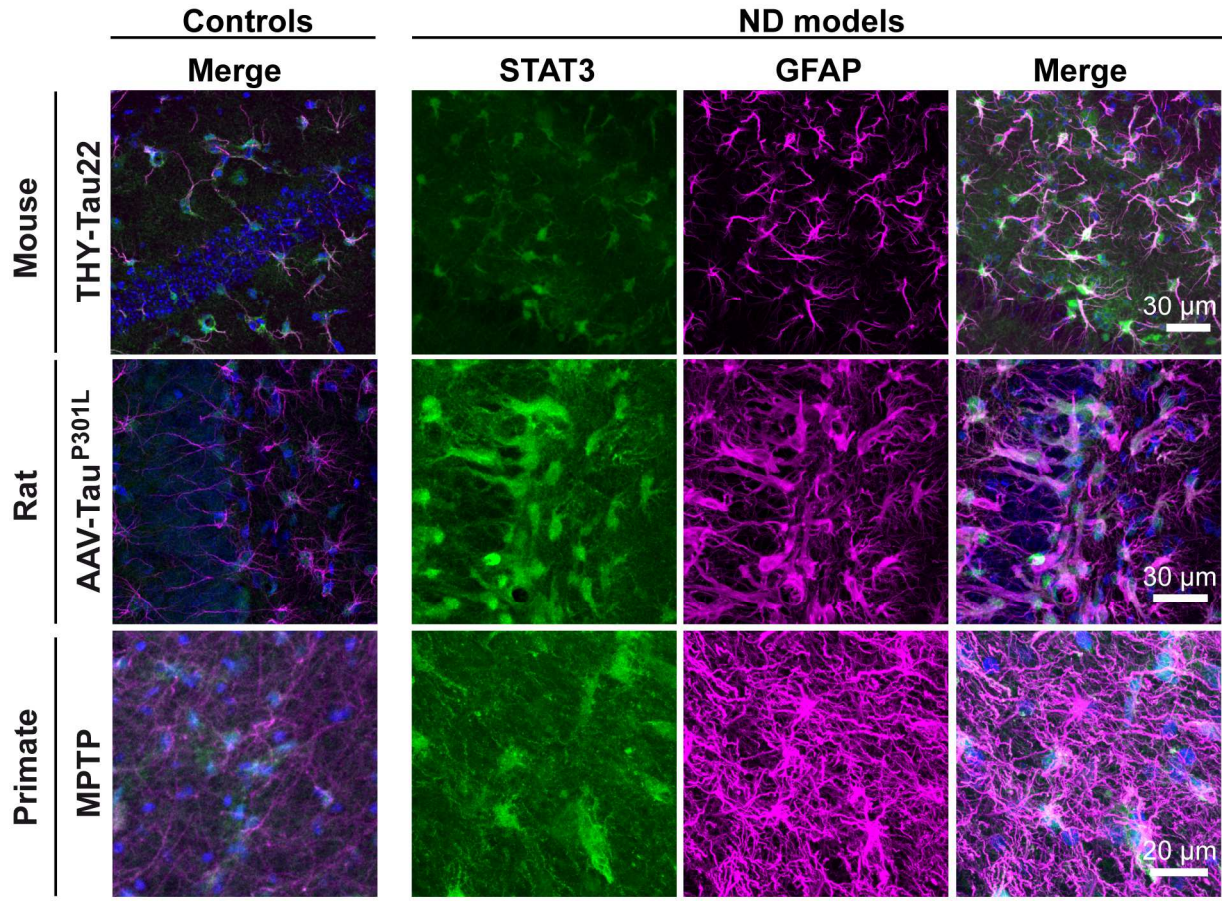

Figure 1. STAT3 is activated in reactive astrocytes of multiple ND models.

Confocal images of astrocytes stained for STAT3 (green) and GFAP (magenta) in 3 animal models of ND and their respective control (see details in Materiel and methods section). STAT3 nuclear accumulation is observed in hypertrophic, $GFAP^{+}$ reactive astrocytes in Thy-Tau-22 mice (Schindowski et al., 2006), in an AAV-based model of tauopathy where Tau^{P301L} is overexpressed in CA1 rat neurons (d'Orange et al., in revision), and in the MPTP primate model of PD. Note that the brain regions analyzed are different between models (CA1 for tauopathies, *substantia nigra* for MPTP). Representative images of N = 3/group.

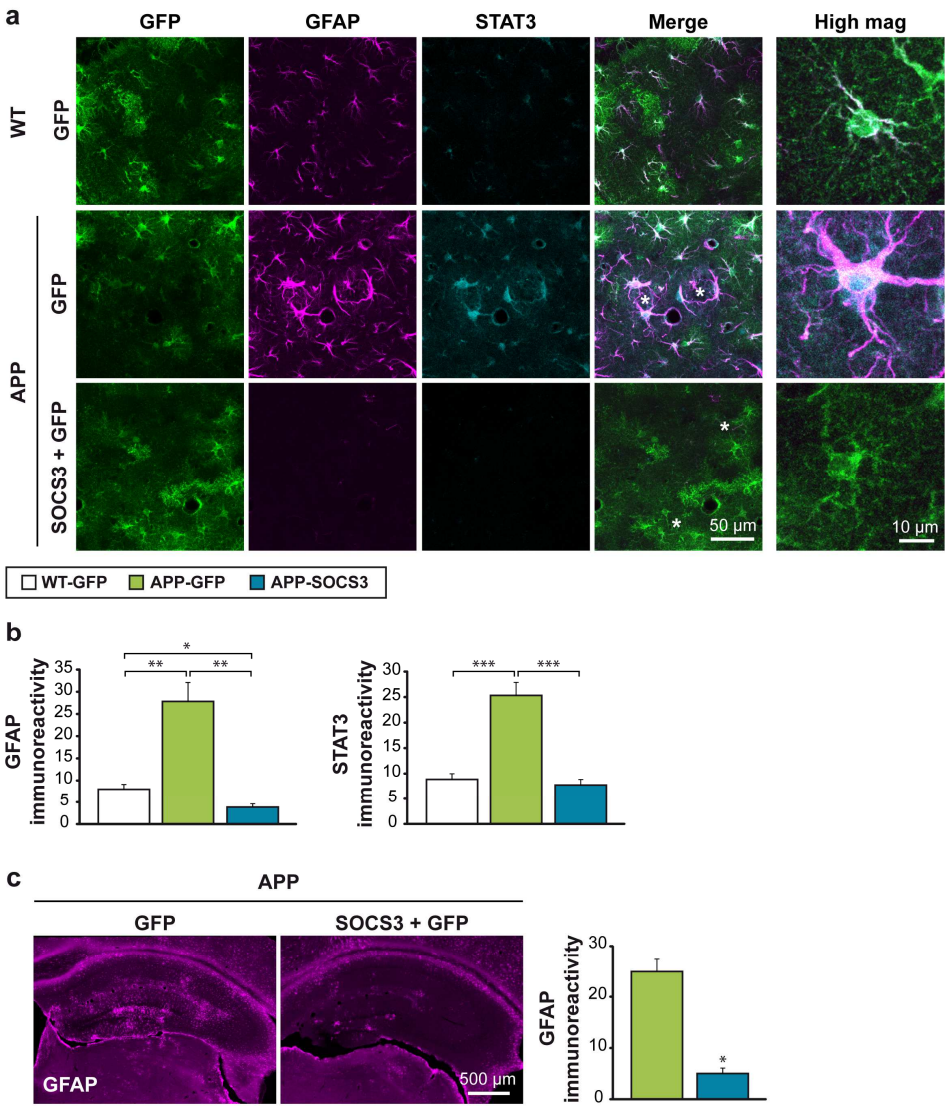

Figure 2. SOCS3 expression in astrocytes prevents the induction of reactive morphological hallmarks in APP mice.

a, Confocal images of astrocytes stained for GFAP (magenta) and STAT3 (cyan) in 12-month-old WT and APP mice. Mice were injected in the CA1 region with a mixture of two AAVs targeting astrocytes and encoding SOCS3 or GFP (SOCS3 + GFP), or only with an AAV encoding GFP (same viral titer). Infected astrocytes express GFP (green). Astrocytes are reactive in APP mice: they are hypertrophic and express GFAP at a higher level than in WT mice. These reactive astrocytes also display STAT3 nuclear accumulation, revealing an activation of the JAK-STAT3 pathway. STAT3 accumulation is even more prominent around amyloid plaques (star). SOCS3 reduces GFAP and STAT3 expression in APP mice. **b,** Quantification of immunofluorescent stainings confirms that SOCS3 normalizes GFAP and STAT3 immunoreactivity in astrocytes even around amyloid plaques. N = 5-7/group. One way ANOVA and Tukey's post hoc test (STAT3) or Kruskall-Wallis and Mann-Whitney tests (GFAP). **c,** AAV-SOCS3 is also able to reverse astrocyte reactivity, when injected in 15 month-old APP mice that already display severe plaque deposition and astrocyte reactivity. N = 3/group. Paired *t* test. * $p < 0.05$, ** $p < 0.01$, *** $p < 0.001$.

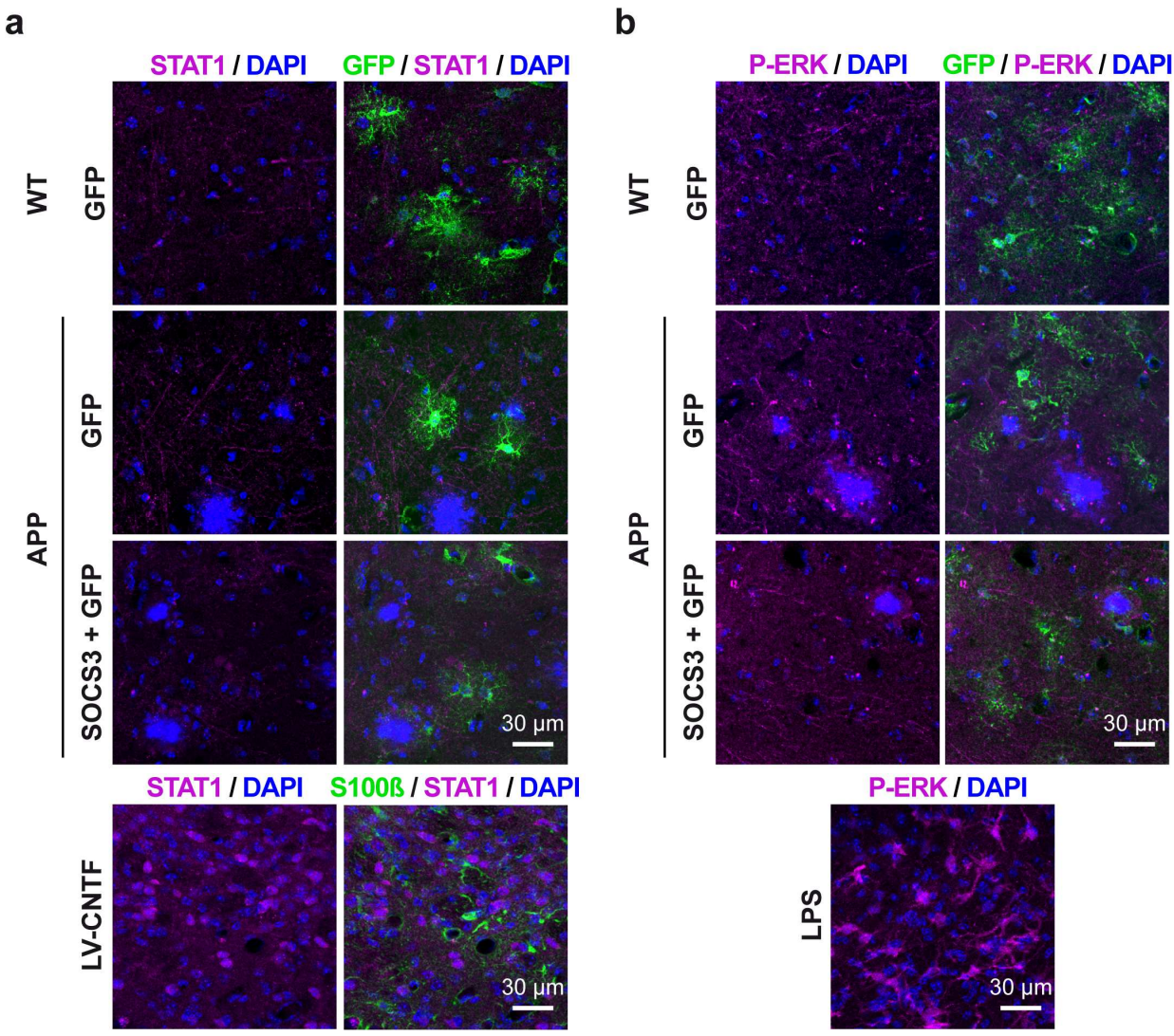

Figure 3. STAT1 and ERK are not activated in APP astrocytes.

Confocal images of astrocytes stained in green for GFP and in magenta for STAT1 (**a**) or P-ERK (**b**) in WT-GFP, APP-GFP and APP-SOCS3 mice. Amyloid plaques are visible in blue with the DAPI staining. Mice injected with LV-CNTF or LPS were included as positive controls for STAT1 and P-ERK staining respectively (see methods). CNTF induces significant nuclear staining in S100β^{-} cells, most probably neurons; while LPS induces ERK phosphorylation in many hypertrophic astrocytes. In contrast, only minimal staining for STAT1 and P-ERK is observed in the hippocampus of WT and APP mice, and none in GFP^{+} astrocytes. Representative images from N = 5-6/group.

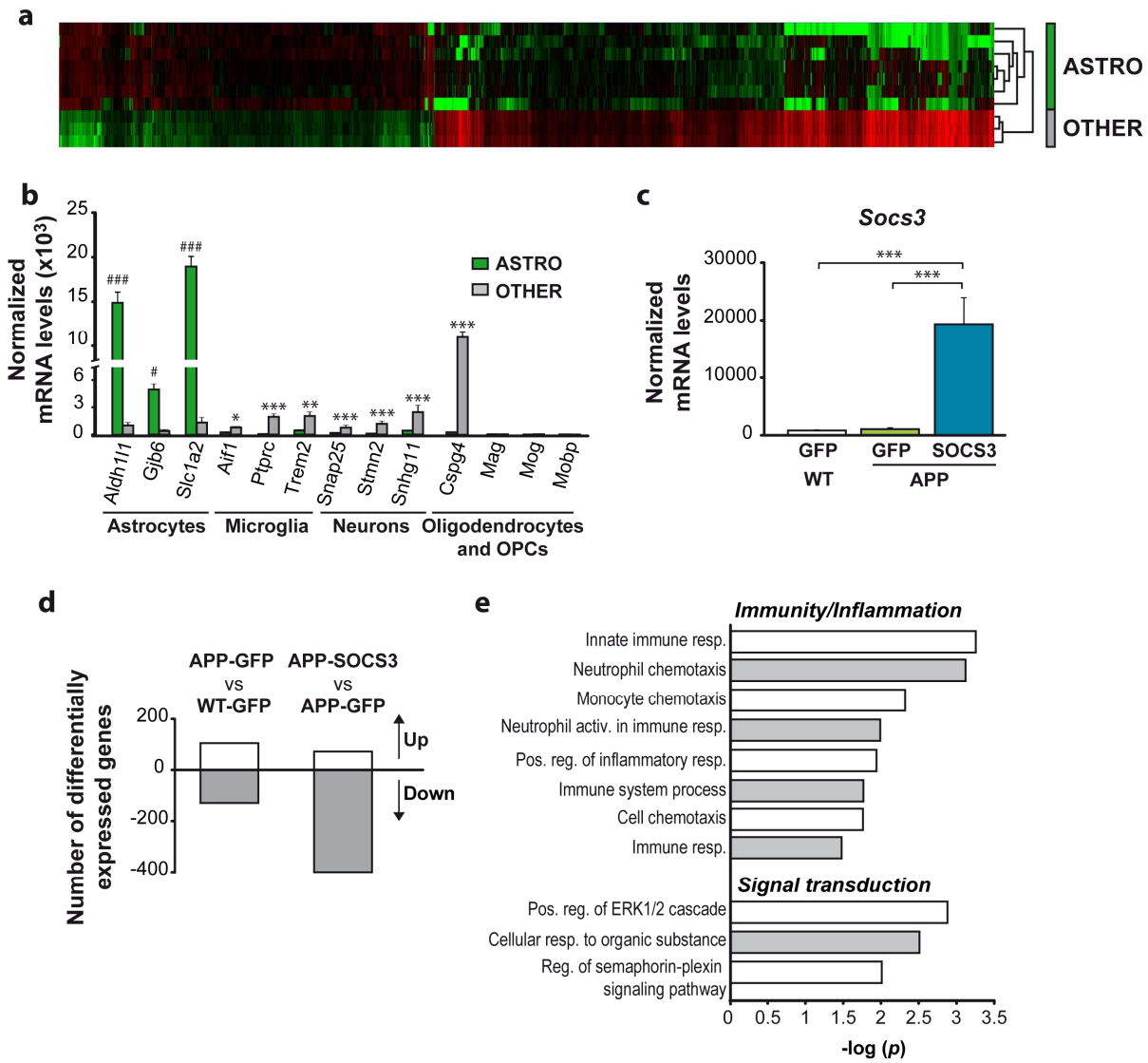

Figure 4. SOCS3 induces significant changes in the transcriptional profile of APP astrocytes.

RNAseq analysis on cells acutely isolated from the hippocampus of 9 month-old WT-GFP, APP-GFP and APP-SOCS3 mice. **a,** Hierarchical clustering of the ~7000 differentially expressed genes between GFP^+ sorted astrocytes (ASTRO) and all GFP-negative cells (OTHER) that comprise microglial cells, neurons, oligodendrocyte precursor cells (OPC) and non-infected astrocytes, reveals a strong segregation. **b,** Analysis of normalized mRNA levels of cell-specific genes validates the sorting procedure. N = 3-7/group. Wald test. **c,** *Socs3* mRNA levels are increased more than 10 times in APP-SOCS3 astrocytes compared to WT-GFP and APP-GFP astrocytes. N = 4-7/group. Wald test. **d,** Hundreds of genes are found differentially expressed between WT-GFP and APP-GFP astrocytes and APP-GFP and APP-SOCS3 astrocytes. Note that SOCS3 preferentially down-regulates gene expression, as expected for an inhibitor of a transcriptional signaling cascade. **e,** Pathway analysis on the 53 genes deregulated in APP-GFP astrocytes and normalized in APP-SOCS3 reveals a specific enrichment in GO terms (biological processes) linked to immunity and inflammation and signaling. Activ. = activity. Pos. = positive. Reg. = regulation. Resp. = response. *<0.05, ** $p < 0.01$, *** $p < 0.001$, $^{\#}$ $p < 1.10^{-20}$, $^{\#\#\#}$ $p < 1.10^{-40}$.

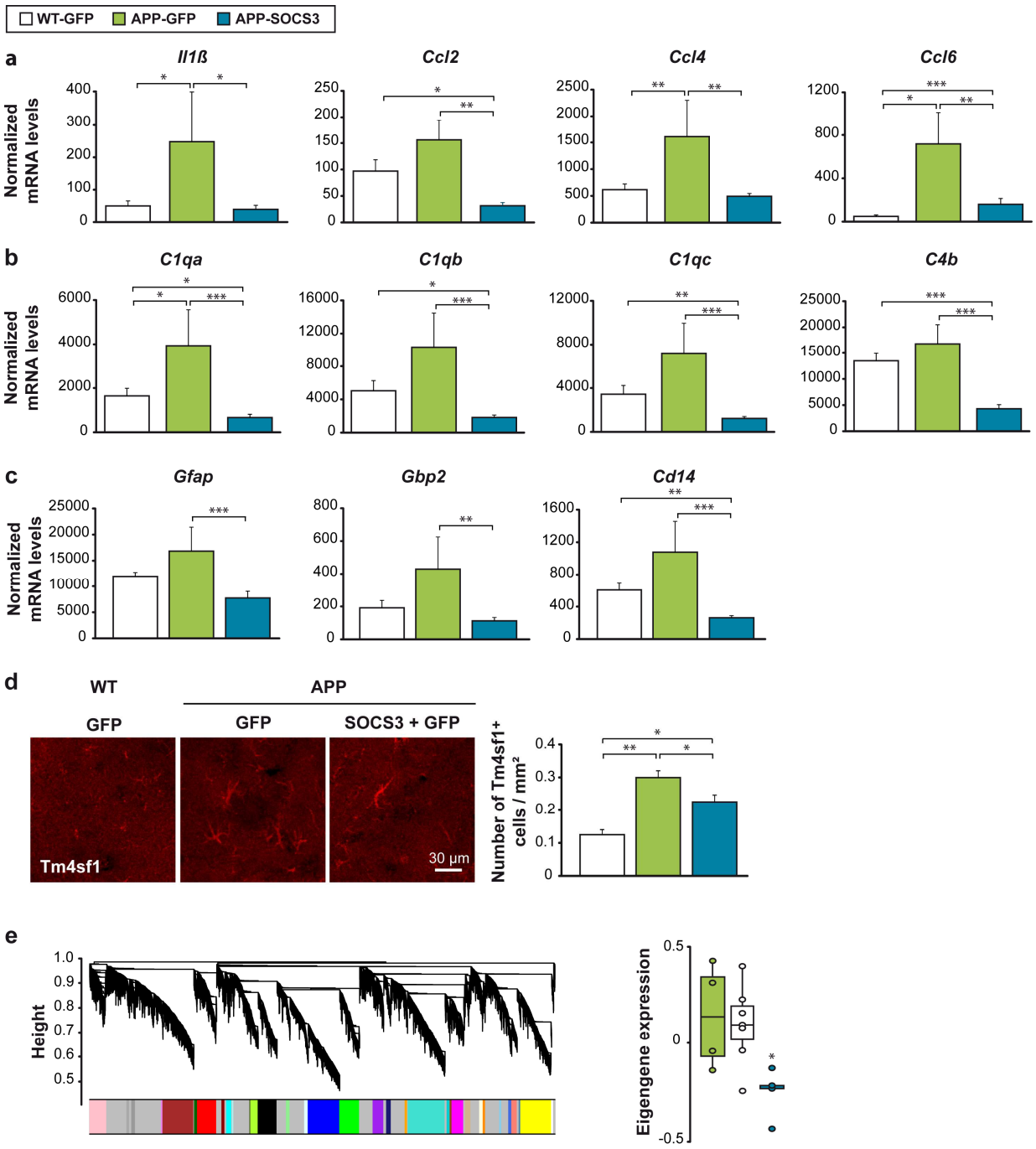

Figure 5. SOCS3 normalizes the transcriptional profile of reactive astrocytes in APP mice.

a-b, Reactive astrocytes in APP-GFP mice overexpress cytokines/chemokines (**a**) and genes of the complement cascade (**b**). SOCS3 normalizes their expression. N = 4-7/group. Wald test. **c,** SOCS3 decreases the expression of pan, A1 and A2 reactive astrocyte genes in APP mice. N = 4-7/group. Wald test. **d,** There are more reactive astrocytes expressing the A2 marker Tm4sf1 in APP-GFP mice than in control WT-GFP mice. SOCS3 reduces the number of Tm4sf1^{+} astrocytes in APP mice. N = 5-8/group. Kruskall-Wallis and Mann-Whitney tests. **e,** Dendrogram obtained by WGCNA. One module out of 19 was differentially expressed between the 3 groups. It is formed by genes that are down-regulated by SOCS3. N = 4-7/group. ANOVA. * $p < 0.05$, ** $p < 0.01$, *** $p < 0.001$.

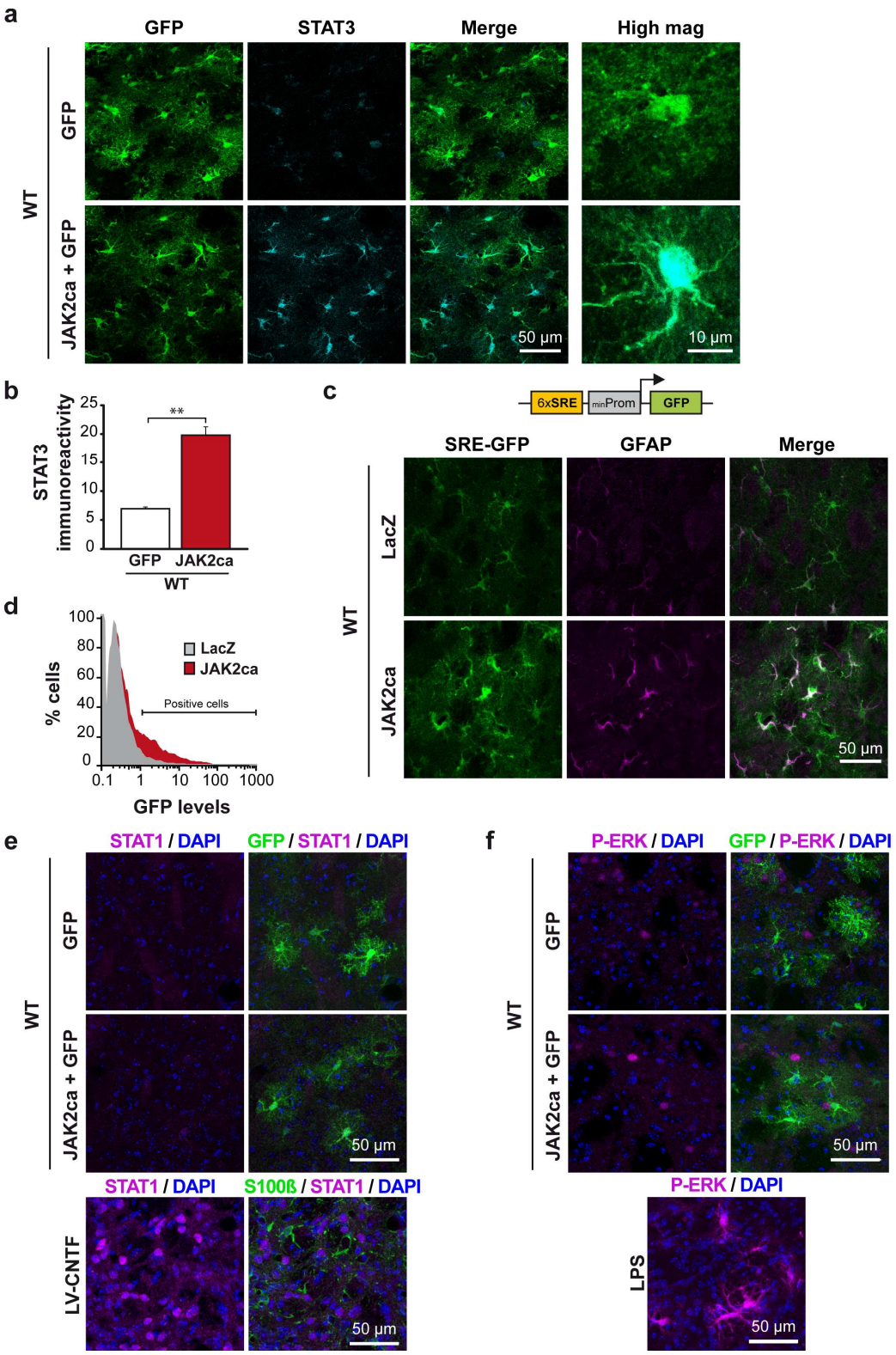

Figure 6. JAK2ca activates the JAK2-STAT3 pathway in striatal astrocytes.

a, Confocal images of striatal sections stained for GFP (green) and STAT3 (cyan) in WT mice injected in the striatum with a mixture of two AAVs encoding JAK2ca or GFP (JAK2ca + GFP), or only with an AAV encoding GFP (same viral titer). JAK2ca induces STAT3 nuclear accumulation in astrocytes. **b,** Quantification of STAT3 immunoreactivity. N = 4/group, paired *t* test. ** $p < 0.01$. **c-d,** JAK2ca expression in striatal astrocytes activates the SRE-GFP reporter, which is composed of 6 SRE driving GFP expression. Astrocytes in the JAK2ca group express higher GFP levels than in the control LacZ

group. This is visible on histological brain sections (**c**) and by FACS of acutely dissociated striatal cells (**d**). Representative images of N = 4/group. **e-f,** Confocal images of astrocytes stained in green for GFP and in magenta for STAT1 (**e**) or P-ERK (**f**) in WT-GFP and WT-JAK2ca mice. JAK2ca does not induce a detectable increased in STAT1 or P-ERK staining in astrocytes. In positive controls, CNTF triggers STAT1 accumulation in the nucleus of cells negative for S100β (stained in green) and LPS induces strong P-ERK immunoreactivity in cells with an astrocyte morphology. Representative images from N = 4/group.

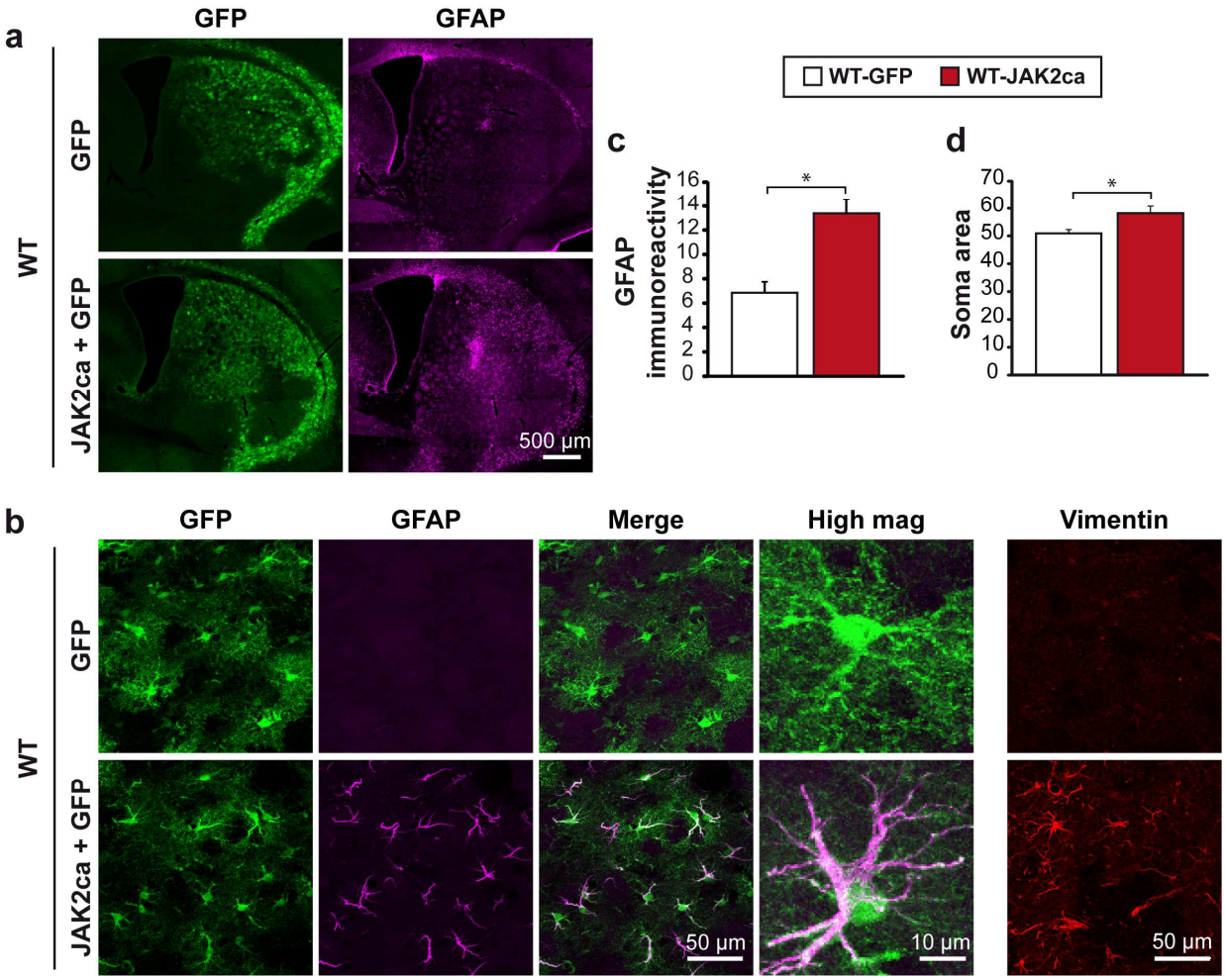

Figure 7. JAK2ca is sufficient to induce hallmarks of astrocyte reactivity in the striatum.

a, Representative 10x-tiled images showing area of infection (GFP^+, green) and GFAP (magenta) immunoreactivity in the striatum of WT mice injected with AAV-GFP or AAV-JAK2ca + AAV-GFP. JAK2ca increases GFAP levels in a large part of the striatum. **b,** Confocal images of astrocytes stained for GFP (green), GFAP (magenta) and vimentin (red) in WT-GFP and WT-JAK2ca mice. JAK2ca increases GFAP and vimentin expression in striatal astrocytes and induces morphological changes. **c,** GFAP immunoreactivity is increased by a factor 2 in JAK2ca-astrocytes N = 4/group, paired *t* test. **d,** Reactive astrocytes in WT-JAK2ca mice are hypertrophic, they have a larger soma. N = 4/group, paired *t* test. * $p < 0.05$.

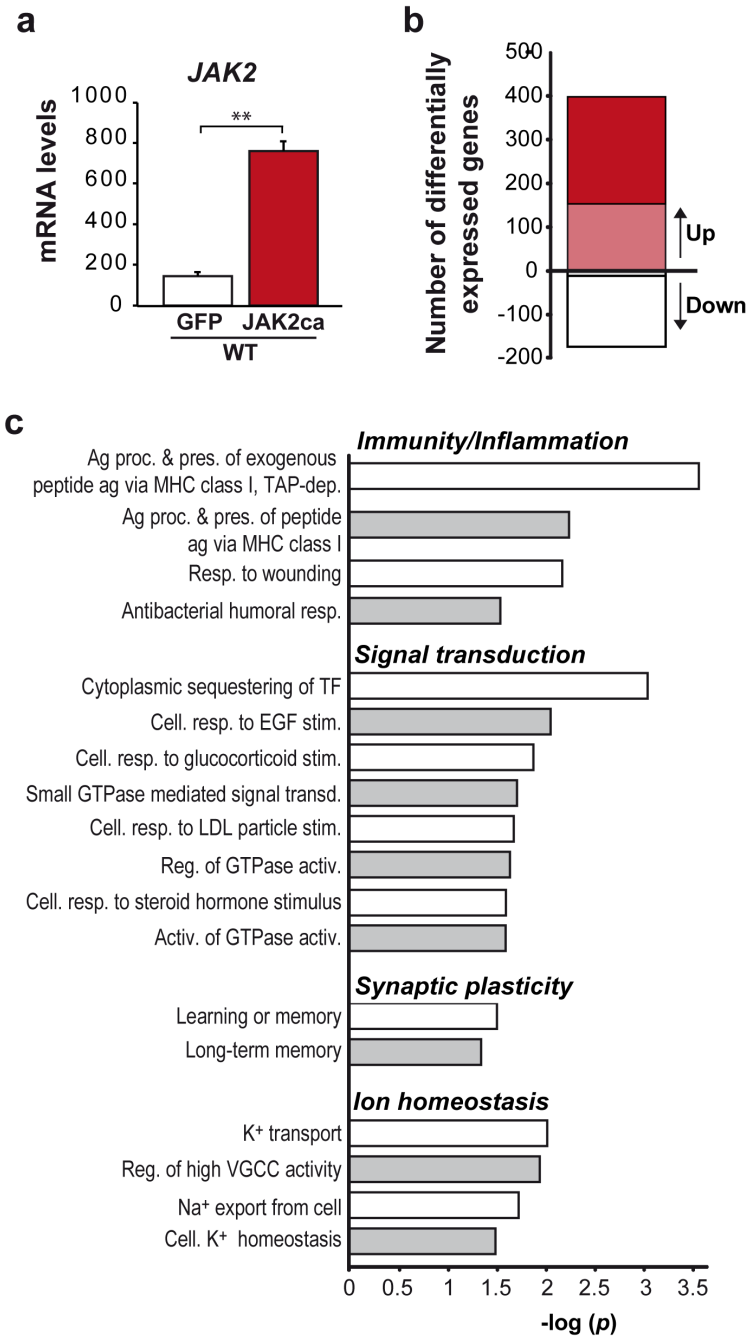

Figure 8. JAK2ca triggers significant transcriptional changes in astrocytes.

Microarray analysis of GFP^+ astrocytes sorted from adult mice injected with AAV-GFP or AAV-JAK2ca + AAV-GFP in the striatum. **a**, AAV-mediated gene transfer of JAK2ca in astrocytes induces a 4-fold increase in their *Jak2* mRNA levels. N = 4/group. Student *t* test. ** $p < 0.01$. **b,** JAK2ca changes the expression of nearly 600 probes, a majority being upregulated by JAK2ca. There are 245 probes significantly induced (red) and 164 probes repressed (white) in JAK2ca-astrocytes compared to control GFP-astrocytes. In addition, 158 probes are undetectable in control astrocytes but are well expressed in JAK2ca astrocytes (pale red). On the opposite, 11 probes were only detected in control astrocytes (grey). **c,** Pathway analysis on the genes regulated by JAK2Ca identifies several enriched biological processes linked to signaling, inflammation and immunity as well as memory and ion homeostasis. Activ. = activity/activation. Ag. = antigene. Cell. = cellular. Pos. = positive. Proc & Pres. = processing and presentation. Reg. = regulation. Resp. = response. Stim. = stimulation.

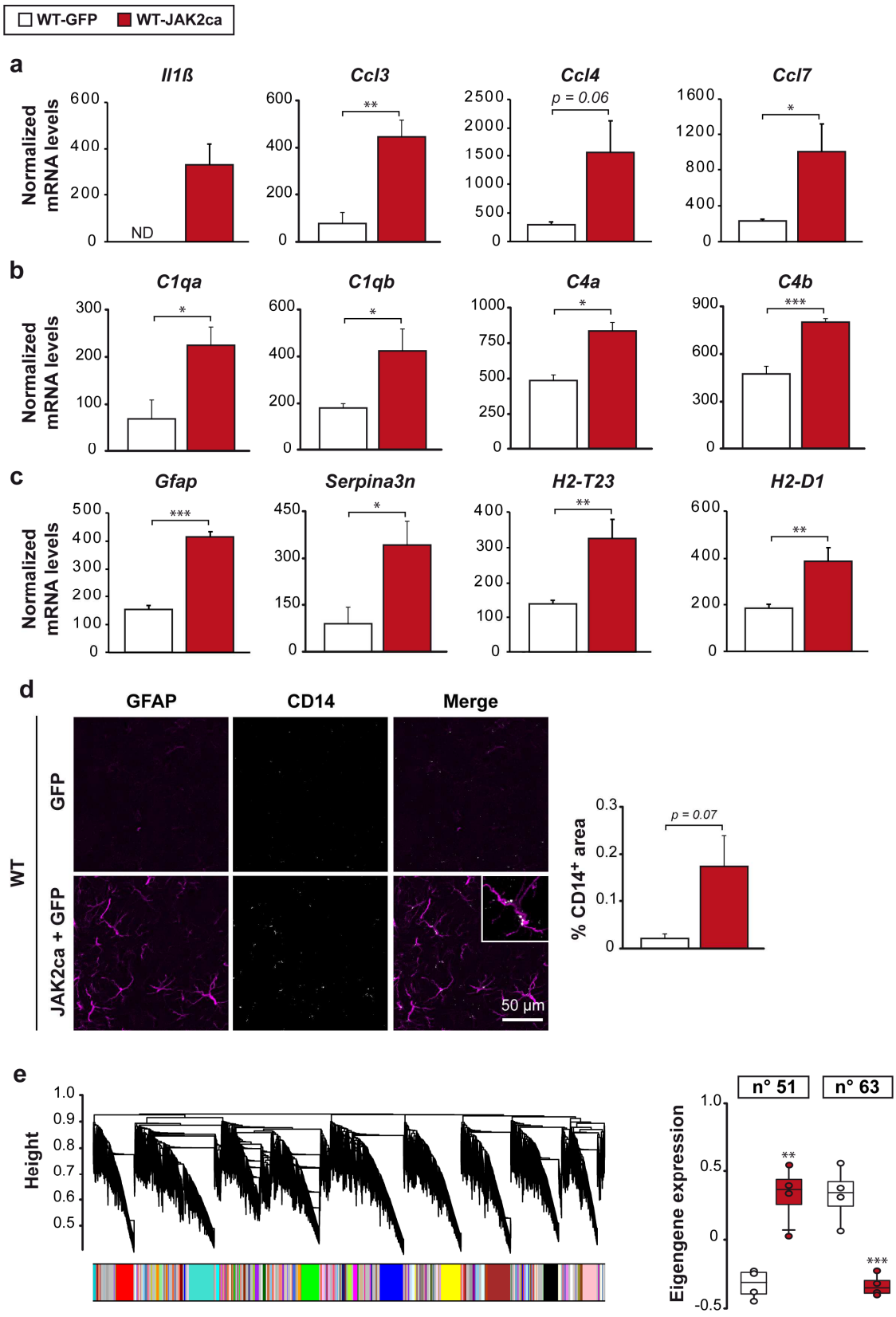

Figure 9. JAK2ca induces a reactive transcriptional profile in astrocytes.

mRNA levels of several cytokines/chemokines (**a**), complement factors (**b**) are higher in JAK2ca-astrocytes than in control GFP-astrocytes. N = 4/group. Student *t* test. **c,** JAK2ca also induces the expression of pan (*Gfap* and *Serpina3n*) and A1 (*H2-T23, H2-D1* and *Srgn)* reactive astrocyte genes. N = 4/group. Student *t* test. **d,** The A2 marker CD14 is increased by JAK2ca in striatal GFAP^{+} reactive

astrocytes. N = 4/group. Paired *t* test. **e**, Dendrogram generated by WGCNA. Eight modules of co-expressed genes that are differentially expressed between GFP and JAK2ca astrocytes are identified. Module n°51 includes genes up-regulated by JAK2ca, while module n°63 includes genes down-regulated by JAK2ca. N = 4/group. ANOVA. * $p < 0.05$, ** $p < 0.01$, *** p<0.001.

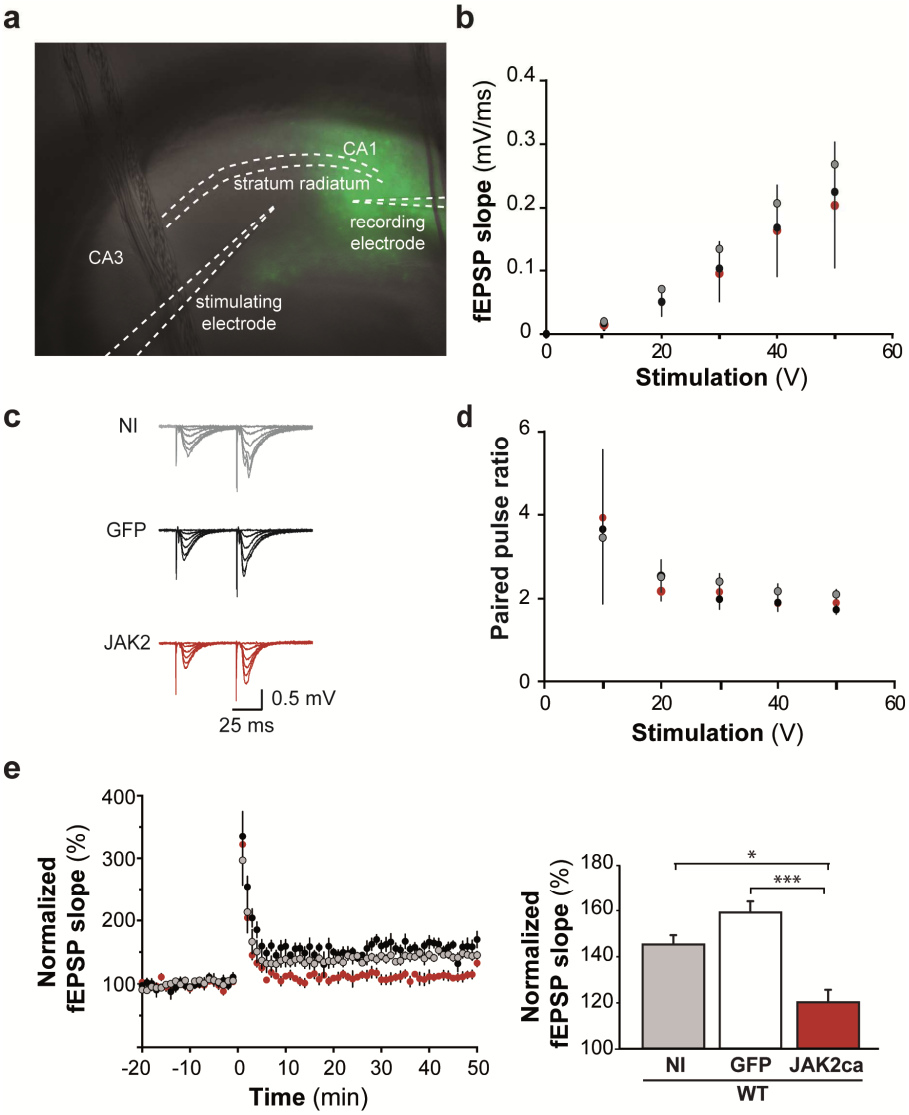

Figure 10. Activation of hippocampal astrocytes by JAK2ca alters synaptic plasticity.

a, Acute hippocampal slices were prepared from the hippocampus of non-injected (NI), WT-GFP and WT-JAK2ca mice. A recording electrode was placed in the GFP^+ CA1 region. **b,** No difference in the input/output relationship was observed between the 3 groups. N = 9-18/group. **c,** Representative traces obtained from the 3 groups when applying a paired-pulse stimulation protocol with increasing voltage. **d,** The paired-pulse ratio was similar in the 3 groups, whatever the voltage. N = 9-18/group. **e,** HFS potentiates fEPSP slopes by 40 to 60% in NI and WT-GFP mice but only by 20% in WT-JAK2ca mice. Left: average traces for each group for 20 min before to 50 min after HFS, induced at time 0. Right: quantification of normalized fEPSP slopes 40 to 50 min post HFS. N = 8-12/group. Kruskal-Wallis and Dunn's test. * p <0.05, *** $p < 0.001$.

TABLES

Name of cohort	Species & Gender	Transgenic line/ strain *(reference)*	Age at injection/ sacrifice	Viral vector type	Viral vectors	Total viral titer/site	Region	Stereotactic coordinates in mm (AP, L, V)
Tau mice	heterozygous female mice	THY-Tau22 *(Schindowski, 2006)*	12 mo	not applicable				
Tau rats	male rats *(d'Orange, 2017)*	Wistar	2 mo / 3 mo	AAV2/8	AAV-UT-GFP AAV-Tau^{P301L}	2.5.10^{10} VG	Hippocampus (posterior CA1)	-5.6, +/-5, -7
MPTP primates	male *Macaca fascicularis*	N/A	5-6 y / 9 mpi	not applicable (MPTP intramuscular injection)				
APP-SOCS3 (histology)	heterozygous male mice	APP/PS1dE9 *(Jankowski, 2004)*	3-5 mo / 12 mo	AAV2/9	AAV-GFP	5.10^{9} VG	Hippocampus (CA1)	-3, +/-3, -1.5
					AAV-SOCS3 + AAV-GFP	4.10^{9} VG + 1.10^{9} VG		
old APP-SOCS3 (histology)			15 mo / 16 mo		AAV-GFP	5.10^{9} VG		
					AAV-SOCS3 + AAV-GFP	4.10^{9} VG + 1.10^{9} VG		
APP-SOCS3 (RNAseq)			2-4 mo / 9 mo		AAV-GFP	7.10^{9} VG		
					AAV-SOCS3 + AAV-GFP	4.10^{9} VG + 3.10^{9} VG		
JAK2ca-striatum (histology, microarray)	male mice	C57bl6	2 mo / 3 mo	AAV2/9	AAV-GFP	5.10^{9} VG	Striatum	1, +/-2, -2.5
					AAV-JAK2ca + AAV-GFP	4.10^{9} VG + 1.10^{9} VG		
JAK2ca-striatum (histology, qPCR)				LV-Mok	LV-GFP	250 ng p24 +		
					LV-JAK2ca + LV-GFP	200 ng p24 + 50 ng p24		
JAK2ca-SRE (histology, FACS)			2 mo / 3 mo	LV-Mok	LV-LacZ + LV-SRE	60 ng p24 + 100 ng p24	Striatum	1, +/-2, -2.5
					LV-JAKca + LV-SRE	60 ng p24 + 100 ng p24		
JAK2ca-hippocampus (histology, electrophysiology)			2 mo / 4 mo	AAV2/9	AAV-GFP	5.10^{9} VG	Hippocampus (CA1)	-3, +/-3, -1.5
					AAV-JAK2ca + AAV-GFP	4.10^{9} VG + 1.10^{9} VG		

Table 1. List of animal cohorts used.

Animals were injected with 3 types of viral vectors: 1) AAV2/9 bearing a GFA_{ABC1D} promoter to target astrocytes; 2) AAV2/8 bearing a CBA promoter to target neurons, and 3) lentiviral vectors pseudotyped with the Mokola (Mok) envelope to target astrocytes (Colin et al., 2009). Viral loads are expressed as VG for AAVs and as ng of the p24 capsid protein for LV. The control group of each cohort is listed first. For transgenic mice, appropriate non-transgenic controls were included as well (see materiel and methods). Depending on the experiment, bilateral injections of the same viruses were performed and controls were generated in different animals. Alternatively, the contralateral brain region was injected with the control virus and the data was analyzed by paired *t* test. Mpi = months post-injection. Mo = month-old. UT = Untranslated.

Symbol	Gene name
Fxyd5 // Mir7050	FXYD domain-containing ion transport regulator 5 // microRNA 7050
Pcp4l1	Purkinje cell protein 4-like 1
Acvrl1	activin A receptor, type II-like 1
Igfbp7	insulin-like growth factor binding protein 7
Ly6e	lymphocyte antigen 6 complex, locus E
Itm2a	integral membrane protein 2A
Gm9817	predicted gene 9817
Arpc1b	actin related protein 2/3 complex, subunit 1B
Serping1	**serine (or cysteine) peptidase inhibitor, clade G, member 1**
Ctsh	cathepsin H
Apod	apolipoprotein D
Slc9a3r2	solute carrier family 9 (sodium/hydrogen exchanger), member 3 regulator 2
Lmo2	LIM domain only 2
Tpm1	tropomyosin 1, alpha
Tmem119	transmembrane protein 119
Rasip1 // Izumo1	Ras interacting protein 1 // izumo sperm-egg fusion 1
Bsg	basigin
Srgn	**serglycin**
Ly6c1	lymphocyte antigen 6 complex, locus C1
Hspb1	**heat shock protein 1**

Table 2: WGCNA: Top 20 most connected genes regulated by SOCS3 in APP astrocytes.

Top 20 most connected genes in the module differentially expressed between WT-GFP, APP-GFP and APP-SOCS3 astrocytes, as identified by WGCNA. Three of the top 20 hub genes, highlighted in bold, are pan or A1 reactive astrocyte genes.

a

Symbol	Gene name
E130014H08Rik	ankyrin repeat domain 44 (Ankrd44)
Gfap	**glial fibrillary acidic protein**
Stim2	stromal interaction molecule 2
Ifitm3	*interferon induced transmembrane protein 3*
Nfkbia	*NFKB inhibitor alpha*
EG381818	
Ccl3	*chemokine (C-C motif) ligand 3*
Prickle3	prickle homolog 3 (Drosophila)
Ctsc	cathepsin C
Bcdo2	beta-carotene 9', 10'-dioxygenase 2
LOC381561	similar to ribosomal protein L31
LOC641240	*h-2 class II histocompatibility antigen, A-U beta chain-like*
Lyzs	lysozyme
scl33870.2_144	
Gfap	**glial fibrillary acidic protein**
Gnb5	*guanine nucleotide binding protein, beta 5, transcript variant 2*
BC048562	
D030049N18Rik	
Plekho2	pleckstrin homology domain containing, family O member 2
Pex14	peroxisomal biogenesis factor 14

b

Symbol	Gene name
Ern1	endoplasmic reticulum to nucleus signaling 1
Golga7	golgi autoantigen, golgin subfamily a, 7, transcript variant 1
Fa2h	fatty acid 2-hydroxylase
Fez1	fasciculation and elongation protein zeta 1 (zygin I)
Car2	carbonic anhydrase 2
Map4k5	mitogen-activated protein kinase kinase kinase kinase 5, transcript variant 2
Carhsp1	calcium regulated heat stable protein 1
Ubp1	upstream binding protein 1
Tm7sf3	transmembrane 7 superfamily member 3
Ppp2r5d	protein phosphatase 2, regulatory subunit B (B56), delta isoform
Efhd1	EF-hand domain family member D1
Sft2d1	SFT2 domain containing 1
Cpox	coproporphyrinogen oxidase
Dpysl5	dihydropyrimidinase-like 5
Fez1	fasciculation and elongation protein zeta 1 (zygin I)
Ubp1	upstream binding protein 1 (Ubp1)
Psmd10	proteasome 26S subunit, non-ATPase, 10
Gltp	glycolipid transfer protein
Piga	phosphatidylinositol glycan anchor biosynthesis, class A
4921517B04Rik	tubulin tyrosine ligase-like family, member 7 (Ttll7)

Table 3: WGCNA: Top 20 most connected genes regulated by JAK2ca in WT astrocytes.

Top 20 most connected genes in the module of genes significantly induced (**a,** module N°51), or down-regulated (**b,** module N°63) in WT-JAK2ca astrocytes compared to WT-GFP astrocytes, as identified by WGCNA. *Gfap* (in bold), the universal marker of reactivity, is present twice within the module N°51, as well as several genes linked to signaling and neuroinflammation (in italics). Some genes appear twice because they were detected by two different probes on the microarray chip.

SUPPLEMENTAL MATERIAL

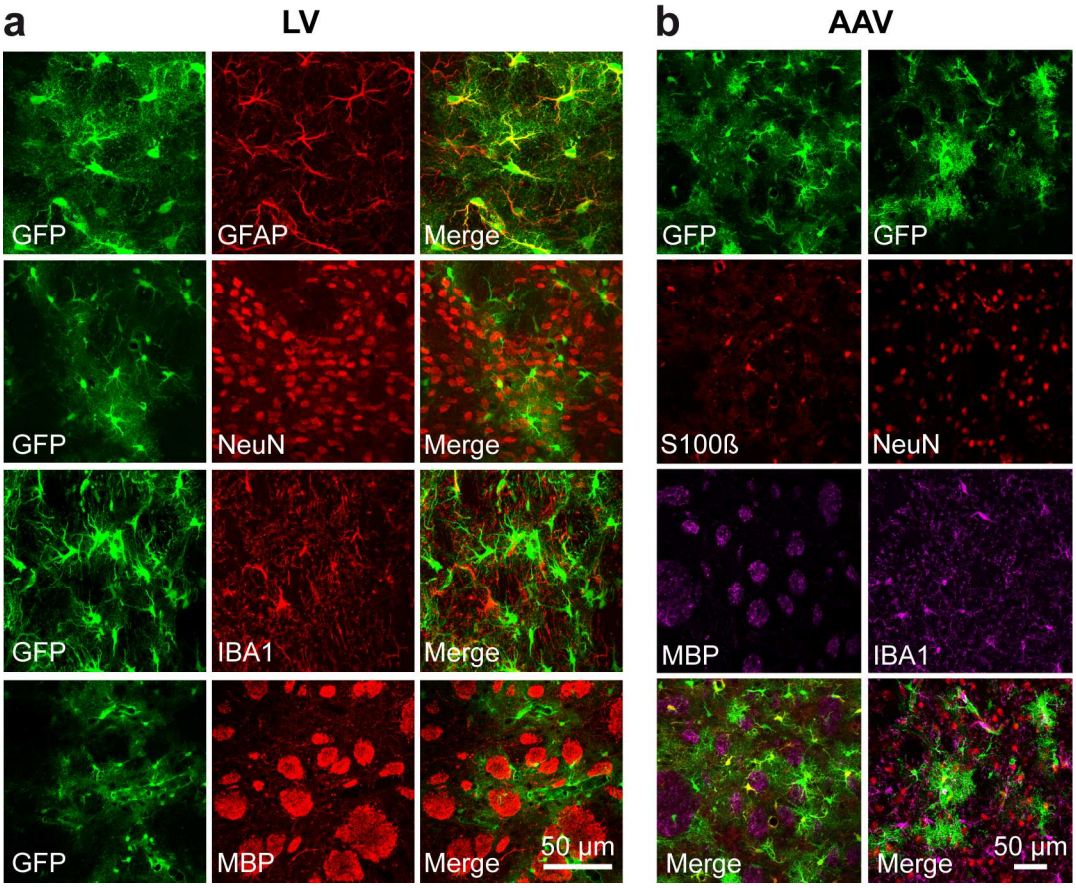

Supplemental figure 1. LV and AAV infect astrocytes selectively.

Injection in the mouse striatum of a LV (**a**) or AAV2/9 (**b**) encoding GFP and targeting astrocytes. GFP^+ cells co-express the astrocytic marker GFAP or S100β, but not the microglial marker IBA1, the neuronal marker NeuN or the oligodendrocyte marker MBP, demonstrating selective astrocyte tropism of the vector used.

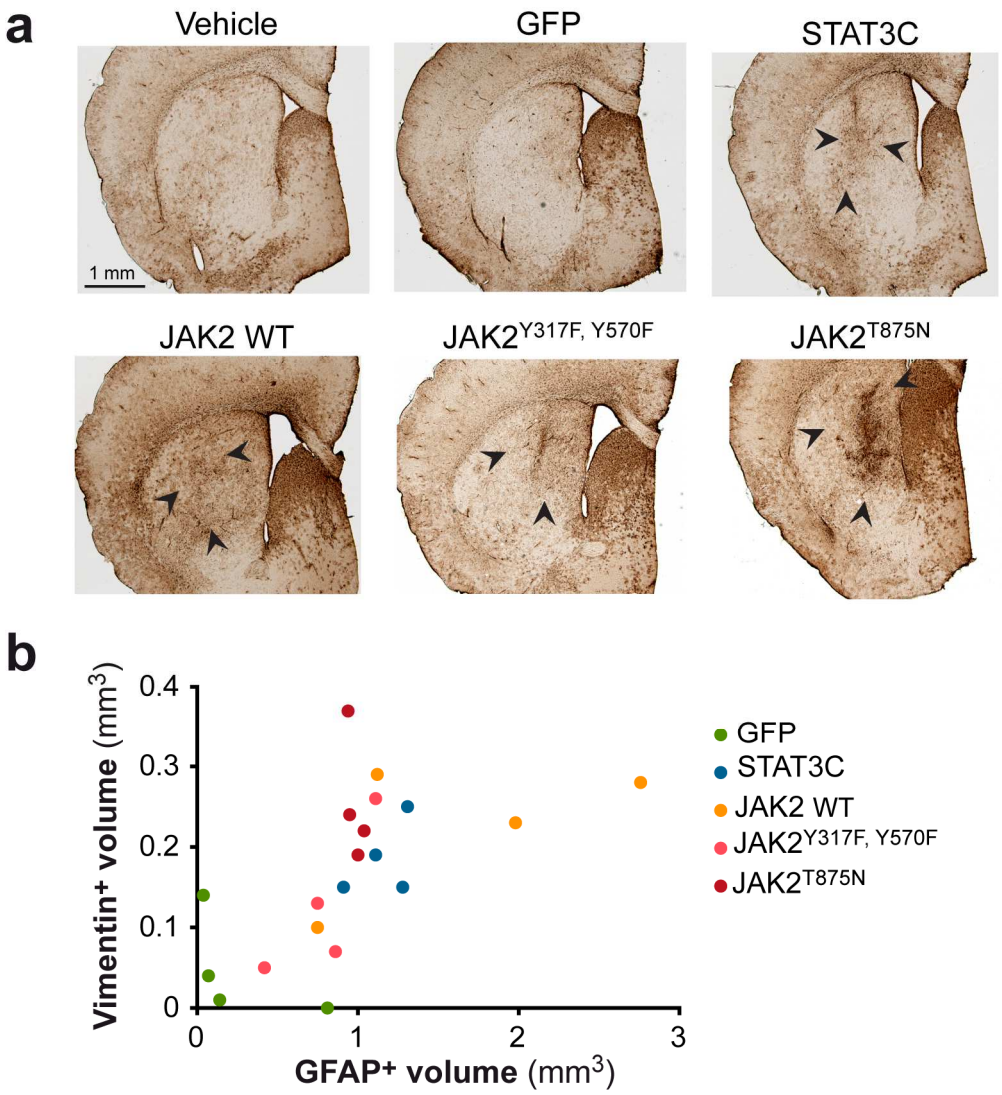

Supplemental figure 2. Overexpression of JAK2 and STAT3 mutants induces astrocyte reactivity in the mouse striatum.

a, Detection of GFAP$^+$ reactive astrocytes on brain sections from mice injected in the striatum with lentiviral vectors encoding WT or mutants constructs of STAT3 (STAT3C), JAK2 [JAK2 WT, JAK2$^{Y317F, Y570F}$, JAK2^{T875N} (JAK2ca)] and controls injected with LV-GFP or with vehicle (PBS, 1% BSA). GFAP expression is comparable in the 2 control groups and upregulated in mice injected with LV encoding STAT3 and JAK2 constructs. **b,** GFAP$^+$ and vimentin$^+$ volumes are higher in the striatum of mice injected with mutants of the JAK2-STAT3 pathway than in the control groups. N = 4/ group.

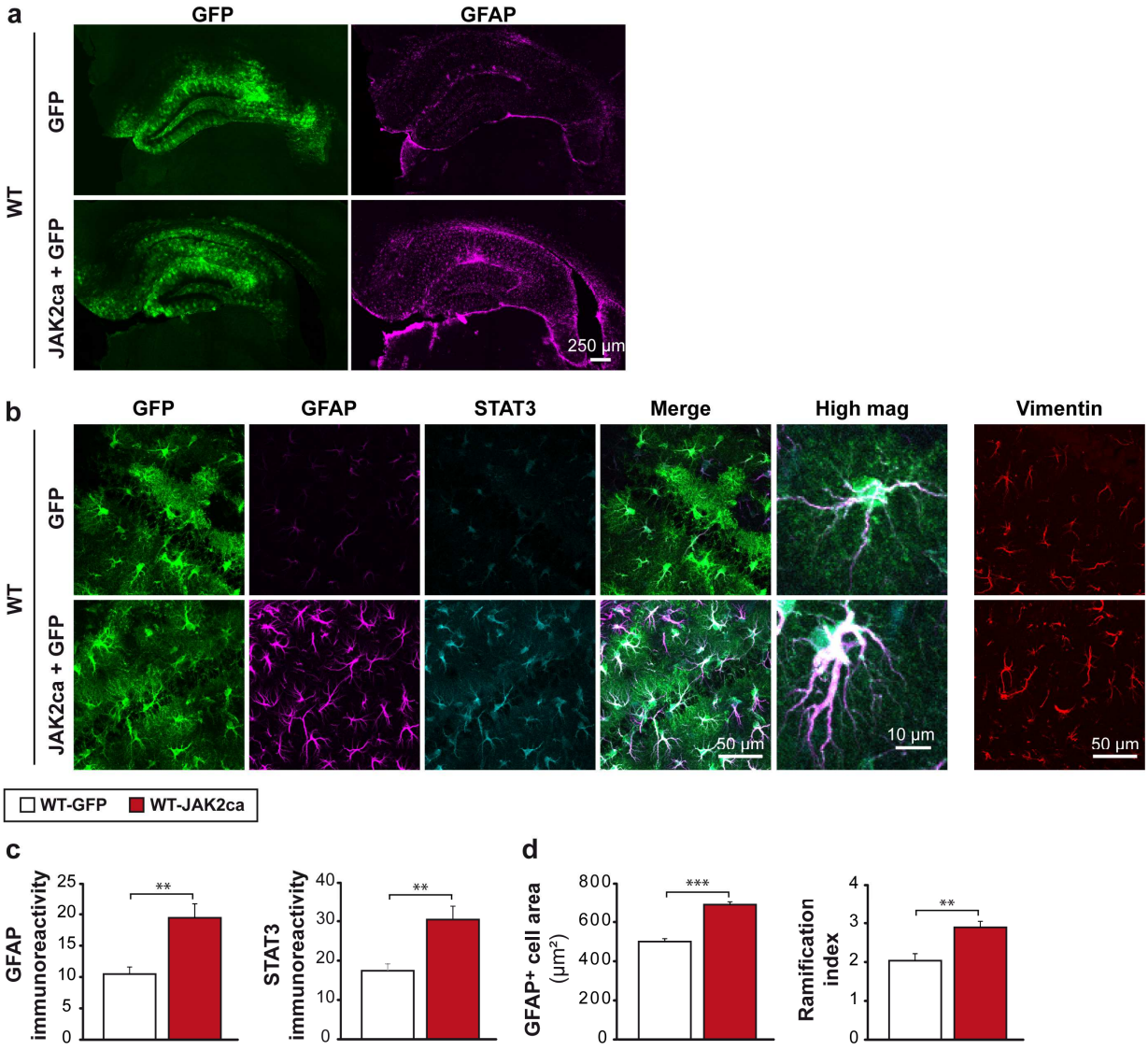

Supplemental figure 3. JAK2ca efficiently induces astrocyte reactivity in the hippocampus.

a, Representative 10x-tiled images showing area of infection (GFP^+, green) and GFAP (magenta) immunoreactivity in the hippocampus of WT mice injected at the same viral titer with AAV-GFP or AAV-JAK2ca + AAV-GFP. JAK2ca increased GFAP immunoreactivity in a large part of the hippocampus. **b,** Confocal images of astrocytes stained for GFP (green), GFAP (magenta) STAT3 (cyan) and vimentin (red) in WT mice. JAK2ca induces GFAP and vimentin overexpression, STAT3 nuclear accumulation and morphological changes in astrocytes. **c,** Quantification of immunostainings confirms that JAK2ca increases GFAP and STAT3 immunoreactivity in astrocytes. N = 4/group. Student *t* test. **d,** Sholl analysis applied to GFAP-labelled astrocytes shows that reactive astrocytes in WT-JAK2ca mice have a larger domain area and a higher ramification index (a measure of cell complexity). N = 5-6/group, Student *t* test. ** $p < 0.01$, *** $p < 0.001$.

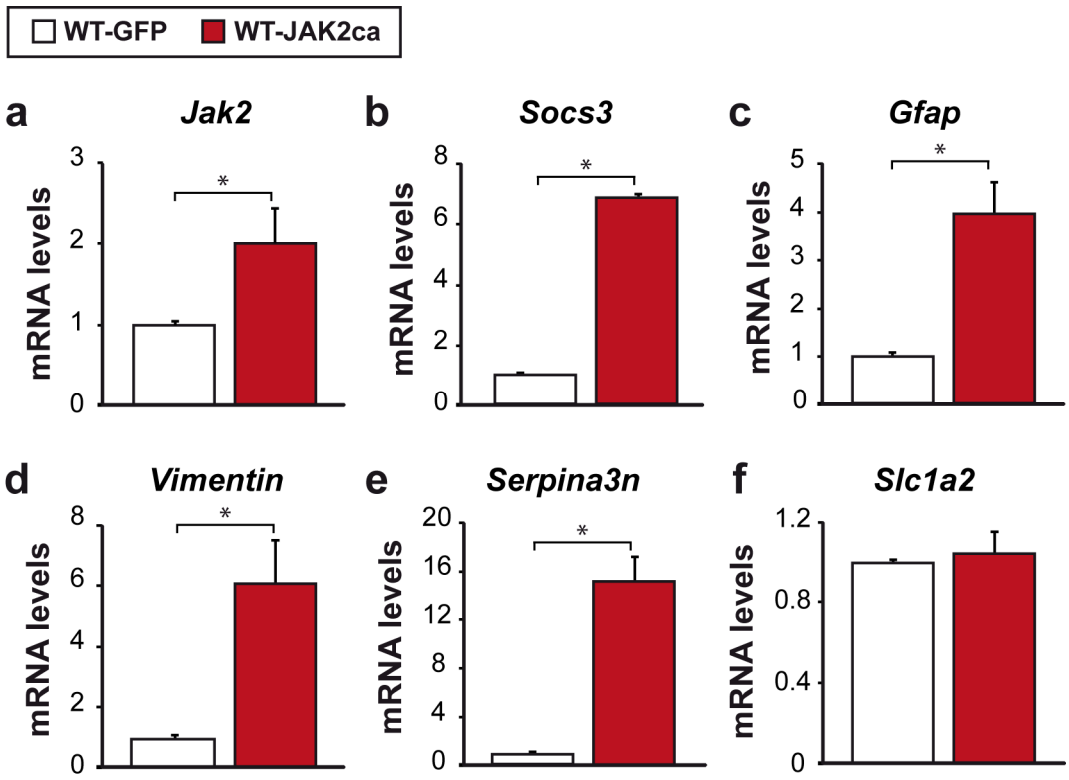

Supplemental figure 4. Validation of microarray data by qRT-PCR on bulk striatum samples.

RT-qPCR analysis on striatum samples from mice injected with LV-GFP or LV-JAK2ca. **a,** Validation of *jak2* overexpression in the JAK2ca-injected group. **b,** *Socs3* mRNA levels are increased in JAK2ca-astrocytes, an indication of activation of the upstream JAK2-STAT3 pathway. **c-f,** Reactive astrocyte markers *Gfap* (**c**), *Vimentin* (**d**) *Serpina3n* (**e**) are selectively upregulated by JAK2ca, whereas another astrocyte marker *Slc1a2* (**f**) is not differentially expressed between JAK2ca and GFP groups. N = 3-7/ group. Mann-Whitney test. * $p < 0.05$.

Gene	Forward primer	Reverse primer
Actin	AGAGGGAAATCGTGCGTGAC	CGATAGTGATGACCTGACCGT
Aldh1l1	TTCGCTGGCTGGTGTGATAAGA	GGTCAAGGTCAGGTTGCGGTT
Gfap	ACGACTATCGCCGCCAACT	GCCGCTCTAGGGACTCGTTC
Jak2	GTCTTGGGATGGCGGTGTTAG	ATTGCTGAATGAATCTGCGAAATCT
Ppia	ATGGCAAATGCTGGACCAAA	GCCTTCTTTCACCTTCCCAAA
Serpina3n	CAACCTTACAGGCCAACCCAT	GGGCACCAAGTAGTCCTAGATGCT
Slc1a2 (Glt1)	GGCAATCCCAAACTCAAGAAGC	GTCACTGTCTGAATCTGCTGGAAAC
Socs3	CGAGAAGATTCCGCTGGTACTGA	TGATCCAGGAACTCCCGAATG
Vimentin	TCGAGGTGGAGCGGGACAAC	TGCAGGGTGCTTTCGGCTTC

Supplemental table 1: Sequences of primers used for qPCR.

ACKNOWLEDGMENTS

This study was supported by CEA, CNRS and grants from the French National Research Agency (grants # 2010-JCJC-1402-1, 2011-BSV4-021-03 and ANR-16-TERC-0016-01), from Fondation Vaincre Alzheimer (grant # FR-15015) (to C.E.), as well as CNRS and INSERM (to S.H.R.O. and A.P). C.E. and A.P. received support from the Fédération pour la Recherche sur le Cerveau.

We thank Profs. Haan, Mayers, Bjørbæk, Shoelson and Yoshimura for sharing the plasmids for JAK2 mutants, SOCS3 and STAT3-C. We are grateful to Pr. L. Buée for sharing the Thy-Tau22 mice.

We thank Prof. N. Déglon for technical input at the initial part of the project. We are grateful to F. Aubry for his pilot experiments on FACS sorting and A. Vautheny for help with immunostainings on Tau mice. We thank D. Gonzales, S. Laumond, J. Tessaire and people at the animal facility of the NeuroCentre Magendie for mouse care.

REFERENCES

Anderson MA, Ao Y, Sofroniew MV (2014) Heterogeneity of reactive astrocytes. Neurosci Lett 565:23-29.

Araque A, Carmignoto G, Haydon PG, Oliet SH, Robitaille R, Volterra A (2014) Gliotransmitters travel in time and space. Neuron 81:728-739.

Aron Badin R, Spinnewyn B, Gaillard MC, Jan C, Malgorn C, Van Camp N, Dolle F, Guillermier M, Boulet S, Bertrand A, Savasta M, Auguet M, Brouillet E, Chabrier PE, Hantraye P (2013) IRC-082451, a novel multitargeting molecule, reduces L-DOPA-induced dyskinesias in MPTP Parkinsonian primates. PLoS One 8:e52680.

Ben Haim L, Carrillo-de Sauvage MA, Ceyzeriat K, Escartin C (2015a) Elusive roles for reactive astrocytes in neurodegenerative diseases. Frontiers in cellular neuroscience 9:278.

Ben Haim L, Ceyzeriat K, Carrillo-de Sauvage MA, Aubry F, Auregan G, Guillermier M, Ruiz M, Petit F, Houitte D, Faivre E, Vandesquille M, Aron-Badin R, Dhenain M, Deglon N, Hantraye P, Brouillet E, Bonvento G, Escartin C (2015b) The JAK/STAT3 Pathway Is a Common Inducer of Astrocyte Reactivity in Alzheimer's and Huntington's Diseases. J Neurosci 35:2817-2829.

Bromberg JF, Wrzeszczynska MH, Devgan G, Zhao Y, Pestell RG, Albanese C, Darnell JE, Jr. (1999) Stat3 as an oncogene. Cell 98:295-303.

Burda JE, Sofroniew MV (2014) Reactive gliosis and the multicellular response to CNS damage and disease. Neuron 81:229-248.

Carrero I, Gonzalo MR, Martin B, Sanz-Anquela JM, Arevalo-Serrano J, Gonzalo-Ruiz A (2012) Oligomers of beta-amyloid protein (Abeta1-42) induce the activation of cyclooxygenase-2 in astrocytes via an interaction with interleukin-1beta, tumour necrosis factor-alpha, and a nuclear factor kappa-B mechanism in the rat brain. Exp Neurol 236:215-227.

Ceyzeriat K, Abjean L, Carrillo-de Sauvage MA, Ben Haim L, Escartin C (2016) The complex STATes of astrocyte reactivity: How are they controlled by the JAK-STAT3 pathway? Neuroscience 330:205-218.

Chung YH, Joo KM, Lim HC, Cho MH, Kim D, Lee WB, Cha CI (2005) Immunohistochemical study on the distribution of phosphorylated extracellular signal-regulated kinase (ERK) in the central nervous system of SOD1G93A transgenic mice. Brain Res 1050:203-209.

Colin A, Faideau M, Dufour N, Auregan G, Hassig R, Andrieu T, Brouillet E, Hantraye P, Bonvento G, Deglon N (2009) Engineered lentiviral vector targeting astrocytes in vivo. Glia 57:667-679.

Crosio C, Valle C, Casciati A, Iaccarino C, Carri MT (2011) Astroglial inhibition of NF-kappaB does not ameliorate disease onset and progression in a mouse model for amyotrophic lateral sclerosis (ALS). PLoS One 6:e17187.

d'Orange M, Aurégan G, Cheramy D, Gaudin-Guérif M, Lieger S, Guillermier M, Stimmer L, Joséphine C, Hérard AS, Gaillard MC, Petit F, Kiessling MC, Schmitz C, Colin M, Buée L, Panayi F, Diguet E, Brouillet E, Hantraye P, Bemelmans AP, Cambon K (in revision) Potentiating tangle formation reduces acute toxicity of soluble Tau species in the rat. Brain.

Dobin A, Davis CA, Schlesinger F, Drenkow J, Zaleski C, Jha S, Batut P, Chaisson M, Gingeras TR (2013) STAR: ultrafast universal RNA-seq aligner. Bioinformatics 29:15-21.

Ehret GB, Reichenbach P, Schindler U, Horvath CM, Fritz S, Nabholz M, Bucher P (2001) DNA binding specificity of different STAT proteins. Comparison of in vitro specificity with natural target sites. J Biol Chem 276:6675-6688.

Escartin C, Brouillet E, Gubellini P, Trioulier Y, Jacquard C, Smadja C, Knott GW, Kerkerian-Le Goff L, Deglon N, Hantraye P, Bonvento G (2006) Ciliary neurotrophic factor activates astrocytes, redistributes their glutamate transporters GLAST and GLT-1 to raft microdomains, and improves glutamate handling in vivo. J Neurosci 26:5978-5989.

Eulenfeld R, Dittrich A, Khouri C, Muller PJ, Mutze B, Wolf A, Schaper F (2012) Interleukin-6 signalling: more than Jaks and STATs. European journal of cell biology 91:486-495.

Fan Y, Mao R, Yang J (2013) NF-kappaB and STAT3 signaling pathways collaboratively link inflammation to cancer. Protein & cell 4:176-185.

Fernandez AM, Jimenez S, Mecha M, Davila D, Guaza C, Vitorica J, Torres-Aleman I (2012) Regulation of the phosphatase calcineurin by insulin-like growth factor I unveils a key role of astrocytes in Alzheimer's pathology. Molecular psychiatry 17:705-718.

Ferreira TA, Blackman AV, Oyrer J, Jayabal S, Chung AJ, Watt AJ, Sjostrom PJ, van Meyel DJ (2014) Neuronal morphometry directly from bitmap images. Nature methods 11:982-984.

Frakes AE, Ferraiuolo L, Haidet-Phillips AM, Schmelzer L, Braun L, Miranda CJ, Ladner KJ, Bevan AK, Foust KD, Godbout JP, Popovich PG, Guttridge DC, Kaspar BK (2014) Microglia induce motor neuron death via the classical NF-kappaB pathway in amyotrophic lateral sclerosis. Neuron 81:1009-1023.

Furman JL, Sama DM, Gant JC, Beckett TL, Murphy MP, Bachstetter AD, Van Eldik LJ, Norris CM (2012) Targeting astrocytes ameliorates neurologic changes in a mouse model of Alzheimer's disease. J Neurosci 32:16129-16140.

Haan S, Wuller S, Kaczor J, Rolvering C, Nocker T, Behrmann I, Haan C (2009) SOCS-mediated downregulation of mutant Jak2 (V617F, T875N and K539L) counteracts cytokine-independent signaling. Oncogene 28:3069-3080.

Hara M, Kobayakawa K, Ohkawa Y, Kumamaru H, Yokota K, Saito T, Kijima K, Yoshizaki S, Harimaya K, Nakashima Y, Okada S (2017) Interaction of reactive astrocytes with type I collagen induces astrocytic scar formation through the integrin-N-cadherin pathway after spinal cord injury. Nat Med 23:818-828.

Heneka MT, Carson MJ, El Khoury J, Landreth GE, Brosseron F, Feinstein DL, Jacobs AH, Wyss-Coray T, Vitorica J, Ransohoff RM, Herrup K, Frautschy SA, Finsen B, Brown GC, Verkhratsky A, Yamanaka K, Koistinaho J, Latz E, Halle A, Petzold GC, Town T, Morgan D, Shinohara ML, Perry VH, Holmes C, Bazan NG, Brooks DJ, Hunot S, Joseph B, Deigendesch N, Garaschuk O, Boddeke E, Dinarello CA, Breitner JC, Cole GM, Golenbock DT, Kummer MP (2015) Neuroinflammation in Alzheimer's disease. Lancet Neurol 14:388-405.

Heneka MT, Kummer MP, Latz E (2014) Innate immune activation in neurodegenerative disease. Nature reviews Immunology 14:463-477.

Hol EM, Pekny M (2015) Glial fibrillary acidic protein (GFAP) and the astrocyte intermediate filament system in diseases of the central nervous system. Current opinion in cell biology 32:121-130.

Hong S, Beja-Glasser VF, Nfonoyim BM, Frouin A, Li S, Ramakrishnan S, Merry KM, Shi Q, Rosenthal A, Barres BA, Lemere CA, Selkoe DJ, Stevens B (2016) Complement and microglia mediate early synapse loss in Alzheimer mouse models. Science 352:712-716.

Hsiao HY, Chen YC, Chen HM, Tu PH, Chern Y (2013) A critical role of astrocyte-mediated nuclear factor-kappaB-dependent inflammation in Huntington's disease. Hum Mol Genet.

Huang da W, Sherman BT, Lempicki RA (2009) Systematic and integrative analysis of large gene lists using DAVID bioinformatics resources. Nature protocols 4:44-57.

Jankowsky JL, Fadale DJ, Anderson J, Xu GM, Gonzales V, Jenkins NA, Copeland NG, Lee MK, Younkin LH, Wagner SL, Younkin SG, Borchelt DR (2004) Mutant presenilins specifically elevate the levels of the 42 residue beta-amyloid peptide in vivo: evidence for augmentation of a 42-specific gamma secretase. Hum Mol Genet 13:159-170.

Jo S, Yarishkin O, Hwang YJ, Chun YE, Park M, Woo DH, Bae JY, Kim T, Lee J, Chun H, Park HJ, Lee DY, Hong J, Kim HY, Oh SJ, Park SJ, Lee H, Yoon BE, Kim Y, Jeong Y, Shim I, Bae YC, Cho J, Kowall NW, Ryu H, Hwang E, Kim D, Lee CJ (2014) GABA from reactive astrocytes impairs memory in mouse models of Alzheimer's disease. Nat Med.

John Lin CC, Yu K, Hatcher A, Huang TW, Lee HK, Carlson J, Weston MC, Chen F, Zhang Y, Zhu W, Mohila CA, Ahmed N, Patel AJ, Arenkiel BR, Noebels JL, Creighton CJ, Deneen B (2017) Identification of diverse astrocyte populations and their malignant analogs. Nat Neurosci 20:396-405.

Kang W, Hebert JM (2011) Signaling pathways in reactive astrocytes, a genetic perspective. Mol Neurobiol 43:147-154.

Kim SK, Nabekura J, Koizumi S (2017) Astrocyte-mediated synapse remodeling in the pathological brain. Glia 65:1719-1727.

Kuipers HF, Yoon J, van Horssen J, Han MH, Bollyky PL, Palmer TD, Steinman L (2017) Phosphorylation of alphaB-crystallin supports reactive astrogliosis in demyelination. Proc Natl Acad Sci U S A 114:E1745-E1754.
Langfelder P, Horvath S (2008) WGCNA: an R package for weighted correlation network analysis. BMC bioinformatics 9:559.
LeComte MD, Shimada IS, Sherwin C, Spees JL (2015) Notch1-STAT3-ETBR signaling axis controls reactive astrocyte proliferation after brain injury. Proc Natl Acad Sci U S A 112:8726-8731.
Lee Y, Messing A, Su M, Brenner M (2008) GFAP promoter elements required for region-specific and astrocyte-specific expression. Glia 56:481-493.
Lian H, Yang L, Cole A, Sun L, Chiang AC, Fowler SW, Shim DJ, Rodriguez-Rivera J, Taglialatela G, Jankowsky JL, Lu HC, Zheng H (2015) NFkappaB-Activated Astroglial Release of Complement C3 Compromises Neuronal Morphology and Function Associated with Alzheimer's Disease. Neuron 85:101-115.
Liddelow SA, Barres BA (2017) Reactive Astrocytes: Production, Function, and Therapeutic Potential. Immunity 46:957-967.
Liddelow SA, Guttenplan KA, Clarke LE, Bennett FC, Bohlen CJ, Schirmer L, Bennett ML, Munch AE, Chung WS, Peterson TC, Wilton DK, Frouin A, Napier BA, Panicker N, Kumar M, Buckwalter MS, Rowitch DH, Dawson VL, Dawson TM, Stevens B, Barres BA (2017) Neurotoxic reactive astrocytes are induced by activated microglia. Nature.
Linossi EM, Babon JJ, Hilton DJ, Nicholson SE (2013) Suppression of cytokine signaling: the SOCS perspective. Cytokine & growth factor reviews 24:241-248.
Love MI, Huber W, Anders S (2014) Moderated estimation of fold change and dispersion for RNA-seq data with DESeq2. Genome Biol 15:550.
Ma X, Reynolds SL, Baker BJ, Li X, Benveniste EN, Qin H (2010) IL-17 enhancement of the IL-6 signaling cascade in astrocytes. J Immunol 184:4898-4906.
Matyash V, Kettenmann H (2010) Heterogeneity in astrocyte morphology and physiology. Brain Res Rev 63:2-10.
Medeiros R, LaFerla FM (2013) Astrocytes: conductors of the Alzheimer disease neuroinflammatory symphony. Exp Neurol 239:133-138.
Mertens C, Darnell JE, Jr. (2007) SnapShot: JAK-STAT signaling. Cell 131:612.
Murray PJ (2007) The JAK-STAT signaling pathway: input and output integration. J Immunol 178:2623-2629.
Nicolas CS, Peineau S, Amici M, Csaba Z, Fafouri A, Javalet C, Collett VJ, Hildebrandt L, Seaton G, Choi SL, Sim SE, Bradley C, Lee K, Zhuo M, Kaang BK, Gressens P, Dournaud P, Fitzjohn SM, Bortolotto ZA, Cho K, Collingridge GL (2012) The Jak/STAT pathway is involved in synaptic plasticity. Neuron 73:374-390.
Noli L, Capalbo A, Ogilvie C, Khalaf Y, Ilic D (2015) Discordant Growth of Monozygotic Twins Starts at the Blastocyst Stage: A Case Study. Stem cell reports 5:946-953.
O'Callaghan JP, Sriram K (2004) Focused microwave irradiation of the brain preserves in vivo protein phosphorylation: comparison with other methods of sacrifice and analysis of multiple phosphoproteins. J Neurosci Methods 135:159-168.
Oddo S, Caccamo A, Shepherd JD, Murphy MP, Golde TE, Kayed R, Metherate R, Mattson MP, Akbari Y, LaFerla FM (2003) Triple-transgenic model of Alzheimer's disease with plaques and tangles: intracellular Abeta and synaptic dysfunction. Neuron 39:409-421.
Oeckl P, Lattke M, Wirth T, Baumann B, Ferger B (2012) Astrocyte-specific IKK2 activation in mice is sufficient to induce neuroinflammation but does not increase susceptibility to MPTP. Neurobiol Dis 48:481-487.
Orre M, Kamphuis W, Osborn LM, Jansen AH, Kooijman L, Bossers K, Hol EM (2014) Isolation of glia from Alzheimer's mice reveals inflammation and dysfunction. Neurobiol Aging 35:2746-2760.
Ortinski PI, Dong J, Mungenast A, Yue C, Takano H, Watson DJ, Haydon PG, Coulter DA (2010) Selective induction of astrocytic gliosis generates deficits in neuronal inhibition. Nat Neurosci 13:584-591.

Panatier A, Vallee J, Haber M, Murai KK, Lacaille JC, Robitaille R (2011) Astrocytes are endogenous regulators of basal transmission at central synapses. Cell 146:785-798.
Robertson SA, Koleva RI, Argetsinger LS, Carter-Su C, Marto JA, Feener EP, Myers MG, Jr. (2009) Regulation of Jak2 function by phosphorylation of Tyr317 and Tyr637 during cytokine signaling. Mol Cell Biol 29:3367-3378.
Rothhammer V, Mascanfroni ID, Bunse L, Takenaka MC, Kenison JE, Mayo L, Chao CC, Patel B, Yan R, Blain M, Alvarez JI, Kebir H, Anandasabapathy N, Izquierdo G, Jung S, Obholzer N, Pochet N, Clish CB, Prinz M, Prat A, Antel J, Quintana FJ (2016) Type I interferons and microbial metabolites of tryptophan modulate astrocyte activity and central nervous system inflammation via the aryl hydrocarbon receptor. Nat Med 22:586-597.
Schindowski K, Bretteville A, Leroy K, Begard S, Brion JP, Hamdane M, Buee L (2006) Alzheimer's disease-like tau neuropathology leads to memory deficits and loss of functional synapses in a novel mutated tau transgenic mouse without any motor deficits. Am J Pathol 169:599-616.
Sharma K, Schmitt S, Bergner CG, Tyanova S, Kannaiyan N, Manrique-Hoyos N, Kongi K, Cantuti L, Hanisch UK, Philips MA, Rossner MJ, Mann M, Simons M (2015) Cell type- and brain region-resolved mouse brain proteome. Nat Neurosci 18:1819-1831.
Shuai K, Liu B (2003) Regulation of JAK-STAT signalling in the immune system. Nature reviews Immunology 3:900-911.
Singh A, Abraham WC (2017) Astrocytes and synaptic plasticity in health and disease. Experimental brain research 235:1645-1655.
Sirko S, Behrendt G, Johansson PA, Tripathi P, Costa M, Bek S, Heinrich C, Tiedt S, Colak D, Dichgans M, Fischer IR, Plesnila N, Staufenbiel M, Haass C, Snapyan M, Saghatelyan A, Tsai LH, Fischer A, Grobe K, Dimou L, Gotz M (2013) Reactive glia in the injured brain acquire stem cell properties in response to sonic hedgehog glia. Cell stem cell 12:426-439.
Srinivasan K, Friedman BA, Larson JL, Lauffer BE, Goldstein LD, Appling LL, Borneo J, Poon C, Ho T, Cai F, Steiner P, van der Brug MP, Modrusan Z, Kaminker JS, Hansen DV (2016) Untangling the brain's neuroinflammatory and neurodegenerative transcriptional responses. Nature communications 7:11295.
Stephan AH, Barres BA, Stevens B (2012) The complement system: an unexpected role in synaptic pruning during development and disease. Annual review of neuroscience 35:369-389.
Tyzack GE, Sitnikov S, Barson D, Adams-Carr KL, Lau NK, Kwok JC, Zhao C, Franklin RJ, Karadottir RT, Fawcett JW, Lakatos A (2014) Astrocyte response to motor neuron injury promotes structural synaptic plasticity via STAT3-regulated TSP-1 expression. Nature communications 5:4294.
Viana da Silva S, Haberl MG, Zhang P, Bethge P, Lemos C, Goncalves N, Gorlewicz A, Malezieux M, Goncalves FQ, Grosjean N, Blanchet C, Frick A, Nagerl UV, Cunha RA, Mulle C (2016) Early synaptic deficits in the APP/PS1 mouse model of Alzheimer's disease involve neuronal adenosine A2A receptors. Nature communications 7:11915.
Volianskis A, Kostner R, Molgaard M, Hass S, Jensen MS (2010) Episodic memory deficits are not related to altered glutamatergic synaptic transmission and plasticity in the CA1 hippocampus of the APPswe/PS1deltaE9-deleted transgenic mice model of ss-amyloidosis. Neurobiol Aging 31:1173-1187.
Wojtowicz AM, Dvorzhak A, Semtner M, Grantyn R (2013) Reduced tonic inhibition in striatal output neurons from Huntington mice due to loss of astrocytic GABA release through GAT-3. Frontiers in neural circuits 7:188.
Wu Z, Guo Z, Gearing M, Chen G (2014) Tonic inhibition in dentate gyrus impairs long-term potentiation and memory in an Alzhiemer's disease model. Nature communications 5:4159.
Yang J, Liao X, Agarwal MK, Barnes L, Auron PE, Stark GR (2007) Unphosphorylated STAT3 accumulates in response to IL-6 and activates transcription by binding to NFkappaB. Genes & development 21:1396-1408.
Zamanian JL, Xu L, Foo LC, Nouri N, Zhou L, Giffard RG, Barres BA (2012) Genomic analysis of reactive astrogliosis. J Neurosci 32:6391-6410.
Zhang Y, Barres BA (2010) Astrocyte heterogeneity: an underappreciated topic in neurobiology. Curr Opin Neurobiol 20:588-594.

Contribution à l'article 1

Cet article rassemble plusieurs études complémentaires menées dans l'équipe. Mon travail expérimental dans cet article a consisté à réaliser les analyses histologiques, biochimiques et transcriptomiques de l'inhibition de la réactivité astrocytaire par SOCS3 dans les souris APP ainsi qu'à la validation de l'induction de la réactivité avec JAK2ca dans les souris WT. J'ai également participé à la rédaction de l'article ainsi qu'à la réalisation de l'ensemble des figures.

Conclusions

Dans cet article, nous avons mis évidence que la voie JAK2-STAT3 est une voie centrale, nécessaire et suffisante pour induire la réactivité astrocytaire. Nous avons développé des outils efficaces et versatiles pour moduler spécifiquement la réactivité astrocytaire, sans directement affecter les autres types cellulaires, en ciblant cette voie par transfert de gène. La surexpression de son inhibiteur SOCS3 dans les astrocytes permet de bloquer la réactivité et même de la reverser dans un modèle murin de la MA. A l'inverse, la surexpression d'une forme constitutivement active de JAK2 dans les astrocytes permet d'induire de nombreuses caractéristiques morphologiques et transcriptionnelles typiques de la réactivité dans des souris WT. Ces outils peuvent donc être utilisés pour induire/amplifier la réactivité ou l'inhiber dans de multiples contextes pathologiques dont la MA, mais également pour étudier les effets propres de la réactivité hors de tout contexte pathologique dans des souris WT.

2. La modulation de la réactivité astrocytaire dans des modèles murins de la MA révèle des effets subtiles et contexte-dépendants

Contexte, objectifs et synthèse de l'article 2

Comme présenté dans le chapitre 5 de l'introduction, l'implication des astrocytes réactifs dans la MA est très controversée. Ces résultats contradictoires peuvent s'expliquer par les multiples stratégies utilisées ainsi que les différents modèles animaux, présentant des contextes pathologiques spécifiques.

Nous avons montré dans l'article 1 que la voie JAK2-STAT3 est nécessaire et suffisante pour contrôler la réactivité astrocytaire. Afin de comprendre si la réactivité astrocytaire a un rôle global bénéfique ou délétère dans la MA, nous avons profité de la versatilité des vecteurs viraux que nous avons utilisé dans l'article 1 pour cibler spécifiquement les astrocytes dans l'hippocampe de souris APP/PS1dE9 (nommées APP dans la suite du manuscrit) et de souris 3xTg-AD (nommées 3xTg). Les souris ont été injectées avec un AAV-SOCS3 pour désactiver les astrocytes ou avec un AAV-JAK2ca pour les suractiver.

Après avoir validé l'efficacité de ces vecteurs dans les deux modèles, nous avons évalué l'effet de la modulation de la réactivité astrocytaire sur différents index de la MA, dans un contexte purement amyloïde (modèle APP/PS1dE9) ainsi que dans un contexte comprenant également la pathologie Tau (modèle 3xTg-AD), comme chez les patients atteints de la MA.

Nous avons ainsi mis en évidence des effets bénéfiques de SOCS3 sur la charge amyloïde dans le modèle APP à 9 mois. Des effets en miroirs ont été obtenus avec JAK2ca. Néanmoins, ces résultats ne semblent s'expliquer ni par une modification de la production de l'Aβ ni par une augmentation de sa dégradation par les enzymes clés ou par des transporteurs tels qu'ApoE. La désactivation astrocytaire n'impacte pas l'accumulation microgliale autour des plaques amyloïdes, ni leur profil transcriptionnel ou leur phagocytose de l'Aβ. De plus, aucune phagocytose par les astrocytes n'a été observée *in vivo.* Dans le modèle 3xTg-AD, étudié à 16-17 mois, aucun effet de la modulation de la réactivité astrocytaire sur la charge amyloïde ou la pathologie Tau n'a été mis en évidence. De façon très intéressante, une altération précoce de la LTP est observée à 8 mois dans les souris 3xTg et restaurée par SOCS3. Ces résultats suggèrent donc que la réactivité astrocytaire est impliquée précocement dans la souffrance neuronale liée à la MA. La réactivité astrocytaire est donc sensible au contexte pathologique et les fonctions affectées ne semblent pas être toujours les mêmes. Mais globalement, la réactivité astrocytaire semble avoir un effet délétère dans la MA.

Article 2

Modulation of astrocyte reactivity in mouse models of Alzheimer's disease reveals context-dependent effects on disease outcomes

Ceyzériat Kelly[1,2], Guillemaud Océane[1,2], Pommier Dylan[3,4#], Matos Marco[3,4#], Petit Fanny[1,2], Pépin Jérémy[1,2], Ben Haim Lucile[1,2], Carrillo-de Sauvage Maria-Angeles[1], Langlais Valentin[3,4], Saint-Georges Thomas[1,2], Bernier Sueva[1,2], Guillermier Martine[1,2], Gaudin Mylène[1,2], Hérard Anne-Sophie[1,2], Joséphine Charlène[1,2], Dechamps Nathalie[5], Bonvento Gilles[1,2], Dhenain Marc[1,2], Cambon K.[1,2], Oliet Stéphane H.R.[3,4], Brouillet Emmanuel[1,2], Flament Julien[1,2], Baijer Jan[5], Hantraye Philippe[1,2], Aude Panatier[3,4], Escartin Carole[1,2]

[1] Commissariat à l'Energie Atomique et aux Energies Alternatives, Département de la Recherche Fondamentale, Institut de Biologie François Jacob, MIRCen, F-92260 Fontenay-aux-Roses, France

[2] Centre National de la Recherche Scientifique, Université Paris-Sud, UMR 9199, Neurodegenerative Diseases Laboratory, F-92260 Fontenay-aux-Roses, France

[3] Neurocentre Magendie, INSERM U1215, 33077 Bordeaux, France

[4] Université de Bordeaux, 33077 Bordeaux, France

[5] Commissariat à l'Energie Atomique et aux Energies Alternatives, Département de la Recherche Fondamentale, Institut de Biologie François Jacob, Institut de Radiobiologie Cellulaire et Moléculaire, Inserm U967, F-92260 Fontenay-aux-Roses, France et Université Paris-Diderot et Université Paris-Sud, Paris, France.

# equal contribution

Key words: Reactive astrocytes – Neurodegenerative diseases – Adeno-associated viruses – Neuroinflammation – JAK-STAT pathway – SOCS3

Corresponding author:
Carole Escartin
MIRCen
18, route du Panorama
92260 Fontenay-aux-roses
carole.escartin@cea.fr

Number of pages: 39
Number of figures: 10
Number of words in Abstract: 271
Introduction: 1083
Discussion: 1858

Conflict of interest
The authors declare no competing financial interests.

ABBREVIATION LIST

3xTg	Triple transgenic mice (3xTg-AD)
AAV	Adeno-associated vectors
ACSF	Artificial cerebrospinal fluid
AD	Alzheimer's disease
ApoE	Apolipoprotein E
APP	Amyloid precursor protein
BACE1	Beta-secretase 1
BSA	Bovine serum albumin
CN	Calcineurin
DAM	Disease-associated microglia
FACS	Fluorescence-activated cell sorting
fEPSP	Field excitatory post-synaptic potentials
GluCEST	Chemical exchange saturation transfer of glutamate
HBSS	Hank's balanced salt solution
HFS	High-frequency stimulation
IDE	Insulin-degrading enzyme
i.p.	Intraperitoneal injection
JAK2	Janus kinase 2
JAK2ca	Constitutively active JAK2
LTP	Long term potentiation
MTRasym	Asymmetrical magnetization transfer ratio
MXO4	Methoxy-XO4
ND	Neurodegenerative diseases
NFAT	Nuclear factor of activated T-cells
NGS	Normal goat serum
NMR	Nuclear magnetic resonance
PBS	Phosphate buffer saline
PBST	0.2% Triton X-100 in PBS
PFA	Paraformaldehyde
RT	Room temperature
STAT3	Signal transducer and activator of transcription 3
SOCS3	Suppressor of cytokine signaling 3
TBST	Tris buffer saline and 0.1% Tween 20
VG	Viral genome
WT	Wild type

ABSTRACT

Neuroinflammation is a hallmark of neurodegenerative diseases (ND) including Alzheimer's disease (AD). This complex process mounts over decades and involves the activation of astrocytes and microglial cells in the brain, and recruitment of peripheral immune cells.

Over the last decades, many studies have explored the role of neuroinflammation in AD pathogenesis. Most of the time, quite unspecific or drastic manipulations are used, targeting multiple cell types in the brain or inducing possible developmental changes or peripheral side effects.

Here, we aim to explore the specific roles of reactive astrocytes in AD by modulating astrocyte reactivity in adult mouse brains. To this aim, we used AAV-gene transfer in astrocytes to manipulate the JAK2-STAT3 cascade, a central cascade for reactivity, in the hippocampus of two mouse models of AD, the APP/PS1dE9 and 3xTg-AD mice.

Inhibition or activation of the JAK2-STAT3 pathway by SOCS3 or a constitutive form of JAK2 modulates astrocyte reactivity accordingly, in the two mouse models. We show that astrocyte reactivity promotes amyloid deposition in APP/PS1dE9 mice. This was not due to changes in microglial molecular profile or phagocytic activity. Interestingly, modulation of astrocyte reactivity in 3xTg-AD did not impact amyloid or Tau pathology. However, inhibition of astrocyte reactivity was able to completely recover deficits in synaptic plasticity at CA3-CA1 synapses in 3xTg-AD mice.

Our original approach to specifically manipulate astrocyte reactivity *in situ* uncovers complex and context-dependent roles for reactive astrocytes in AD. It calls for more experiments to delineate the fine impact of reactivity in each disease situation and on each astrocyte function. Only then we will be able to use these complex yet potent cells for therapeutic purposes.

INTRODUCTION

Alzheimer's disease (AD) is a devastating neurodegenerative disease and the most common form of dementia (Querfurth and LaFerla, 2010). It is characterized by extracellular accumulation of amyloid plaques, Tau hyper-phosphorylation, synaptic alterations and neuronal degeneration. The exact mechanisms responsible for these disease hallmarks are still disputed. There is now a growing recognition that AD is not only caused by cell-autonomous processes within neurons, but that glial cells also play a key role (Heneka et al., 2015, De Strooper and Karran, 2016).

Astrocytes and microglial cells are in charge of key functions in the brain, ranging from neurotransmitter recycling, ion homeostasis, metabolic and trophic support, immune surveillance and debris clearance (Barres, 2008). In the brain of AD patients or in AD animal models, glial cells are reactive and participate in neuroinflammation. Longitudinal brain imaging studies on AD patients or histological analysis of animal models show that glial reactivity may occur at early stages, even before amyloid deposition (Heneka et al., 2005, Hamelin et al., 2016). It thus raises the question of the possible contribution of glial cells to neuronal dysfunction and death in AD. To determine the role of neuroinflammation in AD, various strategies have been used in animal models of AD. They are based on the expression/inhibition of cytokines, pro-inflammatory molecules or intracellular signaling elements (Guillot-Sestier et al., 2015, Krauthausen et al., 2015, Lian et al., 2015, Dansokho et al., 2016, Shi et al., 2017), through injection of recombinant proteins, viral vectors or breeding with mice knock-out for genes linked to neuroinflammation (Zheng et al., 2016). These recent studies have shed new light on the potential contribution of glial cells to AD. However, such strategies classically impact multiple cell types in the brain and sometimes peripheral immune cells, and could have significant development side effects. Most importantly, it is usually not possible to isolate the specific roles played by reactive astrocytes. Given the key supportive functions operated by astrocytes in the normal brain, it is important to understand how their reactive state impact these functions.

Reactive astrocytes are characterized by morphological changes as well as upregulation of intermediate filament proteins [Glial fibrillary acidic protein (GFAP), vimentin, (Hol and Pekny, 2015)]. Much less is known about their functional features and how they impact AD outcomes (Ben Haim et al., 2015a). The study of specific astrocyte function in AD models in cells or *in vivo* reveals multiple changes in specific functions including metabolic support (Allaman et al., 2010, Sancheti et al., 2014), neurotransmitter recycling (Masliah et al., 1996), antioxidant defense (Allaman et al., 2010, Abeti et al., 2011) or regulation of synapses and synaptic transmission (Delekate et al., 2014, Jo et al., 2014, Wu et al., 2014, Lian et al., 2015); for review see (Ben Haim et al., 2015a). From these observations, it is still difficult to determine how reactive astrocytes contribute to AD because these changes are predicted to have either beneficial, detrimental or mixed effects. The inhibition of astrocyte reactivity would better identify the global contribution of reactive astrocytes to AD and determine if they are appropriate therapeutic targets. Knocking out GFAP and vimentin from astrocytes in an attempt to perturb reactivity, exacerbates amyloid plaque formation and neurite dystrophy in AD mice (Kraft et al., 2013). But the effect on plaques was no reproduced in a different cohort (Kamphuis et al., 2015). On the contrary, reduction of astrocyte reactivity by the inhibition of the Calcineurin/Nuclear factor of activated T-cells (CN/NFAT) pathway lowers amyloid deposition and

normalizes synaptic transmission in the same mouse model (Furman et al., 2012). These contradictory results emphasize the need for a better understanding of the role of astrocyte reactivity in AD, using more selective and efficient strategies to manipulate astrocyte reactivity. We recently showed that the Janus kinase 2-Signal transducer and activator of transcription 3 (JAK2-STAT3) pathway is a master regulator of reactivity in astrocytes (Ben Haim et al., 2015a, Ben Haim Ceyzériat et al., submitted). Inhibition of this pathway by overexpression of its inhibitor suppressor of cytokine signaling 3 (SOCS3) by viral gene transfer in astrocytes efficiently blunted and even reversed morphological and molecular hallmarks of astrocyte reactivity in AD mice. Therefore, viral gene transfer of SOCS3 in reactive astrocytes offers a unique possibility to understand the global role of reactivity in AD, by providing an efficient and complete inhibition of reactivity.

In this study, we took advantage of these new viral-vector based strategies to modulate astrocyte reactivity in the hippocampus of murine AD models. We used two complementary mouse models of AD, [APP/PS1dE9 mice (Jankowsky et al., 2004) and 3xTg-AD mice, which also develop Tau pathology (Oddo et al., 2003)] and characterized the consequences of astrocyte modulation at the molecular, biochemical, histological, functional and behavioral levels. We show that reactive astrocytes influence several AD pathological hallmarks, including amyloid deposition and defects in synaptic plasticity, but in a context-dependent manner.

MATERIEL AND METHODS

Animals.

APP/PS1dE9 transgenic mice (APP; http://jaxmice.jax.org/strain/005864.html) harbor a chimeric mouse/human *App* gene with the Swedish mutations K595N and M596L (APPswe) and the human *Psen1* variant lacking exon 9 on a C57BL/6J background. Both transgenes are under the prion promoter (Jankowsky et al., 2004). Non transgenic littermates were used as controls. Triple transgenic AD (3xTg) mice express human APPswe and human TauP301L under a Thy-1 promoter as well as a point mutation on the mouse *Psen1* gene (PS1M146V), on a mixed C57BL/6J x 129Sv background (Oddo et al., 2003). C57BL/6J x 129Sv mice were used as controls. Breeding pairs were obtained from the Mutant Mouse Regional Resource Centers. All experimental protocols were approved by a local ethics committee and submitted to the French Ministry of Education and Research (Approvals # APAFIS#4565-20 16031711426915 v3 and APAFIS#4503-2016031409023019). They were performed in strict accordance with recommendations of the European Union (2010-63/EEC) for the care and use of laboratory animals.

Viral vectors.

Adeno-associated viruses of serotype 9 (AAV2/9) encoding murine SOCS3, JAK2^{T875N} (a constitutive active form of JAK2 (JAK2ca), (JAK2ca, Haan et al., 2009)) or GFP were used. All transgenes were under the control of the GFA_{ABC1D} promoter, a synthetic promoter of GFAP (Lee et al., 2008), which drives transgene expression in astrocytes (**Supplemental Fig. 1b**). AAV-GFP was co-injected with AAV-SOCS3 or AAV-JAK2ca (at the same total viral titer) to visualize infected cells.

Stereotactic injections.

Before surgery, APP mice were anesthetized with an intra-peritoneal (*i.p.*) injection of ketamine (100 mg/kg) and medetomidine (0.25 mg/kg) followed by atipamezole (0.25 mg/kg) injection 45 min after induction. 3xTg mice were anesthetized with a mixture of ketamine (100 mg/kg) and xylazine (10 mg/kg). Subcutaneous injection of lidocaine (7 mg/kg) was also performed at the incision site, 10 min before injections. AAV were diluted in 0.1 M phosphate buffer saline (PBS) with 0.001% pluronic acid, at a final total concentration of 2.5 10^9 viral genome (VG)/µl. Two µl of the viral suspensions were injected at a rate of 0.2 µl/min. Cannula were left in place for 5 min at the end of injection, before being slowly removed and the skin was sutured. Several APP and 3xTg mouse cohorts were analyzed, the number of mice analyzed per group is specified for each outcome measure. Within each cohort, WT mice were injected with AAV-GFP (WT-GFP), at the same total viral titer. Male APP mice were injected at 2-4 months with either AAV-SOCS3 + AAV-GFP (APP-SOCS3 mice) or AAV-JAK2ca + AAV-GFP (APP-JAK2ca mice). APP mice were analyzed at 9-12 months. Similarly, female 3xTg mice were injected at 3-6 months with AAV-GFP, AAV-SOCS3 + AAV-GFP or AAV-JAK2ca + AAV-GFP and post-mortem analysis was done at 16-17 months. For electrophysiological recordings 3xTg mice were injected at 3 months and recordings were performed at 7-8 months. The CA1 region was targeted with the following stereotactic coordinates: antero-posterior (AP) - 2 mm, lateral (L) +/- 2 mm and ventral (V) - 1.2 mm, from dura with tooth bar set at 0 mm. These coordinates were later modified to increase AAV diffusion (AP -3 mm, L +/-3 mm, V -1.5 mm).

Flow cytometry.

Three hours before sacrifice, mice received an *i.p.* injection of 10 mg/kg methoxy-XO4 (MXO4; Tocris, Bristol, UK, diluted at 2.5 mg/ml in 50% DMSO in saline, pH = 12) to label amyloid material and monitor its uptake in cells (Krauthausen et al., 2015). Mice were perfused for 4 min with cold dPBS. Their hippocampus was rapidly collected in Hank's Balanced Salt Solution (HBSS, Sigma, Saint-Louis, MO). Cells were mechanically and enzymatically dissociated with fire-polished Pasteur pipettes and the neural tissue dissociation kit with papaïn (Miltenyi Biotec, Bergisch Gladbach, Germany), following the manufacturer's instructions. After filtration through a 50 µm-filter, cells were centrifuged 10 min at 300 g. Then, myelin removal beads II (Miltenyi Biotec) and MS columns (Miltenyi Biotec) were used to deplete myelin from cell suspensions. Cells were centrifuged at 300 g for 5 min at 4°C and resuspended in 1: 100 Fc block (TruStain FcX™, anti-mouse CD16/32, Biolegend, San Diego, CA) in HBSS for 10 min on ice to prevent antibody binding to Fc receptors. Samples were centrifuged at 300 g for 5 min at 4°C and resuspended in cell staining buffer (Biolegend) with 1: 100 anti-CD11b-PE (eBioscience, San Diego, CA) and 1: 300 anti-CD45-PE-Cy5 (eBioscience) for 30 min on ice, under mild agitation. Cells were centrifuged at 300 g for 5 min at 4°C and resupended in 400 µl HBSS. Cell sorting was performed on a BD Influx cell sorter with the following configuration:

Staining	Lasers	Detectors
Methoxy-XO4	408 nm	450/30
GFP	488 nm	530/40
CD11b-PE	561 nm	594/26
CD45-PECy5	561 nm	670/30

Control samples of unlabeled and of mono-fluorescent brain cells were used to set up detector gains and position sort gates, which were kept constant for all sorted samples. We found that compensation was not required to accurately quantify MXO4, GFP, CD11b-PE ad CD45-PECy5 signals within the same sample. Cells were gated on a forward scatter/side scatter plot, then singlets were selected and finally different cell types were collected. GFP^+ cells represent infected astrocytes (called "*ASTRO"),* $CD11b^+/CD45^+$ cells correspond to microglia. $MXO4^+$ or $MXO4^-$ microglial cells were collected separately from each APP mouse. $GFP^-/CD11b^-/CD45^-$ cells correspond to uninfected astrocytes, neurons, epithelial cells and oligodendrocyte precursor cells, while oligodendrocytes are mostly eliminated with myelin removal. These cells are called "*OTHER*". Cells were centrifuged at 300 g for 5 min at RT, lyzed in 400 µl TRIzol (Invitrogen, Carlsbad, CA) and stored at -80°C before RNA extraction. Every mouse was processed and sorted independently. Typically, 2,000 to 10,000 ASTRO, 15,000 $CD11b^+/CD45^+$ microglial cells and 20,000 to 100,000 OTHER cells were collected from each sample within 10-15 min.

RNA extraction and RT-qPCR.

Sorted cells collected in Trizol were brought to RT and chloroform was added for 3 min. Samples were centrifuged at 12,000 g for 15 min at RT. Aqueous phase was collected and 1 volume of 70% ethanol was added. Samples were transferred onto an RNeasyMin Elute spin column and RNA was purified according to manufacturer's instructions, with on-column DNAse treatment (RNeasy micro kit, Qiagen, Hilden, Germany). RNA was eluted with 14 µl of RNAse-free deionized water and stored at -80°C before analysis. Reverse transcription was performed with the VILO™ kit according to the manufacturer's protocol (SuperScript® VILO™ cDNA synthesis kit, Life Technologies). Samples were diluted 1:5 or 1:20 in H_2O with 100 µg/ml bovine serum albumin (BSA) and mixed with 250 nM of primers and iTaq SYBR®Green (iTaq™ Universal SYBR® Green qPCR SuperMix, Bio-Rad, Hercules, CA) for qPCR. PCR efficiency was between 76 and 140% for each set of primers (sequences shown in **supplementary table 1**). Nuclease-free water and samples without reverse transcription were used as negative controls. Expression levels of genes of interest were normalized to those of control genes with the ΔCt method. The best normalizing genes *(Eef1a1, Actin)* were identified for each set of samples with the Genorm algorithm, according to the criteria defined in (Vandesompele et al., 2002).

Immunohistology.

Mice were killed by an overdose of pentobarbital and one brain hemisphere was rapidly dissected and drop-fixed in 4% paraformaldehyde (PFA). Brains were post-fixed for 24h in 4% PFA, cryoprotected in 30% sucrose solution and cut on a freezing microtome into serial 30 µm coronal sections. Series of slices were stored at -20°C in an anti-freeze solution until used for immunostainings.

Immunofluorescence. Slices were rinsed in PBS for 3x10 min and then blocked in 4.5% normal goat serum (NGS) diluted in PBS with 0.2% Triton X-100 (PBST), for 1h at RT. Slices were incubated overnight at 4°C with the following primary antibodies diluted in 3% NGS/PBST: anti-GFAP-Cy3 (1:1,000, Sigma, #C9205), anti-IBA1 (1:500, Rabbit, Wako, Richmond, VA, #019-19741), anti-MAP2 (1:500, Mouse, Sigma, #M9942), anti-MBP (1:500, Rabbit, Sigma, #M3821), anti-NeuN (1:500, Mouse; Chemicon, Billerica, MA) or anti-Vimentin (1:1,000, Chicken, Abcam, Cambridge, UK,

#ab24525). Slices were rinsed 3x10 min in PBS and incubated with secondary Alexa Fluor-conjugated antibodies (1:500 or 1:1,000, Invitrogen) in 3% NGS/PBST for 1h at RT. After 3 washes in PBS, slices were incubated overnight at 4°C with an anti-GFP biotinylated antibody (1:500, Vector Laboratories, Burlingame, CA, #BA-0702) in 3% NGS/PBST. After 3 rinses with PBS, sections were incubated for 1h at RT with Streptavidine-FITC (1:1,000, ThermoFisher Scientific, Waltham, MA) in 3% NGS/PBST and rinsed 3 times with PBS before being mounted on SuperFrost® Plus (ThermoFisher Scientifc, #J1800AMNZ) slides and coverslipped with Fluorsave™ (Calbiochem, Darmstadt, Germany) or Fluoromount™ (Sigma) medium. With the BAM10 antibody (1:1,000, Mouse, Sigma, #A3981), the mouse on mouse kit (MOM, Vector laboratories) was used, according to the manufacturer's instructions to reduce non-specific background. For MXO4 staining, slices were incubated with 33 µg/ml MXO4 in 0.1 M PBS, for 30 min at RT under mild agitation. After 3 rinses with PBS, a standard protocol for immunofluorescence was performed as described above.

*Immunohistochemistry***.** Slices were rinsed in PBS for 3x10 min and incubated with H_2O_2 (1:100 in H_2O, Sigma) for 20 min at RT to inhibit peroxidases. Slices were then blocked in 4.5% NGS/PBST for 1h at RT. Slices were incubated O/N at RT or 48h at 4°C in 3% NGS/PBST with the following primary antibodies: anti-Aβ42 (1:500, Rabbit, Life Technologies, #44-344), AT8 (1:400; Mouse, ThermoFisher Scientific, MN1020B), HT7 (1:1,000, Mouse, Innogenetics, Zwijnaarde, Belgium, #90204), anti-phospho-Ser422-Tau (1:400, Rabbit, Abcam, #ab79415). After 3x10 min rinses in PBS, slices were incubated for 1h at RT with biotinylated secondary antibodies (1:4,000, or 1:1,000 for anti-phospho-Ser422Tau, Vector Laboratories) in 3% NGS/PBST. They were washed 3x10 min and incubated for 1h at RT with avidin/biotin complexes (1:250 in PBST) and with VIP (Vector Laboratories) after 3 washes with PBS. Slices were mounted on SuperFrost Plus slides and dried O/N at RT. Slices were dehydrated in acetone and xylene and coverslipped with Eukitt mounting medium (Chem-Lab, Zedelmgem, Belgium). For HT7 antibodie, slices were pre-treated with 10 mM citrate buffer for 20 min at 90°C before H_20_2 treatment.

Immunostaining quantification.

GFAP stainings were quantified on 10x-tiled images acquired with an epifluorescence microscope (Leica, Nussloch, Germany; BM6000B). Virally transduced GFP^+ area was manually segmented and the corresponding GFAP mean grey value was measured with Image J. The number and surface of BAM10 or MXO4-labelled plaques was quantified on 10x-tiled fluorescent images with Image J. An automatic detection of objects with intensity and size thresholds was performed on serial sections, after manual segmentation of the hippocampus on each section. Serial sections stained for HT7, Aβ42, AT8 and Phospho-Ser422-Tau were scanned with an Axio scanZ.1 (Zeiss, Oberkochen, Germany). Immunopositive area within manually-segmented hippocampi were automatically detected with an intensity threshold applied with ImageJ.

Stacked confocal images (10 to 13 z-steps of 1 µm, kept constant within a cohort, maximum intensity stack) were acquired with a 40x objective on a Leica TCS SP8 confocal microscope (3 slices per animal and 3 fields per slice). The mean gray value of MAP2 staining was measured on the entire image. The thickness of the CA1 neuronal layer was manually measured on sections stained for NeuN. The number of $Vimentin^+/GFP^+$ cells was counted using image J. For the quantification of MXO4-labelled Aβ in microglia, stack of confocal 0.4 µm images covering the entire height of the plaque were

acquired on 15 $MXO4^+$ plaques per animal (3-4 plaques/slice). The number of $IBA1^+$ microglial cells in direct contact with plaques were counted and the localization of $MXO4^+$ material (membrane or soma) was determined manually.

Protein extraction.

Mice were killed by an overdose of pentobarbital and their brains were rapidly collected. The GFP^+ area was collected with a punch, snap frozen in liquid nitrogen and stored at -80°C until protein extraction. Samples were homogenized by sonication in lysis buffer [50 mM Tris-HCl pH = 7.4, 150 mM NaCl, 1% Triton X-100 with 1:100 phosphatase inhibitors (Sigma, cocktail 2) and 1X protease inhibitors (Roche, Basel, Switzerland); 25 µl/punch] centrifuged at 20,000 g for 20 min at 4°C. The supernatant contains Triton X-100-soluble proteins and was used for western blotting and MSD® ELISA tests.

Western blot.

Protein concentration was measured by the BCA test (Pierce, Waltham, MA). Samples were diluted in loading buffer with DTT (NuPAGE® LDS sample buffer and sample reducing agent, Invitrogen). Ten µg of proteins was loaded on a NuPAGE™ 4-12% Bis-Tris Midi Gel (Life Technologies). Migration was performed at 200 V for 45 min in NuPAGE™ Running Buffer (Invitrogen) and proteins were transferred on a nitrocellulose membrane with an iBlot Gel transfer device (Invitrogen). After 3 x 10 min rinses in Tris buffer saline and 0.1% Tween 20 (TBST), membranes were blocked in 5% milk in TBST for 1h at RT and incubated for 3h at RT, or overnight at 4°C with the following primary antibodies: 6E10 (1:500, Mouse, Covance, Princeton, NJ, #SIG-39320-20), anti-Actin (1:5,000, Mouse, Sigma, #A2066), anti-ApoE (1:1,000, Rabbit, Abcam, #ab20874), anti-BACE1 (1:1,000, Rabbit, Cell signaling, Danvers, MA,#5606P), anti-GAPDH (1:5,000, Rabbit, Cell signaling, #2118), anti-GFAP (1:5,000, Rabbit, Dako, Troy, MI, #Z0334), anti-IDE (1:400, Rabbit, Abcam, #ab32216), anti-PSD95 (1:500, Mouse, BD bioscience, San Jose, CA, #610496) anti-synaptophysin (1:1,000, Mouse, Stressgen, San Diego, CA, #VAM-SV011) and anti-Tubulin α (1:1,000, Sigma, #T5168). After 3x10min washes in TBST, membranes were incubated for 1h at RT with HRP-conjugated secondary antibodies (1:5,000, Vector laboratories) diluted in TBST with 5% milk. Membranes were incubated with the Clarity Western ECL substrate (Bio-Rad) and the signal was detected with a Fusion FX7 camera (ThermoFisher Scientific). Band intensity was quantified with Image J and normalized to actin, tubulin α or GAPDH. Each antibody was used on at least 2 different membranes to confirm the effects. Representative images and quantification from these 2-3 independent blots are shown.

MSD® ELISA tests.

Triton x-100 soluble proteins were diluted in the diluent provided for the V-PLEX Aβ peptide panel kit (6E10 antibody, MSD®, Rockville, MD). For the phospho-Thr231-Tau/Total Tau kit (K15121D, MSD®), samples were diluted in 20 mM Tris HCl pH = 7.4, 150 mM NaCl, 1 mM EDTA, 1 mM EGTA, 1% Triton X-100, with phosphatase and protease inhibitors. For both assays, samples were loaded in triplicate and manufacturer's protocol was followed. Analyte levels were quantified with a standard curve, using the Discovery Workbench4.0, MSD® software, and normalized to the protein content in each well.

Magnetic resonance spectroscopy and imaging.

WT-GFP, APP-GFP and APP-SOCS3 mice were analyzed with an 11.7T Bruker scanner (Bruker, Ettlingen, Germany) at 8-10 months. Mice were anesthetized with 3% isoflurane in a 1:1 gas air/O_2 mixture and positioned in a stereotactic frame to avoid movement. Isoflurane levels were adjusted around 1% to maintain a respiratory rate between 80-100 cycles per min. Body temperature was maintained at 37°C with a regulated water flow system and respiration was monitored with the PC SAM software (Small animal Instruments, Inc., Stony Brook, NY). A quadrature cryoprobe (Bruker, Ettlingen, Germany) was used for radiofrequency transmission and reception. Anatomical images were acquired using T_2-weighted Multi Slices Multi Echos sequence. They were used to position a 6.5 x 1.5 x 2 mm^3 voxel on the hippocampus and proton spectra were acquired using a Localization by Adiabatic Selective Refocusing sequence (echo time/repetition time = 20/5000 ms combined with VAPOR water suppression, acquisition time = 10 min). Spectra were analyzed using LCModel (Provencher, 1993) and 8 metabolites (total N-acetyl-aspartate, glutamate, total choline, glutamine, myo-inositol, lactate, creatine and taurine) were reliably quantified with a Cramér-Rao lower bound below 5%, and normalized to total creatine, set at 8 mM. A protocol for chemical exchange saturation transfer of glutamate (GluCEST) was then applied to acquire maps of glutamate distribution in the dorsal hippocampus, with a resolution of 100 x 100 µm² and a slice thickness of 250 µm. A saturation pulse was applied during T_{sat} = 1 s with an amplitude B_1 = 5 µT and frequency offsets Δω were in a range from -5 ppm to 5 ppm with a step of 1 ppm. B_0 correction was performed using Water Saturation Shift Reference method (Kim et al., 2009) with a weak saturation amplitude (B_1 = 0.2 µT) applied around the water frequency (Δω in a range from −1 ppm to 1 ppm with a step of 0.1 ppm). B_1 homogeneity was achieved by power calibration in the dorsal hippocampus. GluCEST images were processed pixel-by-pixel and analyzed using in-house programs developed on MATLAB software (MathWorks Inc., Natick, MA). Glutamate contribution was isolated by calculating the asymmetrical magnetization transfer ratio (MTRasym) with Δω centered at ± 3 ppm (Pepin et al., 2016). MTRasym was calculated as 100 × [$Msat_{-3\ ppm}$ − $Msat_{+3\ ppm}$] / $Msat_{-5\ ppm}$, with Msat = magnetization acquired with a saturation pulse applied at the indicated ppm.

Electrophysiological recordings.

Transverse hippocampal slices were prepared from 7-8 month-old WT-GFP, 3xTg-GFP and 3xTg-SOCS3 mice, as described previously (Panatier et al., 2011). Mice were anesthetized with 5% isoflurane and decapitated. The brain was rapidly removed and placed in ice-cold artificial cerebrospinal fluid (ACSF) saturated with 95% O_2 and 5% CO_2, containing (in mM): 125 NaCl, 2.5 KCl, 1.25 NaH_2PO_4, 1.3 $MgCl_2$, 2 $CaCl_2$, 26 $NaHCO_3$ and 10 glucose (pH = 7.3; 300-305 mOsmol/kg). A block of tissue containing the hippocampus was prepared and 350 µm transversal hippocampal slices were cut on a vibratome (Leica). Slices were incubated 30 min at 32°C and allowed to recover for at least 1h at RT.

Slices were transferred to a recording immersion chamber and were perfused with ACSF (3 ml/min) at RT during the whole experiment. An incision between CA3 and CA1 regions was made to avoid epileptiform activity caused by the addition of 50 µM picrotoxin in the perfusion bath before recording. CA3 and CA1 areas were identified with differential interference contrast microscopy and the region of interest (GFP^+) was visualized with the epifluorescent mode of the microscope

(Olympus BX50, Tokyo, Japan). Field excitatory postsynaptic potentials (fEPSPs) were evoked by orthodromic stimulations (100 µs, 0.033 Hz) of Schaffer collaterals using a glass pipette filled with ACSF and placed in the *stratum radiatum,* more than 200 µm away from the recording electrode. Then, fEPSPs were recorded with a glass pipette filled with ACSF (2-3 MΩ) and placed in the GFP^+ region, in the *stratum radiatum* of CA1 area. Data were acquired using a Multiclamp 700B amplifier (Molecular Devices, Sunnyvale, CA), digitized with a Digidata 1320A digitizer (Axon Instruments Inc., Sunnyvale, CA), recorded and analysed off line with pClamp and Clampfit 10.3 respectively (Molecular Devices). Recordings were low-pass filtered at 2 kHz and digitized at 10 kHz.
A stable baseline was recorded for at least 20 min before starting the input/output experiment. Long-term potentiation (LTP) was induced after 20 min of baseline recording, by applying a high-frequency stimulation (HFS) protocol (100 Hz train of stimuli for 1 s, repeated 3 times at 20 s interval) in current clamp mode.

Statistical analysis.

Results are expressed as mean ± SEM. Statistical analysis were performed with Statistica software (StatSoft, Tulsa, OK). For each analysis, normality of variables or residues and homoscedasticity were assessed. Paired or unpaired Student's t test were used to compare two groups. One-way ANOVA and Tukey's post hoc test were used to compare 3 groups. If any or both conditions of application were not fulfilled, non-parametric tests were used. Two groups were compared by the Mann-Whitney test and 3 independent groups were compared by a Kruskal-Wallis test followed by a Mann-Whitney test. Percentages were normalized by Arcsin transformation and analyzed with parametric tests. Distribution of plaques according to their size or circularity were compared with a Chi-2 test. The significance level was set at $p < 0.05$.

RESULTS

Targeting the JAK2-STAT3 pathway in hippocampal astrocytes efficiently modulates astrocyte reactivity in APP mice

Three-month old male APP/PS1dE9 mice (hereafter called APP mice), were injected with an AAV2/9 vector encoding *Socs3* under the GFA_{ABC1D} promoter. This viral vector allows a selective transduction of astrocytes, in ~25% of the hippocampus (**Supplemental Fig. 1a, b**). SOCS3 is an inhibitor of the JAK2-STAT3 pathway and we showed that it efficiently blocks astrocyte reactivity in mouse models of ND (Ben Haim et al., 2015b), including in APP mice (Ben Haim Ceyzériat et al., submitted). At the age of 9 months, APP mice infected with the control AAV vector encoding GFP (APP-GFP) displayed higher GFAP expression than WT mice infected with the same control AAV (WT-GFP, **Fig. 1a, b**). In APP mice, hippocampal astrocytes were hypertrophic, which is a hallmark of reactivity. AAV-mediated SOCS3 expression in astrocytes reduced GFAP expression and normalized astrocyte morphology (**Fig. 1a, b, Supplemental Fig. 1c**). In addition, it reduced the number of astrocytes expressing vimentin, another marker of reactivity (**Fig. 1c**). Mirror experiments were performed to over-activate reactive astrocytes by stimulation of the JAK2-STAT3 pathway. APP mice received a hippocampal injection of an AAV2/9 encoding a constitutively active form of JAK2

(JAK2ca), the upstream kinase of the JAK2-STAT3 pathway. Compared with APP-GFP mice, APP-JAK2ca mice displayed enhanced astrocyte reactivity, visible as a two-fold increase in GFAP immunoreactivity and exacerbated enlargement of astrocyte processes (**Fig. 1a, b, Supplemental Fig. 1c**). Modulation of GFAP levels by SOCS3 and JAK2ca was also observed by western blotting on hippocampal samples taken from WT-GFP, APP-GFP, APP-SOCS3 and APP-JAK2ca mice (**Fig. 1d**).

Astrocyte reactivity involves significant transcriptional changes (Zamanian et al., 2012), and we previously showed that SOCS3 was able to normalize the transcriptional profile of reactive astrocytes in APP mice (Ben Haim Ceyzériat et al., submitted). We here aimed to confirm SOCS3 transcriptional effects on reactive astrocyte markers in a different mouse cohort. RT-qPCR was performed on astrocytes acutely isolated from WT-GFP, APP-GFP and APP-SOCS3 hippocampi. Astrocytes were collected by fluorescence-activated cell sorting (FACS), based on their GFP expression (ASTRO fraction). $CD11b^+/CD45^+$ microglial cells were collected separately (see methods). Non-fluorescent cells (including neurons and uninfected astrocytes) were collected as a single fraction called "OTHER". First, we controlled the purity of sorted cells by assessing the expression of cell-type specific markers. *Gfp* and the astrocyte-specific gene *Aldh1l1* were enriched in the ASTRO fraction, while genes specific for microglial cells (*Aif1*), neurons (*Mal2)* and oligodendrocyte precursor cells (*Cspg4*) were all enriched in the OTHER fraction (**Fig. 2a**). Levels of *Mbp,* an oligodendrocyte gene were low in all groups, due to the myelin removal step during cell dissociation (**Fig. 2a**). *Socs3* mRNA levels were nearly undetectable in astrocytes of the WT-GFP and APP-GFP groups, they were increased by more than 200 fold in astrocytes of the APP-SOCS3 group (**Fig. 2b**), demonstrating the efficiency of the AAV-SOCS3 vector. mRNA levels for *Gfap* and *Serpina3n,* two pan-reactive astrocyte markers were higher in astrocytes isolated from the APP-GFP group than in the WT-GFP group (**Fig. 2c**). SOCS3 normalized the expression of these two genes.

These results, in conjunction with our previous genome-wide analysis of SOCS3 effects in astrocytes from APP mice (Ben Haim Ceyzériat et al., submitted) demonstrate that SOCS3 expression in astrocytes efficiently inhibits astrocyte reactivity in APP mice. We next evaluated how the modulation of astrocyte reactivity by JAK2 and SOCS3 impacted amyloid pathology.

Astrocyte reactivity influences amyloid load in APP mice

Astrocyte de-activation by SOCS3 significantly reduced the number of BAM10-positive amyloid plaques present in the hippocampus of 9 month-old APP mice ($p < 0.01$, **Fig. 3a, b**). The reduction in amyloid plaques with SOCS3 was also observed after labelling plaques with methoxy-XO4 (MXO4), a fluorescent Congo red-derivative that binds aggregated amyloid and labels smaller plaques (- 36%, $p < 0.05$, Student *t* test, data not shown, **Fig. 3a**). Importantly, over-activation of astrocytes by JAK2ca had mirror effects ($p < 0.05$, **Fig. 3a, b**). The average plaque size was identical between groups (**Fig. 3c**). A more detailed analysis of plaque features revealed that SOCS3 and JAK2ca affected all categories of plaques (either based on their size, **Fig. 3d**; immunoreactivity or circularity, data not shown), so that the overall distribution of plaques was not different between APP-GFP and APP-SOCS3 or APP-GFP and APP-JAK2 groups (Chi-2 = 0.84 and 0.74 for SOCS3 and JAK2ca respectively, **Fig. 3d**). These results suggest that astrocytes promote the formation of amyloid plaques when they are reactive in AD. This could be due to an enhanced production of Aβ, less clearance of Aβ or plaques, or a combination of these effects.

We measured the levels of Triton X100-soluble Aβ38, Aβ40 and Aβ42 by Mesoscale Discovery (MSD®) assays. Significant levels of both Aβ40 and Aβ42 were detected while Aβ38 levels were nearly undetectable. The levels of Aβ40 and Aβ42 were not significantly impacted by the modulation of astrocyte reactivity, although a trend towards less Aβ40 and Aβ42 was seen with SOCS3 (**Fig. 3e**). A mirror trend was observed with JAK2ca (**Fig. 3e**). The ratio of the most toxic form Aβ42 over Aβ40 was not modified by SOCS3 or JAK2ca (**Fig. 3f**).

We then analyzed the expression of several proteins involved in APP metabolism: the amyloid precursor protein (APP) itself, BACE1, the β-secretase that cleaves APP through the amyloïdogenic pathway, insulin degrading enzyme (IDE) that degrades Aβ and apolipoprotein E (ApoE) a protein secreted by astrocytes, which binds cholesterol and Aβ and promotes their clearance. Human APP was recognized by the 6E10 antibody and was found to be stably expressed across groups (**Fig. 4a**). BACE1, IDE and ApoE were also expressed at similar levels in all groups (**Fig. 4b, c, d**). BACE1 expression was also studied by immunofluorescence of brain slices, and no change in immunoreactivity was observed (data not shown). *ApoE* mRNA levels measured in sorted astrocytes were also found expressed at similar levels in all groups (**Supplemental Fig. 2**). Overall, these results suggest that astrocyte reactivity promotes amyloid deposition without impacting the molecular machinery for Aβ production and clearance.

Modulation of astrocyte reactivity does not impact amyloid uptake by astrocytes and microglial cells

We then studied whether plaque degradation was impacted by the modulation of astrocyte reactivity and could explain the observed changes in amyloid plaque density. We focused on SOCS3 effects, as its lowering effects on amyloid load were the most therapeutically relevant.

Glial cells, and in particular microglial cells, play a key role in plaque elimination (Lee and Landreth, 2010). Microglial cells were first analyzed by immunostaining with IBA1. The typical association of microglial cells around amyloid plaques was observed in APP mice (**Fig. 5a**). There was no difference in IBA1 immunoreactivity between APP-SOCS3 mice and in APP-GFP mice, when measured in the whole hippocampus (p = 0.139, data not shown). Similarly, the number of microglial cells in contact with MXO4-labbeled plaques was not significantly different between groups ($p = 0.6$, **Fig. 5a**).

To measure amyloid uptake by glial cells, mice receive an *i.p.* injection of MXO4 to monitor its accumulation within brain cells by FACS (Krauthausen et al., 2015). Astrocytes were identified by their GFP expression, while labelling with CD11b and CD45 antibodies allowed the identification of microglial cells ($CD11b^+/CD45^+$). The percentages of GFP^+ astrocytes (4%) and microglial cells (14%) were not different between WT-GFP, APP-GFP and APP-SOCS3 groups (**Fig. 5b**). $MXO4^+$ cells were only observed in APP mice and only in $CD11b^+/CD45^+$ microglial cells (**Fig. 5c**). No MXO4 accumulation could be evidenced in GFP^+ astrocytes (**Fig. 5d**). The percentage of microglial cells positive for MXO4 ($CD11b^+/CD45^+/MXO4^+$ cells, **Fig. 5e**) or MXO4 median fluorescent intensity (**Fig. 5f**) were not different between APP-GFP and APP-SOCS3 groups, suggesting that microglial cells have the same capacity to take up MXO4-labeled amyloid material when astrocytes are de-activated by SOCS3.

Because microglial cells could be impacted by cell dissociation and FACS sorting, we also analyzed MXO4 uptake by microglia on fixed brain slices, by quantifying the number of $IBA1^+$ microglial cells

with intracellular MXO4$^+$ material. MXO4$^+$/IBA1$^+$ cells were mainly found in direct contact with MXO4$^+$ amyloid plaques. Only fewer than 5% of microglia cells in contact with plaques were MXO4 negative, revealing an active phagocytosis of amyloid plaques by microglia (**Fig. 5g**). MXO4$^+$ material was either localized at the microglial membrane or within the soma. The localization of MXO4$^+$ within microglia was not different between APP-SOCS3 and APP-GFP groups (**Fig. 5g**).

A sub-class of microglia with active phagocytic capacities was recently described as « disease-associated microglia » (DAM, Keren-Shaul et al., 2017), and it is possible that de-activation of astrocytes with SOCS3 only impacts specific classes of microglial cells like DAM. To explore this possibility, the levels of genes specific for homeostatic microglia (*Ctss* and *C1qb*) and DAM cells were analyzed in MXO4$^-$ and MXO4$^+$ microglial cells. MXO4$^+$ microglia had a gene profile characteristic of DAM (up-regulation of *ApoE* and *Trem2*; downregulation of *Tmem119*) consistent with the strong phagocytic activity of these cells. The expression of SOCS3 in astrocytes did not change the expression of homeostatic microglia or DAM-specific markers (**Supplemental Fig. 2**)

Overall, our analysis of microglial cells show that deactivation of reactive astrocytes by SOCS3 does not does impact their phenotype or phagocytic function.

SOCS3 effects on neuronal and clinical indexes in APP mice

We then determined whether the reduction in amyloid load produced by SOCS3 translated into improved neuronal features and clinical indexes in APP mice. We performed brain imaging on another mouse cohort with nuclear magnetic resonance (NMR) techniques. The concentration of 8 metabolites (total N-acetyl-aspartate, glutamate, total choline, glutamine, myo-inositol, lactate, creatine and taurine) was measured in the hippocampus by NMR spectroscopy (**Fig. 6a**). Only lactate levels were found significantly higher in APP-GFP mice than in WT-GFP mice, suggesting altered brain metabolism (**Fig. 6b**). SOCS3 expression did not restore lactate levels in APP mice. It is possible that SOCS3 has more subtle or local effects that are concealed in a spectroscopy voxel covering the whole hippocampus. The Glutamate Chemical Exchange Saturated Transfer method (GluCEST) was used to generate maps of the excitatory neurotransmitter glutamate in the hippocampus (**Fig. 6c**). No change in glutamate distribution or concentration was observed between the 3 groups, even in the injected CA1 region (**Fig. 6c, d**).

Consistent with a preserved synaptic transmission in 9 month-old APP mice, the levels of the pre- and post-synaptic proteins synaptophysin and PSD95 were found to be expressed at similar levels by western blotting (**Supplemental Fig. 3a**). Similarly, the immunoreactivity for the dendritic protein MAP2 and the thickness of the pyramidal neuronal layer in the CA1 region were not significantly different between groups (**Supplemental Fig. 3b, c**).

Overall, no or very limited molecular, morphological or metabolic alterations were found in our 9 month-old APP mice, precluding in-depth evaluation of the therapeutic effects of SOCS3. We thus turned to another mouse model of AD to further study the functional impact of astrocyte reactivity. We studied 3xTg-AD mice (thereafter called 3xTg mice) that have the advantage of developing amyloid as well as Tau pathology, an important pathological aspect of AD.

Modulation of astrocyte reactivity does not impact amyloid deposition in 3xTg mice

3xTg mice were injected at 6 months and studied 10 months later, when they display both amyloid and Tau pathology. Similar to APP mice, injection of AAV-SOCS3 in the hippocampus of 3xTg mice efficiently reduced astrocyte hypertrophy and normalized GFAP overexpression to levels observed in WT mice injected with an AAV-GFP (**Fig. 7a, b**). Injection of AAV-JAK2ca had mirror effects (**Fig. 7a, b**), confirming that manipulation of the JAK2-STAT3 pathway is a very efficient strategy to modulate astrocyte reactivity in the mouse brain, across disease models. Modulation of GFAP levels in astrocytes was also confirmed by western blot on protein homogenates from WT-GFP, 3xTg-GFP, 3xTg-SOCS3 and 3xTg-JAKca mice (**Fig. 7c**).

In contrast to APP mice, modulation of astrocyte reactivity had no detectable impact on amyloid deposition, as measured by brain sections stained with MXO4 (**Fig. 8a, b**) or with the Aβ42 antibody (data not shown). The number of plaques and their size were identical between groups (**Fig. 8b, c**).

Levels of Triton X-100 soluble Aβ species were analyzed by MSD® assays on protein homogenates prepared from the hippocampus of WT-GFP, 3xTg-GFP, 3xTg-SOCS3 or 3xTg-JAK2ca. At the age of 16 months, only Aβ42 was reliably detected and quantified (Aβ40 was undetectable in 2 to 4 samples/group). Hippocampal Aβ42 concentrations were not significantly modified by SOCS3 or JAK2ca (**Fig. 8d**). Similarly to APP mice, western blotting on the same samples, showed that proteins involved in APP metabolism or clearance (human APP, BACE1, IDE or ApoE) or synaptic proteins (PSD95 and synaptophysin) were expressed at the same level across all groups (**Supplemental Fig. 4**).

Modulation of astrocyte reactivity does not impact Tau pathology in 3xTg mice.

Tau can be phosphorylated on multiple epitopes. Two approaches were used to characterize the effects of astrocyte reactivity on Tau phosphorylation: 1) immunostainings with antibodies against phospho-Ser422-Tau, phospho-Ser202/Thr205-Tau (AT8 antibody) and total human Tau (HT7 antibody) and 2) MSD® assay with antibodies against phospho-Thr231-Tau (AT180 antibody) and total Tau.

First, we controlled by these two methods that total Tau was not altered by SOCS3 or JAK2ca in 3xTg mice (**Fig. 9a, b, c**). Positive staining for phospho-Ser422-Tau and phospho-Ser202/Thr205-Tau was only observed in 3xTg mice, revealing strongly dystrophic neurons and numerous ghost tangles in the hippocampus (**Fig. 9a** and data not shown). Immunoreactivity for these two antibodies was similar between the 3xTg-GFP, 3xTg-SOCS3 and 3xTg-JAK2ca groups (**Fig. 9b** and data not shown). Accordingly, hippocampal concentrations of phospho-Thr231-Tau normalized by total Tau were not impacted by SOCS3 or JAK2ca in 3xTg mice (**Fig. 9c**).

Our data show that the modulation of astrocyte reactivity with SOCS3 and JAK2ca does not influence Tau phosphorylation or amyloid pathology in 16 months old 3xTg mice. These mice also display early defects in synaptic transmission and plasticity in the hippocampus before amyloid deposition (Oddo et al., 2003). Astrocytes are now recognized as active elements of the synapse (Araque et al., 2014). Therefore, we studied the impact of reactivity on synaptic plasticity at the Schaffer collateral-CA1 synapses, in younger 3xTg mice, before overt amyloid deposition or Tau pathology.

Inhibition of astrocyte reactivity by SOCS3 restores synaptic plasticity in 3xTg mice.

Field excitatory post-synaptic potentials (fEPSPs) were recorded in the *stratum radiatum* of the CA1 area of 7-8 months old WT-GFP, 3xTg-GFP and 3xTg-SOCS3 mice. The extracellular recording electrode was placed in the infected, GFP^+ region (**Fig. 10a**). Long-term potentiation (LTP) was induced by stimulation of Schaffer collaterals with 3 high frequency stimulations trains (100 Hz during 1s, 20s interval). As reported before (Oddo et al., 2003), LTP was impaired in 3xTg-GFP mice, in comparison to LTP induced in WT-GFP mice (**Fig. 10b)**. Strikingly, inhibition of astrocyte reactivity by SOCS3 fully recovered LTP (**Fig. 10b**), suggesting that reactive astrocytes play a major role in synaptic plasticity deficits in this model.

DISCUSSION

Our preclinical study performed on two complementary mouse models of AD shows that 1) targeting the JAK2-STAT3 pathway in astrocytes with AAVs is an efficient method to modulate their reactivity *in situ*; 2) reactive astrocytes play subtle and context-dependent roles in AD. In APP mice but not in 3xTg mice, astrocyte reactivity promoted amyloid deposition. In 3xTg mice, astrocyte reactivity de-activation did not modulate Tau pathology, but it restored early deficits in hippocampal LTP. Reactive astrocytes may thus impact different stages and molecular mechanisms of AD pathogenesis.

Reactive astrocytes promotes amyloid deposition in APP mice

Astrocyte reactivity positively influenced the number of amyloid plaques in APP mice without changing their size. This is consistent with the ~30% decrease in amyloid load produced by the inhibition of CN/NFAT pathway in astrocytes, which reduces their reactivity (Furman et al., 2012). In an attempt to identify the mechanisms involved, we studied some molecular and cellular regulators of amyloid deposition and clearance. No change in enzymes or transporters involved in APP metabolism or Aβ clearance was observed. However, the decrease in plaque number was matched with a trend towards lower hippocampal levels of soluble Aβ40 and Aβ42 when astrocytes were de-activated by SOCS3, with mirror effects with JAK2ca. It thus possible that despite stable levels of enzymes involved in APP metabolism, their activity is changed by reactivity, leading to higher production of Aβ and then plaques. Increased Aβ levels may originate from neurons, the major producers of Aβ, but also from astrocytes themselves. Indeed, astrocytes are also able to generate Aβ (Cole and Vassar, 2007, Liao et al., 2016) and reactivity could exacerbate this process. The direct measurement of Aβ production by single cells, as described by Liao *et al*. on astrocytes derived from iPSCs, could solve the question of the origin and levels of Aβ. However, it is uncertain whether such methods could be applied to acutely dissociated cells from adult mouse brains and provide enough sensitivity. Alternatively, astrocytes may uptake amyloid material and degrade amyloid plaques (Wyss-Coray et al., 2003, Koistinaho et al., 2004). However, FACS analysis of amyloid uptake evidenced no MXO4-labelled Aβ in astrocytes (in contrast to ~20% of $MXO4^+$ microglial cells). It is still possible that astrocytes degrade amyloid too quickly to allow detection by our method. It is most likely that astrocyte contribution to amyloid clearance is minor compared to microglia. Intriguingly, microglial cells were not affected by the significant inhibition of astrocyte reactivity with SOCS3.

Microglial cells took up Aβ as efficiently and had normal transcriptional profiles. Therefore, even if astrocytes are de-activated by SOCS3, microglia may receive enough positive signals from aggregated Aβ or dysfunctional neurons to remain activated.

Despite major amyloid deposition, our 9-12 month-old APP mice displayed very limited molecular, cellular and clinical alterations, making it difficult to evaluate the broader therapeutic potential of SOCS3 in AD. No changes in neuronal proteins, synaptic markers or metabolites were found, except a 2-fold increase in lactate levels measured by NMR spectroscopy. According to the astrocyte-to-neuron-lactate shuttle hypothesis, lactate is provided by astrocytes to neurons in conditions of increased energy needs (Belanger et al., 2011). In addition, reactivity is known to change astrocyte metabolism (Escartin et al., 2007, Allaman et al., 2011). However, astrocyte-deactivation by SOCS3 did not impact lactate levels. It is possible that SOCS3 effects are too local, precluding the detection of its effects on global clinical indexes like brain imaging.

Reactive astrocytes restore LTP in 3xTg mice

To further evaluate the effects of astrocyte reactivity modulation in AD, we turned to 3xTg mice that develop Tau pathology as well as early synaptic deficits, before plaque deposition (Oddo et al., 2003). We found that SOCS3 expression in astrocytes fully restored LTP alteration in 3xTg mice. The normalization of LTP with SOCS3 is in agreement with the restoration of several synaptic parameters in 16 month-old APP mice or 8 month-old 5xFAD mice by targeting the CN/NFAT to decrease astrocyte reactivity (Furman et al., 2012, Sompol et al., 2017). What could be the mechanisms involved in SOCS3-mediated rescue of LTP? Astrocytes are known to be important partners of neurons at the synapse. Astrocytes are able to impact synaptic transmission by several mechanisms: modulation of astrocyte coverage, neurotransmitter recycling or release of active molecules called gliotransmitters (Oliet et al., 2001, Panatier et al., 2006, 2011, Pannasch et al., 2014), reviewed in (Araque et al., 2014). In AD mouse models, astrocytes display altered calcium homeostasis and signaling (Kuchibhotla et al., 2009), which result in increased release of purines (Delekate et al., 2014). Other mechanisms of altered gliotransmitter release in AD were described, including higher release of ATP through hemichannels (Yi et al., 2016), of GABA through bestrophin channels or GAT3/4 transporters (Jo et al., 2014, Wu et al., 2014). Alternatively, astrocytes were shown to release the complement factor C3 in AD mice. This disrupted dendrite morphology and synaptic function (Lian et al., 2015). Interestingly, we showed that SOCS3 normalized the expression of several complement factors in APP astrocytes (Ben Haim Ceyzériat et al., submitted). More experiments are needed to tease out the mechanisms involved in SOCS3 beneficial effects on LTP.

Our results further emphasize the disconnection between amyloid deposition (and even Tau pathology in 3xTg mice) from synaptic and neuronal dysfunction. Indeed, the original linear amyloid cascade whereby Aβ first builds up, then triggers Tau hyper-phosphorylation, eventually leading to synaptic dysfunction and neuronal death is now called into question (Herrup, 2015, Musiek and Holtzman, 2015). Opponents to the amyloid cascade stress for example, that synaptic dysfunction may occur before amyloid pathology (as in 3xTg mice), that Tau pathology correlates better with clinical symptoms and that glial cell involvement is overlooked (De Strooper and Karran, 2016). When do reactive astrocytes and neuroinflammation in general, play a role in the pathogenesis of AD? Activated glial cells are thought to appear late in the disease process, following reception of

abnormal signals from dysfunctional neurons or detection of toxic oligomerized or aggregated proteins (see, Ben Haim et al., 2015a, for review). However, positron emission tomography studies on prodromal AD patients suggest that glial reactivity occurs at early stages of disease, before overt signs of amyloid deposition (Heneka et al., 2005, Hamelin et al., 2016). In accordance, our results showing that SOCS3 expression in astrocytes restores LTP in 8 month-old 3xTg mice indicate that reactive astrocytes play a role in early synaptic deficits, before amyloid deposition.

Reactive astrocytes have context-specific effects on disease outcomes

The effects of reactive astrocytes reported in this article are consistent with a deleterious role of these cells in the context of AD (Furman et al., 2012, Jo et al., 2014, Wu et al., 2014, Lian et al., 2015, Sompol et al., 2017). But in fact, it may not be possible to assign a unique, permanent effect of astrocyte reactivity, not even in a single disease. Indeed, our results show than the same experimental manipulation of astrocyte reactivity (modulation of the JAK2-STAT3 pathway) in two AD mouse models, have different effects on the same disease outcome (amyloid plaques) assessed with the same methodology (MXO4 labelling). Astrocyte reactivity is thus a complex process. How can we explain this discrepancy between the two models? In 16 months old 3xTg mice amyloid pathology is accompanied by Tau pathology, while only amyloid pathology occurs in 9 month-old APP mice. This important difference (in addition to other differences between these two models such as genetic background, transgenes) could change mechanisms of amyloid deposition. In addition, mutant Tau in itself influences astrocyte physiology (Dabir et al., 2006, Leyns and Holtzman, 2017) and could further change astrocyte phenotype compared to those in APP mice. Indeed, astrocyte reactivity is a heterogeneous response, encompassing different states (Anderson et al., 2014, Liddelow and Barres, 2017). Recently, a neurotoxic class of reactive astrocytes (termed A1) was characterized *in vitro.* Some reactive astrocytes expressing A1 gene markers were observed in AD patients (Liddelow et al., 2017). However, a nicer version of reactive astrocytes may exist as well (termed A2). Indeed, we and other have also identified significant beneficial roles for reactive astrocytes (Escartin et al., 2006, Escartin et al., 2007, Zamanian et al., 2012, Anderson et al., 2016) including in an AD context (Kraft et al., 2013). The relative proportion of these two classes, as well as other subpopulations of astrocytes, may be different between our two AD models. Therefore, as SOCS3 globally blocks reactivity in astrocytes (Ben Haim Ceyzériat et al., submitted), it may unveil the different impact of these classes on disease outcomes. Finally, to add another level of complexity, it is important to consider that reactivity involves large changes in the transcriptional profile of astrocytes (Zamanian et al., 2012), in particular in AD (Orre et al., 2014, Srinivasan et al., 2016). Interestingly, our RNAseq study showed that SOCS3 normalizes the transcriptional profile of APP astrocytes (Ben Haim Ceyzériat et al., submitted). Among the genes restored by SOCS3, some are expected to have beneficial, detrimental or mixed effects in AD context. For example, SOCS3 reduces the expression of genes of the complement pathway. Recent studies have shown the deleterious roles of complement factors in synapse elimination and neuronal dysfunction (Lian et al., 2015, Hong et al., 2016). However, complement proteins such as C3 may also promote amyloid plaque elimination by acting as chemotactic factors (Shi et al., 2017). Overall, astrocyte reactivity appears as a complex, multifaceted response, with different functional effects on disease outcomes that are highly dependent on the

specific disease context. It may thus be impossible to determine whether definitely and generally, reactive astrocytes are good or bad.

CONCLUSIONS

Our results show that the modulation of astrocyte reactivity by targeting a single core cascade not only impacts late stages of the disease, as found with amyloid deposition in APP mice, but also early synaptic deficits seen in 3xTg mice. Our vector tools offer versatility and efficiency to dissect out the contribution of reactive astrocytes in different disease contexts, without impacting other brain cell types directly. Our experiments underline the complex and subtle actions operated by reactive astrocytes in the diseased brain. More studies are warranted to precisely define therapeutic strategies based on reactive astrocytes in AD.

FIGURES

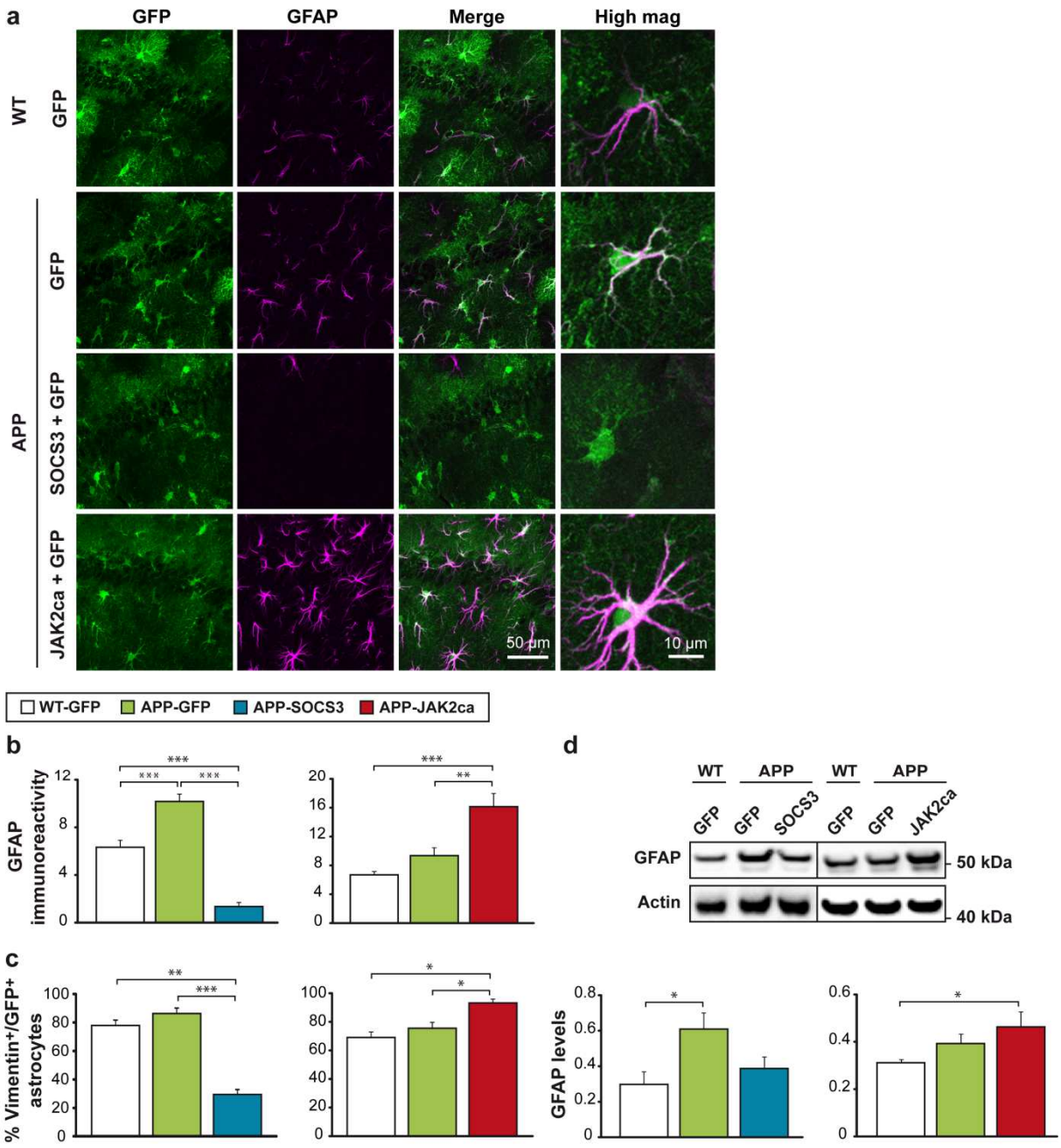

Figure 1. Efficient modulation of astrocyte reactivity by targeting the JAK2-STAT3 pathway in hippocampal astrocytes of APP mice.

a, Representative confocal images of astrocytes stained for GFAP (magenta) in 9 month-old WT and APP mice. Three-month old APP mice and WT littermates were injected in the CA1 region with an AAV targeting astrocytes and encoding GFP, or with two AAVs encoding SOCS3 or GFP (SOCS3 + GFP), or with two AAVs encoding a constitutive form of JAK2 or GFP (JAK2ca + GFP), at the same total viral titer. Co-infection with AAV-GFP allows the identification of infected astrocytes based on their expression of GFP (green). In APP-GFP mice, astrocytes are hypertrophic and overexpress GFAP compared to WT-GFP mice. SOCS3 significantly reduces GFAP levels in APP mice. On the contrary,

JAK2ca increases GFAP levels and exacerbates process enlargement in astrocytes. **b,** Quantification of GFAP immunoreactivity in the hippocampus. N = 5-10/group. One way ANOVA and Tukey's post hoc test. **c,** The proportion of GFP^+ astrocytes overexpressing the reactive marker vimentin is significantly lower in APP-SOCS3 mice and higher in APP-JAK2ca mice than in control APP-GFP mice. N = 3-7/group. One way ANOVA and Tukey's post hoc test on Arcsin transformed ratio. **d,** Western blotting of GFAP in WT and APP mice shows the same pattern of modulation of GFAP levels by SOCS3 and JAK2ca. GFAP levels were normalized by actin. Representative image and quantification from 3 independent membranes. N = 3-7/group. One way ANOVA and Tukey's post hoc test. * $p < 0.05$, ** $p < 0.01$, *** $p < 0.001$.

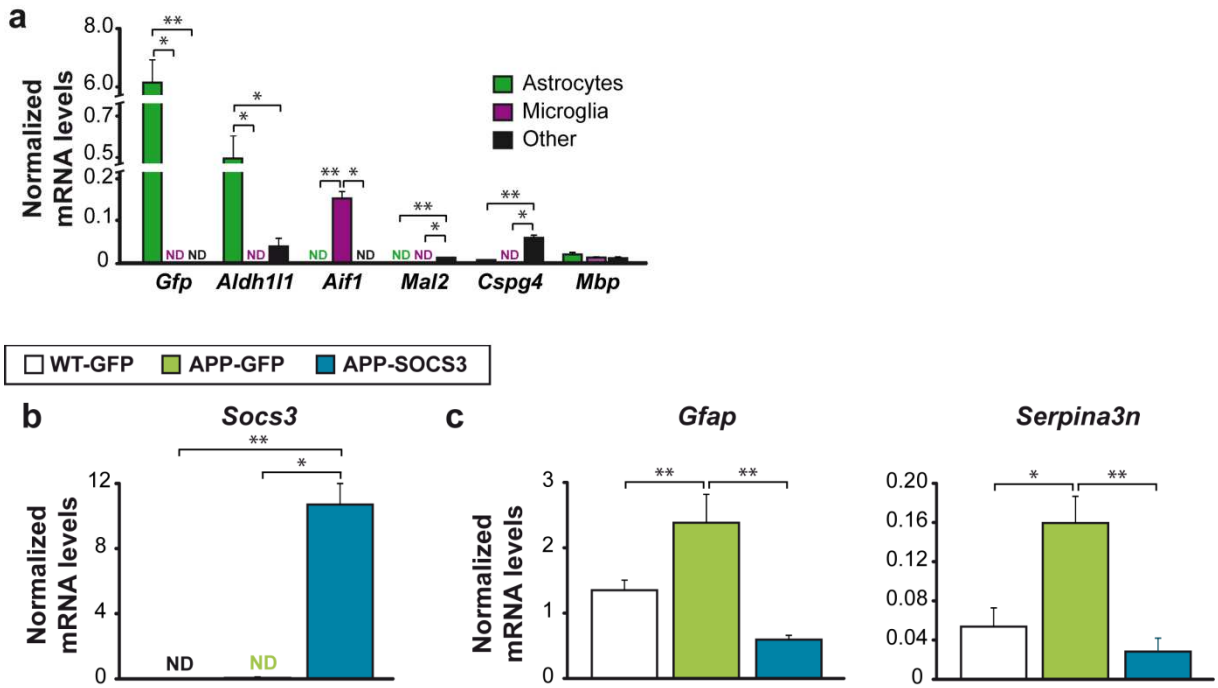

Figure 2. SOCS3 normalizes the expression of reactive markers in APP astrocytes.

RT-qPCR analysis on cells acutely isolated from the hippocampus of WT-GFP, APP-GFP and APP-SOCS3 mice. **a,** mRNA levels for cell-specific genes in GFP^+ sorted astrocytes (ASTRO), $CD11b^+/CD45^+$ microglial cells and all triple negative cells (i.e. neurons, epithelial cells and non-infected astrocytes, called OTHER) validates the sorting procedure. N = 3-7/group. Kruskall-Wallis and Mann-Whitney tests. **b,** *Socs3* mRNA levels are strongly increased by AAV-SOCS3 gene transfer in astrocytes. N = 3-8/group. Kruskall-Wallis and Mann-Whitney tests. **c,** SOCS3 normalizes the expression of *Gfap* and *Serpina3n* in reactive astrocytes of APP mice. N = 4-8/group. One way ANOVA and Tukey's post hoc test (GFAP), and Kruskall-Wallis and Mann-Whitney tests (Serpina3n). ND = Not detectable. * $p < 0.05$, ** $p < 0.01$.

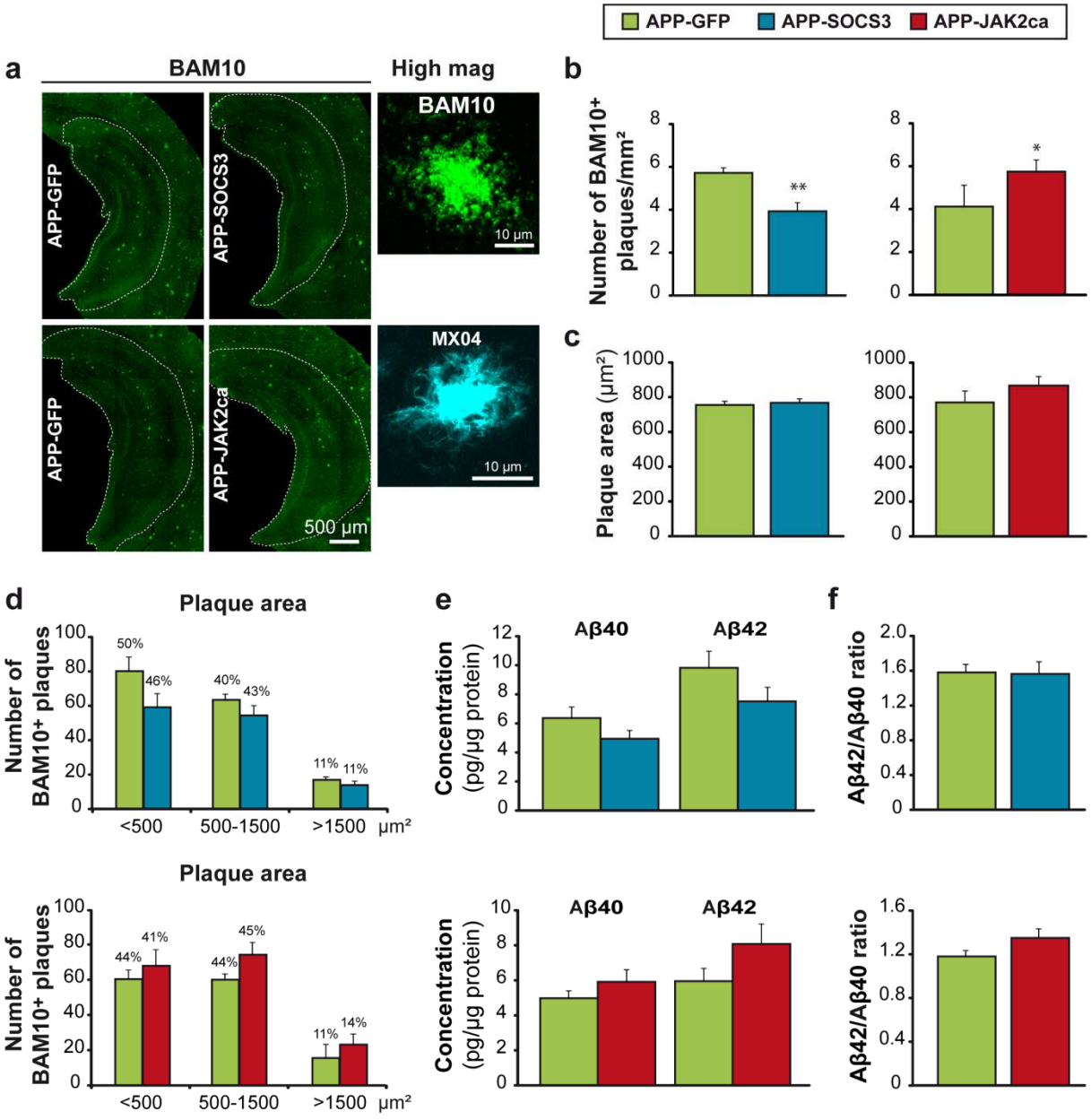

Figure 3. Modulation of astrocyte reactivity impacts amyloid load in APP mice.

a, Representative images of amyloid plaques labelled with an anti-Aβ antibody (BAM10 antibody; green) or with methoxy-XO4 (MXO4; cyan) in APP-GFP, APP-SOCS3 and APP-JAK2ca mice. **b,** Quantification of plaque density in the whole hippocampus. The density of $BAM10^+$ plaques is significantly decreased by SOCS3 and increased by JAK2ca in APP mice. N = 8-9/group. Student *t* test. **c,** The average size of $BAM10^+$ amyloid plaque is similar between groups. N = 8-9/group. Mann-Whitney test. **d,** All plaque size categories are similarly impacted by SOCS3 or JAK2ca. The percentage of each category is indicated on top of each bar. N = 8-9/group. Chi-2 test. **e,** Dosage of Aβ40 and Aβ42 peptide concentrations in Triton-X100 soluble protein homogenates prepared from the infected hippocampus of WT-GFP, APP-GFP, APP-SOCS3 and APP-JAK2ca mice. SOCS3 tends to decrease the concentration of Aβ40 and Aβ42. Conversely, the expression of JAK2ca tends to increase both forms. **f,** Aβ42/Aβ40 ratio were not impacted by SOCS3 or JAK2ca. N = 6-10/group. Student *t* test. * $p < 0.05$, ** $p < 0.01$.

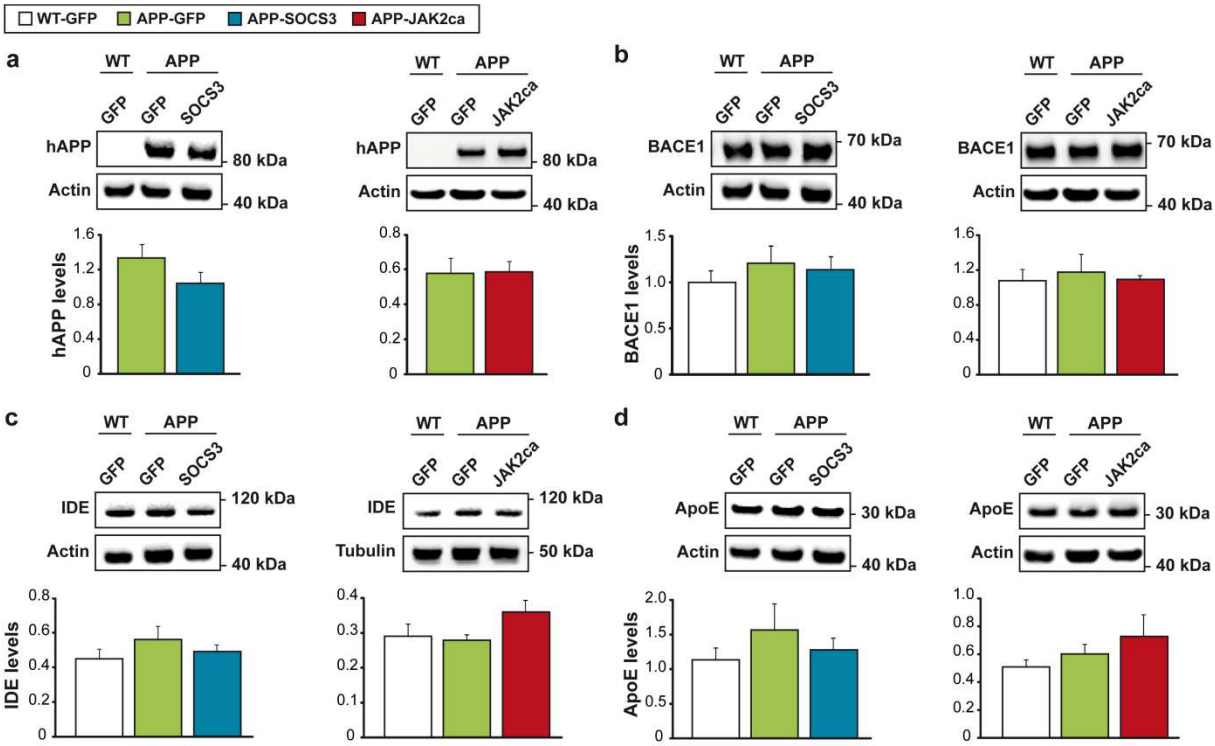

Figure 4. Modulation of astrocyte reactivity does not influence the expression of proteins involved in amyloid metabolism and clearance in APP mice.

a-d, Representative western blottings on protein homogenates prepared from WT-GFP, APP-GFP, APP-SOCS3 and APP-JAK2ca mice. The expression of human (hAPP) (**a**), BACE1 (**b**), IDE (**c**) and ApoE (**d**) are stable across the groups (protein levels are normalized by actin or tubulin α). N = 3-7/group. Kruskall-Wallis test.

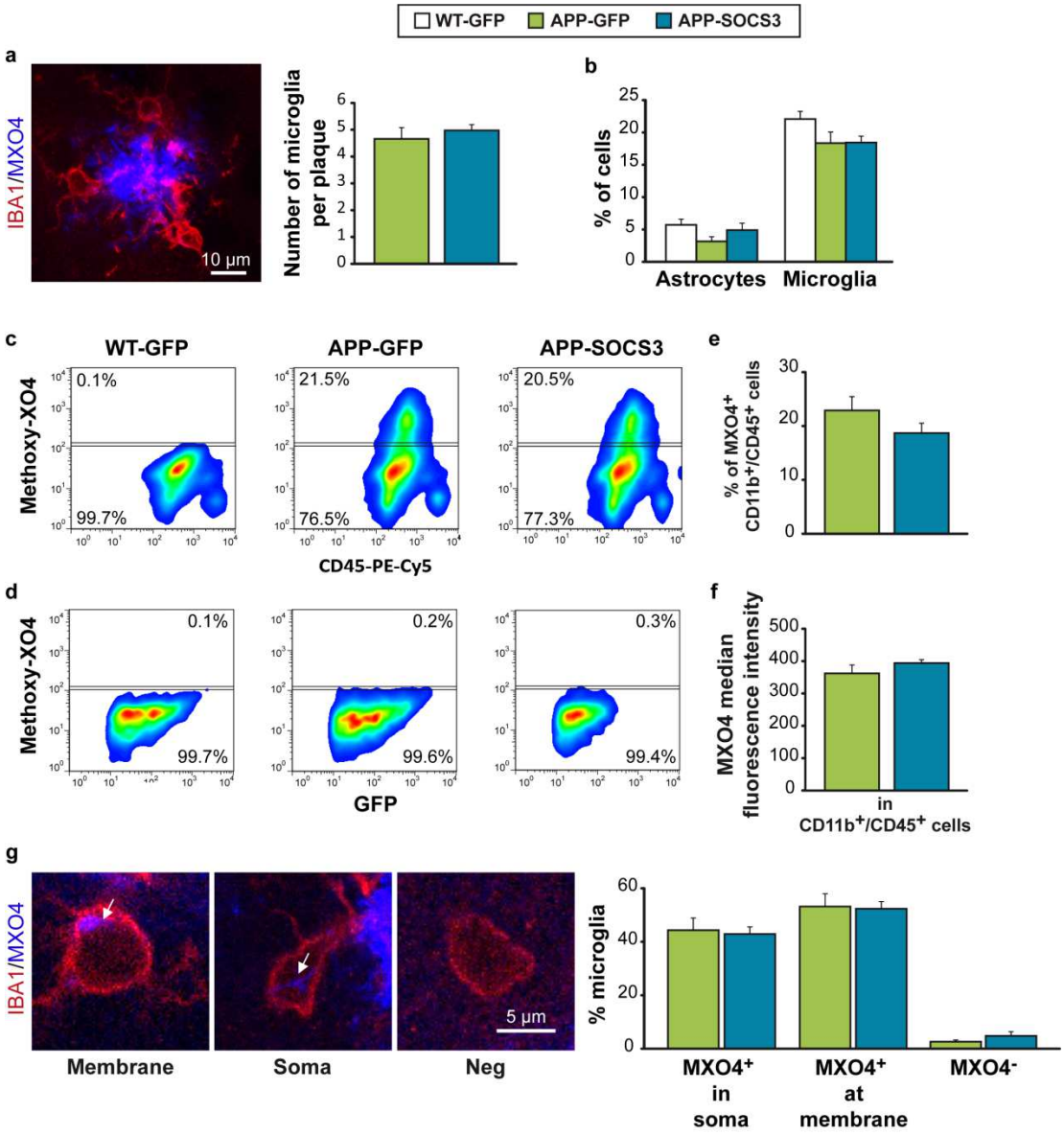

Figure 5. Inhibition of astrocyte reactivity does not change microglia properties.

a, Representative image of IBA1$^+$ microglial cells (red) in direct contact with an amyloid plaque labeled with MXO4 (blue). The number of microglia per plaque is similar between APP-GFP and APP-SOCS3 mice. N = 8-10/group. Mann-Whitney test. **b,** FACS analysis of GFP$^+$ astrocytes and CD11b$^+$/CD45$^+$ microglial cells isolated from the dissociated hippocampus of WT-GFP, APP-GFP and APP-SOCS3 mice, previously injected with MXO4 to detect amyloid uptake. The proportion of these different cell types is similar in the 3 groups. N = 6-10/group. One way ANOVA on Arcsin transformed ratio. **c-d,** Representative gates to analyze uptake of MXO4 labelled amyloid by microglial cells (parent gate = CD11b$^+$ cells) or by astrocytes (parent gate = GFP$^+$ cells). Approximately 20% of microglial cells are MXO4$^+$ (**c**), while no MXO4 uptake is detected in astrocytes (**d**). No difference in the proportion of MXO4$^+$ cells (**e**) or in the intensity of MXO4 staining (**f**) is observed between APP-GFP and APP-SOCS3 mice. N = 6-10/group. Mann-Whitney test. **g,** Confocal images of a 0.4 µm z-section of MXO4 positive material (blue) accumulated in IBA1$^+$ microglial cells (red). Microglial cells in contact with plaques either display MXO4 staining (white arrow) at the membrane, in the cytosol or are MXO4 negative. The proportion of these classes of microglial cells is not different between groups. N = 8-10/group. Student *t* test on Arcsin transformed ratio.

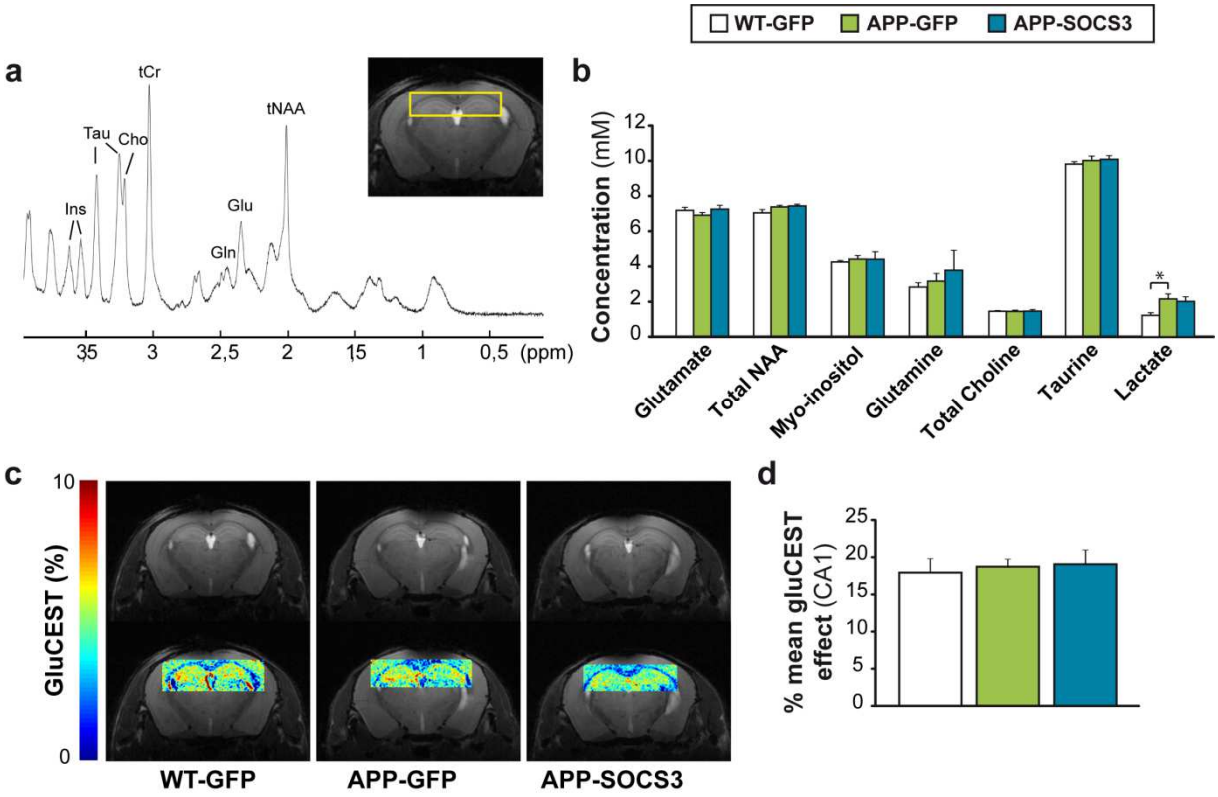

Figure 6. Inhibition of astrocyte reactivity by SOCS3 does not change brain metabolites in APP mice.

a, Evaluation of metabolite concentration and distribution in the hippocampus of WT-GFP, APP-GFP and APP-SOCS3 mice with non-invasive NMR approaches. **b,** Hippocampal concentrations of neuronal metabolites (glutamate and total N-acetyl-aspartate), glial metabolites (myo-inositol, glutamine, total choline), ubiquitous metabolites (lactate and taurine) were quantified and normalized to creatine. These metabolites are stable across the 3 groups. Only lactate levels are significantly higher in APP mice than in WT mice and SOCS3 does not normalize them. N = 6-8/group. One way ANOVA and Tukey's post hoc test. The voxel used for NMR spectroscopy is shown in yellow on the image in **a**. **c,** Representative maps of glutamate levels in the hippocampus generated by GluCEST imaging. **d,** Glutamate levels in CA1 are not different between groups. n=6-7/ group. One way ANOVA. * $p < 0.05$.

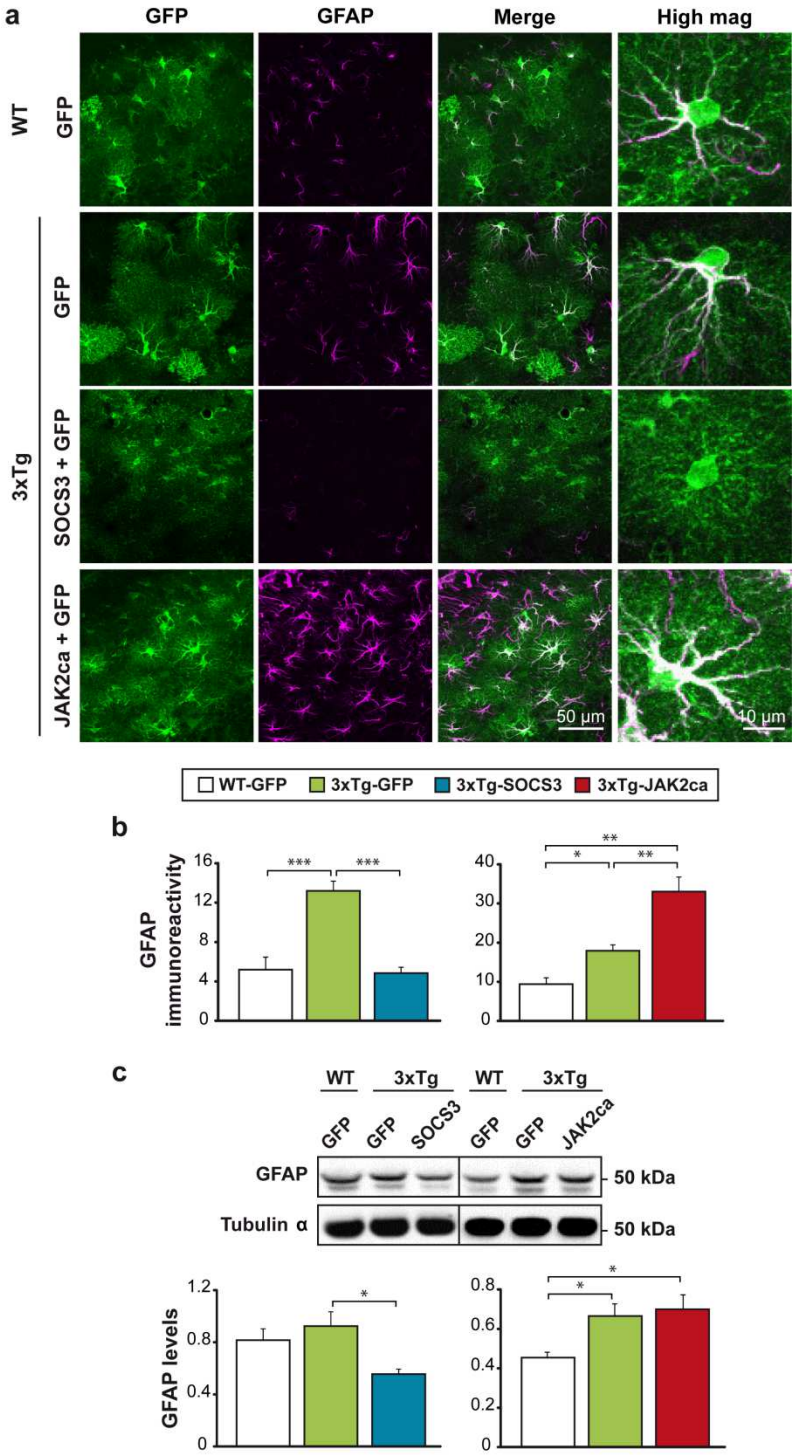

Figure 7. Efficient modulation of astrocyte reactivity in 3xTg mice.

a, Confocal images of GFP^{+} astrocytes (green) stained for GFAP (magenta) in 16 month-old WT and 3xTg mice injected in the CA1 region with AAV-GFP, AAV-SOCS3 + AAV-GFP or AAV-JAK2ca + AAV-GFP (same viral titer). In 3xTg mice, astrocytes display the typical features of reactivity (GFAP overexpression and hypertrophy). SOCS3 significantly reduces GFAP levels, while JAK2ca increases them. **b**, Quantification of GFAP immunoreactivity on hippocampal slices. N = 4-8/group. Kruskall-Wallis and Mann-Whitney tests. **c,** Western blotting and quantification of GFAP levels (normalized by tubulin α) in WT-GFP, 3xTg-GFP, 3xTg-SOCS3 and 3xTg-JAK2ca mice show the same pattern of GFAP modulation by SOCS3 and JAK2ca. N = 7-8/group. One way ANOVA and Tukey's post hoc test. * $p < 0.05$, ** $p < 0.01$, *** $p < 0.001$.

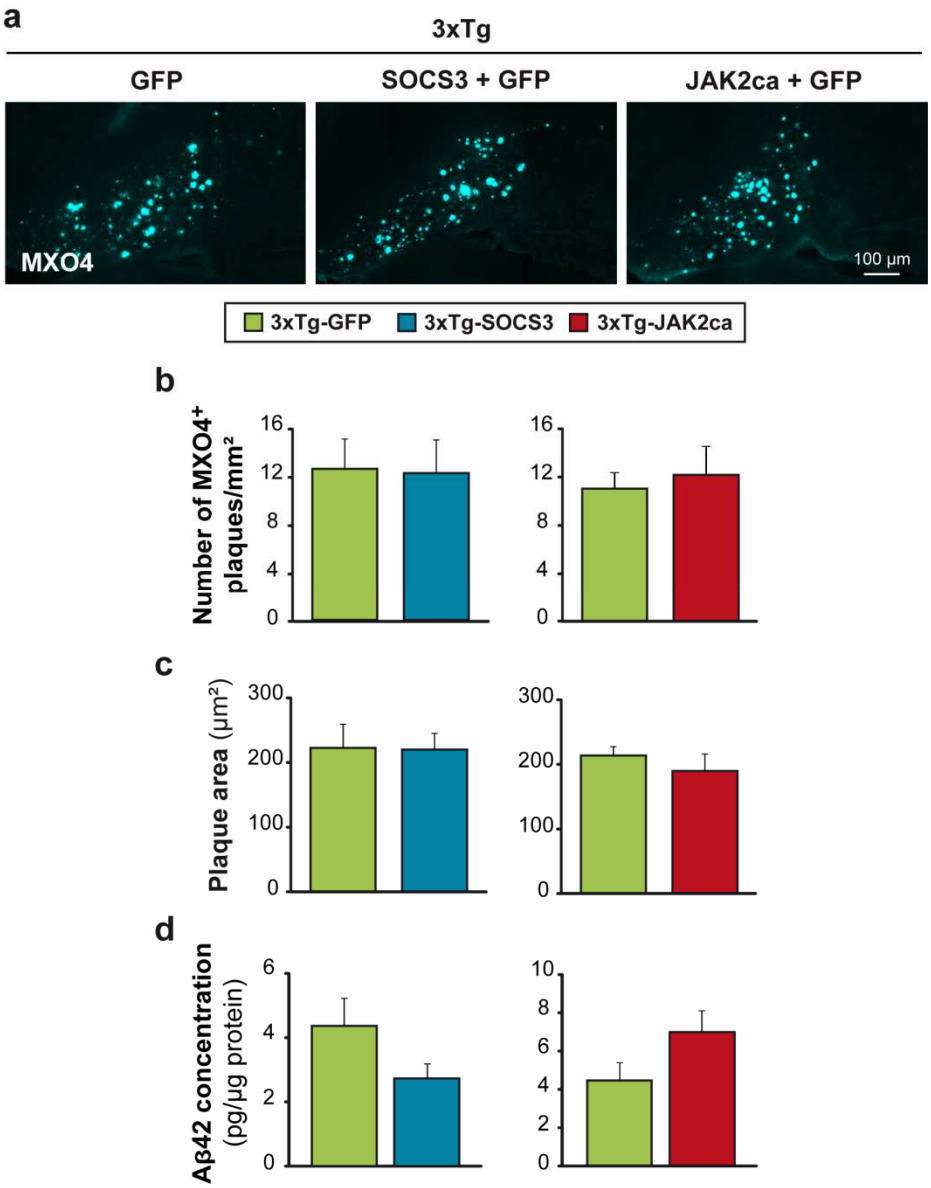

Figure 8. Modulation of astrocyte reactivity does not impact amyloid load in 3xTg mice.

a, Representative images of amyloid plaques labelled with MXO4 (cyan) in 3xTg-GFP, 3xTg-SOCS3 and 3xTg-JAK2ca mice. **b,** Quantification of plaque density in the whole hippocampus shows no change between groups. **c,** The average size of $MXO4^{+}$ amyloid plaques is also similar between groups. N = 7-9/group. Mann-Whitney test. **d,** MSD® measurement of Aβ42 concentration in Triton-X100 soluble protein homogenates prepared from the hippocampus of 3xTg-GFP, 3xTg-SOCS3 and 3xTg-JAK2ca mice. Aβ42 levels are not changed by SOCS3 or JAK2ca in 3xTg mice. N = 7-9/group. Mann-Whitney test.

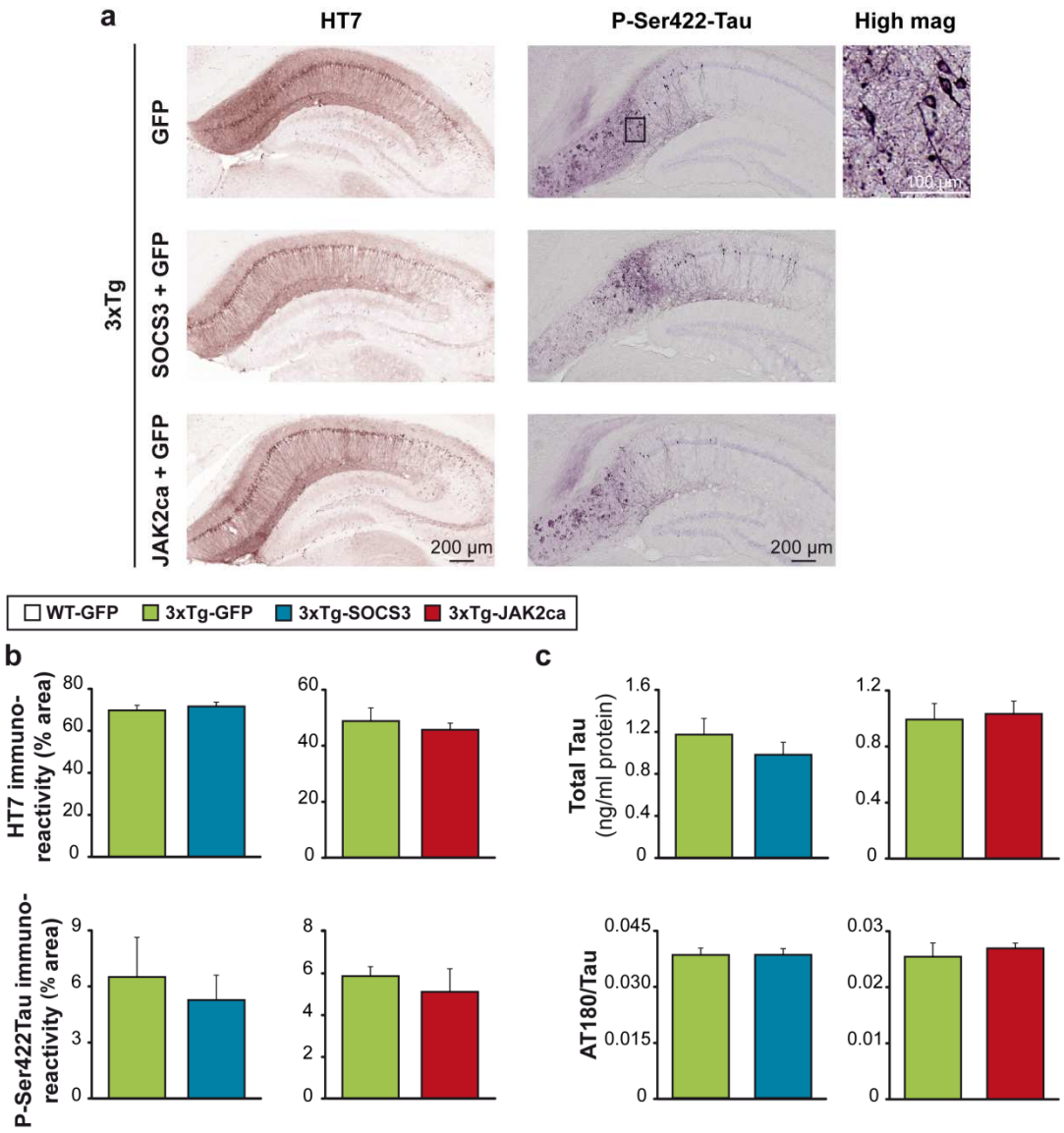

Figure 9. Modulation of astrocyte reactivity does not impact Tau pathology in 3xTg mice.

a, Representative sections of 3xTg-GFP, 3xTg-SOCS3 and 3xTg-JAK2ca mice stained with antibodies against total human Tau (HT7) or phospho-Ser422-Tau antibodies (P-Ser422-Tau). High magnification image illustrates the presence of dystrophic neurons and ghost tangles immunopositive for phospho-Ser422-Tau. **b,** Quantification of the area positive for Tau in the whole hippocampus shows no change between groups for the 2 antibodies. N = 8-9/group. Student *t* test (HT7) or Mann-Whitney test (phospho-Ser422-Tau). **c,** MSD® measurement of phospho-Thr231-Tau (AT180 antibody) and total Tau in protein homogenates prepared from the hippocampus of 3xTg-GFP, 3xTg -SOCS3 and 3xTg-JAK2ca mice. Total Tau and AT180/Tau levels are not changed by SOCS3 or JAK2ca in 3xTg mice. N = 7-9/group. Mann-Whitney test.

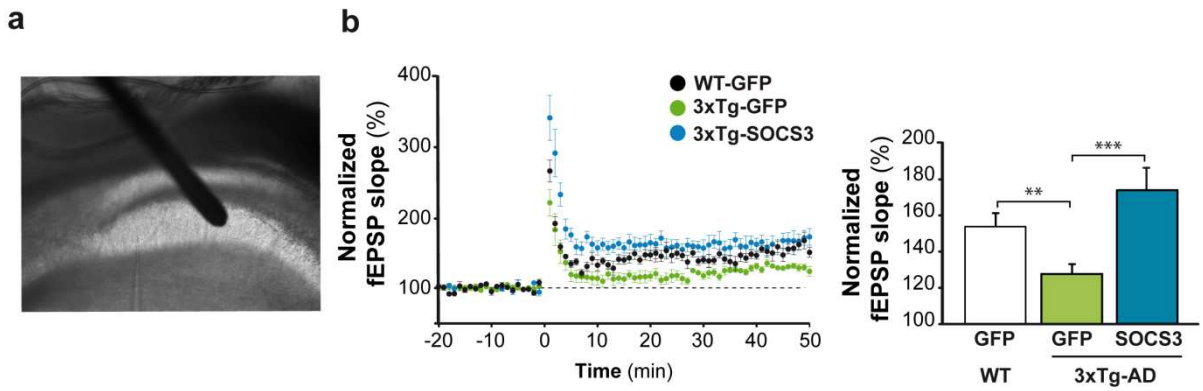

Figure 10. Inhibition of astrocyte reactivity restores LTP.

a. Acute hippocampal slices were prepared from the hippocampus of 7-8 month-old WT-GFP, 3xTg-GFP and 3xTg-SOCS3 mice. A recording electrode was placed in the GFP^+ CA1 region. **b.** HFS failed to induce LTP in 3xTg-GFP mice. De-activation of astrocytes with SOCS3 restored LTP to levels observed in WT-GFP mice. Left panel: average traces for each group for 20 min before to 50 min after HFS, induced at time 0. Right panel: quantification of normalized fEPSP slopes 40 to 50 min post HFS. N = 5-7/group. Kruskal-Wallis and Dunn's multiple comparisons tests. ** $p<0.01$, *** $p<0.001$.

SUPPLEMENTAL MATERIAL

Gene	Forward primer	Reverse primer
Actin	AGAGGGAAATCGTGCGTGAC	CGATAGTGATGACCTGACCGT
Aif1 (Iba1)	CCAGCCTAAGACAACCAGCGTC	GCTGTATTTGGGATCATCGAGGAA
Aldh1l1	TTCGCTGGCTGGTGTGATAAGA	GGTCAAGGTCAGGTTGCGGTT
ApoE	CTGAACCGCTTCTGGGATTACCTG	CATAGTGTCCTCCATCAGTGCCGTC
C1qb	CCACGCAACGGCAAGTTCAC	CGGCCACGAACGAGATTCAC
Cspg4 (Ng2)	AGGGAGCAGGCAAACGAAGA	TGAAGCTGCCACGGATAGGA
Ctss	GGCATGAACGATATGGGAG	TCAGGCAATGTCCGATTAGA
Eef1a1	CTACCCTCCACTTGGTCGCTT	GCAACTGTCTGCCTCATGTCAC
Gfp	TGCAGCTCGCCGACCACTACCA	GCAGGACCATGTGATCGCGCTTC
Gfap	ACGACTATCGCCGCCAACT	GCCGCTCTAGGGACTCGTTC
Mal2	GGCCACCTCCCTGCATGACC	AAGCCAGACCCAAACTGCAACCA
Mbp	CTTCAAAGACAGGCCCTCAG	CCTGTCACCGCTAAAGAAGC
Serpina3n	CAACCTTACAGGCCAACCCAT	GGGCACCAAGTAGTCCTAGATGCT
Socs3	CGAGAAGATTCCGCTGGTACTGA	TGATCCAGGAACTCCCGAATG
Tmem119	GTGTCTAACAGGCCCCAGAA	AGCCACGTGGTATCAAGGAG
Trem2	AATGGGAGCACAGTCATCGCAGA	ACTGGTAGAGGCCCGCGTCAC

Supplemental table 1: Sequence of primers used for qPCR.

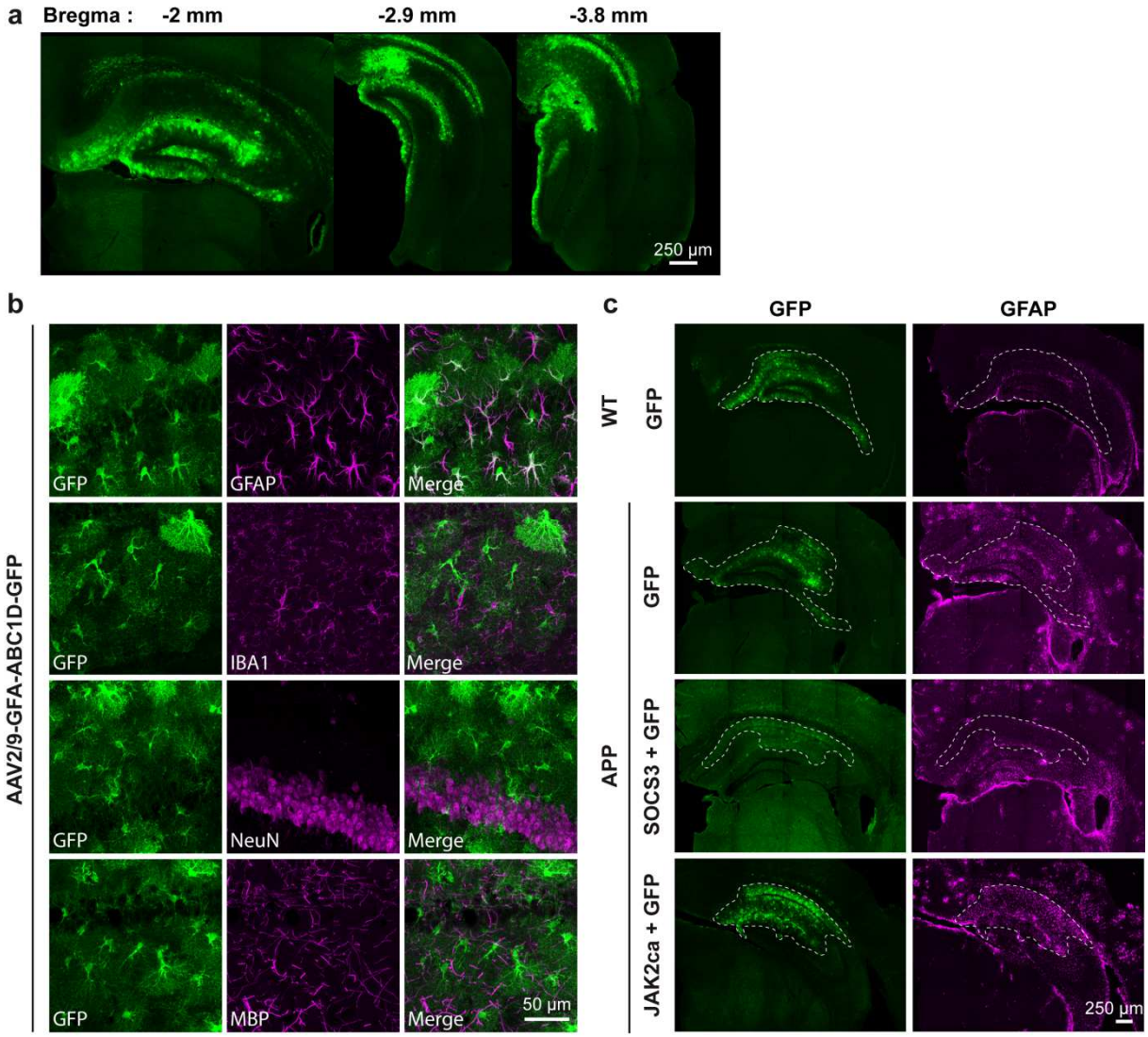

Supplemental figure 1. Widespread modulation of astrocyte reactivity with AAV vectors targeting the JAK2-STAT3 pathway in astrocytes.

a, Injection of AAV-GFP in the hippocampus of WT mice results in a widespread expression of GFP (green) along the antero-posterior axis of the hippocampus. **b,** GFP^+ cells co-express the astrocytic marker GFAP but not the microglial marker IBA1, the neuronal marker NeuN or the oligodendrocyte marker MBP. **c,** AAV-SOCS3 efficiently blunts GFAP expression (magenta), while AAV-JAK2 increase GFAP levels in the hippocampus of APP mice. GFP^+ area (green) displaying infected astrocytes is delineated by white dashes. Note that amyloid plaques are visible in APP mice (especially in the cortex), as clusters of $GFAP^+$ astrocytes.

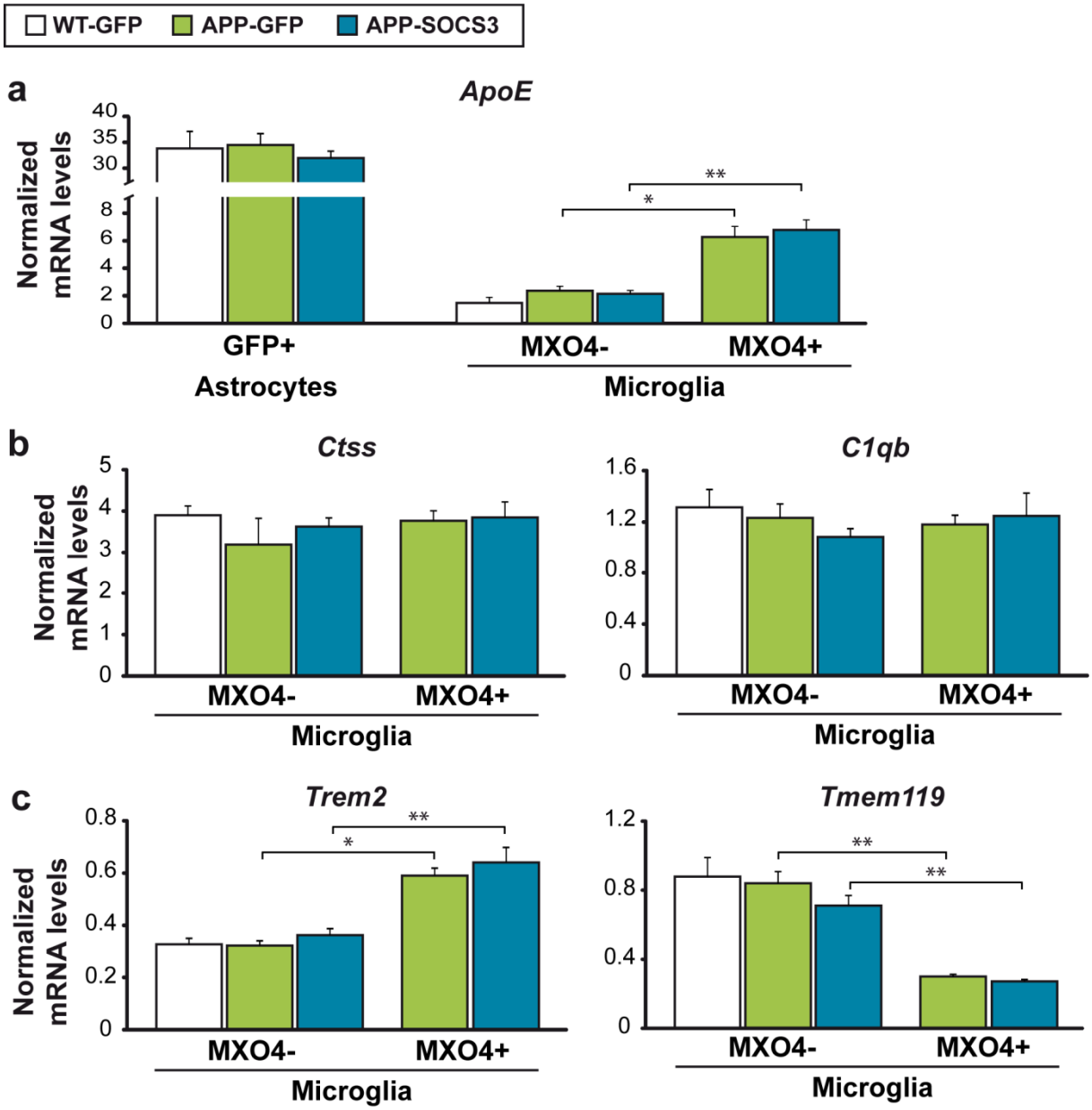

Supplemental figure 2. Inhibition of astrocyte reactivity does not impact the transcriptional profile of microglial cells.

RT-qPCR analysis on cells acutely isolated from the hippocampus of WT-GFP, APP-GFP and APP-SOCS3 mice. **a,** mRNA levels for *Apoe* in GFP^+ astrocytes, $MXO4^-$ or $MXO4^+$ microglial cells. *ApoE* is enriched in astrocytes. Its expression is stable across astrocytes of the 3 groups. *Apoe* is expressed at higher levels in $MXO4^+$ microglia (i.e. phagocytic microglia) than $MXO4^-$ microglia, consistent with DAM transcriptomic profile (Keren-Shaul et al., 2017). **b,** The expression of *Ctss* and *C1qb,* two microglial homeostatic genes, is similar between both types of microglial cells and within the 3 groups. **c,** $MXO4^+$ microglia express higher levels of *Trem2* and lower levels of *Tmem119* than $MXO4^-$ microglial cells, which is again consistent with a DAM transcriptomic profile of $MXO4^+$ microglial cells. Astrocyte de-activation by SOCS3 does not impact the transcriptional profile of either type of microglia. N = 3-8/group. One way ANOVA to compare the 3 groups within $MXO4^-$ cells and Student *t* test to compare two groups within $MXO4^+$ cells. Mann-Whitney test to compare $MXO4^+$ and $MXO4^-$ microglial cells within APP-GFP or APP-SOCS3 groups. * $p < 0.05$, ** $p < 0.01$.

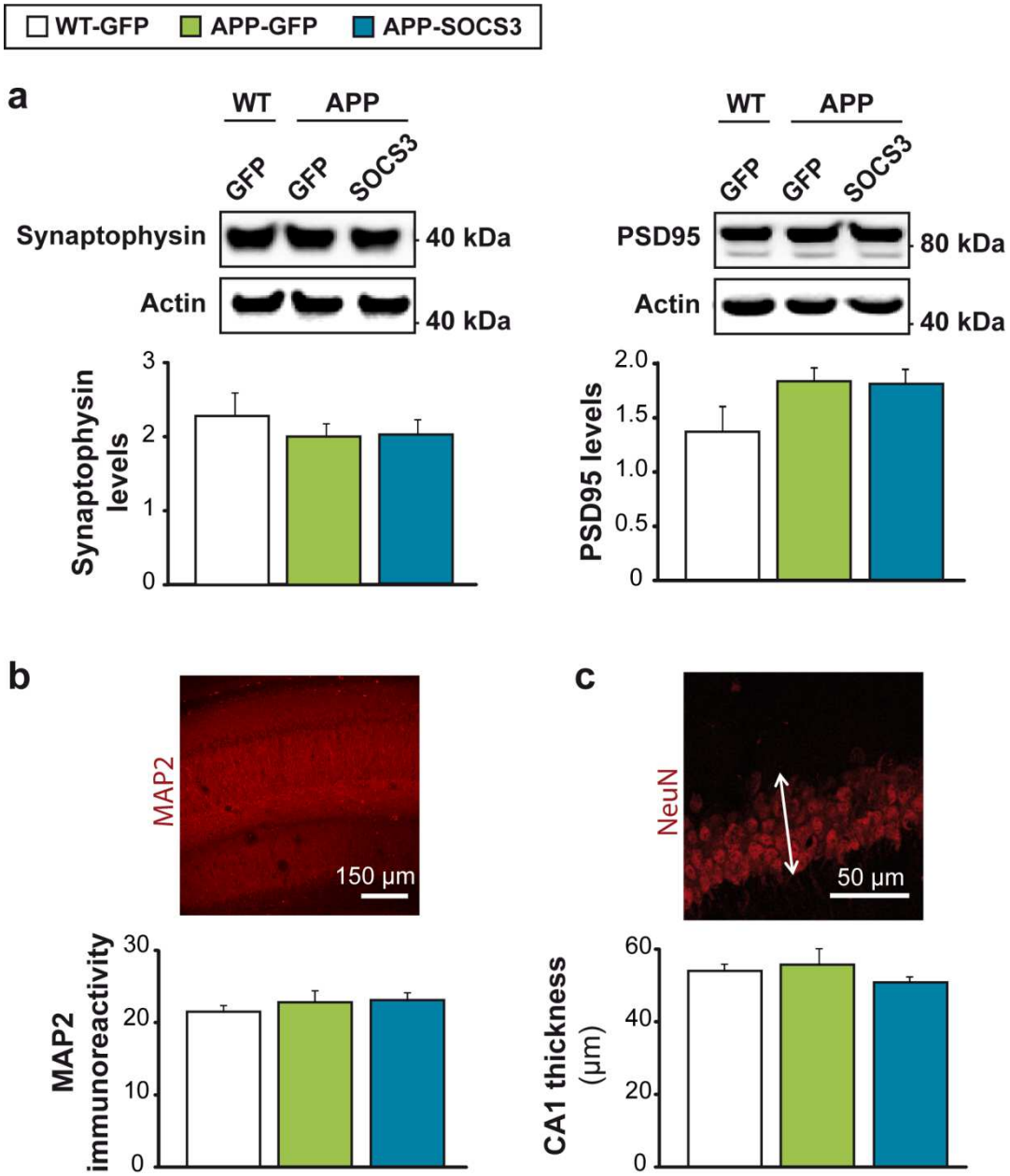

Supplemental figure 3. SOCS3 has no effects on synaptic proteins or neuronal morphological features.

a, Representative western blotting and quantification of synaptic markers in WT-GFP, APP-GFP and APP-SOCS3. Synaptophysin and PSD95 levels are not altered in APP mice or with SOCS3 expression in astrocytes (protein levels are normalized by actin). N = 4-8/group. One way ANOVA. Immunoreactivity for MAP2, a dendritic marker (**b**), or thickness of the CA1 pyramidal cell layer (**c**) are similar in the 3 groups. N = 3-9/group. One way ANOVA.

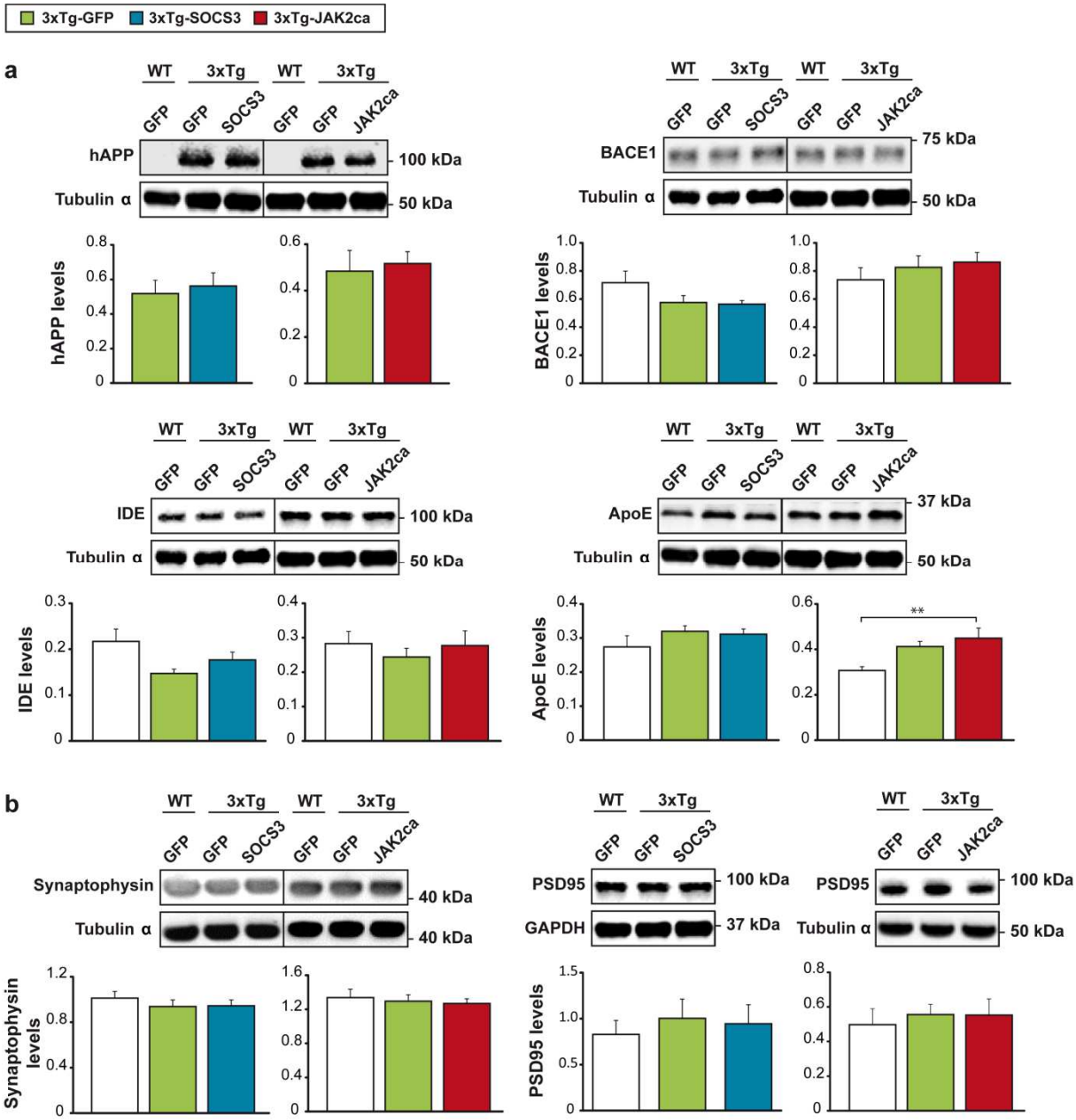

Supplemental figure 4. Modulation of astrocyte reactivity does not impact the expression of proteins involved in Aβ metabolism or clearance and synaptic proteins in 3xTg mice.

a, Representative western blotting and quantification of hAPP and key enzymes (BACE1, IDE) or transporter (ApoE) involved in Aβ production or clearance in WT-GFP, 3xTg-GFP, 3xTg-SOCS3 and 3xTg-JAK2ca. Protein expression is similar between groups. Only ApoE levels are found significantly higher in 3xTg-JAK2ca mice than in WT-GFP mice. N = 3-9/group. One way ANOVA (hAPP, BACE1, IDE) or Kruskall-Wallis test (ApoE). **b,** Synaptophysin and PSD95 levels are not altered in 3xTg mice or with SOCS3 or JAK2ca expression in astrocytes. Protein levels are normalized by GAPDH or tubulin α. N = 4-8/group. Kruskall-Wallis test and Mann-Whitney test. ** $p < 0.01$.

ACKNOWLEDGMENTS

This study was supported by CEA, CNRS and grants from the French National Research Agency (grants # 2010-JCJC-1402-1, 2011-BSV4-021-03 and ANR-16-TERC-0016-01), from Fondation Vaincre Alzheimer (grant # FR-15015) (to C.E.), as well as CNRS and INSERM (to S.H.R.O. and A.P). C.E. and A.P. received support from the Fédération pour la Recherche sur le Cerveau.

K. Ceyzériat and O. Guillemaud are recipients of a doctoral fellowship from the CEA.

We thank Prof. Haan (Univ. Luxembourg) for sharing the JAK2ca cDNA and Dr. Bjørbæk and Dr. Shoelson for sharing the SOCS3 cDNA.

We are grateful to D. Cheramy and Dr. E. Diguet (Servier) for sharing their expertise and equipment for MSD® kits. We thank L. Vincent, K. Bastide, P. Woodling and J.M. Hélies for their help with mouse housing and transfer; C. Garin and C. Dudeffant for help with the APP/PS1dE9 colony. We are grateful to Dr. A. Bémelmans for supervising AAV production and F. Aubry for help with initial AAV vector cloning. We thank D. Gonzales, S. Laumond, J. Tessaire and people at the animal facility of the NeuroCentre Magendie for mouse care and genotyping.

REFERENCES

Abeti R, Abramov AY, Duchen MR (2011) Beta-amyloid activates PARP causing astrocytic metabolic failure and neuronal death. Brain 134:1658-1672.

Allaman I, Belanger M, Magistretti PJ (2011) Astrocyte-neuron metabolic relationships: for better and for worse. Trends Neurosci 34:76-87.

Allaman I, Gavillet M, Belanger M, Laroche T, Viertl D, Lashuel HA, Magistretti PJ (2010) Amyloid-beta aggregates cause alterations of astrocytic metabolic phenotype: impact on neuronal viability. J Neurosci 30:3326-3338.

Anderson MA, Ao Y, Sofroniew MV (2014) Heterogeneity of reactive astrocytes. Neurosci Lett 565:23-29.

Anderson MA, Burda JE, Ren Y, Ao Y, O'Shea TM, Kawaguchi R, Coppola G, Khakh BS, Deming TJ, Sofroniew MV (2016) Astrocyte scar formation aids central nervous system axon regeneration. Nature 532:195-200.

Araque A, Carmignoto G, Haydon PG, Oliet SH, Robitaille R, Volterra A (2014) Gliotransmitters travel in time and space. Neuron 81:728-739.

Barres BA (2008) The mystery and magic of glia: a perspective on their roles in health and disease. Neuron 60:430-440.

Belanger M, Allaman I, Magistretti PJ (2011) Brain energy metabolism: focus on astrocyte-neuron metabolic cooperation. Cell metabolism 14:724-738.

Ben Haim Ceyzériat L, Carrillo de Sauvage MA, A. D, Abjean L, Gipstein P, Derbois C, Palomares MA, Pommier D, Santos M, Guillemaud O, Petit F, Juricek L, Jan C, Veran J, Guillermier M, Auregan G, Dufour N, Joséphine C, Gaillard MC, Dhenain M, Robil N, De la Grange P, Deleuze JF, Hantraye P, Brouillet E, Panatier A, Olaso R, Escartin C (submitted) The JAK2-STAT3 pathway is a master regulator of astrocyte reactivity in neurodegenerative diseases.

Ben Haim L, Carrillo-de Sauvage MA, Ceyzeriat K, Escartin C (2015a) Elusive roles for reactive astrocytes in neurodegenerative diseases. Frontiers in cellular neuroscience 9:278.

Ben Haim L, Ceyzeriat K, Carrillo-de Sauvage MA, Aubry F, Auregan G, Guillermier M, Ruiz M, Petit F, Houitte D, Faivre E, Vandesquille M, Aron-Badin R, Dhenain M, Deglon N, Hantraye P, Brouillet E, Bonvento G, Escartin C (2015b) The JAK/STAT3 Pathway Is a Common Inducer of Astrocyte Reactivity in Alzheimer's and Huntington's Diseases. J Neurosci 35:2817-2829.

Cole SL, Vassar R (2007) The Alzheimer's disease beta-secretase enzyme, BACE1. Molecular neurodegeneration 2:22.

Dabir DV, Robinson MB, Swanson E, Zhang B, Trojanowski JQ, Lee VM, Forman MS (2006) Impaired glutamate transport in a mouse model of tau pathology in astrocytes. J Neurosci 26:644-654.

Dansokho C, Ait Ahmed D, Aid S, Toly-Ndour C, Chaigneau T, Calle V, Cagnard N, Holzenberger M, Piaggio E, Aucouturier P, Dorothee G (2016) Regulatory T cells delay disease progression in Alzheimer-like pathology. Brain 139:1237-1251.

De Strooper B, Karran E (2016) The Cellular Phase of Alzheimer's Disease. Cell 164:603-615.

Delekate A, Fuchtemeier M, Schumacher T, Ulbrich C, Foddis M, Petzold GC (2014) Metabotropic P2Y1 receptor signalling mediates astrocytic hyperactivity in vivo in an Alzheimer's disease mouse model. Nature communications 5:5422.

Escartin C, Brouillet E, Gubellini P, Trioulier Y, Jacquard C, Smadja C, Knott GW, Kerkerian-Le Goff L, Deglon N, Hantraye P, Bonvento G (2006) Ciliary neurotrophic factor activates astrocytes, redistributes their glutamate transporters GLAST and GLT-1 to raft microdomains, and improves glutamate handling in vivo. J Neurosci 26:5978-5989.

Escartin C, Pierre K, Colin A, Brouillet E, Delzescaux T, Guillermier M, Dhenain M, Deglon N, Hantraye P, Pellerin L, Bonvento G (2007) Activation of astrocytes by CNTF induces metabolic plasticity and increases resistance to metabolic insults. J Neurosci 27:7094-7104.

Furman JL, Sama DM, Gant JC, Beckett TL, Murphy MP, Bachstetter AD, Van Eldik LJ, Norris CM (2012) Targeting astrocytes ameliorates neurologic changes in a mouse model of Alzheimer's disease. J Neurosci 32:16129-16140.

Guillot-Sestier MV, Doty KR, Gate D, Rodriguez J, Jr., Leung BP, Rezai-Zadeh K, Town T (2015) Il10 deficiency rebalances innate immunity to mitigate Alzheimer-like pathology. Neuron 85:534-548.

Haan S, Wuller S, Kaczor J, Rolvering C, Nocker T, Behrmann I, Haan C (2009) SOCS-mediated downregulation of mutant Jak2 (V617F, T875N and K539L) counteracts cytokine-independent signaling. Oncogene 28:3069-3080.

Hamelin L, Lagarde J, Dorothee G, Leroy C, Labit M, Comley RA, de Souza LC, Corne H, Dauphinot L, Bertoux M, Dubois B, Gervais P, Colliot O, Potier MC, Bottlaender M, Sarazin M, Clinical It (2016) Early and protective microglial activation in Alzheimer's disease: a prospective study using 18F-DPA-714 PET imaging. Brain 139:1252-1264.

Heneka MT, Carson MJ, El Khoury J, Landreth GE, Brosseron F, Feinstein DL, Jacobs AH, Wyss-Coray T, Vitorica J, Ransohoff RM, Herrup K, Frautschy SA, Finsen B, Brown GC, Verkhratsky A, Yamanaka K, Koistinaho J, Latz E, Halle A, Petzold GC, Town T, Morgan D, Shinohara ML, Perry VH, Holmes C, Bazan NG, Brooks DJ, Hunot S, Joseph B, Deigendesch N, Garaschuk O, Boddeke E, Dinarello CA, Breitner JC, Cole GM, Golenbock DT, Kummer MP (2015) Neuroinflammation in Alzheimer's disease. Lancet Neurol 14:388-405.

Heneka MT, Sastre M, Dumitrescu-Ozimek L, Dewachter I, Walter J, Klockgether T, Van Leuven F (2005) Focal glial activation coincides with increased BACE1 activation and precedes amyloid plaque deposition in APP[V717I] transgenic mice. J Neuroinflammation 2:22.

Herrup K (2015) The case for rejecting the amyloid cascade hypothesis. Nat Neurosci 18:794-799.

Hol EM, Pekny M (2015) Glial fibrillary acidic protein (GFAP) and the astrocyte intermediate filament system in diseases of the central nervous system. Current opinion in cell biology 32:121-130.

Hong S, Beja-Glasser VF, Nfonoyim BM, Frouin A, Li S, Ramakrishnan S, Merry KM, Shi Q, Rosenthal A, Barres BA, Lemere CA, Selkoe DJ, Stevens B (2016) Complement and microglia mediate early synapse loss in Alzheimer mouse models. Science 352:712-716.

Jankowsky JL, Fadale DJ, Anderson J, Xu GM, Gonzales V, Jenkins NA, Copeland NG, Lee MK, Younkin LH, Wagner SL, Younkin SG, Borchelt DR (2004) Mutant presenilins specifically elevate the levels of the 42 residue beta-amyloid peptide in vivo: evidence for augmentation of a 42-specific gamma secretase. Hum Mol Genet 13:159-170.

Jo S, Yarishkin O, Hwang YJ, Chun YE, Park M, Woo DH, Bae JY, Kim T, Lee J, Chun H, Park HJ, Lee DY, Hong J, Kim HY, Oh SJ, Park SJ, Lee H, Yoon BE, Kim Y, Jeong Y, Shim I, Bae YC, Cho J, Kowall NW, Ryu H, Hwang E, Kim D, Lee CJ (2014) GABA from reactive astrocytes impairs memory in mouse models of Alzheimer's disease. Nat Med.

Kamphuis W, Kooijman L, Orre M, Stassen O, Pekny M, Hol EM (2015) GFAP and vimentin deficiency alters gene expression in astrocytes and microglia in wild-type mice and changes the transcriptional response of reactive glia in mouse model for Alzheimer's disease. Glia.

Keren-Shaul H, Spinrad A, Weiner A, Matcovitch-Natan O, Dvir-Szternfeld R, Ulland TK, David E, Baruch K, Lara-Astaiso D, Toth B, Itzkovitz S, Colonna M, Schwartz M, Amit I (2017) A Unique Microglia Type Associated with Restricting Development of Alzheimer's Disease. Cell 169:1276-1290 e1217.

Kim M, Gillen J, Landman BA, Zhou J, van Zijl PC (2009) Water saturation shift referencing (WASSR) for chemical exchange saturation transfer (CEST) experiments. Magn Reson Med 61:1441-1450.

Koistinaho M, Lin S, Wu X, Esterman M, Koger D, Hanson J, Higgs R, Liu F, Malkani S, Bales KR, Paul SM (2004) Apolipoprotein E promotes astrocyte colocalization and degradation of deposited amyloid-beta peptides. Nat Med 10:719-726.

Kraft AW, Hu X, Yoon H, Yan P, Xiao Q, Wang Y, Gil SC, Brown J, Wilhelmsson U, Restivo JL, Cirrito JR, Holtzman DM, Kim J, Pekny M, Lee JM (2013) Attenuating astrocyte activation accelerates plaque pathogenesis in APP/PS1 mice. FASEB J 27:187-198.

Krauthausen M, Kummer MP, Zimmermann J, Reyes-Irisarri E, Terwel D, Bulic B, Heneka MT, Muller M (2015) CXCR3 promotes plaque formation and behavioral deficits in an Alzheimer's disease model. J Clin Invest 125:365-378.

Kuchibhotla KV, Lattarulo CR, Hyman BT, Bacskai BJ (2009) Synchronous hyperactivity and intercellular calcium waves in astrocytes in Alzheimer mice. Science 323:1211-1215.
Lee CY, Landreth GE (2010) The role of microglia in amyloid clearance from the AD brain. Journal of neural transmission 117:949-960.
Lee Y, Messing A, Su M, Brenner M (2008) GFAP promoter elements required for region-specific and astrocyte-specific expression. Glia 56:481-493.
Leyns CEG, Holtzman DM (2017) Glial contributions to neurodegeneration in tauopathies. Molecular neurodegeneration 12:50.
Lian H, Yang L, Cole A, Sun L, Chiang AC, Fowler SW, Shim DJ, Rodriguez-Rivera J, Taglialatela G, Jankowsky JL, Lu HC, Zheng H (2015) NFkappaB-Activated Astroglial Release of Complement C3 Compromises Neuronal Morphology and Function Associated with Alzheimer's Disease. Neuron 85:101-115.
Liao MC, Muratore CR, Gierahn TM, Sullivan SE, Srikanth P, De Jager PL, Love JC, Young-Pearse TL (2016) Single-Cell Detection of Secreted Abeta and sAPPalpha from Human IPSC-Derived Neurons and Astrocytes. J Neurosci 36:1730-1746.
Liddelow SA, Barres BA (2017) Reactive Astrocytes: Production, Function, and Therapeutic Potential. Immunity 46:957-967.
Liddelow SA, Guttenplan KA, Clarke LE, Bennett FC, Bohlen CJ, Schirmer L, Bennett ML, Munch AE, Chung WS, Peterson TC, Wilton DK, Frouin A, Napier BA, Panicker N, Kumar M, Buckwalter MS, Rowitch DH, Dawson VL, Dawson TM, Stevens B, Barres BA (2017) Neurotoxic reactive astrocytes are induced by activated microglia. Nature.
Masliah E, Alford M, DeTeresa R, Mallory M, Hansen L (1996) Deficient glutamate transport is associated with neurodegeneration in Alzheimer's disease. Ann Neurol 40:759-766.
Musiek ES, Holtzman DM (2015) Three dimensions of the amyloid hypothesis: time, space and 'wingmen'. Nat Neurosci 18:800-806.
Oddo S, Caccamo A, Shepherd JD, Murphy MP, Golde TE, Kayed R, Metherate R, Mattson MP, Akbari Y, LaFerla FM (2003) Triple-transgenic model of Alzheimer's disease with plaques and tangles: intracellular Abeta and synaptic dysfunction. Neuron 39:409-421.
Oliet SH, Piet R, Poulain DA (2001) Control of glutamate clearance and synaptic efficacy by glial coverage of neurons. Science 292:923-926.
Orre M, Kamphuis W, Osborn LM, Jansen AH, Kooijman L, Bossers K, Hol EM (2014) Isolation of glia from Alzheimer's mice reveals inflammation and dysfunction. Neurobiol Aging 35:2746-2760.
Panatier A, Theodosis DT, Mothet JP, Touquet B, Pollegioni L, Poulain DA, Oliet SH (2006) Glia-derived D-serine controls NMDA receptor activity and synaptic memory. Cell 125:775-784.
Panatier A, Vallee J, Haber M, Murai KK, Lacaille JC, Robitaille R (2011) Astrocytes are endogenous regulators of basal transmission at central synapses. Cell 146:785-798.
Pannasch U, Freche D, Dallerac G, Ghezali G, Escartin C, Ezan P, Cohen-Salmon M, Benchenane K, Abudara V, Dufour A, Lubke JH, Deglon N, Knott G, Holcman D, Rouach N (2014) Connexin 30 sets synaptic strength by controlling astroglial synapse invasion. Nat Neurosci 17:549-558.
Pepin J, Francelle L, Carrillo-de Sauvage MA, de Longprez L, Gipchtein P, Cambon K, Valette J, Brouillet E, Flament J (2016) In vivo imaging of brain glutamate defects in a knock-in mouse model of Huntington's disease. Neuroimage 139:53-64.
Provencher SW (1993) Estimation of metabolite concentrations from localized in vivo proton NMR spectra. Magn Reson Med 30:672-679.
Querfurth HW, LaFerla FM (2010) Alzheimer's disease. N Engl J Med 362:329-344.
Sancheti H, Patil I, Kanamori K, Diaz Brinton R, Zhang W, Lin AL, Cadenas E (2014) Hypermetabolic state in the 7-month-old triple transgenic mouse model of Alzheimer's disease and the effect of lipoic acid: a 13C-NMR study. J Cereb Blood Flow Metab 34:1749-1760.
Shi Q, Chowdhury S, Ma R, Le KX, Hong S, Caldarone BJ, Stevens B, Lemere CA (2017) Complement C3 deficiency protects against neurodegeneration in aged plaque-rich APP/PS1 mice. Science translational medicine 9.
Sompol P, Furman JL, Pleiss MM, Kraner SD, Artiushin IA, Batten SR, Quintero JE, Simmerman LA, Beckett TL, Lovell MA, Murphy MP, Gerhardt GA, Norris CM (2017) Calcineurin/NFAT

Signaling in Activated Astrocytes Drives Network Hyperexcitability in Abeta-Bearing Mice. J Neurosci 37:6132-6148.
Srinivasan K, Friedman BA, Larson JL, Lauffer BE, Goldstein LD, Appling LL, Borneo J, Poon C, Ho T, Cai F, Steiner P, van der Brug MP, Modrusan Z, Kaminker JS, Hansen DV (2016) Untangling the brain's neuroinflammatory and neurodegenerative transcriptional responses. Nature communications 7:11295.
Vandesompele J, De Preter K, Pattyn F, Poppe B, Van Roy N, De Paepe A, Speleman F (2002) Accurate normalization of real-time quantitative RT-PCR data by geometric averaging of multiple internal control genes. Genome Biol 3:RESEARCH0034.
Wu Z, Guo Z, Gearing M, Chen G (2014) Tonic inhibition in dentate gyrus impairs long-term potentiation and memory in an Alzhiemer's disease model. Nature communications 5:4159.
Wyss-Coray T, Loike JD, Brionne TC, Lu E, Anankov R, Yan F, Silverstein SC, Husemann J (2003) Adult mouse astrocytes degrade amyloid-beta in vitro and in situ. Nat Med 9:453-457.
Yi C, Mei X, Ezan P, Mato S, Matias I, Giaume C, Koulakoff A (2016) Astroglial connexin43 contributes to neuronal suffering in a mouse model of Alzheimer's disease. Cell death and differentiation 23:1691-1701.
Zamanian JL, Xu L, Foo LC, Nouri N, Zhou L, Giffard RG, Barres BA (2012) Genomic analysis of reactive astrogliosis. J Neurosci 32:6391-6410.
Zheng C, Zhou XW, Wang JZ (2016) The dual roles of cytokines in Alzheimer's disease: update on interleukins, TNF-alpha, TGF-beta and IFN-gamma. Translational neurodegeneration 5:7.

Contribution à l'article 2

J'ai réalisé l'ensemble des expériences sur le modèle APP. J'ai également réalisé une partie de l'analyse dans le modèle 3xTg : comportement, validation de la modulation de la réactivité astrocytaire par SOCS3 et JAK2ca, test MSD®, western blot. Cette analyse a été poursuivie par deux étudiants de Master 2 que j'ai supervisés (Thomas Saint-Georges et Océane Guillemaud). En particulier, Océane Guillemaud a réalisé l'analyse des effets de la modulation de la réactivité astrocytaire sur la pathologie Tau. La spectroscopie et l'imagerie par résonance magnétique sur les souris APP ont été réalisées en collaboration avec la plateforme d'imagerie de MIRCen. Les expériences d'électrophysiologie ont été réalisées par l'équipe d'Aude Panatier et Stéphane Oliet (Neurocentre Magendie, Bordeaux). J'ai également participé à la rédaction de l'article ainsi qu'à la réalisation de l'ensemble des figures.

3. Données complémentaires à l'article 2: Evaluation d'index cliniques

Afin de mesurer l'impact de la modulation de la réactivité astrocytaire sur des index plus pertinents pour la clinique, nous avons choisi de mesurer des altérations comportementales (incluant l'anxiété, la mémoire de travail et la mémoire à long terme). Chez les souris 3xTg, les deux groupes (SOCS3 et JAK2ca) ont été analysés, alors que pour les souris APP, nous avons choisi de focaliser notre évaluation clinique uniquement sur une nouvelle cohorte injectée avec l'AAV-SOCS3 car les souris APP-SOCS3 montrent un effet bénéfique au niveau de la pathologie amyloïde.

Altérations comportementales dans les modèles APP/PS1dE9

Le test du labyrinthe en croix a été réalisé afin de mesurer l'anxiété à 9 mois des souris APP et WT injectées avec des vecteurs codant pour SOCS3 + GFP, ou GFP seule. Aucune différence de comportement entre les trois groups n'a été observée. Nous avons ensuite réalisé un test de mémoire hippocampe-dépendant : le test de conditionnement par la peur pour évaluer la mémoire à long terme à 11 mois. Les souris WT font un peu plus de « freezing » que les deux autres groupes avant le choc (8% versus 2% d'immobilisation pour les APP-GFP et APP-SOCS3). Ceci reflète soit une légère anxiété chez les WT, qui n'a pas été visualisée au cours du test du labyrinthe en croix surélevé, soit un manque d'intérêt à visiter le dispositif. Les souris APP-GFP et APP-SOCS3 sont également moins tétanisées après le choc, mais aucune altération de la mémoire à long terme n'a été observée.

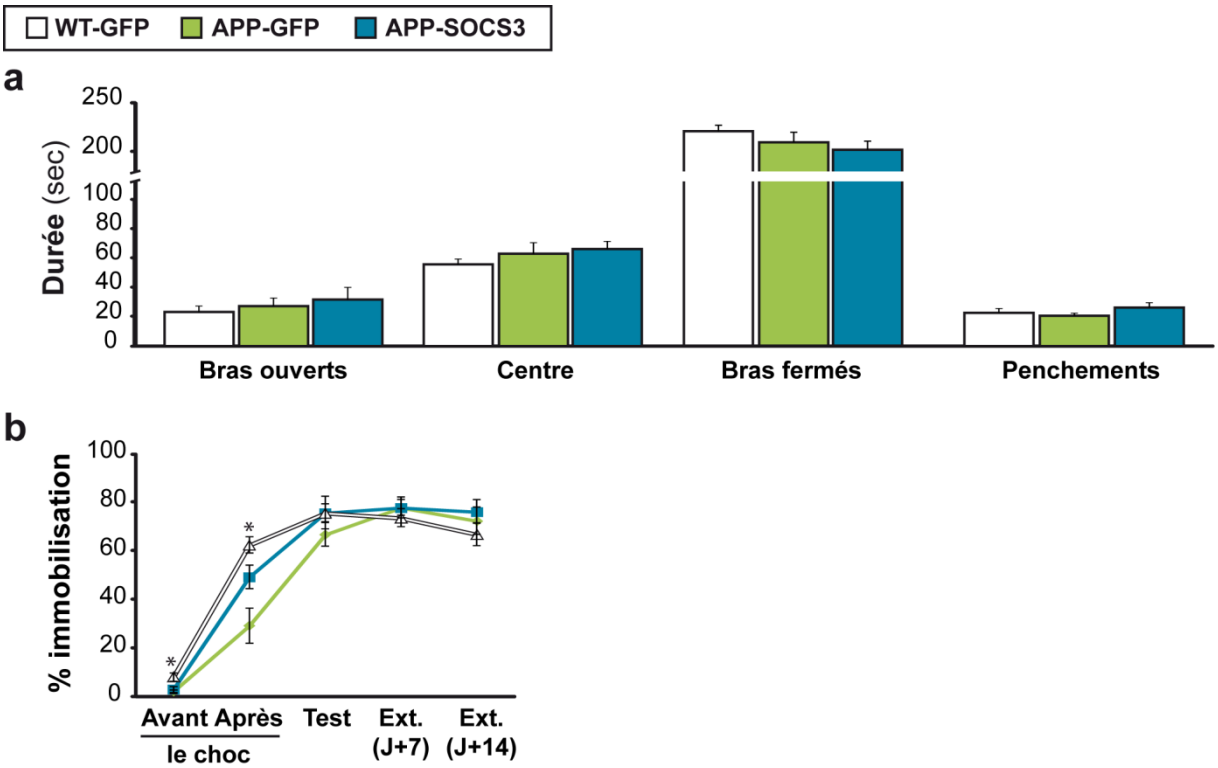

Figure 27 : Aucun déficit comportemental n'est observé dans le modèle APP/PS1dE9 à 9 et 11 mois.

a, Test du labyrinthe en croix surélevé. A 9 mois, les souris APP injectées avec un AAV-GFP passent autant de temps dans les différents bras du dispositif. Elles se penchent également au-dessus des bras ouverts (anxiogènes) comme les souris WT. L'injection d'AAV-SOCS3 n'affecte pas leur comportement. N= 11-13 / groupe. Test de Kruskal-Wallis. **b,** Test du conditionnement par la peur. Les souris APP-GFP restent moins longuement immobiles (« freezing ») que les autres groupes après le choc. Les souris APP-SOCS3 font également moins de « freezing » que les souris WT après le choc, mais aucune différence de mémorisation du choc n'est ensuite observée lors du test (24h après le choc) entre les 3 groupes. Aucune extinction du comportement de peur n'est observée que ce soit 7 ou 14 jours après le choc. N= 7-12 / groupe. Test de Kruskal-Wallis et Mann-Whitney. Abréviations : Ext. = Extinction, J+7 = 7 jours après le test, J+14 = 14 jours après le test.

Aucun de ces tests n'a donc permis de mesurer une altération cognitive dans ce modèle. Il est par conséquent impossible d'évaluer de potentiels effets thérapeutiques. Mais il est important de noter qu'aucun effet toxique de SOCS3 n'est observé.

La modulation de la réactivité astrocytaire semble affecter sensiblement le comportement des souris 3xTg-AD

Les tests du labyrinthe en croix et du labyrinthe en Y ont également été réalisés sur le modèle 3xTg injectées avec des vecteurs codant pour SOCS3 + GFP, ou JAK2ca + GFP, ou GFP seule, à 7-8 mois *(données non montrées)* et à 14-15 mois.

Les altérations du comportement à 7-8 mois suggéraient une plus forte anxiété chez les souris 3xTg-GFP que chez les WT-GFP puisqu'elles avaient tendance à se pencher moins longtemps au-dessus des bras ouverts, environnement anxiogène. Lors du test du labyrinthe en Y, les souris 3xTg-GFP exploraient moins le nouveau bras que le bras familier, suggérant également une altération de la mémoire spatiale de travail chez ces souris. Nous avons donc décidé de réaliser ces tests plus tardivement afin que les altérations cognitives soient plus importantes.

A 14-15 mois, le comportement anxieux (index = temps passé à se pencher au-dessus des bras ouverts ; « head dipping ») des souris 3xTg-GFP par rapport aux WT-GFP n'est toujours pas significatif bien qu'il soit plus important qu'à 7-8 mois. Mais, la désactivation des astrocytes tend à restaurer ce comportement anxieux. A l'inverse, la suractivation des astrocytes semble augmenter le comportement anxieux des souris 3xTg par rapport aux souris WT.

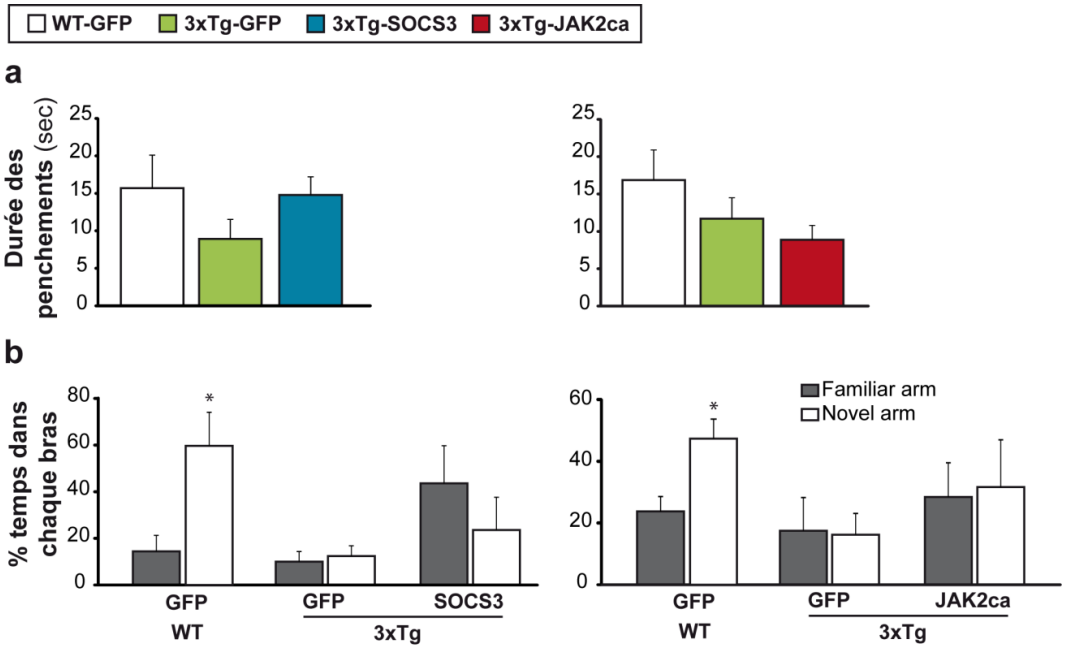

Figure 28 : La modulation de la réactivité astrocytaire semble affecter le comportement anxieux des souris 3xTg-AD mais n'influence pas les déficits mnésiques.

a, Test du labyrinthe en croix surélevé. A 14-15 mois, les souris 3xTg injectées avec un AAV-GFP ont tendance à moins se pencher au-dessus des bras ouverts (anxiogènes) que les souris WT. L'injection de SOCS3 semble corriger ce comportement. A l'inverse, les souris 3xTg-JAK2 ont tendance à se pencher moins longtemps que les deux autres groupes. N= 5-10 / groupe. Test de Kruskal-Wallis. **b,** Test du labyrinthe en Y. Les souris WT explorent préférentiellement le nouveau bras. Par contre, les souris 3xTg ne montrent aucune préférence entre le bras familier et le nouveau bras. Ni SOCS3 ni JAK2ca n'influence cette altération. Test *t* de *student* au sein de chaque bras. N= 4-8 / groupe. ** p<0.05.*

Dans le test du Y maze, les souris WT explorent significativement plus le nouveau bras par rapport au bras familier. Cependant, les souris 3xTg-GFP explorent de façon identique les deux bras, mettant en évidence une altération de leur mémoire de travail. Les souris 3xTg-SOCS3 explorent également de la même façon les deux bras. Aucun effet de JAK2ca n'est observé. La modulation de la réactivité astrocytaire n'impacte donc pas la mémoire de travail des souris 3xTg.

Conclusions

Le ciblage de la voie JAK2-STAT3 est efficace pour inhiber ou amplifier la réactivité astrocytaire dans deux modèles murins de la MA : les modèles APP/PS1dE9 et 3xTg-AD. Ces modèles développent respectivement uniquement la pathologie amyloïde ou allient la pathologie amyloïde et Tau, deux atteintes caractéristiques de la MA. Ils permettent donc d'évaluer l'effet de la réactivité dans deux contextes pathologiques distincts. Nous avons montré que la désactivation de la réactivité astrocytaire par SOCS3 diminue la charge amyloïde dans l'hippocampe de souris APP, sans affecter le métabolisme de l'Aβ ni sa phagocytose par la microglie. Des effets en miroirs ont été observés avec JAK2ca. Néanmoins, de façon intéressante, aucun effet de la modulation astrocytaire n'a été observé sur la charge amyloïde ou la pathologie Tau dans le modèle 3xTg. Par contre, SOCS3 restaure les déficits précoces de LTP dans ce modèle. Ces résultats suggèrent donc que la réactivité astrocytaire est complexe et son implication peut dépendre du stade et du contexte pathologique.

Discussion

Discussion

1. Modulation de la réactivité astrocytaire par transfert de gène

1.1. Comment caractériser la réactivité astrocytaire ?

Les astrocytes réactifs sont caractérisés depuis longtemps par des changements morphologiques dont une hypertrophie du soma et des prolongements ainsi qu'une surexpression de protéines des filaments intermédiaires. La surexpression de la GFAP et de la Vimentine sont reconnues comme marqueurs universels de la réactivité *(Burda and Sofroniew, 2014; Hol and Pekny, 2015)*. Cependant, dans la majorité des études, ces marqueurs sont les seuls étudiés et sont donc insuffisants pour caractériser la réactivité. En effet, les modifications morphologiques sont accompagnées de changements transcriptionnels plus récemment identifiés, qui peuvent dépendre du stimulus pathologique *(Zamanian et al., 2012; Liddelow et al., 2017)*. Il est donc important d'étudier des index de réactivité astrocytaire au-delà des simples changements morphologiques. Néanmoins, des marqueurs fonctionnels liés aux différents stades de la réactivité sont toujours manquants.

Dans nos deux études, nous avons mis en évidence une importante réactivité astrocytaire grâce à l'augmentation de l'expression de la GFAP et de la Vimentine, notamment autour des plaques amyloïdes, dans les modèles APP et 3xTg *(Article 1 et 2)*. Pour aller plus loin, nous avons étudié les modifications transcriptionnelles des astrocytes de souris APP. Nous avons observé une augmentation de l'expression de gènes codant pour des marqueurs de la réactivité induit dans de nombreuses pathologies et quel que soit le stimulus (« PAN-reactive genes » ; *(Liddelow et al., 2017)*) comme *Gfap* et *Serpina3n*, mais aussi de nombreux gènes liés à l'inflammation comme les cytokines *(Il-1ß)* et les chemokines *(Ccl4, Ccl6,)* et liés au complément *(C1qa, C1qb, C1qc, C4b ; Article 1),* précédemment décrits comme surexprimés dans les astrocytes du même modèle mais à un âge plus avancé *(Orre et al., 2014)*. SOCS3 permet donc bien de corriger les modifications morphologiques induites par la réactivité mais aussi de diminuer les molécules majeures de l'inflammation pouvant influencer l'homéostasie du SNC et les autres types cellulaires.

1.2. La voie JAK2-STAT3 est nécessaire et suffisante pour contrôler la réactivité astrocytaire

La réactivité astrocytaire peut être induite par de multiples molécules, comme par exemple les cytokines, les chemokines ou des molécules mal conformées telle que l'Aβ, qui sont libérées par les cellules voisines comme la microglie et les neurones ou par les astrocytes eux-mêmes. Ces molécules peuvent activer de nombreuses voies de signalisation intracellulaires *(**Publication 1 en annexe**)* y compris la voie JAK-STAT3. Son implication dans la réactivité astrocytaire est bien caractérisée dans des modèles aigus *(Sofroniew, 2009; **Publication 2 en annexe**)* mais son rôle dans les maladies neurodégénératives est moins connu. Nous avons mis en évidence en 2015 que la voie JAK-STAT3 est activée dans les astrocytes dans plusieurs modèles de maladies neurodégénératives, tels que la maladie de Huntington et la MA, et ce dans plusieurs espèces et régions cérébrales *(**Publication 3 en annexe**).* Afin d'étudier l'activation de la voie, nous mesurons classiquement l'expression de STAT3, majoritairement exprimé dans les astrocytes *(**Publication 3 en annexe**, Article 1 et 2).* Comme STAT3 s'accumule dans le noyau et induit sa propre transcription *(Levy and Darnell, 2002 ; **Publication 2 en annexe**),* la surexpression de STAT3 reflète l'activation de la voie JAK-STAT3. Il serait plus direct de mesurer la forme phosphorylée de STAT3 (P-STAT3), présente lors de l'activation de la voie, mais P-STAT3 n'est pas détectable dans nos modèles progressifs de maladies neurodégénératives. Cependant, la surexpression de STAT3 corrèle bien avec l'expression de P-STAT3, comme observé dans un modèle chronique où une forte réactivité est induite par des vecteurs viraux codant pour le CNTF *(données non présentées).*

Le rôle central de la voie JAK2-STAT3 dans la réactivité astrocytaire est appuyé par l'efficacité de nos vecteurs viraux pour moduler de la réactivité astrocytaire. En effet, nous avons étudié l'effet de la surexpression de SOCS3 ou d'une forme constitutivement active de JAK2 (JAK2ca) spécifiquement dans les astrocytes sur les différents index morphologiques et transcriptionnels liés à la réactivité *(Article 1 et 2).* L'expression de SOCS3 désactive efficacement les astrocytes dans ces deux modèles *(Cf §1.1 de la discussion).* A l'inverse, l'expression de JAK2ca augmente l'expression de la GFAP et de la Vimentine dans les deux modèles et dans l'hippocampe ou le striatum de souris WT, démontrant bien l'efficacité de ce second vecteur viral pour (sur)activer les astrocytes.

Ces outils nous ont donc permis de démontrer l'importance de la voie JAK2-STAT3 dans l'induction de la réactivité astrocytaire et nous permettent de moduler spécifiquement la réactivité astrocytaire. Nous avons également montré leur versatilité puisque SOCS3 permet la désactivation des astrocytes dans plusieurs maladies neurodégénératives (maladie de Huntington, et MA) et dans différentes espèces *(**Publication 3 en annexe** et Article 1).* La voie JAK2-STAT3 est donc nécessaire et suffisante pour induire la réactivité astrocytaire dans les maladies neurodégénératives dont la MA.

1.3. Avantages et limites des vecteurs viraux pour moduler la voie JAK2-STAT3

Parmi les vecteurs de transfert de gènes, les AAV sont couramment utilisés pour cibler le SNC puisqu'ils présentent de nombreux avantages *(Kantor et al., 2014)*. La particule virale est de petite taille favorisant sa bonne diffusion dans le parenchyme cérébral et les AAV semblent être moins inflammatoires que les lentivirus (utilisés dans la ***publication 3* en annexe** et certaines expériences de l'article 1). De plus, l'expression du transgène peut être contrôlée temporellement et spatialement, selon l'âge et le site d'injection. Cette stratégie est plus facile à mettre en œuvre et n'a aucun effet sur le développement quand les virus sont injectés chez l'adulte, contrairement à certains modèles transgéniques. Il existe de nombreux sérotypes présentant des tropismes cellulaires différents *(Serguera and Bemelmans, 2014)*. Nous utilisons le sérotype 9 car il est plus efficace pour exprimer des protéines d'intérêts dans les astrocytes de l'hippocampe *(Kootstra and Verma, 2003)*. De plus, le choix d'un promoteur spécifiquement astrocytaire *(*GFA-abc1d : promoteur synthétique de la GFAP ; *Lee et al., 2008)* permet également d'éviter les effets sur le système périphérique, d'autant que la voie JAK2-STAT3 est une voie ubiquitaire *(**Publication 2 en annexe**)*. Enfin, les vecteurs viraux sont des outils versatiles, qui peuvent être utilisés facilement dans différents modèles mais également différentes espèces *(**Publication 3 en annexe**, Article 1).*

Les AAV ont été injectés dans la région CA1 de l'hippocampe des deux premiers lots de souris APP-SOCS3 et APP-JAK2ca, région fortement impliquée dans les processus d'encodage et la consolidation de la mémoire qui sont altérés dans la MA *(Deng et al., 2010)*. Cependant, la diffusion du vecteur viral reste généralement limitée à cette région. Ceci peut s'expliquer par l'organisation très structurée des différentes couches cellulaires de l'hippocampe. Afin d'améliorer cette diffusion et de pouvoir observer des effets plus importants, nous avons modifié les coordonnées d'injection pour infecter également les astrocytes autour du gyrus denté et du *stratum lacunosum*, régions où les plaques amyloïdes s'avèrent être plus abondantes dans ce modèle. Les souris 3xTg ont également été injectées dans l'hippocampe postérieur afin de cibler le *subiculum*, région dans laquelle les plaques amyloïdes sont nombreuses. Au final, 25 % de l'hippocampe est infecté par les vecteurs. Ce volume d'infection est basé sur l'expression de la GFP, visible par histologie. Il est donc possible que nous sous-estimions le nombre d'astrocytes infectés. Néanmoins, au cours d'autres études dans le laboratoire, nous avons trié par FACS environ 20000 astrocytes à partir d'un hippocampe de souris Aldh1l1-GFP (souris transgéniques dans lesquelles l'expression de la GFP est sous le contrôle du promoteur astrocytaire Aldh1l1), alors qu'environ 5000 astrocytes sont GFP^+ dans nos souris injectées avec des AAV-GFP, ce qui est en accord avec une infection de 25 % de l'hippocampe.

Afin d'augmenter la zone d'infection, nous pourrions injecter une plus grande quantité ou un plus grand volume de virus. Cependant, ce projet visant à étudier l'impact de la neuroinflammation sur la MA, il est important que les vecteurs utilisés ne déclenchent pas ce processus en eux-mêmes comme décrit par Ortinski et collaborateurs *(Ortinski et al., 2010)*. Des expériences de dose-réponse avaient été préalablement réalisées au laboratoire afin de déterminer la dose de virus pouvant être injectée sans provoquer de neuroinflammation. Une autre stratégie serait de modifier le promoteur pour

d'augmenter le niveau d'expression des transgènes ou d'utiliser un autre sérotype d'AAV qui diffuserait mieux dans le parenchyme cérébral. Cette dernière stratégie fait l'objet de recherches au sein du laboratoire.

Enfin, il est à noter que nous ne pouvons pas détecter les transgènes SOCS3 ou JAK2ca par immunomarquage ou western blot, malgré le test de plusieurs anticorps. Nous avons donc systématiquement co-injecté le vecteur viral codant pour le transgène d'intérêt (SOCS3 ou JAK2ca) avec un second vecteur codant pour la GFP. Pour toutes les expériences, nous avons injecté les deux vecteurs au ratio 4 : 1 (transgène : GFP) afin de garder la charge virale constante entre les groupes d'intérêts et les groupes contrôles, injectés uniquement avec un AAV-GFP. Plus de 99 % de co-expression des deux vecteurs avait été mesurée par FACS préalablement à ce projet, à l'aide de co-injections de vecteurs AAV-GFP et AAV-tdTomato. La co-injection d'un vecteur codant pour la GFP permet donc de visualiser la zone d'infection et l'expression du transgène d'intérêt. Elle présente également l'avantage de permettre la visualisation de l'intégralité de la morphologie des astrocytes infectés.

2. La modulation de la réactivité astrocytaire affecte sensiblement certains index cliniques de la MA

Les modifications fonctionnelles associées à la réactivité astrocytaire sont nombreuses. Elles incluent des altérations de l'homéostasie du glutamate *(Masliah et al., 1996)*, du métabolisme énergétique *(Merlini et al., 2011)*, du métabolisme du cholestérol *(Bu, 2009)* mais également une modification de leur « sécrétome » (ROS *(Abramov et al., 2004)*, cytokines et chemokines *(Orre et al., 2014)*, molécules du complément *(Barnum, 1995)*, etc). Pour revue, voir la ***publication 1*** **en annexe**. Chacune de ces modifications fonctionnelles astrocytaires est susceptible de participer à la souffrance neuronale observée dans la MA. Plusieurs études ont mis en évidence un rôle bénéfique (Kraft et al., 2013) ou délétère *(Fernandez et al., 2012; Furman et al., 2012; Sompol et al., 2017)* de la réactivité astrocytaire sur les fonctions neuronales voire même sur les fonctions cognitives de souris modèles de la MA. Néanmoins, comme discuté en introduction, la modulation de la réactivité astrocytaire n'a été que très peu caractérisée et les outils utilisés ne permettent pas toujours de s'assurer que les effets observés sont bien liés uniquement à l'inhibition de la réactivité *(Cf §5.1 de l'introduction)*. Contrairement à ces outils, nos vecteurs viraux ciblent une voie centrale, nécessaire et suffisante pour induire la réactivité astrocytaire. Ils nous permettent donc d'étudier spécifiquement l'impact de la modulation de la réactivité astrocytaire sur différents index pathologiques. Nous nous sommes notamment intéressés à des index d'intégrité neuronale et à des index fonctionnels comme la transmission glutamatergique à la synapse CA3/CA1, région infectée par nos vecteurs viraux ou les concentrations de métabolites hippocampiques *(Article 2)*.

2.1. Difficulté du modèle APP/PS1dE9

Nous avons étudié différents index structuraux afin d'évaluer de potentielles altérations neuronales dans le modèle APP à 9 mois *(Article 2)*. Aucune modification du marquage dendritique MAP2 ou de l'épaisseur de CA1 n'a été mise en évidence par histologie. Par western blot, nous avons mesuré l'expression de marqueurs pré et post-synaptiques (synaptophysine et PSD95), mais ceux-ci ne sont pas modifiés, bien que certaines études décrivent une altération de ces marqueurs en histologie dès 3 mois dans ce modèle *(Hong et al., 2016)*. Aucun effet toxique de SOCS3 ou de JAK2ca n'a été observé. Afin d'obtenir des données plus fonctionnelles, il serait intéressant de réaliser des expériences d'électrophysiologie pour de vérifier si ces souris présentent une altération de LTP et de voir si SOCS3 restaure ce déficit, comme observé dans les souris 3xTg-SOCS3. Cependant, ces souris présentent des déficits précoces mais seulement de la LTP transitoire *(Volianskis et al., 2010)* ou plus tard au niveau des cellules pyramidales de CA3 *(Viana da Silva et al., 2016)*. Les altérations de LTP à la synapse CA3/CA1, étudiée dans les 3xTg, n'apparaissent qu'à un stade très avancé de la pathologie *(Volianskis et al., 2010 ; Métais et al., 2014)*.

De plus, par spectroscopie par résonnance magnétique, nous avons mesuré plusieurs métabolites astrocytaires (myo-inositol, choline, glutamine), neuronaux (NAA, glutamate) ou ubiquitaires (taurine, créatine, lactate) *(Simmons et al., 1991 ; Griffin et al., 2002)*. Seule la concentration du lactate est significativement augmentée dans les souris APP par rapport aux souris WT. SOCS3 n'influence pas cette concentration. Cette augmentation est traditionnellement considérée comme signe de « souffrance neuronale » mais selon l'hypothèse de la « lactate shuttle », le lactate est libéré par les astrocytes lors d'une activité neuronale accrue. Outre son rôle métabolique pour subvenir aux besoins énergétiques des neurones *(Allaman et al., 2011)*, le lactate pourrait participer à la formation de la mémoire *(Suzuki et al., 2011)*. Cette augmentation de lactate dans les souris APP n'est donc pas nécessairement délétère. De plus, la réactivité impacte le métabolisme des astrocytes *(Escartin et al., 2007)*. Il est donc surprenant que SOCS3 n'influence pas cette augmentation de lactate. Néanmoins, il est possible que la désactivation soit trop locale pour que son effet soit visible sur l'ensemble de l'hippocampe *(Cf paragraphe précèdent)*.

Enfin, contrairement à ce qui est décrit dans la littérature *(Kilgore et al., 2010 ; Ma et al., 2012)*, nos souris APP ne présentent aucune altération cognitive détectable (anxiété, mémoire à long terme) à 9 et 11 mois, du moins dans les tests réalisés. L'utilisation de ce modèle à cet âge se révèle donc peu adaptée à l'étude du potentiel thérapeutique de l'AAV-SOCS3. Il est important de noter que la puissance statistique de ces tests comportementaux est très faible (~20%), ce qui n'exclue pas l'existence d'effets comportementaux de SOCS3 masqués par la grande variabilité de réponse aux tests employés. Il serait donc indispensable d'augmenter le nombre d'animaux par groupe afin de pouvoir conclure, ou d'identifier des tests qui génèrent des réponses moins variables. Néanmoins, si ces données s'avèrent exactes, ces différences avec la littérature pourraient s'expliquer par une dérive génétique de la colonie maintenue au laboratoire. De plus, les expériences de comportement ont été réalisées pendant une période de travaux qui ont probablement stressé les souris, ce qui a pu

altérer les performances des souris WT et donc atténuer les différences avec les souris APP. Il serait donc aussi intéressant de réaliser à nouveau ces tests comportementaux sur une cohorte plus âgée.

2.2. SOCS3 restaure la plasticité synaptique dans les souris 3xTg-AD

Dans le modèle 3xTg, aucune altération des marqueurs pré- et post-synaptiques n'a été mise en évidence par western blot à 16-17 mois *(Article 2)*. Tout comme dans le modèle APP, aucune toxicité des transgènes SOCS3 ou JAK2ca n'a été observée. En revanche, les expériences d'électrophysiologie ont mis en évidence une altération précoce de la LTP à la synapse CA3-CA1 dans ce modèle à 8 mois, avant même l'apparition des plaques amyloïdes ou de formes hyperphosphorylées de Tau. Ces données sont en accord avec celles de la littérature *(Oddo et al., 2003a)*.

La réactivité astrocytaire, bien que souvent associée aux plaques amyloïdes, est observée avant leur apparition dans certains modèles de la MA *(Heneka et al., 2005)*. De façon très intéressante, l'expression de SOCS3 dans les astrocytes corrige les déficits de LTP dans le modèle 3xTg *(Article 2)*. Les astrocytes étant un partenaire actif de la synapse tri-partite *(Araque et al., 2014)*, les altérations morphologiques et fonctionnelles liées à la réactivité peuvent avoir un impact sur le fonctionnement de la synapse. En effet, d'un point de vue simplement morphologique, la réactivité peut affecter la couverture des PAP à la synapse, modulant la recapture du glutamate *(Oliet et al., 2001)*. La réactivité astrocytaire induit également une diminution des transporteurs astrocytaires au glutamate *(Masliah et al., 2000)* et module la libération des gliotransmetteurs *(Jo et al., 2014 ; Wu et al., 2014)*, pouvant altérer directement la LTP. L'effet direct de la réactivité sur la LTP est également démontré par nos résultats obtenus sur les WT-JAK2ca *(Article 1).* En effet, la surexpression de JAK2ca induit une réactivité astrocytaire, hors de tout contexte pathologique et engendre des déficits de LTP, semblables à ceux observés dans le modèle 3xTg. De plus amples études, faisant partie du projet de thèse d'Océane Guillemaud, sont prévues afin d'identifier les mécanismes moléculaires entrant en jeu dans cette restauration.

D'un point de vue comportemental, les effets de la modulation de la réactivité astrocytaire sont très modestes *(données complémentaires à l'article 2)*. Les souris 3xTg semblent plus anxieuses que les souris WT. L'injection d'AAV-SOCS3 tend à corriger ce comportement anxieux. A l'inverse, la surexpression de JAK2ca semble amplifier l'anxiété des souris. Une altération de la mémoire spatiale de travail à 7-8 mois *(données non montrées)* et à 14-15 mois est observée dans les souris 3xTg. Néanmoins, ni SOCS3 ni JAK2ca ne restaure ce déficit. Ces résultats suggèrent que la réactivité astrocytaire n'a pas d'effet sur la mémoire spatiale de travail. Ceci serait surprenant puisque SOCS3 restaure les déficits de LTP, décrite comme étant à la base de l'apprentissage et de la mémoire *(Malenka and Bear, 2004)*. Cependant, il est possible que la zone impactée par SOCS3 soit trop limitée pour avoir un effet sur cette atteinte mnésique. La LTP pourrait être restaurée uniquement localement. Les synapses adjacentes, impliquant des astrocytes non infectés, pourraient être toujours altérées, et SOCS3 serait alors non suffisant pour compenser ces déficits sur l'ensemble de la circuiterie. En effet, notre stratégie ne cible que 25 % de l'hippocampe. Notre stratégie cellulaire

n'est donc pas forcément adaptée pour mettre en évidence des effets au niveau du comportement. De plus, l'hippocampe n'est pas la seule région impliquée dans les processus mnésiques. Par exemple, la LTP dans l'amygdale basolatérale entre en jeu dans la mémoire associée au conditionnement par la peur *(Sigurdsson et al., 2007)*. Enfin, la LTP n'est pas le seul mécanisme de formation de la mémoire. D'autres formes de plasticité synaptiques interviennent dans l'hippocampe, comme la dépression à long terme *(Neves et al., 2008)*. Néanmoins, il est important de noter que la puissance statistique de ces tests comportementaux reste faible (~20-60%). Comme pour les tests effectués sur les souris APP/PS1dE9, il serait donc nécessaire d'augmenter le nombre d'animaux par groupe afin de pouvoir conclure.

3. Quels mécanismes sont impliqués dans la modulation de la charge amyloïde dans les souris APP/PS1dE9 ?

Nous avons mis en évidence que la désactivation des astrocytes diminue sensiblement le nombre de plaques amyloïdes $BAM10^{+}$ sans affecter la taille moyenne de celles-ci, dans le modèle APP. Ces résultats ont été confirmés avec un second marqueur de plaques amyloïdes, le méthoxy-XO4. De plus, la concentration de peptides Aβ40 et Aβ42 tend à être également diminuée par SOCS3. La même analyse pour les souris APP-JAK2ca révèle un effet en miroir par rapport aux APP-SOCS3. L'ensemble de ces résultats suggèrent un rôle délétère des astrocytes réactifs dans la pathologie amyloïde au cours de la MA *(Article 2)* et sont en accord avec la réduction de la charge amyloïde observée par Furman *et al.,* en interférant avec la réactivité astrocytaire par la voie NFAT/Calcineurine *(Furman et al., 2012)*.

Nous avons étudié quatre hypothèses majeures pour expliquer l'effet de la modulation de la réactivité astrocytaire sur la charge amyloïde : 1/ Les peptides Aβ ne s'agrègent pas, restant sous forme soluble, 2/ La modulation de la réactivité astrocytaire impacte le métabolisme (production et dégradation) de l'Aβ, 3/ La modulation de la réactivité astrocytaire impacte indirectement la microglie et sa capacité de phagocytose de l'Aβ, 4/ La réactivité astrocytaire influence le recrutement des cellules immunitaires périphériques, qui pourraient aussi être impliquées dans la dégradation de l'Aβ *(Figure 29)*.

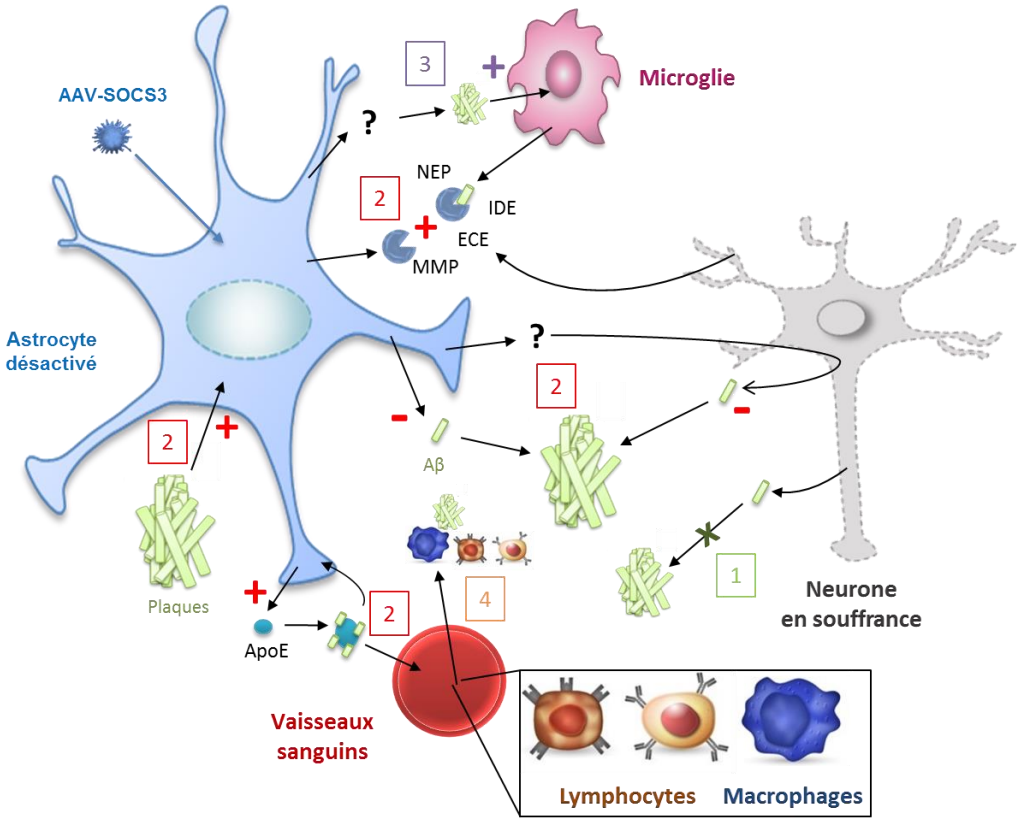

Figure 29 : Par quels mécanismes la charge amyloïde est-elle impactée par la réactivité astrocytaire ?
Schéma représentant les hypothèses de travail dans le cas où les astrocytes sont désactivés par SOCS3. L'expression de SOCS3 dans les astrocytes diminue la charge amyloïde. Quatre hypothèses majeures peuvent expliquer cette diminution : 1) L'Aβ ne s'agrège pas, 2) SOCS3 impacte le métabolisme de l'Aβ, 3) les astrocytes désactivés augmentent la phagocytose microgliale de l'Aβ, 4) SOCS3 augmente le recrutement des cellules immunitaires périphériques. Abréviations : NEP = Néprylisine, IDE = « Insulin-degrading enzyme », MMP = Matrix métalloprotéinase, ECE = « Endothelin-converting enzyme », ApoE = Apolipoprotéine.

3.1. La modulation de la réactivité astrocytaire n'impacte ni l'agrégation ni le métabolisme de l'Aβ

Les résultats des mesures ELISA des taux d'Aβ, même s'ils ne sont pas significatifs, tendent à invalider la première hypothèse et seraient plutôt en faveur de la seconde. En effet, ils montrent que la concentration de peptides Aβ40 et Aβ42 solubles tend à être également diminuée par SOCS3, ce qui pourrait réduire leur agrégation sous forme de plaques amyloïdes. JAK2ca induit des effets en miroir. Il est important de noter que nous n'avons pas exploré en détail les différentes formes d'Aβ. Le test MSD® effectué permet de mesurer les formes solubles dans le Triton X-100 (probablement les formes monomériques et petits oligomères) alors que les formes les plus agrégées (majorité des oligomères, fibrilles et plaques amyloïdes) ne sont pas solubles dans ce tampon de lyse *(Xia et al., 2009; Bao et al., 2012)*. L'Aβ agrégé a été par ailleurs solubilisé dans un tampon 5 M guanidine et collecté. La concentration en Aβ40 et Aβ42 dans cette fraction « Guanidine soluble » a été également mesurée par test MSD®. Cependant, ces concentrations étaient très variables, et nous avons choisi de ne pas les présenter.

Une étude a mis en évidence une diminution l'expression de BACE1, impliqué dans la synthèse de l'Aβ, lorsque les astrocytes sont désactivés *(Furman et al., 2012)*. Ces résultats sont associés à une diminution de la charge amyloïde dans le modèle APP/PS1dE9. Cependant, nous n'avons observé aucune modulation des enzymes clés (BACE1, APH1A, PS1, PS2) dans la production de l'Aβ par western blot sur des homogénats totaux ou par analyse transcriptomique sur des astrocytes triés, dans les souris APP par rapport aux WT *(Article 2 et données non montrées).* De plus, SOCS3 ou JAK2ca n'influencent pas leur expression. Les mêmes observations ont été faites pour des enzymes et des transporteurs impliqués dans les voies de dégradation de l'Aβ tels qu'IDE et ApoE, ou ADAM10, qui est impliqué dans la voie non amyloïdogénique. Néanmoins, nous ciblons spécifiquement les astrocytes, qui sont loin d'être les producteurs majoritaires d'Aβ ou d'IDE et ADAM10 par rapport à la microglie ou aux neurones *(Hickman et al., 2008 ; Yuan et al., 2017)*. Nous prévoyons donc d'étudier l'expression de ces enzymes spécifiquement dans la microglie et dans la fraction « OTHER » (qui inclue les neurones) par qPCR. Par contre, ApoE est très majoritairement produit par les astrocytes *(Bu, 2009)*. La désactivation astrocytaire n'impacte donc pas cette voie d'élimination de l'Aβ. Cependant, nous avons mesuré le niveau d'expression de ces enzymes clés dans le métabolisme de l'APP mais il serait également nécessaire d'étudier leur activité enzymatique.

Enfin, une accumulation de vacuoles autophagiques a été décrite dans le cerveau de patients et des modèles murins de la MA *(Nixon et al., 2005)*. Ces vacuoles présentent une accumulation d'APP, PS1 et BACE, qui sont nécessaires et suffisants à la génération de peptides Aβ *(Yu et al., 2004, 2005)*. De façon intéressante, nous observons une augmentation de l'expression de nombreux gènes lysosomaux lorsque les astrocytes deviennent réactifs (*Laptm5, Ctss, CD68, Hexb* ; *Données de RNAseq non présentées*). L'expression de la majorité de ces gènes est restaurée par SOCS3. On peut donc supposer qu'à cause d'une dysfonction de l'autophagie, les astrocytes réactifs dégradent moins efficacement l'Aβ et participent même à sa production. SOCS3 inhiberait donc directement cette voie de production. Mais ce mécanisme est certainement minoritaire dans la production d'Aβ et n'est donc sûrement pas le seul en jeu.

3.2. SOCS3 n'influence ni la recapture de l'Aβ par la microglie ni le recrutement des cellules immunitaires périphériques

La troisième hypothèse s'appuie sur le fait que les astrocytes et la microglie communiquent finement via la libération de cytokines et chemokines. Plusieurs études ont en effet observé une modulation de l'activation de la microglie et de la réactivité astrocytaire via l'expression de cytokines *(Kiyota et al., 2010, 2012)*. De plus, l'expression de nombreuses cytokines dans les astrocytes est fortement impactée par la réactivité *(Orre et al., 2014; Bagyinszky et al., 2017).* Basée sur la surexpression d'IBA1, aucune activation microgliale n'a été observée dans les souris APP sauf très localement au niveau des plaques amyloïdes. SOCS3 et JAK2ca ne semblent pas affecter la morphologie de la microglie. Il est intéressant de noter que le profil transcriptomique de la microglie à proximité des plaques (microglie $MX04^{+}$) est différent de celui des cellules microgliales $MXO4^{-}$ *(Article 2).* Une surexpression de marqueurs tels que *Trem2* ou *Apoe* et une baisse d'expression de *Tmem119* sont

observées dans les cellules microgliales MXO4^{+}, correspondant au profil transcriptionnel des DAM *(Keren-Shaul et al., 2017)*. SOCS3 n'affecte pas ce profil transcriptionnel. Ces résultats sont surprenants puisque de nombreux gènes dont l'expression est diminuée par SOCS3 sont liés à la réponse immunitaire innée et à l'inflammation *(Analyse d'ontologie des gènes ; Article 1).* Il est possible que les signaux émis par les neurones en souffrance, les astrocytes non infectés ou les peptides Aβ, soient encore trop importants pour que la désactivation astrocytaire réduise la réactivité microgliale.

De plus, il est très bien décrit dans la littérature que la microglie participe à la dégradation des plaques *(Lee and Landreth, 2010 ; Figure 22).* En plus des gènes codant pour des cytokines, de nombreux gènes liés au complément *(C1qa, C1qb, C1qc, C4b)* sont modulés par la réactivité et restaurés par SOCS3 *(Article 1)*. La désactivation ou l'amplification de la réactivité astrocytaire pourrait donc modifier finement la signalisation intercellulaire et moduler ainsi la dégradation des plaques amyloïdes, comme supposé dans de précédentes études *(Chakrabarty et al., 2015 ; Lian et al., 2016)*. Nous avons montré par cytométrie en flux que l'activité phagocytaire de la microglie n'est pas modulée par la désactivation des astrocytes. En plus de confirmer les résultats obtenus en FACS, la quantification par immunomarquage met en évidence que seulement 5% des cellules microgliales en contact avec une plaque amyloïde sont MXO4^{-}. Ces résultats démontrent donc déjà une phagocytose très active par la microglie dans les souris APP. La diminution de la charge amyloïde n'est donc pas due à une augmentation de cette voie de dégradation dans la microglie.

De plus, contrairement aux nombreuses études *in vitro (Shaffer et al., 1995 ; Wyss-Coray et al., 2003 ; Nielsen et al., 2009),* et aux quelques études *in vivo (Wyss-Coray et al., 2003 ; Koistinaho et al., 2004 ; Iram et al., 2016),* nous n'avons mis en évidence aucune phagocytose d'Aβ par les astrocytes. Cependant, il est possible que le métabolisme des astrocytes pour dégrader l'Aβ soit plus ou moins rapide que celui de la microglie. Nous avons effectué des expériences complémentaires d'injection du MXO4 à différents temps avant le sacrifice (injection 1h ou 24h ; *données non montrées*). Le délai de 1h ne permet pas d'observer de la recapture de MXO4 par les astrocytes ou par la microglie. Ce délai est certainement trop court pour le que MXO4 diffuse jusqu'au SNC et marque suffisamment d'Aβ pour qu'il soit détectable ou pour que la microglie le phagocyte. Avec l'injection 24h avant le sacrifice, les mêmes résultats qu'avec le délai de 3h ont été obtenus. En effet, la même proportion de cellules microgliales MXO4^{+} est observée, mais aucun astrocyte n'est MXO4^{+}, suggérant bien que les astrocytes ne phagocytent pas l'Aβ *in vivo,* dans le modèle APP.

Enfin, la quatrième hypothèse est basée sur la modulation des cellules immunitaires périphériques. En effet, l'augmentation de la production de cytokines par les astrocytes réactifs *(Orre et al., 2014 ; données de RNAseq présentées dans l'article 1)* pourrait altérer la perméabilité de la BHE *(Desai et al., 2002 ; Bowman et al., 2007)*, permettant une modulation des cellules du SNC par les cellules immunitaires périphériques *(Persidsky et al., 2006)*, voire même l'entrée de macrophages *(Mildner et al., 2011)*, et ainsi une modulation de la charge amyloïde. Nous avons observé par FACS la présence d'une population cellulaire CD11b^{+} qui exprime fortement CD45 *(données non montrées)*, caractéristique des cellules immunitaires périphériques, certainement des lymphocytes *(Sedgwick et*

al., 1991). La proportion de cette population reste constante entre les souris WT et les souris APP, suggérant que le recrutement des cellules immunitaires périphériques n'est pas augmenté dans ce modèle, comme décrit dans de précédentes études *(Dansokho et al., 2016 ; Martin et al., 2017)*. Néanmoins, SOCS3 diminue non seulement un grand nombre de gènes codant pour des cytokines, chemokines mais réduit également de façon majoritaire d'autres gènes liés à la chemotaxie des monocytes et des neutrophiles, et plus généralement au recrutement des leucocytes *(Article 1),* suggérant donc plutôt que SOCS3 diminue le recrutement des cellules immunitaires périphériques. Notre analyse par FACS est en accord avec ces données puisque SOCS3 tend effectivement à diminuer cette population $CD11b^{+}/CD45^{high}$ *(données non montrées)*. La diminution des plaques amyloïdes lorsque les astrocytes sont désactivés ne semble donc pas impliquer les cellules du système immunitaire périphérique. Néanmoins, la population $CD11b^{+}/CD45^{high}$ correspond à une très faible fraction cellulaire (~0,5-1% des cellules). La pertinence de ces variations reste donc à confirmer. De plus, la proportion de cette population cellulaire dépend de l'efficacité de l'élimination des leucocytes périvasculaires au moment de la perfusion des souris. De plus amples études sont donc nécessaires afin de : 1) identifier plus précisément le type cellulaire observé en FACS en réalisant par exemple des marquages complémentaires pour caractériser ces cellules, 2) confirmer l'absence d'augmentation de l'infiltration de cellules périphériques et l'absence d'effet de SOCS3 sur ce recrutement par des marquages histologiques.

4. Complexité de la réactivité astrocytaire

4.1. Les astrocytes réactifs agissent-ils différemment selon le contexte pathologique ?

Contrairement à l'effet observé dans les souris APP, le nombre de plaques amyloïdes $MXO4^{+}$ est inchangé, que les astrocytes réactifs surexpriment SOCS3 ou JAK2ca dans les souris 3xTg. Les mêmes résultats ont été obtenus avec un second marquage anti-Aβ42 *(données non montrées).* De plus, nous avons étudié différents sites de phosphorylations de la protéine Tau ainsi que son agrégation, mais aucun effet n'a été observé *(Article 2)*.

Trois hypothèses peuvent être émises pour expliquer les effets différents de la réactivité astrocytaire sur la pathologie amyloïde entre ces 2 modèles. 1/ Le sexe diffère entre les deux modèles (souris APP/PS1dE9 mâles, et souris 3xTg femelles). Le sexe semble influencer les différents partenaires de la neuroinflammation *(Nelson and Lenz, 2017 ; Schwarz and Bilbo, 2012)* et pourrait donc en partie expliquer cette différence entre les deux modèles. Il serait intéressant d'étudier l'effet de la désactivation des astrocytes réactifs sur des souris de l'autre sexe pour chaque modèle. 2/ La pathologie amyloïde se développe avant la pathologie Tau dans les souris 3xTg *(Oddo et al., 2003a)*. Les astrocytes réactifs pourraient donc être impliqués transitoirement dans la mise en place ou la progression de la pathologie amyloïde au cours des phases précoces puis perdre leur effet délétère

quand la pathologie Tau se rajoute à la pathologie amyloïde. Afin de tester cette hypothèse, une nouvelle étude sur des souris 3xTg âgées de 8 mois, âge étudié en électrophysiologie, est en cours. 3/ Deux grandes classes d'astrocytes réactifs (A1 et A2) ont été identifiées récemment. Les astrocytes A1 sont neurotoxiques car ils perdent une majorité de leurs fonctions de soutien aux neurones *(Liddelow et al., 2017)* alors que les astrocytes A2 présenteraient des propriétés bénéfiques par exemple en faveur de la repousse axonale *(Zamanian et al., 2012)*. Leur présence dépend du stimulus pathologique. Comme le modèle 3xTg développe les deux pathologies (amyloïde et Tau), le contexte pathologique est différent de celui des APP. Les fonctions modulées par SOCS3 pourraient donc ne pas être les mêmes.

4.2. SOCS3 inhibe des marqueurs d'astrocytes réactifs A1 et A2

Par analyse RNAseq, nous avons mis en évidence que l'expression de marqueurs A1 *(Serping1, H2-D1 et Gbp2)* et A2 *(Cd14 et Tm4sf1)* est induite dans les souris APP par rapport aux souris WT *(Article 1)*. La réactivité astrocytaire semble donc bien hétérogène dans le modèle APP puisqu'elle implique l'induction de marqueurs de type A1 et A2. De façon très intéressante, SOCS3 diminue l'expression des deux types de marqueurs. Grâce à des marquages histologiques, nous avons confirmé au niveau protéique la surexpression de Tm4sf1 dans les souris APP ; expression qui est diminuée par SOCS3. Les marquages histologiques testés pour certains marqueurs d'astrocytes réactifs A1 ne fonctionnant pas, nous n'avons pas pu confirmer la diminution de marqueurs A1 avec SOCS3. Néanmoins, l'ensemble de ces données démontrent encore une fois l'efficacité de nos vecteurs viraux pour désactiver les astrocytes.

Comme exposé dans le paragraphe précédent, les effets de la modulation de la réactivité astrocytaire sur la charge amyloïde sont différents entre les deux modèles. Il serait donc très intéressant d'étudier l'expression de ces marqueurs A1 et A2 dans le modèle 3xTg afin de pouvoir comparer leur expression à celle mesurée dans les APP et ainsi observé l'impact du contexte pathologique. Nous avons prévu d'étudier l'expression des deux marqueurs A2 (Tm4sf1 et CD14) par histologie. Il serait aussi intéressant d'étudier ces marqueurs précocement dans les 3xTg, avant l'apparition de la pathologie Tau, afin de voir s'ils sont différentiellement exprimés. Cette étude permettrait aussi de voir si le profil transcriptionnel des astrocytes de souris 3xTg, n'ayant pas encore développées la pathologie Tau, est similaire à celui des astrocytes de souris APP.

Cette classification est très récente, elle nécessite d'être développée et raffinée. En effet, suffit-il de détecter l'expression d'un seul marqueur A1 pour classer l'astrocyte parmi le phénotype A1 ? Ou faut-il que la cellule exprime l'ensemble des marqueurs ? De plus, comme décrit par l'équipe de B. Barres, on ne peut pas toujours classer de façon stricte les astrocytes réactifs dans une classe *(Liddelow et al., 2017)*. En effet, un même astrocyte peut exprimer des marqueurs des deux types de classe. Cette classification représente deux états extrêmes de la réactivité et n'est donc pas suffisante pour décrire l'hétérogénéité astrocytaire. Une controverse équivalente a lieu depuis plusieurs années pour les classes de microglie M1 (pro-inflammatoires) et M2 (anti-inflammatoires) *(Varnum and Ikezu, 2012)*. Une transition du phénotype M1 vers le phénotype M2 était souvent

proposée, mais il est maintenant plutôt admis qu'il ne s'agit pas d'un *continuum* mais de plusieurs états, induits par différents stimuli pathologiques *(Ransohoff, 2016)*. La classification des astrocytes réactifs risque donc d'évoluer et se complexifier de la même façon.

4.3. Importance de comprendre la réactivité astrocytaire hors de tout contexte pathologique

La réactivité astrocytaire semble donc très hétérogène *(Article 1)* et sensible au contexte pathologique *(Article 2)*. Les études de l'impact de la réactivité astrocytaire sur le développement et la progression de la MA sont de plus en plus nombreuses mais montrent des effets contradictoires selon la stratégie expérimentale et le modèle utilisés. Afin de mieux comprendre le rôle de la réactivité astrocytaire dans la MA, ne faudrait-il donc pas d'abord étudier la réactivité astrocytaire en absence de tout contexte pathologique ? Grâce à l'expression de JAK2ca spécifiquement dans les astrocytes, nous pouvons induire une importante réactivité astrocytaire dans des souris sauvages. En particulier, des marqueurs d'astrocytes A1 sont détectés par microarray dans les astrocytes JAK2ca (injectées dans le striatum ; gènes *H2-T23, H2-D1* et *Srgn*). Une augmentation de CD14, marqueur A2, dans les astrocytes striataux surexprimant JAK2ca *(Article 1*) est observée, mettant en évidence également la présence d'astrocytes réactifs A2. La voie JAK2-STAT3 module donc la réactivité astrocytaire au-delà des marqueurs A1 et A2.

Ce modèle, présenté pour la première fois dans l'article 1, nous permettra de mieux comprendre les effets propres de la réactivité astrocytaire. Par exemple, comme décrit précédemment, nous avons mis en évidence une altération de la LTP dans des souris WT injectées avec l'AAV-JAK2ca *(Article 1 ; §2.2 de la discussion)*. Ces données suggèrent un possible rôle direct de la réactivité dans les altérations de LTP observées dans de nombreuses maladies neurodégénératives. Les mécanismes entrant en jeu dans cette altération pourront donc être étudiés précisément, sans avoir l'impact d'autres paramètres, tels que la présence de plaques ou de DNF, dus à la pathologie.

Conclusion générale

Conclusion générale

Les astrocytes sont des cellules essentielles au bon fonctionnement du cerveau. Ils ont de multiples rôles de soutien aux neurones mais participent aussi activement à la transmission synaptique. En conditions pathologiques comme dans la maladie d'Alzheimer, les astrocytes deviennent réactifs. Au-delà des changements morphologiques induits, comme l'hypertrophie du soma et des prolongements, et la surexpression de protéines des filaments intermédiaires, la réactivité entraîne des changements transcriptionnels et fonctionnels mal connus. De ce fait, leur implication globale bénéfique ou délétère dans la MA est débattue.

Afin de comprendre leur rôle dans cette pathologie, il est essentiel d'identifier les voies de signalisation contrôlant la réactivité afin de pouvoir la manipuler pour favoriser ensuite les fonctions bénéfiques des astrocytes. Dans ce projet, nous avons mis en évidence grâce à des outils innovants que la voie JAK2-STAT3 est nécessaire et suffisante pour induire et maintenir la réactivité astrocytaire dans de nombreuses maladies neurodégénératives. Grâce à des vecteurs viraux surexprimant SOCS3, inhibiteur endogène de la voie, ou une forme constitutivement active de la kinase JAK2, nous sommes capables respectivement d'inhiber ou d'induire les modifications morphologiques classiques de la réactivité décrites précédemment (hypertrophie et surexpression de protéines des filaments intermédiaires) mais également de moduler le transcriptome des astrocytes.

De plus, nous avons utilisé ces outils dans deux modèles murins de la MA (le modèle APP/PS1dE9 et le modèle 3xTg-AD) afin de mieux comprendre le rôle de la réactivité dans ces modèles. La désactivation des astrocytes par SOCS3 induit une diminution du nombre de plaques amyloïdes et tend à diminuer la concentration des formes solubles des peptides Aβ, formes les plus toxiques. A l'inverse, l'amplification de la réactivité par JAK2ca provoque des effets en miroir. Ces résultats supposent donc que la réactivité astrocytaire est délétère dans ce modèle. Nous avons étudié certains mécanismes pouvant expliquer l'effet de la modulation de la réactivité astrocytaire sur la charge amyloïde dans le modèle APP/PS1dE9. Aucune modulation de l'expression des enzymes et transporteurs clés impliqués dans le métabolisme (production ou dégradation) de l'Aβ n'a été observée. De plus, malgré la modulation de nombreux gènes codant pour des cytokines et chemokines, impliquées dans la communication intracellulaire entre les astrocytes et la microglie, SOCS3 n'influence pas la phagocytose microgliale de l'Aβ.

De façon intéressante, ni SOCS3 ni JAK2ca n'a d'effet sur la pathologie amyloïde ou la pathologie Tau dans le modèle 3xTg-AD. Ces résultats suggèrent des effets différents de la réactivité astrocytaire en fonction du contexte pathologique. Néanmoins, SOCS3 restaure les altérations de la LTP dans le modèle 3xTg-AD, mettant tout de même en avant un rôle délétère précoce des astrocytes réactifs dans ce second modèle. Il a été récemment décrit deux classes d'astrocytes réactifs : les astrocytes A1, délétères et les astrocytes A2, plutôt bénéfiques, dont la présence majoritaire dépend du stimulus induisant la réactivité *(Liddelow et al., 2017)*. Nous avons évalué l'effet de SOCS3 sur

différents marqueurs de ces deux populations par analyse transcriptomique. Des marqueurs A1 et A2 sont induits dans les astrocytes de l'hippocampe dans le modèle APP/PS1dE9 et SOCS3 diminue leur expression. Nous devons maintenant étudier cette hétérogénéité dans le modèle 3xTg afin de voir si ces populations sont différemment induites dans un contexte pathologique alliant amyloïde et Tau.

Au vu de cette importante hétérogénéité et donc complexité de la réactivité astrocytaire, qui est contexte-dépendante, les astrocytes réactifs ne semblent pas être une cible thérapeutique évidente dans le contexte de la MA. Il est nécessaire de mieux comprendre les effets propres de la réactivité, hors de tout contexte pathologique, afin d'identifier les fonctions astrocytaires clés, bénéfiques à la survie et bon fonctionnement neuronal, et les mécanismes qui les contrôlent. Nous pourrons alors envisager de moduler ces fonctions astrocytaires spécifiques à des fins thérapeutiques.

Perspectives

A court terme, plusieurs marquages par histologie sont prévus afin de mieux caractériser l'hétérogénéité astrocytaire au sein et entre les deux modèles murins de la MA utilisés. Nous étudierons notamment l'expression des marqueurs A2 précédemment cités (Tm4sf1 et CD14) et le développement de marquages A1 est en cours. La validation par qPCR de l'expression de certains gènes d'intéret, observés en RNAseq comme étant modulés dans la MA et restoré par SOCS3, est en cours. Nous allons également mesurer la concentration des peptides Aβ42 dans des souris 3xTg agées seulement de 8 mois, avant l'apparition de la pathologie Tau et à l'âge où SOCS3 restaure la LTP. Cette expérience nous permettra d'identifier si l'impact délétère des astrocytes réactifs est transitoire et dépendant de la présence de la pathologie Tau.

L'expression des gènes codant pour différentes enzymes impliquées dans le métabolisme de l'Aβ devrait être mesuré spécifiquement dans les différents types cellulaires (astrocytes, microglie, neurones présents dans la fraction « Other ») par qPCR. Il serait également important de mesurer l'activité de ces enzymes pour s'assurer que la modulation de charge amyloïde n'est pas due à une modification de sa production ou de sa dégradation.

A plus long terme, les altérations fonctionelles induites par l'expression de JAK2ca dans les astrocytes de souris WT seront aussi étudiées par biochimie, histologie et transcriptomique. Ces données permettront d'étudier l'effet propre de la réactivité en s'affranchissant de l'impact des protéines mal conformées, comme l'Aβ et Tau hyperphosphorylée, sur les cellules avoisinnantes ou sur les astrocytes eux-mêmes et des signaux produits par les neurones en soufrance et les autres partenaires de la neuroinflammation.

Enfin, mieux comprendre les voies de signalisations impliquées dans l'induction des différentes classes d'astrocytes réactifs apparait également comme une question centrale suite à ce projet. En effet, la voie JAK2-STAT3 induit globalement la réactivité. L'identification des effecteurs induisant par exemple des astrocytes réactifs de type A2 (protecteurs) pourrait permettre de favoriser des fonctions astrocytaires en faveur de la survie et de l'activité neuronale dans le cadre de la MA.

Annexes

Publication 1

frontiers in Cellular Neuroscience

REVIEW
published: 03 August 2015
doi: 10.3389/fncel.2015.00278

Elusive roles for reactive astrocytes in neurodegenerative diseases

Lucile Ben Haim[1,2], *Maria-Angeles Carrillo-de Sauvage*[1,2], *Kelly Ceyzériat*[1,2] and *Carole Escartin*[1,2]*

[1] Commissariat à l'Energie Atomique et aux Energies Alternatives, Département des Sciences du Vivant, Institut d'Imagerie Biomédicale, MIRCen, Fontenay-aux-Roses, France, [2] Neurodegenerative Diseases Laboratory, Centre National de la Recherche Scientifique, Université Paris-Sud, UMR 9199, Fontenay-aux-Roses, France

Astrocytes play crucial roles in the brain and are involved in the neuroinflammatory response. They become reactive in response to virtually all pathological situations in the brain such as axotomy, ischemia, infection, and neurodegenerative diseases (ND). Astrocyte reactivity was originally characterized by morphological changes (hypertrophy, remodeling of processes) and the overexpression of the intermediate filament glial fibrillary acidic protein (GFAP). However, it is unclear how the normal supportive functions of astrocytes are altered by their reactive state. In ND, in which neuronal dysfunction and astrocyte reactivity take place over several years or decades, the issue is even more complex and highly debated, with several conflicting reports published recently. In this review, we discuss studies addressing the contribution of reactive astrocytes to ND. We describe the molecular triggers leading to astrocyte reactivity during ND, examine how some key astrocyte functions may be enhanced or altered during the disease process, and discuss how astrocyte reactivity may globally affect ND progression. Finally we will consider the anticipated developments in this important field. With this review, we aim to show that the detailed study of reactive astrocytes may open new perspectives for ND.

Keywords: astrocyte reactivity, neuron-astrocyte interactions, neuroinflammation, Alzheimer's disease, Huntington's disease, amyotrophic lateral sclerosis, Parkinson's disease

OPEN ACCESS

Edited by:
James Francis Curtin, Dublin Institute of Technology, Ireland

Reviewed by:
De-Lai Qiu, YanBian University, China
Dmitry Lim, Università del Piemonte Orientale Amedeo Avogadro, Italy

***Correspondence:**
Carole Escartin, MIRCen UMR9199, Batiment 61, 18, Route du Panorama, 92260 Fontenay-aux-roses, France
carole.escartin@cea.fr

Received: *13 May 2015*
Accepted: *06 July 2015*
Published: *03 August 2015*

Citation:
Ben Haim L, Carrillo-de Sauvage M-A, Ceyzériat K and Escartin C (2015) Elusive roles for reactive astrocytes in neurodegenerative diseases. Front. Cell. Neurosci. 9:278. doi: 10.3389/fncel.2015.00278

Introduction

Astrocytes become reactive in response to virtually all pathological conditions in the central nervous system (CNS), both following acute injuries (stroke, trauma) and during progressive diseases (tumors, epilepsy and ND see **Box 1** and **Table 1**). Astrocyte reactivity is observed in many mammalian and bird species. In non-mammalian species, which have low number of or no parenchymal astrocytes, it is unclear whether *bona fide* astrocyte reactivity exists (Appel, 2013). Yet, in lampreys, newts and frogs, astrocyte-like cells react to injury and form a glial bridge promoting axonal regeneration (Bloom, 2014). In Drosophila, glial cells with some typical astrocyte functions display strong phagocytic activity and morphological changes following neuronal degeneration (Freeman, 2015).

Astrocyte reactivity involves morphological, transcriptional and functional changes that we will try to cover in this review. For the sake of clarity, we will focus primarily on Alzheimer's (AD) and Huntington's diseases (HD), as well as amyotrophic lateral sclerosis (ALS) and Parkinson's disease (PD). In particular, we aim to illustrate that astrocyte reactivity is a shared and central feature in ND that requires further characterization.

BOX 1 | Terminology and definitions

"Neuroinflammation" defines the state of reactivity of astrocytes and microglia induced by pathological conditions. It may be associated with the recruitment of peripheral macrophages and lymphocytes. Reactive astrocytes and microglia mediate the innate immune responses in the brain (Heneka et al., 2014).

In this review, the term "***astrogliosis"*** will not be used because it implies the notion of astrocyte proliferation. In fact, in most injury or disease models, astrocytes do not proliferate (see Section Do Reactive Astrocytes Proliferate in ND?) and thus, reactive astrogliosis is a confounding term.

"***Astrocyte reactivity***" or "***reactive astrocytes"*** refer to astrocytes that respond to any pathological condition in the CNS. Astrocytes are considered reactive when they become hypertrophic and overexpress the intermediate filament GFAP. This "minimal definition" of reactive astrocytes is thus based on the two most universal hallmarks of reactivity, but this does not exclude that additional transcriptional, morphological and functional changes occur in a disease-specific manner, as discussed later in this review. Astrocyte reactivity involves the activation of a transcriptional program triggered by specific signaling cascades (see Section How Do Astrocytes Become Reactive?) that results in long-lasting changes in morphology and function, persisting over several hours, days or even decades. This should be distinguished from **"activated astrocytes,"** which are stimulated by exposure to neurotransmitters, for example. This transient response involves intracellular Ca^{2+} on the millisecond to second time scale, and is sometimes accompanied by subtle morphological changes (Bernardinelli et al., 2014), but not long term increases in GFAP gene expression or morphological hypertrophy.

"***Glial scar***" is a specific form of astrocyte reactivity, which is irreversible and involves major morphological remodeling of reactive astrocytes along the disrupted parenchyma.

"Resting astrocytes" will be used to denote astrocytes that are not reactive. However, it does not mean that astrocytes are inactive; instead, it refers to a non-disease state, or a "homeostically active" state.

TABLE 1 | Reactive astrocytes are found in vulnerable brain regions in animal models and patients with ND.

		When	Where	References	Comments
AD	Patients	Before clinical symptoms. GFAP levels increase with Braak stage	Entorhinal cortex and hippocampus. Gradual progression to temporal, frontal and parietal lobes	Simpson et al., 2010; Carter et al., 2012	
	Murine models	May start before amyloid deposition. Prominent when plaques are formed	Primarily around amyloid plaques. (Brain region depends on the model)	Heneka et al., 2005; Duyckaerts et al., 2008; Olabarria et al., 2010	Astrocytes located far from plaques are atrophied in 3xTg-AD mice
HD	Patients	Already visible at grade 0 in putamen.	Primarily in caudate and putamen. Later in motor cortex, globus pallidus, thalamus, hippocampus	Vonsattel et al., 1985; Faideau et al., 2010	
	Murine models	Late or no reactivity	Striatum	Tong et al., 2014; Ben Haim et al., 2015	Strong reactivity in models with neuronal death (Lenti-Htt82Q or toxins)
ALS	Patients	Before motor symptoms	Ventral and dorsal horns in the spinal cord. Lateral descending corticospinal tracts, subcortical white matter, cortical gray matter in the brain	Maragakis and Rothstein, 2006; Philips and Robberecht, 2011	
	Murine models	Before motor symptoms	Pattern similar to that in patients	Hall et al., 1998; Barbeito et al., 2004; Maragakis and Rothstein, 2006	
PD	Patients	Follows dopaminergic cell death	*Substantia nigra*, correlates with the severity of neuronal loss	Forno et al., 1992; Damier et al., 1993	
	MPTP- monkeys	Follows dopaminergic cell death	*Substantia nigra*	Barcia et al., 2004	
	MPTP-mice 6-OHDA rats	Follows microglial activation, peaks at 4–5 days after intoxication	*Substantia nigra* and striatum	Sheng et al., 1993; Kohutnicka et al., 1998; Hirsch and Hunot, 2009	

It has been very difficult to distinguish the contribution of astrocytes from that of microglia because they usually become reactive in concert and both are involved in neuroinflammation (see definitions in **Box 1**). However, they have quite different functions in the brain in normal conditions; therefore, they may also play different roles during ND. Cell-type specific approaches based on viral vectors or transgenesis offer a unique opportunity to understand the roles of reactive astrocytes (Davila et al., 2013). In this review, we will focus on reactive astrocytes in ND. Excellent reviews recently published on microglia in ND can be found elsewhere (Hanisch and Kettenmann, 2007; Heneka et al., 2014).

Reactive Astrocytes in ND: Definitions and General Considerations

A Brief History

In 1856, Rudolf Virchow first described "neuroglia" as a connective tissue with embedded nerve cells (Virchow, 1856). The development of microscopic and histological techniques by Camilo Golgi, Santiago Ramón y Cajal and Pio del Rio Hortega later revealed the morphology of astrocytes and their extraordinary diversity (Somjen, 1988; Kettenmann and Ransom, 2004). The first description of astrocyte reactivity also dates from the nineteenth century, when Virchow reported that the spinal cord tissue was more fibrillar in neurosyphilis patients than in healthy individuals (Weigert, 1895; Oberheim et al., 2008). The concept of astrocyte reactivity truly emerged with the discovery of the intermediate filament (IF) protein GFAP (Eng et al., 1971) and the development of immunohistological staining for this protein (Eng et al., 2000). Strong GFAP expression in astrocytes became the hallmark of reactivity (Bignami and Dahl, 1976), even though other IF such as vimentin and nestin are also upregulated by reactive astrocytes.

Morphological Changes

Another cardinal feature of astrocyte reactivity is hypertrophy, which was reported by early neuropathologists. Reactive astrocytes display an enlarged cell body and processes (Wilhelmsson et al., 2006). In addition, astrocyte arborization is reorganized with reactivity: the number of primary processes changes (Wilhelmsson et al., 2006) or they polarize toward the site of injury (Bardehle et al., 2013) or toward amyloid plaques in AD (see below).

Less is known about the thin distal processes in astrocytes called perisynaptic processes (PAP), which contact synapses. PAP are dynamic and they influence synaptic transmission in physiological conditions (Oliet et al., 2001; Genoud et al., 2006; Bernardinelli et al., 2014). It is experimentally challenging to monitor morphological changes in PAP that are smaller than the diffraction limit. New microscopy techniques will allow the study of PAP with higher resolution in both resting and reactive astrocytes (Panatier et al., 2014).

Astrocytes occupy separate and non-overlapping spatial domains (Bushong et al., 2002). This organization seems fairly insensitive to reactivity during ND because an increase in domain overlap occurs only after severe insults such as recurring epilepsy, but not in AD models (Oberheim et al., 2008).

Reactive Astrocytes in Commonly Studied ND

AD is the most common form of dementia, characterized by cognitive deficits including learning impairment and memory loss (Querfurth and Laferla, 2010). The brains of AD patients display extracellular amyloid depositions composed of amyloid β (Aβ) peptides and intracellular neurofibrillary tangles formed by hyperphosphorylated Tau protein. AD is characterized by severe neuronal loss; primarily located in the hippocampus and the entorhinal cortex (Querfurth and Laferla, 2010). More than 100 transgenic mouse models of AD are now available (Duyckaerts et al., 2008, see also www.alzforum.org). Most involve the expression of mutated amyloid precursor protein (APP), presenilin 1 (PS1), PS2 and/or Tau, and they replicate some neuropathological features and functional alterations of AD as well as memory deficits (Gotz and Ittner, 2008). Astrocyte reactivity can be detected in the brain of AD patients with imaging and proteomic techniques before the onset of symptoms (Owen et al., 2009; Carter et al., 2012). Similarly, foci of reactive astrocytes are detected at early stages in some mouse models, even before amyloid deposition (Heneka et al., 2005). Reactive astrocytes are usually found around amyloid plaques (Nagele et al., 2003; Wyss-Coray et al., 2003, **Table 1**). However, plaques can also be devoid of reactive astrocytes and patches of reactive astrocytes may be found in the absence of plaques in patients (Simpson et al., 2010). In addition, atrophied astrocytes may be located at a distance from plaques in some mouse models (Olabarria et al., 2010, see **Tables 1**, **2**).

HD is a fatal genetic ND caused by an autosomal dominant mutation, involving the expansion of glutamine (Q) repeats in the protein huntingtin (Htt). HD patients present psychiatric, cognitive and motor symptoms, the most characteristic being progressive chorea (Vonsattel et al., 1985). HD is characterized by the extensive loss of GABAergic neurons in the caudate and putamen (striatum) and by mutant Htt (mHtt) aggregates. Many HD transgenic mouse models exist, which were generated by expressing mHtt under the endogenous Htt promoter (knock-in) or using various transgenic constructs (see **Table 2**). Astrocyte reactivity is an early feature of HD because GFAP immunoreactivity is detected in the striatum of presymptomatic carriers and it increases with disease progression (Faideau et al., 2010). Strikingly, no clear evidence of astrocyte reactivity exists in most HD models (Tong et al., 2014; Ben Haim et al., 2015, **Table 1**). Instead, HD astrocytes show functional alterations (see Section What Do Reactive Astrocytes Do or Fail to Do During ND?) in the absence of the main features of reactivity (hypertrophy and high GFAP expression).

ALS is characterized by the progressive loss of upper motor neurons in the motor cortex and lower motor neurons in the spinal cord and brainstem, resulting in progressive muscle atrophy, weakness and spasticity (Rothstein et al., 1992). Murine models overexpressing mutated forms of superoxide dismutase 1 (mSOD1), identified in familial forms of ALS, develop progressive motor neurodegeneration that mimics the pathogenic features of ALS (Turner and Talbot, 2008, **Table 2**). More recently, new genetic loci associated with familial ALS have been identified, like the *43 kDa transactivation-response DNA-binding protein (TDP-43)*, and new mouse models are being developed (Robberecht and Philips, 2013). Reactive astrocytes are observed in both ALS patients and models (**Table 1**). They appear in vulnerable regions and the degree of reactivity correlates with the level of neurodegeneration (Barbeito et al., 2004).

PD is characterized by the loss of dopaminergic neurons in the substantia nigra (SN), resulting in dopamine deficiency in the striatum and alteration of the basal ganglia circuitry. This causes major motor symptoms, such as akinesia, bradykinesia, tremor, rigidity and postural instability (Agid, 1991), as well as non-motor alterations such as cognitive fluctuations (Witjas

TABLE 2 | Main behavioral, cellular, and molecular features of several mouse models of ND.

Disease modeled	Model	Species	Genetic construct	Promoter	Lifespan	Major symptoms	Histopathological features	Vulnerable brain regions	Original references
AD	APP/PS1dE9	Mouse	Mo/hu APP_{Swe}, Hu PSEN1 deltaE9	MoPrP	Normal	Spatial memory impairment Reduced LTP	Extracellular Aβ depositions No extensive neuronal death	Hippocampus Cortex	Jankowsky et al., 2004
	3xTg-AD	Mouse	$HuAPP_{Swe}$, Mo $PSEN1^{M146V}$, Hu $MAPT^{P301L}$,	MoThy1.2 (for APP and MAPT); endogenous moPSEN1 promoter (for PSEN1)	Normal	Spatial memory impairment Reduced basal synaptic transmission and LTP	Extracellular Aβ depositions Tau pathology in CA1 neurons No extensive neuronal death	Subiculum Hippocampus Entorhinal cortex	Oddo et al., 2003
	Tg2576	Mouse	$HuAPP_{Swe}$	Hamster PrP	Normal	Spatial memory impairment Reduced LTP	Extracellular Aβ depositions No extensive neuronal death	Hippocampus Frontal, entorhinal and occipital cortex	Hsiao et al., 1996
	APPPS1	Mouse	Mo/hu APP_{Swe}; Hu $PSEN1^{L166P}$	Mo Thy1	Normal	Spatial memory impairment Reduced LTP	Extracellular Aβ depositions Local neuronal death in the dentate gyrus Altered dendritic spine morphology	Hippocampus Cortex	Radde et al., 2006
HD	R6/2	Mouse	Exon 1 of huHtt with 150 CAG	1 kb huHtt	10–13 weeks	Altered motor coordination and gait Involuntary movements Seizures Cognitive deficits (selective discrimination learning, contextual fear conditioning) Alteration of MSN electrophysiology	NII Striatal atrophy No extensive neuronal death Alteration of MSN morphology	Striatum Motor cortex	Mangiarini et al., 1997
	Hdh140	Mouse	Knock-in of Mo/hu exon 1 Htt with 140 CAG	Endogenous moHtt promoter	Normal	Altered motor coordination Alteration of MSN electrophysiology	NII Striatal atrophy Low expression of neuronal transcripts	Striatum Motor cortex	Menalled et al., 2003
	zQ175	Mouse	Knock-in of Mo/hu exon 1 Htt with 175 CAG (derived from Hdh140)	Endogenous moHtt promoter	Normal	Altered motor coordination Cognitive deficits (selective discrimination learning)	NII Striatal atrophy Low expression of neuronal transcripts	Striatum Motor cortex	Menalled et al., 2012
	BACHD	Mouse	Full length huHtt with 97 CAG/CAA	HuHtt	Normal	Altered motor coordination Alteration of MSN electrophysiology	Extranuclear aggregates Striatal and cortical atrophy No extensive neuronal death	Striatum Motor cortex	Gray et al., 2008
	Lenti-Htt82Q (lentiviral-based)	Mouse	Lentiviral vector encoding 171 first amino acids of huHtt with 82 Q	PGK	Normal	Behavioral alterations not tested in mice	Cytoplasmic and nuclear inclusions MSN loss	Striatum	De Almeida et al., 2002

(Continued)

TABLE 2 | Continued

Disease modeled	Model	Species	Genetic construct	Promoter	Lifespan	Major symptoms	Histopathological features	Vulnerable brain regions	Original references
ALS	SOD1G93A	Mouse	$HuSOD1^{G93A}$	HuSOD1	5 months	Weight loss Hindlimb weakness Progressive paralysis	Loss of ventral SC motor neurons Degeneration of ventral root axons SOD1 inclusions in the SC and brain	Spinal cord Motor cortex	Gurney et al., 1994
	SOD1G93A	Rat	$HuSOD1^{G93A}$	HuSOD1	3–4 months	Abnormal gait Quick hindlimb paralysis Weight loss Muscle atrophy and denervation	Loss of ventral SC motor neurons Degeneration of ventral root axons Vacuolar degeneration SOD1 inclusions in the SC and brain	Spinal cord Brain	Howland et al., 2002
PD	MPTP	Mouse	N/A	N/A	N/A	Altered rearing and coordination	Loss of DA neurons Reduced dopamine levels in striatum	SNpc Striatum	Heikkila et al., 1984
	MPTP	Non-human primate	N/A	N/A	N/A	Bradykinesia, rigidity, tremor	Loss of DA neurons Reduced dopamine levels in caudate-putamen	SNpc Caudate putamen	Burns et al., 1983

Common mouse models of ND were included in the table if they are mentioned at least twice in the text. APPSwe, KM670/671NL (Swedish mutation); DA, dopaminergic. Hu, human; Mo, mouse; MSN, medium-sized spiny neurons; NII, neuronal intranuclear inclusions; PGK, phosphoglycerate kinase; PrP, Prion Protein; Q, glutamine, SNpc, Substantia nigra pars reticulata.

et al., 2002). The first animal models of PD were based on toxins that specifically induce the degeneration of dopaminergic neurons in the SN pars compacta (SNpc) in rodents or primates (e.g., 6-hydroxydopamine [6-OHDA], 1-methyl-4-phenyl-1,2,3,6-tetrahydropyridine [MPTP] or rotenone). Transgenic mice harboring genes mutated in familial PD (α-synuclein, leucine-rich repeat kinase 2…) were subsequently developed (Beal, 2010, see **Table 2**). The involvement of microglial cells in PD has been more extensively studied than that of astrocytes. Yet, astrocyte reactivity is detected in the SNpc of patients with PD, individuals intoxicated with MPTP and in animal models (Forno et al., 1992; Hirsch and Hunot, 2009, **Table 1**).

Do Reactive Astrocytes Proliferate in ND?

The original definition of astrocyte reactivity included the notion of proliferation. The idea that reactive astrocytes proliferate is based on the misleading observation that the number of $GFAP^+$ cells increases after injury (Dimou and Gotz, 2014). Most astrocytes in the adult mouse CNS express GFAP at undetectable levels under physiological conditions. Upon injury or disease, reactive astrocytes upregulate GFAP, leading to an increased number of $GFAP^+$ cells. Recent evidence based on BrdU incorporation or Ki67 labeling reveals that astrocyte proliferation is very limited, especially in ND. The exact value depends on the model, age and detection method. For example, reactive astrocytes do not proliferate in the APP/PS1dE9 mouse model of AD (Kamphuis et al., 2012), and represent less than 3% of total proliferating cells in the APPPS1 mouse model of AD (Sirko et al., 2013) and less than 7% in a model of ALS (Lepore et al., 2008a). Proliferating astrocytes account for only 1% of total gray matter astrocytes in APPPS1 mice (Sirko et al., 2013). In the temporal cortex of AD patients, $GFAP^+$ cells were carefully quantified by co-labeling with ubiquitous astrocyte markers (glutamine synthase [GS] or aldehyde dehydrogenase 1 family, member L1). This analysis confirms that the high density of $GFAP^+$ cells is explained by enhanced GFAP expression and cortical atrophy (Serrano-Pozo et al., 2013).

Can Astrocyte Reactivity be Reproduced *In vitro*?

With the development of *in vitro* systems to study astrocytes (McCarthy and De Vellis, 1980), it became possible to study reactive astrocytes in a dish. Human astrocytes can also be grown *in vitro*, either from fetuses or biopsies (Sharif and Prevot, 2012) or generated from induced pluripotent stem cells, including from patients (Krencik and Ullian, 2013). Generally, primary astrocytes are exposed to cytokines such as interleukins (IL), tumor necrosis factor alpha (TNFα) and interferon gamma (IFNγ), which induce many transcriptional and functional changes (Sofroniew, 2009; Sofroniew and Vinters, 2010). Describing them all is beyond the scope of this review. The main limitation to *in vitro* studies is that astrocytes in a dish show signs of reactivity, even in the absence of stimulus. They express high levels of GFAP and usually have a flat, polygonal morphology, very different from the bushy morphology observed *in situ*. This precludes the identification of the hallmarks of astrocyte reactivity. Co-culture with neurons triggers a stellate morphology and low GFAP expression, suggesting that neurons

release factors that maintain astrocytes in a resting state (see Section The Molecular Triggers of Reactivity). More recently, new methods have been developed to reduce astrocyte reactivity *in vitro*, such as exposure to heparin-binding EGF-like growth factor (Foo et al., 2011) or 3D polymer matrix (Puschmann et al., 2013). Given the above-mentioned limitations, we will focus on results obtained in animal models, or even more relevant, in patient brains.

How Do Astrocytes Become Reactive?

The Molecular Triggers of Reactivity

Astrocyte reactivity is triggered by any alteration in brain homeostasis. Astrocytes are equipped with many receptors and intracellular signaling cascades to respond quickly to changes in their environment (Buffo et al., 2010; Burda and Sofroniew, 2014). They express many receptors, including pattern recognition receptors (PRR), that detect abnormal signals in the extracellular space (viral or bacterial molecules, serum proteins, aggregated proteins such as Aβ…), increased concentrations of some molecules (cytokines, chemokines, purines) and even the absence of "normal" signals from neighboring cells (growth factors, neurotransmitters…) (Buffo et al., 2010; Burda and Sofroniew, 2014; Kigerl et al., 2014). Indeed, astrocytes, like microglia, seem to be actively maintained in a resting state. For instance, knocking out fibroblast growth factor (FGF) receptors or β1 integrin (a subunit of the integrin receptor family that binds extracellular matrix molecules) in astrocytes, results in astrocyte reactivity in absence of pathological stimuli (Robel et al., 2009; Kang et al., 2014).

Extracellular molecules inducing astrocyte reactivity have primarily been studied in acute injury models involving scar formation (Burda and Sofroniew, 2014). Such acute lesions involve the breach of the blood-brain-barrier (BBB) and infiltration of immune cells. By contrast, these events occur very progressively in ND, if ever (Zlokovic, 2008). Therefore, although some molecular triggers are shared between acute injuries and ND, molecules such as endothelins or serum proteins are probably not involved in the initiation of astrocyte reactivity in ND.

The exact molecular triggers that occur during the initial stages of ND, before significant neurodegeneration takes place, are unknown. It is probable that glial cells (both astrocytes and microglial cells) can detect even mild neuronal dysfunction (altered neurotransmission, release of stress signals, and abnormally folded proteins). Indeed, astrocytes are very well positioned at the tripartite synapse to detect abnormal synaptic activity and microglial cells permanently monitor the brain parenchyma. Once activated by such signals, glial cells further release active molecules to set up a reactive state. For example, purines, pro-inflammatory cytokines and growth factors may be released by reactive astrocytes and, in even larger amounts by activated microglia (Buffo et al., 2010, see Section Release of Active Molecules).

Importantly, in ND, mutant proteins (e.g., mHtt, mSOD1) may be directly expressed by astrocytes or toxic proteins (Aβ, hyperphosphorylated tau, α-synuclein) can be taken up by astrocytes and activate them (see **Figure 1**). Lentiviral-mediated expression of mHtt specifically in striatal astrocytes increases GFAP expression and induces cellular hypertrophy (Faideau et al., 2010). Similarly, the expression of $SOD1^{G86R}$, α-$synuclein^{A53T}$, or tau (either WT or P301L mutant) in astrocytes, induces their reactivity (Gong et al., 2000; Dabir et al., 2006; Gu et al., 2010). The precise molecular mechanisms linking the accumulation of intracellular toxic proteins in astrocytes to reactivity remain to be characterized (see **Figure 1**). Cytosolic PRR that can detect intracellular "danger associated molecular patterns" have been described in microglial cells, but much less is known about their role in astrocytes (Heneka et al., 2014).

Other molecular triggers of reactivity (e.g., cytokines, growth factors, purines), bind to their cognate receptors at the astrocyte membrane and activate various intracellular signaling cascades. These include the Janus Kinase/Signal Transducer and Activator of Transcription (JAK/STAT) pathway, the Nuclear Factor of Kappa light polypeptide gene enhancer in B-cells (NF-κB) pathway, the calcineurin (CN) pathways and the Mitogen-Activated Protein Kinase (MAPK) pathway (**Figure 1**).

The JAK/STAT3 Pathway

The JAK/STAT3 pathway is a ubiquitous cascade that predominantly mediates cytokine signaling in cells. It regulates the expression of genes involved in many functions including cell growth, proliferation, differentiation and inflammation. Cytokines of the interleukin family (e.g., IL-6, ciliary neurotrophic factor [CNTF] and leukemia inhibitory factor) signal through specific cell-surface receptors possessing the glycoprotein 130 receptor (gp130) subunit. Upon binding, they trigger the assembly of multimeric receptors, leading to the phosphorylation and nuclear translocation of STAT3, and the transcription of its target genes (Levy and Darnell, 2002 and see **Figure 1** for a detailed description of the pathway). Interestingly, the JAK/STAT3 pathway also controls the onset of astrogliogenesis during brain development (He et al., 2005), by promoting the expression of mature astrocyte genes such as *gfap* and *S100*β (Kanski et al., 2014).

It is well established that the JAK/STAT3 pathway mediates astrocyte reactivity and scar formation in models of acute injuries (Okada et al., 2006; Herrmann et al., 2008). Fewer studies have been performed in ND models. Phospho-STAT3 (pSTAT3) is detected in the nucleus of reactive astrocytes (as well as microglia and motor neurons) in the spinal cord of mouse models and patients with ALS (Shibata et al., 2009, 2010). STAT3 accumulates in the nucleus of reactive astrocytes in the hippocampus of transgenic mouse models of AD and in the striatum of murine and primate models of HD (Ben Haim et al., 2015). Activation of the STAT3 pathway seems to be a universal feature of astrocyte reactivity in ND models, shared between disease models, brain regions and animal species (**Figure 2**). Pharmacological inhibition of JAK2 in the MPTP mouse model of PD significantly decreases pSTAT3 and GFAP levels, suggesting that the JAK/STAT3 pathway is required to induce astrocyte reactivity (Sriram et al., 2004). However, this pathway is active in all brain cells; therefore,

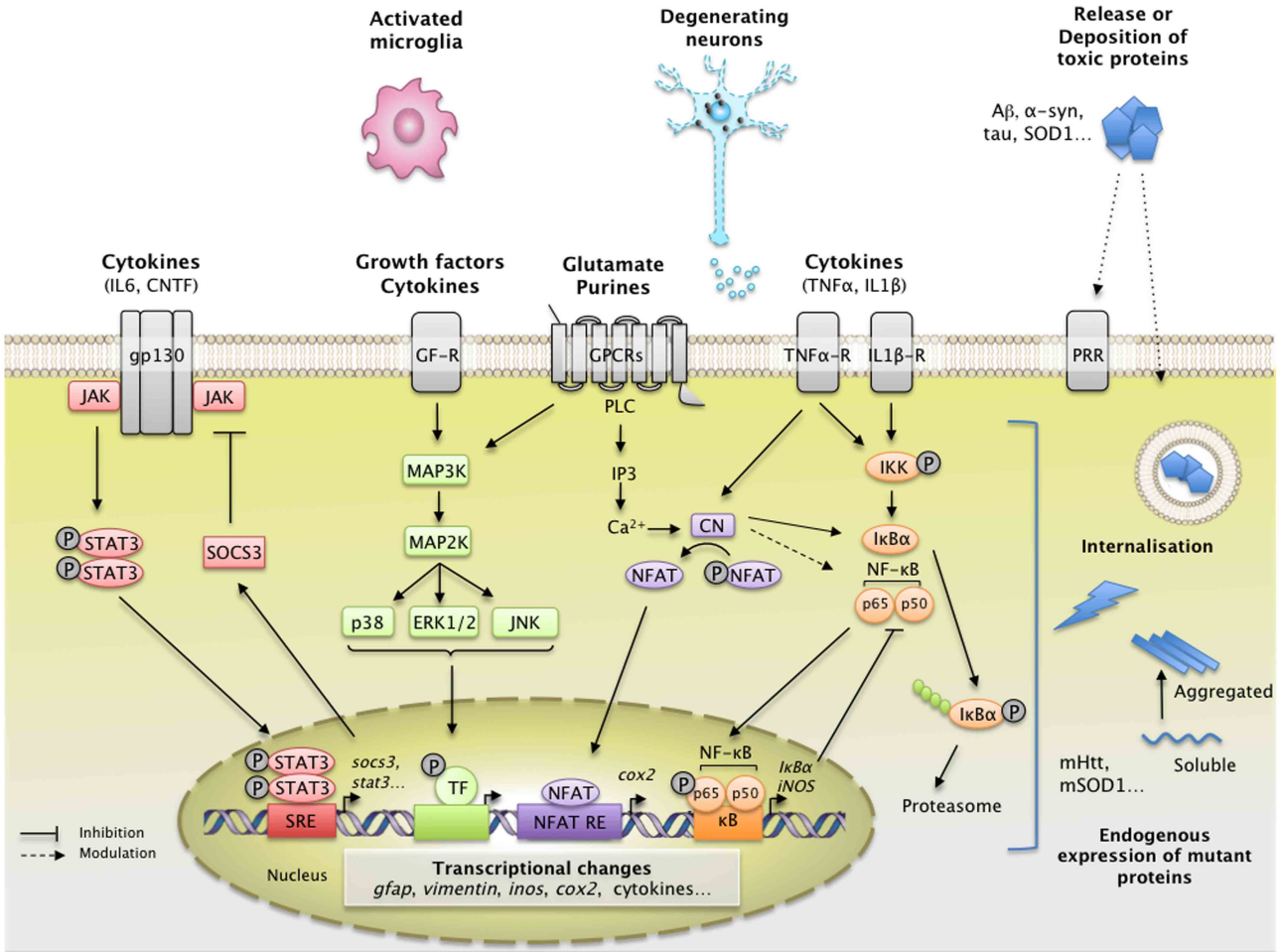

FIGURE 1 | Main extracellular stimuli and intracellular signaling pathways leading to astrocyte reactivity in ND. Dysfunctional neurons, activated microglia, and astrocytes themselves release a wide range of molecules, which bind specific receptors at the astrocyte plasma membrane. These signals activate intracellular pathways such as the JAK/STAT3 pathway (in red), the NF-κB pathway (in orange), the CN/NFAT pathway (in purple), or the MAPK pathway (in green). **The JAK/STAT3 pathway** is activated by interleukins such as IL-6 or CNTF. Upon cytokine binding, the kinase JAK is activated and STAT3 is recruited to the gp-130 receptor. JAK phosphorylates STAT3, which dimerizes and translocates to the nucleus, where it binds consensus sequences (STAT responsive element, SRE) in the promoter region of its target genes. In astrocytes, the JAK/STAT3 pathway regulates the transcription of *gfap, vimentin,* and *stat3* itself. STAT3 also induces the expression of SOCS3, the endogenous inhibitor of the JAK/STAT3 pathway, which mediates an inhibitory feedback loop. **The NF-κB pathway** is activated by pro-inflammatory cytokines such as TNFα and IL-1β. The canonical NF-κB pathway involves the activation of the IKK complex by receptor-bound protein kinases, leading to the phosphorylation of IκBα, the master inhibitor of NF-κB. Upon phosphorylation, IκBα is polyubiquinated and targeted to the proteasome for degradation. The NF-κB subunits p50 and p65 then translocate to the nucleus, where they activate the transcription of various target genes such as inducible nitric oxide synthase and *cox2*. Like the JAK/STAT3 pathway, NF-κB induces the transcription of its own inhibitor, IκBα. **The CN/NFAT pathway** is activated by cytokines such as TNFα or by glutamate. CN is a Ca^{2+}-dependent phosphatase with many regulatory effects on the NF-κB pathway depending on the initial trigger and cellular context. CN also activates NFAT by dephosphorylation. NFAT binds specific promoter sequences and activates the expression of target genes (*cox2*). **The MAPK pathway** is activated by growth factors and cytokines which initiate a phosphorylation cascade. Upon activation, ERK1/2, p38 and c-jun also regulate gene transcription through the activation of a specific set of transcription factors (TF). ND are characterized by intracellular and/or extracellular depositions of pathologic proteins (such as Aβ, Tau, and mHtt, which are shown in blue). In ND, pathological proteins can either be endogenously expressed or internalized by astrocytes. They represent "danger associated molecular patterns" that bind specific pattern recognition receptors (PRR) at the membrane or within astrocytes. These abnormal proteins can interfere with intracellular signaling pathways, activating or inhibiting various signaling proteins (represented as lightning, see Section Additional levels of Complexity and **Figure 3**). The precise molecular mechanisms involved in astrocytes are mostly unknown. These complex signaling cascades strongly affect the astrocyte transcriptome and lead to astrocyte reactivity. Abbreviations: NFAT RE, NFAT responsive element; GF-R, Growth factor receptor; GPCR, G-protein coupled receptor.

non-specific effects of JAK2 inhibitors on other cell types cannot be ruled out. To overcome this limitation, we used lentiviral vectors to overexpress suppressor of cytokine signaling 3 (SOCS3), the endogenous inhibitor of the JAK/STAT3 pathway, selectively in astrocytes of the adult mouse brain. SOCS3 overexpression prevented the nuclear accumulation of STAT3

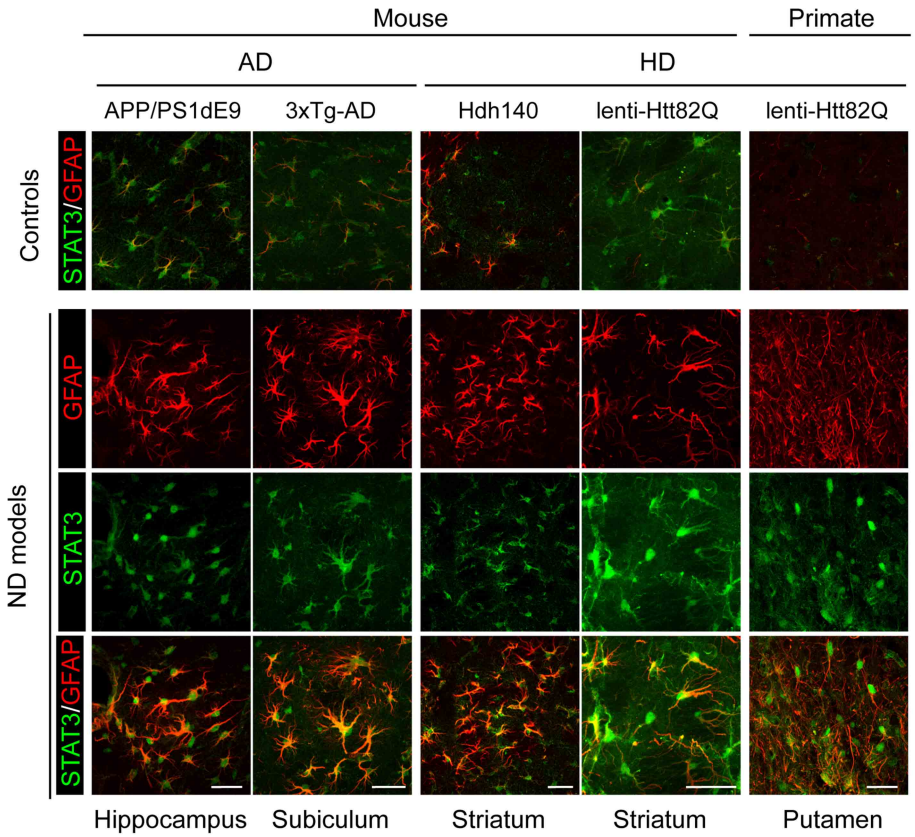

FIGURE 2 | Activation of the JAK/STAT3 pathway is a common feature of astrocyte reactivity in various ND models. Images of brain sections from several models of AD and HD (APP/PS1dE9 mice, 3xTg-AD mice, Hdh140 mice, and the murine and primate lenti-Htt82Q-based models of HD). For all ND models, STAT3 (green) accumulates in the nucleus of reactive astrocytes labeled with GFAP (red) in specific vulnerable regions (as indicated at the bottom). The first line shows the merged STAT3 (green)/GFAP (red) staining in age-matched control animals for each model. Scale bars: 20 μm (mouse) and 40 μm (primate). Adapted from Ben Haim et al. (2015).

and GFAP upregulation in mouse models of ND. Furthermore, SOCS3-expressing astrocytes displayed a resting morphology, showing that the JAK/STAT3 pathway is responsible for astrocyte reactivity in these models (Ben Haim et al., 2015). Interestingly, a recent paper showed that the *Drosophila* ortholog of STAT3 also modulates the reactivity of glial cells following injury (Doherty et al., 2014). Therefore, the JAK/STAT3 pathway is a conserved and central pathway for astrocyte reactivity.

The NF-κB Pathway

The NF-κB pathway is another pathway associated with neuroinflammation. It is involved in many cellular processes including immune responses, inflammation, cell division and apoptosis (Mattson and Meffert, 2006 see **Figure 1** for a detailed description of the pathway). This pathway is activated by several known pro-inflammatory agents (e.g., lipopolysaccharide [LPS], IL-1β, TNFα) (Kaltschmidt et al., 2005). The NF-κB pathway is found activated during ND. Following microinjection of Aβ1-42 oligomers into the rat cortex, NF-κB activation is detected in some $GFAP^+$ astrocytes, along with cyclooxygenase 2 (COX2) and IL-1β, two NF-κB target genes (Carrero et al., 2012). NF-κB accumulates in astrocyte nuclei in the R6/2 model of HD (Hsiao et al., 2013) and in the spinal cord of ALS patients (Migheli et al., 1997). However, experiments involving an NF-κB-GFP reporter construct in ALS mice demonstrate that this pathway is predominantly active in microglial cells in the spinal cord (Frakes et al., 2014). In fact, the NF-κB pathway seems to be active in many cell types other than reactive astrocytes during ND. NF-κB is activated in dopaminergic neurons in the SNpc of PD patients (Hunot et al., 1997), in peripheral immune cells in patients with HD (Trager et al., 2014) and, in hippocampal and entorhinal cortex neurons of AD patients, but not in glial cells (Terai et al., 1996; Kaltschmidt et al., 1997; Ferrer et al., 1998). Overall, this ubiquitous cascade is found activated in various cell types including astrocytes but these observations do not prove that NF-κB is required for astrocyte reactivity. In a mouse model of ALS, Crosio et al. found that inhibiting NF-κB signaling selectively in astrocytes only transiently attenuated their reactivity at the onset of disease (Crosio et al., 2011).

Overall, the NF-κB pathway is activated in ND and plays a key role in microglial activation, but this cascade does not seem essential to initiate astrocyte reactivity. Further studies in other models are needed to understand the role of NF-κB pathway in astrocyte reactivity during ND.

The Phosphatase Calcineurin

The Ca^{2+}/calmodulin-dependent serine/threonine phosphatase CN regulates gene expression by modulating transcription factors such as nuclear factor of activated T-cells (NFATs) and NF-κB (Furman and Norris, 2014). CN is a ubiquitous protein, although it is expressed at high levels in the brain. It regulates growth, differentiation and various cellular processes in T-cells, osteoclasts and myocytes (Hogan et al., 2003 and see **Figure 1** for a detailed description of the pathway).

CN is activated in inflammatory conditions. Several studies have linked the CN/NFAT pathway to astrocyte reactivity, in particular in AD. Indeed, CN immunoreactivity is high in reactive astrocytes in aged mice and around amyloid plaques both in AD patients and mouse models (Furman and Norris, 2014). Activated NFAT1 and 3, two downstream targets of CN, are found in both neurons and astrocytes in AD brains (Abdul et al., 2009).

The effects of CN on astrocyte reactivity are extremely complex and context-dependent because CN can both trigger and prevent reactivity (Furman and Norris, 2014). On the one hand, overexpression of constitutively active CN (caCN) in primary rat hippocampal astrocytes induces morphological and transcriptional changes reminiscent of astrocyte reactivity *in vivo* (Norris et al., 2005). Viral-mediated overexpression of VIVIT, a blocking peptide that inhibits NFAT, attenuates astrocyte reactivity around amyloid depositions in APP/PS1dE9 mice (Furman et al., 2012). But on the other hand, caCN expression in astrocytes reduces GFAP induction following brain injury or LPS injection (Fernandez et al., 2007), and in APP/PS1 mice (Fernandez et al., 2012). This discrepancy between the pro- and anti-reactivity action of CN may be controlled by its signaling partners (Fernandez et al., 2012; Furman and Norris, 2014): its downstream targets (NF-κB vs. NFAT for example) as well as its activators. Indeed, Aβ and IGF-1 both activate CN in cultured astrocytes, but they have opposite effects on the NF-κB pathway (Pons and Torres-Aleman, 2000; Lim et al., 2013).

Overall, CN appears to modulate rather than induce astrocyte reactivity. Whether the effects of CN are conserved in other models and ND remains to be assessed.

The MAPK Pathway

The binding of growth factors (such as FGF, EGF, and TGFα), cytokines or extracellular matrix proteins to their specific cell-surface receptors activates the MAPK pathway (Jeffrey et al., 2007). This is mediated by the activation of small GTP-ase proteins (RAS) and the successive phosphorylation of MAP3K, MAP2K, and MAPK. There are three main phosphorylation cascades, with p38, ERK1/2 or JNK as downstream effectors (see **Figure 1** for a detailed description of the pathway). All result in the activation of different transcription factors by phosphorylation. Cellular stress and extracellular matrix proteins such as integrins activate the c-jun N-terminal kinase (JNK) cascade, whereas cytokines such as IL-1β activate p38 (Jeffrey et al., 2007).

The MAPK pathway is activated in many cell types in ND patients and models. Reactive astrocytes contain active forms of p38, JNK and ERK in mouse models and/or in patients with ALS (Migheli et al., 1997; Tortarolo et al., 2003; Bendotti et al., 2004; Chung et al., 2005). However, in ALS mice, p38 is also activated in motor neurons and microglial cells (Tortarolo et al., 2003). Similarly, p38 and JNK are activated both in neurons and reactive astrocytes in the brain of patients with various tauopathies (Ferrer et al., 2001). In AD patients, phosphorylated forms of p38 are observed in neurons and glial cells around plaques (Hensley et al., 1999) but only in microglial cells in a mouse model (Koistinaho et al., 2002). Several MAPK inhibitors have been tested in an attempt to reduce neuroinflammation in pathological conditions; however, they are thought to act on reactive microglia (Kaminska et al., 2009).

Overall, although the MAPK pathway is activated in many cell types in ND patients and mouse models, to the best of our knowledge, there is no evidence showing that it is directly involved in the initiation of astrocyte reactivity in ND.

Additional Levels of Complexity

Interactions between Pathways

There are many levels of crosstalk between these intracellular signaling pathways (**Figures 1**, **3**). For instance, depending on the specific cellular environment, STAT3 and NF-κB pathways may interfere with each other through direct physical interaction, perform reciprocal inhibition through their respective inhibitors, or cooperate in the regulation of transcription of target genes (Grivennikov and Karin, 2010; Oeckinghaus et al., 2011). Similar interactions between STAT3 and ERK have been reported *in vitro* (Jain et al., 1998). In astrocyte cultures, the stimulation of purinergic receptors by specific agonists results in STAT3 phosphorylation, suggesting crosstalk between STAT3 and purinergic signaling cascades (Washburn and Neary, 2006). Similarly, several members of the MAPK family may interact with the NF-κB pathway. For example, p38 is a co-factor for NF-κB activation (Hoesel and Schmid, 2013). However, most of these mechanisms were described in cell lines, using cytokine stimulation or expression of constitutively active mutant proteins. Whether these interactions occur in reactive astrocytes *in vivo* remains to be demonstrated, especially in ND.

In addition, transcription factors such as STAT3 can also bind non-consensus sequences and interact with co-factors or epigenetic regulators, which represent an additional level of transcriptional regulation (Hutchins et al., 2013). Zamanian et al. recently showed that astrocyte reactivity induced by LPS injection or ischemia in the mouse brain induces the expression of hundreds of genes (Zamanian et al., 2012). Only a subset of these genes was common between the two models, illustrating the diversity of the transcriptional changes that may occur in reactive astrocytes, depending on the trigger and cellular environment (see **Figure 3**).

MicroRNA

MicroRNAs (miRNA) are non-coding RNA involved in the post-transcriptional regulation of gene expression. Several studies have linked changes in miRNA expression to astrocyte reactivity

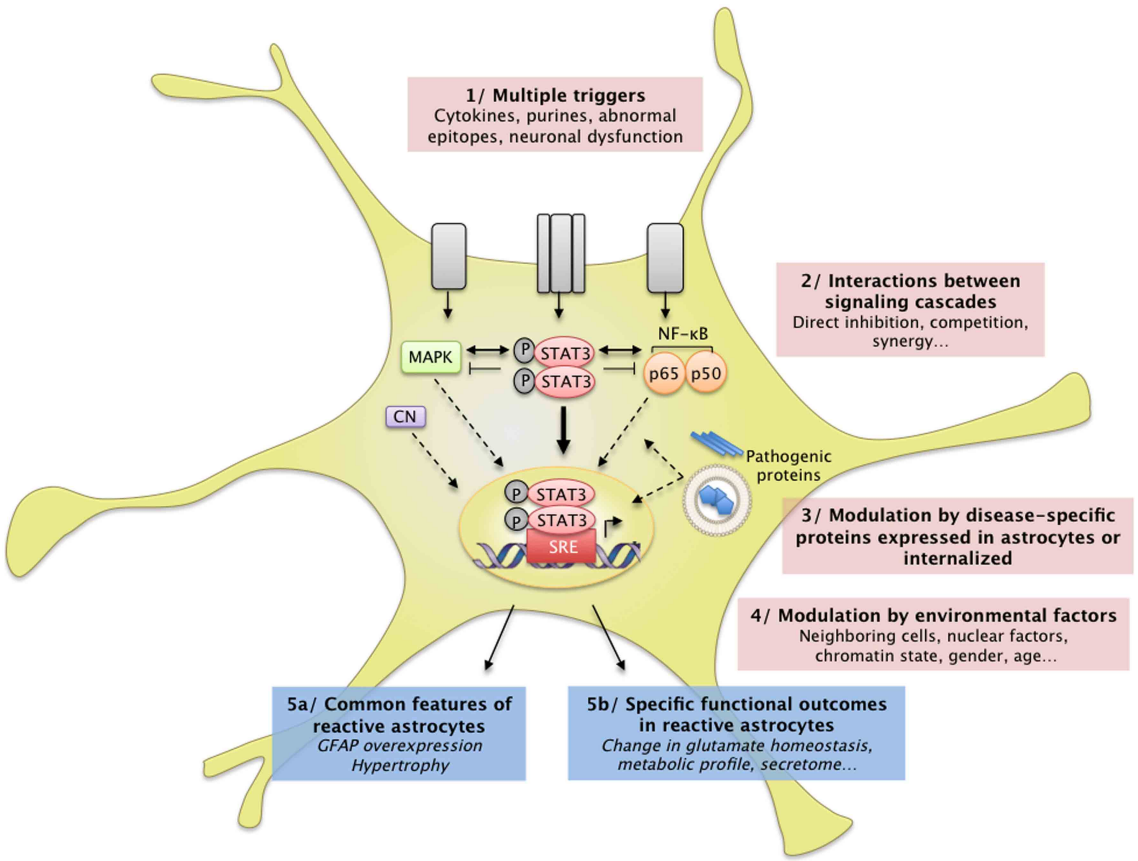

FIGURE 3 | Complex interactions between intracellular cascades result in a unique pattern of astrocyte reactivity in ND. (1) Many signals can trigger astrocyte reactivity (see Section How do Astrocytes become Reactive? and **Figure 1**) such as cytokines, purines or abnormal epitopes like aggregated proteins. Astrocytes may also react to the absence of "resting signals" from neighboring cells, which occurs with neuronal death in ND. (2) These molecular signals are detected by specific receptor complexes at the astrocyte membrane, which activate several signaling cascades such as the JAK/STAT3 pathway, the NF-κB pathway, and the MAP kinase pathway (see also **Figure 1**). These pathways and their effectors interact either directly or indirectly, in the cytoplasm, in the nucleus, or on DNA promoter regions (see Section Additional Levels of Complexity). Recent studies support the idea that these cascades eventually converge on the JAK/STAT3 pathway, triggering a transcriptional program of reactivity in astrocytes. This program is modulated at several levels. (3) Disease-specific proteins (mHtt, mSOD1) endogenously expressed in astrocytes as well as internalized aggregated proteins (Aβ) can directly interfere with these signaling cascades or with transcriptional activity. (4) Several environmental factors may also affect the transcriptional program in reactive astrocytes, such as nuclear factors (other transcription factors, chromatin state) and environmental factors (age, sex). In the brain, dialog with other cell types or the specific brain regions involved is another potential level of modulation. These complex signaling cascades result in (5a) common features of astrocyte reactivity such as the upregulation of GFAP and cellular hypertrophy and (5b) disease-specific outcomes. This scheme illustrates how several signals can converge on a central signaling cascade that, in turn, is modulated in a disease- and environment-specific manner to produce a particular functional outcome.

(Bhalala et al., 2013). For example, the expression of particular miRNA increases in parallel with markers of reactivity, in the brains of patients and models of AD (Li et al., 2011) and in mouse astrocytes after spinal cord injury (Bhalala et al., 2012). Furthermore, miR145 reduces GFAP expression (Wang et al., 2015), whereas miR181 controls the expression of several cytokines in astrocytes (Hutchison et al., 2013). These miRNAs can also modulate signaling cascades including the NF-κB (Cui et al., 2010) and JAK/STAT pathways (Witte and Muljo, 2014). Overall, miRNAs, by regulating gene networks, add another level of control to astrocyte reactivity, which requires further investigation in ND.

The Effects of Mutant Proteins

Interestingly, mutant proteins involved in familial forms of ND may also interfere directly with intracellular cascades and thus affect signaling that reaches the nucleus (**Figure 3**). For example, wild-type Htt plays a role in NF-κB nuclear transport (Marcora and Kennedy, 2010) and mHtt impairs NF-κB signaling in astrocytes (Chou et al., 2008). In addition, mHtt interacts with the inhibitor of κB kinase (IKK) and inhibits IKK activity and NF-κB signaling (Khoshnan et al., 2004). Finally, ND are associated with dysfunction of the ubiquitin proteasome system (UPS, see Section Processing of Mutant Proteins), which is responsible for the degradation of IκB, the master inhibitor of

NF-κB (Oeckinghaus et al., 2011, **Figure 1**). JAK proteins can also be targeted to the UPS by SOCS3 (Kershaw et al., 2014). Alterations in the UPS may thus indirectly influence the activity of several signaling cascades within astrocytes.

In conclusion, astrocyte reactivity can be triggered by many extracellular or intracellular signals. Although several signaling pathways are activated in reactive astrocytes, they seem to converge on the JAK/STAT3 pathway (**Figure 3**). Other cascades such as the NF-kB pathway or CN may regulate, rather than induce, astrocyte reactivity in ND. These signaling pathways result in massive transcriptional changes that may affect many astrocyte functions.

What Do Reactive Astrocytes Do or Fail to Do during ND?

Insights from Cytokine-induced Astrocyte Reactivity

As a first attempt to elucidate the functional changes occurring in reactive astrocytes, cytokines and pro-inflammatory agents were overexpressed directly in the brain to induce reactivity. This was achieved by the injection of recombinant proteins, viral vector-mediated gene transfer or through transgenic mice overexpressing the protein of interest. Clearly, many functional changes are triggered by exposure to these molecules (Sofroniew, 2014). In addition to astrocytes, microglial cells also become activated and peripheral immune cells can be recruited within the brain parenchyma. Interestingly, reactivity can be selectively induced in astrocytes, leaving microglial cells virtually unaffected, by overexpressing the cytokine CNTF (Lavisse et al., 2012), or through the genetic ablation of β1-integrin in astrocytes (Robel et al., 2009). Such approaches have contributed to identify functional changes occurring in reactive astrocytes, including changes in glutamate homeostasis (Escartin et al., 2006; Beurrier et al., 2010), energy metabolism (Escartin et al., 2007; Carrillo-De Sauvage et al., 2015) and K^+ homeostasis (Seidel et al., 2014; Robel et al., 2015); see Liberto et al. (2004) for a general review.

More relevant to ND, experiments have also been performed with disease-causing agents like Aβ or mHtt to decipher the functional changes occurring in reactive astrocytes during ND.

Insights from Disease Models

In the following paragraphs, we will present several astrocyte functions that are known to be modified by reactivity, instead of describing each ND separately, to illustrate the existence of shared mechanisms between several ND.

Glutamate Homeostasis

Alteration of glutamate uptake is probably one of the best documented and earliest described dysfunction of astrocytes in ND (Maragakis and Rothstein, 2004; Soni et al., 2014). Indeed, astrocytes are responsible for most glutamate uptake at synapses, through transporters encoded by *excitatory amino acid transporter gene 1 and 2* (EAAT1 and 2, also called GLAST and GLT1 in rodents) (Danbolt, 2001). Inefficient glutamate uptake leads to over-stimulation of glutamate receptors, which causes excitotoxic cell death in neurons. Excitotoxicity is a well-described pathological mechanism in ND (Maragakis and Rothstein, 2004).

Pioneering work from the Rothstein laboratory showed that glutamate transport is impaired in synaptosomes from patients with ALS (Rothstein et al., 1992). EAAT2 protein levels are low in the spinal cord and motor cortex of patients with familial or sporadic ALS (Rothstein et al., 1995) and animal models expressing mSOD1 (Bendotti et al., 2001; Howland et al., 2002), even before neuronal loss (Howland et al., 2002).

EAAT2 mRNA (Arzberger et al., 1997) and protein (Faideau et al., 2010) levels are also decreased in the caudate and putamen of patients with HD, depending on the disease stage (Faideau et al., 2010). In the prefrontal cortex of patients with HD, the uptake of glutamate is significantly impaired (Hassel et al., 2008). Such alterations are reproduced in mouse and fly models of HD (Lievens et al., 2001, 2005). Importantly, selective expression of mHtt in striatal astrocytes is sufficient to reduce GLT-1 expression, alters glutamate uptake and is associated with the dysfunction of striatal neurons (Faideau et al., 2010) and motor abnormalities (Bradford et al., 2009). Thus, alteration of glutamate uptake in astrocytes contributes to the neuronal toxicity observed in HD.

Alteration of glutamate homeostasis is also thought to contribute to the pathogenesis of AD. Binding of [^{3}H] aspartate (a transportable analog of glutamate that does not bind to glutamate receptors) is reduced in the midfrontal cortex of patients with AD (Masliah et al., 1996). In a transgenic mouse model of AD, aspartate binding and glutamate transporter levels are lower than in WT littermates (Masliah et al., 2000). However, mRNA levels of glutamate transporters were unaffected in this model, suggesting that post-transcriptional modifications are involved. Indeed, in protein lysates from AD brains and Aβ-treated synaptosomes, EAAT2 is oxidized, which may impair its function (Lauderback et al., 2001). In addition, alternative EAAT2 splice variants with reduced glutamate transport capability (Scott et al., 2011) and abnormal detergent-insoluble EAAT2 (Woltjer et al., 2010) are found in vulnerable brain regions of AD patients. Finally, in brain slices, $A\beta_{1-42}$ treatment results in the internalization of GLT-1, which reduces glutamate clearance by astrocytes (Scimemi et al., 2013). Therefore, transcriptional, post-transcriptional and post-translational mechanisms account for the dysregulation of EAATs in AD.

The low expression and poor functionality of EAATs appears to be a truly universal feature of ND. Expression of the human tau protein under the GFAP promoter decreases EAAT expression in the brainstem and the spinal cord and impairs glutamate transport in synaptosomal preparations from the spinal cord (Dabir et al., 2006). The selective expression of α-synuclein^{A53T} in astrocytes also reduces GLT-1 levels in both pre-symptomatic and symptomatic mice and triggers the death of dopaminergic neurons in the SNpc (Gu et al., 2010).

Once taken up from the synaptic cleft by astrocytes, glutamate is metabolized into glutamine by GS. Glutamine is then transported back to neurons and used for the production of glutamate and GABA (Danbolt, 2001). GS expression is low in the temporal cortex of patients with AD (Le Prince et al., 1995) and

in the hippocampus of 3xTg-AD mice (Olabarria et al., 2011). GS mRNA levels are also lower in R6/2 mice (Lievens et al., 2001) and in BACHD mice (Boussicault et al., 2014) than in WT littermates. In the mouse hippocampus, the reduction in GS expression in reactive astrocytes triggers GABA depletion and neuronal hyper-excitability (Ortinski et al., 2010). Therefore, alterations of the glutamate-glutamine cycle may directly contribute to neuronal dysfunction in ND.

Altogether, it is well established that glutamate homeostasis is altered in ND, both in patients and animal models. In addition to its action on synaptic receptors, glutamate also serves as a metabolic signal to promote glucose uptake (Pellerin and Magistretti, 1994). Therefore, any alteration of glutamate homeostasis is likely to affect brain energy metabolism.

Energy Metabolism

Astrocytes are involved in complex metabolic interactions with neurons (Allaman et al., 2011). Their strategic location at the interface between intracerebral blood vessels and synapses make them ideally positioned to deliver neurons with blood-borne metabolic substrates, according to their energy needs (see Belanger et al., 2011, for review). It is still unclear how the morphological changes associated with reactivity affect blood vessels coverage and metabolite uptake by astrocytes. Several metabolic pathways such as the glutamate-glutamine cycle, cholesterol metabolism and glutathione production, are compartmentalized between neurons and astrocytes. This confers astrocytes with a pivotal regulatory role. Energy deficits are a common hallmark of various ND (Lin and Beal, 2006), suggesting that some metabolic interactions are altered when astrocytes become reactive in ND.

Glucose metabolism

Glucose is by far the preferred energy substrate for the brain. According to the astrocyte-to-neuron lactate shuttle hypothesis, in conditions of increased neuronal activity, more glucose is taken up by astrocytes and oxidized through glycolysis and redistributed to neurons in the form of lactate (Pellerin and Magistretti, 1994). Positron emission tomography (PET) imaging shows that cerebral glucose metabolism is impaired in HD and AD patients (Grafton et al., 1992; Fukuyama et al., 1994). However, it is not known whether such metabolic deficits originate from reactive astrocytes.

A comprehensive autoradiography analysis suggests that regional glucose metabolism is reorganized in aged BACHD mice (decreased glucose uptake in the striatum, increased in the hypothalamus). Neuron-astrocyte insert co-cultures were performed to identify the cellular origin of such deficits. They showed that expression of mHtt in astrocytes does not affect their own rate of glucose uptake. However, it impairs glucose uptake in neurons, regardless of their genotype, suggesting that HD astrocytes indirectly regulate neuronal metabolism by diffusible factors (Boussicault et al., 2014). In ALS, lactate was identified as one of the molecules that are released differently when astrocytes are reactive. $SOD1^{G93A}$ mice express lower levels of the astrocytic lactate transporter Slc16a4 than WT mice, which reduces lactate release in the spinal cord. Decreased lactate production is also observed in spinal astrocytes from familial ALS patients (Ferraiuolo et al., 2011), and may be deleterious to neurons relying on this metabolic supply.

Astrocyte metabolism can be studied by NMR on brain extracts after i.p. injection of ^{13}C-labeled acetate in animal models because this compound is metabolized preferentially by astrocytes (see Section Reactive Astrocytes as Biomarkers). Astrocytic "hyper-metabolism," characterized by high incorporation of ^{13}C into metabolic intermediates is observed in the brain of 7-month old 3xTg-AD mice (Sancheti et al., 2014) and in the cortex of a mouse model of a tauopathy (Nilsen et al., 2013). But opposite changes are observed in the frontal cortex in a rat model of AD (McGill-R-thy1-APP) (Nilsen et al., 2014). Also in favor of a decreased metabolic activity in reactive astrocytes, the transfer of glutamine to glutamate is reduced in 3xTg-AD mice (Sancheti et al., 2014). Similar conflicting effects of Aβ on astrocyte oxidative metabolism were reported in culture (see Allaman et al., 2010, and references therein). Overall, the metabolic changes occurring in reactive astrocytes during ND are quite contrasted, depending on the ND, the animal model and the stage of the disease considered.

Besides glucose uptake, many studies report mitochondrial dysfunction in ND (Lin and Beal, 2006). Some studies suggest that not only neurons display mitochondrial failure in ND, but reactive astrocytes too. Motori et al. performed an elegant imaging study of reactive astrocytes following stab wound injury. They reported that mitochondria undergo more fission events in reactive than in resting astrocytes (Motori et al., 2013). The exposure of pro-inflammatory cytokines had the same effect on mitochondria *in vitro* and resulted in impaired respiratory activity and reactive oxygen species (ROS) production (Motori et al., 2013). Transcriptomic analysis of astrocytes from AD patients indicates that mitochondrial genes, such as those involved in tricarboxylic acid cycle, are expressed at lower levels than in astrocytes of age-matched control individuals (Sekar et al., 2015). The exposure of astrocytes to Aβ reduces their mitochondrial membrane potential, which activates toxic enzymes such as poly (ADP-ribose) polymerase 1 and nicotinamide adenine dinucleotide phosphate (NADPH) oxidase, a potent pro-oxidant enzyme (Abeti et al., 2011). Similarly, mitochondrial respiration is altered in astrocytes isolated from the spinal cord of ALS rats, probably because of increased oxidative stress (Cassina et al., 2008). Therefore, although transient beneficial changes occur in reactive astrocytes during ND, overall, they display altered metabolism that may result in ROS production (see Section Antioxidants and ROS).

Cholesterol metabolism

Cholesterol, the most common steroid in humans, is a structural component of cell membranes and a precursor of steroid hormones. It also contributes to synapse formation and neuronal activity; therefore, defects in cholesterol homeostasis may have severe consequences on brain function (Pfrieger and Ungerer, 2011). Cholesterol synthesis and degradation are highly compartmentalized in astrocytes and neurons, respectively (Pfrieger and Ungerer, 2011). In particular, astrocytes express

high levels of apolipoprotein E (ApoE) that carries cholesterol to neurons (Bu, 2009).

The ε4 allele of the *ApoE* gene is the major risk factor for sporadic AD. It increases the probability of developing AD by a factor of 3–4 (Corder et al., 1993). ApoE influences the pathogenesis of AD at multiple levels, by regulating cholesterol metabolism, APP processing and Aβ clearance (Bu, 2009). ApoE is a chaperone for the binding of Aβ to the low density lipoprotein receptor or low density lipoprotein receptor-related protein 1 on astrocytes (Koistinaho et al., 2004). This is an important route for Aβ clearance (see Section Processing of Mutant Proteins). In astrocytes from aged APP/PS1dE9 mice, there is a widespread reduction in the expression of enzymes and transporters linked to cholesterol metabolism including ApoE, suggesting a decrease capacity to clear Aβ in these mice (Orre et al., 2014).

Cholesterol biosynthesis is low in the brain of several mouse models of HD (Valenza et al., 2010). In primary astrocytes from HD mice, mRNA levels of genes for cholesterol biogenesis and efflux are substantially lower than in control astrocytes. In addition, lower amounts of ApoE are secreted by HD *in vitro* and it forms smaller lipoprotein particles in the cerebrospinal fluid of HD mice (Valenza et al., 2010). The impairment in cholesterol biosynthesis correlates with the number of CAG repeats, the amount of mHtt (Leoni and Caccia, 2014) and is eventually toxic to HD neurons (Valenza et al., 2015).

Connexin-based networks of astrocytes

Astrocytes form multicellular networks connected by their gap junctions composed of connexins. These networks are involved in K^+ buffering but also deliver metabolic substrates to active synapses (Rouach et al., 2008).

The expression of astrocyte connexin (Cx) and astroglial coupling through gap junction channels is changed in reactive astrocytes in ND (Giaume et al., 2010). Cx43 expression is high in the caudate of HD patients (Vis et al., 1998) and around amyloid plaques in the cortex of AD patients (Nagy et al., 1996). Similarly, Cx43 expression is higher in the spinal cord of $SOD1^{G93A}$ mice (Cui et al., 2014), in two mouse models of AD (Mei et al., 2010) and in the MPTP model of PD (Rufer et al., 1996), than in their respective controls. Cx30 expression is also altered in ND models and patients, although the direction of the change is context dependent. Cx30 is expressed at low levels in the striatum of a rat and primate pharmacological model of PD (Charron et al., 2014) but is highly expressed in a mouse model of AD (Mei et al., 2010) and in AD patients (Nagy et al., 1996). However, in most cases, the functional effects on the astrocyte network and especially on metabolite trafficking was not assessed (Escartin and Rouach, 2013). Increased coupling may be beneficial for the delivery of metabolites. However, Cx also form hemichannels, through which several active molecules or gliotransmitters are released (Giaume et al., 2010; Bosch and Kielian, 2014). High Cx expression in reactive astrocytes in ND may thus lead to the excessive release of ATP or glutamate (Bosch and Kielian, 2014). This would maintain microglial cells in an active state and cause excitotoxicity in nearby neurons (see Section Release of Active Molecules and **Figure 4**).

Ion Homeostasis

Buffering of K^+

Astrocytes buffer K^+ by specific channels and transporters, which are enriched in PAP and vascular endfeet. The maintenance of K^+ homeostasis by astrocytes is essential for synaptic transmission and appears to be altered in ND. The mRNA expression of several K^+ channels is lower in astrocytes isolated from APP/PS1dE9 than from WT mice (Orre et al., 2014). Protein levels of Kir4.1, an inward rectifier K^+ channel, are decreased in the spinal cord of ALS mice (Kaiser et al., 2006) and in the striatum of R6/2 and zQ175 mice, two models of HD (Tong et al., 2014). Restoration of Kir4.1 levels through viral gene transfer in striatal astrocytes improves some of the neurological features in R6/2 mice (Tong et al., 2014). Importantly, astrocytes do not display the hallmarks of reactivity in these HD mice (see **Table 1**), suggesting that astrocytes can be dysfunctional before being "fully" reactive.

Ca^{2+} homeostasis

Several studies have reported alterations of Ca^{2+} homeostasis in reactive astrocytes in ND models, especially in AD (Vincent et al., 2010). Spontaneous Ca^{2+} transients are more frequent in slices from Tg2576 mice overexpressing APP than in controls (Pirttimaki et al., 2013). Hyperactive Ca^{2+} transients and waves can also be observed by two-photon live imaging with Ca^{2+} dyes in several mouse models of AD (Takano et al., 2007; Kuchibhotla et al., 2009; Delekate et al., 2014). Astrocytes from $SOD1^{G93A}$ ALS mice also display enhanced Ca^{2+} transients following stimulation of mGluR5 receptors (Martorana et al., 2012) or exposure to ATP (Kawamata et al., 2014). Store-operated accumulation of Ca^{2+} in the endoplasmic reticulum may be responsible for these altered Ca^{2+} responses (Kawamata et al., 2014).

Deregulation of Ca^{2+} in reactive astrocytes may elicit profound changes in various Ca^{2+}-dependent processes such as intracellular signaling cascades, proteolysis and gliotransmitter release.

Release of Active Molecules

Astrocytes interact with neighboring cells by releasing many molecules involved in cell-to-cell signaling, trophic support or antioxidant defense. The overall "secretome" of astrocytes is strongly altered by their reactivity (**Figure 4**). Some of these neuroactive molecules like glutamate, purines or GABA are neurotransmitters, and are thus called gliotransmitters when released by astrocytes (Araque et al., 2014).

Gliotransmitters

The release mode of gliotransmitters and their physiological relevance is a matter of intense debate (Araque et al., 2014; Sloan and Barres, 2014). The study of gliotransmission *in situ* is particularly difficult because most of these molecules are also released by neurons.

Glutamate is one of the best studied gliotransmitters. FRET-based imaging shows that cultured astrocytes release glutamate in response to recombinant Aβ1–42 or Aβ isolated from the brain of AD patients. This phenomenon is Ca^{2+}-dependent and is deleterious to neighboring neurons (Talantova et al., 2013). Glutamate release elicited by mechanical stimulation is more

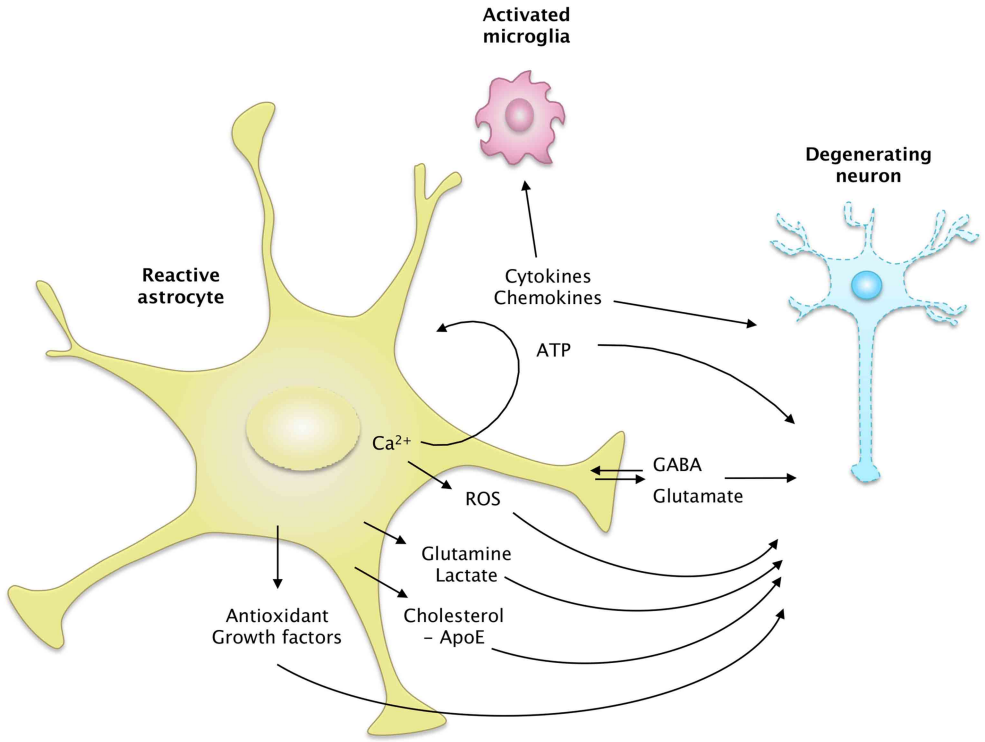

FIGURE 4 | The secretome of reactive astrocytes. Astrocytes secrete many active molecules that influence neuronal survival and synaptic activity. Reactivity affects the pattern of secreted molecules, and thus alters neuron-astrocyte communications. In ND, reactive astrocytes may secrete higher levels of antioxidants, such as glutathione and its precursors or metabolic substrates. These changes would promote neuron survival. However, reactive astrocytes may also release fewer trophic molecules such as cholesterol, growth factors or glutamine and produce more ROS than resting astrocytes. The regulation of glutamate and GABA homeostasis may also be altered by reactivity, due to a change in their release but also their uptake. Intracellular Ca^{2+} levels are deregulated in ND, which may stimulate the release of gliotransmitters such as glutamate and ATP. Reactive astrocytes also produce more cytokines, which activate microglial cells or act as paracrine factors, maintaining glial cells in a chronically reactive state.

important in cortical astrocytes isolated from BACHD mice than in their WT counterparts (Lee et al., 2013). Interestingly, the cytokine TNFα plays many regulatory roles at the excitatory synapse; it directly scales synaptic transmission and potentiates glutamate release by astrocytes (see Santello and Volterra, 2012, for review). TNFα levels are elevated in patients and animal models of ND (see Section Cytokines and Inflammatory Molecules), which may stimulate the non-physiological release of glutamate by reactive astrocytes. Unexpectedly, glutamate release in response to TNFα is impaired in hippocampal slices from AD mice harboring numerous Aβ plaques and reactive astrocytes (Rossi et al., 2005). The authors hypothesized that the intracellular cascades downstream from the TNFα receptor were altered in reactive astrocytes in this model (Rossi et al., 2005). Overall, additional studies are still needed, especially *in vivo*, to determine precisely how the release of glutamate by reactive astrocytes is changed in ND, and how it modulates synaptic transmission (Agulhon et al., 2012).

GABA is yet another gliotransmitter that was recently implicated in ND. Reactive astrocytes release more GABA than resting astrocytes, which contributes to cognitive impairment in two mouse models of AD (Jo et al., 2014; Wu et al., 2014). Excessive GABA released by reactive astrocytes results in the tonic inhibition of dentate gyrus granule cells in the hippocampus of AD mice. Inhibition of GABA synthesis or pharmacological blockade of GABA transporters restores synaptic plasticity and memory deficits in these mice (Jo et al., 2014; Wu et al., 2014). By contrast, GABA release by astrocytes appears to be defective in HD. Electrophysiological recordings on slices show that both $GABA_A$ (postsynaptic) and $GABA_B$ (presynaptic) currents are lower in R6/2 and zQ175 mice than in control mice. This results in a lower GABA-mediated tonic inhibition of striatal neurons. Pharmacological manipulation of the GABA transporter-3 (GAT-3), which is preferentially expressed by astrocytes, suggests that HD astrocytes have an impaired capacity to release GABA through GAT-3 (Wojtowicz et al., 2013).

Purines are another class of gliotransmitters, comprising ATP and its metabolite adenosine, which is generated extracellularly by ectonucleotidases. Stimulation of primary astrocyte cultures with Aβ induces the release of ATP (Jung et al., 2012) via Cx43 hemichannels (Orellana et al., 2011). Recently, it was shown that reactive astrocytes around amyloid plaques in the cortex of APPPS1 mice release more ATP via hemichannels than their WT counterparts. ATP, degraded into adenosine, acts as an autocrine signal on astrocyte P2Y1 receptors and elicits Ca^{2+} hyperactivity (Delekate et al., 2014). Cultured astrocytes from SOD^{G93A} mice

also release more ATP than those from WT mice, which is toxic to co-cultured motor neurons (Kawamata et al., 2014).

Cytokines and inflammatory molecules

The levels of pro-inflammatory cytokines are higher in vulnerable brain regions and in the cerebrospinal fluid in ND patients than in healthy individuals (Lucin and Wyss-Coray, 2009; Heneka et al., 2014). However, many cell-types such as activated microglia or peripheral immune cells may produce these molecules. Transcriptional analysis performed on laser-captured $GFAP^+$ reactive astrocytes from APP/PS1dE9 mice reveal that these cells express high levels of several cytokines (Orre et al., 2014). The number of genes induced and the fold-increase in expression are higher in astrocytes than in microglial cells, showing that reactive astrocytes may contribute significantly to the production of cytokines during AD. However, the absolute expression level of these cytokines remains lower in reactive astrocytes than in microglia. Some of these cytokines act as recruiting signals for peripheral immune cells or promote BBB permeability (Farina et al., 2007; Sofroniew, 2015). In ALS, a major increase in the transcription of inflammatory molecules is well established, including in astrocytes derived from both familial and sporadic forms of the disease (Haidet-Phillips et al., 2011). These astrocytes are toxic to motor neurons in co-culture systems.

In microglia, the maturation of some cytokines like IL-1β is operated in the cytosol by the inflammasome. Aβ phagocytosis activates the NOD-like receptor protein (NLRP) 3 inflammasome in these cells (Halle et al., 2008), thereby linking the internalization of pathologic proteins with the release of pro-inflammatory cytokines in ND. Only two recent studies suggest that in astrocytes, stimulation of the inflammasome also triggers IL-1β production (Minkiewicz et al., 2013; Zeis et al., 2015).

Finally, reactive astrocytes overexpress molecules of the complement system in AD mice (Orre et al., 2014), which can alter dendrite morphology, Ca^{2+} homeostasis and excitatory synaptic responses in neurons, at least *in vitro* (Lian et al., 2015). In AD and HD patients, components of the complement system are overexpressed (Singhrao et al., 1999; Lian et al., 2015); however they are not necessarily produced by astrocytes only.

Trophic factors

Astrocytes secrete various factors exhibiting trophic effects on neurons, such as growth factors (e.g., CNTF, brain-derived neurotrophic factor [BDNF], nerve growth factor [NGF], FGF), neurosteroids, and adhesion molecules involved in neurite outgrowth (Muller et al., 1995; Sofroniew and Vinters, 2010). Inadequate synthesis and release of such factors may contribute to neuronal toxicity observed in HD. The expression of mHtt in primary cultures of cortical astrocytes impairs BDNF production in astrocytes. Levels of mature BDNF in the medium are thus low under these conditions, which limits neurite development of primary cortical neurons (Wang et al., 2012). Similarly, transcription and release of the chemokine (C-C motif) ligand 5 (CCL5/RANTES), which promotes neurite outgrowth and neuronal survival, is also impaired by the expression of mHtt in cultured astrocytes (Chou et al., 2008). CCL5/RANTES accumulates in the cytosol of astrocytes in HD patients and in two mouse models of HD (Chou et al., 2008). Although reactive astrocytes secrete more trophic factors such as NGF in ALS rodent models and patients (Pehar et al., 2004; Ferraiuolo et al., 2011), it may nonetheless have unexpected detrimental consequences on nearby neurons. Indeed, vulnerable motor neurons in ALS express the specific p75 neurotrophin receptor isoform, and its stimulation by NGF triggers apoptosis instead of trophic actions (Pehar et al., 2004).

Antioxidants and ROS

Astrocytes are important for defense against ROS because they express many detoxifying enzymes and transporters (Vargas and Johnson, 2009; Allaman et al., 2011). They produce high levels of antioxidants for neurons, including ascorbic acid (AA, also known as vitamin C), glutathione and its precursors. The antioxidant action of astrocytes is crucial for neurons, because oxidative respiration produces high levels of ROS. Indeed, oxidative stress contributes to neuronal dysfunction in several ND (Belanger et al., 2011). The expression of many detoxifying enzymes and transporters are controlled by the master regulator NF-E2 related factor-2 (Nrf2), a transcription factor which translocates to the nucleus and binds specific promoter sequences in response to oxidative stress (Vargas and Johnson, 2009). Reactive astrocytes found in the spinal cord of early symptomatic ALS rats show high levels of Nrf2 expression and nuclear translocation (Vargas et al., 2005). Although high Nrf2 activity may be beneficial for neurons exposed to oxidative stress, this endogenous antioxidant response does not offer sufficient protection. Indeed, Nrf2 activity can be further enhanced in astrocytes by genetic manipulation, which improves disease outcome in animal models of ALS (Vargas et al., 2008), PD (Chen et al., 2009; Gan et al., 2012), and HD (Calkins et al., 2010).

The release of AA by astrocytes is altered in HD (Rebec, 2013). In the R6/2 mouse model of HD, extracellular AA levels are lower than in age-matched WT mice but only during behavioral activity (Rebec et al., 2002). Accordingly, mHtt expression in astrocytes (and not in neurons) is sufficient to trigger oxidative stress in neurons by diffusible factors (Boussicault et al., 2014). In fact, reactive astrocytes may not only produce fewer antioxidant molecules during ND, they may also release more pro-oxidant factors. Exposure to Aβ stimulates the pentose phosphate pathway in astrocytes *in vitro*; yet they release more ROS than in control conditions and are toxic to co-cultured neurons even without physical contact (Allaman et al., 2010). Furthermore, reactive astrocytes overexpress inducible NO synthase (NOS), including in the brain of AD patients (Heneka et al., 2014). Aβ peptides also cause a loss of mitochondrial membrane potential in astrocytes, which is associated with the activation of NADPH oxidase and excessive ROS production (Abramov et al., 2004). Accordingly, mitochondria from mSOD1 astrocytes produce large amounts of superoxide radicals, causing motor neuron death in co-culture, which is prevented by pre-incubation with antioxidants and NOS inhibitors (Cassina et al., 2008). Similarly, rodent astrocytes expressing a mutant form of TDP43 induce nitrosative stress in motoneurons and kill them (Rojas et al., 2014). Overall, ROS production by reactive astrocytes exposed

to toxic or mutant disease-specific proteins seems to be another deleterious mechanism common to several ND.

Processing of Mutant Proteins

Aggregation of intra- or extra-cellular misfolded proteins is a central feature of ND. However, the exact role of aggregate formation is still debated. Soluble forms of mutant proteins are now considered to be the most toxic forms, and their aggregation may be instead a protective mechanism that prevents them from interfering with important intracellular partners (Ross and Poirier, 2004).

Misfolded proteins are degraded by two major intracellular pathways: autophagy and the UPS. Autophagy involves the formation of intra-cytoplasmic vesicles that may also envelop organelles. Engulfed elements are completely degraded by proteases such as cathepsins after fusion with a lysosome. Alternatively, the UPS forms a protease complex to which proteins are addressed by specific ubiquitin tags. Both pathways are altered in ND (Dantuma and Bott, 2014; Ghavami et al., 2014).

The UPS has been extensively studied in neurons in models of ND and is even a target of neuroprotection (Margulis and Finkbeiner, 2014; Popovic et al., 2014). Much less is known about the UPS in astrocytes (Jansen et al., 2014). Protein aggregates are mainly found in neurons, suggesting that astrocytes are more efficient than neurons at handling toxic proteins (Jansen et al., 2014). Indeed, a study based on a reporter system showed that the UPS is more active in glial cells than in neurons *in vitro* and *in vivo* (Tydlacka et al., 2008). During ND, the UPS in astrocytes may become less efficient than in healthy conditions because UPS subunits are down-regulated in astrocytes from AD patients (Simpson et al., 2011). In addition, during ND, reactive astrocytes may express a specific form of the proteasome, called the immunoproteasome, which is formed by the cytokine-inducible subunits β1i, β2i, and β5i. The immunoproteasome is detected in reactive astrocytes around amyloid plaques in AD patients and APP/PS1dE9 mice (Orre et al., 2013) and in the spinal cord of SOD^{G93A} mice (Puttaparthi and Elliott, 2005). The immunoproteasome is involved in antigen presentation (Jansen et al., 2014), but its functional role in reactive astrocytes during ND is not yet known. Invalidation of the B1i subunit of the immunoproteaseome does not influence disease outcome in SOD^{G93A} mice (Puttaparthi et al., 2007).

In AD, reactive astrocytes play yet another role in the clearance of extracellular Aβ. More than a decade ago, it was shown that astrocytes are able to internalize amyloid plaques and Aβ peptides (Funato et al., 1998; Nagele et al., 2003; Wyss-Coray et al., 2003). They do so by phagocytosis or by internalizing Aβ bound to membrane receptors, including ApoE receptors (Koistinaho et al., 2004; Thal, 2012, see Section Cholesterol Metabolism). The astrocytic protein ApoE also promotes Aβ extrusion through the BBB or along the perivascular space (Bu, 2009, and see Section Cholesterol Metabolism). Intracellular vesicles containing Aβ are addressed to lysosomes for degradation and the enhancement of lysosomal biogenesis selectively in astrocytes attenuates amyloid-related disease in a mouse model of AD (Xiao et al., 2014).

Aβ may also be degraded extracellularly, and astrocytes produce some Aβ-degrading enzymes such as insulin-degrading enzyme (IDE), neprilysin or matrix metalloproteinase 2 and 9 (MMP9). Neprilysin and IDE are overexpressed in reactive astrocytes in contact with plaques in AD brains (Apelt et al., 2003; Dorfman et al., 2010) and MMP9 is overexpressed in mouse models of AD (Yan et al., 2006). However, reactive astrocytes may eventually become overwhelmed as the disease progresses because they undergo cell lysis and form extracellular deposits containing neuronal-derived Aβ peptides (Nagele et al., 2003).

Alternatively, it was suggested that reactive astrocytes may contribute to Aβ production by overexpressing β-site APP cleaving enzyme 1 (BACE1), the rate limiting enzyme for Aβ production. Strong BACE1 expression is observed in reactive astrocytes in patients and several mouse models of AD, and following exposure to pro-inflammatory cytokines, which can directly activate the BACE1 promoter (Cole and Vassar, 2007). However, it is unknown how the amount of Aβ produced by astrocytes compares with the large pool of Aβ generated by neurons.

Regarding HD, we found that blocking astrocyte reactivity by overexpressing SOCS3 significantly promoted the formation of mHtt aggregates in the mouse striatum (Ben Haim et al., 2015). A recent study performed in *Drosophila* also reported that reactive glia are able to phagocyte mHtt expressed in neurons (Pearce et al., 2015). These results suggest that reactive astrocytes may participate in the processing of mHtt and its aggregation in neurons, but the exact molecular mechanisms need to be established.

How Do Reactive Astrocytes Globally Contribute to ND?

We have seen that many changes occur in astrocytes during ND, which makes it extremely difficult to get a clear view of their impact on the disease. In addition, the reactive status of astrocytes is not always directly reported in studies. Therefore, to evaluate the overall contribution of reactive astrocytes to ND, experimental designs that interfere with astrocyte reactivity provide a valuable insight into this difficult question (**Table 3**).

Intermediate Filament KO

Given that the upregulation of IF is a hallmark of astrocyte reactivity, transgenic mice knockout (KO) for GFAP or Vim or double KO were initially generated and tested in acute injuries. Disruption of reactive astrocyte cytoskeleton was also studied in ND models and was found to shorten the lifespan of the $SOD1^{H46R}$ mouse model of ALS (Yoshii et al., 2011). Studies involving the genetic ablation of GFAP and vimentin in APP/PS1dE9 mice gave conflicting results, with one reporting increased amyloid load and dystrophic neurites (Kraft et al., 2013), and another showing no effect on amyloid load in the cortex (Kamphuis et al., 2015). However, knocking out IF affects several basal functions in astrocytes (Shibuki et al., 1996) and results in many transcriptional changes (Kamphuis et al., 2015).

TABLE 3 | Main genetic approaches to block reactive astrocytes in mouse models of ND.

Approach	Construct	ND	ND model	Effect on astrocyte reactivity	Effects on disease outcomes	References
Disruption of cytoskeleton in reactive astrocytes	gfap$^{-/-}$	ALS	SOD1^{H46R} mice	No change in vimentin protein levels No data on astrocyte morphology	Shorter lifespan No effect on motor symptoms	Yoshii et al., 2011
	gfap$^{-/-}$ vimentin$^{-/-}$	AD	APP/PS1dE9 mice	Lower astrocyte hypertrophy	Higher amyloid load More dystrophic neurites	Kraft et al., 2013
					No effect on amyloid load	Kamphuis et al., 2015
Ablation of proliferating astrocytes	gfap-tk	ALS	SOD1^{G93A}	No change in the number of GFAP^{+} cells in the ventral SC No data on astrocyte morphology	No effect on survival, disease onset, duration No effect on motor function No effect on neuronal loss	Lepore et al., 2008a
Inhibition of the JAK/STAT3 pathway	lenti-socs3	HD	Lenti-Htt82Q	Lower GFAP and vimentin expression (mRNA and protein) Resting-like morphology	No effect on neuronal loss More mHtt aggregates	Ben Haim et al., 2015
Inhibition of the NF-kB pathway	hGFAP-Cre x IKKβ $^{fl/fl}$	ALS	SOD1^{G93A} mice	No data on astrocyte phenotype	No effect on survival No effect on motor performances	Frakes et al., 2014
	AAV-IκBα-SR	ALS	SOD1^{G93A} mice	No data on astrocyte phenotype	No effect on survival No effect on motor performances No effect on neuron survival *in vitro*	Frakes et al., 2014
	hGFAP-IκBα-DR	ALS	SOD1^{G93A} mice	Temporary lower number of GFAP^{+} cells (at disease onset)	No effect on survival No effect on motor performances	Crosio et al., 2011
	lenti-DN-IKKγ	HD	R6/2 mice	No data on astrocyte phenotype	Improved motor and cognitive deficits, Less severe MSN atrophy	Hsiao et al., 2013
Inhibition of CN/NFAT signaling	AAV-VIVIT	AD	APP/PS1dE9	Trend of lower GFAP levels (protein) Reduced astrocyte hypertrophy	Improved cognitive deficits Improved synaptic transmission Lower amyloid load	Furman et al., 2012
Constitutive activation of CN	mGFAP-caCN	AD	APP/PS1	Fewer GFAP^{+} cells Lower GFAP levels (protein and mRNA) Reduced astrocyte hypertrophy around plaques	Reduced cognitive deficits Lower amyloid load	Fernandez et al., 2012

Abbreviations: AAV, adeno-associated viral vector; caCN, constitutively active form of calcineurin; DN, dominant negative; IκBα, nuclear factor of kappa light polypeptide gene enhancer in B-cells inhibitor alpha; IKKβ, IκBα kinase alpha; MSN, medium-sized spiny neurons; SC, spinal cord; SR, super repressor; tk, thymidine kinase; DR, degradation resistant.

Upregulation of IF is only a hallmark of reactivity; therefore, their removal from astrocytes will not necessarily block other molecular cascades associated with reactivity.

Ablation of Proliferative Astrocytes

Another strategy developed to evaluate the contribution of reactive astrocytes to CNS injury is the ablation of proliferating astrocytes. This approach involves the expression of the viral enzyme thymidine kinase (TK) under the GFAP promoter, in presence of the drug ganciclovir (Bush et al., 1999). Ganciclovir is metabolized by TK-expressing cells into a base analog that blocks DNA replication, thus inducing the death of proliferating cells. This system has been extensively used to evaluate the effects of glial scar formation in acute injury models (Sofroniew, 2009). These studies demonstrate that glial scar-forming astrocytes act as a barrier to limit immune cell extravasation in the CNS parenchyma. However, in the progressive SOD1^{G93A} mouse model of ALS, ablation of proliferating astrocytes has no effect on disease outcomes (Lepore et al., 2008a), probably because of the small number of proliferating astrocytes in this model (see Section Do Reactive Astrocytes Proliferate in ND?).

Manipulation of Intracellular Signaling Pathways

A third strategy to study reactive astrocytes is to block intracellular signaling pathways controlling reactivity.

The JAK/STAT3 Pathway

Several transgenic mice have been generated to block the JAK/STAT3 pathway in reactive astrocytes. They are based on the conditional KO of STAT3 following the expression of the Cre recombinase under the GFAP or nestin promoter (Okada et al., 2006; Herrmann et al., 2008). Most of these studies have focused on acute injuries with glial scar formation and found that reactive astrocytes mainly exert beneficial functions. By contrast, few studies have investigated the contribution of the JAK/STAT3 pathway in reactive astrocytes in ND, using pharmacological or viral-based approaches. In the MPTP mouse model of PD, pharmacological inhibition of JAK2 reduces astrocyte reactivity. However, this inhibitor does not influence tyrosine hydroxylase levels in the striatum, suggesting that reactive astrocytes do not contribute to dopaminergic loss in this model (Sriram et al., 2004). In a mouse model of HD, viral-mediated overexpression of SOCS3 in reactive astrocytes did not influence neuronal death but promoted the formation of mHtt aggregates (Ben Haim et al., 2015). This intriguing result suggests that reactive astrocytes affect the processing and aggregation of mHtt, which is key pathological mechanism in HD (see Section Processing of Mutant Proteins).

The NF-κB Pathway

In ALS, two independent studies reported that inhibition of the NF-κB pathway in reactive astrocytes does not influence disease phenotype in $SOD1^{G93A}$ mice (Crosio et al., 2011; Frakes et al., 2014). To block this pathway in astrocytes, Frakes et al. crossed mice KO for IKKβ in astrocytes ($GFAP\text{-}Ikkb^{fl/fl}$) with $SOD1^{G93A}$ mice or they overexpressed a dominant negative form of IκBα (AAV-IκB-SR) in astrocytes by viral gene transfer. The inhibition of the NF-κB pathway in reactive astrocytes did not influence motor neuron survival in culture or in the spinal cord of $SOD1^{G93A}$ mice (Frakes et al., 2014), probably because this pathway is mainly active in microglia.

The role of the NF-κB pathway in reactive astrocytes has also been studied in HD. A dominant negative form of IKKγ (DN-IKKγ) was overexpressed by lentiviral gene transfer in the striatum of R6/2 mice to block NF-κB signaling. DN-IKKγ overexpression improved motor performance and prevented shrinkage of striatal neurons in HD mice (Hsiao et al., 2013). However, DN-IKKγ expression was not restricted to astrocytes and may thus have acted in other cell types such as microglia.

The CN/NFAT Pathway

CN is activated upon inflammatory stimulation and regulates gene expression through the transcription factors NFATs and NF-κB (Furman and Norris, 2014). Expression of caCN in astrocytes of APP/PS1 mice reduces astrocyte reactivity, Aβ levels and the number of amyloid plaques. These effects are associated with improved cognitive functions (Fernandez et al., 2012). The beneficial effects of CN are mediated by the inhibition of the NF-κB pathway and subsequent production of pro-inflammatory cytokines (Fernandez et al., 2012). Viral-mediated gene transfer of the blocking peptide VIVIT was used to inhibit NFAT signaling in hippocampal astrocytes in APP/PS1dE9 mice (Furman et al., 2012). VIVIT limited astrocyte hypertrophy, prevented the accumulation of Aβ and improved synaptic plasticity and cognitive functions in AD mice (Furman et al., 2012). These results suggest that reactive astrocytes play detrimental roles in AD. However, VIVIT may be secreted by infected astrocytes; therefore, it is not possible to exclude the involvement of other cell types, especially because CN is permanently activated in neurons in the Tg2576 mouse model of AD (D'Amelio et al., 2011).

In conclusion, several approaches have been used to determine the contribution of reactive astrocytes to ND progression. The overall picture is still unclear because reactive astrocytes have been shown to be beneficial, detrimental or to have no effect, depending on the experimental approach chosen, the molecular target (e.g., IF, signaling cascades) and the disease model (**Table 3**). Some of these approaches rely on pharmacological inhibitors or transgenic mice lacking cell-type specificity or that might involve developmental effects (with non-inducible Cre expression for example). To better delineate the roles of reactive astrocytes in ND, it will be interesting to target pivotal signaling cascades and to use cell-type specific and versatile tools like viral vectors to interfere with astrocyte reactivity in different ND models.

Ongoing Questions, Future Directions

Heterogeneity of Reactive Astrocytes

One of the next challenges in the field is to deal with the functional heterogeneity of astrocytes. Indeed, like neurons, astrocytes display remarkable heterogeneity regarding their density, morphology (Emsley and Macklis, 2006), transcriptional profile (Bachoo et al., 2004), and expression of transporters, channels, receptors and transcription factors (Matyash and Kettenmann, 2010). Astrocyte reactivity is also quite heterogeneous both between and within brain regions (Anderson et al., 2014). Such heterogeneity is best explored in acute injury models, because injury can be inflicted in different brain regions. In the spinal cord for example, astrocytes from the ventral horn do not migrate into a dorsal stab wound, even for very close lesions (Tsai et al., 2012). Even within the same sub-region of the mouse cerebral cortex, astrocytes respond heterogeneously to stab wound injury. A very elegant study based on live two-photon microscopy demonstrated that almost all astrocytes become hypertrophic and overexpress GFAP following injury; however, some had their processes polarized toward the lesion, others proliferated (less than 15%), and some remain static (Bardehle et al., 2013). In ND, reactive astrocytes in contact with plaques have a more pronounced reactive morphology than those at a distance, which correlates with larger transcriptional changes (Orre et al., 2014). In the 3xTg-AD model of AD, astrocytes at distance from plaques may even be atrophic (Olabarria et al., 2010). Overall, the heterogeneity of reactive astrocytes at the regional, sub-regional and cellular level needs to be thoroughly investigated in animal models and patients taking advantage

of modern techniques such as two-photon microscopy and cell-specific transcriptomic analysis. Indeed, it remains unclear how such heterogeneity is established during development or disease and how it contributes to the local vulnerability of neighboring neurons in ND (Molofsky et al., 2012).

Reactive Astrocytes in the Clinics

Reactive Astrocytes as Biomarkers

Given that astrocytes are able to sense even mild neuronal dysfunction and to become reactive, they represent attractive biomarkers for the diagnosis and monitoring of ND. Reactive astrocytes can be imaged in brain slices or in living mice by the expression of a reporter gene (GFP, luciferase) under the control of the GFAP promoter (see O'Brien et al., 2013, for a complete review). For clinical applications, non-invasive image techniques to monitor reactive astrocytes are still under development.

PET provides a way to quantify neuroinflammation through radiolabeled tracers that bind to glial cells. The most common target for neuroinflammation is the peripheral benzodiazepine receptor or translocator protein 18 kDa (TSPO) (see Chauveau et al., 2008). Activated microglia express high levels of TSPO but, as recently demonstrated, reactive astrocytes also overexpress this protein (Lavisse et al., 2012). Therefore, TSPO radioligands do not discriminate between reactive microglia and reactive astrocytes, but they are nonetheless a valuable imaging approach to identify early neuroinflammation in ND patients (Venneti et al., 2006). Radiotracers that target astrocyte metabolism, such as [1-^{11}C]-octanoate (Kuge et al., 2000) and [2-^{18}F]-fluoroacetate (Marik et al., 2009) have also been evaluated in models of glioblastoma and ischemia. It remains to be established whether they can detect progressive astrocyte reactivity in ND patients. Another molecular target is monoamine oxidase B (MAO-B), which is highly expressed in reactive astrocytes. The binding of ^{11}C-DED, a MAO-B radioligand is high in patients with ALS (Johansson et al., 2007), and patients with mild cognitive impairment or AD (Carter et al., 2012). However, this enzyme is also found in serotonergic neurons, which could contribute to this signal. Overall, new PET radiotracers with higher specificity for reactive astrocytes are needed and recent transcriptomic studies on reactive astrocytes may help to identify new targets.

Nuclear magnetic resonance (NMR) techniques are an attractive alternative to monitor astrocyte reactivity *in situ*. Increased T1 relaxation time is observed by magnetic resonance imaging (MRI) in acute models of ischemia and excitotoxicity. Arundic acid, an inhibitor of astrocyte reactivity, normalizes it, but the molecular basis for such changes in NMR signals is unclear (Sibson et al., 2008). NMR-spectroscopy (MRS) allows the quantification of abundant brain metabolites, including myo-inositol, glutamine and choline which are enriched in glial cells. In a model of selective astrocyte reactivity in the rat brain, myo-inositol and choline levels are higher whereas glutamine levels are lower than in controls, suggesting that reactivity leads to the complex re-structuring of metabolic pathways (Carrillo-De Sauvage et al., 2015). High concentrations of myo-inositol are also commonly observed in ND models and patients, which correlates with neuroinflammation (Choi et al., 2007). However, the exact contribution of reactive astrocytes to these NMR signals is unknown because of the concomitant activation of microglial cells or other pathological events in ND.

More cellular selectivity may be achieved by MRS techniques after the infusion of ^{13}C-labeled metabolic substrates such as glucose or acetate. Indeed, acetate is preferentially oxidized by astrocytes and its metabolic fate can be monitored by MRS (De Graaf et al., 2011). Furthermore, the rate of astrocytic tricarboxylic acid cycle and of the glutamate/glutamine cycle can be estimated by modeling (Lebon et al., 2002). ^{13}C-acetate injection coupled with *ex vivo* MRS analysis was performed recently in several rodent models of AD (see Section Cholesterol Metabolism). ^{13}C-MRS may be translated to the clinics although it remains quite an expensive and sophisticated approach (Ross et al., 2003).

Reactive Astrocytes as Therapeutic Targets

The above-mentioned changes in reactive astrocytes make these cells alternative or complementary therapeutic targets to neurons for ND (Escartin and Bonvento, 2008). For example, strategies enhancing glutamate uptake in astrocytes may prevent excitotoxicity, which is common to all ND (Soni et al., 2014). High-throughput screening identified β-lactam antibiotics as potent inducers of glutamate uptake by astrocytes (Rothstein et al., 2005). The β-lactam antibiotic ceftriaxone is neuroprotective *in vitro* and *in vivo* in models of ALS (Rothstein et al., 2005) and HD (Miller et al., 2008). A phase I clinical trial with ceftriaxone in ALS patients gave promising results, but they were not confirmed in the phase II-III stage (Cudkowicz et al., 2014). Another astrocyte-based therapeutic strategy involves grafting astrocyte progenitors close to vulnerable neurons to provide them with global support (Lepore et al., 2008b). Interestingly, some pharmacological agents tested or used in clinics to target neurons may also affect astrocyte functions. Indeed, neurons and astrocytes share many membrane receptors, transporters and signaling pathways. For example, activators of the Nrf2 pathway like curcumin may enhance antioxidant defense in the brain by acting within astrocytes (Vargas and Johnson, 2009).

Therapeutic strategies tested so far for ND have largely focused on neurons and have been mostly unsuccessful to date (Huang and Mucke, 2012; Wild and Tabrizi, 2014). Only symptomatic treatments are offered to patients and their efficacy of some decreases with disease progression (e.g., acetylcholine esterase inhibitors for AD, L-DOPA supplementation for PD). No treatment truly prevents neurons from degenerating. In light of their many actions on neurons, strategies targeting reactive astrocytes may effectively sustain neuronal function and hence survival during ND. However, given the complex changes that occur in reactive astrocytes during ND, complete ablation of astrocyte reactivity may be counterproductive because these cells also display beneficial adaptative changes during disease. Identifying the complex interplay between shared intracellular pathways mediating reactivity and disease specific signals may enable the design of selective therapeutic cocktails to engage reactive astrocytes in protective actions (**Figure 3**).

Conclusions

Overall, this review illustrates the multifaceted and complex roles of reactive astrocytes during ND. Astrocyte reactivity appears as a conserved response that is initially beneficial but is later corrupted by disease-specific alterations. Huge progress has been made recently as a result of the heightened interest in glial cells, and the development of innovative and cell type-specific approaches. However, these cells remain enigmatic, and many aspects of their physiology need to be clarified. Although the molecular pathways leading to astrocyte reactivity during ND have been described, it is crucial to elucidate what disease-, region- and environmental-specific mechanisms control the functional outcomes associated with astrocyte reactivity (**Figure 3**). In any case, considering reactive astrocytes as key partners in neuronal dialog during ND opens new avenues for neuroscience and biomedical research.

Acknowledgments

CE is supported by French National Research Agency Grants 2010-JCJC-1402-1 and 2011-BSV4-021-03, CEA, and CNRS. LB and KC are recipients of a PhD fellowship from the Atomic Energy and Alternative Energies Commission (Irtelis program). We apologize for not being able to cite all original studies relevant to this review, due to space limitations.

References

Abdul, H. M., Sama, M. A., Furman, J. L., Mathis, D. M., Beckett, T. L., Weidner, A. M., et al. (2009). Cognitive decline in Alzheimer's disease is associated with selective changes in calcineurin/NFAT signaling. *J. Neurosci.* 29, 12957–12969. doi: 10.1523/JNEUROSCI.1064-09.2009

Abeti, R., Abramov, A. Y., and Duchen, M. R. (2011). Beta-amyloid activates PARP causing astrocytic metabolic failure and neuronal death. *Brain* 134, 1658–1672. doi: 10.1093/brain/awr104

Abramov, A. Y., Canevari, L., and Duchen, M. R. (2004). Beta-amyloid peptides induce mitochondrial dysfunction and oxidative stress in astrocytes and death of neurons through activation of NADPH oxidase. *J. Neurosci.* 24, 565–575. doi: 10.1523/JNEUROSCI.4042-03.2004

Agid, Y. (1991). Parkinson's disease: pathophysiology. *Lancet* 337, 1321–1324. doi: 10.1016/0140-6736(91)92989-F

Agulhon, C., Sun, M. Y., Murphy, T., Myers, T., Lauderdale, K., and Fiacco, T. A. (2012). Calcium signaling and gliotransmission in normal vs. reactive astrocytes. *Front. Pharmacol.* 3:139. doi: 10.3389/fphar.2012.00139

Allaman, I., Belanger, M., and Magistretti, P. J. (2011). Astrocyte-neuron metabolic relationships: for better and for worse. *Trends Neurosci.* 34, 76–87. doi: 10.1016/j.tins.2010.12.001

Allaman, I., Gavillet, M., Belanger, M., Laroche, T., Viertl, D., Lashuel, H. A., et al. (2010). Amyloid-beta aggregates cause alterations of astrocytic metabolic phenotype: impact on neuronal viability. *J. Neurosci.* 30, 3326–3338. doi: 10.1523/JNEUROSCI.5098-09.2010

Anderson, M. A., Ao, Y., and Sofroniew, M. V. (2014). Heterogeneity of reactive astrocytes. *Neurosci. Lett.* 565, 23–29. doi: 10.1016/j.neulet.2013.12.030

Apelt, J., Ach, K., and Schliebs, R. (2003). Aging-related down-regulation of neprilysin, a putative beta-amyloid-degrading enzyme, in transgenic Tg2576 Alzheimer-like mouse brain is accompanied by an astroglial upregulation in the vicinity of beta-amyloid plaques. *Neurosci. Lett.* 339, 183–186. doi: 10.1016/S0304-3940(03)00030-2

Appel, B. (2013). "Nonmammalian vertebrate glia," in *Neuroglia*, eds H. Kettenmann and B. R. Ransom (New York, NY: Oxford University Press), 24–31.

Araque, A., Carmignoto, G., Haydon, P. G., Oliet, S. H., Robitaille, R., and Volterra, A. (2014). Gliotransmitters travel in time and space. *Neuron* 81, 728–739. doi: 10.1016/j.neuron.2014.02.007

Arzberger, T., Krampfl, K., Leimgruber, S., and Weindl, A. (1997). Changes of NMDA receptor subunit (NR1, NR2B) and glutamate transporter (GLT1) mRNA expression in Huntington's disease–an *in situ* hybridization study. *J. Neuropathol. Exp. Neurol.* 56, 440–454. doi: 10.1097/00005072-199704000-00013

Bachoo, R. M., Kim, R. S., Ligon, K. L., Maher, E. A., Brennan, C., Billings, N., et al. (2004). Molecular diversity of astrocytes with implications for neurological disorders. *Proc. Natl. Acad. Sci. U.S.A.* 101, 8384–8389. doi: 10.1073/pnas.0402140101

Barbeito, L. H., Pehar, M., Cassina, P., Vargas, M. R., Peluffo, H., Viera, L., et al. (2004). A role for astrocytes in motor neuron loss in amyotrophic lateral sclerosis. *Brain Res. Brain Res. Rev.* 47, 263–274. doi: 10.1016/j.brainresrev.2004.05.003

Barcia, C., Sanchez Bahillo, A., Fernandez-Villalba, E., Bautista, V., Poza, Y. P. M., Fernandez-Barreiro, A., et al. (2004). Evidence of active microglia in substantia nigra pars compacta of parkinsonian monkeys 1 year after MPTP exposure. *Glia* 46, 402–409. doi: 10.1002/glia.20015

Bardehle, S., Kruger, M., Buggenthin, F., Schwausch, J., Ninkovic, J., Clevers, H., et al. (2013). Live imaging of astrocyte responses to acute injury reveals selective juxtavascular proliferation. *Nat. Neurosci.* 16, 580–586. doi: 10.1038/nn.3371

Beal, M. F. (2010). Parkinson's disease: a model dilemma. *Nature* 466, S8–10. doi: 10.1038/466S8a

Belanger, M., Allaman, I., and Magistretti, P. J. (2011). Brain energy metabolism: focus on astrocyte-neuron metabolic cooperation. *Cell Metab.* 14, 724–738. doi: 10.1016/j.cmet.2011.08.016

Ben Haim, L., Ceyzeriat, K., Carrillo-De Sauvage, M. A., Aubry, F., Auregan, G., Guillermier, M., et al. (2015). The JAK/STAT3 Pathway is a common inducer of astrocyte reactivity in Alzheimer's and Huntington's diseases. *J. Neurosci.* 35, 2817–2829. doi: 10.1523/JNEUROSCI.3516-14.2015

Bendotti, C., Atzori, C., Piva, R., Tortarolo, M., Strong, M. J., Debiasi, S., et al. (2004). Activated p38MAPK is a novel component of the intracellular inclusions found in human amyotrophic lateral sclerosis and mutant SOD1 transgenic mice. *J. Neuropathol. Exp. Neurol.* 63, 113–119.

Bendotti, C., Tortarolo, M., Suchak, S. K., Calvaresi, N., Carvelli, L., Bastone, A., et al. (2001). Transgenic SOD1 G93A mice develop reduced GLT-1 in spinal cord without alterations in cerebrospinal fluid glutamate levels. *J. Neurochem.* 79, 737–746. doi: 10.1046/j.1471-4159.2001.00572.x

Bernardinelli, Y., Randall, J., Janett, E., Nikonenko, I., Konig, S., Jones, E. V., et al. (2014). Activity-dependent structural plasticity of perisynaptic astrocytic domains promotes excitatory synapse stability. *Curr. Biol.* 24, 1679–1688. doi: 10.1016/j.cub.2014.06.025

Beurrier, C., Faideau, M., Bennouar, K. E., Escartin, C., Kerkerian-Le Goff, L., Bonvento, G., et al. (2010). Ciliary neurotrophic factor protects striatal neurons against excitotoxicity by enhancing glial glutamate uptake. *PLoS ONE* 5:e8550. doi: 10.1371/journal.pone.0008550

Bhalala, O. G., Pan, L., Sahni, V., McGuire, T. L., Gruner, K., Tourtellotte, W. G., et al. (2012). microRNA-21 regulates astrocytic response following spinal cord injury. *J. Neurosci.* 32, 17935–17947. doi: 10.1523/JNEUROSCI.3860-12.2012

Bhalala, O. G., Srikanth, M., and Kessler, J. A. (2013). The emerging roles of microRNAs in CNS injuries. *Nat. Rev. Neurol.* 9, 328–339. doi: 10.1038/nrneurol.2013.67

Bignami, A., and Dahl, D. (1976). The astroglial response to stabbing. Immunofluorescence studies with antibodies to astrocyte-specific protein (GFA) in mammalian and submammalian vertebrates. *Neuropathol. Appl. Neurobiol.* 2, 99–110. doi: 10.1111/j.1365-2990.1976.tb00488.x

Bloom, O. (2014). Non-mammalian model systems for studying neuro-immune interactions after spinal cord injury. *Exp. Neurol.* 258, 130–140. doi: 10.1016/j.expneurol.2013.12.023

Bosch, M., and Kielian, T. (2014). Hemichannels in neurodegenerative diseases: is there a link to pathology? *Front. Cell. Neurosci.* 8:242. doi: 10.3389/fncel.2014.00242

Boussicault, L., Herard, A. S., Calingasan, N., Petit, F., Malgorn, C., Merienne, N., et al. (2014). Impaired brain energy metabolism in the BACHD mouse model of Huntington's disease: critical role of astrocyte-neuron interactions. *J. Cereb. Blood Flow Metab.* 34, 1500–1510. doi: 10.1038/jcbfm.2014.110

Bradford, J., Shin, J. Y., Roberts, M., Wang, C. E., Li, X. J., and Li, S. (2009). Expression of mutant huntingtin in mouse brain astrocytes causes age-dependent neurological symptoms. *Proc. Natl. Acad. Sci. U.S.A.* 106, 22480–22485. doi: 10.1073/pnas.0911503106

Bu, G. (2009). Apolipoprotein E and its receptors in Alzheimer's disease: pathways, pathogenesis and therapy. *Nat. Rev. Neurosci.* 10, 333–344. doi: 10.1038/nrn2620

Buffo, A., Rolando, C., and Ceruti, S. (2010). Astrocytes in the damaged brain: molecular and cellular insights into their reactive response and healing potential. *Biochem. Pharmacol.* 79, 77–89. doi: 10.1016/j.bcp.2009.09.014

Burda, J. E., and Sofroniew, M. V. (2014). Reactive gliosis and the multicellular response to CNS damage and disease. *Neuron* 81, 229–248. doi: 10.1016/j.neuron.2013.12.034

Burns, R. S., Chiueh, C. C., Markey, S. P., Ebert, M. H., Jacobowitz, D. M., and Kopin, I. J. (1983). A primate model of parkinsonism: selective destruction of dopaminergic neurons in the pars compacta of the substantia nigra by N-methyl-4-phenyl-1,2,3,6-tetrahydropyridine. *Proc. Natl. Acad. Sci. U.S.A.* 80, 4546–4550. doi: 10.1073/pnas.80.14.4546

Bush, T. G., Puvanachandra, N., Horner, C. H., Polito, A., Ostenfeld, T., Svendsen, C. N., et al. (1999). Leukocyte infiltration, neuronal degeneration, and neurite outgrowth after ablation of scar-forming, reactive astrocytes in adult transgenic mice. *Neuron* 23, 297–308. doi: 10.1016/S0896-6273(00)80781-3

Bushong, E. A., Martone, M. E., Jones, Y. Z., and Ellisman, M. H. (2002). Protoplasmic astrocytes in CA1 stratum radiatum occupy separate anatomical domains. *J. Neurosci.* 22, 183–192.

Calkins, M. J., Vargas, M. R., Johnson, D. A., and Johnson, J. A. (2010). Astrocyte-specific overexpression of Nrf2 protects striatal neurons from mitochondrial complex II inhibition. *Toxicol. Sci.* 115, 557–568. doi: 10.1093/toxsci/kfq072

Carrero, I., Gonzalo, M. R., Martin, B., Sanz-Anquela, J. M., Arevalo-Serrano, J., and Gonzalo-Ruiz, A. (2012). Oligomers of beta-amyloid protein (Abeta1-42) induce the activation of cyclooxygenase-2 in astrocytes via an interaction with interleukin-1beta, tumour necrosis factor-alpha, and a nuclear factor kappa-B mechanism in the rat brain. *Exp. Neurol.* 236, 215–227. doi: 10.1016/j.expneurol.2012.05.004

Carrillo-De Sauvage, M.-A., Flament, J., Bramoulle, Y., Ben Haim, L., Guillermier, M., Berniard, A., et al. (2015). *The neuroprotective agent CNTF decreases neuronal metabolites in the rat striatum: an in vivo multimodal magnetic resonance imaging study. J. Cereb. Blood Flow Metab.* 35, 917–921. doi: 10.1038/jcbfm.2015.48

Carter, S. F., Scholl, M., Almkvist, O., Wall, A., Engler, H., Langstrom, B., et al. (2012). Evidence for astrocytosis in prodromal Alzheimer disease provided by 11C-deuterium-L-deprenyl: a multitracer PET paradigm combining 11C-Pittsburgh compound B and 18F-FDG. *J. Nucl. Med.* 53, 37–46. doi: 10.2967/jnumed.110.087031

Cassina, P., Cassina, A., Pehar, M., Castellanos, R., Gandelman, M., De Leon, A., et al. (2008). Mitochondrial dysfunction in SOD1G93A-bearing astrocytes promotes motor neuron degeneration: prevention by mitochondrial-targeted antioxidants. *J. Neurosci.* 28, 4115–4122. doi: 10.1523/JNEUROSCI.5308-07.2008

Charron, G., Doudnikoff, E., Canron, M. H., Li, Q., Vega, C., Marais, S., et al. (2014). Astrocytosis in parkinsonism: considering tripartite striatal synapses in physiopathology? *Front. Aging Neurosci.* 6:258. doi: 10.3389/fnagi.2014.00258

Chauveau, F., Boutin, H., Van Camp, N., Dolle, F., and Tavitian, B. (2008). Nuclear imaging of neuroinflammation: a comprehensive review of [11C]PK11195 challengers. *Eur. J. Nucl. Med. Mol. Imaging* 35, 2304–2319. doi: 10.1007/s00259-008-0908-9

Chen, P. C., Vargas, M. R., Pani, A. K., Smeyne, R. J., Johnson, D. A., Kan, Y. W., et al. (2009). Nrf2-mediated neuroprotection in the MPTP mouse model of Parkinson's disease: critical role for the astrocyte. *Proc. Natl. Acad. Sci. U.S.A.* 106, 2933–2938. doi: 10.1073/pnas.0813361106

Choi, J. K., Dedeoglu, A., and Jenkins, B. G. (2007). Application of MRS to mouse models of neurodegenerative illness. *NMR Biomed.* 20, 216–237. doi: 10.1002/nbm.1145

Chou, S. Y., Weng, J. Y., Lai, H. L., Liao, F., Sun, S. H., Tu, P. H., et al. (2008). Expanded-polyglutamine huntingtin protein suppresses the secretion and production of a chemokine (CCL5/RANTES) by astrocytes. *J. Neurosci.* 28, 3277–3290. doi: 10.1523/JNEUROSCI.0116-08.2008

Chung, Y. H., Joo, K. M., Lim, H. C., Cho, M. H., Kim, D., Lee, W. B., et al. (2005). Immunohistochemical study on the distribution of phosphorylated extracellular signal-regulated kinase (ERK) in the central nervous system of SOD1G93A transgenic mice. *Brain Res.* 1050, 203–209. doi: 10.1016/j.brainres.2005.05.060

Cole, S. L., and Vassar, R. (2007). The Alzheimer's disease beta-secretase enzyme, BACE1. *Mol. Neurodegener.* 2, 22. doi: 10.1186/1750-1326-2-22

Corder, E. H., Saunders, A. M., Strittmatter, W. J., Schmechel, D. E., Gaskell, P. C., Small, G. W., et al. (1993). Gene dose of apolipoprotein E type 4 allele and the risk of Alzheimer's disease in late onset families. *Science* 261, 921–923. doi: 10.1126/science.8346443

Crosio, C., Valle, C., Casciati, A., Iaccarino, C., and Carri, M. T. (2011). Astroglial inhibition of NF-kappaB does not ameliorate disease onset and progression in a mouse model for amyotrophic lateral sclerosis (ALS). *PLoS ONE* 6:e17187. doi: 10.1371/journal.pone.0017187

Cudkowicz, M. E., Titus, S., Kearney, M., Yu, H., Sherman, A., Schoenfeld, D., et al. (2014). Safety and efficacy of ceftriaxone for amyotrophic lateral sclerosis: a multi-stage, randomised, double-blind, placebo-controlled trial. *Lancet Neurol.* 13, 1083–1091. doi: 10.1016/S1474-4422(14)70222-4

Cui, J. G., Li, Y. Y., Zhao, Y., Bhattacharjee, S., and Lukiw, W. J. (2010). Differential regulation of interleukin-1 receptor-associated kinase-1 (IRAK-1) and IRAK-2 by microRNA-146a and NF-kappaB in stressed human astroglial cells and in Alzheimer disease. *J. Biol. Chem.* 285, 38951–38960. doi: 10.1074/jbc.M110.178848

Cui, Y., Masaki, K., Yamasaki, R., Imamura, S., Suzuki, S. O., Hayashi, S., et al. (2014). Extensive dysregulations of oligodendrocytic and astrocytic connexins are associated with disease progression in an amyotrophic lateral sclerosis mouse model. *J. Neuroinflammation* 11, 42. doi: 10.1186/1742-2094-11-42

Dabir, D. V., Robinson, M. B., Swanson, E., Zhang, B., Trojanowski, J. Q., Lee, V. M., et al. (2006). Impaired glutamate transport in a mouse model of tau pathology in astrocytes. *J. Neurosci.* 26, 644–654. doi: 10.1523/JNEUROSCI.3861-05.2006

D'Amelio, M., Cavallucci, V., Middei, S., Marchetti, C., Pacioni, S., Ferri, A., et al. (2011). Caspase-3 triggers early synaptic dysfunction in a mouse model of Alzheimer's disease. *Nat. Neurosci.* 14, 69–76. doi: 10.1038/nn.2709

Damier, P., Hirsch, E. C., Zhang, P., Agid, Y., and Javoy-Agid, F. (1993). Glutathione peroxidase, glial cells and Parkinson's disease. *Neuroscience* 52, 1–6. doi: 10.1016/0306-4522(93)90175-F

Danbolt, N. C. (2001). Glutamate uptake. *Prog. Neurobiol.* 65, 1–105. doi: 10.1016/S0301-0082(00)00067-8

Dantuma, N. P., and Bott, L. C. (2014). The ubiquitin-proteasome system in neurodegenerative diseases: precipitating factor, yet part of the solution. *Front. Mol. Neurosci.* 7:70. doi: 10.3389/fnmol.2014.00070

Davila, D., Thibault, K., Fiacco, T. A., and Agulhon, C. (2013). Recent molecular approaches to understanding astrocyte function. *Front. Cell. Neurosci.* 7:272. doi: 10.3389/fncel.2013.00272

De Almeida, L. P., Ross, C. A., Zala, D., Aebischer, P., and Deglon, N. (2002). Lentiviral-mediated delivery of mutant huntingtin in the striatum of rats induces a selective neuropathology modulated by polyglutamine repeat size, huntingtin expression levels, and protein length. *J. Neurosci.* 22, 3473–3483.

De Graaf, R. A., Rothman, D. L., and Behar, K. L. (2011). State of the art direct 13C and indirect 1H-[13C] NMR spectroscopy *in vivo*. A practical guide. *NMR Biomed.* 24, 958–972. doi: 10.1002/nbm.1761

Delekate, A., Fuchtemeier, M., Schumacher, T., Ulbrich, C., Foddis, M., and Petzold, G. C. (2014). Metabotropic P2Y1 receptor signalling mediates astrocytic hyperactivity *in vivo* in an Alzheimer's disease mouse model. *Nat. Commun.* 5, 5422. doi: 10.1038/ncomms6422

Dimou, L., and Gotz, M. (2014). Glial cells as progenitors and stem cells: new roles in the healthy and diseased brain. *Physiol. Rev.* 94, 709–737. doi: 10.1152/physrev.00036.2013

Doherty, J., Sheehan, A. E., Bradshaw, R., Fox, A. N., Lu, T. Y., and Freeman, M. R. (2014). PI3K signaling and Stat92E converge to modulate glial responsiveness to axonal injury. *PLoS Biol.* 12:e1001985. doi: 10.1371/journal.pbio.1001985

Dorfman, V. B., Pasquini, L., Riudavets, M., Lopez-Costa, J. J., Villegas, A., Troncoso, J. C., et al. (2010). Differential cerebral deposition of IDE and NEP in sporadic and familial Alzheimer's disease. *Neurobiol. Aging* 31, 1743–1757. doi: 10.1016/j.neurobiolaging.2008.09.016

Duyckaerts, C., Potier, M. C., and Delatour, B. (2008). Alzheimer disease models and human neuropathology: similarities and differences. *Acta Neuropathol.* 115, 5–38. doi: 10.1007/s00401-007-0312-8

Emsley, J. G., and Macklis, J. D. (2006). Astroglial heterogeneity closely reflects the neuronal-defined anatomy of the adult murine CNS. *Neuron Glia Biol.* 2, 175–186. doi: 10.1017/S1740925X06000202

Eng, L. F., Ghirnikar, R. S., and Lee, Y. L. (2000). Glial fibrillary acidic protein: GFAP-thirty-one years (1969-2000). *Neurochem. Res.* 25, 1439–1451. doi: 10.1023/A:1007677003387

Eng, L. F., Vanderhaeghen, J. J., Bignami, A., and Gerstl, B. (1971). An acidic protein isolated from fibrous astrocytes. *Brain Res.* 28, 351–354. doi: 10.1016/0006-8993(71)90668-8

Escartin, C., and Bonvento, G. (2008). Targeted activation of astrocytes: a potential neuroprotective strategy. *Mol. Neurobiol.* 38, 231–241. doi: 10.1007/s12035-008-8043-y

Escartin, C., Brouillet, E., Gubellini, P., Trioulier, Y., Jacquard, C., Smadja, C., et al. (2006). Ciliary neurotrophic factor activates astrocytes, redistributes their glutamate transporters GLAST and GLT-1 to raft microdomains, and improves glutamate handling *in vivo*. *J. Neurosci.* 26, 5978–5989. doi: 10.1523/JNEUROSCI.0302-06.2006

Escartin, C., Pierre, K., Colin, A., Brouillet, E., Delzescaux, T., Guillermier, M., et al. (2007). Activation of astrocytes by CNTF induces metabolic plasticity and increases resistance to metabolic insults. *J. Neurosci.* 27, 7094–7104. doi: 10.1523/JNEUROSCI.0174-07.2007

Escartin, C., and Rouach, N. (2013). Astroglial networking contributes to neurometabolic coupling. *Front. Neuroenergetics* 5:4. doi: 10.3389/fnene.2013.00004

Faideau, M., Kim, J., Cormier, K., Gilmore, R., Welch, M., Auregan, G., et al. (2010). *In vivo* expression of polyglutamine-expanded huntingtin by mouse striatal astrocytes impairs glutamate transport: a correlation with Huntington's disease subjects. *Hum. Mol. Genet.* 19, 3053–3067. doi: 10.1093/hmg/ddq212

Farina, C., Aloisi, F., and Meinl, E. (2007). Astrocytes are active players in cerebral innate immunity. *Trends Immunol.* 28, 138–145. doi: 10.1016/j.it.2007.01.005

Fernandez, A. M., Fernandez, S., Carrero, P., Garcia-Garcia, M., and Torres-Aleman, I. (2007). Calcineurin in reactive astrocytes plays a key role in the interplay between proinflammatory and anti-inflammatory signals. *J. Neurosci.* 27, 8745–8756. doi: 10.1523/JNEUROSCI.1002-07.2007

Fernandez, A. M., Jimenez, S., Mecha, M., Davila, D., Guaza, C., Vitorica, J., et al. (2012). Regulation of the phosphatase calcineurin by insulin-like growth factor I unveils a key role of astrocytes in Alzheimer's pathology. *Mol. Psychiatry* 17, 705–718. doi: 10.1038/mp.2011.128

Ferraiuolo, L., Higginbottom, A., Heath, P. R., Barber, S., Greenald, D., Kirby, J., et al. (2011). Dysregulation of astrocyte-motoneuron cross-talk in mutant superoxide dismutase 1-related amyotrophic lateral sclerosis. *Brain* 134, 2627–2641. doi: 10.1093/brain/awr193

Ferrer, I., Blanco, R., Carmona, M., and Puig, B. (2001). Phosphorylated mitogen-activated protein kinase (MAPK/ERK-P), protein kinase of 38 kDa (p38-P), stress-activated protein kinase (SAPK/JNK-P), and calcium/calmodulin-dependent kinase II (CaM kinase II) are differentially expressed in tau deposits in neurons and glial cells in tauopathies. *J. Neural Transm.* 108, 1397–1415. doi: 10.1007/s007020100016

Ferrer, I., Marti, E., Lopez, E., and Tortosa, A. (1998). NF-kB immunoreactivity is observed in association with beta A4 diffuse plaques in patients with Alzheimer's disease. *Neuropathol. Appl. Neurobiol.* 24, 271–277. doi: 10.1046/j.1365-2990.1998.00116.x

Foo, L. C., Allen, N. J., Bushong, E. A., Ventura, P. B., Chung, W. S., Zhou, L., et al. (2011). Development of a method for the purification and culture of rodent astrocytes. *Neuron* 71, 799–811. doi: 10.1016/j.neuron.2011.07.022

Forno, L. S., Delanney, L. E., Irwin, I., Di Monte, D., and Langston, J. W. (1992). Astrocytes and Parkinson's disease. *Prog. Brain Res.* 94, 429–436. doi: 10.1016/S0079-6123(08)61770-7

Frakes, A. E., Ferraiuolo, L., Haidet-Phillips, A. M., Schmelzer, L., Braun, L., Miranda, C. J., et al. (2014). Microglia induce motor neuron death via the classical NF-kappaB pathway in amyotrophic lateral sclerosis. *Neuron* 81, 1009–1023. doi: 10.1016/j.neuron.2014.01.013

Freeman, M. R. (2015). Drosophila central nervous system Glia. *Cold Spring Harb. Perspect Biol.* doi: 10.1101/cshperspect.a020552. [Epub ahead of print].

Fukuyama, H., Ogawa, M., Yamauchi, H., Yamaguchi, S., Kimura, J., Yonekura, Y., et al. (1994). Altered cerebral energy metabolism in Alzheimer's disease: a PET study. *J. Nucl. Med.* 35, 1–6.

Funato, H., Yoshimura, M., Yamazaki, T., Saido, T. C., Ito, Y., Yokofujita, J., et al. (1998). Astrocytes containing amyloid beta-protein (Abeta)-positive granules are associated with Abeta40-positive diffuse plaques in the aged human brain. *Am. J. Pathol.* 152, 983–992.

Furman, J. L., and Norris, C. M. (2014). Calcineurin and glial signaling: neuroinflammation and beyond. *J. Neuroinflammation* 11, 158. doi: 10.1186/s12974-014-0158-7

Furman, J. L., Sama, D. M., Gant, J. C., Beckett, T. L., Murphy, M. P., Bachstetter, A. D., et al. (2012). Targeting astrocytes ameliorates neurologic changes in a mouse model of Alzheimer's disease. *J. Neurosci.* 32, 16129–16140. doi: 10.1523/JNEUROSCI.2323-12.2012

Gan, L., Vargas, M. R., Johnson, D. A., and Johnson, J. A. (2012). Astrocyte-specific overexpression of Nrf2 delays motor pathology and synuclein aggregation throughout the CNS in the alpha-synuclein mutant (A53T) mouse model. *J. Neurosci.* 32, 17775–17787. doi: 10.1523/JNEUROSCI.3049-12.2012

Genoud, C., Quairiaux, C., Steiner, P., Hirling, H., Welker, E., and Knott, G. W. (2006). Plasticity of astrocytic coverage and glutamate transporter expression in adult mouse cortex. *PLoS Biol.* 4:e343. doi: 10.1371/journal.pbio.0040343

Ghavami, S., Shojaei, S., Yeganeh, B., Ande, S. R., Jangamreddy, J. R., Mehrpour, M., et al. (2014). Autophagy and apoptosis dysfunction in neurodegenerative disorders. *Prog. Neurobiol.* 112, 24–49. doi: 10.1016/j.pneurobio.2013.10.004

Giaume, C., Koulakoff, A., Roux, L., Holcman, D., and Rouach, N. (2010). Astroglial networks: a step further in neuroglial and gliovascular interactions. *Nat. Rev. Neurosci.* 11, 87–99. doi: 10.1038/nrn2757

Gong, Y. H., Parsadanian, A. S., Andreeva, A., Snider, W. D., and Elliott, J. L. (2000). Restricted expression of G86R Cu/Zn superoxide dismutase in astrocytes results in astrocytosis but does not cause motoneuron degeneration. *J. Neurosci.* 20, 660–665.

Gotz, J., and Ittner, L. M. (2008). Animal models of Alzheimer's disease and frontotemporal dementia. *Nat. Rev. Neurosci.* 9, 532–544. doi: 10.1038/nrn2420

Grafton, S. T., Mazziotta, J. C., Pahl, J. J., St George-Hyslop, P., Haines, J. L., Gusella, J., et al. (1992). Serial changes of cerebral glucose metabolism and caudate size in persons at risk for Huntington's disease. *Arch. Neurol.* 49, 1161–1167. doi: 10.1001/archneur.1992.00530350075022

Gray, M., Shirasaki, D. I., Cepeda, C., Andre, V. M., Wilburn, B., Lu, X. H., et al. (2008). Full-length human mutant huntingtin with a stable polyglutamine repeat can elicit progressive and selective neuropathogenesis in BACHD mice. *J. Neurosci.* 28, 6182–6195. doi: 10.1523/JNEUROSCI.0857-08.2008

Grivennikov, S. I., and Karin, M. (2010). Dangerous liaisons: STAT3 and NF-kappaB collaboration and crosstalk in cancer. *Cytokine Growth Factor Rev.* 21, 11–19. doi: 10.1016/j.cytogfr.2009.11.005

Gu, X. L., Long, C. X., Sun, L., Xie, C., Lin, X., and Cai, H. (2010). Astrocytic expression of Parkinson's disease-related A53T alpha-synuclein causes neurodegeneration in mice. *Mol. Brain* 3, 12. doi: 10.1186/1756-6606-3-12

Gurney, M. E., Pu, H., Chiu, A. Y., Dal Canto, M. C., Polchow, C. Y., Alexander, D. D., et al. (1994). Motor neuron degeneration in mice that express a human Cu,Zn superoxide dismutase mutation. *Science* 264, 1772–1775. doi: 10.1126/science.8209258

Haidet-Phillips, A. M., Hester, M. E., Miranda, C. J., Meyer, K., Braun, L., Frakes, A., et al. (2011). Astrocytes from familial and sporadic ALS patients are toxic to motor neurons. *Nat. Biotechnol.* 29, 824–828. doi: 10.1038/nbt.1957

Hall, E. D., Oostveen, J. A., and Gurney, M. E. (1998). Relationship of microglial and astrocytic activation to disease onset and progression in a transgenic model of familial ALS. *Glia* 23, 249–256.

Halle, A., Hornung, V., Petzold, G. C., Stewart, C. R., Monks, B. G., Reinheckel, T., et al. (2008). The NALP3 inflammasome is involved in the innate immune response to amyloid-beta. *Nat. Immunol.* 9, 857–865. doi: 10.1038/ni.1636

Hanisch, U. K., and Kettenmann, H. (2007). Microglia: active sensor and versatile effector cells in the normal and pathologic brain. *Nat. Neurosci.* 10, 1387–1394. doi: 10.1038/nn1997

Hassel, B., Tessler, S., Faull, R. L., and Emson, P. C. (2008). Glutamate uptake is reduced in prefrontal cortex in Huntington's disease. *Neurochem. Res.* 33, 232–237. doi: 10.1007/s11064-007-9463-1

He, F., Ge, W., Martinowich, K., Becker-Catania, S., Coskun, V., Zhu, W., et al. (2005). A positive autoregulatory loop of Jak-STAT signaling controls the onset of astrogliogenesis. *Nat. Neurosci.* 8, 616–625. doi: 10.1038/nn1440

Heikkila, R. E., Hess, A., and Duvoisin, R. C. (1984). Dopaminergic neurotoxicity of 1-methyl-4-phenyl-1,2,5,6-tetrahydropyridine in mice. *Science* 224, 1451–1453. doi: 10.1126/science.6610213

Heneka, M. T., Kummer, M. P., and Latz, E. (2014). Innate immune activation in neurodegenerative disease. *Nat. Rev. Immunol.* 14, 463–477. doi: 10.1038/nri3705

Heneka, M. T., Sastre, M., Dumitrescu-Ozimek, L., Dewachter, I., Walter, J., Klockgether, T., et al. (2005). Focal glial activation coincides with increased BACE1 activation and precedes amyloid plaque deposition in APP[V717I] transgenic mice. *J. Neuroinflammation* 2, 22. doi: 10.1186/1742-2094-2-22

Hensley, K., Floyd, R. A., Zheng, N. Y., Nael, R., Robinson, K. A., Nguyen, X., et al. (1999). p38 kinase is activated in the Alzheimer's disease brain. *J. Neurochem.* 72, 2053–2058. doi: 10.1046/j.1471-4159.1999.0722053.x

Herrmann, J. E., Imura, T., Song, B., Qi, J., Ao, Y., Nguyen, T. K., et al. (2008). STAT3 is a critical regulator of astrogliosis and scar formation after spinal cord injury. *J. Neurosci.* 28, 7231–7243. doi: 10.1523/JNEUROSCI.1709-08.2008

Hirsch, E. C., and Hunot, S. (2009). Neuroinflammation in Parkinson's disease: a target for neuroprotection? *Lancet Neurol.* 8, 382–397. doi: 10.1016/S1474-4422(09)70062-6

Hoesel, B., and Schmid, J. A. (2013). The complexity of NF-kappaB signaling in inflammation and cancer. *Mol. Cancer* 12, 86. doi: 10.1186/1476-4598-12-86

Hogan, P. G., Chen, L., Nardone, J., and Rao, A. (2003). Transcriptional regulation by calcium, calcineurin, and NFAT. *Genes Dev.* 17, 2205–2232. doi: 10.1101/gad.1102703

Howland, D. S., Liu, J., She, Y., Goad, B., Maragakis, N. J., Kim, B., et al. (2002). Focal loss of the glutamate transporter EAAT2 in a transgenic rat model of SOD1 mutant-mediated amyotrophic lateral sclerosis (ALS). *Proc. Natl. Acad. Sci. U.S.A.* 99, 1604–1609. doi: 10.1073/pnas.032539299

Hsiao, H. Y., Chen, Y. C., Chen, H. M., Tu, P. H., and Chern, Y. (2013). A critical role of astrocyte-mediated nuclear factor-kappaB-dependent inflammation in Huntington's disease. *Hum. Mol. Genet.* 22, 1826–1842. doi: 10.1093/hmg/ddt036

Hsiao, K., Chapman, P., Nilsen, S., Eckman, C., Harigaya, Y., Younkin, S., et al. (1996). Correlative memory deficits, Abeta elevation, and amyloid plaques in transgenic mice. *Science* 274, 99–102. doi: 10.1126/science.274.5284.99

Huang, Y., and Mucke, L. (2012). Alzheimer mechanisms and therapeutic strategies. *Cell* 148, 1204–1222. doi: 10.1016/j.cell.2012.02.040

Hunot, S., Brugg, B., Ricard, D., Michel, P. P., Muriel, M. P., Ruberg, M., et al. (1997). Nuclear translocation of NF-kappaB is increased in dopaminergic neurons of patients with parkinson disease. *Proc. Natl. Acad. Sci. U.S.A.* 94, 7531–7536. doi: 10.1073/pnas.94.14.7531

Hutchins, A. P., Diez, D., Takahashi, Y., Ahmad, S., Jauch, R., Tremblay, M. L., et al. (2013). Distinct transcriptional regulatory modules underlie STAT3′s cell type-independent and cell type-specific functions. *Nucleic Acids Res.* 41, 2155–2170. doi: 10.1093/nar/gks1300

Hutchison, E. R., Kawamoto, E. M., Taub, D. D., Lal, A., Abdelmohsen, K., Zhang, Y., et al. (2013). Evidence for miR-181 involvement in neuroinflammatory responses of astrocytes. *Glia* 61, 1018–1028. doi: 10.1002/glia.22483

Jain, N., Zhang, T., Fong, S. L., Lim, C. P., and Cao, X. (1998). Repression of Stat3 activity by activation of mitogen-activated protein kinase (MAPK). *Oncogene* 17, 3157–3167. doi: 10.1038/sj.onc.1202238

Jankowsky, J. L., Fadale, D. J., Anderson, J., Xu, G. M., Gonzales, V., Jenkins, N. A., et al. (2004). Mutant presenilins specifically elevate the levels of the 42 residue beta-amyloid peptide *in vivo*: evidence for augmentation of a 42-specific gamma secretase. *Hum. Mol. Genet.* 13, 159–170. doi: 10.1093/hmg/ddh019

Jansen, A. H., Reits, E. A., and Hol, E. M. (2014). The ubiquitin proteasome system in glia and its role in neurodegenerative diseases. *Front. Mol. Neurosci.* 7:73. doi: 10.3389/fnmol.2014.00073

Jeffrey, K. L., Camps, M., Rommel, C., and Mackay, C. R. (2007). Targeting dual-specificity phosphatases: manipulating MAP kinase signalling and immune responses. *Nat. Rev. Drug Discov.* 6, 391–403. doi: 10.1038/nrd2289

Jo, S., Yarishkin, O., Hwang, Y. J., Chun, Y. E., Park, M., Woo, D. H., et al. (2014). GABA from reactive astrocytes impairs memory in mouse models of Alzheimer's disease. *Nat. Med.* 20, 886–896. doi: 10.1038/nm.3639

Johansson, A., Engler, H., Blomquist, G., Scott, B., Wall, A., Aquilonius, S. M., et al. (2007). Evidence for astrocytosis in ALS demonstrated by [11C](L)-deprenyl-D2 PET. *J. Neurol. Sci.* 255, 17–22. doi: 10.1016/j.jns.2007.01.057

Jung, E. S., An, K., Hong, H. S., Kim, J. H., and Mook-Jung, I. (2012). Astrocyte-originated ATP protects Abeta(1-42)-induced impairment of synaptic plasticity. *J. Neurosci.* 32, 3081–3087. doi: 10.1523/JNEUROSCI.6357-11.2012

Kaiser, M., Maletzki, I., Hulsmann, S., Holtmann, B., Schulz-Schaeffer, W., Kirchhoff, F., et al. (2006). Progressive loss of a glial potassium channel (KCNJ10) in the spinal cord of the SOD1 (G93A) transgenic mouse model of amyotrophic lateral sclerosis. *J. Neurochem.* 99, 900–912. doi: 10.1111/j.1471-4159.2006.04131.x

Kaltschmidt, B., Uherek, M., Volk, B., Baeuerle, P. A., and Kaltschmidt, C. (1997). Transcription factor NF-kappaB is activated in primary neurons by amyloid beta peptides and in neurons surrounding early plaques from patients with Alzheimer disease. *Proc. Natl. Acad. Sci. U.S.A.* 94, 2642–2647. doi: 10.1073/pnas.94.6.2642

Kaltschmidt, B., Widera, D., and Kaltschmidt, C. (2005). Signaling via NF-kappaB in the nervous system. *Biochim. Biophys. Acta* 1745, 287–299. doi: 10.1016/j.bbamcr.2005.05.009

Kaminska, B., Gozdz, A., Zawadzka, M., Ellert-Miklaszewska, A., and Lipko, M. (2009). MAPK signal transduction underlying brain inflammation and gliosis as therapeutic target. *Anat. Rec.* 292, 1902–1913. doi: 10.1002/ar.21047

Kamphuis, W., Kooijman, L., Orre, M., Stassen, O., Pekny, M., and Hol, E. M. (2015). *GFAP* and vimentin deficiency alters gene expression in astrocytes and microglia in wild-type mice and changes the transcriptional response of reactive glia in mouse model for Alzheimer's disease. *Glia* 63, 1036–1056. doi: 10.1002/glia.22800

Kamphuis, W., Orre, M., Kooijman, L., Dahmen, M., and Hol, E. M. (2012). Differential cell proliferation in the cortex of the APPswePS1dE9 Alzheimer's disease mouse model. *Glia* 60, 615–629. doi: 10.1002/glia.22295

Kang, W., Balordi, F., Su, N., Chen, L., Fishell, G., and Hebert, J. M. (2014). Astrocyte activation is suppressed in both normal and injured brain by FGF signaling. *Proc. Natl. Acad. Sci. U.S.A.* 111, E2987–E2995. doi: 10.1073/pnas.1320401111

Kanski, R., Van Strien, M. E., Van Tijn, P., and Hol, E. M. (2014). A star is born: new insights into the mechanism of astrogenesis. *Cell. Mol. Life Sci.* 71, 433–447. doi: 10.1007/s00018-013-1435-9

Kawamata, H., Ng, S. K., Diaz, N., Burstein, S., Morel, L., Osgood, A., et al. (2014). Abnormal intracellular calcium signaling and SNARE-dependent exocytosis contributes to SOD1G93A astrocyte-mediated toxicity in amyotrophic lateral sclerosis. *J. Neurosci.* 34, 2331–2348. doi: 10.1523/JNEUROSCI.2689-13.2014

Kershaw, N. J., Laktyushin, A., Nicola, N. A., and Babon, J. J. (2014). Reconstruction of an active SOCS3-based E3 ubiquitin ligase complex *in vitro*: identification of the active components and JAK2 and gp130 as substrates. *Growth Factors* 32, 1–10. doi: 10.3109/08977194.2013.877005

Kettenmann, H., and Ransom, B. R. (2004). "The concept of neuroglia: a historical perspective," in *Neuroglia*, eds H. Kettenmann and B. R. Ransom (New York, NY: Oxford University Press), 1–16. doi: 10.1093/acprof:oso/9780195152227.001.0001

Khoshnan, A., Ko, J., Watkin, E. E., Paige, L. A., Reinhart, P. H., and Patterson, P. H. (2004). Activation of the IkappaB kinase complex and nuclear factor-kappaB contributes to mutant huntingtin neurotoxicity. *J. Neurosci.* 24, 7999–8008. doi: 10.1523/JNEUROSCI.2675-04.2004

Kigerl, K. A., De Rivero Vaccari, J. P., Dietrich, W. D., Popovich, P. G., and Keane, R. W. (2014). Pattern recognition receptors and central nervous system repair. *Exp. Neurol.* 258, 5–16. doi: 10.1016/j.expneurol.2014.01.001

Kohutnicka, M., Lewandowska, E., Kurkowska-Jastrzebska, I., Czlonkowski, A., and Czlonkowska, A. (1998). Microglial and astrocytic involvement in a murine model of Parkinson's disease induced by 1-methyl-4-phenyl-1,2,3,6-tetrahydropyridine (MPTP). *Immunopharmacology* 39, 167–180. doi: 10.1016/S0162-3109(98)00022-8

Koistinaho, M., Kettunen, M. I., Goldsteins, G., Keinanen, R., Salminen, A., Ort, M., et al. (2002). Beta-amyloid precursor protein transgenic mice that harbor diffuse A beta deposits but do not form plaques show increased ischemic vulnerability: role of inflammation. *Proc. Natl. Acad. Sci. U.S.A.* 99, 1610–1615. doi: 10.1073/pnas.032670899

Koistinaho, M., Lin, S., Wu, X., Esterman, M., Koger, D., Hanson, J., et al. (2004). Apolipoprotein E promotes astrocyte colocalization and degradation of deposited amyloid-beta peptides. *Nat. Med.* 10, 719–726. doi: 10.1038/nm1058

Kraft, A. W., Hu, X., Yoon, H., Yan, P., Xiao, Q., Wang, Y., et al. (2013). Attenuating astrocyte activation accelerates plaque pathogenesis in APP/PS1 mice. *FASEB J.* 27, 187–198. doi: 10.1096/fj.12-208660

Krencik, R., and Ullian, E. M. (2013). A cellular star atlas: using astrocytes from human pluripotent stem cells for disease studies. *Front. Cell. Neurosci.* 7:25. doi: 10.3389/fncel.2013.00025

Kuchibhotla, K. V., Lattarulo, C. R., Hyman, B. T., and Bacskai, B. J. (2009). Synchronous hyperactivity and intercellular calcium waves in astrocytes in Alzheimer mice. *Science* 323, 1211–1215. doi: 10.1126/science.1169096

Kuge, Y., Kawashima, H., Minematsu, K., Hasegawa, Y., Yamaguchi, T., Miyake, Y., et al. (2000). [1-11C]Octanoate as a PET tracer for studying ischemic stroke: evaluation in a canine model of thromboembolic stroke with positron emission tomography. *Biol. Pharm. Bull.* 23, 984–988. doi: 10.1248/bpb.23.984

Lauderback, C. M., Hackett, J. M., Huang, F. F., Keller, J. N., Szweda, L. I., Markesbery, W. R., et al. (2001). The glial glutamate transporter, GLT-1, is oxidatively modified by 4-hydroxy-2-nonenal in the Alzheimer's disease brain: the role of Abeta1-42. *J. Neurochem.* 78, 413–416. doi: 10.1046/j.1471-4159.2001.00451.x

Lavisse, S., Guillermier, M., Herard, A. S., Petit, F., Delahaye, M., Van Camp, N., et al. (2012). Reactive Astrocytes Overexpress TSPO and are detected by TSPO positron emission tomography imaging. *J. Neurosci.* 32, 10809–10818. doi: 10.1523/JNEUROSCI.1487-12.2012

Le Prince, G., Delaere, P., Fages, C., Lefrancois, T., Touret, M., Salanon, M., et al. (1995). Glutamine synthetase (GS) expression is reduced in senile dementia of the Alzheimer type. *Neurochem. Res.* 20, 859–862. doi: 10.1007/BF00969698

Lebon, V., Petersen, K. F., Cline, G. W., Shen, J., Mason, G. F., Dufour, S., et al. (2002). Astroglial contribution to brain energy metabolism in humans revealed by 13C nuclear magnetic resonance spectroscopy: elucidation of the dominant pathway for neurotransmitter glutamate repletion and measurement of astrocytic oxidative metabolism. *J. Neurosci.* 22, 1523–1531.

Lee, W., Reyes, R. C., Gottipati, M. K., Lewis, K., Lesort, M., Parpura, V., et al. (2013). Enhanced Ca(2+)-dependent glutamate release from astrocytes of the BACHD Huntington's disease mouse model. *Neurobiol. Dis.* 58, 192–199. doi: 10.1016/j.nbd.2013.06.002

Leoni, V., and Caccia, C. (2014). Study of cholesterol metabolism in Huntington's disease. *Biochem. Biophys. Res. Commun.* 446, 697–701. doi: 10.1016/j.bbrc.2014.01.188

Lepore, A. C., Dejea, C., Carmen, J., Rauck, B., Kerr, D. A., Sofroniew, M. V., et al. (2008a). Selective ablation of proliferating astrocytes does not affect disease outcome in either acute or chronic models of motor neuron degeneration. *Exp. Neurol.* 211, 423–432. doi: 10.1016/j.expneurol.2008.02.020

Lepore, A. C., Rauck, B., Dejea, C., Pardo, A. C., Rao, M. S., Rothstein, J. D., et al. (2008b). Focal transplantation-based astrocyte replacement is neuroprotective in a model of motor neuron disease. *Nat. Neurosci.* 11, 1294–1301. doi: 10.1038/nn.2210

Levy, D. E., and Darnell, J. E. Jr. (2002). Stats: transcriptional control and biological impact. *Nat. Rev. Mol. Cell Biol.* 3, 651–662. doi: 10.1038/nrm909

Li, Y. Y., Cui, J. G., Hill, J. M., Bhattacharjee, S., Zhao, Y., and Lukiw, W. J. (2011). Increased expression of miRNA-146a in Alzheimer's disease transgenic mouse models. *Neurosci. Lett.* 487, 94–98. doi: 10.1016/j.neulet.2010.09.079

Lian, H., Yang, L., Cole, A., Sun, L., Chiang, A. C., Fowler, S. W., et al. (2015). NFkappaB-Activated astroglial release of complement C3 compromises neuronal morphology and function associated with Alzheimer's Disease. *Neuron* 85, 101–115. doi: 10.1016/j.neuron.2014.11.018

Liberto, C. M., Albrecht, P. J., Herx, L. M., Yong, V. W., and Levison, S. W. (2004). Pro-regenerative properties of cytokine-activated astrocytes. *J. Neurochem.* 89, 1092–1100. doi: 10.1111/j.1471-4159.2004.02420.x

Lievens, J. C., Rival, T., Iche, M., Chneiweiss, H., and Birman, S. (2005). Expanded polyglutamine peptides disrupt EGF receptor signaling and glutamate transporter expression in Drosophila. *Hum. Mol. Genet.* 14, 713–724. doi: 10.1093/hmg/ddi067

Lievens, J. C., Woodman, B., Mahal, A., Spasic-Boscovic, O., Samuel, D., Kerkerian-Le Goff, L., et al. (2001). Impaired glutamate uptake in the R6 Huntington's disease transgenic mice. *Neurobiol. Dis.* 8, 807–821. doi: 10.1006/nbdi.2001.0430

Lim, D., Iyer, A., Ronco, V., Grolla, A. A., Canonico, P. L., Aronica, E., et al. (2013). Amyloid beta deregulates astroglial mGluR5-mediated calcium signaling via calcineurin and Nf-kB. *Glia* 61, 1134–1145. doi: 10.1002/glia.22502

Lin, M. T., and Beal, M. F. (2006). Mitochondrial dysfunction and oxidative stress in neurodegenerative diseases. *Nature* 443, 787–795. doi: 10.1038/nature05292

Lucin, K. M., and Wyss-Coray, T. (2009). Immune activation in brain aging and neurodegeneration: too much or too little? *Neuron* 64, 110–122. doi: 10.1016/j.neuron.2009.08.039

Mangiarini, L., Sathasivam, K., Mahal, A., Mott, R., Seller, M., and Bates, G. P. (1997). Instability of highly expanded CAG repeats in mice transgenic for the Huntington's disease mutation. *Nat. Genet.* 15, 197–200. doi: 10.1038/ng0297-197

Maragakis, N. J., and Rothstein, J. D. (2004). Glutamate transporters: animal models to neurologic disease. *Neurobiol. Dis.* 15, 461–473. doi: 10.1016/j.nbd.2003.12.007

Maragakis, N. J., and Rothstein, J. D. (2006). Mechanisms of Disease: astrocytes in neurodegenerative disease. *Nat. Clin. Pract. Neurol.* 2, 679–689. doi: 10.1038/ncpneuro0355

Marcora, E., and Kennedy, M. B. (2010). The Huntington's disease mutation impairs Huntingtin's role in the transport of NF-kappaB from the synapse to the nucleus. *Hum. Mol. Genet.* 19, 4373–4384. doi: 10.1093/hmg/ddq358

Margulis, J., and Finkbeiner, S. (2014). Proteostasis in striatal cells and selective neurodegeneration in Huntington's disease. *Front. Cell. Neurosci.* 8:218. doi: 10.3389/fncel.2014.00218

Marik, J., Ogasawara, A., Martin-McNulty, B., Ross, J., Flores, J. E., Gill, H. S., et al. (2009). PET of glial metabolism using 2-18F-fluoroacetate. *J. Nucl. Med.* 50, 982–990. doi: 10.2967/jnumed.108.057356

Martorana, F., Brambilla, L., Valori, C. F., Bergamaschi, C., Roncoroni, C., Aronica, E., et al. (2012). The BH4 domain of Bcl-X(L) rescues astrocyte degeneration in amyotrophic lateral sclerosis by modulating intracellular calcium signals. *Hum. Mol. Genet.* 21, 826–840. doi: 10.1093/hmg/ddr513

Masliah, E., Alford, M., Deteresa, R., Mallory, M., and Hansen, L. (1996). Deficient glutamate transport is associated with neurodegeneration in Alzheimer's disease. *Ann. Neurol.* 40, 759–766. doi: 10.1002/ana.410400512

Masliah, E., Alford, M., Mallory, M., Rockenstein, E., Moechars, D., and Van Leuven, F. (2000). Abnormal glutamate transport function in mutant amyloid precursor protein transgenic mice. *Exp. Neurol.* 163, 381–387. doi: 10.1006/exnr.2000.7386

Mattson, M. P., and Meffert, M. K. (2006). Roles for NF-kappaB in nerve cell survival, plasticity, and disease. *Cell Death Differ.* 13, 852–860. doi: 10.1038/sj.cdd.4401837

Matyash, V., and Kettenmann, H. (2010). Heterogeneity in astrocyte morphology and physiology. *Brain Res. Rev.* 63, 2–10. doi: 10.1016/j.brainresrev.2009.12.001

McCarthy, K. D., and De Vellis, J. (1980). Preparation of separate astroglial and oligodendroglial cell cultures from rat cerebral tissue. *J. Cell Biol.* 85, 890–902. doi: 10.1083/jcb.85.3.890

Mei, X., Ezan, P., Giaume, C., and Koulakoff, A. (2010). Astroglial connexin immunoreactivity is specifically altered at beta-amyloid plaques in beta-amyloid precursor protein/presenilin1 mice. *Neuroscience* 171, 92–105. doi: 10.1016/j.neuroscience.2010.08.001

Menalled, L. B., Kudwa, A. E., Miller, S., Fitzpatrick, J., Watson-Johnson, J., Keating, N., et al. (2012). Comprehensive behavioral and molecular characterization of a new knock-in mouse model of Huntington's disease: zQ175. *PLoS ONE* 7:e49838. doi: 10.1371/journal.pone.0049838

Menalled, L. B., Sison, J. D., Dragatsis, I., Zeitlin, S., and Chesselet, M. F. (2003). Time course of early motor and neuropathological anomalies in a knock-in mouse model of Huntington's disease with 140 CAG repeats. *J. Comp. Neurol.* 465, 11–26. doi: 10.1002/cne.10776

Migheli, A., Piva, R., Atzori, C., Troost, D., and Schiffer, D. (1997). c-Jun, JNK/SAPK kinases and transcription factor NF-kappa B are selectively activated in astrocytes, but not motor neurons, in amyotrophic lateral sclerosis.

J. Neuropathol. Exp. Neurol. 56, 1314–1322. doi: 10.1097/00005072-199712000-00006

Miller, B. R., Dorner, J. L., Shou, M., Sari, Y., Barton, S. J., Sengelaub, D. R., et al. (2008). Up-regulation of GLT1 expression increases glutamate uptake and attenuates the Huntington's disease phenotype in the R6/2 mouse. *Neuroscience* 153, 329–337. doi: 10.1016/j.neuroscience.2008.02.004

Minkiewicz, J., De Rivero Vaccari, J. P., and Keane, R. W. (2013). Human astrocytes express a novel NLRP2 inflammasome. *Glia* 61, 1113–1121. doi: 10.1002/glia.22499

Molofsky, A. V., Krencik, R., Ullian, E. M., Tsai, H. H., Deneen, B., Richardson, W. D., et al. (2012). Astrocytes and disease: a neurodevelopmental perspective. *Genes Dev.* 26, 891–907. doi: 10.1101/gad.188326.112

Motori, E., Puyal, J., Toni, N., Ghanem, A., Angeloni, C., Malaguti, M., et al. (2013). Inflammation-induced alteration of astrocyte mitochondrial dynamics requires autophagy for mitochondrial network maintenance. *Cell Metab.* 18, 844–859. doi: 10.1016/j.cmet.2013.11.005

Muller, H. W., Junghans, U., and Kappler, J. (1995). Astroglial neurotrophic and neurite-promoting factors. *Pharmacol. Ther.* 65, 1–18. doi: 10.1016/0163-7258(94)00047-7

Nagele, R. G., D'Andrea, M. R., Lee, H., Venkataraman, V., and Wang, H. Y. (2003). Astrocytes accumulate A beta 42 and give rise to astrocytic amyloid plaques in Alzheimer disease brains. *Brain Res.* 971, 197–209. doi: 10.1016/S0006-8993(03)02361-8

Nagy, J. I., Li, W., Hertzberg, E. L., and Marotta, C. A. (1996). Elevated connexin43 immunoreactivity at sites of amyloid plaques in Alzheimer's disease. *Brain Res.* 717, 173–178. doi: 10.1016/0006-8993(95)01526-4

Nilsen, L. H., Rae, C., Ittner, L. M., Gotz, J., and Sonnewald, U. (2013). Glutamate metabolism is impaired in transgenic mice with tau hyperphosphorylation. *J. Cereb. Blood Flow Metab.* 33, 684–691. doi: 10.1038/jcbfm.2012.212

Nilsen, L. H., Witter, M. P., and Sonnewald, U. (2014). Neuronal and astrocytic metabolism in a transgenic rat model of Alzheimer's disease. *J. Cereb. Blood Flow Metab.* 34, 906–914. doi: 10.1038/jcbfm.2014.37

Norris, C. M., Kadish, I., Blalock, E. M., Chen, K. C., Thibault, V., Porter, N. M., et al. (2005). Calcineurin triggers reactive/inflammatory processes in astrocytes and is upregulated in aging and Alzheimer's models. *J. Neurosci.* 25, 4649–4658. doi: 10.1523/JNEUROSCI.0365-05.2005

Oberheim, N. A., Tian, G. F., Han, X., Peng, W., Takano, T., Ransom, B., et al. (2008). Loss of astrocytic domain organization in the epileptic brain. *J. Neurosci.* 28, 3264–3276. doi: 10.1523/JNEUROSCI.4980-07.2008

O'Brien, E. R., Howarth, C., and Sibson, N. R. (2013). The role of astrocytes in CNS tumors: pre-clinical models and novel imaging approaches. *Front. Cell Neurosci.* 7:40. doi: 10.3389/fncel.2013.00040

Oddo, S., Caccamo, A., Shepherd, J. D., Murphy, M. P., Golde, T. E., Kayed, R., et al. (2003). Triple-transgenic model of Alzheimer's disease with plaques and tangles: intracellular Abeta and synaptic dysfunction. *Neuron* 39, 409–421. doi: 10.1016/S0896-6273(03)00434-3

Oeckinghaus, A., Hayden, M. S., and Ghosh, S. (2011). Crosstalk in NF-kappaB signaling pathways. *Nat. Immunol.* 12, 695–708. doi: 10.1038/ni.2065

Okada, S., Nakamura, M., Katoh, H., Miyao, T., Shimazaki, T., Ishii, K., et al. (2006). Conditional ablation of Stat3 or Socs3 discloses a dual role for reactive astrocytes after spinal cord injury. *Nat. Med.* 12, 829–834. doi: 10.1038/nm1425

Olabarria, M., Noristani, H. N., Verkhratsky, A., and Rodriguez, J. J. (2010). Concomitant astroglial atrophy and astrogliosis in a triple transgenic animal model of Alzheimer's disease. *Glia* 58, 831–838. doi: 10.1002/glia.20967

Olabarria, M., Noristani, H. N., Verkhratsky, A., and Rodriguez, J. J. (2011). Age-dependent decrease in glutamine synthetase expression in the hippocampal astroglia of the triple transgenic Alzheimer's disease mouse model: mechanism for deficient glutamatergic transmission? *Mol. Neurodegener.* 6, 55. doi: 10.1186/1750-1326-6-55

Oliet, S. H., Piet, R., and Poulain, D. A. (2001). Control of glutamate clearance and synaptic efficacy by glial coverage of neurons. *Science* 292, 923–926. doi: 10.1126/science.1059162

Orellana, J. A., Shoji, K. F., Abudara, V., Ezan, P., Amigou, E., Saez, P. J., et al. (2011). Amyloid beta-induced death in neurons involves glial and neuronal hemichannels. *J. Neurosci.* 31, 4962–4977. doi: 10.1523/JNEUROSCI.6417-10.2011

Orre, M., Kamphuis, W., Dooves, S., Kooijman, L., Chan, E. T., Kirk, C. J., et al. (2013). Reactive glia show increased immunoproteasome activity in Alzheimer's disease. *Brain* 136, 1415–1431. doi: 10.1093/brain/awt083

Orre, M., Kamphuis, W., Osborn, L. M., Jansen, A. H., Kooijman, L., Bossers, K., et al. (2014). Isolation of glia from Alzheimer's mice reveals inflammation and dysfunction. *Neurobiol. Aging* 35, 2746–2760. doi: 10.1016/j.neurobiolaging.2014.06.004

Ortinski, P. I., Dong, J., Mungenast, A., Yue, C., Takano, H., Watson, D. J., et al. (2010). Selective induction of astrocytic gliosis generates deficits in neuronal inhibition. *Nat. Neurosci.* 13, 584–591. doi: 10.1038/nn.2535

Owen, J. B., Di Domenico, F., Sultana, R., Perluigi, M., Cini, C., Pierce, W. M., et al. (2009). Proteomics-determined differences in the concanavalin-A-fractionated proteome of hippocampus and inferior parietal lobule in subjects with Alzheimer's disease and mild cognitive impairment: implications for progression of AD. *J. Proteome Res.* 8, 471–482. doi: 10.1021/pr800667a

Panatier, A., Arizono, M., and Nagerl, U. V. (2014). Dissecting tripartite synapses with STED microscopy. *Philos. Trans. R. Soc. Lond. B Biol. Sci.* 369:20130597. doi: 10.1098/rstb.2013.0597

Pearce, M. M., Spartz, E. J., Hong, W., Luo, L., and Kopito, R. R. (2015). Prion-like transmission of neuronal huntingtin aggregates to phagocytic glia in the Drosophila brain. *Nat. Commun.* 6, 6768. doi: 10.1038/ncomms7768

Pehar, M., Cassina, P., Vargas, M. R., Castellanos, R., Viera, L., Beckman, J. S., et al. (2004). Astrocytic production of nerve growth factor in motor neuron apoptosis: implications for amyotrophic lateral sclerosis. *J. Neurochem.* 89, 464–473. doi: 10.1111/j.1471-4159.2004.02357.x

Pellerin, L., and Magistretti, P. J. (1994). Glutamate uptake into astrocytes stimulates aerobic glycolysis: a mechanism coupling neuronal activity to glucose utilization. *Proc. Natl. Acad. Sci. U.S.A.* 91, 10625–10629. doi: 10.1073/pnas.91.22.10625

Pfrieger, F. W., and Ungerer, N. (2011). Cholesterol metabolism in neurons and astrocytes. *Prog. Lipid Res.* 50, 357–371. doi: 10.1016/j.plipres.2011.06.002

Philips, T., and Robberecht, W. (2011). Neuroinflammation in amyotrophic lateral sclerosis: role of glial activation in motor neuron disease. *Lancet Neurol.* 10, 253–263. doi: 10.1016/S1474-4422(11)70015-1

Pirttimaki, T. M., Codadu, N. K., Awni, A., Pratik, P., Nagel, D. A., Hill, E. J., et al. (2013). alpha7 Nicotinic receptor-mediated astrocytic gliotransmitter release: Abeta effects in a preclinical Alzheimer's mouse model. *PLoS ONE* 8:e81828. doi: 10.1371/journal.pone.0081828

Pons, S., and Torres-Aleman, I. (2000). Insulin-like growth factor-I stimulates dephosphorylation of ikappa B through the serine phosphatase calcineurin (protein phosphatase 2B). *J. Biol. Chem.* 275, 38620–38625. doi: 10.1074/jbc.M004531200

Popovic, D., Vucic, D., and Dikic, I. (2014). Ubiquitination in disease pathogenesis and treatment. *Nat. Med.* 20, 1242–1253. doi: 10.1038/nm.3739

Puschmann, T. B., Zanden, C., De Pablo, Y., Kirchhoff, F., Pekna, M., Liu, J., et al. (2013). Bioactive 3D cell culture system minimizes cellular stress and maintains the *in vivo*-like morphological complexity of astroglial cells. *Glia* 61, 432–440. doi: 10.1002/glia.22446

Puttaparthi, K., and Elliott, J. L. (2005). Non-neuronal induction of immunoproteasome subunits in an ALS model: possible mediation by cytokines. *Exp. Neurol.* 196, 441–451. doi: 10.1016/j.expneurol.2005.08.027

Puttaparthi, K., Van Kaer, L., and Elliott, J. L. (2007). Assessing the role of immuno-proteasomes in a mouse model of familial ALS. *Exp. Neurol.* 206, 53–58. doi: 10.1016/j.expneurol.2007.03.024

Querfurth, H. W., and Laferla, F. M. (2010). Alzheimer's disease. *N. Engl. J. Med.* 362, 329–344. doi: 10.1056/NEJMra0909142

Radde, R., Bolmont, T., Kaeser, S. A., Coomaraswamy, J., Lindau, D., Stoltze, L., et al. (2006). Abeta42-driven cerebral amyloidosis in transgenic mice reveals early and robust pathology. *EMBO Rep.* 7, 940–946. doi: 10.1038/sj.embor.7400784

Rebec, G. V. (2013). Dysregulation of corticostriatal ascorbate release and glutamate uptake in transgenic models of Huntington's disease. *Antioxid. Redox Signal.* 19, 2115–2128. doi: 10.1089/ars.2013.5387

Rebec, G. V., Barton, S. J., and Ennis, M. D. (2002). Dysregulation of ascorbate release in the striatum of behaving mice expressing the Huntington's disease gene. *J Neurosci* 22:RC202.

Robberecht, W., and Philips, T. (2013). The changing scene of amyotrophic lateral sclerosis. *Nat. Rev. Neurosci.* 14, 248–264. doi: 10.1038/nrn3430

Robel, S., Buckingham, S. C., Boni, J. L., Campbell, S. L., Danbolt, N. C., Riedemann, T., et al. (2015). Reactive astrogliosis causes the development of spontaneous seizures. *J. Neurosci.* 35, 3330–3345. doi: 10.1523/JNEUROSCI.1574-14.2015

Robel, S., Mori, T., Zoubaa, S., Schlegel, J., Sirko, S., Faissner, A., et al. (2009). Conditional deletion of beta1-integrin in astroglia causes partial reactive gliosis. *Glia* 57, 1630–1647. doi: 10.1002/glia.20876

Rojas, F., Cortes, N., Abarzua, S., Dyrda, A., and Van Zundert, B. (2014). Astrocytes expressing mutant SOD1 and TDP43 trigger motoneuron death that is mediated via sodium channels and nitroxidative stress. *Front. Cell. Neurosci.* 8:24. doi: 10.3389/fncel.2014.00024

Ross, B., Lin, A., Harris, K., Bhattacharya, P., and Schweinsburg, B. (2003). Clinical experience with 13C MRS *in vivo*. *NMR Biomed.* 16, 358–369. doi: 10.1002/nbm.852

Ross, C. A., and Poirier, M. A. (2004). Protein aggregation and neurodegenerative disease. *Nat. Med.* 10(Suppl.), S10–S17. doi: 10.1038/nm1066

Rossi, D., Brambilla, L., Valori, C. F., Crugnola, A., Giaccone, G., Capobianco, R., et al. (2005). Defective tumor necrosis factor-alpha-dependent control of astrocyte glutamate release in a transgenic mouse model of Alzheimer disease. *J. Biol. Chem.* 280, 42088–42096. doi: 10.1074/jbc.M504124200

Rothstein, J. D., Martin, L. J., and Kuncl, R. W. (1992). Decreased glutamate transport by the brain and spinal cord in amyotrophic lateral sclerosis. *N. Engl. J. Med.* 326, 1464–1468. doi: 10.1056/NEJM199205283262204

Rothstein, J. D., Patel, S., Regan, M. R., Haenggeli, C., Huang, Y. H., Bergles, D. E., et al. (2005). Beta-lactam antibiotics offer neuroprotection by increasing glutamate transporter expression. *Nature* 433, 73–77. doi: 10.1038/nature03180

Rothstein, J. D., Van Kammen, M., Levey, A. I., Martin, L. J., and Kuncl, R. W. (1995). Selective loss of glial glutamate transporter GLT-1 in amyotrophic lateral sclerosis. *Ann. Neurol.* 38, 73–84. doi: 10.1002/ana.410380114

Rouach, N., Koulakoff, A., Abudara, V., Willecke, K., and Giaume, C. (2008). Astroglial metabolic networks sustain hippocampal synaptic transmission. *Science* 322, 1551–1555. doi: 10.1126/science.1164022

Rufer, M., Wirth, S. B., Hofer, A., Dermietzel, R., Pastor, A., Kettenmann, H., et al. (1996). Regulation of connexin-43, GFAP, and FGF-2 is not accompanied by changes in astroglial coupling in MPTP-lesioned, FGF-2-treated parkinsonian mice. *J. Neurosci. Res.* 46, 606–617.

Sancheti, H., Patil, I., Kanamori, K., Diaz Brinton, R., Zhang, W., Lin, A. L., et al. (2014). Hypermetabolic state in the 7-month-old triple transgenic mouse model of Alzheimer's disease and the effect of lipoic acid: a 13C-NMR study. *J. Cereb. Blood Flow Metab.* 34, 1749–1760. doi: 10.1038/jcbfm.2014.137

Santello, M., and Volterra, A. (2012). TNFalpha in synaptic function: switching gears. *Trends Neurosci.* 35, 638–647. doi: 10.1016/j.tins.2012.06.001

Scimemi, A., Meabon, J. S., Woltjer, R. L., Sullivan, J. M., Diamond, J. S., and Cook, D. G. (2013). Amyloid-beta1-42 slows clearance of synaptically released glutamate by mislocalizing astrocytic GLT-1. *J. Neurosci.* 33, 5312–5318. doi: 10.1523/JNEUROSCI.5274-12.2013

Scott, H. A., Gebhardt, F. M., Mitrovic, A. D., Vandenberg, R. J., and Dodd, P. R. (2011). Glutamate transporter variants reduce glutamate uptake in Alzheimer's disease. *Neurobiol. Aging* 32, 553.e1-11. doi: 10.1016/j.neurobiolaging.2010.03.008

Seidel, J. L., Faideau, M., Aiba, I., Pannasch, U., Escartin, C., Rouach, N., et al. (2014). Ciliary neurotrophic factor (CNTF) activation of astrocytes decreases spreading depolarization susceptibility and increases potassium clearance. *Glia* 63, 91–103. doi: 10.1002/glia.22735

Sekar, S., McDonald, J., Cuyugan, L., Aldrich, J., Kurdoglu, A., Adkins, J., et al. (2015). Alzheimer's disease is associated with altered expression of genes involved in immune response and mitochondrial processes in astrocytes. *Neurobiol. Aging* 36, 583–591. doi: 10.1016/j.neurobiolaging.2014.09.027

Serrano-Pozo, A., Gomez-Isla, T., Growdon, J. H., Frosch, M. P., and Hyman, B. T. (2013). A phenotypic change but not proliferation underlies glial responses in Alzheimer disease. *Am. J. Pathol.* 182, 2332–2344. doi: 10.1016/j.ajpath.2013.02.031

Sharif, A., and Prevot, V. (2012). Isolation and culture of human astrocytes. *Methods Mol. Biol.* 814, 137–151. doi: 10.1007/978-1-61779-452-0_11

Sheng, J. G., Shirabe, S., Nishiyama, N., and Schwartz, J. P. (1993). Alterations in striatal glial fibrillary acidic protein expression in response to 6-hydroxydopamine-induced denervation. *Exp. Brain Res.* 95, 450–456. doi: 10.1007/BF00227138

Shibata, N., Kakita, A., Takahashi, H., Ihara, Y., Nobukuni, K., Fujimura, H., et al. (2009). Activation of signal transducer and activator of transcription-3 in the spinal cord of sporadic amyotrophic lateral sclerosis patients. *Neurodegener. Dis.* 6, 118–126. doi: 10.1159/000213762

Shibata, N., Yamamoto, T., Hiroi, A., Omi, Y., Kato, Y., and Kobayashi, M. (2010). Activation of STAT3 and inhibitory effects of pioglitazone on STAT3 activity in a mouse model of SOD1-mutated amyotrophic lateral sclerosis. *Neuropathology* 30, 353–360. doi: 10.1111/j.1440-1789.2009.01078.x

Shibuki, K., Gomi, H., Chen, L., Bao, S., Kim, J. J., Wakatsuki, H., et al. (1996). Deficient cerebellar long-term depression, impaired eyeblink conditioning, and normal motor coordination in GFAP mutant mice. *Neuron* 16, 587–599. doi: 10.1016/S0896-6273(00)80078-1

Sibson, N. R., Lowe, J. P., Blamire, A. M., Martin, M. J., Obrenovitch, T. P., and Anthony, D. C. (2008). Acute astrocyte activation in brain detected by MRI: new insights into T(1) hypointensity. *J. Cereb. Blood Flow Metab.* 28, 621–632. doi: 10.1038/sj.jcbfm.9600549

Simpson, J. E., Ince, P. G., Lace, G., Forster, G., Shaw, P. J., Matthews, F., et al. (2010). Astrocyte phenotype in relation to Alzheimer-type pathology in the ageing brain. *Neurobiol. Aging* 31, 578–590. doi: 10.1016/j.neurobiolaging.2008.05.015

Simpson, J. E., Ince, P. G., Shaw, P. J., Heath, P. R., Raman, R., Garwood, C. J., et al. (2011). Microarray analysis of the astrocyte transcriptome in the aging brain: relationship to Alzheimer's pathology and APOE genotype. *Neurobiol. Aging* 32, 1795–1807. doi: 10.1016/j.neurobiolaging.2011.04.013

Singhrao, S. K., Neal, J. W., Morgan, B. P., and Gasque, P. (1999). Increased complement biosynthesis by microglia and complement activation on neurons in Huntington's disease. *Exp. Neurol.* 159, 362–376. doi: 10.1006/exnr.1999.7170

Sirko, S., Behrendt, G., Johansson, P. A., Tripathi, P., Costa, M., Bek, S., et al. (2013). Reactive glia in the injured brain acquire stem cell properties in response to sonic hedgehog glia. *Cell Stem Cell* 12, 426–439. doi: 10.1016/j.stem.2013.01.019

Sloan, S. A., and Barres, B. A. (2014). Looks can be deceiving: reconsidering the evidence for gliotransmission. *Neuron* 84, 1112–1115. doi: 10.1016/j.neuron.2014.12.003

Sofroniew, M. V. (2009). Molecular dissection of reactive astrogliosis and glial scar formation. *Trends Neurosci.* 32, 638–647. doi: 10.1016/j.tins.2009.08.002

Sofroniew, M. V. (2014). Multiple roles for astrocytes as effectors of cytokines and inflammatory mediators. *Neuroscientist* 20, 160–172. doi: 10.1177/1073858413504466

Sofroniew, M. V. (2015). Astrocyte barriers to neurotoxic inflammation. *Nat. Rev. Neurosci.* 16, 249–263. doi: 10.1038/nrn3898

Sofroniew, M. V., and Vinters, H. V. (2010). Astrocytes: biology and pathology. *Acta Neuropathol.* 119, 7–35. doi: 10.1007/s00401-009-0619-8

Somjen, G. G. (1988). Nervenkitt: notes on the history of the concept of neuroglia. *Glia* 1, 2–9. doi: 10.1002/glia.440010103

Soni, N., Reddy, B. V., and Kumar, P. (2014). GLT-1 transporter: an effective pharmacological target for various neurological disorders. *Pharmacol. Biochem. Behav.* 127, 70–81. doi: 10.1016/j.pbb.2014.10.001

Sriram, K., Benkovic, S. A., Hebert, M. A., Miller, D. B., and O'callaghan, J. P. (2004). Induction of gp130-related cytokines and activation of JAK2/STAT3 pathway in astrocytes precedes up-regulation of glial fibrillary acidic protein in the 1-methyl-4-phenyl-1,2,3,6-tetrahydropyridine model of neurodegeneration: key signaling pathway for astrogliosis *in vivo*? *J. Biol. Chem.* 279, 19936–19947. doi: 10.1074/jbc.M309304200

Takano, T., Han, X., Deane, R., Zlokovic, B., and Nedergaard, M. (2007). Two-photon imaging of astrocytic Ca2+ signaling and the microvasculature in experimental mice models of Alzheimer's disease. *Ann. N.Y. Acad. Sci.* 1097, 40–50. doi: 10.1196/annals.1379.004

Talantova, M., Sanz-Blasco, S., Zhang, X., Xia, P., Akhtar, M. W., Okamoto, S., et al. (2013). Abeta induces astrocytic glutamate release, extrasynaptic NMDA receptor activation, and synaptic loss. *Proc. Natl. Acad. Sci. U.S.A.* 110, E2518–E2527. doi: 10.1073/pnas.1306832110

Terai, K., Matsuo, A., and McGeer, P. L. (1996). Enhancement of immunoreactivity for NF-kappa B in the hippocampal formation and cerebral cortex of Alzheimer's disease. *Brain Res.* 735, 159–168. doi: 10.1016/0006-8993(96)00310-1

Thal, D. R. (2012). The role of astrocytes in amyloid beta-protein toxicity and clearance. *Exp. Neurol.* 236, 1–5. doi: 10.1016/j.expneurol.2012.04.021

Tong, X., Ao, Y., Faas, G. C., Nwaobi, S. E., Xu, J., Haustein, M. D., et al. (2014). Astrocyte Kir4.1 ion channel deficits contribute to neuronal dysfunction in Huntington's disease model mice. *Nat. Neurosci.* 17, 694–703. doi: 10.1038/nn.3691

Tortarolo, M., Veglianese, P., Calvaresi, N., Botturi, A., Rossi, C., Giorgini, A., et al. (2003). Persistent activation of p38 mitogen-activated protein kinase in a mouse model of familial amyotrophic lateral sclerosis correlates with disease progression. *Mol. Cell. Neurosci.* 23, 180–192. doi: 10.1016/S1044-7431(03)00022-8

Trager, U., Andre, R., Lahiri, N., Magnusson-Lind, A., Weiss, A., Grueninger, S., et al. (2014). HTT-lowering reverses Huntington's disease immune dysfunction caused by NFkappaB pathway dysregulation. *Brain* 137, 819–833. doi: 10.1093/brain/awt355

Tsai, H. H., Li, H., Fuentealba, L. C., Molofsky, A. V., Taveira-Marques, R., Zhuang, H., et al. (2012). Regional astrocyte allocation regulates CNS synaptogenesis and repair. *Science* 337, 358–362. doi: 10.1126/science.1222381

Turner, B. J., and Talbot, K. (2008). Transgenics, toxicity and therapeutics in rodent models of mutant SOD1-mediated familial ALS. *Prog. Neurobiol.* 85, 94–134. doi: 10.1016/j.pneurobio.2008.01.001

Tydlacka, S., Wang, C. E., Wang, X., Li, S., and Li, X. J. (2008). Differential activities of the ubiquitin-proteasome system in neurons versus glia may account for the preferential accumulation of misfolded proteins in neurons. *J. Neurosci.* 28, 13285–13295. doi: 10.1523/JNEUROSCI.4393-08.2008

Valenza, M., Leoni, V., Karasinska, J. M., Petricca, L., Fan, J., Carroll, J., et al. (2010). Cholesterol defect is marked across multiple rodent models of Huntington's disease and is manifest in astrocytes. *J. Neurosci.* 30, 10844–10850. doi: 10.1523/JNEUROSCI.0917-10.2010

Valenza, M., Marullo, M., Di Paolo, E., Cesana, E., Zuccato, C., Biella, G., et al. (2015). Disruption of astrocyte-neuron cholesterol cross talk affects neuronal function in Huntington's disease. *Cell Death Differ.* 22, 690–702. doi: 10.1038/cdd.2014.162

Vargas, M. R., Johnson, D. A., Sirkis, D. W., Messing, A., and Johnson, J. A. (2008). Nrf2 activation in astrocytes protects against neurodegeneration in mouse models of familial amyotrophic lateral sclerosis. *J. Neurosci.* 28, 13574–13581. doi: 10.1523/JNEUROSCI.4099-08.2008

Vargas, M. R., and Johnson, J. A. (2009). The Nrf2-ARE cytoprotective pathway in astrocytes. *Expert Rev. Mol. Med.* 11, e17. doi: 10.1017/S1462399409001094

Vargas, M. R., Pehar, M., Cassina, P., Martinez-Palma, L., Thompson, J. A., Beckman, J. S., et al. (2005). Fibroblast growth factor-1 induces heme oxygenase-1 via nuclear factor erythroid 2-related factor 2 (Nrf2) in spinal cord astrocytes: consequences for motor neuron survival. *J. Biol. Chem.* 280, 25571–25579. doi: 10.1074/jbc.M501920200

Venneti, S., Lopresti, B. J., and Wiley, C. A. (2006). The peripheral benzodiazepine receptor (Translocator protein 18kDa) in microglia: from pathology to imaging. *Prog. Neurobiol.* 80, 308–322. doi: 10.1016/j.pneurobio.2006.10.002

Vincent, A. J., Gasperini, R., Foa, L., and Small, D. H. (2010). Astrocytes in Alzheimer's disease: emerging roles in calcium dysregulation and synaptic plasticity. *J. Alzheimers. Dis.* 22, 699–714. doi: 10.3233/JAD-2010-101089

Virchow, R. (1856). *Gesammelte Abhandlungen zur wissenschaftlichen Medizin*. Frankfurt: Verlag von Meidinger Sohn & Comp.

Vis, J. C., Nicholson, L. F., Faull, R. L., Evans, W. H., Severs, N. J., and Green, C. R. (1998). Connexin expression in Huntington's diseased human brain. *Cell Biol. Int.* 22, 837–847. doi: 10.1006/cbir.1998.0388

Vonsattel, J. P., Myers, R. H., Stevens, T. J., Ferrante, R. J., Bird, E. D., and Richardson, E. P. Jr. (1985). Neuropathological classification of Huntington's disease. *J. Neuropathol. Exp. Neurol.* 44, 559–577. doi: 10.1097/00005072-198511000-00003

Wang, C. Y., Yang, S. H., and Tzeng, S. F. (2015). MicroRNA-145 as one negative regulator of astrogliosis. *Glia* 63, 194–205. doi: 10.1002/glia.22743

Wang, L., Lin, F., Wang, J., Wu, J., Han, R., Zhu, L., et al. (2012). Expression of mutant N-terminal huntingtin fragment (htt552-100Q) in astrocytes suppresses the secretion of BDNF. *Brain Res.* 1449, 69–82. doi: 10.1016/j.brainres.2012.01.077

Washburn, K. B., and Neary, J. T. (2006). P2 purinergic receptors signal to STAT3 in astrocytes: difference in STAT3 responses to P2Y and P2X receptor activation. *Neuroscience* 142, 411–423. doi: 10.1016/j.neuroscience.2006.06.034

Weigert, C. (1895). "Beiträge zur Kenntnis der normalen menschlichen Neuroglia," in *Zeitschrift für Psychologie und Physiologie der Sinnesorgane*, ed Liepmann (Frankfurt: Moritz Diesterweg).

Wild, E. J., and Tabrizi, S. J. (2014). Targets for future clinical trials in Huntington's disease: what's in the pipeline? *Mov. Disord.* 29, 1434–1445. doi: 10.1002/mds.26007

Wilhelmsson, U., Bushong, E. A., Price, D. L., Smarr, B. L., Phung, V., Terada, M., et al. (2006). Redefining the concept of reactive astrocytes as cells that remain within their unique domains upon reaction to injury. *Proc. Natl. Acad. Sci. U.S.A.* 103, 17513–17518. doi: 10.1073/pnas.0602841103

Witjas, T., Kaphan, E., Azulay, J. P., Blin, O., Ceccaldi, M., Pouget, J., et al. (2002). Nonmotor fluctuations in Parkinson's disease: frequent and disabling. *Neurology* 59, 408–413. doi: 10.1212/WNL.59.3.408

Witte, S., and Muljo, S. A. (2014). Integrating non-coding RNAs in JAK-STAT regulatory networks. *JAKSTAT* 3, e28055. doi: 10.4161/jkst.28055

Wojtowicz, A. M., Dvorzhak, A., Semtner, M., and Grantyn, R. (2013). Reduced tonic inhibition in striatal output neurons from Huntington mice due to loss of astrocytic GABA release through GAT-3. *Front. Neural Circuits* 7:188. doi: 10.3389/fncir.2013.00188

Woltjer, R. L., Duerson, K., Fullmer, J. M., Mookherjee, P., Ryan, A. M., Montine, T. J., et al. (2010). Aberrant detergent-insoluble excitatory amino acid transporter 2 accumulates in Alzheimer disease. *J. Neuropathol. Exp. Neurol.* 69, 667–676. doi: 10.1097/NEN.0b013e3181e24adb

Wu, Z., Guo, Z., Gearing, M., and Chen, G. (2014). Tonic inhibition in dentate gyrus impairs long-term potentiation and memory in an Alzhiemer's disease model. *Nat. Commun.* 5, 4159. doi: 10.1038/ncomms5159

Wyss-Coray, T., Loike, J. D., Brionne, T. C., Lu, E., Anankov, R., Yan, F., et al. (2003). Adult mouse astrocytes degrade amyloid-beta *in vitro* and *in situ*. *Nat. Med.* 9, 453–457. doi: 10.1038/nm838

Xiao, Q., Yan, P., Ma, X., Liu, H., Perez, R., Zhu, A., et al. (2014). Enhancing astrocytic lysosome biogenesis facilitates abeta clearance and attenuates amyloid plaque pathogenesis. *J. Neurosci.* 34, 9607–9620. doi: 10.1523/JNEUROSCI.3788-13.2014

Yan, P., Hu, X., Song, H., Yin, K., Bateman, R. J., Cirrito, J. R., et al. (2006). Matrix metalloproteinase-9 degrades amyloid-beta fibrils *in vitro* and compact plaques *in situ*. *J. Biol. Chem.* 281, 24566–24574. doi: 10.1074/jbc.M602440200

Yoshii, Y., Otomo, A., Pan, L., Ohtsuka, M., and Hadano, S. (2011). Loss of glial fibrillary acidic protein marginally accelerates disease progression in a SOD1(H46R) transgenic mouse model of ALS. *Neurosci. Res.* 70, 321–329. doi: 10.1016/j.neures.2011.03.006

Zamanian, J. L., Xu, L., Foo, L. C., Nouri, N., Zhou, L., Giffard, R. G., et al. (2012). Genomic analysis of reactive astrogliosis. *J. Neurosci.* 32, 6391–6410. doi: 10.1523/JNEUROSCI.6221-11.2012

Zeis, T., Allaman, I., Gentner, M., Schroder, K., Tschopp, J., Magistretti, P. J., et al. (2015). Metabolic gene expression changes in astrocytes in Multiple Sclerosis cerebral cortex are indicative of immune-mediated signaling. *Brain Behav. Immun.* doi: 10.1016/j.bbi.2015.04.013. [Epub ahead of print].

Zlokovic, B. V. (2008). The blood-brain barrier in health and chronic neurodegenerative disorders. *Neuron* 57, 178–201. doi: 10.1016/j.neuron.2008.01.003

Conflict of Interest Statement: The authors declare that the research was conducted in the absence of any commercial or financial relationships that could be construed as a potential conflict of interest.

Publication 2

Neuroscience 330 (2016) 205–218

NEUROSCIENCE FOREFRONT REVIEW

THE COMPLEX STATES OF ASTROCYTE REACTIVITY: HOW ARE THEY CONTROLLED BY THE JAK–STAT3 PATHWAY?

KELLY CEYZÉRIAT, [a,b] **LAURENE ABJEAN,** [a,b] **MARÍA-ANGELES CARRILLO-DE SAUVAGE,** [a,b] **LUCILE BEN HAIM** [a,b,c] **AND CAROLE ESCARTIN** [a,b]*

[a] *Commissariat à l'Energie Atomique et aux Energies Alternatives (CEA), Département de la Recherche Fondamentale (DRF), Institut d'Imagerie Biomédicale (I2BM), MIRCen, F-92260 Fontenay-aux-Roses, France*

[b] *Centre National de la Recherche Scientifique (CNRS), Université Paris-Sud, UMR 9199, Neurodegenerative Diseases Laboratory, F-92260 Fontenay-aux-Roses, France*

[c] *Eli and Edythe Broad Institute for Stem Cell Research and Regeneration Medicine, University of California, San Francisco, CA 94143, USA*

Abstract—Astrocytes play multiple important roles in brain physiology. In pathological conditions, they become reactive, which is characterized by morphological changes and upregulation of intermediate filament proteins. Besides these descriptive hallmarks, astrocyte reactivity involves significant transcriptional and functional changes that are far from being fully understood. Most importantly, astrocyte reactivity seems to encompass multiple states, each having a specific influence on surrounding cells and disease progression. These diverse functional states of reactivity must be regulated by subtle signaling networks. Many signaling cascades have been associated with astrocyte reactivity, but among them, the JAK–STAT3 pathway is emerging as a central regulator. In this review, we aim (i) to show that the JAK–STAT3 pathway plays a key role in the control of astrocyte reactivity, (ii) to illustrate that STAT3 is a pleiotropic molecule operating multiple functions in reactive astrocytes, and (iii) to suggest that each specific functional state of reactivity is governed by complex molecular interactions within astrocytes, which converge on STAT3. More research is needed to precisely identify the signaling networks controlling the diverse states of astrocyte reactivity. Only then, we will be able to precisely delineate the therapeutic potential of reactive astrocytes in each neurological disease context.

Key words: reactive astrocytes, STAT3, JAK–STAT pathway, neurological diseases, signaling cascades.

Contents

*Correspondence to: C. Escartin, UMR9199, MIRCen, Bat 61, 18, route du Panorama, 92260 Fontenay-aux-Roses, France.
E-mail addresses: Kelly.ceyzeriat@cea.fr (K. Ceyzériat), Laurene.abjean@cea.fr (L. Abjean), maria.carrillo@cea.fr (M.-A. Carrillo-de Sauvage), Lucile.BenHaim@ucsf.edu (L. Ben Haim), carole.escartin@cea.fr (C. Escartin).

Abbreviations: AD, Alzheimer's disease; ALS, amyotrophic lateral sclerosis; CNS, central nervous system; CNTF, ciliary neurotrophic factor; Cx43, connexin 43; DN, dominant negative; EGF, epidermal growth factor; ETC, electron transport chain; GFAP, glial fibrillary acidic protein; GPCR, G-protein-coupled receptor; HD, Huntington's disease; HDAC, histone deacetylase; IL, interleukin; JAK, janus kinase; KO, knock out; Lcn2, lipocalin 2; LPS, lipopolysaccharide; Lys, lysine; MAPK, mitogen-activated protein kinase; MCAO, middle cerebral artery occlusion; MMP, matrix metallo-proteinase; MPTP, 1-methyl-4-phenyl-1,2,3,6-tetrahydropyridine; MS, multiple sclerosis; mSTAT3, mitochondrial STAT3; MnSOD, manganese superoxide dismutase; ND, neurodegenerative diseases; NF-κB, nuclear factor kappa-light-chain-enhancer of activated B cells; PD, Parkinson's disease; PIAS, protein inhibitor of activated STAT; PKR, protein kinase R; PTM, post-translational modifications; ROS, reactive oxygen species; SCI, spinal cord injury; Ser, serine; Shh, Sonic Hedgehog; SOCS, suppressor of cytokine signaling; SRE, STAT3-responsive element; STAT, signal transducer and activator of transcription; TBI, traumatic brain injury; TSP1, thrombospondin-1; Tyr, tyrosine; UCP, uncoupling protein.

http://dx.doi.org/10.1016/j.neuroscience.2016.05.043
0306-4522/

INTRODUCTION

In response to the multiple pathological conditions that affect the central nervous system (CNS), astrocytes become reactive. This response develops after acute injuries such as ischemia, traumatic brain injury (TBI), spinal cord injury (SCI) or infection, as well as under progressive conditions like neurodegenerative diseases (ND) or multiple sclerosis (MS). Astrocyte reactivity was initially characterized by morphological changes (hypertrophy of soma and processes) and by the upregulation of intermediate filament proteins such as glial fibrillary acidic protein (GFAP) or vimentin. Besides these two hallmarks, astrocyte reactivity involves multiple transcriptional and functional changes that are still being elucidated (Burda and Sofroniew, 2014; Pekny and Pekna, 2014; Ben Haim et al., 2015a). Importantly, astrocyte reactivity is now recognized as a heterogeneous response resulting in various functional states depending on the disease context. In fact, it is important to note that reactivity is not the only change observed in astrocytes during diseases. For example, astrocytes may be dystrophic in the brain of patients with schizophrenia or even degenerate following encephalopathies. They may directly be hit by the disease and dysfunction, like in Alexander's disease, which is caused by mutations in the *gfap* gene (Verkhratsky et al., 2015; Pekny et al., 2016).

Given the multiple roles operated by astrocytes in physiological conditions (Parpura et al., 2012), the functional changes occurring with reactivity could have major consequences on surrounding cells like neurons or microglial cells and influence disease progression. Therefore, it is crucial to unravel the signaling cascades controlling the specific states of astrocyte reactivity.

Multiple pathways are associated with astrocyte reactivity (Buffo et al., 2010; Kang and Hebert, 2011; Ben Haim et al., 2015a). Among them, the janus kinase-signal transducer and activator of transcription 3 (JAK–STAT3) pathway seems to play a central role that we will cover in this review.

We will focus on the roles of STAT3 in astrocytes during various brain diseases, but we will also describe data from other cell types in the CNS or peripheral organs, when they give insight into the functions of the JAK–STAT3 pathway. Indeed, seminal discoveries on this cascade were made in cell cultures in the fields of Immunology and Oncology. Although very potent, *in vitro* studies have serious limitations when applied to the brain, because of the significant phenotypic changes occurring when brain cells are isolated in a dish. This is especially true for primary astrocytes that tend to become reactive without stimulation (Ben Haim et al., 2015a). In this review, we will thus present *in vivo* studies whenever possible, and landmark *in vitro* studies to illustrate the complex roles played by STAT3 in the control of astrocyte reactivity. We will (i) show that the JAK–STAT3 pathway plays a key role in the control of astrocyte reactivity, (ii) illustrate that STAT3 is a pleiotropic molecule operating multiple functions in reactive astrocytes and (iii) propose that each specific functional state of reactivity is governed by complex molecular interactions within astrocytes, which converge on STAT3.

THE JAK–STAT3 PATHWAY

A linear, canonical JAK–STAT3 pathway from the membrane to the nucleus

The JAK–STAT pathway is a ubiquitous, evolutionarily conserved signaling cascade, present in various species from *Dictyostelium* and *Drosophila* to mammals (Decker and Kovarik, 2000). It was discovered more than twenty years ago, as the cascade mediating interferon effects (Darnell et al., 1994; Stark and Darnell, 2012). There are four JAKs (JAK1-3, and TYK2) and seven STATs (STAT1-4, 5A, 5B, and 6) in mammals (Darnell, 1997). STAT3 was sequenced and cloned in 1994 (Akira et al., 1994; Zhong et al., 1994b). STAT3 is well expressed in the brain (Zhong et al., 1994a) and has been the most extensively STAT studied in the context of astrocyte reactivity.

The canonical JAK–STAT3 pathway is activated by the binding of polypeptides such as cytokines, hormones or growth factors to their multimeric receptor (Mertens and Darnell, 2007, Fig. 1). Conformational changes on the intracellular tail of the receptor bring the kinase domains of two JAKs in apposition (Brooks et al., 2014). JAKs are receptor-associated tyrosine (Tyr) kinases that phosphorylate each other and the receptor on several residues. The latent transcription factor STAT3 is then recruited to the phosphorylated receptor through its Src homology 2 (SH2) domain and is transphosphorylated by JAK on Tyr705 (Lim and Cao, 2006). Phospho-STAT3 proteins dimerize and accumulate in the nucleus. There, dimers of phospho-STAT3 bind specific sequences called STAT3-responsive elements (SRE) in the promoter of target genes and induce their transcription (Shuai et al., 1993; Darnell, 1997). These transcriptional changes impact cell growth, proliferation, differentiation and survival. This pathway is particularly important during development and immune responses, and its dysregulation is involved in cancer and immune diseases (see, Yu et al., 2009; O'Shea et al., 2013, for a complete review, as this will not be developed here). Activation of the JAK–STAT3 pathway increases the expression of several elements of the pathway, including *stat3* itself, which promotes a positive feedback loop (Hutchins et al., 2013).

Additional branching points on the pathway increase the complexity of STAT3 signaling cascades

Besides the linear "canonical" pathway, STAT3 is connected to alternative signaling cascades within the cell (Fig. 1).

First, some G-protein-coupled receptors (GPCRs), which are seven-transmembrane domain receptors for growth factors or purines, may be coupled to JAKs and phosphorylate STAT3 (Mertens and Darnell, 2007). Alternatively, STAT3 can be phosphorylated on Tyr705 by other upstream kinases than JAKs (Fig. 1). They include receptors with an intrinsic Tyr kinase activity, like the receptor for epidermal growth factor (EGF), and non-receptor Tyr kinases, which are usually cytoplasmic and of viral origin, such as v-src (Mertens and Darnell, 2007).

In addition, STAT3 can be phosphorylated on Serine 727 (Ser727) by various Ser kinases, especially by mitogen-activated protein kinases (MAPK) (Wen et al., 1995; Decker and Kovarik, 2000). Depending on the

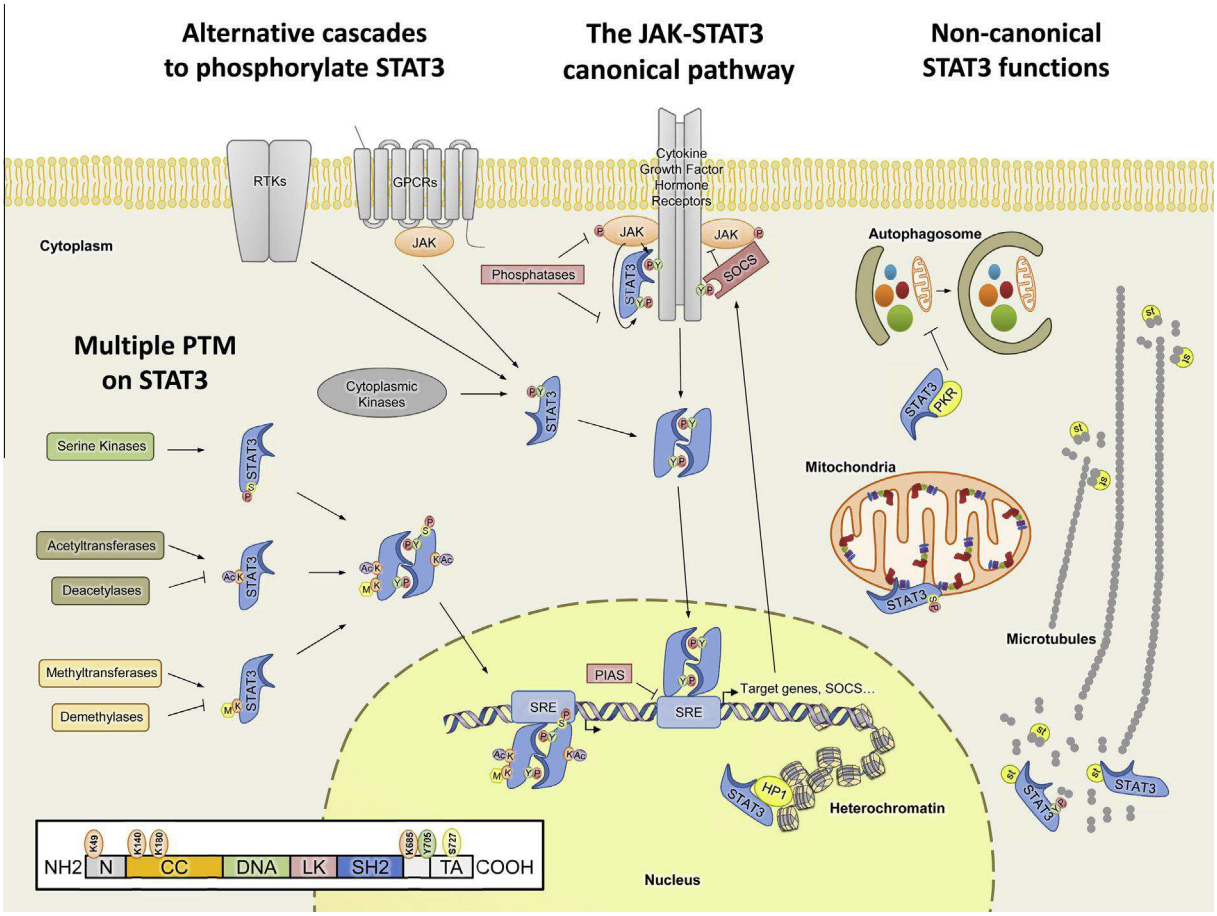

Fig. 1. STAT3 is a signaling hub. STAT3 is involved in complex signaling cascades within the cell. The **canonical JAK–STAT3 pathway** (center), is triggered by the binding of cytokines, hormones or growth factors to their multimeric receptors (e.g. receptors for IL, growth hormone, CNTF or LIF). It causes conformational changes and activation of JAKs bound to the receptor. JAKs phosphorylate the receptor and then STAT3, after its recruitment to the phosphorylated receptor through its SH2 domain. Tyr705-phospho-STAT3 dimerizes and accumulates in the nucleus where it recognizes SRE in the promoter region of target genes, inducing their transcription. STAT3 is involved in **alternative signaling cascades** (left). It can be directly phosphorylated on Tyr705 by receptors with an intrinsic Tyr kinase activity (RTK, e.g. receptors for EGF or platelet-derived growth factor) or by cytoplasmic kinases like v-src. Alternatively, GPCRs (which include receptors for purines, growth factors like angiotensin, or for chemokines like CCL5), can trigger Tyr705 phosphorylation by JAK (Reich and Liu, 2006; Mertens and Darnell, 2007). STAT3 may also be phosphorylated at Ser727 by Ser kinases such as MAP kinases. **Additional PTMs** on STAT3 include Lys acetylations, which are regulated by acetyltransferases (like p300/CBP) and deacetylases (like HDACs) and methylations, which are regulated by methyltransferases (like EZH2 or SET9) and demethylases (like LSD1). These PTMs may occur in the cytoplasm or in the nucleus. Overall, multiple isoforms of STATS with different sets of PTMs (two are represented on the left) can be present in the nucleus, each with its own transcriptional activity. Even unphosphorylated STAT3 may activate the transcription of some genes. Finally, STAT3 performs **non-canonical functions** through non-transcriptional mechanisms (right). STAT3 contributes to the maintenance of cellular shape and migration by preventing stathmins (st) from sequestering tubulin and destabilizing microtubule networks. STAT3 is also present in the mitochondria where it regulates energy production, antioxidant defense and apoptosis. The phosphorylation of Ser727 appears to be important for these functions (Yang and Rincon, 2016). STAT3 also represses autophagy by inhibiting PKR and stabilizes heterochromatin by binding to HP1. The JAK–STAT3 pathway is inhibited by at least three mechanisms: (i) dephosphorylation of the receptors, JAKs and STAT3 by phosphatases like SHP2, (ii) direct inhibition of JAKs by SOCS proteins and (iii) inhibition of DNA binding by PIAS in the nucleus. It is important to note that most of these cascades, PTMs and non-canonical functions have been primarily studied in cell types other than astrocytes. They are rather unexplored in the context of astrocyte reactivity. **Insert**: STAT3 is composed of several functional domains: the N terminal domain (N), the coiled-coiled domain (CC), the DNA binding domain (DNA) and the linker domain (LK). The SH2 domain binds to phospho-Tyr on the receptor and on other STATs for dimer formation. The transactivator domain (TA) is responsible for transcriptional induction. Tyr705 (Y705) and Ser727 (S727) are represented, as well as the main Lys that are acetylated or methylated. Ac = acetylation; M = methylation; P = phosphorylation; K = lysine; S = serine; Y = tyrosine. For other abbreviations, see main text.

experimental conditions (stimulus, promoter studied, cell type), phosphorylation at Ser727 has positive or negative effects on Tyr705-dependent transcription (Decker and Kovarik, 2000). Activation of STAT3 via P2Y receptors was reported in astrocyte cultures, resulting in the phosphorylation of both Tyr705 and Ser727 (Washburn and Neary, 2006). Other toxic stimuli were reported to trigger Ser727 phosphorylation like TBI (Oliva et al., 2012, see Fig. 2), or lipopolysaccharide (LPS, Moravcova et al., 2016).

Lastly, besides phosphorylations, STAT3 is subjected to multiple other post-translational modifications (PTM, see Fig. 1) that modulate its transcriptional activity (Lim and Cao, 2006). STAT3 is acetylated on several Lysine (Lys) residues. Acetylation levels are regulated by the balance of activity between histone acetyl-transferases like p300/CREB binding protein and deacetylases like histone deacetylases (HDAC, Zhuang, 2013). Acetylation of Lys685 by p300 promotes STAT3 dimerization, nuclear

localization and transcriptional activation (Wang et al., 2005; Yuan et al., 2005). STAT3 acetylation was recently observed in hypothalamic neurons (Chen et al., 2015) and cultured microglia (Eufemi et al., 2015) but its physiological role in astrocytes is largely unexplored. STAT3 may also be methylated on several Lys residues, which influences the pattern of genes regulated by STAT3 (Yang et al., 2010; Kim et al., 2013; Dasgupta et al., 2015). *In vitro* studies suggest that even non-phosphorylated STAT3 is able to increase the transcription of specific genes (Yang and Stark, 2008).

Overall, STAT3 represents a hub for multiple signaling cascades that converge towards the nucleus to modulate transcriptional activity.

STAT3 has non-canonical functions independent of transcription

Another layer of complexity in STAT3 signaling was discovered more recently, when STAT3 was found to be more than a simple transcription factor (see, Gao and Bromberg, 2006, and Fig. 1). In the nucleus, STAT3 also induces global chromatin remodeling (Li, 2008). STAT3 is able to interact with microtubules to regulate their stability (Ng et al., 2006, and section "STAT3 modulates astrocyte morphology and migration"). In the cytoplasm, STAT3 may also participate in the control of the autophagic flux by binding to protein kinase R (PKR, Shen et al., 2012, and section "Other important functions for STAT3 in astrocytes") or contribute to long term depression in hippocampal neurons, by yet unknown mechanisms independent of transcription (Nicolas et al., 2012). Last, STAT3 is found in mitochondria where it modulates their functions (Yang and Rincon, 2016, and section "STAT3 regulates mitochondrial functions").

It is important to note that most of these alternative, non-transcriptional STAT3 functions have been characterized in cancer and immune cells *in vitro* (Mohr et al., 2012). Whether they also occur in astrocytes *in situ*, is mostly unknown.

Retro-controls on the JAK–STAT3 pathway

The JAK–STAT3 pathway is tightly regulated by phosphatases, suppressors of cytokine signaling (a family of eight members SOCS1–7 and CIS) and protein inhibitors of activated STAT (PIAS) (Heinrich et al., 2003, and see Fig. 1). Protein Tyr phosphatases like Src homology 2 domain-containing phosphatase 2 (SHP2) terminate signal transduction at the different steps of the pathway. They may dephosphorylate the receptor, JAKs or STAT3, including within the nucleus (Heinrich et al., 2003; Mertens and Darnell, 2007). SOCS proteins inhibit JAK–STAT3 signaling by two mechanisms: they either promote ubiquitination of JAKs and their associated receptors, targeting them for proteasome degradation or they directly inhibit JAK activity (Babon et al., 2014). The second mechanism is more prominent in the case of SOCS1 and 3, the two most studied SOCSs (Babon et al., 2014). SOCS3 is a very efficient inhibitor of the JAK2–STAT3 pathway, thanks to its capacity to bind JAK2 and the activated, phosphorylated receptor concomitantly, acting as a pseudo-substrate for JAK2 (Kershaw et al., 2013). SOCS3 expression is strongly induced by the JAK–STAT3 pathway, operating a retro-control on the pathway. On the contrary, the expression of PIAS is constitutive. PIAS3 interacts with phosphorylated STAT3 in the nucleus and reduces its binding to DNA (Chung et al., 1997; Lim and Cao, 2006).

Box 1: An extensive toolbox to study the JAK–STAT3 pathway

There are many molecular tools and techniques to study the JAK–STAT3 pathway in the brain.

A. To evidence the activation of the pathway with biochemical & histological techniques:

Standard and widely used techniques applied to *in vitro* or *in vivo* samples include (see Fig. 2 for examples):

- Detection of phosphorylated active forms (e.g. gp130, JAK, STAT3). Phospho-specific antibodies may be used for western blotting, ELISA or immunostaining on slices, cultured cells or cell suspensions for cytometry analysis.
- Detection of STAT3 nuclear translocation by immunostaining or subcellular fractionation.
- Detection of transcriptional induction of target genes by RT-qPCR (e.g. *socs3, stat3*).
- Detection of STAT3 binding to specific DNA sequences by electromobility shift assay or chromatin immunoprecipitation.

B. To monitor the activity of the pathway with reporter systems

- **To monitor transcriptional induction:** Consensus SRE ($TTG(N)_3CAA$), coupled with a minimal promoter control the expression of a fluorescent protein or an enzyme whose activity is easily measured (e.g. luciferase, alkaline phosphatase, β-galactosidase). Such reporters are generally used *in vitro* but, they could be used to produce viral vectors (Gabel et al., 2010) to infect brain cells or to generate transgenic reporter mice.
- **To monitor STAT3 intracellular trafficking:** STAT3 is tagged with a fluorescent protein, and its subcellular location and trafficking is monitored by time-lapse fluorescent microscopy or fluorescent recovery after photobleaching (FRAP, Selvaraj et al., 2012).
- **To monitor the formation of protein complexes:** Förster resonance energy transfer (FRET) imaging can be used to reveal protein-protein interactions, for example, when STAT3 dimerizes (Kretzschmar et al., 2004) or when JAK2 is activated at the growth hormone receptor (Brooks et al., 2014).

C. To modulate the JAK–STAT3 pathway

- **Pharmacological inhibitors:** They are numerous inhibitors of JAKs and STAT3. They were initially developed for the treatment of cancer and immune diseases (Yu et al., 2009; O'Shea et al., 2013). AG490 and Stattic are two commonly used inhibitors of JAK2 and STAT3 respectively (Meydan et al., 1996; Schust et al., 2006). Their use may be limited by poor blood brain barrier penetration and their potential side-effects on multiple cell types in the brain and periphery.
- **Conditional KO:** Given the important developmental and peripheral roles of the pathway, conditional recombination is required to restrict expression of the Cre recombinase to astrocytes by specific promoters such as the *gfap* promoter (Herrmann et al., 2008). It is also advisable to control the time window of recombination with *tet*-operated promoters or by using tamoxifen inducible Cre (Pfrieger and Slezak, 2012).
- **Expression of inhibitors or dominant negative mutants:** Several mutant forms of STAT3 have been developed. They act as dominant negatives [e.g. $STAT3^{Y705F}$, STAT3D with a mutation in the DNA binding domain (Nakajima et al., 1996; He et al., 2005; Kohro et al., 2015)]. Alternatively, expression of endogenous inhibitors like SOCS3 in astrocytes prevents STAT3 activation (Ben Haim et al., 2015b).
- **Expression of constitutively active mutants:** Introduction of two cysteine residues by point mutation in STAT3 was used to create STAT3-C, a mutant that should be capable of auto-dimerization by disulfide bonds (Bromberg et al., 1999). Recent studies suggest that STAT3-C still needs to be phosphorylated to bind DNA, but it does so with greater efficacy (Li and Shaw, 2006).

THE JAK–STAT3 PATHWAY IS A UNIVERSAL INDUCER OF ASTROCYTE REACTIVITY

Astrocytes become reactive in response to various pathological conditions affecting the CNS. While several signaling cascades are found activated in reactive astrocytes over the course of diseases or following injuries (Kang and Hebert, 2011; Ben Haim et al., 2015a), STAT3 appears as a key regulator of astrocyte reactivity.

Activation of the JAK–STAT3 pathway in acute diseases

STAT3 activation is detected by its phosphorylation, nuclear translocation and/or nuclear accumulation (Box 1). Activated STAT3 is observed in reactive astrocytes in various acute injury models, including TBI (Li and Shaw, 2006; Oliva et al., 2012 and see Fig. 2), excitotoxicity (Acarin et al., 2000), neonatal white matter injury (Nobuta et al., 2012), neuropathic pain (Tsuda et al., 2011), axotomy (Xia et al., 2002; Schubert et al., 2005; Tyzack et al., 2014), infection with scrapie (Na et al., 2007), glaucoma (Zhang et al., 2013), epilepsy (Choi et al., 2003b; Xu et al., 2011), ischemia (Justicia et al., 2000; Choi et al., 2003a) and after exposure to neurotoxins (Sriram et al., 2004; O'Callaghan et al., 2014) or LPS (Gautron et al., 2002). The activation of upstream cascades was explored in some studies: JAK2 and the cytokine receptor gp130 are also phosphorylated in a rat TBI model (Oliva et al., 2012, and see Fig. 2); JAK2 (but not JAK1 or Tyk2) is also activated by the injection of the neurotoxin 1-methyl-4-phenyl-1,2,3,6-tetrahydropyridine (MPTP, Sriram et al., 2004).

Overall, there is ample evidence that activation of the JAK–STAT3 pathway is associated with astrocyte reactivity. However, to demonstrate that STAT3 is really required for astrocyte reactivity, it is necessary to interfere with it (see Box 1). This was nicely demonstrated in the case of the glial scar, a dense structure of cells that aggregate at the site of parenchyma disruption (Sofroniew, 2009; Pekny and Pekna, 2014; Ben Haim et al., 2015a). Conditional knock-out (KO) of *stat3* in reactive astrocytes (*Nestin-Cre* × *stat3*$^{fl/fl}$) reduces glial scar formation while *socs3* deletion (*Nestin-Cre* × *socs3*$^{fl/fl}$) has opposite effects (Okada et al., 2006). Similarly, *stat3* KO in astrocytes (*Gfap-Cre* × *stat3*$^{fl/fl}$) attenuates GFAP upregulation and disrupts glial scar formation after SCI (Herrmann et al., 2008; Wanner et al., 2013).

STAT3 is also responsible for astrocyte reactivity in acute disease models without glial scarring. For example, pharmacological inhibition of JAK2 decreases STAT3 activation and astrocyte reactivity after hypoxic-ischemic damage in the neonatal mouse brain (Hristova et al., 2016), in the epileptic rat hippocampus (Xu et al., 2011), after MPTP injection (Sriram et al., 2004) and in a model of peripheral nerve injury (Tsuda et al., 2011). Khoro et al. later used viral gene transfer of a dominant negative (DN) form of STAT3 to inhibit this cascade more specifically in spinal astrocytes after peripheral nerve injury in mice. They demonstrate that this pathway contributes to astrocyte reactivity, as the mRNA levels of *gfap*, *vimentin* and *socs3* were reduced by STAT3-DN (Kohro et al., 2015). Genetic studies based on *Gfap-Cre* × *stat3*$^{fl/fl}$ transgenic mice further established the importance of STAT3 for astrocyte reactivity. By contrast to controls, transgenic mice display reduced astrocyte hypertrophy and GFAP upregulation following neonatal white matter injury in the brain (Nobuta et al., 2012) and spinal cord (Monteiro de Castro et al., 2015), axotomy (Tyzack et al., 2014), in a model of chronic itch (Shiratori-Hayashi et al., 2015) or after exposure to a range of neurotoxins causing neuronal death in different brain regions and species (O'Callaghan et al., 2014). Interestingly, STAT3 involvement in astrocyte reactivity is conserved in *Drosophila*. Stat92E, the *Drosophila* homolog of STAT3, controls glial reactivity after axonal injury (Doherty et al., 2014).

These results show that STAT3 is a central regulator of glial reactivity, conserved across evolution, as well as between disease conditions.

Activation of the JAK–STAT3 pathway in ND

In progressive pathological conditions such as ND, where astrocyte reactivity, neuroinflammation and neuronal death are gradually established over years, STAT3 appears to play a central role as well. STAT3 activation is reported in reactive astrocytes of patients with MS (Lu et al., 2013) or amyotrophic lateral sclerosis (ALS, Shibata et al., 2009). Similarly, STAT3 activation is found in mouse models of ALS (Shibata et al., 2010) and Alzheimer's disease (AD, Ben Haim et al., 2015b and see Fig. 2), in pharmacological models of Parkinson's disease (PD, Sriram et al., 2004; O'Callaghan et al., 2014) and in mouse and primate models of Huntington's disease (HD, Ben Haim et al., 2015b).

While STAT3 activation is consistently detected in reactive astrocytes in ND models, few studies have investigated its role in the establishment of astrocyte reactivity (see Ben Haim et al., 2015a for review). Pharmacological inhibition of JAK2 and astrocyte-specific KO of *stat3* in the MPTP model of PD attenuates astrocyte reactivity (Sriram et al., 2004; O'Callaghan et al., 2014). A similar reduction in reactivity is observed with JAK2 inhibition in a pharmacological model of HD based on striatal injection of an excitotoxin (Ignarro et al., 2013). To improve cell-type specificity, our group used lentiviral vectors to overexpress SOCS3 selectively in astrocytes, in mouse models of AD and HD (Ben Haim et al., 2015b). SOCS3 overexpression prevented STAT3 activation and GFAP upregulation in astrocytes of AD and HD mice. Furthermore, SOCS3-expressing astrocytes displayed resting-like morphology, demonstrating that the JAK–STAT3 pathway is a key pathway mediating astrocyte reactivity in ND models.

The JAK–STAT3 pathway is a central mediator of astrocyte reactivity in a variety of pathological conditions in the CNS. What are the functional outcomes of this cascade in reactive astrocytes?

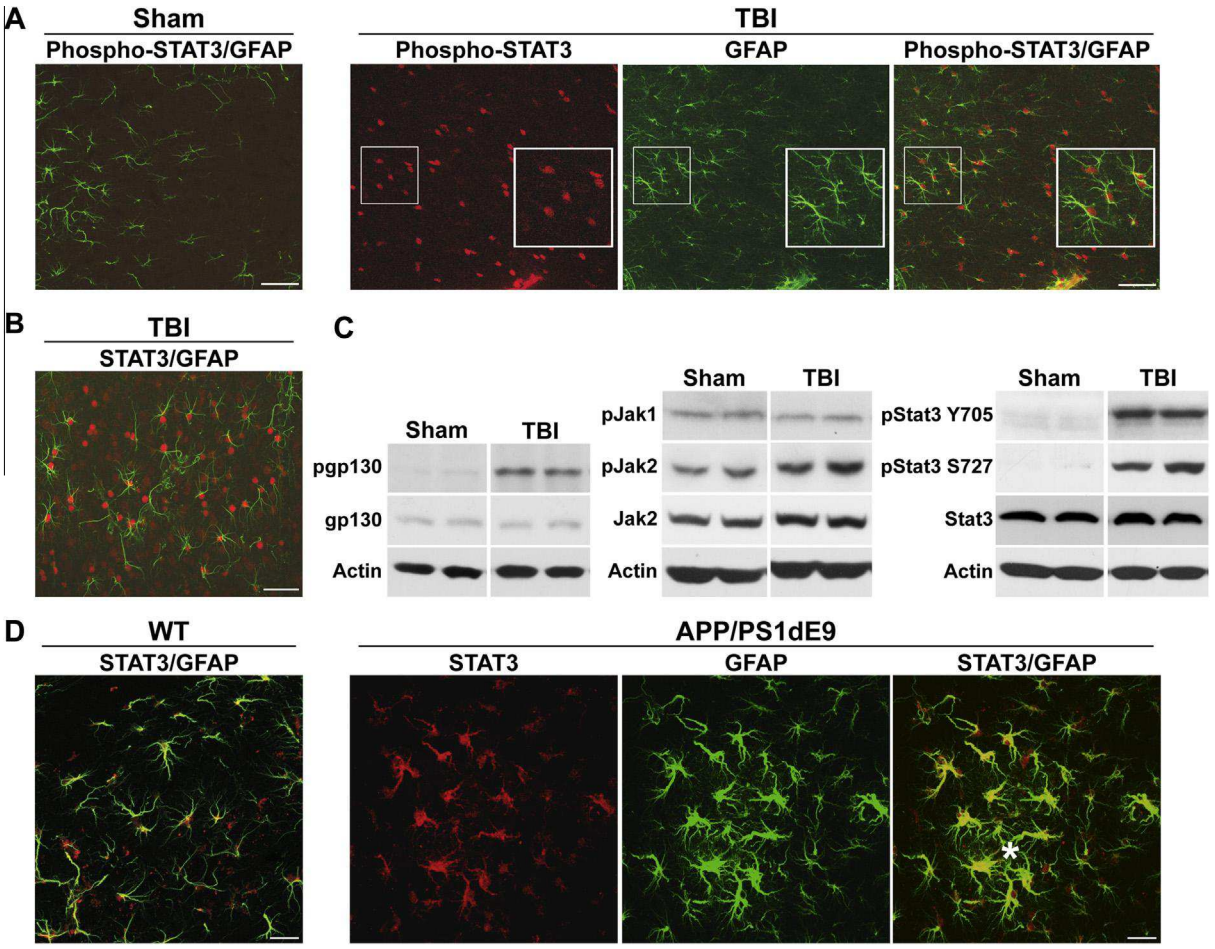

Fig. 2. The JAK–STAT3 pathway is activated in reactive astrocytes in two models of brain disease. A In a model of TBI, the phosphorylated form of STAT3 (red) accumulates in reactive astrocytes overexpressing GFAP (green). Sham-operated rats display low GFAP and no phospho-STAT3 immunoreactivity. **B.** In the cortex exposed to TBI, activation of the JAK–STAT3 pathway is also detected by accumulation of total STAT3 in the nucleus of astrocytes. **C.** In this model, Oliva et al. explored the upstream cascades responsible for STAT3 activation. TBI induces phosphorylation of the gp130 receptor (pgp130), as well as JAK2 (pJAK2) but not JAK1 (pJAK1). Interestingly, STAT3 is phosphorylated at Tyr705 as well as Ser727 (**A, B**: 6 h post TBI, **C:** 3 h post TBI, modified from, Oliva et al., 2012). In more progressive models, the detection of STAT3 phosphorylation is sometimes difficult, as it is usually quite transient and prone to post-mortem dephosphorylation (O'Callaghan and Sriram, 2004). Yet, accumulation of STAT3 in the nucleus of reactive astrocytes is observed in many disease models (Ben Haim et al., 2015a). **D.** For example, STAT3 activation (red) is observed in GFAP$^+$ reactive astrocytes (green), in the hippocampus of APP/PS1dE9 mice, a transgenic model of AD. Reactive astrocytes with strong STAT3 activation are especially visible around amyloid plaques (star). GFAP and STAT3 staining is low in wildtype (WT) littermates. Scale bars: A, B = 50 μm, D = 25 μm.

WHAT DOES STAT3 DO IN ASTROCYTES?

STAT3 induces the expression of intermediate filament proteins

One of the best-known target genes of STAT3 is *gfap*, whose induction in astrocytes is the primary hallmark of their reactive state (Hol and Pekny, 2015). As described in section "The JAK–STAT3 pathway is a universal inducer of astrocyte", pharmacological inhibition or genetic invalidation of *stat3,* consistently prevents or reduces the increase in *gfap* mRNA and/or protein levels in astrocytes following induction of reactivity. In fact, levels of GFAP are also reduced by STAT3 inhibition or invalidation in non-lesioned groups (Herrmann et al., 2008; Wanner et al., 2013; Levine et al., 2015), suggesting that STAT3 controls the basal expression of GFAP. The human *gfap* promoter is well characterized; it displays at least one SRE that contributes to high GFAP expression in multiple brain regions (Yeo et al., 2013). These SRE are conserved in the rodent *gfap* promoter (Nakashima et al., 1999). Vimentin, another intermediate filament characteristic of reactive as well as immature astrocytes, is similarly regulated by STAT3 (Herrmann et al., 2008).

Interestingly, STAT3-mediated induction of intermediate filaments in reactive astrocytes recapitulates an important signaling cascade occurring at the time of astrogliogenesis (Kanski et al., 2014). The JAK–STAT3 pathway is inhibited during neurogenesis and activation of STAT3 coincides with the expression of glial markers GFAP and S100β at E18.5 in mice (He et al., 2005). STAT3 binds to the *gfap* promoter and increases GFAP expression in cortical progenitors (Bonni et al., 1997). STAT3-dependent induction of GFAP is modulated by the pattern of histone and DNA methyla-

tion of the *gfap* promoter (Takizawa et al., 2001; Song and Ghosh, 2004).

STAT3 controls proliferation of a subset of reactive astrocytes

The JAK–STAT3 pathway is involved in normal proliferation of neuronal precursor cells during development (Kim et al., 2010) and abnormal proliferation of cancer cells (de la Iglesia et al., 2009; Yu et al., 2009). Does STAT3 also promote the proliferation of reactive astrocytes?

Recent studies show that contrary to the common belief, proliferation of reactive astrocytes is quite limited, being transient or involving only a small percentage of astrocytes (5–10%), especially in chronic diseases or injuries that do not involve rupture of the blood brain barrier (Dimou and Gotz, 2014). These subsets of proliferative astrocytes are located in specific niches, in contact with the vasculature (Bardehle et al., 2013) or the lesion core (Wanner et al., 2013; LeComte et al., 2015) and display stem cell properties (Sirko et al., 2013). There is some indirect evidence that STAT3 controls the proliferation of reactive astrocytes. JAK inhibitors reduce the number of proliferating reactive astrocytes following spinal nerve injury (Tsuda et al., 2011). The formation of the glial scar, which is composed of newly proliferated astrocytes, is also altered in *Gfap-Cre* × *stat3*$^{fl/fl}$ transgenic mice (Wanner et al., 2013; Anderson et al., 2016).

By which mechanisms does STAT3 control astrocyte proliferation? In cancer cells, it is well known that STAT3 promotes the expression of cell cycle genes, like cyclin D1 (Yu et al., 2009), and this regulation also occurs in cultured astrocytes (Sarafian et al., 2010). In addition, STAT3 activates the expression of anti-apoptotic genes (Sarafian et al., 2010, see section "STAT3 regulates mitochondrial functions"), which may promote the survival of proliferating reactive astrocytes. More recently, Lecomte et al. showed that following middle cerebral artery occlusion (MCAO), STAT3 is activated within a subset of reactive astrocytes sensitive to Notch signaling. STAT3 promotes the expression of the endothelin B receptor, which acts in an autocrine manner to stimulate the proliferation of this subset of cells (LeComte et al., 2015).

Of note, it was shown recently that the morphogen Sonic Hedgehog (Shh), which is abundant in the cerebrospinal fluid, also controls the proliferation of reactive astrocytes and their stem cell potential after invasive injuries (Sirko et al., 2013). Whether and how the Shh cascade interacts with STAT3 in astrocytes is unknown.

STAT3 regulates the secretome of reactive astrocytes

In immune cells, STAT3 is an established transcriptional activator of cytokines (Yu et al., 2009). In astrocytes as well, STAT3 regulates the production of cytokines and chemokines during reactivity.

Pharmacological inhibition of the JAK–STAT3 pathway reduces mRNA levels of *interleukin 6 (IL-6), IL-1β, IL-4* and *vascular endothelial growth factor* by astrocytes made reactive by high glucose concentration in culture (Wang et al., 2012). Likewise, expression of a siRNA against STAT3 reduces LPS-mediated induction of the chemokines Ccl20, Cx3cl1, Cxcl5 and Cxcl10 in primary astrocytes. Similar effects are observed *in vivo*, after intrathecal injection of the STAT3 inhibitor Stattic, in a LPS model of inflammation (Liu et al., 2013).

Lipocalin-2 (Lcn2) is one of the proteins released by reactive astrocytes (Zamanian et al., 2012). Its specific function in the brain is still unclear (Jha et al., 2015), but it may serve as an inflammatory mediator, as shown under chronic itch conditions (Shiratori-Hayashi et al., 2015). Lcn2 production by reactive astrocytes is dependent upon STAT3, as demonstrated by pharmacological inhibition in cultured astrocytes and astrocyte-specific KO of *stat3* in mice (Shiratori-Hayashi et al., 2015).

Molecules released by reactive astrocytes may further activate microglial cells or recruit immune cells from the periphery, contributing to a feed forward effect on neuroinflammation. Indeed, specific inhibition of the JAK–STAT3 pathway in astrocytes by SOCS3 reduces the mRNA levels of the microglial markers *Iba1* and *CD11b* in a mouse model of HD (Ben Haim et al., 2015b). Likewise, the astrocyte-specific KO of *stat3* reduces microglial reactivity induced by hypoxia–ischemia (Hristova et al., 2016). The factors released by astrocytes in a STAT3-dependant manner do not only activate microglial cells but also modulate their activity. For example, reactive astrocytes release yet unidentified factors that reduce the production of transforming growth factor β by microglia in culture (Nobuta et al., 2012).

The STAT3-dependent release of proteins by reactive astrocytes not only impacts microglial cells but also neurons. For example, facial nucleus axotomy increases mRNA levels of *thrombospondin-1* (*tsp1*, a secreted protein promoting synapse formation and stability during development) in reactive astrocytes. This induction is reduced in *Gfap-Cre* × *stat3*$^{fl/fl}$ mice, which is associated with decreased synapse number and activity in neighboring neurons. Therefore, reactive astrocytes produce TSP1 in a STAT3-dependent manner, as further demonstrated by the direct binding of STAT3 to the *tsp1* promoter in astrocyte cultures (Tyzack et al., 2014). Recently, Anderson et al. showed that reactive astrocytes forming the glial scar after SCI, express a range of molecules in a STAT3-dependent manner (like chondroitin surface proteoglycans), which overall have axon-growth promoting effects (Anderson et al., 2016).

STAT3 modulates astrocyte morphology and migration

STAT3 plays a role in the migration of multiple cell types including glioblastoma cells (Zhang et al., 2015) and reactive astrocytes (Okada et al., 2006). The deletion of *Stat3* in reactive astrocytes (*Nestin-Cre* × *stat3*$^{fl/fl}$) reduces the migration of reactive astrocytes after *in vitro* scratch injury. Impaired migration after SCI could be responsible for the altered wound closure and enhanced infiltration of inflammatory cells observed in these mice. The opposite is observed in *Nestin-Cre* × *socs3*$^{fl/fl}$ mice whose astrocytes display a quicker migration *in vitro* and an efficient compaction of the lesion in the spinal cord (Okada

et al., 2006). In different cell types, STAT3 regulates the transcription of genes implicated in matrix remodeling such as matrix metallo-proteinases MMP-1, MMP-2 and MMP-10 and the zinc transporter LIV-1, which regulates the expression of the adhesion molecule E-cadherin (Gao and Bromberg, 2006). In the spinal cord as well, *Nestin-Cre* × *stat3*$^{fl/fl}$ mice exposed to SCI display lower mRNA levels of LIV-1 than wild-type littermates, and a concomitant increase in E-cadherin levels (Okada et al., 2006). The impairment of cell migration may thus be explained by the altered expression of cell adhesion proteins in absence of STAT3. But STAT3 may also regulate migration by non-canonical mechanisms. In neuronal cell lines and in fibroblasts, STAT3 was shown to interact with stathmin, a cytoplasmic protein that binds to tubulin and prevents its assembly into microtubules (Ng et al., 2006). The interaction of STAT3 with stathmin is also observed in cultured motoneurons, it promotes microtubule stability and axonal elongation. Intriguingly, this interaction requires Tyr705 phosphorylation but no transcriptional regulation (Selvaraj et al., 2012). It is currently unknown whether such non-canonical effects of STAT3 are involved in the migration of reactive astrocytes.

In fact, reactive astrocytes display limited capacity to migrate towards an injury site (Bardehle et al., 2013; Wanner et al., 2013); instead, astrocyte reactivity is characterized by striking morphological changes (hypertrophy, reorientation of processes). Such morphological plasticity appears to be regulated by STAT3 as well. During glial scar formation following SCI, the reorientation of astrocyte processes parallel to the lesion and the formation of bundles between apposed astrocytes are important to "corral" immune cells and fibroblasts. These morphological changes are disturbed in *Gfap-Cre* × *stat3*$^{fl/fl}$ mice (Wanner et al., 2013). Following axotomy of the facial nucleus, reactive astrocytes increase their coverage of axotomized neuronal cell bodies, a response found altered in *stat3* KO astrocytes (Tyzack et al., 2014). Similarly, STAT3 induces the expression of growth associated protein 43, which contributes to increased process arborization in primary rat astrocytes exposed to LPS (Hung et al., 2016), confirming STAT3 importance for different types of morphological rearrangements. It is noteworthy that in neurons, STAT3 is also an important regulator of morphology and it promotes axonal regrowth (Moore and Goldberg, 2011).

STAT3 regulates mitochondrial functions

Interestingly, a pool of STAT3 proteins is present at the mitochondria (mSTAT3) and interacts with the complexes I and II of the electron transport chain (ETC) in the murine heart and liver (Wegrzyn et al., 2009). The KO of *stat3* in cultured B cells reduces complex I and II activities, which is restored by viral gene transfer of *stat3* (Wegrzyn et al., 2009). Strikingly, the effects of mSTAT3 on the ETC are mediated by its mitochondrial localization and its phosphorylation on Ser727 and not by its transcriptional activity. In other experimental conditions however, STAT3 does modulate metabolism by transcriptional regulation of genes involved in glycolysis and mitochondrial respiration. In particular, STAT3 induces the expression of hypoxia inducible factor 1α, which promotes glycolysis over mitochondrial respiration (Demaria et al., 2010).

Does STAT3 play similar roles in astrocytes? Sarafian et al. found that cultured astrocytes from *Gfap-Cre* × *stat3*$^{fl/fl}$ mice display lower mitochondrial mass and membrane potential and reduced ATP production (Sarafian et al., 2010). Inhibition of JAK2 by AG490 in wildtype astrocytes reproduces the decrease in mitochondrial membrane potential, suggesting that STAT3 operates through a canonical cascade involving JAK2 phosphorylation. The expression of several ETC enzymes is decreased in *stat3* KO astrocytes, further confirming that STAT3 regulation of astrocyte metabolism is controlled at the transcriptional level.

STAT3 may also lower the production of reactive oxygen species (ROS) by the mitochondria, although the mechanisms are still unclear (Szczepanek et al., 2012; Yang and Rincon, 2016). Indeed, *stat3* KO astrocytes display increased generation of ROS and reduced levels of the antioxidant glutathione (Sarafian et al., 2010). STAT3 also promotes ROS detoxification by activating the expression of several antioxidant genes. For example in the mouse brain, STAT3 directly binds to the promoter of the manganese superoxide dismutase (MnSOD) gene, a mitochondrial enzyme that metabolizes superoxide anions (Jung et al., 2009). Inhibition of the JAK2–STAT3 pathway by AG490 or STAT3 decoy DNA in leptin-treated cultures of hippocampal neurons reduces MnSOD expression and increases ROS production (Guo et al., 2008). Other transcriptional targets of STAT3 include the uncoupling proteins (UCP), which are able to decrease mitochondrial ROS production (Negre-Salvayre et al., 1997). In astrocyte cultures treated with leukemia inhibitory factor (LIF), STAT3 is activated, binds to the *ucp2* promoter and increases its transcription. This new pool of *ucp2* mRNA can be later mobilized by astrocytes exposed to oxidative stress to quickly produce UCP2 protein (Lapp et al., 2014).

Lastly, STAT3 may have an anti-apoptotic action on the mitochondria. In cardiomyocytes, STAT3 prevents the formation of the mitochondrial permeability transition pore (Boengler et al., 2010) and enhances cell resistance to apoptotic stimuli (Szczepanek et al., 2012). As for metabolic regulation and antioxidant defense, the anti-apoptotic effect of STAT3 is governed both by a direct action at the mitochondria, through interactions with components of the mitochondrial permeability transition pore, and by transcriptional regulation in the nucleus (Szczepanek et al., 2012). STAT3 promotes the expression of anti-apoptotic genes like *bcl-xl* in neurons (Guo et al., 2008) and of *bcl2* in astrocytes (Sarafian et al., 2010; Gu et al., 2016).

Other important functions for STAT3 in astrocytes

There are a few additional functions regulated by STAT3 that are important for brain homeostasis or response to injury.

Ozog et al. found that activation of the JAK2–STAT3 pathway by ciliary neurotrophic factor (CNTF) increases mRNA and protein levels of connexin 43 (Cx43),

resulting in an enhanced gap junction-coupling between astrocytes (Ozog et al., 2004). They identified three putative SRE on the *cx43* promoter. Interestingly, CNTF-mediated increase in Cx43 levels is also observed in reactive astrocytes of the rat brain (Escartin et al., 2006). Gap junction coupling plays key roles in the normal and diseased brain, modulating synaptic transmission and metabolic supply to neurons (Giaume et al., 2010).

Recently, STAT3 was found to regulate autophagy, a key homeostatic mechanism whose alteration is linked to many brain diseases (Choi et al., 2013). Cytoplasmic STAT3, through a transcription-independent mechanism involving the binding to PKR, tonically suppresses autophagy in cell lines (Shen et al., 2012, see Fig. 1). STAT3 also regulates the expression of genes involved in the control of the autophagic flux (You et al., 2015).

Finally, Doherty et al. reported that Stat92E regulates the ability of glial cells to engulf debris of dead neurons by enhancing the expression of the *Draper* receptor in *Drosophila* (Doherty et al., 2014). Interestingly, they report that the upstream activator of Stat92E is the G-protein Rac1, and not the JAK homologue, suggesting that in *Drosophila* glia, non-canonical pathways operate as well.

Overall, the range of astrocyte functions regulated by STAT3 is extremely large, and most of them appear to be of great importance for neuronal survival in disease conditions.

HOW DOES STAT3 GENERATE SO MANY FUNCTIONAL OUTCOMES?

Previous paragraphs illustrate a puzzling fact: a unique pathway is able to control diverse functions ranging from cell proliferation to morphological remodeling in many cell types and organs. Even within reactive astrocytes, STAT3 mediates various effects depending on the disease, brain region or model studied. How does a single protein trigger so many functional outcomes?

An easy explanation is that STAT3 does not act alone. Besides the JAK–STAT3 pathway, other signaling cascades may be activated in reactive astrocytes (Buffo et al., 2010; Kang and Hebert, 2011; Ben Haim et al., 2015a) and STAT3 may interact with other transcription factors in the nucleus (Hutchins et al., 2013).

Interactions between the JAK–STAT3 pathway and other cascades

For example, the MAPK pathways and the nuclear factor-kappa-light-chain-enhancer of activated B cells (NF-κB) pathway are sometimes found activated in reactive astrocytes (Ben Haim et al., 2015a). For example, IL-6 activates the MAPK and STAT3 pathways, and the equilibrium between the two is controlled by a Tyr motif on the IL-6 receptor (Eulenfeld et al., 2012). Many interactions may take place between the JAK–STAT3 and these other pathways (Yu et al., 2009): they may act in synergy on the same target genes, activate one another in cascade (e.g. STAT3 target genes are activators of the NF-κB pathway, and reciprocally) or regulate one other (e.g. MAPKs phosphorylate STAT3 on Ser727, modulating its transcriptional activity). Conversely, these pathways can inhibit one another or compete for binding sequences on gene promoters (Oeckinghaus et al., 2011).

The interaction between the JAK–STAT3 pathway and other signaling cascades is particularly well studied in the context of astrogliogenesis. The JAK–STAT3 pathway interacts with the fibroblast growth factor 2 pathway (Song and Ghosh, 2004), the Notch/Hes pathway (Kamakura et al., 2004), and the bone morphogenetic protein-2/Smad1 pathway (Nakashima et al., 1999), to activate the *gfap* promoter during development (see, Kanski et al., 2014 for a recent review).

The pattern of activation of these cascades in a disease-specific manner may underlie the diverse transcriptional and functional outcomes observed in reactive astrocytes.

A signaling code

Even without resorting to interactions with other signaling cascades, the canonical JAK–STAT3 pathway has already a large potential for complexity and signaling subtleties. There are many ligands, acting on different receptors, activating several JAKs; STAT3 can form heterodimers with other STATs, and the pathway is retro-controlled by several inhibitors (see details in section "The JAK–STAT3 pathway"). New modulators or interactors of the pathway are still being discovered (Icardi et al., 2012; Matsuda et al., 2015). Overall, there is an immense potential for signaling complexity within the JAK–STAT3 pathway (Ernst and Jenkins, 2004).

The upstream ligands activating STAT3 influence the resulting transcriptional and functional effects. For example, IL-6 and IL-10, two cytokines relying on STAT3 as their effector, have opposite effects on inflammatory processes. Computational modeling and experiments on dendritic cells revealed that this could be explained by different temporal profiles of STAT3 activation, resulting in different transcriptional outcomes (Braun et al., 2013). An emerging theme in cell signaling is that the intensity, duration, frequency and pattern of receptor stimulation encode information that translates into different transcriptional profiles (Lemmon et al., 2016).

Another level of complexity resides in the numerous PTMs on STAT3 (see Fig. 1). The pattern of PTMs constitutes a molecular code that significantly impacts the profile of genes regulated at a given time by STAT3 (see section "Additional branching points on the pathway increase the complexity of STAT3 signaling cascades").

Finally, the non-canonical actions that STAT3 performs outside of the nucleus may further diversify STAT3 functional outputs in reactive astrocytes. How these non-canonical functions are regulated in the context of astrocyte reactivity is an open question.

Overall, the JAK–STAT3 pathway is composed of multiple elements that can generate significant signaling

complexity and contribute to the observed diversity in astrocyte reactivity.

Differential abilities to engage in STAT3 signaling

The functional outcomes mediated by STAT3 may be influenced by the cell's ability to mediate STAT3 signaling. Indeed, depending on the specific status of the cell, its response to the same stimulus on the JAK–STAT3 pathway will be different. Many factors can influence the capacity of a cell to efficiently operate the JAK–STAT3 pathway, including the abundance of pathway inhibitors, its epigenetic status, the activity of molecular machinery involved in signal transduction (e.g. nuclear import, ATP-dependent phosphorylation) and termination (e.g. nuclear export, phosphatase activity, degradation by the proteasome).

For example, the JAK–STAT3 pathway will be more or less active, depending on how much of SOCS and PIAS inhibitors are present and located at the right place to inhibit this pathway. SOCS3 is strongly induced by the JAK–STAT3 pathway, depending on the "signaling history" of the cell, the abundance of SOCS3 will vary (Linossi and Nicholson, 2015).

STAT3 binding to promoters is influenced by DNA and histone methylation, a regulation well described in the context of astrogliogenesis (Kanski et al., 2014, and section "STAT3 induces the expression of intermediate filament proteins"). Therefore, it is expected that the epigenetic status of the cell will impact the transcriptional outcomes of the JAK–STAT3 pathway.

The disease context itself may influence how a cell is able to respond to a stimulation of the JAK–STAT3 pathway. For example in *Drosophila*, the formation of tau aggregates in glia reduces STAT-dependent promoter activity (Colodner and Feany, 2010). Likewise, the amyloid β protein reduces the activity of the JAK–STAT3 pathway in neurons (Chiba et al., 2009).

Global impairment in the cell's ability to engage in a STAT3 response may occur in brain diseases. Several elements of the JAK–STAT3 pathway are sensitive to ROS, which are produced in many brain diseases (Duhe, 2013). Likewise, there is a consistent alteration in energy production in ND (Lin and Beal, 2006), which could affect the multiple energy-dependent steps of this cascade (e.g. phosphorylation, nuclear translocation, transcriptional induction). The activity of the JAK–STAT3 pathway is reduced in white matter astrocytes exposed to hypoxia (Raymond et al., 2011) and in the mouse brain after MCAO (Jung et al., 2009), confirming the importance of energy supply for proper STAT3 signaling. Finally, the nucleocytoplasmic transport is altered in some ND, due to the scavenging of key components of this system in toxic protein aggregates (Da Cruz and Cleveland, 2016), and this could directly prevent STAT3 signaling to the nucleus.

Therefore, depending on the disease and its stage of evolution, astrocytes will have variable intrinsic capabilities to trigger a STAT3-dependent response. This probably also contributes to the significant heterogeneity of the functional responses of reactive astrocytes in each disease context.

CONCLUSIONS AND PERSPECTIVES

Over the last decade, it has become clear that the JAK–STAT3 pathway, a signaling cascade initially described in the immune system, is very important for astrocyte development and response to injury. A thorough molecular dissection of the multiple interactors and regulators of this cascade has been performed in cell lines. It is now time to integrate this knowledge in the study of astrocyte response *in vivo*, and this is not a simple task (see Box 2). STAT3 appears to orchestrate numerous molecular and functional changes in reactive astrocytes. Much remains to be done to understand how a central signaling cascade mediates so many functional outcomes in astrocytes.

Deciphering the molecular code of astrocyte reactivity holds promising prospects for basic and medical science. It would make it possible to understand how the brain responds to each disease situation and to develop novel, efficient and, specific therapeutic strategies.

Box 2: Future questions and challenges

- What are the **endogenous activators** of this pathway during brain diseases (e.g. cytokines, growth factors, danger associated molecular patterns)?
- What is the **time course** of activation of the JAK–STAT3 pathway in reactive astrocytes, in relation to microglial activation or neuronal death?
- What are the **effects of PTMs** on STAT3 in reactive astrocytes?
- What are the **non-canonical functions of STAT3 in reactive astrocytes**, unrelated to transcriptional regulation?
- Can we define the networks of signaling cascades that control **each specific functional state** in reactive astrocytes?
- Can this pathway be **targeted for therapeutic purposes**?

Acknowledgments—L.B.H. and K.C. are recipients of a PhD fellowship from the CEA (IRTELIS program). L.A. holds a PhD fellowship from the "Region Ile-de-France" via the "DIM Cerveau et Pensée".

C.E. was supported by French National Research Agency Grants 2010-JCJC-1402-1 and 2011-BSV4-021-03, CEA and CNRS. The authors wish to thank the LECMA-Vaincre Alzheimer organization (Grant FR-15015) and the Fédération pour la Recherche sur le Cerveau (FRC) for financial support.
We apologize for not being able to cite all original studies relevant to the topic of this review, due to space limitations. We thank Dr. S. Williams for proofreading the manuscript. We thank Dr. C. Atkins for providing the original images for Fig. 2A-C.

REFERENCES

Acarin L, Gonzalez B, Castellano B (2000) STAT3 and NFkappaB activation precedes glial reactivity in the excitotoxically injured young cortex but not in the corresponding distal thalamic nuclei. J Neuropathol Exp Neurol 59:151–163.

Akira S, Nishio Y, Inoue M, Wang XJ, Wei S, Matsusaka T, Yoshida K, Sudo T, Naruto M, Kishimoto T (1994) Molecular cloning of APRF, a novel IFN-stimulated gene factor 3 p91-related transcription factor involved in the gp130-mediated signaling pathway. Cell 77:63–71.

Anderson MA, Burda JE, Ren Y, Ao Y, O'Shea TM, Kawaguchi R, Coppola G, Khakh BS, Deming TJ, Sofroniew MV (2016) Astrocyte scar formation aids central nervous system axon regeneration. Nature.

Babon JJ, Varghese LN, Nicola NA (2014) Inhibition of IL-6 family cytokines by SOCS3. Semin Immunol 26:13–19.

Bardehle S, Kruger M, Buggenthin F, Schwausch J, Ninkovic J, Clevers H, Snippert HJ, Theis FJ, Meyer-Luehmann M, Bechmann I, Dimou L, Gotz M (2013) Live imaging of astrocyte responses to acute injury reveals selective juxtavascular proliferation. Nat Neurosci 16:580–586.

Ben Haim L, Carrillo-de Sauvage MA, Ceyzeriat K, Escartin C (2015a) Elusive roles for reactive astrocytes in neurodegenerative diseases. Front Cell Neurosci 9:278.

Ben Haim L, Ceyzeriat K, Carrillo-de Sauvage MA, Aubry F, Auregan G, Guillermier M, Ruiz M, Petit F, Houitte D, Faivre E, Vandesquille M, Aron-Badin R, Dhenain M, Deglon N, Hantraye P, Brouillet E, Bonvento G, Escartin C (2015b) The JAK/STAT3 pathway is a common inducer of astrocyte reactivity in Alzheimer's and Huntington's diseases. J Neurosci 35:2817–2829.

Boengler K, Hilfiker-Kleiner D, Heusch G, Schulz R (2010) Inhibition of permeability transition pore opening by mitochondrial STAT3 and its role in myocardial ischemia/reperfusion. Basic Res Cardiol 105:771–785.

Bonni A, Sun Y, Nadal-Vicens M, Bhatt A, Frank DA, Rozovsky I, Stahl N, Yancopoulos GD, Greenberg ME (1997) Regulation of gliogenesis in the central nervous system by the JAK-STAT signaling pathway. Science 278:477–483.

Braun DA, Fribourg M, Sealfon SC (2013) Cytokine response is determined by duration of receptor and signal transducers and activators of transcription 3 (STAT3) activation. J Biol Chem 288:2986–2993.

Bromberg JF, Wrzeszczynska MH, Devgan G, Zhao Y, Pestell RG, Albanese C, Darnell Jr JE (1999) Stat3 as an oncogene. Cell 98:295–303.

Brooks AJ, Dai W, O'Mara ML, Abankwa D, Chhabra Y, Pelekanos RA, Gardon O, Tunny KA, Blucher KM, Morton CJ, Parker MW, Sierecki E, Gambin Y, Gomez GA, Alexandrov K, Wilson IA, Doxastakis M, Mark AE, Waters MJ (2014) Mechanism of activation of protein kinase JAK2 by the growth hormone receptor. Science 344:1249783.

Buffo A, Rolando C, Ceruti S (2010) Astrocytes in the damaged brain: molecular and cellular insights into their reactive response and healing potential. Biochem Pharmacol 79:77–89.

Burda JE, Sofroniew MV (2014) Reactive gliosis and the multicellular response to CNS damage and disease. Neuron 81:229–248.

Chen Y, Wu R, Chen HZ, Xiao Q, Wang WJ, He JP, Li XX, Yu XW, Li L, Wang P, Wan XC, Tian XH, Li SJ, Yu X, Wu Q (2015) Enhancement of hypothalamic STAT3 acetylation by nuclear receptor Nur77 dictates leptin sensitivity. Diabetes 64:2069–2081.

Chiba T, Yamada M, Sasabe J, Terashita K, Shimoda M, Matsuoka M, Aiso S (2009) Amyloid-beta causes memory impairment by disturbing the JAK2/STAT3 axis in hippocampal neurons. Mol Psychiatry 14:206–222.

Choi AM, Ryter SW, Levine B (2013) Autophagy in human health and disease. N Engl J Med 368:1845–1846.

Choi JS, Kim SY, Cha JH, Choi YS, Sung KW, Oh ST, Kim ON, Chung JW, Chun MH, Lee SB, Lee MY (2003a) Upregulation of gp130 and STAT3 activation in the rat hippocampus following transient forebrain ischemia. Glia 41:237–246.

Choi JS, Kim SY, Park HJ, Cha JH, Choi YS, Kang JE, Chung JW, Chun MH, Lee MY (2003b) Upregulation of gp130 and differential activation of STAT and p42/44 MAPK in the rat hippocampus following kainic acid-induced seizures. Brain Res Mol Brain Res 119:10–18.

Chung CD, Liao J, Liu B, Rao X, Jay P, Berta P, Shuai K (1997) Specific inhibition of Stat3 signal transduction by PIAS3. Science 278:1803–1805.

Colodner KJ, Feany MB (2010) Glial fibrillary tangles and JAK/STAT-mediated glial and neuronal cell death in a Drosophila model of glial tauopathy. J Neurosci 30:16102–16113.

Da Cruz S, Cleveland DW (2016) Cell Biology. Disrupted nuclear import–export in neurodegeneration. Science 351:125–126.

Darnell Jr JE (1997) STATs and gene regulation. Science 277:1630–1635.

Darnell Jr JE, Kerr IM, Stark GR (1994) Jak-STAT pathways and transcriptional activation in response to IFNs and other extracellular signaling proteins. Science 264:1415–1421.

Dasgupta M, Dermawan JK, Willard B, Stark GR (2015) STAT3-driven transcription depends upon the dimethylation of K49 by EZH2. Proc Natl Acad Sci USA 112:3985–3990.

de la Iglesia N, Puram SV, Bonni A (2009) STAT3 regulation of glioblastoma pathogenesis. Curr Mol Med 9:580–590.

Decker T, Kovarik P (2000) Serine phosphorylation of STATs. Oncogene 19:2628–2637.

Demaria M, Giorgi C, Lebiedzinska M, Esposito G, D'Angeli L, Bartoli A, Gough DJ, Turkson J, Levy DE, Watson CJ, Wieckowski MR, Provero P, Pinton P, Poli V (2010) A STAT3-mediated metabolic switch is involved in tumour transformation and STAT3 addiction. Aging 2:823–842.

Dimou L, Gotz M (2014) Glial cells as progenitors and stem cells: new roles in the healthy and diseased brain. Physiol Rev 94: 709–737.

Doherty J, Sheehan AE, Bradshaw R, Fox AN, Lu TY, Freeman MR (2014) PI3K signaling and Stat92E converge to modulate glial responsiveness to axonal injury. PLoS Biol 12:e1001985.

Duhe RJ (2013) Redox regulation of Janus kinase: the elephant in the room. Jak-Stat 2:e26141.

Ernst M, Jenkins BJ (2004) Acquiring signalling specificity from the cytokine receptor gp130. Trends Genet 20:23–32.

Escartin C, Brouillet E, Gubellini P, Trioulier Y, Jacquard C, Smadja C, Knott GW, Kerkerian-Le Goff L, Deglon N, Hantraye P, Bonvento G (2006) Ciliary neurotrophic factor activates astrocytes, redistributes their glutamate transporters GLAST and GLT-1 to raft microdomains, and improves glutamate handling in vivo. J Neurosci 26:5978–5989.

Eufemi M, Cocchiola R, Romaniello D, Correani V, Di Francesco L, Fabrizi C, Maras B, Schinina ME (2015) Acetylation and phosphorylation of STAT3 are involved in the responsiveness of microglia to beta amyloid. Neurochem Int 81:48–56.

Eulenfeld R, Dittrich A, Khouri C, Muller PJ, Mutze B, Wolf A, Schaper F (2012) Interleukin-6 signalling: more than Jaks and STATs. Eur J Cell Biol 91:486–495.

Gabel K, Bednorz NL, Klemmt P, Vafaizadeh V, Borghouts C, Groner B (2010) Visualization of Stat3 and Stat5 transactivation activity with specific response element dependent reporter constructs integrated into lentiviral gene transfer vectors. Horm Mol Biol Clin Investig 1:127–137.

Gao SP, Bromberg JF (2006) Touched and moved by STAT3. Science's STKE 2006.

Gautron L, Lafon P, Chaigniau M, Tramu G, Laye S (2002) Spatiotemporal analysis of signal transducer and activator of transcription 3 activation in rat brain astrocytes and pituitary following peripheral immune challenge. Neuroscience 112:717–729.

Giaume C, Koulakoff A, Roux L, Holcman D, Rouach N (2010) Astroglial networks: a step further in neuroglial and gliovascular interactions. Nat Rev Neurosci 11:87–99.

Gu Y, He M, Zhou X, Liu J, Hou N, Bin T, Zhang Y, Li T, Chen J (2016) Endogenous IL-6 of mesenchymal stem cell improves behavioral outcome of hypoxic-ischemic brain damage neonatal rats by supressing apoptosis in astrocyte. Sci Rep 6:18587.

Guo Z, Jiang H, Xu X, Duan W, Mattson MP (2008) Leptin-mediated cell survival signaling in hippocampal neurons mediated by JAK STAT3 and mitochondrial stabilization. J Biol Chem 283:1754–1763.

He F, Ge W, Martinowich K, Becker-Catania S, Coskun V, Zhu W, Wu H, Castro D, Guillemot F, Fan G, de Vellis J, Sun YE (2005) A positive autoregulatory loop of Jak-STAT signaling controls the onset of astrogliogenesis. Nat Neurosci 8:616–625.

Heinrich PC, Behrmann I, Haan S, Hermanns HM, Muller-Newen G, Schaper F (2003) Principles of interleukin (IL)-6-type cytokine signalling and its regulation. Biochem J 374:1–20.

Herrmann JE, Imura T, Song B, Qi J, Ao Y, Nguyen TK, Korsak RA, Takeda K, Akira S, Sofroniew MV (2008) STAT3 is a critical regulator of astrogliosis and scar formation after spinal cord injury. J Neurosci 28:7231–7243.

Hol EM, Pekny M (2015) Glial fibrillary acidic protein (GFAP) and the astrocyte intermediate filament system in diseases of the central nervous system. Curr Opin Cell Biol 32:121–130.

Hristova M, Rocha-Ferreira E, Fontana X, Thei L, Buckle R, Christou M, Hompoonsup S, Gostelow N, Raivich G, Peebles D (2016) Inhibition of Signal Transducer and Activator of Transcription 3 (STAT3) reduces neonatal hypoxic–ischaemic brain damage. J Neurochem 136:981–994.

Hung CC, Lin CH, Chang H, Wang CY, Lin SH, Hsu PC, Sun YY, Lin TN, Shie FS, Kao LS, Chou CM, Lee YH (2016) Astrocytic GAP43 Induced by the TLR4/NF-kappaB/STAT3 Axis Attenuates Astrogliosis-Mediated Microglial Activation and Neurotoxicity. J Neurosci 36:2027–2043.

Hutchins AP, Diez D, Takahashi Y, Ahmad S, Jauch R, Tremblay ML, Miranda-Saavedra D (2013) Distinct transcriptional regulatory modules underlie STAT3's cell type-independent and cell type-specific functions. Nucleic Acids Res 41:2155–2170.

Icardi L, Mori R, Gesellchen V, Eyckerman S, De Cauwer L, Verhelst J, Vercauteren K, Saelens X, Meuleman P, Leroux-Roels G, De Bosscher K, Boutros M, Tavernier J (2012) The Sin3a repressor complex is a master regulator of STAT transcriptional activity. Proc Natl Acad Sci USA 109:12058–12063.

Ignarro RS, Vieira AS, Sartori CR, Langone F, Rogerio F, Parada CA (2013) JAK2 inhibition is neuroprotective and reduces astrogliosis after quinolinic acid striatal lesion in adult mice. J Chem Neuroanat 48–49:14–22.

Jha MK, Lee S, Park DH, Kook H, Park KG, Lee IK, Suk K (2015) Diverse functional roles of lipocalin-2 in the central nervous system. Neurosci Biobehav Rev 49:135–156.

Jung JE, Kim GS, Narasimhan P, Song YS, Chan PH (2009) Regulation of Mn-superoxide dismutase activity and neuroprotection by STAT3 in mice after cerebral ischemia. J Neurosci 29:7003–7014.

Justicia C, Gabriel C, Planas AM (2000) Activation of the JAK/STAT pathway following transient focal cerebral ischemia: signaling through Jak1 and Stat3 in astrocytes. Glia 30:253–270.

Kamakura S, Oishi K, Yoshimatsu T, Nakafuku M, Masuyama N, Gotoh Y (2004) Hes binding to STAT3 mediates crosstalk between Notch and JAK-STAT signalling. Nat Cell Biol 6:547–554.

Kang W, Hebert JM (2011) Signaling pathways in reactive astrocytes, a genetic perspective. Mol Neurobiol 43:147–154.

Kanski R, van Strien ME, van Tijn P, Hol EM (2014) A star is born: new insights into the mechanism of astrogenesis. Cell Mol Life Sci 71:433–447.

Kershaw NJ, Murphy JM, Liau NP, Varghese LN, Laktyushin A, Whitlock EL, Lucet IS, Nicola NA, Babon JJ (2013) SOCS3 binds specific receptor-JAK complexes to control cytokine signaling by direct kinase inhibition. Nat Struct Mol Biol 20:469–476.

Kim E, Kim M, Woo DH, Shin Y, Shin J, Chang N, Oh YT, Kim H, Rheey J, Nakano I, Lee C, Joo KM, Rich JN, Nam DH, Lee J (2013) Phosphorylation of EZH2 activates STAT3 signaling via STAT3 methylation and promotes tumorigenicity of glioblastoma stem-like cells. Cancer Cell 23:839–852.

Kim YH, Chung JI, Woo HG, Jung YS, Lee SH, Moon CH, Suh-Kim H, Baik EJ (2010) Differential regulation of proliferation and differentiation in neural precursor cells by the Jak pathway. Stem Cells 28:1816–1828.

Kohro Y, Sakaguchi E, Tashima R, Tozaki-Saitoh H, Okano H, Inoue K, Tsuda M (2015) A new minimally-invasive method for microinjection into the mouse spinal dorsal horn. Sci Rep 5:14306.

Kretzschmar AK, Dinger MC, Henze C, Brocke-Heidrich K, Horn F (2004) Analysis of Stat3 (signal transducer and activator of transcription 3) dimerization by fluorescence resonance energy transfer in living cells. Biochem J 377:289–297.

Lapp DW, Zhang SS, Barnstable CJ (2014) Stat3 mediates LIF-induced protection of astrocytes against toxic ROS by upregulating the UPC2 mRNA pool. Glia 62:159–170.

LeComte MD, Shimada IS, Sherwin C, Spees JL (2015) Notch1-STAT3-ETBR signaling axis controls reactive astrocyte proliferation after brain injury. Proc Natl Acad Sci USA 112:8726–8731.

Lemmon MA, Freed DM, Schlessinger J, Kiyatkin A (2016) The dark side of cell signaling: positive roles for negative regulators. Cell 164:1172–1184.

Levine J, Kwon E, Paez P, Yan W, Czerwieniec G, Loo JA, Sofroniew MV, Wanner IB (2015) Traumatically injured astrocytes release a proteomic signature modulated by STAT3-dependent cell survival. Glia.

Li L, Shaw PE (2006) Elevated activity of STAT3C due to higher DNA binding affinity of phosphotyrosine dimer rather than covalent dimer formation. J Biol Chem 281:33172–33181.

Li WX (2008) Canonical and non-canonical JAK-STAT signaling. Trends Cell Biol 18:545–551.

Lim CP, Cao X (2006) Structure, function, and regulation of STAT proteins. Mol BioSyst 2:536–550.

Lin MT, Beal MF (2006) Mitochondrial dysfunction and oxidative stress in neurodegenerative diseases. Nature 443:787–795.

Linossi EM, Nicholson SE (2015) Kinase inhibition, competitive binding and proteasomal degradation: resolving the molecular function of the suppressor of cytokine signaling (SOCS) proteins. Immunol Rev 266:123–133.

Liu X, Tian Y, Lu N, Gin T, Cheng CH, Chan MT (2013) Stat3 inhibition attenuates mechanical allodynia through transcriptional regulation of chemokine expression in spinal astrocytes. PLoS One 8:e75804.

Lu JQ, Power C, Blevins G, Giuliani F, Yong VW (2013) The regulation of reactive changes around multiple sclerosis lesions by phosphorylated signal transducer and activator of transcription. J Neuropathol Exp Neurol 72:1135–1144.

Matsuda T, Muromoto R, Sekine Y, Togi S, Kitai Y, Kon S, Oritani K (2015) Signal transducer and activator of transcription 3 regulation by novel binding partners. World J Biol Chem 6:324–332.

Mertens C, Darnell Jr JE (2007) SnapShot: JAK-STAT signaling. Cell 131:612.

Meydan N, Grunberger T, Dadi H, Shahar M, Arpaia E, Lapidot Z, Leeder JS, Freedman M, Cohen A, Gazit A, Levitzki A, Roifman CM (1996) Inhibition of acute lymphoblastic leukaemia by a Jak-2 inhibitor. Nature 379:645–648.

Mohr A, Chatain N, Domoszlai T, Rinis N, Sommerauer M, Vogt M, Muller-Newen G (2012) Dynamics and non-canonical aspects of JAK/STAT signalling. Eur J Cell Biol 91:524–532.

Monteiro de Castro G, Deja NA, Ma D, Zhao C, Franklin RJ (2015) Astrocyte activation via Stat3 signaling determines the balance of oligodendrocyte versus schwann cell remyelination. Am J Pathol 185:2431–2440.

Moore DL, Goldberg JL (2011) Multiple transcription factor families regulate axon growth and regeneration. Dev Neurobiol 71:1186–1211.

Moravcova S, Cervena K, Pacesova D, Bendova Z (2016) Identification of STAT3 and STAT5 proteins in the rat suprachiasmatic nucleus and the day/night difference in astrocytic STAT3 phosphorylation in response to lipopolysaccharide. J Neurosci Res 94:99–108.

Na YJ, Jin JK, Kim JI, Choi EK, Carp RI, Kim YS (2007) JAK-STAT signaling pathway mediates astrogliosis in brains of scrapie-infected mice. J Neurochem 103:637–649.

Nakajima K, Yamanaka Y, Nakae K, Kojima H, Ichiba M, Kiuchi N, Kitaoka T, Fukada T, Hibi M, Hirano T (1996) A central role for

Stat3 in IL-6-induced regulation of growth and differentiation in M1 leukemia cells. EMBO J 15:3651–3658.
Nakashima K, Yanagisawa M, Arakawa H, Kimura N, Hisatsune T, Kawabata M, Miyazono K, Taga T (1999) Synergistic signaling in fetal brain by STAT3-Smad1 complex bridged by p300. Science 284:479–482.
Negre-Salvayre A, Hirtz C, Carrera G, Cazenave R, Troly M, Salvayre R, Penicaud L, Casteilla L (1997) A role for uncoupling protein-2 as a regulator of mitochondrial hydrogen peroxide generation. FASEB J 11:809–815.
Ng DC, Lin BH, Lim CP, Huang G, Zhang T, Poli V, Cao X (2006) Stat3 regulates microtubules by antagonizing the depolymerization activity of stathmin. J Cell Biol 172:245–257.
Nicolas CS, Peineau S, Amici M, Csaba Z, Fafouri A, Javalet C, Collett VJ, Hildebrandt L, Seaton G, Choi SL, Sim SE, Bradley C, Lee K, Zhuo M, Kaang BK, Gressens P, Dournaud P, Fitzjohn SM, Bortolotto ZA, Cho K, Collingridge GL (2012) The Jak/STAT pathway is involved in synaptic plasticity. Neuron 73:374–390.
Nobuta H, Ghiani CA, Paez PM, Spreuer V, Dong H, Korsak RA, Manukyan A, Li J, Vinters HV, Huang EJ, Rowitch DH, Sofroniew MV, Campagnoni AT, de Vellis J, Waschek JA (2012) STAT3-mediated astrogliosis protects myelin development in neonatal brain injury. Ann Neurol 72:750–765.
O'Callaghan JP, Kelly KA, VanGilder RL, Sofroniew MV, Miller DB (2014) Early activation of STAT3 regulates reactive astrogliosis induced by diverse forms of neurotoxicity. PLoS One 9:e102003.
O'Callaghan JP, Sriram K (2004) Focused microwave irradiation of the brain preserves in vivo protein phosphorylation: comparison with other methods of sacrifice and analysis of multiple phosphoproteins. J Neurosci Methods 135:159–168.
O'Shea JJ, Holland SM, Staudt LM (2013) JAKs and STATs in immunity, immunodeficiency, and cancer. N Engl J Med 368:161–170.
Oeckinghaus A, Hayden MS, Ghosh S (2011) Crosstalk in NF-kappaB signaling pathways. Nat Immunol 12:695–708.
Okada S, Nakamura M, Katoh H, Miyao T, Shimazaki T, Ishii K, Yamane J, Yoshimura A, Iwamoto Y, Toyama Y, Okano H (2006) Conditional ablation of Stat3 or Socs3 discloses a dual role for reactive astrocytes after spinal cord injury. Nat Med 12:829–834.
Oliva Jr AA, Kang Y, Sanchez-Molano J, Furones C, Atkins CM (2012) STAT3 signaling after traumatic brain injury. J Neurochem 120:710–720.
Ozog MA, Bernier SM, Bates DC, Chatterjee B, Lo CW, Naus CC (2004) The complex of ciliary neurotrophic factor-ciliary neurotrophic factor receptor alpha up-regulates connexin43 and intercellular coupling in astrocytes via the Janus tyrosine kinase/signal transducer and activator of transcription pathway. Mol Biol Cell 15:4761–4774.
Parpura V, Heneka MT, Montana V, Oliet SH, Schousboe A, Haydon PG, Stout Jr RF, Spray DC, Reichenbach A, Pannicke T, Pekny M, Pekna M, Zorec R, Verkhratsky A (2012) Glial cells in (patho)physiology. J Neurochem 121:4–27.
Pekny M, Pekna M (2014) Astrocyte reactivity and reactive astrogliosis: costs and benefits. Physiol Rev 94:1077–1098.
Pekny M, Pekna M, Messing A, Steinhauser C, Lee JM, Parpura V, Hol EM, Sofroniew MV, Verkhratsky A (2016) Astrocytes: a central element in neurological diseases. Acta Neuropathol 131:323–345.
Pfrieger FW, Slezak M (2012) Genetic approaches to study glial cells in the rodent brain. Glia 60:681–701.
Raymond M, Li P, Mangin JM, Huntsman M, Gallo V (2011) Chronic perinatal hypoxia reduces glutamate-aspartate transporter function in astrocytes through the Janus kinase/signal transducer and activator of transcription pathway. J Neurosci 31:17864–17871.
Reich NC, Liu L (2006) Tracking STAT nuclear traffic. Nat Rev Immunol 6:602–612.
Sarafian TA, Montes C, Imura T, Qi J, Coppola G, Geschwind DH, Sofroniew MV (2010) Disruption of astrocyte STAT3 signaling decreases mitochondrial function and increases oxidative stress in vitro. PLoS One 5:e9532.
Schubert KO, Naumann T, Schnell O, Zhi Q, Steup A, Hofmann HD, Kirsch M (2005) Activation of STAT3 signaling in axotomized neurons and reactive astrocytes after fimbria-fornix transection. Exp Brain Res 165:520–531.
Schust J, Sperl B, Hollis A, Mayer TU, Berg T (2006) Stattic: a small-molecule inhibitor of STAT3 activation and dimerization. Chem Biol 13:1235–1242.
Selvaraj BT, Frank N, Bender FL, Asan E, Sendtner M (2012) Local axonal function of STAT3 rescues axon degeneration in the pmn model of motoneuron disease. J Cell Biol 199:437–451.
Shen S, Niso-Santano M, Adjemian S, Takehara T, Malik SA, Minoux H, Souquere S, Marino G, Lachkar S, Senovilla L, Galluzzi L, Kepp O, Pierron G, Maiuri MC, Hikita H, Kroemer R, Kroemer G (2012) Cytoplasmic STAT3 represses autophagy by inhibiting PKR activity. Mol Cell 48:667–680.
Shibata N, Kakita A, Takahashi H, Ihara Y, Nobukuni K, Fujimura H, Sakoda S, Sasaki S, Iwata M, Morikawa S, Hirano A, Kobayashi M (2009) Activation of signal transducer and activator of transcription-3 in the spinal cord of sporadic amyotrophic lateral sclerosis patients. Neuro-degenerat Dis 6:118–126.
Shibata N, Yamamoto T, Hiroi A, Omi Y, Kato Y, Kobayashi M (2010) Activation of STAT3 and inhibitory effects of pioglitazone on STAT3 activity in a mouse model of SOD1-mutated amyotrophic lateral sclerosis. Neuropathology: official journal of the Japanese Society of. Neuropathology 30:353–360.
Shiratori-Hayashi M, Koga K, Tozaki-Saitoh H, Kohro Y, Toyonaga H, Yamaguchi C, Hasegawa A, Nakahara T, Hachisuka J, Akira S, Okano H, Furue M, Inoue K, Tsuda M (2015) STAT3-dependent reactive astrogliosis in the spinal dorsal horn underlies chronic itch. Nat Med 21:927–931.
Shuai K, Ziemiecki A, Wilks AF, Harpur AG, Sadowski HB, Gilman MZ, Darnell JE (1993) Polypeptide signalling to the nucleus through tyrosine phosphorylation of Jak and Stat proteins. Nature 366:580–583.
Sirko S, Behrendt G, Johansson PA, Tripathi P, Costa M, Bek S, Heinrich C, Tiedt S, Colak D, Dichgans M, Fischer IR, Plesnila N, Staufenbiel M, Haass C, Snapyan M, Saghatelyan A, Tsai LH, Fischer A, Grobe K, Dimou L, Gotz M (2013) Reactive glia in the injured brain acquire stem cell properties in response to sonic hedgehog [corrected]. Cell Stem Cell 12:426–439.
Sofroniew MV (2009) Molecular dissection of reactive astrogliosis and glial scar formation. Trends Neurosci 32:638–647.
Song MR, Ghosh A (2004) FGF2-induced chromatin remodeling regulates CNTF-mediated gene expression and astrocyte differentiation. Nat Neurosci 7:229–235.
Sriram K, Benkovic SA, Hebert MA, Miller DB, O'Callaghan JP (2004) Induction of gp130-related cytokines and activation of JAK2/STAT3 pathway in astrocytes precedes up-regulation of glial fibrillary acidic protein in the 1-methyl-4-phenyl-1,2,3,6-tetrahydropyridine model of neurodegeneration: key signaling pathway for astrogliosis in vivo? J Biol Chem 279:19936–19947.
Stark GR, Darnell Jr JE (2012) The JAK-STAT pathway at twenty. Immunity 36:503–514.
Szczepanek K, Lesnefsky EJ, Larner AC (2012) Multi-tasking: nuclear transcription factors with novel roles in the mitochondria. Trends Cell Biol 22:429–437.
Takizawa T, Nakashima K, Namihira M, Ochiai W, Uemura A, Yanagisawa M, Fujita N, Nakao M, Taga T (2001) DNA methylation is a critical cell-intrinsic determinant of astrocyte differentiation in the fetal brain. Dev. Cell 1:749–758.
Tsuda M, Kohro Y, Yano T, Tsujikawa T, Kitano J, Tozaki-Saitoh H, Koyanagi S, Ohdo S, Ji RR, Salter MW, Inoue K (2011) JAK-STAT3 pathway regulates spinal astrocyte proliferation and neuropathic pain maintenance in rats. Brain 134:1127–1139.
Tyzack GE, Sitnikov S, Barson D, Adams-Carr KL, Lau NK, Kwok JC, Zhao C, Franklin RJ, Karadottir RT, Fawcett JW, Lakatos A (2014) Astrocyte response to motor neuron injury promotes structural synaptic plasticity via STAT3-regulated TSP-1 expression. Nat Commun 5:4294.
Verkhratsky A, Steardo L, Parpura V, Montana V (2015) Translational potential of astrocytes in brain disorders. Progr Neurobiol.

Wang J, Li G, Wang Z, Zhang X, Yao L, Wang F, Liu S, Yin J, Ling EA, Wang L, Hao A (2012) High glucose-induced expression of inflammatory cytokines and reactive oxygen species in cultured astrocytes. Neuroscience 202:58–68.

Wang R, Cherukuri P, Luo J (2005) Activation of Stat3 sequence-specific DNA binding and transcription by p300/CREB-binding protein-mediated acetylation. J Biol Chem 280:11528–11534.

Wanner IB, Anderson MA, Song B, Levine J, Fernandez A, Gray-Thompson Z, Ao Y, Sofroniew MV (2013) Glial scar borders are formed by newly proliferated, elongated astrocytes that interact to corral inflammatory and fibrotic cells via STAT3-dependent mechanisms after spinal cord injury. J Neurosci 33:12870–12886.

Washburn KB, Neary JT (2006) P2 purinergic receptors signal to STAT3 in astrocytes: Difference in STAT3 responses to P2Y and P2X receptor activation. Neuroscience 142:411–423.

Wegrzyn J, Potla R, Chwae YJ, Sepuri NB, Zhang Q, Koeck T, Derecka M, Szczepanek K, Szelag M, Gornicka A, Moh A, Moghaddas S, Chen Q, Bobbili S, Cichy J, Dulak J, Baker DP, Wolfman A, Stuehr D, Hassan MO, Fu XY, Avadhani N, Drake JI, Fawcett P, Lesnefsky EJ, Larner AC (2009) Function of mitochondrial Stat3 in cellular respiration. Science 323:793–797.

Wen Z, Zhong Z, Darnell Jr JE (1995) Maximal activation of transcription by Stat1 and Stat3 requires both tyrosine and serine phosphorylation. Cell 82:241–250.

Xia XG, Hofmann HD, Deller T, Kirsch M (2002) Induction of STAT3 signaling in activated astrocytes and sprouting septal neurons following entorhinal cortex lesion in adult rats. Mol Cell Neurosci 21:379–392.

Xu Z, Xue T, Zhang Z, Wang X, Xu P, Zhang J, Lei X, Li Y, Xie Y, Wang L, Fang M, Chen Y (2011) Role of signal transducer and activator of transcription-3 in up-regulation of GFAP after epilepsy. Neurochem Res 36:2208–2215.

Yang J, Huang J, Dasgupta M, Sears N, Miyagi M, Wang B, Chance MR, Chen X, Du Y, Wang Y, An L, Wang Q, Lu T, Zhang X, Wang Z, Stark GR (2010) Reversible methylation of promoter-bound STAT3 by histone-modifying enzymes. Proc Natl Acad Sci USA 107:21499–21504.

Yang J, Stark GR (2008) Roles of unphosphorylated STATs in signaling. Cell Res 18:443–451.

Yang R, Rincon M (2016) Mitochondrial Stat3, the Need for Design Thinking. Int J Biol Sci 12:532–544.

Yeo S, Bandyopadhyay S, Messing A, Brenner M (2013) Transgenic analysis of GFAP promoter elements. Glia 61:1488–1499.

You L, Wang Z, Li H, Shou J, Jing Z, Xie J, Sui X, Pan H, Han W (2015) The role of STAT3 in autophagy. Autophagy 11:729–739.

Yu H, Pardoll D, Jove R (2009) STATs in cancer inflammation and immunity: a leading role for STAT3. Nat Rev Cancer 9:798–809.

Yuan ZL, Guan YJ, Chatterjee D, Chin YE (2005) Stat3 dimerization regulated by reversible acetylation of a single lysine residue. Science 307:269–273.

Zamanian JL, Xu L, Foo LC, Nouri N, Zhou L, Giffard RG, Barres BA (2012) Genomic analysis of reactive astrogliosis. J Neurosci 32:6391–6410.

Zhang S, Li W, Wang W, Zhang SS, Huang P, Zhang C (2013) Expression and activation of STAT3 in the astrocytes of optic nerve in a rat model of transient intraocular hypertension. PLoS One 8:e55683.

Zhang Y, Ni S, Huang B, Wang L, Zhang X, Li X, Wang H, Liu S, Hao A, Li X (2015) Overexpression of SCLIP promotes growth and motility in glioblastoma cells. Cancer Biol Ther 16:97–105.

Zhong Z, Wen Z, Darnell Jr JE (1994a) Stat3 and Stat4: members of the family of signal transducers and activators of transcription. Proc Natl Acad Sci USA 91:4806–4810.

Zhong Z, Wen Z, Darnell Jr JE (1994b) Stat3: a STAT family member activated by tyrosine phosphorylation in response to epidermal growth factor and interleukin-6. Science 264:95–98.

Zhuang S (2013) Regulation of STAT signaling by acetylation. Cell Signal 25:1924–1931.

(Accepted 19 May 2016)
(Available online 27 May 2016)

Publication 3

Development/Plasticity/Repair

The JAK/STAT3 Pathway Is a Common Inducer of Astrocyte Reactivity in Alzheimer's and Huntington's Diseases

Lucile Ben Haim,[1,2] Kelly Ceyzériat,[1,2] Maria Angeles Carrillo-de Sauvage,[1,2] Fabien Aubry,[1,2] Gwennaëlle Auregan,[1,2] Martine Guillermier,[1,2] Marta Ruiz,[1,2] Fanny Petit,[1,2] Diane Houitte,[1,2] Emilie Faivre,[1,2] Matthias Vandesquille,[1,2] Romina Aron-Badin,[1,2] Marc Dhenain,[1,2] Nicole Déglon,[1,2] Philippe Hantraye,[1,2] Emmanuel Brouillet,[1,2] Gilles Bonvento,[1,2] and Carole Escartin[1,2]

[1]Commissariat à l'Energie Atomique et aux Energies Alternatives (CEA), Département des Sciences du Vivant (DSV), Institut d'Imagerie Biomédicale (I2BM), Molecular Imaging Research Center (MIRCen), F-92260 Fontenay-aux-Roses, France, and [2]Centre National de la Recherche Scientifique (CNRS), Université Paris-Sud, UMR 9199, Neurodegenerative Diseases Laboratory, F-92260 Fontenay-aux-Roses, France

Astrocyte reactivity is a hallmark of neurodegenerative diseases (ND), but its effects on disease outcomes remain highly debated. Elucidation of the signaling cascades inducing reactivity in astrocytes during ND would help characterize the function of these cells and identify novel molecular targets to modulate disease progression. The Janus kinase/signal transducer and activator of transcription 3 (JAK/STAT3) pathway is associated with reactive astrocytes in models of acute injury, but it is unknown whether this pathway is directly responsible for astrocyte reactivity in progressive pathological conditions such as ND. In this study, we examined whether the JAK/STAT3 pathway promotes astrocyte reactivity in several animal models of ND. The JAK/STAT3 pathway was activated in reactive astrocytes in two transgenic mouse models of Alzheimer's disease and in a mouse and a nonhuman primate lentiviral vector-based model of Huntington's disease (HD). To determine whether this cascade was instrumental for astrocyte reactivity, we used a lentiviral vector that specifically targets astrocytes *in vivo* to overexpress the endogenous inhibitor of the JAK/STAT3 pathway [suppressor of cytokine signaling 3 (SOCS3)]. SOCS3 significantly inhibited this pathway in astrocytes, prevented astrocyte reactivity, and decreased microglial activation in models of both diseases. Inhibition of the JAK/STAT3 pathway within reactive astrocytes also increased the number of huntingtin aggregates, a neuropathological hallmark of HD, but did not influence neuronal death. Our data demonstrate that the JAK/STAT3 pathway is a common mediator of astrocyte reactivity that is highly conserved between disease states, species, and brain regions. This universal signaling cascade represents a potent target to study the role of reactive astrocytes in ND.

Key words: **animal models; lentiviral vector; neurodegenerative diseases; reactive astrocytes; SOCS3; STAT3**

Introduction

In response to multiple pathological conditions, astrocytes undergo molecular, morphological, and functional changes, referred to as astrocyte reactivity (Sofroniew and Vinters, 2010). They become hypertrophic, upregulate intermediate filament proteins, including GFAP and vimentin, and display functional alterations that are still not fully understood. Astrocyte reactivity occurs in both acute and progressive pathological conditions and is a hallmark of multiple neurodegenerative diseases (ND; Sofroniew and Vinters, 2010). Astrocyte reactivity develops in vulnerable regions at the early stages of ND and progresses along with neurological symptoms and cell death. Reactive astrocytes are observed in close proximity to amyloid depositions in both patients with Alzheimer's disease (AD) and mouse models of AD (Probst et al., 1982; Itagaki et al., 1989). They are also found in the striatum and cortex of patients with Huntington's disease (HD) and some mouse models of HD (Vonsattel et al., 1985; Yu et al., 2003; Faideau et al., 2010).

The involvement of reactive astrocytes in disease progression is highly controversial. Although they are generally considered as detrimental for neuronal function, several studies suggest that reactive astrocytes may have beneficial effects and promote neuronal survival (Escartin and Bonvento, 2008; Hamby and Sofroniew, 2010). In any case, elucidation of the precise molecular cascades that lead to astrocyte reactivity may help identify potential therapeutic targets to modulate disease progression.

Received Aug. 21, 2014; revised Dec. 8, 2014; accepted Dec. 31, 2014.

Author contributions: L.B.H. and C.E. designed research; L.B.H., K.C., M.A.C.d.S., F.A., G.A., M.G., M.R., F.P., D.H., R.A.-B., and C.E. performed research; E.F., M.V., M.D., N.D., P.H., E.B., and G.B. contributed unpublished reagents/analytic tools; L.B.H. and C.E. analyzed data; L.B.H. and C.E. wrote the paper.

This work was supported by French National Research Agency Grants 2010-JCJC-1402-1 and 2011-BSV4-021-03 (C.E.), 2011-MALZ-003-02 (G.B.), and 2011-INBS-0011 NeurATRIS (P.H.), the Association France Alzheimer (G.B. and M.D.), CEA, and CNRS. L.B.H. was a recipient of a PhD fellowship from the CEA (Irtelis program). We thank Dr. C. Bjørbæk and Dr. S. E. Shoelson for providing us with the pcDNA3-SOCS3 plasmid. We thank N. Dufour, C. Joséphine, and Dr. A. Bémelmans for viral vector production. We are grateful to P. Gipchtein and Dr. C. Jan for their help with immunostainings and Dr. M. C. Gaillard for technical advice on qRT-PCR analysis. We thank T. Kortulewski and L. Irbah for providing training and technical advice for confocal analysis.

The authors declare no competing financial interests.

Correspondence should be addressed to Carole Escartin, MIRCen 18, route du Panorama, F-92260 Fontenay-aux-Roses, France. E-mail: carole.escartin@cea.fr.

N. Déglon's present address: Laboratory of Cellular and Molecular Neurotherapies, Department of Clinical Neurosciences, Lausanne University Hospital, CH-1015 Lausanne, Switzerland.

DOI:10.1523/JNEUROSCI.3516-14.2015

 0270-6474/15/352817-13$15.00/0

Astrocytes can sense many extracellular signals, such as cytokines, growth factors, nucleotides, endothelins, or ephrins, that activate various intracellular signaling pathways, such as the mitogen-activated protein kinase, the nuclear factor κB (NF-κB), and the Janus kinase/signal transducer and activator of transcription (JAK/STAT) pathways (Kang and Hébert, 2011). Among them, the JAK/STAT3 pathway appears as a central player in the induction of astrocyte reactivity. It is activated by a variety of cytokines and growth factors that signal through the gp130 receptor (Levy and Darnell, 2002). Activation of the JAK/STAT3 pathway has been observed in reactive astrocytes in several conditions of acute injury (Justicia et al., 2000; Okada et al., 2006; Herrmann et al., 2008; O'Callaghan et al., 2014) and in patients and mouse models of amyotrophic lateral sclerosis (ALS; Shibata et al., 2009, 2010). However, it remains to be demonstrated whether the JAK/STAT3 pathway is directly responsible for astrocyte reactivity during progressive pathological conditions such as ND.

In this study, we show that the JAK/STAT3 pathway is activated in reactive astrocytes in several mouse and nonhuman primate models of AD and HD. Overexpression of suppressor of cytokine signaling 3 (SOCS3), the endogenous inhibitor of the JAK/STAT3 pathway in astrocytes *in vivo*, inhibited this pathway and prevented astrocyte reactivity. It also reduced microglial activation and increased the formation of mutant huntingtin (Htt) aggregates but did not affect neuronal death. These results identify the JAK/STAT3 pathway as a universal inducer of astrocyte reactivity, and its modulation affects several pathological features in ND.

Materials and Methods

Transgenic mouse models. Amyloid precursor protein (APP)/Presenilin 1 (PS1) mice [B6.Cg-Tg (APPswe, PSEN1dE9) 85Dbo (http://jaxmice.jax.org/strain/005864.html)] harbor the chimeric mouse/human APP gene with Swedish mutations K594N and M595L (APPswe) and the human PS1 variant lacking exon 9 on a C57BL/6J (http://jaxmice.jax.org/strain/000664.html) background (Jankowsky et al., 2004). APP/PS1dE9 breeding pairs were obtained from The Jackson Laboratory. Triple transgenic AD (3xTg-AD) mice express the mutated human APPswe, PS1M146V, and tauP301L transgenes on a mixed 129Sv (http://jaxmice.jax.org/strain/002448.html) and C57BL/6J background (Oddo et al., 2003). Breeding pairs of 3xTg-AD mice were obtained from the Mutant Mouse Regional Resource Centers. We used 8-month-old APP/PS1dE9 heterozygous females, 12-month-old 3xTg-AD homozygous females, and their respective age-matched wild-type (WT) control mice. Genotyping by PCR was performed at 4–6 weeks of age for APP/PS1dE9 mice. All experimental procedures were approved by a local ethics committee and submitted to the French Ministry of Education and Research (Approval 10-057). They were performed in strict accordance with the recommendations of the European Union (86/609/EEC) for the care and use of laboratory animals.

Lentiviral vectors and injections in mice. We used self-inactivated lentiviral vectors containing the central polypurine tract sequence, the mouse phosphoglycerate kinase I promoter, and the woodchuck postregulatory element sequence. We used two types of vectors to mediate transgene expression in either neurons or astrocytes. To target neurons, lentiviral vectors were pseudotyped with the G-protein of the vesicular stomatitis virus (Naldini et al., 1996). To target astrocytes, lentiviral vectors were pseudotyped with the G-protein of the Mokola lyssaviruses and contained four copies of the target sequence of the neuronal miRNA124 to repress transgene expression in neurons (Colin et al., 2009). Lentiviral vectors are referred to as "lenti-name of the transgene" in the subsequent sections of this manuscript. Neuron-targeted vectors encoded the first 171 N-terminal amino acids of human Htt cDNA with either 18 (lenti-Htt18Q) or 82 (lenti-Htt82Q) polyglutamine repeats (de Almeida et al., 2002). Astrocyte-targeted vectors encoded either the enhanced green fluorescent protein cDNA (lenti-GFP) or the murine SOCS3 cDNA (lenti-SOCS3; Bjørbaek et al., 1998).

The production and titration of these lentiviruses have been described previously (Hottinger et al., 2000). Lentiviral vectors were diluted in 0.1 M PBS with 1% BSA at a final concentration of 100 ng p24/μl. Mice were anesthetized with a mixture of ketamine (150 mg/kg) and xylazine (10 mg/kg). Lidocaine (5 mg/kg) was injected subcutaneously under the scalp 5 min before the beginning of surgery. C57BL/6J and 3xTg-AD mice received bilateral stereotaxic injections of diluted lentiviral vectors in the striatum or the subiculum, respectively, administered by a 10 μl Hamilton syringe via a 34 gauge blunt needle. The stereotaxic coordinates used were as follows: for the striatum, anteroposterior (AP), +1 mm; lateral (L), ±2 mm from bregma; ventral (V), −2.5 mm from the dura; and for the subiculum, AP, −2.92 mm; L, ±1.5 mm; V, −1.5 mm, with ear bars set at 4 mm and a tooth bar set at 0 mm. Mice received a total volume of 2.5 or 3.5 μl per injection site at a rate of 0.25 μl/min. At the end of the injection, the needle was left in place for 5 min before being removed slowly. The skin was sutured, and mice were allowed to recover.

For the lentiviral vector-based HD model (de Almeida et al., 2002), 8-week-old male C57BL/6J mice were injected with lenti-Htt18Q (100 ng of p24) and lenti-GFP (150 ng of p24) in the left striatum and with lenti-Htt82Q (100 ng of p24) and lenti-GFP (150 ng of p24) in the right striatum.

To inhibit the JAK/STAT3 pathway in the HD model, 8-week-old male C57BL/6 mice were injected bilaterally in the striatum with lenti-Htt82Q (150 ng of p24) and coinjected with the control lenti-GFP (200 ng of p24) in the left striatum and with lenti-SOCS3 (150 ng of p24) and lenti-GFP (50 ng of p24) in the right striatum. To inhibit the JAK/STAT3 pathway in the AD model, 7- to 8-month-old 3xTg-AD female mice were injected in the subiculum with either lenti-GFP (250 ng of p24) or lenti-SOCS3 (200 ng of p24) and lenti-GFP (50 ng of p24). Coinjections with lenti-GFP were performed to visualize the infected area and the morphology of infected cells as SOCS3 cannot be detected by immunohistochemistry because of the lack of specific antibodies. Postmortem analysis was performed 6 weeks after injection for HD mice and 4.5 months after injection for 3xTg-AD mice.

Primate model of HD. Three adult male cynomolgus monkeys (*Macaca fascicularis*, 4.2 ± 0.08 kg) were used in this study according to European (European Union Directive 86/609/EEC) and French (French Act Rural Code R 214-87-131) regulations. The animal facility was approved by veterinarian inspectors (Authorization 92-032-02) and complies with Standards for Humane Care and Use of Laboratory Animals of the Office of Laboratory Animal Welfare (A5826-01).

Magnetic resonance imaging (MRI) was performed on each macaque to calculate stereotaxic coordinates for lentiviral injection. MRI was performed on a 7 Tesla scanner (Varian) with the following parameters: TR, 15 ms; TE, 5500 ms; TI, 10 ms; flip angle, 90°; and 0.45 × 0.45 × 1 mm with coronal acquisition on a 256 × 256 × 40 matrix. For lentiviral injections, animals were anesthetized with a mixture of ketamine (10 mg/kg) and xylazine (1 mg/kg) and were kept under intravenous infusion of propofol (1% Rapinovet, 0.05–0.25 $mg \cdot kg^{-1} \cdot min^{-1}$) throughout the procedure with continuous monitoring of cardiac and respiratory frequencies, blood pressure, and temperature. Animals were placed in a custom-made stereotaxic frame, and a KDS injection micropump connected to a Hamilton syringe and a 26 gauge needle were used to perform five bilateral injections of 5 μl of lenti-Htt82Q at a rate of 1 μl/min. The injection sites comprised two deposits in the precommissural caudate [anterior commissure (AC) +5, AC +3)] and three deposits in the commissural and postcommissural (AC −2, AC −5) putamen. Postmortem analysis was performed 16–18 months later.

Immunofluorescence. For histological processing, animals were killed with an overdose of sodium pentobarbital. Animals were either perfused transcardially with 4% paraformaldehyde (PFA) or their brains were postfixed for 24 h in 4% PFA. Brains were cryoprotected by incubation in a 30% sucrose solution. Coronal brain sections (mice, 30 μm; monkey, 40 μm) were cut on a freezing microtome, collected serially, and stored at −20°C until additional analysis. Antigen retrieval protocols were used for STAT3 and 4G8 staining. For STAT3 immunofluorescence, slices were permeabilized with 100% methanol at −20°C for 20 min. For 4G8 staining, slices were pretreated in 70% formic acid for 5 min. Sections were then blocked with 4.5% normal goat serum (Sigma) and incubated

with primary antibodies directed against the following proteins: 4G8 (1:500, mouse; Signet Covance), EM48 (1:200, mouse; Millipore Bioscience Research Reagents), GFAP–Cy3 (1:1000, mouse; Invitrogen), IBA1 (1:1000, rabbit; Wako), S100β (1:500, mouse; Invitrogen), STAT3 (STAT3α, 1:200, rabbit; Cell Signaling Technology), and vimentin (1:1000, chicken; Abcam). Anti-STAT3 antibody was diluted in Signal Boost antibody diluent (Cell Signaling Technology). Brain sections were incubated for 36 h with STAT3 antibody and overnight at 4°C for all other antibodies. After rinsing, brain slices were incubated for 1–2 h at room temperature with fluorescent secondary Alexa Fluor-conjugated antibodies (Invitrogen). Slices were stained with DAPI (1:2000; Sigma), mounted with FluorSave reagent (Calbiochem), and analyzed by either epifluorescence (DM6000; Leica) or confocal microscopy (LSM 510 by Zeiss; and TCS SPE or SP8 by Leica).

Immunohistochemistry. Brain slices were pretreated in 0.3% H_2O_2, blocked in 4.5% NGS (Sigma), and incubated overnight at 4°C with primary antibodies directed against DARPP32 (1:1000, rabbit; Santa Cruz Biotechnology) or EM48 (1:200). After rinsing, brain slices were incubated with biotinylated secondary antibodies (Vector Laboratories) for 1 h at room temperature. Finally, they were incubated with the Vectastain Elite ABC Kit (Vector Laboratories) and revealed with the DAB kit (Vector Laboratories).

Cytochrome c oxidase histochemistry. Brain slices were incubated in 0.1 M PB, 4% sucrose, 0.05% DAB (Sigma), and 0.03% cytochrome *c* (Sigma) for 6 h at room temperature.

qRT-PCR. Mice were killed with an overdose of sodium pentobarbital. Mouse brains were rapidly collected and sliced into 1-mm-thick coronal sections with a brain matrix. The GFP-positive (GFP^+) area on each slice was dissected with 1-mm-diameter punches (Ted Pella) under a fluorescence macroscope (MacroFluo; Leica). Punches were stored in RNA Later (Sigma) until additional processing. Total RNA was isolated from striatal punches with TRIzol (Invitrogen), and cDNA was synthesized from 0.2 μg of RNA with the VILO kit (Invitrogen) and diluted at 0.3 ng/μl. The Platinum SYBR Green qPCR SuperMix UDG (Invitrogen) was used to perform qRT-PCR. Three housekeeping genes were tested, and the peptidylprolyl isomerase A (*cyclophilin A*) gene was selected as the best normalizing gene, because it showed the minimal, nonsignificant, variation between groups. The abundance of each transcript of interest was then normalized to the abundance of *cyclophilin A* with the ΔCt method. The efficiency of qRT-PCR were between 85 and 110% for each set of primers. Distilled water and RT-negative reactions were used as negative controls. The sequences of oligonucleotides used for qRT-PCR are as follows: *aif1* (*iba1*), forward, CCAGCCTAAGACAACCAGCGTC and reverse, GCTGTATTTGGGATCATCGAGGAA; *ccl2*, forward, ACCAGCACCAGCCAACTCT and reverse, AGGCCCAGAAGCATGACA; *cyclophilin A*, forward, ATGGCAAATGCTGGACCAAA and reverse, GCCTTCTTTCACCTTCCCAAA; *gfap*, forward, ACGACTATCGCCGCCAACT and reverse, GCCGCTCTAGGGACTCGTTC; *itgam* (*CD11b*), forward, GGGAGAATGCTGCGAAGA and reverse, GCTGGCTTAGATGCGATGG; *socs3*, forward, CGAGAAGATTCCGCTGGTACTGA and reverse, TGATCCAGGAACTCCCGAATG; and *vimentin*, forward, TCGAGGTGGAGCGGGACAAC and reverse, TGCAGGGTGCTTTCGGCTTC.

Western blotting. Mice were killed with an overdose of sodium pentobarbital, and their brains were rapidly collected and sliced into 1-mm-thick coronal sections with a brain matrix. The striatum or the dorsal hippocampus were dissected out. Samples were then homogenized with a glass homogenizer in 50 mM Tris-HCl, pH 7.4, 100 mM NaCl, and 1% SDS, with protease (Roche) and phosphatase (Sigma) inhibitor cocktails. Protein concentration was determined by the BCA method. Protein samples were diluted in NuPAGE LDS sample buffer with NuPAGE Sample Reducing agent (Life Technologies), boiled for 5 min, loaded on a 4–12% Bis-Tris gel, submitted to SDS-PAGE, and transferred to a nitrocellulose membrane, with an iBlot transfer device (Life Technologies). Membranes were blotted overnight at 4°C with antibodies against GAPDH (1:4000, mouse; Abcam) or IκBα (1:500, mouse; Cell Signaling Technology) diluted in Tris-buffered saline with 0.1% Tween 20 and 5% BSA. After rinsing, secondary antibodies coupled to horseradish peroxidase were incubated with the membrane for 1 h (for IκBα, 1:500, Cell Signaling Technology; and for GAPDH, 1:5000, Vector Laboratories). Antibody binding was detected by a Fusion FX7 camera system (Thermo Fisher Scientific) after incubation with the enhanced chemiluminescence Clarity substrate (Bio-Rad). Band intensity for IκBα were measured with NIH Image J (http://imagej.nih.gov/ij/) and normalized to GAPDH. Positive controls for NF-κB pathway activation were included. They were prepared from HeLa cells treated with TNFα (Cell Signaling Technology).

Quantification of immunostainings. Immunofluorescent staining was quantified from stacked confocal images (18 steps; Z-step, 1 μm, maximum intensity stack) acquired with the 40× objective on three slices per mouse and three fields on each slice. The $GFAP^+$ area was measured on each 40× Z-stack image with the threshold function of NIH Image J. $GFAP^+$ and $IBA1^+$ areas were divided by the area of the image and expressed as a percentage. The average number of $GFAP^+$ cells expressing STAT3 in the nucleus ($nSTAT3^+/GFAP^+$ cells) was quantified on these images. In lenti-GFP-injected mice, we also quantified the average number of GFP^+ infected astrocytes coexpressing STAT3 ($GFP^+/STAT3^+$ cells), GFAP ($GFP^+/GFAP^+$ cells), or S100β ($GFP^+/S100\beta^+$ cells). Finally, astrocyte soma was manually segmented, and the corresponding mean gray value for STAT3 staining was measured with NIH Image J. We then determined the number of cells with a mean gray value for STAT3 over a fixed threshold for each experiment. These cells were considered as cells expressing high levels of STAT3. Unfortunately, the presence of autofluorescent puncta in the subiculum made it impossible to quantify reliably the intensity of STAT3 staining in 3xTg-AD mice and WT controls. Microscope settings and NIH Image J thresholds were identical for all images and mice, within each experiment. Immunohistochemical stainings were quantified on bright-field images, acquired with the 2.5× (COX and DARPP32 stainings) or 10× (EM48 staining) objectives, on five to eight serial sections per mice. The lesion was detected by a loss of DARPP32 and COX staining and was manually segmented with NIH Image J on each slice. The lesion volume was calculated with the Cavalieri method (Damiano et al., 2013). $EM48^+$ aggregates were automatically detected on each image with the threshold function of the Morphostrider analysis software (Explora Nova), as described previously (Francelle et al., 2014). From these measurements, the average size and the total number of aggregates were calculated.

Statistical analysis. Results are expressed as mean ± SEM. Statistical analysis was performed with Statview software. We used Student's *t* test to compare two experimental groups and a Student's paired *t* test for left–right comparisons. The fraction of cells expressing high levels of STAT3 was normalized by the arcsine transformation, before applying a Student's *t* test. The results of qRT-PCR were analyzed using two-way (Htt length and treatment) ANOVA test and Scheffé *post hoc* test. The significance level was set at $p < 0.05$.

Results

Astrocyte reactivity is observed in vulnerable brain regions in AD and HD mouse models

Reactive astrocytes overexpressing GFAP were found around $4G8^+$ amyloid depositions in both the APP/PS1dE9 and the 3xTg-AD transgenic mouse models of AD, consistent with previous findings (Oddo et al., 2003; Ruan et al., 2009). In particular, astrocytes overexpressed GFAP and displayed hypertrophic processes in the stratum lacunosum moleculare and the dentate gyrus of 8-month-old APP/PS1d9 mice (Figs. 1*A*, 2*A*,*B*). We quantified this phenomenon by counting the number of pixels that were positive for GFAP staining on confocal images of the hippocampus. The $GFAP^+$ area was four times larger in APP/PS1d9 mice than in WT mice ($p = 0.0010$, df = 5, Student's *t* test; Fig. 1*B*). Astrocytes in APP/PS1dE9 mice also strongly expressed vimentin (Fig. 2*B*). The APP/PS1dE9 mouse is a quickly evolving model of AD, with substantial deposits of amyloid at 6 months of age (Jankowsky et al., 2004). Thus, we analyzed astrocyte reactivity in 3xTg-AD mice, a more progressive model of AD. We observed astrocyte reactivity around amyloid depositions primarily

in the subicular region of the hippocampus, in female 3xTg-AD mice at 12 months of age (Figs. 1*C*, 3*A*,*B*). In this region, the GFAP$^+$ area was 13-fold larger in 3xTg-AD mice than in age-matched controls ($p < 0.0001$, df = 6, Student's *t* test; Fig. 1*D*). Furthermore, astrocytes displayed a reactive morphology with enlarged soma and processes and overexpressed vimentin, which was nearly undetectable in WT mice (Fig. 3*B*).

We also characterized astrocyte reactivity in mouse models of HD. We studied two HD transgenic mouse models, N171-82Q mice (Schilling et al., 1999) and Hdh140 knock-in HD mice (Menalled et al., 2003). Although these models recapitulate the typical features of HD, we found that they displayed undetectable or very late astrocyte reactivity in the striatum and cortex, similar to what has been described in other mouse models (Tong et al., 2014). Thus, we focused on a lentiviral-based model of HD that has been used extensively (Ruiz and Déglon, 2012). This model reproduces both neuronal death and strong astrocyte reactivity in the striatum, as observed in HD patients (Faideau et al., 2010). C57BL/6 mice were injected in the left striatum with a lentiviral vector encoding normal Htt with 18 glutamines (lenti-Htt18Q) and in the right striatum with a lentiviral vector encoding mutant Htt (mHtt) with 82 glutamines (lenti-Htt82Q). Mice were studied 6 weeks later. As described previously (Faideau et al., 2010; Francelle et al., 2014), overexpression of Htt82Q in neurons led to the formation of intraneuronal EM48$^+$ aggregates of mHtt (Fig. 1*E*). In the lenti-Htt82Q-injected striatum, astrocytes strongly upregulated both GFAP and vimentin relative to the contralateral striatum injected with lenti-Htt18Q (Figs. 1*E*, 4*A*). The GFAP$^+$ area within the injected area was six times larger in the Htt82Q side than in the Htt18Q side ($p = 0.0098$, df = 5, Student's paired *t* test; Fig. 1*F*).

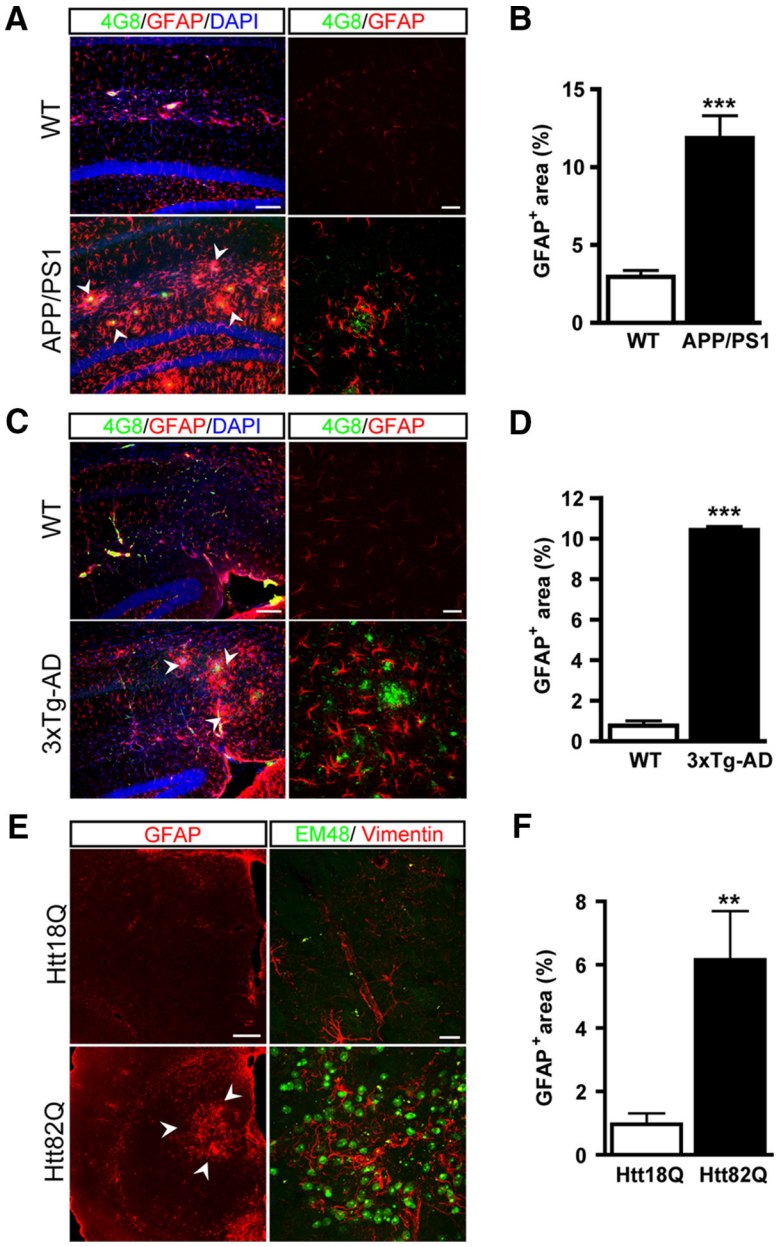

Figure 1. Mouse models of AD and HD display astrocyte reactivity in vulnerable regions of the brain. ***A–C***, Images of brain sections from mouse models of AD showing double staining for amyloid plaques (4G8, green) and astrocytes (GFAP, red). ***A***, GFAP is strongly expressed in hippocampal astrocytes of 8-month-old APP/PS1dE9 mice around amyloid depositions (arrowheads) in the stratum lacunosum moleculare and the dentate gyrus. ***B***, Quantification of the GFAP$^+$ area in the hippocampus of APP/PS1dE9 and WT mice. ***C***, In the subiculum, 3xTg-AD mice display amyloid depositions that are surrounded by GFAP$^+$ reactive astrocytes (arrowheads). ***D***, Quantification of the GFAP$^+$ area in the subiculum of 12-month-old 3xTg-AD mice and age-matched WT mice. ***E***, Mice injected with lenti-Htt82Q in the striatum display EM48$^+$ aggregates of mHtt (green). Expression of the mHtt in striatal neurons leads to astrocyte reactivity (arrowheads) as shown by increased GFAP and vimentin staining (red). ***F***, Quantification of the GFAP$^+$ area in the lenti-Htt82Q-injected striatum relative to the control striatum injected with lenti-Htt18Q. $n = 3–6$ per group. $^{**}p < 0.01$, $^{***}p < 0.001$. Scale bars: ***A*** and ***C***, left, 100 μm; right, 20 μm; ***E***, left, 200 μm; right, 20 μm.

The JAK/STAT3 pathway is activated in reactive astrocytes in AD and HD mouse models

We next evaluated whether astrocyte reactivity observed in these models was associated with activation of the JAK/STAT3 pathway. The phosphorylated form of STAT3 (pSTAT3) was undetectable by immunofluorescence or Western blotting in these progressive models of ND. After activation, pSTAT3 translocates to the nucleus in which it induces the transcription of a set of target genes, including the *Stat3* gene itself (Campbell et al., 2014). Thus, we considered STAT3 nuclear localization and increased immunoreactivity as indexes of JAK/STAT3 pathway activation, as reported previously (Escartin et al., 2006; Tyzack et al., 2014). This also enabled us to identify cell types displaying an active JAK/STAT3 pathway. To validate this surrogate marker of JAK/STAT3 pathway activation, we used ciliary neurotrophic factor (CNTF), a well known activator of this pathway (Bonni et al., 1993) in astrocytes (Escartin et al., 2006). Besides increasing STAT3 phosphorylation, CNTF overexpression in the mouse striatum increased STAT3 levels in the nucleus of reactive astrocytes (data not shown). Interestingly, STAT3 staining was observed predominantly in astrocytes in all models of ND. In

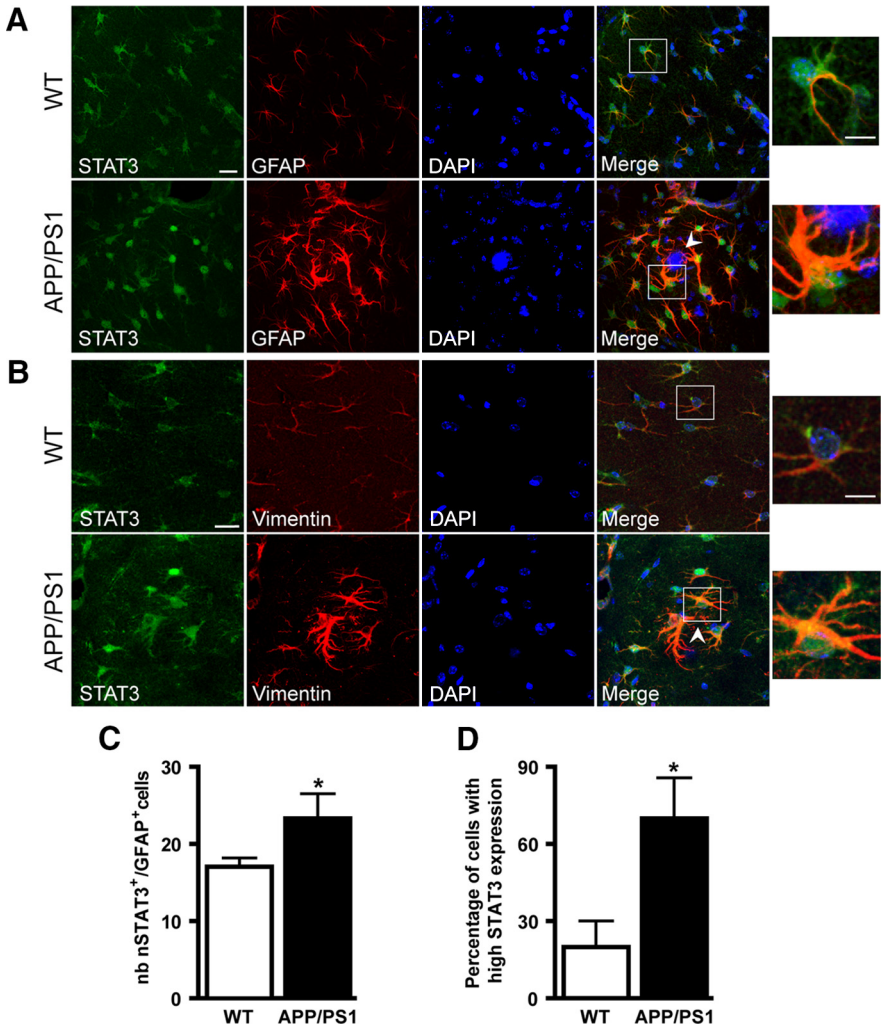

Figure 2. The JAK/STAT3 pathway is activated in reactive astrocytes in APP/PS1dE9 mice. ***A***, ***B***, Images of brain sections from 8-month-old APP/PS1dE9 mice showing double staining for STAT3 (green) and reactive astrocyte markers (***A***, GFAP; ***B***, vimentin). APP/PS1dE9 mice display reactive astrocytes that overexpress GFAP, vimentin, and STAT3 around amyloid plaques (arrowhead) in the hippocampus. STAT3 accumulates in the nucleus of reactive astrocytes (see enlargement). ***C***, The number of GFAP$^+$ astrocytes coexpressing STAT3 in the nucleus (nSTAT3$^+$/GFAP$^+$ cells) is significantly higher in APP/PS1dE9 mice than in WT mice. ***D***, The percentage of cells showing strong staining for STAT3 is higher in APP/PS1dE9 mice than in WT mice. $n = 3$–4 per group. $^*p < 0.05$. Scale bars: 20 μm; enlargements, 5 μm.

8-month-old APP/PS1dE9 mice, there was an accumulation of STAT3 in the nucleus of GFAP$^+$ and vimentin$^+$ reactive astrocytes, whereas in age-matched WT mice, STAT3 was expressed at the basal level throughout the astrocyte cytoplasm (Fig. 2*A*,*B*). The number of GFAP$^+$ astrocytes expressing STAT3 in the nucleus (nSTAT3$^+$/GFAP$^+$ cells) was higher in APP/PS1dE9 mice than in age-matched WT mice ($p = 0.0235$, df = 5, Student's *t* test; Fig. 2*C*). We also measured STAT3 immunoreactivity in astrocyte cell bodies. The percentage of cells with high STAT3 expression was more than threefold higher in APP/PS1dE9 mice than in WT mice, reflecting STAT3 activation in this mouse model of AD ($p = 0.0226$, df = 5, Student's *t* test; Fig. 2*D*).

In the subiculum of 12-month-old female 3xTg-AD mice, there was also a strong increase in STAT3 immunoreactivity in the nucleus of reactive astrocytes overexpressing GFAP and vimentin (Fig. 3*A*,*B*). The number of astrocytes coexpressing GFAP and STAT3 in the nucleus was >10-fold higher in 3xTg-AD mice than in age-matched WT mice ($p < 0.0001$, df = 6, Student's *t* test; Fig. 3*C*).

We then investigated whether the JAK/STAT3 pathway was also activated in the mouse model of HD. STAT3 staining was strongly upregulated in reactive astrocytes found in the lenti-Htt82Q-injected striatum (Fig. 4*A*). Indeed, there were four times more nSTAT3$^+$/GFAP$^+$ astrocytes in the Htt82Q striatum than in the Htt18Q striatum ($p = 0.0004$, df = 5, Student's paired *t* test; Fig. 4*B*). Cells expressing high levels of STAT3 were also more abundant in the Htt82Q striatum than in the Htt18Q striatum ($p = 0.0060$, df = 5, Student's paired *t* test; Fig. 4*C*). We sought to evaluate whether the JAK/STAT3 pathway was also activated in reactive astrocytes in other species. We took advantage of the fact that lentiviral vectors can be used in several animal species, including nonhuman primates. Injection of lenti-Htt82Q in the macaque putamen leads to the formation of mHtt aggregates, neuronal death, and motor symptoms (Palfi et al., 2007). We found that the injection of lenti-Htt82Q into the macaque putamen induced the formation of EM48$^+$ aggregates of mHtt and led to strong astrocyte reactivity (Fig. 5). There was a prominent accumulation of STAT3 in the nucleus of GFAP$^+$ reactive astrocytes. In contrast, at a distance from the injection area, resting astrocytes of the same animal expressed nearly undetectable levels of both GFAP and STAT3 (Fig. 5).

These results suggest that the JAK/STAT3 pathway is a common signaling cascade for astrocyte reactivity in several models of ND, which involve different pathological mechanisms, brain regions, and animal species.

The NF-κB pathway is not activated in 3xTg-AD mice and in the lentiviral-based model of HD

Other pathways, such as NF-κB, have been associated with astrocyte reactivity (Kang and Hébert, 2011). Therefore, we used Western blotting to measure the abundance of IκBα, the master inhibitor of the NF-κB pathway, which is degraded during pathway activation (Hayden and Ghosh, 2008).

We performed this experiment with 3xTg-AD mice and lenti-Htt82Q-injected mice, because astrocyte reactivity was the strongest in these models. In 3xTg-AD mice, the abundance of IκBα normalized to GAPDH was similar to that in WT mice ($p = 0.4037$, df = 8, Student's *t* test; Fig. 6*A*), whereas the positive control of cells treated with the cytokine TNFα displayed the expected decrease in IκBα levels (Fig. 6*A*,*B*). Similarly, the abundance of IκBα normalized to GAPDH was not different between the Htt18Q striatum and the Htt82Q striatum ($p = 0.8062$, df = 5, Student's paired *t* test; Fig. 6*B*).

The JAK/STAT3 pathway is responsible for astrocyte reactivity in AD and HD models

To establish that the JAK/STAT3 pathway was responsible for astrocyte reactivity, we inhibited this pathway by overexpressing

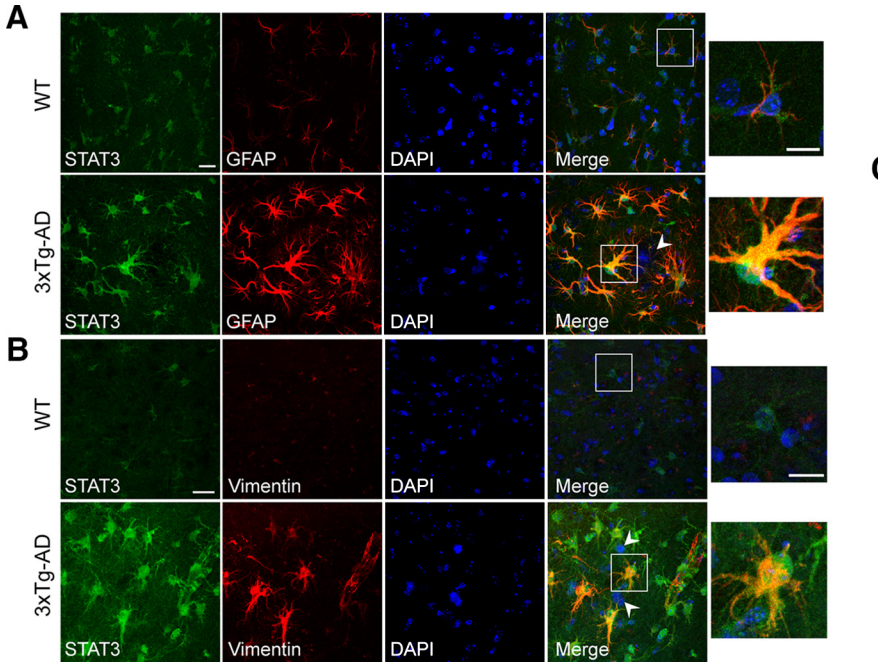

Figure 3. The JAK/STAT3 pathway is activated in reactive astrocytes in 3xTg-AD mice. ***A***, ***B***, Images of brain sections from the subiculum of 12-month-old 3xTg-AD mice. STAT3 (green) accumulates in the nucleus of reactive astrocytes labeled with GFAP (***A***, red) or vimentin (***B***, red), especially around amyloid plaques (arrowheads). ***C***, The number of nSTAT3$^+$/GFAP$^+$ cells is significantly higher in 3xTg-AD mice than in age-matched WT controls. $n = 3$–5 per group. $^{***}p < 0.001$. Scale bars: 20 μm; enlargements, 5 μm.

its endogenous inhibitor SOCS3 through selective lentiviral gene transfer in astrocytes. SOCS3 blocks STAT association with JAK2 (Kershaw et al., 2013) and prevents its phosphorylation, operating a negative feedback on the JAK/STAT3 pathway (Starr et al., 1997).

We used Mokola-pseudotyped lentiviral vectors that selectively target astrocytes (Colin et al., 2009; Figs. 7*F*, 8*G*) We did not detect transgene expression in other brain cell types, such as IBA1$^+$ microglia (Fig. 9*A*), NeuN$^+$ neurons, NG2$^+$ oligodendrocyte progenitors, or MBP$^+$ myelinating oligodendrocytes (data not shown). In addition, we checked that infection of astrocytes with a control lentiviral vector (lenti-GFP) did not lead to their activation in the striatum of WT mice or in the subiculum of 3xTg-AD mice. In both models, GFAP expression was similar between lenti-GFP controls and non-injected mice (data not shown).

We first tested whether SOCS3 overexpression in astrocytes was able to inhibit the JAK/STAT3 pathway. We used CNTF to strongly induce STAT3 phosphorylation, and we found that coinjection with lenti-SOCS3 significantly reduced pSTAT3 levels by Western blot (data not shown). We detected SOCS3 overexpression by qRT-PCR after lenti-SOCS3 injection (100-fold increase; Fig. 8*I*), but we were not able to show SOCS3 expression by immunohistochemistry because of the lack of specific antibodies. Therefore, for each experiment, we coinjected lenti-GFP with lenti-SOCS3 to visualize infected cells and their morphology. Indeed, we found that injection of two lentiviral vectors leads to a large majority of infected astrocytes coexpressing the two transgenes (88.7 ± 2%). Control mice were injected with lenti-GFP alone, at the same total virus load.

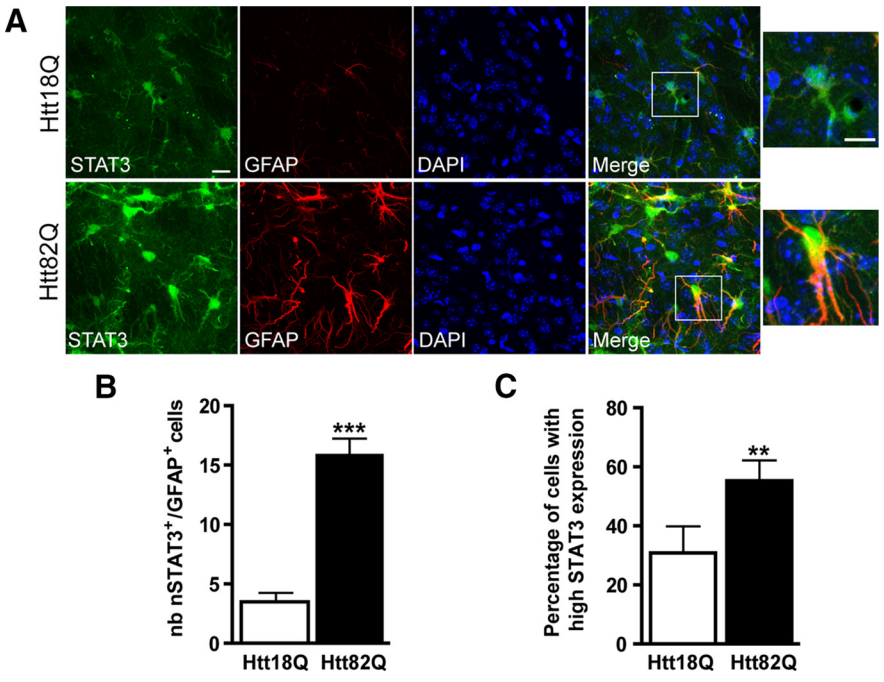

Figure 4. The JAK/STAT3 pathway is activated in reactive astrocytes in the mouse model of HD. ***A***, Images of brain sections showing double staining for GFAP (red) and STAT3 (green) on mouse brain sections, 6 weeks after the infection of striatal neurons with lenti-Htt18Q or lenti-Htt82Q. Astrocytes in the Htt82Q striatum are hypertrophic and express higher levels of STAT3 in their nucleus relative to resting astrocytes in the Htt18Q striatum. ***B***, ***C***, The number of nSTAT3$^+$/GFAP$^+$ cells (***B***) and the percentage of cells displaying strong staining for STAT3 (***C***) are significantly higher in the Htt82Q striatum than in the Htt18Q striatum. $n = 6$. $^{**}p < 0.01$, $^{***}p < 0.001$. Scale bars: 20 μm; enlargements, 5 μm.

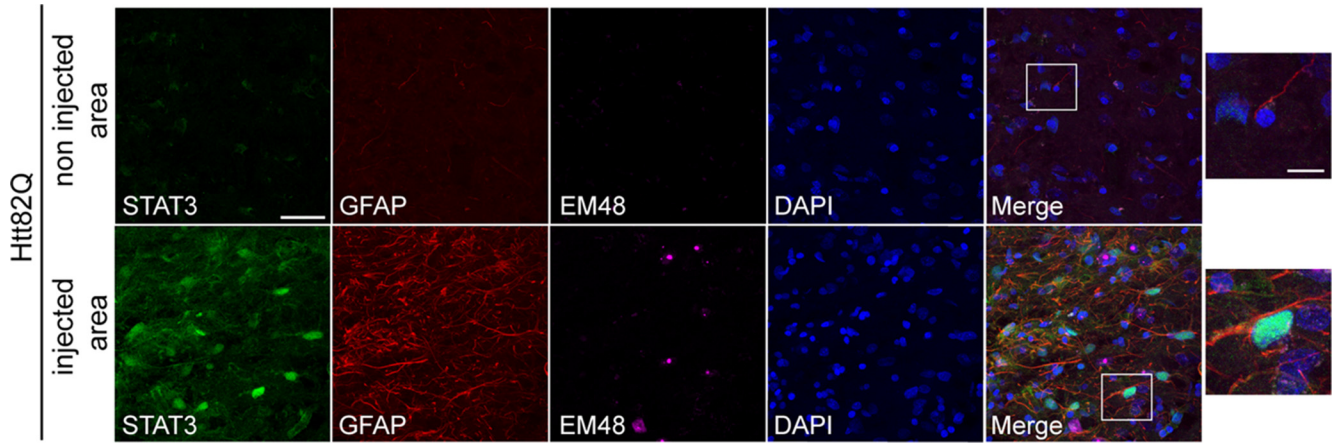

Figure 5. The JAK/STAT3 pathway is activated in reactive astrocytes in the primate model of HD. ***A***, Images of brain sections from macaques injected with lenti-Htt82Q in the putamen showing triple staining for STAT3 (green), GFAP (red), and EM48 (magenta). Seventeen months after infection with lenti-Htt82Q in the putamen, EM48$^+$ aggregates of mHtt are observed, as well as prominent astrocyte reactivity. The immunoreactivity for STAT3 is much stronger in GFAP$^+$ reactive astrocytes than in resting astrocytes found outside the injected area in the same animal. Images are representative of all three macaques. Scale bars: 40 μm; enlargement, 10 μm.

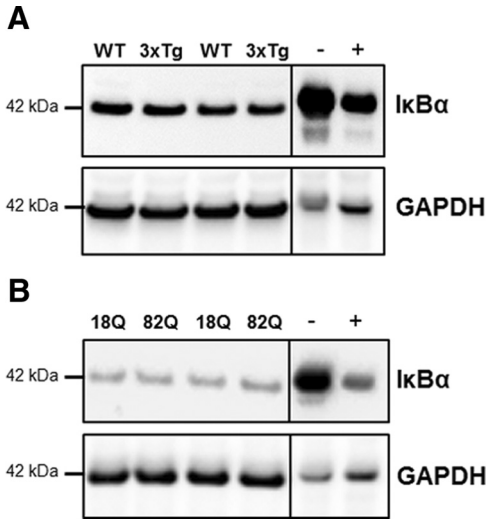

Figure 6. The NF-κB pathway is not activated in 3xTg-AD mice and the lentiviral-based model of HD. Western blot for IκBα and GAPDH in 3xTg-AD mice (3xTg) or their age-matched WT controls (***A***) or mice injected in the left striatum with lenti-Htt18Q (18Q) and in the right striatum with lenti-Htt82Q (82Q; ***B***). IκBα expression is similar between 3xTg-AD and WT mice and between the left and right striatum of mice injected with lenti-Htt. The abundance of IκBα is lower in HeLa cells treated with TNFα (positive control, +) than in untreated cells (negative control, −). $n = 4–6$ mice per group.

We injected lenti-SOCS3 plus lenti-GFP or lenti-GFP alone into the subiculum of 7- to 8-month-old 3xTg-AD mice, and we analyzed the mice 4.5 months later. The subiculum was chosen because it is the region displaying the most prominent accumulation of amyloid plaques and astrocyte reactivity at this age (Oddo et al., 2003; Fig. 1*C*). In 3xTg-AD mice, SOCS3 strongly decreased STAT3 expression in astrocytes (Fig. 7*A*). The number of GFP$^+$ astrocytes showing STAT3 immunoreactivity in the nucleus was significantly lower in mice coinfected with lenti-SOCS3 than in those infected with lenti-GFP alone ($p = 0.0375$, df = 6, Student's *t* test; Fig. 7*B*). SOCS3 overexpression visibly reduced GFAP expression in the subiculum (Fig. 7*C*). GFAP expression was 73% lower in the SOCS3 group than in the GFP controls, although this difference was not statistically significant ($p = 0.0827$, df = 6, Student's *t* test; Fig. 7*D*). There were significantly fewer GFP$^+$ astrocytes coexpressing GFAP in the SOCS3 group than in the control (−94%, $p = 0.0149$, df = 6, Student's *t* test; Fig. 7*E*). GFP expression in infected astrocytes allowed us to visualize their morphology in both groups. Astrocytes in the subiculum of 3xTg-AD mice displayed a morphology characteristic of reactive astrocytes with enlarged soma and large GFAP$^+$ primary processes (Fig. 7*A*,*C*,*F*). In contrast, SOCS3-infected astrocytes displayed complex ramifications composed of thin cytoplasmic processes organized radially around the soma (Fig. 7*A*,*C*,*F*), typical of resting astrocytes of the mouse brain (Wilhelmsson et al., 2006). We also performed immunostaining for S100β, a ubiquitous marker of astrocytes, to verify that SOCS3 did not globally impair protein expression in astrocytes. The number of GFP$^+$/S100β^+ astrocytes was similar between 3xTg-AD mice injected with lenti-SOCS3 or lenti-GFP (Fig. 7*F*,*G*).

We performed the same experiment with the lentiviral-based model of HD. C57BL/6 mice were injected with lenti-Htt82Q and lenti-GFP in the left striatum and with lenti-Htt82Q, lenti-SOCS3, and lenti-GFP in the right striatum at the same total virus load. Again, SOCS3 efficiently prevented the activation of the JAK/STAT3 pathway in astrocytes (Fig. 8*A*). The number of infected cells coexpressing STAT3 was 87% lower in the striatum injected with lenti-SOCS3 than in the control striatum ($p = 0.0072$, df = 3, Student's paired *t* test; Fig. 8*B*). In addition, the percentage of cells highly fluorescent for STAT3 was strongly reduced by SOCS3 ($p = 0.0118$, df = 3, Student's paired *t* test; Fig. 8*C*). SOCS3-expressing astrocytes displayed a bushy morphology with thin cytoplasmic processes and numerous ramifications, whereas reactive astrocytes in the control striatum showed enlarged and tortuous primary processes (Fig. 8*A*,*D*,*G*). Inhibition of the JAK/STAT3 pathway by SOCS3 prevented the increase of GFAP expression in the lenti-Htt82Q-injected area (Fig. 8*D*). The GFAP$^+$ area was 86% smaller in the striatum injected with lenti-SOCS3 than in the control striatum ($p = 0.0035$, df = 3, Student's paired *t* test; Fig. 8*E*). In addition, the number of GFP$^+$/GFAP$^+$ cells was significantly decreased by SOCS3 ($p = 0.0036$, df = 3, Student's paired *t* test, Fig. 8*F*). On the contrary, the number of GFP$^+$/S100β^+ astrocytes was not altered by SOCS3 (Fig. 8*G*,*H*).

Activation of the JAK/STAT3 pathway results in the transcriptional activation of many genes, including *gfap* and *vimentin*. Therefore, we studied the mRNA abundance of reactive astrocyte markers to characterize further the effect of SOCS3 expression in astrocytes. We only used the lentiviral-based HD model, because

the infected area in the subiculum of 3xTg-AD mice was too small to be dissected out for qRT-PCR analysis. We studied the effects of lenti-SOCS3 on mice injected with lenti-Htt18Q or lenti-Htt82Q compared with the control vector lenti-GFP by performing a two-way (Htt length and treatment) ANOVA. *gfap* mRNA was induced more than twofold by lenti-Htt82Q (Fig. 8*J*), consistent with immunofluorescence results. Expression of SOCS3 in astrocytes normalized the expression of *gfap* to levels comparable with controls ($p = 0.0254$ for Htt length × treatment effect, df = 1, two-way ANOVA; Fig. 8*J*). A similar pattern was observed with *vimentin* mRNA ($p = 0.0018$ for Htt length × treatment effect, df = 1, two-way ANOVA; Fig. 8*K*). Importantly, SOCS3 overexpression in mice injected with the control lentiviral vector lenti-Htt18Q did not change *gfap* or *vimentin* expression, showing that SOCS3 has no effect in resting astrocytes. These results suggest that inhibition of the JAK/STAT3 pathway in reactive astrocytes restores a resting-like status to astrocytes.

Preventing astrocyte reactivity reduces neuroinflammation

We then evaluated how the inhibition of astrocyte reactivity affected other pathological features (neuroinflammation, protein aggregation, and neuronal death).

We first studied the expression of IBA1, a marker of microglia that is upregulated during microglial activation attributable to both transcriptional regulation and morphological changes (Sieber et al., 2013). The IBA1$^+$ area was 38% smaller in the striatum injected with lenti-SOCS3 than in the control striatum ($p = 0.0397$, df = 5, Student's paired *t* test; Fig. 9*A*,*B*). A similar effect was observed in the subiculum of 3xTg-AD mice injected with lenti-SOCS3, although it did not reach significance (−44%, $p = 0.1800$, df = 5, Student's *t* test; data not shown). We also studied the neuroinflammatory response at the transcriptional level. The expression of the microglial marker *aif1* (*iba1*) was increased 2.3-fold by Htt82Q and reduced by SOCS3 ($p = 0.0048$ for Htt length × treatment effect, df = 1, two-way ANOVA; Fig. 9*C*). Similarly, the marker for reactive microglia *itgam* (CD11b) and the chemokine *ccl2* were increased 2.3- and 4.1-fold, respectively, by Htt82Q and reduced to control levels by SOCS3 ($p = 0.0165$ and $p < 0.0001$, respectively, for Htt length × treatment effect, df = 1, two-way ANOVA; Fig.

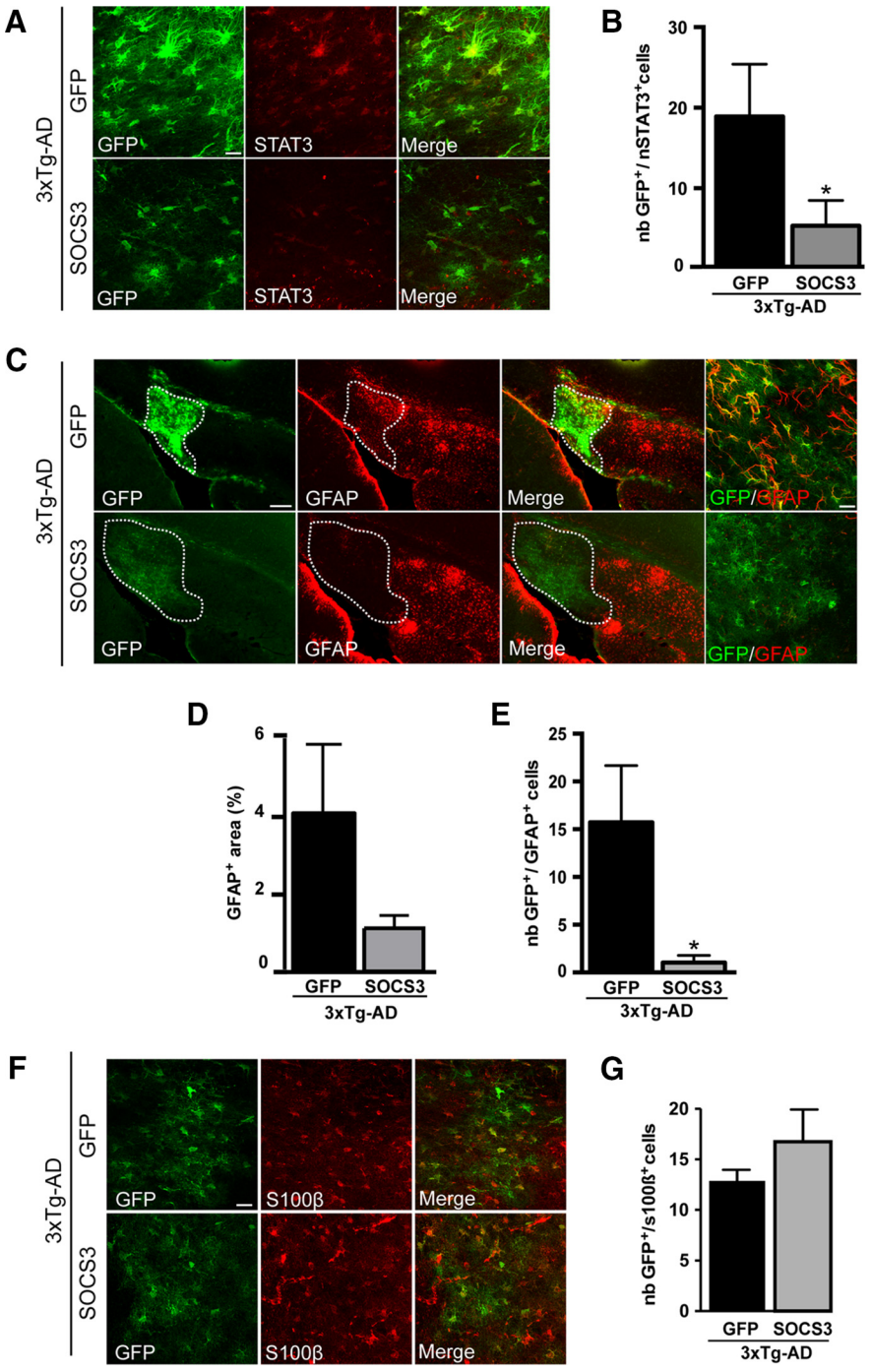

Figure 7. The JAK/STAT3 pathway is responsible for astrocyte reactivity in 3xTg-AD mice. ***A***, Images of double staining for GFP (green) and STAT3 (red) in 7- to 8-month-old 3xTg-AD mice injected in the subiculum with lenti-GFP or lenti-SOCS3 plus lenti-GFP (same total virus load). STAT3 expression becomes undetectable in astrocytes infected with lenti-SOCS3. ***B***, The number of GFP$^+$ astrocytes coexpressing STAT3 in the nucleus (GFP$^+$/nSTAT3$^+$ cells) is significantly lower in the SOCS3 group than in the GFP control group. ***C***, Images of GFP (green) and GFAP (red) staining in brain sections from 3xTg-AD mice injected with lenti-GFP or lenti-SOCS3 plus lenti-GFP in the subiculum. Lenti-SOCS3 injection strongly reduces GFAP expression in the injected area (delimited by white dots) in 3xTg-AD mice. Note that infected astrocytes in the SOCS3 group have a bushy morphology typical of resting astrocytes, whereas cells in the GFP group are hypertrophic with enlarged primary processes. ***D***, Quantification of the GFAP$^+$ area in 3xTg-AD mice injected with lenti-SOCS3 plus lenti-GFP or lenti-GFP alone. ***E***, The number of GFP$^+$ astrocytes coexpressing GFAP is significantly lower in the SOCS3 group than in the GFP control group. ***F***, Immunofluorescent labeling for the astrocyte marker S100β. ***G***, Quantification of the number of infected astrocytes coexpressing S100β (GFP$^+$/S100β^+ cells) shows that its expression is not altered by SOCS3. $n = 3$–5 per group. *$p < 0.05$. Scale bars: ***A*** and ***F***, 20 μm; ***C***, left, 500 μm; right, 20 μm. Infected astrocytes in both groups are identified by their expression of GFP.

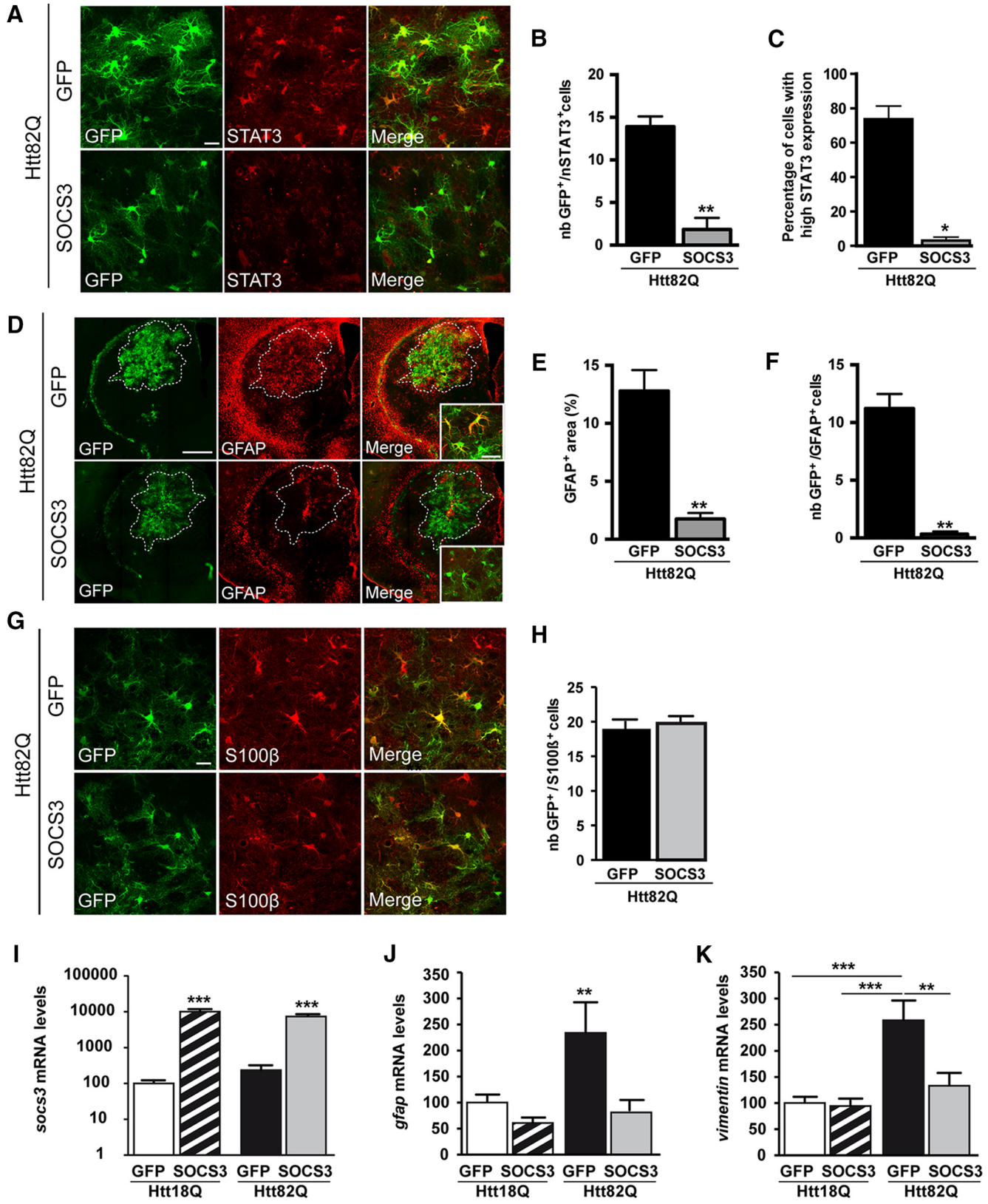

Figure 8. The JAK/STAT3 pathway is responsible for astrocyte reactivity in the lentiviral-based mouse model of HD. ***A***, Immunofluorescent staining of GFP (green) and STAT3 (red) in mice injected in the left striatum with lenti-Htt82Q plus lenti-GFP and the right striatum with lenti-Htt82Q plus lenti-SOCS3 plus lenti-GFP. STAT3 expression becomes undetectable in astrocytes infected with lenti-SOCS3. ***B***, ***C***, The number of GFP $^{+}$/nSTAT3 $^{+}$ astrocytes (***B***) and the percentage of cells showing strong staining for STAT3 (***C***) is significantly lower in the right striatum injected with lenti-SOCS3 than in the control striatum. ***D***, SOCS3 expression strongly reduces GFAP expression (red) in the injected area (GFP $^{+}$, green). Infected astrocytes in the SOCS3 group display thin processes and complex ramifications, unlike hypertrophic reactive astrocytes in the control group. ***E***, Quantification confirms that the GFAP $^{+}$ area is significantly smaller in the striatum injected with lenti-SOCS3 than in the control striatum. ***F***, The number of GFP $^{+}$ astrocytes coexpressing GFAP is significantly lower in the striatum expressing SOCS3 than in the control striatum. ***G***, Immunofluorescent staining for the astrocyte marker S100β (red). ***H***, The number of GFP $^{+}$/S100β $^{+}$ cells is not different between the two groups. ***I–K***, qRT-PCR analysis on mice injected in the striatum (*Figure legend continues.*)

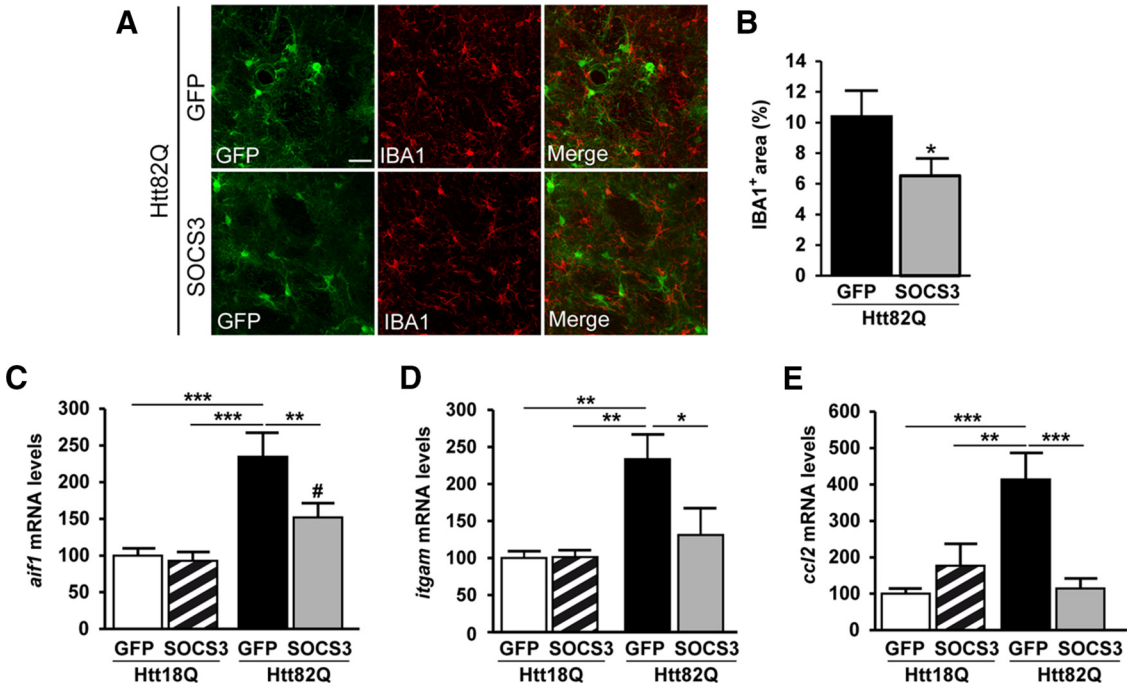

Figure 9. Preventing astrocyte reactivity reduces microglial activation. ***A***, Immunofluorescent staining of GFP (green) and IBA1 (red) in mice injected in the left striatum with lenti-Htt82Q plus lenti-GFP and the right striatum with lenti-Htt82Q plus lenti-SOCS3 plus lenti-GFP. ***B***, Quantification shows that the IBA1$^+$ area is significantly smaller in the striatum injected with lenti-SOCS3 than in the control striatum. ***C–E***, qRT-PCR analysis on mice injected in the striatum with lenti-Htt18Q plus lenti-GFP, lenti-Htt18Q plus lenti-SOCS3 plus lenti-GFP, lenti-Htt82Q plus lenti-GFP, or lenti-Htt82Q plus lenti-SOCS3 plus lenti-GFP (same total virus load). The expression of *aif1* (*iba1*; ***C***), *itgam* (*CD11b*; ***D***), and *ccl2* (***E***) is induced by lenti-Htt82Q and is reduced by SOCS3. $n = 4–11$ per group. $^*p < 0.05$, $^{**}p < 0.01$, $^{***}p < 0.001$, $^{\#}p < 0.05$ versus Htt18Q plus GFP and Htt18Q plus SOCS3. Scale bar, 20 μm.

9*D*,*E*). These results suggest that inhibition of astrocyte reactivity reduces the neuroinflammatory response.

Preventing astrocyte reactivity modulates HD pathology

Finally, we evaluated the effects of SOCS3 on neuronal death and mHtt aggregation. Htt82Q induced a lesion detected by a loss of DARPP32 staining and COX activity. SOCS3 did not change the size of the lesion as measured with these two markers ($p = 0.2088$ and $p = 0.1508$, respectively, df = 10, Student's paired *t* test; Fig. 10). However, SOCS3 significantly increased the number of EM48$^+$ mHtt aggregates ($p = 0.0409$, df = 10, Student's paired *t* test; Fig. 10). The average size of EM48$^+$ aggregates was not different between the GFP and SOCS3 groups (GFP, 10.20 ± 0.30 μm^2; SOCS3, 10.60 ± 0.48 μm^2, $p = 0.3638$).

Overall, our results identify the JAK/STAT3 pathway as a pivotal and universal signaling cascade for astrocyte reactivity in various models of ND. Inhibition of the JAK/STAT3 pathway in reactive astrocytes influences several disease outcomes in the context of HD.

Discussion

Activation of the JAK/STAT3 pathway is a universal feature of astrocyte reactivity

The JAK/STAT3 pathway is known to trigger astrocyte reactivity in models of acute injury (Kang and Hébert, 2011). We aimed to decipher the role of the JAK/STAT3 pathway in astrocyte reactivity during progressive pathological conditions, such as ND.

Active pSTAT3 could not be detected by immunohistochemistry; therefore, we used increased STAT3 expression and nuclear localization as alternative indicators of pathway activation, as described previously by us and others (Escartin et al., 2006; Tyzack et al., 2014). The absence of pSTAT3 immunoreactivity was not attributable to a technical problem because we were able to detect it with the positive control CNTF. Instead, it may be attributable to the models of ND themselves, which are progressive and may involve low, transient, or asynchronous phosphorylation of STAT3. We show that the JAK/STAT3 pathway is activated in reactive astrocytes in mouse models of both AD and HD and in a primate model of HD.

Importantly, the etiology of the two ND studied here is very different and involves particular vulnerable brain regions. Thus, activation of the JAK/STAT3 pathway appears to be a universal feature of astrocyte reactivity, observed in multiple brain disorders, both acute and progressive. Both resting and reactive astrocytes are now considered as highly heterogeneous cells in terms of their morphological or functional features (Anderson et al., 2014). However, our results suggest that the molecular cascades triggering reactivity are in fact highly conserved between disease states, species, and brain regions.

In addition to the three mouse models studied here, we examined astrocyte reactivity in two transgenic mouse models of HD. Both N171-82Q and Hdh140 mice display behavioral abnormalities and striatal atrophy. However, we did not observe substantial astrocyte reactivity in end-stage N171-82Q mice or before 17 months of age in Hdh140 mice. Interestingly, the JAK/STAT3 pathway was also found activated in the few reactive astrocytes of the old Hdh140 mouse. This limited astrocyte reactivity in HD transgenic mice is consistent with the literature (Tong et al.,

←

(*Figure legend continued.*) with lenti-Htt18Q plus lenti-GFP, lenti-Htt18Q plus lenti-SOCS3 plus lenti-GFP, lenti-Htt82Q plus lenti-GFP, or lenti-Htt82Q plus lenti-SOCS3 plus lenti-GFP (same total virus load). ***I***, *Socs3* mRNA is overexpressed >100 times after lenti-SOCS3 injection. The expression of *gfap* (***J***) and *vimentin* (***K***) is induced by lenti-Htt82Q and is restored to levels observed in the Htt18Q controls by the expression of SOCS3. Note that lenti-SOCS3 has no effect in resting astrocytes. $n = 4–11$ per group. $^*p < 0.05$, $^{**}p < 0.01$, $^{***}p < 0.001$. Scale bars: ***A*** and ***G***, 20 μm; ***D***, 500 μM; enlargement, 20 μm.

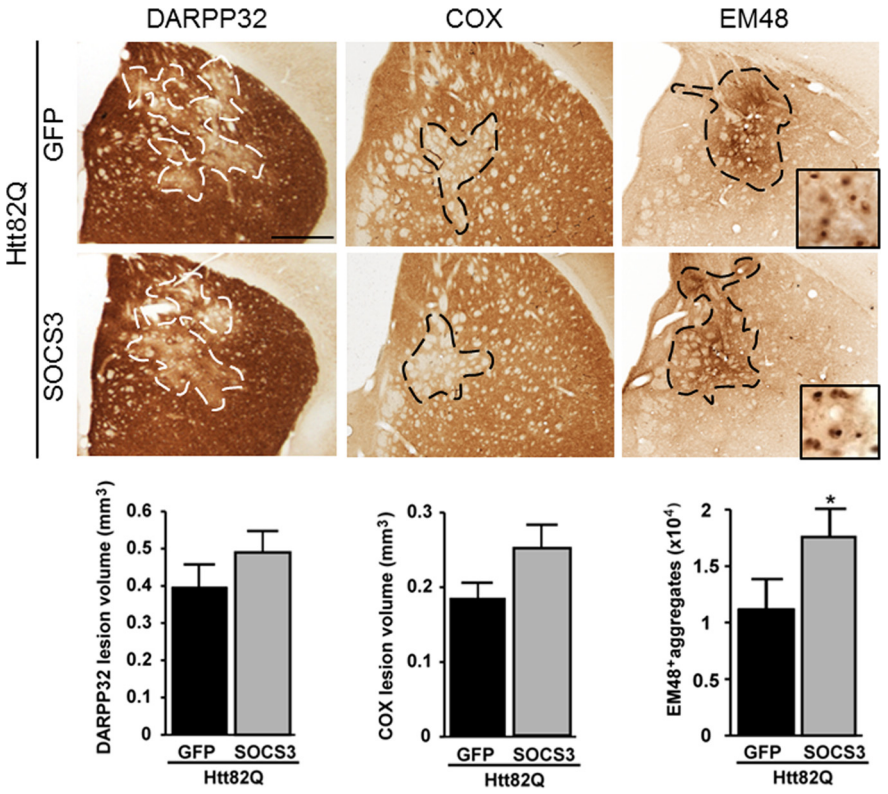

Figure 10. Preventing astrocyte reactivity modulates HD pathology. Immunostaining of the striatal neuronal marker DARPP32 and histochemistry of COX in mice injected in the left striatum with lenti-Htt82Q plus lenti-GFP and in the right striatum with lenti-Htt82Q plus lenti-SOCS3 plus lenti-GFP. mHtt aggregates are detected by immunostaining with EM48 in the same mice, and they form nuclear inclusions (see enlargement). Quantification of the lesion size and the number of EM48$^+$ aggregates. SOCS3 increases the number of EM48$^+$ aggregates. $n = 11$. $^*p < 0.05$. Scale bar, 500 μm.

2014) but differs greatly from what is observed in HD patients (Faideau et al., 2010). This discrepancy may be related to the absence of massive neuronal death in HD transgenic models. Thus, we focused on the lentiviral-based model of HD that reproduces neuronal death in the striatum, along with strong astrocyte reactivity.

Astrocyte reactivity in ND models is mediated by the JAK/STAT3 pathway

By immunohistological and biochemical techniques, it was shown that the JAK/STAT3 pathway is activated in reactive astrocytes in several models of acute injury (Justicia et al., 2000; Xia et al., 2002) and in ALS (Shibata et al., 2010). Experiments involving pharmacological inhibitors of the JAK/STAT3 pathway later suggested that this pathway was needed for astrocyte reactivity, including in the MPTP model of PD (Sriram et al., 2004). However, the JAK/STAT3 pathway is active in all brain cells; therefore, it is possible that such inhibitors affect other cell types besides astrocytes. More recently, genetic approaches have been developed to knock out the expression of STAT3 specifically in astrocytes with the Cre–LoxP system. STAT3 conditional knock-out strongly reduces astrocyte reactivity after acute injuries (Okada et al., 2006; Herrmann et al., 2008; Tyzack et al., 2014). However, the use of a non-inducible Cre recombinase expressed under a *nestin* or *gfap* promoter may trigger side effects, because these promoters are active during embryonic development (Alvarez-Buylla et al., 2001). In contrast, our strategy based on SOCS3 overexpression by lentiviral gene transfer results in an efficient inhibition of the JAK/STAT3 pathway specifically in astrocytes of the adult brain. Indeed, SOCS3 was able to prevent the accumulation of STAT3 in the nucleus of reactive astrocytes in ND models and to blunt the strong phosphorylation of STAT3 induced by CNTF. This selective approach allowed us to demonstrate that the JAK/STAT3 pathway is responsible for astrocyte reactivity in two models of ND.

In agreement with a pivotal role of the JAK/STAT3 pathway for astrocyte reactivity, we observed no evidence for an activation of the NF-κB pathway in these models. This pathway is associated with astrocyte reactivity in acute disorders, such as spinal cord injury (Kang and Hébert, 2011). In AD and HD, the NF-κB pathway is altered in neurons (Chiba et al., 2009; Khoshnan and Patterson, 2011) but is activated in the peripheral immune cells of HD patients (Träger et al., 2014) and in astrocytes in mouse models of both diseases (Hsiao et al., 2013; Medeiros and LaFerla, 2013). However, the specific requirement of this pathway for the establishment of reactivity in astrocytes has not been tested in these NDs. The NF-κB pathway is activated mainly in microglial cells in the SOD^{G93A} mouse model of ALS (Frakes et al., 2014). Indeed, inhibition of the NF-κB pathway in astrocytes reduced their reactivity very moderately and only transiently (Crosio et al., 2011). In both studies, inhibition of the NF-κB pathway in astrocytes did not influence disease outcomes, further suggesting that this pathway does not play a major role in reactive astrocytes during ND.

There are multiple levels of crosstalk between the NF-κB and the JAK/STAT3 pathways (Fan et al., 2013). It is possible that the NF-κB pathway secondarily activates the JAK/STAT3 pathway or that STAT3 inhibits the NF-κB pathway (Yu et al., 2002). Although other signaling pathways may be active in astrocytes or in other cell types during the disease, our experiments based on the specific inhibition by SOCS3 in astrocytes show that the JAK/STAT3 pathway is ultimately responsible for triggering astrocyte reactivity in these ND.

Viral vectors are versatile tools; therefore, our approach based on a lentiviral vector encoding an inhibitor of the JAK/STAT3 pathway could be easily extended to any animal model of brain disease, including those affecting different brain regions. However, one limitation is that lentiviral vectors may transduce a small number of cells, especially in the subiculum, preventing qRT-PCR or biochemical analysis by Western blotting.

What are the effects of STAT3-mediated astrocyte reactivity?

The JAK/STAT3 pathway is a ubiquitous signaling pathway involved in cell proliferation, survival, and differentiation (Levy and Darnell, 2002). In adult astrocytes, activation of the JAK/STAT3 pathway increases the expression of cytoskeletal proteins, such as GFAP and vimentin, as observed here, but many other genes could be induced, as shown in reactive astrocytes after ischemia or LPS injection *in vivo* (Zamanian et al., 2012). In particular, reactive astrocytes may release several signaling molecules,

such as cytokines or chemokines, that affect neighboring cells, including microglial cells (Burda and Sofroniew, 2014). Indeed, we found an increased expression of neuroinflammation markers in the lenti-based model of HD, which was restored to basal levels by SOCS3. This observation suggests that reactive astrocytes are responsible for microglial activation in this model and illustrates the complex dialog occurring between glial cells in ND.

Blunting astrocyte reactivity by SOCS3 also increased the number of mHtt aggregates, suggesting that reactive astrocytes participate in mHtt processing and aggregation. Because those mHtt aggregates are found mainly in neurons, such an effect necessarily involves neuron-to-astrocyte communication. Interestingly, it was reported recently that mHtt can propagate between neurons (Pecho-Vrieseling et al., 2014), opening the possibility that it may also be exchanged between neurons and glial cells. More experiments are needed to decipher the molecular mechanisms responsible for the control of mHtt clearance by reactive astrocytes.

It is still highly debated how mHtt inclusions contribute to neuronal death: it may be toxic, protective, or without effect (Arrasate and Finkbeiner, 2012). We show that increasing the number of mHtt aggregates does not influence the lesion, which is in favor of a disconnection between mHtt aggregates and neuronal death. Indeed, the inclusions of mHtt measured here are only the end products of mHtt metabolism, and it is now believed that soluble or oligomeric mHtt are the toxic species (Leitman et al., 2013).

We show that interfering with astrocyte reactivity influences two important features of HD (neuroinflammation and mHtt aggregation) but did not affect neuronal death. However, we cannot exclude that the lentiviral-based model of HD is too severe to allow restoration by the modulation of astrocyte and microglia reactivity or mHtt aggregation.

A similar thorough evaluation of SOCS3 effects could not be performed in the 3xTg-AD model because the volume targeted with lenti-SOCS3 was too small to provide a reliable quantification of disease indexes, such as amyloid load. There are conflicting reports on the role of reactive astrocytes in AD (Furman et al., 2012; Kraft et al., 2013). It may be clarified by inhibiting the JAK/STAT3 pathway, identified here as an instrumental cascade to promote reactivity, and assessing the consequences on AD outcomes.

Our study extends previous findings obtained in acute models of injury and suggests that the JAK/STAT3 pathway is a universal signaling cascade involved in virtually all pathological situations in the brain. Manipulation of the JAK/STAT3 pathway is a promising strategy to study the functional features of reactive astrocyte, as well as their contribution to disease progression, particularly in the context of ND.

References

Alvarez-Buylla A, García-Verdugo JM, Tramontin AD (2001) A unified hypothesis on the lineage of neural stem cells. Nat Rev Neurosci 2:287–293. CrossRef Medline

Anderson MA, Ao Y, Sofroniew MV (2014) Heterogeneity of reactive astrocytes. Neurosci Lett 565:23–29. CrossRef Medline

Arrasate M, Finkbeiner S (2012) Protein aggregates in Huntington's disease. Exp Neurol 238:1–11. CrossRef Medline

Bjørbaek C, Elmquist JK, Frantz JD, Shoelson SE, Flier JS (1998) Identification of SOCS-3 as a potential mediator of central leptin resistance. Mol Cell 1:619–625. CrossRef Medline

Bonni A, Frank DA, Schindler C, Greenberg ME (1993) Characterization of a pathway for ciliary neurotrophic factor signaling to the nucleus. Science 262:1575–1579. CrossRef Medline

Burda JE, Sofroniew MV (2014) Reactive gliosis and the multicellular response to CNS damage and disease. Neuron 81:229–248. CrossRef Medline

Campbell IL, Erta M, Lim SL, Frausto R, May U, Rose-John S, Scheller J, Hidalgo J (2014) Trans-signaling is a dominant mechanism for the pathogenic actions of interleukin-6 in the brain. J Neurosci 34:2503–2513. CrossRef Medline

Chiba T, Yamada M, Sasabe J, Terashita K, Shimoda M, Matsuoka M, Aiso S (2009) Amyloid-beta causes memory impairment by disturbing the JAK2/STAT3 axis in hippocampal neurons. Mol Psychiatry 14:206–222. CrossRef Medline

Colin A, Faideau M, Dufour N, Auregan G, Hassig R, Andrieu T, Brouillet E, Hantraye P, Bonvento G, Déglon N (2009) Engineered lentiviral vector targeting astrocytes in vivo. Glia 57:667–679. CrossRef Medline

Crosio C, Valle C, Casciati A, Iaccarino C, Carrì MT (2011) Astroglial inhibition of NF-kappaB does not ameliorate disease onset and progression in a mouse model for amyotrophic lateral sclerosis (ALS). PLoS One 6:e17187. CrossRef Medline

Damiano M, Diguet E, Malgorn C, D'Aurelio M, Galvan L, Petit F, Benhaim L, Guillermier M, Houitte D, Dufour N, Hantraye P, Canals JM, Alberch J, Delzescaux T, Déglon N, Beal MF, Brouillet E (2013) A role of mitochondrial complex II defects in genetic models of Huntington's disease expressing N-terminal fragments of mutant huntingtin. Hum Mol Genet 22:3869–3882. CrossRef Medline

de Almeida LP, Ross CA, Zala D, Aebischer P, Déglon N (2002) Lentiviral-mediated delivery of mutant huntingtin in the striatum of rats induces a selective neuropathology modulated by polyglutamine repeat size, huntingtin expression levels, and protein length. J Neurosci 22:3473–3483. Medline

Escartin C, Bonvento G (2008) Targeted activation of astrocytes: a potential neuroprotective strategy. Mol Neurobiol 38:231–241. CrossRef Medline

Escartin C, Brouillet E, Gubellini P, Trioulier Y, Jacquard C, Smadja C, Knott GW, Kerkerian-Le Goff L, Déglon N, Hantraye P, Bonvento G (2006) Ciliary neurotrophic factor activates astrocytes, redistributes their glutamate transporters GLAST and GLT-1 to raft microdomains, and improves glutamate handling in vivo. J Neurosci 26:5978–5989. CrossRef Medline

Faideau M, Kim J, Cormier K, Gilmore R, Welch M, Auregan G, Dufour N, Guillermier M, Brouillet E, Hantraye P, Déglon N, Ferrante RJ, Bonvento G (2010) In vivo expression of polyglutamine-expanded huntingtin by mouse striatal astrocytes impairs glutamate transport: a correlation with Huntington's disease subjects. Hum Mol Genet 19:3053–3067. CrossRef Medline

Fan Y, Mao R, Yang J (2013) NF-kappaB and STAT3 signaling pathways collaboratively link inflammation to cancer. Protein Cell 4:176–185. CrossRef Medline

Frakes AE, Ferraiuolo L, Haidet-Phillips AM, Schmelzer L, Braun L, Miranda CJ, Ladner KJ, Bevan AK, Foust KD, Godbout JP, Popovich PG, Guttridge DC, Kaspar BK (2014) Microglia induce motor neuron death via the classical NF-kappaB pathway in amyotrophic lateral sclerosis. Neuron 81:1009–1023. CrossRef Medline

Francelle L, Galvan L, Gaillard MC, Guillermier M, Houitte D, Bonvento G, Petit F, Jan C, Dufour N, Hantraye P, Elalouf JM, de Chaldee M, Deglon N, Brouillet E (2014) Loss of the thyroid hormone binding protein Crym renders striatal neurons more vulnerable to mutant huntingtin in Huntington's disease. Hum Mol Genet. Advance online publication. Retrieved January 8, 2015. doi:10.1093/hmg/ddu571. CrossRef Medline

Furman JL, Sama DM, Gant JC, Beckett TL, Murphy MP, Bachstetter AD, Van Eldik LJ, Norris CM (2012) Targeting astrocytes ameliorates neurologic changes in a mouse model of Alzheimer's disease. J Neurosci 32:16129–16140. CrossRef Medline

Hamby ME, Sofroniew MV (2010) Reactive astrocytes as therapeutic targets for CNS disorders. Neurotherapeutics 7:494–506. CrossRef Medline

Hayden MS, Ghosh S (2008) Shared principles in NF-kappaB signaling. Cell 132:344–362. CrossRef Medline

Herrmann JE, Imura T, Song B, Qi J, Ao Y, Nguyen TK, Korsak RA, Takeda K, Akira S, Sofroniew MV (2008) STAT3 is a critical regulator of astrogliosis and scar formation after spinal cord injury. J Neurosci 28:7231–7243. CrossRef Medline

Hottinger AF, Azzouz M, Déglon N, Aebischer P, Zurn AD (2000) Complete and long-term rescue of lesioned adult motoneurons by lentiviral-mediated expression of glial cell line-derived neurotrophic factor in the facial nucleus. J Neurosci 20:5587–5593. Medline

Hsiao HY, Chen YC, Chen HM, Tu PH, Chern Y (2013) A critical role of astrocyte-mediated nuclear factor-kappaB-dependent inflammation in Huntington's disease. Hum Mol Genet 22:1826–1842. CrossRef Medline

Itagaki S, McGeer PL, Akiyama H, Zhu S, Selkoe D (1989) Relationship of microglia and astrocytes to amyloid deposits of Alzheimer disease. J Neuroimmunol 24:173–182. CrossRef Medline

Jankowsky JL, Fadale DJ, Anderson J, Xu GM, Gonzales V, Jenkins NA, Copeland NG, Lee MK, Younkin LH, Wagner SL, Younkin SG, Borchelt DR (2004) Mutant presenilins specifically elevate the levels of the 42 residue beta-amyloid peptide in vivo: evidence for augmentation of a 42-specific gamma secretase. Hum Mol Genet 13:159–170. CrossRef Medline

Justicia C, Gabriel C, Planas AM (2000) Activation of the JAK/STAT pathway following transient focal cerebral ischemia: signaling through Jak1 and Stat3 in astrocytes. Glia 30:253–270. CrossRef Medline

Kang W, Hébert JM (2011) Signaling pathways in reactive astrocytes, a genetic perspective. Mol Neurobiol 43:147–154. CrossRef Medline

Kershaw NJ, Murphy JM, Liau NP, Varghese LN, Laktyushin A, Whitlock EL, Lucet IS, Nicola NA, Babon JJ (2013) SOCS3 binds specific receptor-JAK complexes to control cytokine signaling by direct kinase inhibition. Nat Struct Mol Biol 20:469–476. CrossRef Medline

Khoshnan A, Patterson PH (2011) The role of IkappaB kinase complex in the neurobiology of Huntington's disease. Neurobiol Dis 43:305–311. CrossRef Medline

Kraft AW, Hu X, Yoon H, Yan P, Xiao Q, Wang Y, Gil SC, Brown J, Wilhelmsson U, Restivo JL, Cirrito JR, Holtzman DM, Kim J, Pekny M, Lee JM (2013) Attenuating astrocyte activation accelerates plaque pathogenesis in APP/PS1 mice. FASEB J 27:187–198. CrossRef Medline

Leitman J, Ulrich Hartl F, Lederkremer GZ (2013) Soluble forms of polyQ-expanded huntingtin rather than large aggregates cause endoplasmic reticulum stress. Nat Commun 4:2753. CrossRef Medline

Levy DE, Darnell JE Jr (2002) Stats: transcriptional control and biological impact. Nat Rev Mol Cell Biol 3:651–662. CrossRef Medline

Medeiros R, LaFerla FM (2013) Astrocytes: conductors of the Alzheimer disease neuroinflammatory symphony. Exp Neurol 239:133–138. CrossRef Medline

Menalled LB, Sison JD, Dragatsis I, Zeitlin S, Chesselet MF (2003) Time course of early motor and neuropathological anomalies in a knock-in mouse model of Huntington's disease with 140 CAG repeats. J Comp Neurol 465:11–26. CrossRef Medline

Naldini L, Blömer U, Gallay P, Ory D, Mulligan R, Gage FH, Verma IM, Trono D (1996) In vivo gene delivery and stable transduction of nondividing cells by a lentiviral vector. Science 272:263–267. CrossRef Medline

O'Callaghan JP, Kelly KA, VanGilder RL, Sofroniew MV, Miller DB (2014) Early activation of STAT3 regulates reactive astrogliosis induced by diverse forms of neurotoxicity. PLoS One 9:e102003. CrossRef Medline

Oddo S, Caccamo A, Shepherd JD, Murphy MP, Golde TE, Kayed R, Metherate R, Mattson MP, Akbari Y, LaFerla FM (2003) Triple-transgenic model of Alzheimer's disease with plaques and tangles: intracellular Abeta and synaptic dysfunction. Neuron 39:409–421. CrossRef Medline

Okada S, Nakamura M, Katoh H, Miyao T, Shimazaki T, Ishii K, Yamane J, Yoshimura A, Iwamoto Y, Toyama Y, Okano H (2006) Conditional ablation of Stat3 or Socs3 discloses a dual role for reactive astrocytes after spinal cord injury. Nat Med 12:829–834. CrossRef Medline

Palfi S, Brouillet E, Jarraya B, Bloch J, Jan C, Shin M, Condé F, Li XJ, Aebischer P, Hantraye P, Déglon N (2007) Expression of mutated huntingtin fragment in the putamen is sufficient to produce abnormal movement in non-human primates. Mol Ther 15:1444–1451. CrossRef Medline

Pecho-Vrieseling E, Rieker C, Fuchs S, Bleckmann D, Esposito MS, Botta P, Goldstein C, Bernhard M, Galimberti I, Müller M, Lüthi A, Arber S, Bouwmeester T, van der Putten H, Di Giorgio FP (2014) Transneuronal propagation of mutant huntingtin contributes to non-cell autonomous pathology in neurons. Nat Neurosci 17:1064–1072. CrossRef Medline

Probst A, Ulrich J, Heitz PU (1982) Senile dementia of Alzheimer type: astroglial reaction to extracellular neurofibrillary tangles in the hippocampus. An immunocytochemical and electron-microscopic study. Acta Neuropathol 57:75–79. CrossRef Medline

Ruan L, Kang Z, Pei G, Le Y (2009) Amyloid deposition and inflammation in APPswe/PS1dE9 mouse model of Alzheimer's disease. Curr Alzheimer Res 6:531–540. CrossRef Medline

Ruiz M, Déglon N (2012) Viral-mediated overexpression of mutant huntingtin to model HD in various species. Neurobiol Dis 48:202–211. CrossRef Medline

Schilling G, Becher MW, Sharp AH, Jinnah HA, Duan K, Kotzuk JA, Slunt HH, Ratovitski T, Cooper JK, Jenkins NA, Copeland NG, Price DL, Ross CA, Borchelt DR (1999) Intranuclear inclusions and neuritic aggregates in transgenic mice expressing a mutant N-terminal fragment of huntingtin. Hum Mol Genet 8:397–407. CrossRef Medline

Shibata N, Kakita A, Takahashi H, Ihara Y, Nobukuni K, Fujimura H, Sakoda S, Sasaki S, Iwata M, Morikawa S, Hirano A, Kobayashi M (2009) Activation of signal transducer and activator of transcription-3 in the spinal cord of sporadic amyotrophic lateral sclerosis patients. Neurodegener Dis 6:118–126. CrossRef Medline

Shibata N, Yamamoto T, Hiroi A, Omi Y, Kato Y, Kobayashi M (2010) Activation of STAT3 and inhibitory effects of pioglitazone on STAT3 activity in a mouse model of SOD1-mutated amyotrophic lateral sclerosis. Neuropathology 30:353–360. CrossRef Medline

Sieber MW, Jaenisch N, Brehm M, Guenther M, Linnartz-Gerlach B, Neumann H, Witte OW, Frahm C (2013) Attenuated inflammatory response in triggering receptor expressed on myeloid cells 2 (TREM2) knock-out mice following stroke. PLoS One 8:e52982. CrossRef Medline

Sofroniew MV, Vinters HV (2010) Astrocytes: biology and pathology. Acta Neuropathol 119:7–35. CrossRef Medline

Sriram K, Benkovic SA, Hebert MA, Miller DB, O'Callaghan JP (2004) Induction of gp130-related cytokines and activation of JAK2/STAT3 pathway in astrocytes precedes up-regulation of glial fibrillary acidic protein in the 1-methyl-4-phenyl-1,2,3,6-tetrahydropyridine model of neurodegeneration: key signaling pathway for astrogliosis in vivo? J Biol Chem 279:19936–19947. CrossRef Medline

Starr R, Willson TA, Viney EM, Murray LJ, Rayner JR, Jenkins BJ, Gonda TJ, Alexander WS, Metcalf D, Nicola NA, Hilton DJ (1997) A family of cytokine-inducible inhibitors of signalling. Nature 387:917–921. CrossRef Medline

Tong X, Ao Y, Faas GC, Nwaobi SE, Xu J, Haustein MD, Anderson MA, Mody I, Olsen ML, Sofroniew MV, Khakh BS (2014) Astrocyte Kir4.1 ion channel deficits contribute to neuronal dysfunction in Huntington's disease model mice. Nat Neurosci 17:694–703. CrossRef Medline

Träger U, Andre R, Lahiri N, Magnusson-Lind A, Weiss A, Grueninger S, McKinnon C, Sirinathsinghji E, Kahlon S, Pfister EL, Moser R, Hummerich H, Antoniou M, Bates GP, Luthi-Carter R, Lowdell MW, Björkqvist M, Ostroff GR, Aronin N, Tabrizi SJ (2014) HTT-lowering reverses Huntington's disease immune dysfunction caused by NFkappaB pathway dysregulation. Brain 137:819–833. CrossRef Medline

Tyzack GE, Sitnikov S, Barson D, Adams-Carr KL, Lau NK, Kwok JC, Zhao C, Franklin RJ, Karadottir RT, Fawcett JW, Lakatos A (2014) Astrocyte response to motor neuron injury promotes structural synaptic plasticity via STAT3-regulated TSP-1 expression. Nat Commun 5:4294. CrossRef Medline

Vonsattel JP, Myers RH, Stevens TJ, Ferrante RJ, Bird ED, Richardson EP Jr (1985) Neuropathological classification of Huntington's disease. J Neuropathol Exp Neurol 44:559–577. CrossRef Medline

Wilhelmsson U, Bushong EA, Price DL, Smarr BL, Phung V, Terada M, Ellisman MH, Pekny M (2006) Redefining the concept of reactive astrocytes as cells that remain within their unique domains upon reaction to injury. Proc Natl Acad Sci U S A 103:17513–17518. CrossRef Medline

Xia XG, Hofmann HD, Deller T, Kirsch M (2002) Induction of STAT3 signaling in activated astrocytes and sprouting septal neurons following entorhinal cortex lesion in adult rats. Mol Cell Neurosci 21:379–392. CrossRef Medline

Yu ZX, Li SH, Evans J, Pillarisetti A, Li H, Li XJ (2003) Mutant huntingtin causes context-dependent neurodegeneration in mice with Huntington's disease. J Neurosci 23:2193–2202. Medline

Yu Z, Zhang W, Kone BC (2002) Signal transducers and activators of transcription 3 (STAT3) inhibits transcription of the inducible nitric oxide synthase gene by interacting with nuclear factor kappaB. Biochem J 367:97–105. CrossRef Medline

Zamanian JL, Xu L, Foo LC, Nouri N, Zhou L, Giffard RG, Barres BA (2012) Genomic analysis of reactive astrogliosis. J Neurosci 32:6391–6410. CrossRef Medline

Publication 4

Ce manuscript a été soumis au journal CNS drugs et est en cours de révisions.

Targeting Neuroinflammation to Treat Alzheimer's Disease

Ardura-Fabregat A[1*], Boddeke EWGM[2*], Boza-Serrano A[3*], Brioschi S[4*], Ceyzériat K[5,6*], Dansoko C[7*], Dierkes T[7,8*], Gelders G[9*], Heneka MT[7,10*], Hoeijmakers L.[11*], Hoffmann A[12*], Iaccarino L[13,14*], Jahnert S[10*], Kuhbandner K[12*], Landreth G[15*], Lonnemann N[16*], Löschmann PA[17*], McManus R[7*], Paulus A[3*], Reemst K[11*], Sanchez-Caro JM[7*], Van der Perren A[9*], Vautheny A[5,6*], Venegas C[10*], Webers A[10*], Weydt P[10*], Wijasa TS[7*], Xianyuan X[18,19*], Yiyi Y[3*]

[1] Institute of Neuropathology, Faculty of Medicine, University of Freiburg, Freiburg, Germany

[2] Department of Neuroscience, Section Medical Physiology, University of Groningen, University Medical Center Groningen, Groningen, the Netherlands

[3] Experimental Neuroinflammation laboratory, Department of Experimental Medical Sciences, Biomedical Centrum (BMC), Lund University, Sweden

[4] Department of Psychiatry and Psychotherapy, Medical Center University of Freiburg, Faculty of Medicine University of Freiburg, Germany

[5] Commissariat à l'Energie Atomique et aux Energies Alternatives (CEA), Département de la Recherche Fondamentale (DRF), Institut de biologie François Jacob, MIRCen, F-92260 Fontenay-aux-Roses, France

[6] Centre National de la Recherche Scientifique (CNRS), Université Paris-Sud, UMR 9199, Neurodegenerative Diseases Laboratory, F-92260 Fontenay-aux-Roses, France

[7] German Center for Neurodegenerative Diseases (DZNE), Sigmund Freud Str. 27, 53127, Bonn, Germany

[8] Institute of Innate Immunity, Biomedical Centre, University hospital Bonn, Sigmund-Freud-Str. 25, Bonn 53127, Germany

[9] KU Leuven, Laboratory for Neurobiology and Gene Therapy, Department of Neurosciences, Leuven, Belgium

[10] Department of Neurodegenerative Disease and Gerontopsychiatry/Neurology, University of Bonn Medical Center, Sigmund-Freud Str. 25, 53127, Bonn, Germany

[11] Swammerdam Institute for Life Sciences, Center for Neuroscience (SILS-CNS), University of Amsterdam, the Netherlands

[12] Department of Molecular Neurology, University Hospital Erlangen, Friedrich-Alexander-Universität Erlangen-Nürnberg, Erlangen, Germany

[13] Vita-Salute San Raffaele University, Milan, Italy

[14] In Vivo Human Molecular and Structural Neuroimaging Unit, Division of Neuroscience, IRCCS San Raffaele Scientific Institute, Milan, Italy

[15] Stark Neuroscience Research Institute, Indiana University School of Medicine, Indianapolis, IN 46202, USA

[16] Technische Universität Braunschweig, Zoological Institute, Department of Cellular Neurobiology, Braunschweig, Germany

[17] Pfizer Deutschland GmbH, Berlin, Germany

[18] Biomedical Center (BMC), Biochemistry, Ludwig-Maximilians-University Munich, 81377 Munich, Germany

[19] Graduate School of Systemic Neuroscience, Ludwig- Maximilians- University, Munich, 82152 Munich, Germany

- equally contributing authors

Correspondence:

Michael T. Heneka
Prof. of Clinical Neuroscience
Dept. of Neurodegenerative Disease and Gerontopsychiatry
Sigmund-Freud Str. 25
53127 Bonn
Germany
(p) +49 228 28713091
(e) michael.heneka@ukbonn.de
(w) henekalab.com

ABSTRACT

Over the past decades, research on Alzheimer's disease has been dominated by studying pathomechanisms linked to two of the major pathological hallmarks, extracellular deposition of beta-amyloid peptides and intraneuronal formation of neurofibrills. Very recently a third disease component, the neuroinflammatory reaction of cerebral innate immune cells has become focus of intense research, based on new findings from genetic, pre-clinical and clinical studies. Various proteins arising during neurodegenerative processes, including beta-amyloid, tau, heat shock proteins, chromogranin and several others act as danger-associated molecular patterns, that upon ligation of pattern recognition receptors induced inflammatory signaling pathways that ultimately lead to the production and release of immune mediators, that may harbour beneficial effects, but ultimately may compromize neuronal function and cause cell death. The current review, that has been assembled by participants of the Chiclana Summer School on Neuroinflammation 2016, provides an overview about our current understanding and knowledge on related immune processes, their mutual interaction with neurodegneration and possible future therapeutic targets.

INTRODUCTION

Dementias and related diseases of cognitive decline pose an enormous and growing disease burden on our societies and health economy. According to the most recent *WHO Global Disease Burden Report* deaths from neurological diseases have risen by 114% over the past 20 years to 1.2 Mio in 2010(World Health Organization, 2008). The increase is largely driven by neurodegenerative diseases such as *Alzheimer's dementia* and *Parkinson's disease* and by an ageing population in general. Not surprisingly the development of strategies to curb this frightening surge is a high priority for life science research. The responsible allocation of these resources requires the identification of valid therapeutic targets. The immune system is particularly alluring in this regard. The contribution of the immune system and peripheral infections to cognitive decline remains incompletely understood, but the past 15 years have established a key role for inflammation in the progression of age-related neurodegeneration. The immune privilege of the brain is clearly not absolute, and cells of the central nervous system are sensitive to both the inflammatory events occurring within and outside of the brain.

Here we summarize the current state of neuroinflammation research from cellular to molecular mechanisms as they pertain to the pathogenesis of Alzheimer's disease and outline how this might be leveraged into preventive strategies and therapeutic approaches to stem the daunting surge in dementia diseases facing our society.

Cellular players

Microglia

Microglia are the principal innate immune cells in the brain, and they are often considered the macrophages of the central nervous system (CNS). Recent studies have shed light on their origin from erythromyeloid (EMPs) progenitors from the yolk sac (Ginhoux et al., 2010; Kierdorf et al., 2013), which migrate into the brain at embryonic day 7.5 where they further differentiate into microglial cells (Ginhoux et al., 2010). Microglia exhibit the capacity to self-renewal within the brain (Ajami et al., 2007; Tay et al., 2016) likely arising from a newly identified progenitor (Elmore et al., 2014). Microglia continuously survey their microenvironment and monitor ongoing synaptic activity including synapse remodeling, debris clearance, trophic support for neurons and drive a major part of the innate immune response. Microglia react to pathological triggers via pathogen associated molecular patterns (PAMPs) or danger associated molecular patterns (DAMPs) (Baroja-Mazo et al., 2014; Koenigsknecht-Talboo and Landreth, 2005;

Sondag et al., 2009). Microglia are also phagocytic cells, and can ingest Aβ through a range of cell surface receptors including CD14, TLR2, TLR4, α6β1 integrin, CD47 and scavenger receptors, such as CD36 (Bamberger et al., 2003; Ries and Sastre, 2016; Tahara et al., 2006; Wilkinson and El Khoury, 2012). It has been suggested that in AD, a key factor in the accumulation of Aβ throughout the brain is the failure of microglia to remove extracellular amyloid (Hickman et al., 2008; Thériault et al., 2015; Weiner and Frenkel, 2006). Indeed in cortical tissue specimens from AD patients, the microglia surrounding plaques are impaired at Aβ uptake (Frackowiak et al., 1992; Krabbe et al., 2013; Thériault et al., 2015). Newly developed Positron Emission Tomography (PET) techniques employ radioligands to detect activated microglia *in vivo* (Jacobs et al., 2012; Stefaniak and O'Brien, 2016; Varley et al., 2015). Many tracers target the 18 kDa Translocator Protein (TSPO) (Jacobs et al., 2012), an outer mitochondrial membrane protein present in microglia, which is upregulated during activation (Lavisse et al., 2012; Liu et al., 2014; Venneti et al., 2006). The ^{11}C-PK11195 ligand was the first and prototypical TSPO ligand, while second-generation tracers have been more recently developed with improved signal-to-noise ratio (Chauveau et al., 2008). A common polymorphism, however, significantly influences the binding affinity of these new compounds (Owen et al., 2012), thus making genetic screening a necessary step for accurate quantification (Turkheimer et al., 2015). TSPO up - regulation has been described in prodromal AD and in manifest AD dementia, using both ^{11}C-PK11195 (Cagnin et al., 2001; Edison et al., 2008; Fan et al., 2015a; Okello et al., 2009) and second-generation tracers (Hamelin et al., 2016; Kreisl et al., 2013; Suridjan et al., 2015; Varrone et al., 2015; Yasuno et al., 2012) in regions known to be affected by AD pathology and beyond. Mixed evidence has emerged regarding the relationship between *in vivo* microglial activation and amyloid-β plaque burden (Edison et al., 2008; Fan et al., 2015b; Hamelin et al., 2016; Okello et al., 2009; Yokokura et al., 2011).

Astrocytes

Under pathological conditions astrocytes exhibit morphological changes including hypertrophy and upregulation of glial fibrillary acidic protein (GFAP). Astrocytes can detect aggregated proteins such as amyloid-β (Aβ) or respond to inflammatory molecules (e.g cytokines, chemokines, see below). Indeed significant astrocyte reactivity has been reported in sporadic AD (Carter et al., 2012; Choo et al., 2014; Santillo et al., 2011) and familial AD (Rodriguez-Vieitez et al., 2016). Similar to microglia, reactive astrocytes can polarize their processes around amyloid plaques and are capable of amyloid plaque degradation (Nagele et al., 2003; Wyss-Coray et al., 2003). Altered calcium signaling (Vincent et al., 2010), impaired glutamate homeostasis (Masliah et al., 1996; Scimemi et al., 2013) and increased production of inflammatory mediators by astrocytes are also observed in AD.

Oligodendrocytes

The involvement of oligodendrocytes in AD remains incompletely understood, although there is emerging evidence that these cells contribute to the pathogenesis and progression of neurodegenerative disorders including AD (Ettle et al., 2016). Bartzokis and colleagues demonstrated that the loss of myelin integrity normally occurring during aging was strongly aggravated in human presenilin-1 familial, preclinical and sporadic AD cases, particularly near Aβ-plaques (Bartzokis, 2004, 2011; Bartzokis et al., 2004; Mitew et al., 2010). In addition, focal loss of oligodendrocytes was observed in sporadic cases of AD. In transgenic mouse models of AD this demyelination was also found, specifically at the core of Aβ plaques (Mitew et al., 2010). Focal oligodendrocyte loss was also detected in Tg2576 and APP/PS1 transgenic mice (Mitew et al., 2010), a phenomenon which may negatively influence cortical processing and neurite formation. Several cellular processes such as neuroinflammation, oxidative stress and/or apoptosis may contribute to oligodendrocyte dysfunction and death (Mitew et al., 2010). In addition, Aβ can impair the survival and maturation of oligodendrocyte progenitor cells and the formation of the myelin sheath (Desai et al., 2010).

Myeloid cells other than microglia

In addition to microglia, a variety of other monocytic cells are found in the brain, including perivascular cells, meningeal macrophages, choroid plexus macrophages and peripheral blood-derived monocytes (Prinz and Priller, 2014). These cells

may, under certain circumstances, also phagocyte and degrade amyloid plaques in a transgenic model of AD (Simard et al., 2006). Migration of peripheral monocytes is dependent on CCR2, as receptor ablation in Tg2576 mice results in decreased recruitment of these cells, and a corresponding increase in amyloid pathology (El Khoury et al., 2007). In contrast, blocking TGFβ signaling increased peripheral myeloid cell infiltration into the CNS and significantly reduced in amyloid burden (Town et al., 2008). Glatiramer acetate also increased recruitment of peripheral monocytes to the CNS, which reduced amyloid deposition. Ablation of bone-marrow derived myeloid cells in this very model exacerbated amyloid pathology (Koronyo et al., 2015). However, when resident microglia are ablated from the APP/PS1 and APP23 mouse models, the recruitment of peripheral myeloid cells is not sufficient to clear amyloid load (Prokop et al., 2015; Varvel et al., 2015). Furthermore a recent parabiosis experiment found no evidence of monocyte infiltration around amyloid plaques (Wang et al., 2016). Thus, the extent of myeloid infiltration into the brain and the contribution to damage or clearance of pathological proteins is still not fully understood. A particularly critical aspect of this particular work is the complexity and toxicity of experimental approaches used.

PAMPs and DAMPs: Inducers and modulators of neuroinflammation in Alzheimer's disease

During periods of pathogen invasion or tissue damage, pathogen-associated molecular patterns (PAMPs) and danger-associated molecular patterns (DAMPs) are produced to alert the immune system of the host and trigger an appropriate response to the insult.

DAMPs encompass a diverse class of molecules. A well-characterized group of DAMPs consists of intracellular proteins that are expressed at a basal level within a cell and are released after injury. These include high-mobility group protein B1 (HMGB1), S100 proteins, heat shock proteins (HSPs), chromogranin A and Aβ. A second class of DAMPs is comprised of nucleic acids and nucleotide derivatives, such as mitochondrial DNA (mt-DNA), DNA and ATP (Bianchi, 2007). In contrast, PAMPs mainly include microbial molecules that are normally not present in human cells, such as lipid A, flagellin, lipoproteins from Gram-positive and Gram-negative bacteria, bacterial DNA containing particular CpG motifs and fragments of bacterial peptidoglycan (Vance et al., 2009).

Both, PAMPs and DAMPs contribute to neuroinflammation in AD. Aβ can induce inflammatory responses (Salminen et al., 2009) via activation of pattern recognition receptors (PRRs) of the innate immunity system including TLR2 (Liu et al., 2012), TLR4 and TLR6, as well as their co-receptors, CD36, CD14 and CD47. Neutralization by CD14 antibodies reduced the Aβ-induced microglial activation (Fassbender et al., 2004). Furthermore, the NLRP1 and NLRP3 inflammasome can sense a range of aggregated proteins; such as Aβ (Halle et al., 2008) . Indeed, lack of NLRP3 and caspase-1 protected mice from AD pathology (Halle et al., 2008; Heneka et al., 2013).

HMGB1 levels are increased in AD brains, and are associated with senile plaques, promoting its stabilization (Takata et al., 2003). It has been shown that microglia stimulation by HMGB1 reduced Aβ phagocytosis (Takata et al., 2003). HMGB1 promotes the migration and proliferation of immune cells through the binding to advanced glycation end products receptors (RAGE) and TLRs (Degryse et al., 2001). HMGB1 can also act in concert with other factors such chemokines, growth factors and PAMPs, together promoting immune system activation (Bianchi, 2009; Castellani et al., 2014).

Chromogranin A is associated with microglial activation in neurodegeneration (Ciesielski-Treska et al., 2001; Kingham et al., 1999), it induces the release of IL-1□, indicating that TLRs and the NLRP3 inflammasome are involved in this pathway (Terada et al., 2010). In AD, increased levels of chromogranin A are observed in senile plaque dystrophic neurites (Weiler et al., 1990). Interestingly, at least in vitro, the immunestimulatory potential is almost identical to the one of bacterial LPS (Taupenot et al., 1995).

Many S100 proteins are involved in AD including S100A9, S100A8 and S100B. S100A8 and S100A9 form a complex, which is increased in the brain and CSF of human AD patients (Maezawa et al., 2011; Reed-Geaghan et al., 2009) and can activate

microglia through TLR4. In addition, S100A8-mediated inflammatory stimuli are connected with the upregulation of the □-site APP-cleaving enzyme BACE1, which is involved in the APP processing (Heneka et al., 2015a; Kummer et al., 2014). S100B has been observed in A□ plaques and in the CSF (Van Eldik and Griffin, 1994; Moran et al., 2003) and overexpression human S100B exacerbates amyloidosis and gliosis in the Tg2576 AD mouse model (Mori et al., 2010).

Likewise, mt-DNA and DNA can be released from the cells and act as DAMPs upon entering the blood flow, causing inflammation (Thundyil and Lim, 2015). Mt-DNA can bind to TLR-9 and mediate the release of TNFα and type I IFNs (Hauser et al., 2010). In addition, cell free DNA can bind to TLR and non-TLR receptors. Upon TLR binding, DNA activates the NFκB pathway thereby promoting pro-inflammatory cytokine production (Barbalat et al., 2011). DNA can also bind to the absent in melanoma 2 (AIM2) inflammasome, releasing IL-1β, through the caspase-1 activation pathway.

HSPs bind to several receptors, such as TLR2 and TLR4, resulting in the production of inflammatory cytokines such as TNFα and IL-1β (Asea et al., 2002; Basu et al., 2000; Luong et al., 2012). Furthermore, HSPs may also exert beneficial effects in AD, thus, HSP70 can bind to APP and reduce the secretion of Aβ1-40 and Aβ1-42 through interference of with the APP processing pathway (Yang et al., 1998). HSP70, together with HSP90 can also interact with tau and Aβ oligomers and degrade them by employing proteasomal degradation (Dickey et al., 2009).

Endogenous modulators

Neurotransmitters can act as endogenous modulators, such as adenosine triphosphate (ATP), glutamate, dopamine and various neurotrophic factors, e.g. brain-derived neurotrophic factor (BDNF) and nerve growth factor (NGF). Microglial cells are equipped with a plethora of neurotransmitter receptors, which makes them a primary target, in particular for site of non-synaptic release (Pocock and Kettenmann, 2007).

In AD there is a decline in ATP production from neurons. Mitochondrial dysfunction as evidenced by reduced ATP is related to oxidative stress in AD pathology (Moreira et al., 2010). Oxidative stress can also initiate inflammatory responses and contributes to the etiopathology of AD (Mao et al., 2012).

Glutamatergic neurotransmission is disturbed due to an increased amount of soluble Aβ oligomers in AD(De Felice et al., 2008). The possible inflammatory process occurs subsequently through activation of microglia with TNFα release, synergizing with NMDA-mediated neurodegeneration (Wenk et al., 2006). However, the modulation of glutamate can be either pro- or anti-inflammatory depending on the expression of different groups of GluRs on microglia and most likely on the astroglial uptake capabilities, too(Farso et al., 2009; Kaushal and Schlichter, 2008).

Dopamine mediates the activation of microglia possibly by triggering the MAP kinase-NFκB cascade and inducing neurotoxicity towards dopaminergic neurons (Beaulieu and Gainetdinov, 2011; Lee et al., 2004). In general acetylcholine prevents the inflammatory response in microglia via α7 nicotinic acetylcholine receptors, mediated by the PLC/IP3/Ca2+ signaling pathway (Suzuki et al., 2006). In AD patients, significant loss of cholinergic neurons is tightly related to the progression of the disease. Failure in cholinergic neurotransmission decreases the cholinergic input to microglia, which in turn results in microglial activation (Carnevale et al., 2007; Wang et al., 2003). In addition, stimulation of microglia with norepinephrine suppressed inflammation through cAMP/PKA signaling cascades (Heneka et al., 2010; Tanaka et al., 2002). Of note, the locus ceruelus, the chief source of NA in the human brain, degenerates very early. Thus, its projection regions, most dominantly the limbic system and neocortex experience decreasing NA levels. Modeling this in rodents, increased Aβ-induced inflammation (Heneka et al., 2002, 2003) and substantially increased neuronal death and memory deficits (Heneka et al., 2006). Using 2 photon laser microscopy, it was demonstrated that depletion of NA in APP/PS1 transgenic mice, caused a complete inhibition of microglial Aβ clearance and subsequently an increase in the number and volume of Aβ deosits (Heneka et al., 2010). Replenishing cortical and hippocampal NA levels by treatment with the NA precursor, L-threo-DOPS, partly rescued this phenotype.

The levels of BDNF and NGF are severely altered in the brains of AD patients. BDNF is released by activated microglia and inhibits the release of TNF-α and IFN-γ, while promoting the expression of anti-inflammatory cytokines IL-4, IL10 and IL-11 (Makar et al., 2009). However, an *in vitro* study also shows prolonged microglial activation through a positive feedback loop by autocrine BDNF (Zhang et al., 2014). Together, this demonstrates that BDNF may modulate inflammation at various levels. In addition, evidence from a human microglial cell line suggests that NGF synthesis is potentially stimulated by inflammatory signals (cytokines and complement factors), as well as by exposure to Aβ25-35, through NFκB-dependent and -independent mechanisms (Heese et al., 1998).

Inflammatory mediators

Cytokines

Cytokines are released by glial cells, such as astrocytes and microglia, during the every inflammatory challenge (Orre et al., 2014; Su et al., 2016; Wyss-Coray and Rogers, 2012). Many cytokines, such as IL-1β and IL-12 have been related to the progression of AD pathology (Dursun et al., 2015; Sciacca et al., 2003). Increased IL-1β serum levels have been linked to AD and patients suffering from mild cognitive impairment, a putative prophase of dementia (Dursun et al., 2015; Forlenza et al., 2009). Several studies have reported associations between IL-1β polymorphisms and the onset of AD pathology(Payão et al., 2012; Sciacca et al., 2003; Yuan et al., 2013), and linking both IL-1β polymorphisms and APOEε4 to higher levels of IL-1β in the blood and sleep disturbance in patients (Yin et al., 2016). IL-12 is related to the regulation of the adaptive and the innate immune system (Trinchieri et al., 2003) and an IL-12 polymorphism has been linked to AD in a Han Chinese population(Zhu et al., 2014). Indeed Vom Berg *et al.*, suggested that inhibition of the IL-12/IL-23 pathway may attenuate AD pathology and cognitive deficits due to the decrease in the IL-12p40 subunit and its receptor activity (Vom Berg et al., 2012). In this study, the concentration of IL-12p40 was increased in the CSF of AD patients. Regarding anti-inflammatory cytokines, IL-10 deletion attenuates AD-related deficits such as altered synaptic integrity and behavioral deficits in APP/PS1 mice(Guillot-Sestier et al., 2015). Chakrabarty et al showed that the overexpression of IL-10 using adeno-associated viruses (AAV) increases amyloid deposition, behavioral deficits, synaptic alterations and impaired microglial phagocytosis of Aβ in the APP transgenic mouse model(Chakrabarty et al., 2015).

Another major regulator of inflammation is the transforming growth factor beta (TGF-β). Increased TGF-β is observed in amyloid plaques (van der Wal et al., 1993) and in the CSF of AD patients(Chao et al., 1994; Zetterberg et al., 2004). However, this cytokine has a dual role in AD. Overexpression of TGF-β *in vivo* induces Aβ deposition in cerebral blood vessels but it may also decrease microgliosis while increasing Aβ phagocytosis (Wyss-Coray et al., 2001). A link between TGF-β and neuro-fibrillary tangles (NFT) has also been reported (Chalmers and Love, 2007).

Chemokines

Chemokines participate in the chemoattraction of immune cells from the periphery to the brain and in the attraction and activation of resident glial cells. In AD, chemokines play a dual role as they are implicated in both the resolution and the propagation of pathology (Le Thuc et al., 2015). The most intensively studied chemokines in AD are CX3C chemokine ligand 1 (CX3CL1) and chemokine ligand 2 (CCL2).

CX3CL1, also termed fractalkine, is expressed by neurons, whereas its receptor, CX3CR1, is predominantly expressed by microglia (Cardona et al., 2006; Harrison et al., 1998). The participation of this chemokine in the pathophysiology of AD is complex since CX3CL1/CX3CR1 signaling can have a beneficial role in a context of tau pathology (Bhaskar et al., 2010; Cho et al., 2011; Nash et al., 2013) or a detrimental role in an amyloid context (Lee et al., 2010). In fact, in an amyloid model, deficiency of CX3CR1 decreased Aβ deposition (Lee et al., 2010), whereas it worsened tau pathology and cognitive performance (Bhaskar et al., 2010; Cho et al., 2011). Moreover, the expression of CX3CL1 is increased in tau-injured neurons whereas it is decreased in brains of APP transgenic mice (Duan et al., 2008). However, in patients the level of CX3CL1 is inversely correlated

with AD severity (Kim et al., 2008). Together this may point to the possibility that the same inflammatory mediator may adopt various different, if not opposing effects and qualities during disease progression.

CCL2 has also been associated with a dominant role in chronic inflammation (Sokolova et al., 2009). A recent study demonstrated that the CCL2/CCR2 pathway of astrocyte-induced microglial activation is associated with "M1-polarised" and enhanced microglial activity (He et al., 2016). In AD, CCL2 levels were increased in mild, but not severe AD, suggesting that elevated CCL2 may play a pathogenic role during early AD stages (Galimberti et al., 2006). In keeping with this, Westin et al. showed that CCL2 marks a faster cognitive decline in early disease stages (Westin et al., 2012). Kiyota et al. found accelerated neurodegeneration in APP/CCL2 transgenic mice, indirectly suggesting that a direct inhibition of CCL2 signalling may modify microglial activation, resulting in lower Aβ deposition and improving behavioural outcomes (Kiyota et al., 2009). CCL2 overexpression accelerated oligomeric and diffuse Aβ deposition and caused spatial and working memory deficits by affecting Aβ seeding in Tg2576 mice (Kiyota et al., 2009).

Other mediators

Nitric oxide (NO) is synthesized by three different isoforms of nitric oxide synthase (NOS). Each isoform plays a role in either AD progression or prevention, suggesting that NO can be neuroprotective or neurotoxic. High doses of LPS induced robust CNS inflammation and microglia-induced release of NO. NO in the CNS can influence many signaling pathways including protein nitrosylation, impairment of long-term potentiation or inhibition of mitochondrial respiration. The impact of NO signaling depends on the local cellular environment. In the AD brain, NO mainly derives from the inducible isoform of NOS, NOS2, which is being expressed by neurons(Vodovotz et al., 1996), microglia and astrocytes (Heneka et al., 2001a). Nitrosative stress has been shown to affect all types of cellular proteins, including but not restricted to synaptic proteins. Posttranslational protein modification can take place either by s-nitrosylation of cysteine residues or by nitration of tyrosine residues. Importantly, Aβ itself represents a nitration target at tyrosine 10 of its amino acid sequence. Nitration at this position strongly increases the peptides propensity to aggregate and nitrated Aβ predominantly resides in the core of the deposits, suggesting that this mechanisms contributes to the initiation of deposition (Kummer et al., 2011).

Effect of neuroinflammation on neuronal function

Cytokines and synaptic scaling

Mechanisms of synaptic plasticity are strongly influenced by basal levels of cytokines(Yirmiya and Goshen, 2011). Emblematic is the case of "synaptic scaling", a well-defined form of homeostatic plasticity which regulates the density of glutamate receptors at presynaptic and postsynaptic sites (Turrigiano, 2008). A homeostatic reduction of neuronal excitability by withdrawal of glutamate receptors is termed "down-scaling", whereas the increase of neuronal excitability (by accumulation of glutamate receptors) is known as "up-scaling". TNF-α has been shown to support synaptic up-scaling by increasing AMPA receptor-dependent miniature excitatory postsynaptic currents (mEPSC). Importantly, TNFα required for up-scaling synapses is derived from glial cells (Stellwagen and Malenka, 2006) and not from neurons themselves. Such evidence implies that glial cells are able to release cytokines in response to changes of neuronal activity. By contrast, enhanced release of inflammatory cytokines, for instance during a chronic peripheral inflammation, can disrupt the physiological mechanisms of synaptic plasticity, promoting neuronal hyper-excitability and increased susceptibility to seizures generation (Riazi et al., 2008).

A growing body of evidence demonstrates that microglia can actively respond to increased neuronal excitability and microglial processes make physical contact with excitatory synapses (Dissing-Olesen et al., 2014; Eyo et al., 2014; Fontainhas et al., 2011; Li et al., 2012). This type of microglia-synapse interaction has been shown to reduce neuronal excitability (Ji et al., 2013; Zhang et al., 2014), potentially as a form of a regulatory mechanism for

preventing glutamatergic excitotoxicity(Eyo et al., 2014).

Microglia and synaptic pruning

Microglia can actively participate in remodeling synaptic connections (''synaptic pruning''). A pathological form of synaptic pruning may represent a commonly shared mechanism among several neurological conditions of different nature*:* Thus, a recent study in a murine model of chronic-stress, showed electron-dense (dark) microglia co-localized with synaptic terminals. This microglial phenotype, that is associated with synaptic pruning, appeared clearly reactive possibly accounting for an increased loss of synapses during chronic inflammation(Bisht et al., 2016). Microglia may also remove synapses through a complement-dependent manner in a mouse model of West-Nile-Virus-induced neuroinflammation (Vasek et al., 2016). Mice with either a deficit in microglia number ($IL34^{-/-}$) or a deficiency of complement components (such as C3 protein or complement receptor 3 knock-out) were protected from inflammation-induced synaptic loss(Vasek et al., 2016).

An alternative hypothesis suggests that pathological pruning of synapses during inflammation may also represent a form of "tissue remodeling" for auto-protective purposes (Chen et al., 2012). A recent study suggested that upon LPS injection, microglia pruned preferentially GABAergic terminals, thereby increasing excitatory synaptic activity and induction of neurotrophic pathways in downstream neurons. This mchanism has been interpreted as an attempt to promote neuronal viability in a pathological context, although at the expense of a temporary imbalance of synaptic connectivity(Chen et al., 2014).

In mouse models of Aβ deposition, complement protein C1q was elevated as early as 1 month of age in both DG and frontal cortex. At this time point neither plaques nor synaptic loss became detectable. At later age (3-4 months old mice) the number of synapses decreased significantly, however, synaptic loss was rescued almost completely in the absence of either C1q, C3 or CR3. Additionally, ICV injection of oligomeric Aβ in wild-type mice induced synapse loss and activated a phagocytic phenotype in microglia. additionally, synapse loss in response to oligomeric Aβ was neither in C1q nor in CR3 knock-out mice observed (Hong et al., 2016).

Similar findings have been obtained in a mouse model deficient for the *progranulin gene*, typically associated with frontotemporal dementia (FTD) in humans(Baker et al., 2006; Cruts et al., 2006). Lack of progranulin has been shown to trigger an exaggerated inflammatory reaction in microglia and macrophages(Yin et al., 2010). Interestingly, the brain of progranulin-deficient mice showed increased levels of complement proteins, a prominent pro-phagocytic activation of microglia and enhanced pruning of synapses(Lui et al., 2016).

Inflammation and neurogenesis

Under homeostasis, immunological signals can actively shape adult neurogenesis. Microglia were shown to rapidly engulf and remove apoptotic neuronal progenitors, importantly, without any trace of inflammatory reaction (Abiega et al., 2016; Sierra et al., 2010) . Other evidences have pinpointed a close interplay between different immune proteins and the neurogenic process(Boulanger, 2009; Deverman and Patterson, 2009). IL-1β has often received particular attention due to its anti-neurogenic activity (Gemma et al., 2007; Green and Nolan, 2012; Guadagno et al., 2015; Koo and Duman, 2008; Wu et al., 2013; Zhang et al., 2013; Zunszain et al., 2012). One could assume that microglia are primarily responsible for this reduction of neurogenesis during inflammatory challenges. An interesting molecular player is the CX3C axis between neurons and microglia, which is known to preserve the microglial "resting" phenotype under physiological conditions (Biber et al., 2007; Hellwig et al., 2013). Several consistent findings showed reduced neurogenesis in CX3CR1-deficient mice, along with increased NFkB activation and IL-1β expression in microglia (Maggi et al., 2011; Reshef et al., 2014; Rogers et al., 2011; Sellner et al., 2016). Consistently, when an inflammatory challenge is applied under CX3CR1-deficient conditions, microglia release an increased and uncontrolled amount of inflammatory mediators and free radicals, causing neurotoxicity and cognitive/behavioral deficits (Cardona et al., 2006; Corona et al., 2013). Interestingly, during ageing, neurons decrease expression of CX3CL1 (Bachstetter et al., 2011), which likely would result in a general downregulation of the CX3C axis and pro-inflammatory skewing of microglia (Damani et al.,

2011; Hefendehl et al., 2014). Pro-inflammatory microglial priming has been suggested as a possible mechanism leading to the dysregulated microglial function and the ensuing stepwise decline of neurogenesis (and potentially neurodegeneration) during senility (Eggen et al., 2013; Gemma and Bachstetter, 2013; Harry, 2013; Niraula et al., 2017; Perry, 2010; Raj et al., 2014; Wong, 2013). In contrast, several lines of evidence are pointing towards the pro-neurogenic function of microglia, especially during the period of early brain development. These indications suggest that microglia play an important role during brain development, axonal guidance and formation of neuronal networks.

Astrocytes and glutamate reuptake

In the CNS, extracellular levels of glutamate are tightly regulated by astrocytes in order to modulate glutamate receptor activity and prevent potential excitotoxicity (Dong et al., 2009). Once in the synaptic cleft, glutamate in excess is promptly scavenged by the "Excitatory-Amino-Acid-Transporters" (EAATs) expressed on both neurons and astrocytes (Clements et al., 1992). The astrocytic EAAT2 is thought to be responsible for about the 90% of all glutamate uptake in the brain (Danbolt, 2001; Holmseth et al., 2009). There are no synaptic enzymes which otherwise would degrade glutamate. Therefore, astrocyte-mediated glutamate uptake represents the primary mechanism for the homeostatic regulation of glutamate bioavailability (Popoli et al., 2011). Impairment of glutamate uptake causes *excitotoxicity* characterized by overload of cellular calcium, generation of free radicals and protein/lipid oxidation. Notably, astrocyte glutamate transporters (EAAT1 and EAAT2) were shown to be reduced in the cortex and hippocampus of AD patients (Masliah et al., 1996; Scott et al., 2011). Moreover, Aβ-induced neurotoxicity in-vivo has been associated with NMDAR-dependent excitotoxicity (Miguel-Hidalgo et al., 2002).

In conclusion, pharmaceutical compounds aiming to modulate glutamate excitotoxicity have revealed a certain therapeutic potential for neurodegenerative diseases.

Modifiable risk factors for AD

Infections

Infection represents an important risk factor in the progression of dementia and AD (Iwashyna et al., 2010; McManus and Heneka, 2017). Multiple infections double the risk of developing dementia (Dunn et al., 2005) and in AD patients, peripheral infection results in accelerated cognitive decline (Holmes et al., 2003, 2009). The frequency of various infections including pneumonia, urinary tract infections, and respiratory tract infections is higher in individuals with AD than compared to healthy, elderly controls (Natalwala et al., 2008). Indeed, pneumonia is one of the most common causes of death in AD (Fitzpatrick et al., 2005; Foley et al., 2015; Magaki et al., 2014). In contrast, vaccination against influenza and other infectious conditions significantly lowered the risk of developing AD (Tyas et al., 2001; Verreault et al., 2001).

A number of specific viral, bacterial and fungal infections have been found in the AD brain, and may be implicated in AD development. One example is herpes simplex virus type 1 (HSV-1) (Jamieson et al., 1991, 1992; Wozniak et al., 2005) which is an AD risk factor in people carrying the *APOE4* allele (Honjo et al., 2009; Itzhaki et al., 1997). *Chlamydia pneumonia* is a Gram-negative bacteria found in the AD brain (Gérard et al., 2005, 2006), where it can infect microglia, astrocytes and neurons (Gérard et al., 2006). Interestingly fungal protein and DNA has been identified in the AD brain and CSF, too (Alonso et al., 2014, 2015). Co-infection with many fungi was observed, with fungal material identified inside neuronal cells and in many regions of the post-mortem AD brain (Pisa et al., 2015a, 2015b). However, the significance of these findings remains unclear to date and several factors including postmortem time and handling should be considered before prematurely drawing conclusions. Systemic inflammation certainly impacts on the brain, which is not at all "immune-privileged" as our textbook reading still suggests. Thus, higher rates of cognitive decline were observed in AD patients with acute systemic inflammation (Holmes et al., 2009). Leaky gut could be one of the drivers of systemic inflammation, and it is directly related to a dysbalance of gut microbiota (Jakobsson et al., 2015).

Traumatic brain injury

Traumatic brain injury (TBI) results in damaged blood vessels, axons, nerve cells and glia of the brain in a focal, multifocal or diffuse pattern resulting in impaired brain function (Faden and Loane, 2015; Faden et al., 2016). A single moderate or severe TBI may increase the risk of developing late-onset AD, while repetitive mild TBI (e.g. through contact sport) is associated with an elevated risk of chronic traumatic encephalopathy (Smith et al., 2013a; Washington et al., 2016). Two key meta-analyses of case-control studies found a significant association between moderate-severe TBI and AD (Fleminger et al., 2003; Mortimer et al., 1991). Furthermore, animal and human studies support an abnormal accumulation of AD-related pathological proteins including soluble and insoluble Aβ and hyperphosphorylated tau aggregates, following TBI (Johnson et al., 2012; Smith et al., 1999). Aggregation and deposition of Aβ is accelerated after an acute TBI event, with changes just 24 hours to 2 months after injury (Bennett et al., 2013; Chen et al., 2004; Iwata et al., 2002; Shishido et al., 2016; Smith et al., 1999) and was associated with memory impairments in 3xTg-AD mice (Shishido et al., 2016). Aberrant tau phosphorylation was also described in several models after TBI (Kane et al., 2012; Luong et al., 2012; McAteer et al., 2016; Petraglia et al., 2014) (Kane et al., 2012; Luo et al., 2014; McAteer et al., 2016; Petraglia et al., 2014). The formation of misfolded Aβ and tau oligomeric seeds triggered by TBI may lead to spreading of the pathology in a prion-like manner, causing a faster and more severe onset of the disease (Gerson et al., 2016).

Smoking and Alzheimer's disease

A recent meta-analysis study showed that smoking is associated with a 1.7-fold higher risk for AD (Cataldo et al., 2010), with a correlation between smoking intensity and duration (Tyas et al., 2001). It is estimated that today, smoking accounts for 4.7 million AD cases worldwide (Barnes and Yaffe, 2011). Various *in vitro* and *in vivo* studies suggest that sustained cigarette smoke exposure facilitates the production of regional Aβ and tau pathology (Giunta et al., 2012; Moreno-Gonzalez et al., 2013). Cigarette smoke can increase oxidative stress (Baldeiras et al., 2010; Ho et al., 2012; Seet et al., 2011), affecting cerebrovascular dysfunction (Gons et al., 2011), neuroinflammation (Moreno-Gonzalez et al., 2013) as well as protein misfolding and aggregation (Kenche et al., 2013; Shen et al., 2008).

Physical activity in Alzheimer's disease

A case-control study showed AD patients were less active in their midlife (Friedland et al., 2001). Physical inactivity is accompanied with several secondary effects including obesity, metabolic syndrome, diabetes type 2, and cardiovascular disease (Booth et al., 2008). In contrast, regular physical exercise positively influences neurogenesis, brain plasticity and metabolic function, reduces levels of pro-inflammatory cytokines and oxidative stress (Baker et al., 2010; Nascimento et al., 2014; Radak et al., 2010) and can alter disease-related biomarkers in patients with dementia (Jensen et al., 2015).

Analysis of different animal models suggests positive effects of physical exercise on BDNF levels, oxidative stress and even Aβ and tau pathology, resulting in delayed disease onset and progression (Kim et al., 2014; Leem et al., 2009; Marosi et al., 2012; Um et al., 2008). Although, physical exercise may not benefit all patient populations equally (Jensen et al., 2015; Smith et al., 2013b). Some studies report a stronger effect of physical activity among *APOE4* carriers in comparison to non-carriers (Etnier et al., 2007; Rovio et al., 2005; Schuit et al., 2001), while others could not replicate these results (Cheng et al., 2014; Eggermont et al., 2009; Podewils et al., 2005).

Diet & Obesity

Many specific dietary components have been studied in relation to AD. In clinical studies, higher intake of unsaturated fatty acids, antioxidants, vitamins B12 and folate have been associated with a lower risk for AD and cognitive decline (Commenges et al., 2000; Morris, 2012; Wang et al., 2001). However, the opposite or even no effect has also been found for these factors (Crystal et al., 1994; Engelhart et al., 2002; Luchsinger et al., 2003). Instead of focusing on individual dietary components, the effect of overall dietary patterns (which incorporates nutrient interaction) has been examined, including the Mediterranean Diet (MeDi) (Willett et al., 1995), Dietary Approaches to Stop Hypertension (DASH)

(Tangney et al., 2014) and the Mediterranean-DASH Intervention for Neurodegenerative Delay (MIND) (Morris et al., 2015a). These studies point towards diet as a protective effect against cognitive decline and development of AD (Morris et al., 2015b, 2015c, Scarmeas et al., 2006a, 2006b, 2009, Tangney et al., 2011, 2014; Tsivgoulis et al., 2013).

In contrast, overnutrition can lead to obesity, which in turn has been associated with AD development. Obesity is characterized by leptin and insulin resistance, leading to impaired energy metabolism and chronic inflammation (Schmidt et al., 2015). This chronic inflammatory status can cause cellular stress and neurodegeneration and is thought to be the link between obesity and its adverse effects on cognitive performance and AD development (Cai, 2013; Elias et al., 2005; Engelhart et al., 2004; Tan et al., 2007; Waldstein and Katzel, 2006). Most importantly, some of these effects may occur in midlife already. Thus, increased BMI and saggital abdominal diameter in 40-45 year old males was associated with an increased AD risk in later life (Whitmer et al., 2008).

Life-time distress

Life-time frequency of stress exposure is consistently associated with the incidence of mild cognitive impairment (MCI) and is suggested to increase the risk for late-onset AD (Johansson et al., 2014; Wilson et al., 2003, 2007). Particularly, higher levels of the stress hormone cortisol are associated with an accelerated age-related decline in cognition (Arsenault-Lapierre et al., 2010; Comijs et al., 2010). The hypothalamic – pituitary – adrenal (HPA) axis regulates the release of cortisol in humans or the equivalent corticosterone in rodents. This system is dysregulated in AD patients, with higher cortisol levels in blood plasma and CSF of AD subjects compared to age-matched controls (Arsenault-Lapierre et al., 2010; Csernansky et al., 2006).

Interestingly, exposing rodents to stressful experiences increases corticosterone levels and glucocorticoid receptor activation, resulting in aggravation of AD related neuropathologies in various transgenic models (Baglietto-Vargas et al., 2015; Dong et al., 2008; Green et al., 2006; Huang et al., 2015; Jeong et al., 2006; Rothman et al., 2012). Microglia are highly responsive to glucocorticoids, with abundant glucocorticoid receptor expression levels (Sierra et al., 2008). Furthermore, glucocorticoids can induce a pro-inflammatory microglial phenotype upon stress, especially following a secondary inflammatory challenge(Busillo and Cidlowski, 2013; Perez Nievas et al., 2011; Walker et al., 2013).

Diabetes mellitus

Type-II-diabetes (T2D) affects approximately 370 million people world-wide, accounting for 90 – 95 % of all diabetic patients (Verdile et al., 2015). The disease is characterized by hyperglycaemia, insulin resistance and relative lack of insulin (Kandimalla et al., 2017). People suffering from T2D had a 73 % greater risk of developing dementia (Biessels et al., 2014) and they have decreased brain volume in both the white and grey matter of the temporal and frontal lobes (Brundel et al., 2014; Moran et al., 2013). Cortical and hippocampal atrophies were also observed in diabetes mice (db/db) (Ramos-Rodriguez et al., 2014).

Importantly, insulin resistance leads to the generation of neurofibrillary tangles via decreased activation of protein kinase B, resulting in ineffective inhibition of glycogen synthase kinase 3 thus mediating tau phosphorylation and formation of neurofibrillary tangles (Kroner, 2009; Lizcano and Alessi, 2002). In addition, due to the amount of insulin in diabetes patients the insulin-degrading enzyme is sequestered away from Aβ, which fosters the accumulation of Aβ in the brain (Haque and Nazir, 2014; Qiu and Folstein, 2006). T2D patients have impaired immunological defense mechanisms, resulting in frequent infections that may contribute to the development of AD (C et al., 2017). The concentration of pro-inflammatory cytokines in the CSF is increased in T2D patients (Fishel et al., 2005), indeed chronic subacute inflammation can also induce insulin resistance and cause T2D (Shoelson et al., 2006).

Protection by anti-inflammatory strategies

Past and present strategies

Various anti-inflammatory therapeutic approaches have been performed to modify AD progression in the past two decades, ranging from non-steroidal

anti-inflammatory drugs (NSAIDs) to TNFα inhibition. One of those approaches is the Alzheimer's Disease Anti-inflammatory Prevention Trial (ADAPT). This trial was constructed to question whether non-steroidal anti-inflammatory drugs (NSAIDs) could prevent or delay the onset of AD, and whether the treatments could worsen cognitive decline associated with aging (Meinert and Breitner, 2008).

Early epidemiological studies had suggested that long-term medication with NSAIDs decreases risk of AD development (Andersen et al., 1995; Breitner et al., 1994; Gasparini et al., 2004; Stewart et al., 1997). Additionally, strong experimental evidence has emerged supporting the positive effect of NSAIDs in AD animal models (Heneka et al., 2015a; Shadfar et al., 2015). NSAIDs have been shown to reduce beta-amyloid secretion and accumulation both in vitro and in vivo, to modulate γ-secretase activity, to exert an anti-inflamatory effect and to improve cognitive function in AD mouse models (Carreras et al., 2013; Heneka et al., 2005; Kukar et al., 2007; Lim et al., 2001; McKee et al., 2008; Weggen et al., 2001).

However, most NSAIDs have not convincingly shown any beneficial effects during clinical trials in AD patients. Only a small, early study using indometacin on AD patients(Rogers et al., 1993), which has not been replicated, and a follow up analysis from the ADAPT research group using naproxen (Breitner et al., 2011) have shown positive effects.

PPARγ-agonism has consistently been shown to reduce the production of inflammatory cytokines and amyloid accumulation in AD mouse models (Heneka et al., 2001b, 2005; Hu et al., 2012; Landreth and Heneka, 2001; Mandrekar-Colucci and Landreth, 2011). Rosiglitazone has been described to induce activation of the ERK pathway leading to cognitive enhancement in AD models (Alaynick, 2008; Denner et al., 2012; Inestrosa and Toledo, 2008; Jahrling et al., 2014). Pioglitazone has been found to improve cognition and cerebral blood flow in mild AD (Sato et al., 2011). Additionally, pioglitazone treatment reduced dementia risk in initially non-insulin dependent diabetes mellitus patients in a case-control study (Heneka et al., 2015b). However, no significant effect was detected on a randomized pilot clinical trial for the safety of this drug on AD patients (Geldmacher et al., 2011). Rosigitazone has been described to delay cognitive decline in early AD and MCI patients (Watson et al., 2005). Another study found an improvement in cognitive function using pioglitazone that was restricted to ApoE epsilon4 non-carriers (Risner et al., 2006).

Trials with other anti-inflammatory drugs such as prednisone, hydroxychroloquine, simvastatin, atorvastatin and aspirin have been performed but shown no significant positive cognitive effects on AD patients (Aisen et al., 2000; Feldman et al., 2010; Heneka et al., 2015b; Simons et al., 2002; Sparks et al., 2005; Van Gool et al., 2001).

Drug	Participants	Duration of treat.	Dose	Main effect	Ref.
Indometacin	28 AD dementia patients	6 months	100-150 mg daily versus placebo	Positive effects on a battery of psychometric tests	*Rogers et al. 1993*
Indometacin	51 Patients wth mild-to-moderate AD	1 year	100mg daily with omeprazole versus placebo	Not significant effect on ADAS-cog score	*De Jong et al. 2008*
Naproxen sodium or rofecoxib	351 patients with mild-to-moderate AD	1 year	220mg Naproxen twice daily or rofecoxib 25mg once daily versus placebo	Not significant effect on ADAS-cog score	*Aisen et al. 2003*
Nimesulide	40 AD dementia patients	3 months	100mg	Not apparent effect on a composite of cognitive, behavioural and functional outcomes	*Aisen et al. 2002*
Rofecoxib	1457 MCI patients	4 years	25 mg once daily versus placebo	Not significant effect on ADAS-cog score	*Thal et al. 2005*
Celecoxib or naproxen sodium	2528 healthy individuals with family history of AD	1-3 years	100 mg twice daily of naproxen sodium 220mg twice daily versus placebo	Not significant effect on a battery of neuropsychological tests	*Martin et al. 2008*
Celecoxib or naproxen sodium	2071 participants randomized in ADAPT	2-4 years follow up after termination of treatment	Follow up	Not significant effect for celecoxib. Reduced AD onset and CSF tau to $A\beta_{1-42}$ ratio for naproxen.	*Breitner et al. 2011*
Celecoxib or naproxen sodium	1537 participants randomized in ADAPT	5-7 years follows up after termination of treatment	Follow up	Not significant delay on onset of AD	*ADAPT research Group. 2013*

Table 1. Randomized clinical trials of NSAIDs in patients with Alzheimer's disease. AD=Alzheimer's disease. ADAS-Cog=Alzheimer Disease Assessment Scale-cognitive portion. MCI=mild cognitive impairment. ADAPT= Alzheimer's Disease Anti-infl amatory. Treat=Treatment. Adapted from Heneka et al. 2015.

Inhibiting TNFα signaling has also become an interesting and promising approach to treat AD. Infliximab (an antibody against TNFα already approved for other indications) was found to reduce Aβ plaques and tau pathology in APP/PS1 mice and has also been described to enhance cognitive function after intrathecal administration in a clinical case report (Shi et al., 2011a, 2011b). Additionally, two small pilot clinical studies using a different TNFα inhibititor, etanercept, showed cognitive improvement in AD patients (Tobinick and Gross, 2008; Tobinick et al., 2006). These studies however use small sample sizes, open-label design and lack a placebo group. Thus, a bigger well-designed placebo-controlled study is necessary to assess the possible utility of TNFα in AD (Shadfar et al., 2015).

Future strategies

Recently, fenamate NSAIDs including Mefenamic acid here found to inhibit NLRP3 selectively through the inhibition of volume regulated ion channels (VRAC channels), inhibiting cognitive impairments in rodent models of Alzheimer disease (Daniels et al., 2016). Mefanamic acid is already in the market and used for abdominal pain in premenstrual syndrome. MCC950, a new potent NLRP3-selective inhibitor has been developed but is not yet available for clinical use (Coll et al., 2015). Anakinra, an IL-1 receptor antagonist and a neutralizing antibody, canakinumab, have been proposed to work inhibiting this NLRP3 axis, but price-benefit and bioavailability in the brain remains a concern (Dinarello et al., 2012).

CSP-1103 (Also known as CHF 5074 or Itanapraced), is now in Phase III clinical trials as a microglia modulator. It may inhibit Aβ plaque deposition, reduce tau pathology, restore normal microglial function by increasing phagocytosis and decreasing production of pro-inflammatory cytokines (Porrini et al., 2015).

Some other new therapeutic targets have been proposed. MAPKα inhibitors (e.g. VX-745) would reduce IL-1β levels (Alam, 2015)(Clinicaltrials.gov/record NCT02423200). Administration of low dose IL-2 would increase plaque-associated microglia and increase cognition (Dansokho et al., 2016). C3aR antagonist SB290157 would act decreasing amyloid load and microgliosis (Mathieu et al., 2005). PD-1 inhibitors would reduce plaque load and improve cognition (Baruch et al., 2016). Blocking IL-12 and IL-23's p40 common subunit would decrease amyloid burden (Hu et al., 2012; Teng et al., 2015; Vom Berg et al., 2012). A CD33 inhibitor would promote microglial phagocytosis of Aβ (Griciuc et al., 2013).

SUMMARY AND CONCLUSIONS

Neuroinflammation in AD is likely to arise from the recognition of Aβ by pattern recognition receptors on the surface of innate immune cells in the brain. Once initiated ongoing inflammation and neurodegeneration will unleash further factors, which themeselves act as danger-associated molecular patterns and thereby contribute to the persisting and chronic type of sterile immune reaction in the brain. Several mechanisms of interaction by which inflammatory processes contribute to disease progression have been identified. Given the early deposition of Aβ, decades prior to first mnestic and cognitive deficits, makes it likely that such mechanisms may represent explorable therapeutic targets. Next to the identification of the most suited mode and site of intervention models, which better address the human cerebral innate immune system and biomarkers hereof, need to be identified.

REFERENCES

Abiega, O., Beccari, S., Diaz-Aparicio, I., Nadjar, A., Layé, S., Leyrolle, Q., Gómez-Nicola, D., Domercq, M., Pérez-Samartín, A., Sánchez-Zafra, V., et al. (2016). Neuronal Hyperactivity Disturbs ATP Microgradients, Impairs Microglial Motility, and Reduces Phagocytic Receptor Expression Triggering Apoptosis/Microglial Phagocytosis Uncoupling. PLoS Biol. *14*, e1002466.

Aisen, P.S., Davis, K.L., Berg, J.D., Schafer, K., Campbell, K., Thomas, R.G., Weiner, M.F., Farlow, M.R., Sano, M., Grundman, M., et al. (2000). A randomized controlled trial of prednisone in Alzheimer's disease. Alzheimer's Disease Cooperative Study. Neurology *54*, 588–593.

Ajami, B., Bennett, J.L., Krieger, C., Tetzlaff, W., and Rossi, F.M.V. (2007). Local self-renewal can sustain CNS microglia maintenance and function throughout adult life. Nat. Neurosci. *10*, 1538–1543.

Alam, J.J. (2015). Selective Brain-Targeted Antagonism of p38 MAPKα Reduces Hippocampal IL-1β Levels and Improves Morris Water Maze Performance in Aged Rats. J. Alzheimers Dis. JAD *48*, 219–227.

Alaynick, W.A. (2008). Nuclear receptors, mitochondria and lipid metabolism. Mitochondrion *8*, 329–337.

Alonso, R., Pisa, D., Marina, A.I., Morato, E., Rábano, A., and Carrasco, L. (2014). Fungal infection in patients with Alzheimer's disease. J. Alzheimers Dis. JAD *41*, 301–311.

Alonso, R., Pisa, D., Rábano, A., Rodal, I., and Carrasco, L. (2015). Cerebrospinal Fluid from Alzheimer's Disease Patients Contains Fungal Proteins and DNA. J. Alzheimers Dis. JAD *47*, 873–876.

Andersen, K., Launer, L.J., Ott, A., Hoes, A.W., Breteler, M.M., and Hofman, A. (1995). Do nonsteroidal anti-inflammatory drugs decrease the risk for Alzheimer's disease? The Rotterdam Study. Neurology *45*, 1441–1445.

Arsenault-Lapierre, G., Chertkow, H., and Lupien, S. (2010). Seasonal effects on cortisol secretion in normal aging, mild cognitive impairment and Alzheimer's disease. Neurobiol. Aging *31*, 1051–1054.

Asea, A., Rehli, M., Kabingu, E., Boch, J.A., Bare, O., Auron, P.E., Stevenson, M.A., and Calderwood, S.K. (2002). Novel signal transduction pathway utilized by extracellular HSP70: role of toll-like receptor (TLR) 2 and TLR4. J. Biol. Chem. *277*, 15028–15034.

Bachstetter, A.D., Morganti, J.M., Jernberg, J.,

Schlunk, A., Mitchell, S.H., Brewster, K.W., Hudson, C.E., Cole, M.J., Harrison, J.K., Bickford, P.C., et al. (2011). Fractalkine and CX 3 CR1 regulate hippocampal neurogenesis in adult and aged rats. Neurobiol. Aging *32*, 2030–2044.
Baglietto-Vargas, D., Chen, Y., Suh, D., Ager, R.R., Rodriguez-Ortiz, C.J., Medeiros, R., Myczek, K., Green, K.N., Baram, T.Z., and LaFerla, F.M. (2015). Short-term modern life-like stress exacerbates Aβ-pathology and synapse loss in 3xTg-AD mice. J. Neurochem. *134*, 915–926.
Baker, L.D., Frank, L.L., Foster-Schubert, K., Green, P.S., Wilkinson, C.W., McTiernan, A., Plymate, S.R., Fishel, M.A., Watson, G.S., Cholerton, B.A., et al. (2010). Effects of aerobic exercise on mild cognitive impairment: a controlled trial. Arch. Neurol. *67*, 71–79.
Baker, M., Mackenzie, I.R., Pickering-Brown, S.M., Gass, J., Rademakers, R., Lindholm, C., Snowden, J., Adamson, J., Sadovnick, A.D., Rollinson, S., et al. (2006). Mutations in progranulin cause tau-negative frontotemporal dementia linked to chromosome 17. Nature *442*, 916–919.
Baldeiras, I., Santana, I., Proença, M.T., Garrucho, M.H., Pascoal, R., Rodrigues, A., Duro, D., and Oliveira, C.R. (2010). Oxidative damage and progression to Alzheimer's disease in patients with mild cognitive impairment. J. Alzheimers Dis. JAD *21*, 1165–1177.
Bamberger, M.E., Harris, M.E., McDonald, D.R., Husemann, J., and Landreth, G.E. (2003). A cell surface receptor complex for fibrillar beta-amyloid mediates microglial activation. J. Neurosci. Off. J. Soc. Neurosci. *23*, 2665–2674.
Barbalat, R., Ewald, S.E., Mouchess, M.L., and Barton, G.M. (2011). Nucleic acid recognition by the innate immune system. Annu. Rev. Immunol. *29*, 185–214.
Barnes, D.E., and Yaffe, K. (2011). The projected effect of risk factor reduction on Alzheimer's disease prevalence. Lancet Neurol. *10*, 819–828.
Baroja-Mazo, A., Martín-Sánchez, F., Gomez, A.I., Martínez, C.M., Amores-Iniesta, J., Compan, V., Barberà-Cremades, M., Yagüe, J., Ruiz-Ortiz, E., Antón, J., et al. (2014). The NLRP3 inflammasome is released as a particulate danger signal that amplifies the inflammatory response. Nat. Immunol. *15*, 738–748.
Bartzokis, G. (2004). Age-related myelin breakdown: a developmental model of cognitive decline and Alzheimer's disease. Neurobiol. Aging *25*, 5-18-62.
Bartzokis, G. (2011). Alzheimer's disease as homeostatic responses to age-related myelin breakdown. Neurobiol. Aging *32*, 1341–1371.
Bartzokis, G., Lu, P.H., and Mintz, J. (2004). Quantifying age-related myelin breakdown with MRI: novel therapeutic targets for preventing cognitive decline and Alzheimer's disease. J. Alzheimers Dis. JAD *6*, S53-59.
Baruch, K., Deczkowska, A., Rosenzweig, N., Tsitsou-Kampeli, A., Sharif, A.M., Matcovitch-Natan, O., Kertser, A., David, E., Amit, I., and Schwartz, M. (2016). PD-1 immune checkpoint blockade reduces pathology and improves memory in mouse models of Alzheimer's disease. Nat. Med. *22*, 135–137.
Basu, S., Binder, R.J., Suto, R., Anderson, K.M., and Srivastava, P.K. (2000). Necrotic but not apoptotic cell death releases heat shock proteins, which deliver a partial maturation signal to dendritic cells and activate the NF-kappa B pathway. Int. Immunol. *12*, 1539–1546.
Bhaskar, K., Konerth, M., Kokiko-Cochran, O.N., Cardona, A., Ransohoff, R.M., and Lamb, B.T. (2010). Regulation of tau pathology by the microglial fractalkine receptor. Neuron *68*, 19–31.
Bianchi, M.E. (2007). DAMPs, PAMPs and alarmins: all we need to know about danger. J. Leukoc. Biol. *81*, 1–5.
Bianchi, M.E. (2009). HMGB1 loves company. J. Leukoc. Biol. *86*, 573–576.
Biber, K., Neumann, H., Inoue, K., and Boddeke, H.W.G.M. (2007). Neuronal "On" and "Off" signals control microglia. Trends Neurosci. *30*, 596–602.
Biessels, G.J., Strachan, M.W.J., Visseren, F.L.J., Kappelle, L.J., and Whitmer, R.A. (2014). Dementia and cognitive decline in type 2 diabetes and prediabetic stages: towards targeted interventions. Lancet Diabetes Endocrinol. *2*, 246–255.
Bisht, K., Sharma, K.P., Lecours, C., Sánchez, M.G., El Hajj, H., Milior, G., Olmos-Alonso, A., Gómez-Nicola, D., Luheshi, G., Vallières, L., et al. (2016). Dark microglia: A new phenotype predominantly associated with pathological states. Glia *64*, 826–839.
Booth, F.W., Laye, M.J., Lees, S.J., Rector, R.S., and Thyfault, J.P. (2008). Reduced physical activity and risk of chronic disease: the biology behind the consequences. Eur. J. Appl. Physiol. *102*, 381–390.
Boulanger, L.M. (2009). Immune proteins in brain development and synaptic plasticity. Neuron *64*, 93–109.
Breitner, J.C., Gau, B.A., Welsh, K.A., Plassman, B.L., McDonald, W.M., Helms, M.J., and Anthony, J.C. (1994). Inverse association of anti-inflammatory treatments and Alzheimer's disease: initial results of a co-twin control study. Neurology *44*, 227–232.
Breitner, J.C., Baker, L.D., Montine, T.J.,

Meinert, C.L., Lyketsos, C.G., Ashe, K.H., Brandt, J., Craft, S., Evans, D.E., Green, R.C., et al. (2011). Extended results of the Alzheimer's disease anti-inflammatory prevention trial. Alzheimers Dement. J. Alzheimers Assoc. *7*, 402–411.
Brundel, M., Kappelle, L.J., and Biessels, G.J. (2014). Brain imaging in type 2 diabetes. Eur. Neuropsychopharmacol. J. Eur. Coll. Neuropsychopharmacol. *24*, 1967–1981.
Busillo, J.M., and Cidlowski, J.A. (2013). The five Rs of glucocorticoid action during inflammation: ready, reinforce, repress, resolve, and restore. Trends Endocrinol. Metab. TEM *24*, 109–119.
C, W., G, X., Sa, T., Wj, F., and Ct, L. (2017). Transcriptional profiles of type 2 diabetes in human skeletal muscle reveal insulin resistance, metabolic defects, apoptosis, and molecular signatures of immune activation in response to infections. Biochem. Biophys. Res. Commun. *482*, 282–288.
Cagnin, A., Brooks, D.J., Kennedy, A.M., Gunn, R.N., Myers, R., Turkheimer, F.E., Jones, T., and Banati, R.B. (2001). In-vivo measurement of activated microglia in dementia. Lancet Lond. Engl. *358*, 461–467.
Cai, D. (2013). Neuroinflammation and neurodegeneration in overnutrition-induced diseases. Trends Endocrinol. Metab. TEM *24*, 40–47.
Cardona, A.E., Pioro, E.P., Sasse, M.E., Kostenko, V., Cardona, S.M., Dijkstra, I.M., Huang, D., Kidd, G., Dombrowski, S., Dutta, R., et al. (2006). Control of microglial neurotoxicity by the fractalkine receptor. Nat. Neurosci. *9*, 917–924.
Carreras, I., McKee, A.C., Choi, J.-K., Aytan, N., Kowall, N.W., Jenkins, B.G., and Dedeoglu, A. (2013). R-flurbiprofen improves tau, but not Aß pathology in a triple transgenic model of Alzheimer's disease. Brain Res. *1541*, 115–127.
Carter, S.F., Schöll, M., Almkvist, O., Wall, A., Engler, H., Långström, B., and Nordberg, A. (2012). Evidence for astrocytosis in prodromal Alzheimer disease provided by 11C-deuterium-L-deprenyl: a multitracer PET paradigm combining 11C-Pittsburgh compound B and 18F-FDG. J. Nucl. Med. Off. Publ. Soc. Nucl. Med. *53*, 37–46.
Castellani, P., Balza, E., and Rubartelli, A. (2014). Inflammation, DAMPs, tumor development, and progression: a vicious circle orchestrated by redox signaling. Antioxid. Redox Signal. *20*, 1086–1097.
Cataldo, J.K., Prochaska, J.J., and Glantz, S.A. (2010). Cigarette smoking is a risk factor for Alzheimer's Disease: an analysis controlling for tobacco industry affiliation. J. Alzheimers Dis. JAD *19*, 465–480.
Chakrabarty, P., Li, A., Ceballos-Diaz, C., Eddy, J.A., Funk, C.C., Moore, B., DiNunno, N., Rosario, A.M., Cruz, P.E., Verbeeck, C., et al. (2015). IL-10 alters immunoproteostasis in APP mice, increasing plaque burden and worsening cognitive behavior. Neuron *85*, 519–533.
Chalmers, K.A., and Love, S. (2007). Neurofibrillary tangles may interfere with Smad 2/3 signaling in neurons. J. Neuropathol. Exp. Neurol. *66*, 158–167.
Chao, C.C., Ala, T.A., Hu, S., Crossley, K.B., Sherman, R.E., Peterson, P.K., and Frey, W.H. (1994). Serum cytokine levels in patients with Alzheimer's disease. Clin. Diagn. Lab. Immunol. *1*, 433–436.
Chauveau, F., Boutin, H., Van Camp, N., Dollé, F., and Tavitian, B. (2008). Nuclear imaging of neuroinflammation: a comprehensive review of [11C]PK11195 challengers. Eur. J. Nucl. Med. Mol. Imaging *35*, 2304–2319.
Chen, Z., Jalabi, W., Shpargel, K.B., Farabaugh, K.T., Dutta, R., Yin, X., Kidd, G.J., Bergmann, C.C., Stohlman, S.A., and Trapp, B.D. (2012). Lipopolysaccharide-induced microglial activation and neuroprotection against experimental brain injury is independent of hematogenous TLR4. J. Neurosci. Off. J. Soc. Neurosci. *32*, 11706–11715.
Chen, Z., Jalabi, W., Hu, W., Park, H.-J., Gale, J.T., Kidd, G.J., Bernatowicz, R., Gossman, Z.C., Chen, J.T., Dutta, R., et al. (2014). Microglial displacement of inhibitory synapses provides neuroprotection in the adult brain. Nat. Commun. *5*, 4486.
Cheng, S.-T., Chow, P.K., Song, Y.-Q., Yu, E.C.S., Chan, A.C.M., Lee, T.M.C., and Lam, J.H.M. (2014). Mental and physical activities delay cognitive decline in older persons with dementia. Am. J. Geriatr. Psychiatry Off. J. Am. Assoc. Geriatr. Psychiatry *22*, 63–74.
Cho, S.H., Sun, B., Zhou, Y., Kauppinen, T.M., Halabisky, B., Wes, P., Ransohoff, R.M., and Gan, L. (2011). CX3CR1 protein signaling modulates microglial activation and protects against plaque-independent cognitive deficits in a mouse model of Alzheimer disease. J. Biol. Chem. *286*, 32713–32722.
Choo, I.L.H., Carter, S.F., Schöll, M.L., and Nordberg, A. (2014). Astrocytosis measured by ^{11}C-deprenyl PET correlates with decrease in gray matter density in the parahippocampus of prodromal Alzheimer's patients. Eur. J. Nucl. Med. Mol. Imaging *41*, 2120–2126.
Ciesielski-Treska, J., Ulrich, G., Chasserot-Golaz, S., Zwiller, J., Revel, M.O., Aunis, D., and Bader, M.F. (2001). Mechanisms underlying neuronal

death induced by chromogranin A-activated microglia. J. Biol. Chem. *276*, 13113–13120.
Clements, J.D., Lester, R.A., Tong, G., Jahr, C.E., and Westbrook, G.L. (1992). The time course of glutamate in the synaptic cleft. Science *258*, 1498–1501.
Coll, R.C., Robertson, A.A.B., Chae, J.J., Higgins, S.C., Muñoz-Planillo, R., Inserra, M.C., Vetter, I., Dungan, L.S., Monks, B.G., Stutz, A., et al. (2015). A small-molecule inhibitor of the NLRP3 inflammasome for the treatment of inflammatory diseases. Nat. Med. *21*, 248–255.
Comijs, H.C., Gerritsen, L., Penninx, B.W.J.H., Bremmer, M.A., Deeg, D.J.H., and Geerlings, M.I. (2010). The association between serum cortisol and cognitive decline in older persons. Am. J. Geriatr. Psychiatry Off. J. Am. Assoc. Geriatr. Psychiatry *18*, 42–50.
Commenges, D., Scotet, V., Renaud, S., Jacqmin-Gadda, H., Barberger-Gateau, P., and Dartigues, J.F. (2000). Intake of flavonoids and risk of dementia. Eur. J. Epidemiol. *16*, 357–363.
Corona, A.W., Norden, D.M., Skendelas, J.P., Huang, Y., O'Connor, J.C., Lawson, M., Dantzer, R., Kelley, K.W., and Godbout, J.P. (2013). Indoleamine 2,3-dioxygenase inhibition attenuates lipopolysaccharide induced persistent microglial activation and depressive-like complications in fractalkine receptor (CX(3)CR1)-deficient mice. Brain. Behav. Immun. *31*, 134–142.
Cruts, M., Gijselinck, I., van der Zee, J., Engelborghs, S., Wils, H., Pirici, D., Rademakers, R., Vandenberghe, R., Dermaut, B., Martin, J.-J., et al. (2006). Null mutations in progranulin cause ubiquitin-positive frontotemporal dementia linked to chromosome 17q21. Nature *442*, 920–924.
Crystal, H.A., Ortof, E., Frishman, W.H., Gruber, A., Hershman, D., and Aronson, M. (1994). Serum vitamin B12 levels and incidence of dementia in a healthy elderly population: a report from the Bronx Longitudinal Aging Study. J. Am. Geriatr. Soc. *42*, 933–936.
Csernansky, J.G., Dong, H., Fagan, A.M., Wang, L., Xiong, C., Holtzman, D.M., and Morris, J.C. (2006). Plasma cortisol and progression of dementia in subjects with Alzheimer-type dementia. Am. J. Psychiatry *163*, 2164–2169.
Damani, M.R., Zhao, L., Fontainhas, A.M., Amaral, J., Fariss, R.N., and Wong, W.T. (2011). Age-related alterations in the dynamic behavior of microglia. Aging Cell *10*, 263–276.
Danbolt, N.C. (2001). Glutamate uptake. Prog. Neurobiol. *65*, 1–105.
Daniels, M.J.D., Rivers-Auty, J., Schilling, T., Spencer, N.G., Watremez, W., Fasolino, V., Booth, S.J., White, C.S., Baldwin, A.G., Freeman, S., et al. (2016). Fenamate NSAIDs inhibit the NLRP3 inflammasome and protect against Alzheimer's disease in rodent models. Nat. Commun. *7*, 12504.
Dansokho, C., Ait Ahmed, D., Aid, S., Toly-Ndour, C., Chaigneau, T., Calle, V., Cagnard, N., Holzenberger, M., Piaggio, E., Aucouturier, P., et al. (2016). Regulatory T cells delay disease progression in Alzheimer-like pathology. Brain J. Neurol. *139*, 1237–1251.
De Felice, F.G., Wu, D., Lambert, M.P., Fernandez, S.J., Velasco, P.T., Lacor, P.N., Bigio, E.H., Jerecic, J., Acton, P.J., Shughrue, P.J., et al. (2008). Alzheimer's disease-type neuronal tau hyperphosphorylation induced by A beta oligomers. Neurobiol. Aging *29*, 1334–1347.
Degryse, B., Bonaldi, T., Scaffidi, P., Müller, S., Resnati, M., Sanvito, F., Arrigoni, G., and Bianchi, M.E. (2001). The high mobility group (HMG) boxes of the nuclear protein HMG1 induce chemotaxis and cytoskeleton reorganization in rat smooth muscle cells. J. Cell Biol. *152*, 1197–1206.
Denner, L.A., Rodriguez-Rivera, J., Haidacher, S.J., Jahrling, J.B., Carmical, J.R., Hernandez, C.M., Zhao, Y., Sadygov, R.G., Starkey, J.M., Spratt, H., et al. (2012). Cognitive enhancement with rosiglitazone links the hippocampal PPARγ and ERK MAPK signaling pathways. J. Neurosci. Off. J. Soc. Neurosci. *32*, 16725–16735a.
Desai, M.K., Mastrangelo, M.A., Ryan, D.A., Sudol, K.L., Narrow, W.C., and Bowers, W.J. (2010). Early oligodendrocyte/myelin pathology in Alzheimer's disease mice constitutes a novel therapeutic target. Am. J. Pathol. *177*, 1422–1435.
Deverman, B.E., and Patterson, P.H. (2009). Cytokines and CNS development. Neuron *64*, 61–78.
Dickey, C., Kraft, C., Jinwal, U., Koren, J., Johnson, A., Anderson, L., Lebson, L., Lee, D., Dickson, D., de Silva, R., et al. (2009). Aging analysis reveals slowed tau turnover and enhanced stress response in a mouse model of tauopathy. Am. J. Pathol. *174*, 228–238.
Dinarello, C.A., Simon, A., and van der Meer, J.W.M. (2012). Treating inflammation by blocking interleukin-1 in a broad spectrum of diseases. Nat. Rev. Drug Discov. *11*, 633–652.
Dissing-Olesen, L., LeDue, J.M., Rungta, R.L., Hefendehl, J.K., Choi, H.B., and MacVicar, B.A. (2014). Activation of neuronal NMDA receptors triggers transient ATP-mediated microglial process outgrowth. J. Neurosci. Off. J. Soc. Neurosci. *34*, 10511–10527.
Dong, H., Yuede, C.M., Yoo, H.-S., Martin, M.V., Deal, C., Mace, A.G., and Csernansky, J.G. (2008). Corticosterone and related receptor expression are associated with increased beta-

amyloid plaques in isolated Tg2576 mice. Neuroscience *155*, 154–163.
Dong, X., Wang, Y., and Qin, Z. (2009). Molecular mechanisms of excitotoxicity and their relevance to pathogenesis of neurodegenerative diseases. Acta Pharmacol. Sin. *30*, 379–387.
Duan, R.S., Yang, X., Chen, Z.G., Lu, M.O., Morris, C., Winblad, B., and Zhu, J. (2008). Decreased fractalkine and increased IP-10 expression in aged brain of APPswe transgenic mice. Neurochem. Res. *33*, 1085–1089.
Dunn, N., Mullee, M., Perry, V.H., and Holmes, C. (2005). Association between dementia and infectious disease: evidence from a case-control study. Alzheimer Dis. Assoc. Disord. *19*, 91–94.
Dursun, E., Gezen-Ak, D., Hanağası, H., Bilgiç, B., Lohmann, E., Ertan, S., Atasoy, İ.L., Alaylıoğlu, M., Araz, Ö.S., Önal, B., et al. (2015). The interleukin 1 alpha, interleukin 1 beta, interleukin 6 and alpha-2-macroglobulin serum levels in patients with early or late onset Alzheimer's disease, mild cognitive impairment or Parkinson's disease. J. Neuroimmunol. *283*, 50–57.
Edison, P., Archer, H.A., Gerhard, A., Hinz, R., Pavese, N., Turkheimer, F.E., Hammers, A., Tai, Y.F., Fox, N., Kennedy, A., et al. (2008). Microglia, amyloid, and cognition in Alzheimer's disease: An [11C](R)PK11195-PET and [11C]PIB-PET study. Neurobiol. Dis. *32*, 412–419.
Eggen, B.J.L., Raj, D., Hanisch, U.-K., and Boddeke, H.W.G.M. (2013). Microglial phenotype and adaptation. J. Neuroimmune Pharmacol. Off. J. Soc. NeuroImmune Pharmacol. *8*, 807–823.
Eggermont, L.H.P., Swaab, D.F., Hol, E.M., and Scherder, E.J.A. (2009). Walking the line: a randomised trial on the effects of a short term walking programme on cognition in dementia. J. Neurol. Neurosurg. Psychiatry *80*, 802–804.
El Khoury, J., Toft, M., Hickman, S.E., Means, T.K., Terada, K., Geula, C., and Luster, A.D. (2007). Ccr2 deficiency impairs microglial accumulation and accelerates progression of Alzheimer-like disease. Nat. Med. *13*, 432–438.
Van Eldik, L.J., and Griffin, W.S. (1994). S100 beta expression in Alzheimer's disease: relation to neuropathology in brain regions. Biochim. Biophys. Acta *1223*, 398–403.
Elias, M.F., Elias, P.K., Sullivan, L.M., Wolf, P.A., and D'Agostino, R.B. (2005). Obesity, diabetes and cognitive deficit: The Framingham Heart Study. Neurobiol. Aging *26 Suppl 1*, 11–16.
Elmore, M.R.P., Najafi, A.R., Koike, M.A., Dagher, N.N., Spangenberg, E.E., Rice, R.A., Kitazawa, M., Matusow, B., Nguyen, H., West, B.L., et al. (2014). Colony-stimulating factor 1 receptor signaling is necessary for microglia viability, unmasking a microglia progenitor cell in the adult brain. Neuron *82*, 380–397.
Engelhart, M.J., Geerlings, M.I., Ruitenberg, A., Van Swieten, J.C., Hofman, A., Witteman, J.C.M., and Breteler, M.M.B. (2002). Diet and risk of dementia: Does fat matter? Neurology *59*, 1915–1921.
Engelhart, M.J., Geerlings, M.I., Meijer, J., Kiliaan, A., Ruitenberg, A., van Swieten, J.C., Stijnen, T., Hofman, A., Witteman, J.C.M., and Breteler, M.M.B. (2004). Inflammatory proteins in plasma and the risk of dementia: the rotterdam study. Arch. Neurol. *61*, 668–672.
Etnier, J.L., Caselli, R.J., Reiman, E.M., Alexander, G.E., Sibley, B.A., Tessier, D., and McLemore, E.C. (2007). Cognitive performance in older women relative to ApoE-epsilon4 genotype and aerobic fitness. Med. Sci. Sports Exerc. *39*, 199–207.
Ettle, B., Schlachetzki, J.C.M., and Winkler, J. (2016). Oligodendroglia and Myelin in Neurodegenerative Diseases: More Than Just Bystanders? Mol. Neurobiol. *53*, 3046–3062.
Eyo, U.B., Peng, J., Swiatkowski, P., Mukherjee, A., Bispo, A., and Wu, L.-J. (2014). Neuronal hyperactivity recruits microglial processes via neuronal NMDA receptors and microglial P2Y12 receptors after status epilepticus. J. Neurosci. Off. J. Soc. Neurosci. *34*, 10528–10540.
Faden, A.I., and Loane, D.J. (2015). Chronic neurodegeneration after traumatic brain injury: Alzheimer disease, chronic traumatic encephalopathy, or persistent neuroinflammation? Neurother. J. Am. Soc. Exp. Neurother. *12*, 143–150.
Faden, A.I., Wu, J., Stoica, B.A., and Loane, D.J. (2016). Progressive inflammation-mediated neurodegeneration after traumatic brain or spinal cord injury. Br. J. Pharmacol. *173*, 681–691.
Fan, Z., Aman, Y., Ahmed, I., Chetelat, G., Landeau, B., Ray Chaudhuri, K., Brooks, D.J., and Edison, P. (2015a). Influence of microglial activation on neuronal function in Alzheimer's and Parkinson's disease dementia. Alzheimers Dement. J. Alzheimers Assoc. *11*, 608–621.e7.
Fan, Z., Okello, A.A., Brooks, D.J., and Edison, P. (2015b). Longitudinal influence of microglial activation and amyloid on neuronal function in Alzheimer's disease. Brain J. Neurol. *138*, 3685–3698.
Farso, M.C., O'Shea, R.D., and Beart, P.M. (2009). Evidence group I mGluR drugs modulate the activation profile of lipopolysaccharide-exposed microglia in culture. Neurochem. Res. *34*, 1721–1728.

Fassbender, K., Walter, S., Kühl, S., Landmann, R., Ishii, K., Bertsch, T., Stalder, A.K., Muehlhauser, F., Liu, Y., Ulmer, A.J., et al. (2004). The LPS receptor (CD14) links innate immunity with Alzheimer's disease. FASEB J. Off. Publ. Fed. Am. Soc. Exp. Biol. *18*, 203–205.
Feldman, H.H., Doody, R.S., Kivipelto, M., Sparks, D.L., Waters, D.D., Jones, R.W., Schwam, E., Schindler, R., Hey-Hadavi, J., DeMicco, D.A., et al. (2010). Randomized controlled trial of atorvastatin in mild to moderate Alzheimer disease: LEADe. Neurology *74*, 956–964.
Fishel, M.A., Watson, G.S., Montine, T.J., Wang, Q., Green, P.S., Kulstad, J.J., Cook, D.G., Peskind, E.R., Baker, L.D., Goldgaber, D., et al. (2005). Hyperinsulinemia provokes synchronous increases in central inflammation and beta-amyloid in normal adults. Arch. Neurol. *62*, 1539–1544.
Fitzpatrick, A.L., Kuller, L.H., Lopez, O.L., Kawas, C.H., and Jagust, W. (2005). Survival following dementia onset: Alzheimer's disease and vascular dementia. J. Neurol. Sci. *229–230*, 43–49.
Fleminger, S., Oliver, D.L., Lovestone, S., Rabe-Hesketh, S., and Giora, A. (2003). Head injury as a risk factor for Alzheimer's disease: the evidence 10 years on; a partial replication. J. Neurol. Neurosurg. Psychiatry *74*, 857–862.
Foley, N.C., Affoo, R.H., and Martin, R.E. (2015). A systematic review and meta-analysis examining pneumonia-associated mortality in dementia. Dement. Geriatr. Cogn. Disord. *39*, 52–67.
Fontainhas, A.M., Wang, M., Liang, K.J., Chen, S., Mettu, P., Damani, M., Fariss, R.N., Li, W., and Wong, W.T. (2011). Microglial morphology and dynamic behavior is regulated by ionotropic glutamatergic and GABAergic neurotransmission. PloS One *6*, e15973.
Forlenza, O.V., Diniz, B.S., Talib, L.L., Mendonça, V.A., Ojopi, E.B., Gattaz, W.F., and Teixeira, A.L. (2009). Increased serum IL-1beta level in Alzheimer's disease and mild cognitive impairment. Dement. Geriatr. Cogn. Disord. *28*, 507–512.
Frackowiak, J., Wisniewski, H.M., Wegiel, J., Merz, G.S., Iqbal, K., and Wang, K.C. (1992). Ultrastructure of the microglia that phagocytose amyloid and the microglia that produce beta-amyloid fibrils. Acta Neuropathol. (Berl.) *84*, 225–233.
Friedland, R.P., Fritsch, T., Smyth, K.A., Koss, E., Lerner, A.J., Chen, C.H., Petot, G.J., and Debanne, S.M. (2001). Patients with Alzheimer's disease have reduced activities in midlife compared with healthy control-group members. Proc. Natl. Acad. Sci. U. S. A. *98*, 3440–3445.
Galimberti, D., Fenoglio, C., Lovati, C., Venturelli, E., Guidi, I., Corrà, B., Scalabrini, D., Clerici, F., Mariani, C., Bresolin, N., et al. (2006). Serum MCP-1 levels are increased in mild cognitive impairment and mild Alzheimer's disease. Neurobiol. Aging *27*, 1763–1768.
Gasparini, L., Ongini, E., and Wenk, G. (2004). Non-steroidal anti-inflammatory drugs (NSAIDs) in Alzheimer's disease: old and new mechanisms of action. J. Neurochem. *91*, 521–536.
Geldmacher, D.S., Fritsch, T., McClendon, M.J., and Landreth, G. (2011). A randomized pilot clinical trial of the safety of pioglitazone in treatment of patients with Alzheimer disease. Arch. Neurol. *68*, 45–50.
Gemma, C., and Bachstetter, A.D. (2013). The role of microglia in adult hippocampal neurogenesis. Front. Cell. Neurosci. *7*, 229.
Gemma, C., Bachstetter, A.D., Cole, M.J., Fister, M., Hudson, C., and Bickford, P.C. (2007). Blockade of caspase-1 increases neurogenesis in the aged hippocampus. Eur. J. Neurosci. *26*, 2795–2803.
Gérard, H.C., Wildt, K.L., Whittum-Hudson, J.A., Lai, Z., Ager, J., and Hudson, A.P. (2005). The load of Chlamydia pneumoniae in the Alzheimer's brain varies with APOE genotype. Microb. Pathog. *39*, 19–26.
Gérard, H.C., Dreses-Werringloer, U., Wildt, K.S., Deka, S., Oszust, C., Balin, B.J., Frey, W.H., Bordayo, E.Z., Whittum-Hudson, J.A., and Hudson, A.P. (2006). Chlamydophila (Chlamydia) pneumoniae in the Alzheimer's brain. FEMS Immunol. Med. Microbiol. *48*, 355–366.
Gerson, J., Castillo-Carranza, D.L., Sengupta, U., Bodani, R., Prough, D.S., DeWitt, D.S., Hawkins, B.E., and Kayed, R. (2016). Tau Oligomers Derived from Traumatic Brain Injury Cause Cognitive Impairment and Accelerate Onset of Pathology in Htau Mice. J. Neurotrauma *33*, 2034–2043.
Ginhoux, F., Greter, M., Leboeuf, M., Nandi, S., See, P., Gokhan, S., Mehler, M.F., Conway, S.J., Ng, L.G., Stanley, E.R., et al. (2010). Fate mapping analysis reveals that adult microglia derive from primitive macrophages. Science *330*, 841–845.
Giunta, B., Deng, J., Jin, J., Sadic, E., Rum, S., Zhou, H., Sanberg, P., and Tan, J. (2012). EVALUATION OF HOW CIGARETTE SMOKE IS A DIRECT RISK FACTOR FOR ALZHEIMER'S DISEASE. Technol. Innov. *14*, 39–48.
Gons, R.A.R., van Norden, A.G.W., de Laat, K.F., van Oudheusden, L.J.B., van Uden, I.W.M.,

Zwiers, M.P., Norris, D.G., and de Leeuw, F.-E. (2011). Cigarette smoking is associated with reduced microstructural integrity of cerebral white matter. Brain J. Neurol. *134*, 2116–2124.
Green, H.F., and Nolan, Y.M. (2012). Unlocking mechanisms in interleukin-1β-induced changes in hippocampal neurogenesis--a role for GSK-3β and TLX. Transl. Psychiatry *2*, e194.
Green, K.N., Billings, L.M., Roozendaal, B., McGaugh, J.L., and LaFerla, F.M. (2006). Glucocorticoids increase amyloid-beta and tau pathology in a mouse model of Alzheimer's disease. J. Neurosci. Off. J. Soc. Neurosci. *26*, 9047–9056.
Griciuc, A., Serrano-Pozo, A., Parrado, A.R., Lesinski, A.N., Asselin, C.N., Mullin, K., Hooli, B., Choi, S.H., Hyman, B.T., and Tanzi, R.E. (2013). Alzheimer's disease risk gene CD33 inhibits microglial uptake of amyloid beta. Neuron *78*, 631–643.
Guadagno, J., Swan, P., Shaikh, R., and Cregan, S.P. (2015). Microglia-derived IL-1β triggers p53-mediated cell cycle arrest and apoptosis in neural precursor cells. Cell Death Dis. *6*, e1779.
Guillot-Sestier, M.-V., Doty, K.R., Gate, D., Rodriguez, J., Leung, B.P., Rezai-Zadeh, K., and Town, T. (2015). Il10 deficiency rebalances innate immunity to mitigate Alzheimer-like pathology. Neuron *85*, 534–548.
Halle, A., Hornung, V., Petzold, G.C., Stewart, C.R., Monks, B.G., Reinheckel, T., Fitzgerald, K.A., Latz, E., Moore, K.J., and Golenbock, D.T. (2008). The NALP3 inflammasome is involved in the innate immune response to amyloid-beta. Nat. Immunol. *9*, 857–865.
Hamelin, L., Lagarde, J., Dorothée, G., Leroy, C., Labit, M., Comley, R.A., de Souza, L.C., Corne, H., Dauphinot, L., Bertoux, M., et al. (2016). Early and protective microglial activation in Alzheimer's disease: a prospective study using 18F-DPA-714 PET imaging. Brain J. Neurol. *139*, 1252–1264.
Haque, R., and Nazir, A. (2014). Insulin-degrading enzyme: a link between Alzheimer's and type 2 diabetes mellitus. CNS Neurol. Disord. Drug Targets *13*, 259–264.
Harrison, J.K., Jiang, Y., Chen, S., Xia, Y., Maciejewski, D., McNamara, R.K., Streit, W.J., Salafranca, M.N., Adhikari, S., Thompson, D. a, et al. (1998). Role for neuronally derived fractalkine in mediating interactions between neurons and CX3CR1-expressing microglia. Proc. Natl. Acad. Sci. U. S. A. *95*, 10896–10901.
Harry, G.J. (2013). Microglia during development and aging. Pharmacol. Ther. *139*, 313–326.
Hauser, C.J., Sursal, T., Rodriguez, E.K., Appleton, P.T., Zhang, Q., and Itagaki, K. (2010). Mitochondrial damage associated molecular patterns from femoral reamings activate neutrophils through formyl peptide receptors and P44/42 MAP kinase. J. Orthop. Trauma *24*, 534–538.
He, M., Dong, H., Huang, Y., Lu, S., Zhang, S., Qian, Y., and Jin, W. (2016). Astrocyte-derived CCL2 is associated with m1 activation and recruitment of cultured microglial cells. Cell. Physiol. Biochem. *38*, 859–870.
Heese, K., Hock, C., and Otten, U. (1998). Inflammatory signals induce neurotrophin expression in human microglial cells. J. Neurochem. *70*, 699–707.
Hefendehl, J.K., Neher, J.J., Sühs, R.B., Kohsaka, S., Skodras, A., and Jucker, M. (2014). Homeostatic and injury-induced microglia behavior in the aging brain. Aging Cell *13*, 60–69.
Hellwig, S., Heinrich, A., and Biber, K. (2013). The brain's best friend: microglial neurotoxicity revisited. Front. Cell. Neurosci. *7*, 71.
Heneka, M.T., Wiesinger, H., Dumitrescu-Ozimek, L., Riederer, P., Feinstein, D.L., and Klockgether, T. (2001a). Neuronal and glial coexpression of argininosuccinate synthetase and inducible nitric oxide synthase in Alzheimer disease. J. Neuropathol. Exp. Neurol. *60*, 906–916.
Heneka, M.T., Landreth, G.E., and Feinstein, D.L. (2001b). Role for peroxisome proliferator-activated receptor-gamma in Alzheimer's disease. Ann. Neurol. *49*, 276.
Heneka, M.T., Galea, E., Gavriluyk, V., Dumitrescu-Ozimek, L., Daeschner, J., O'Banion, M.K., Weinberg, G., Klockgether, T., and Feinstein, D.L. (2002). Noradrenergic depletion potentiates beta -amyloid-induced cortical inflammation: implications for Alzheimer's disease. J. Neurosci. Off. J. Soc. Neurosci. *22*, 2434–2442.
Heneka, M.T., Gavrilyuk, V., Landreth, G.E., O'Banion, M.K., Weinberg, G., and Feinstein, D.L. (2003). Noradrenergic depletion increases inflammatory responses in brain: effects on IkappaB and HSP70 expression. J. Neurochem. *85*, 387–398.
Heneka, M.T., Sastre, M., Dumitrescu-Ozimek, L., Hanke, A., Dewachter, I., Kuiperi, C., O'Banion, K., Klockgether, T., Van Leuven, F., and Landreth, G.E. (2005). Acute treatment with the PPARgamma agonist pioglitazone and ibuprofen reduces glial inflammation and Abeta1-42 levels in APPV717I transgenic mice. Brain J. Neurol. *128*, 1442–1453.
Heneka, M.T., Ramanathan, M., Jacobs, A.H., Dumitrescu-Ozimek, L., Bilkei-Gorzo, A., Debeir, T., Sastre, M., Galldiks, N., Zimmer, A., Hoehn,

M., et al. (2006). Locus ceruleus degeneration promotes Alzheimer pathogenesis in amyloid precursor protein 23 transgenic mice. J. Neurosci. Off. J. Soc. Neurosci. *26*, 1343–1354.
Heneka, M.T., Nadrigny, F., Regen, T., Martinez-Hernandez, A., Dumitrescu-Ozimek, L., Terwel, D., Jardanhazi-Kurutz, D., Walter, J., Kirchhoff, F., Hanisch, U.-K., et al. (2010). Locus ceruleus controls Alzheimer's disease pathology by modulating microglial functions through norepinephrine. Proc. Natl. Acad. Sci. U. S. A. *107*, 6058–6063.
Heneka, M.T., Kummer, M.P., Stutz, A., Delekate, A., Schwartz, S., Vieira-Saecker, A., Griep, A., Axt, D., Remus, A., Tzeng, T.-C., et al. (2013). NLRP3 is activated in Alzheimer's disease and contributes to pathology in APP/PS1 mice. Nature *493*, 674–678.
Heneka, M.T., Golenbock, D.T., and Latz, E. (2015a). Innate immunity in Alzheimer's disease. Nat. Immunol. *16*, 229–236.
Heneka, M.T., Fink, A., and Doblhammer, G. (2015b). Effect of pioglitazone medication on the incidence of dementia. Ann. Neurol. *78*, 284–294.
Hickman, S.E., Allison, E.K., and El Khoury, J. (2008). Microglial dysfunction and defective beta-amyloid clearance pathways in aging Alzheimer's disease mice. J. Neurosci. Off. J. Soc. Neurosci. *28*, 8354–8360.
Ho, Y.-S., Yang, X., Yeung, S.-C., Chiu, K., Lau, C.-F., Tsang, A.W.-T., Mak, J.C.-W., and Chang, R.C.-C. (2012). Cigarette Smoking Accelerated Brain Aging and Induced Pre-Alzheimer-Like Neuropathology in Rats. PLOS ONE *7*, e36752.
Holmes, C., El-Okl, M., Williams, A.L., Cunningham, C., Wilcockson, D., and Perry, V.H. (2003). Systemic infection, interleukin 1beta, and cognitive decline in Alzheimer's disease. J. Neurol. Neurosurg. Psychiatry *74*, 788–789.
Holmes, C., Cunningham, C., Zotova, E., Woolford, J., Dean, C., Kerr, S., Culliford, D., and Perry, V.H. (2009). Systemic inflammation and disease progression in Alzheimer disease. Neurology *73*, 768–774.
Holmseth, S., Scott, H.A., Real, K., Lehre, K.P., Leergaard, T.B., Bjaalie, J.G., and Danbolt, N.C. (2009). The concentrations and distributions of three C-terminal variants of the GLT1 (EAAT2; slc1a2) glutamate transporter protein in rat brain tissue suggest differential regulation. Neuroscience *162*, 1055–1071.
Hong, S., Beja-Glasser, V.F., Nfonoyim, B.M., Frouin, A., Li, S., Ramakrishnan, S., Merry, K.M., Shi, Q., Rosenthal, A., Barres, B.A., et al. (2016). Complement and microglia mediate early synapse loss in Alzheimer mouse models. Science *352*, 712–716.
Honjo, K., van Reekum, R., and Verhoeff, N.P.L.G. (2009). Alzheimer's disease and infection: do infectious agents contribute to progression of Alzheimer's disease? Alzheimers Dement. J. Alzheimers Assoc. *5*, 348–360.
Hu, W.T., Holtzman, D.M., Fagan, A.M., Shaw, L.M., Perrin, R., Arnold, S.E., Grossman, M., Xiong, C., Craig-Schapiro, R., Clark, C.M., et al. (2012). Plasma multianalyte profiling in mild cognitive impairment and Alzheimer disease. Neurology *79*, 897–905.
Huang, H., Wang, L., Cao, M., Marshall, C., Gao, J., Xiao, N., Hu, G., and Xiao, M. (2015). Isolation Housing Exacerbates Alzheimer's Disease-Like Pathophysiology in Aged APP/PS1 Mice. Int. J. Neuropsychopharmacol. *18*.
Inestrosa, N.C., and Toledo, E.M. (2008). The role of Wnt signaling in neuronal dysfunction in Alzheimer's Disease. Mol. Neurodegener. *3*, 9.
Itzhaki, R.F., Lin, W.R., Shang, D., Wilcock, G.K., Faragher, B., and Jamieson, G.A. (1997). Herpes simplex virus type 1 in brain and risk of Alzheimer's disease. Lancet Lond. Engl. *349*, 241–244.
Iwashyna, T.J., Ely, E.W., Smith, D.M., and Langa, K.M. (2010). Long-term cognitive impairment and functional disability among survivors of severe sepsis. JAMA *304*, 1787–1794.
Jacobs, A.H., Tavitian, B., and INMiND consortium (2012). Noninvasive molecular imaging of neuroinflammation. J. Cereb. Blood Flow Metab. Off. J. Int. Soc. Cereb. Blood Flow Metab. *32*, 1393–1415.
Jahrling, J.B., Hernandez, C.M., Denner, L., and Dineley, K.T. (2014). PPARγ recruitment to active ERK during memory consolidation is required for Alzheimer's disease-related cognitive enhancement. J. Neurosci. Off. J. Soc. Neurosci. *34*, 4054–4063.
Jakobsson, H.E., Rodríguez-Piñeiro, A.M., Schütte, A., Ermund, A., Boysen, P., Bemark, M., Sommer, F., Bäckhed, F., Hansson, G.C., and Johansson, M.E.V. (2015). The composition of the gut microbiota shapes the colon mucus barrier. EMBO Rep. *16*, 164–177.
Jamieson, G.A., Maitland, N.J., Wilcock, G.K., Craske, J., and Itzhaki, R.F. (1991). Latent herpes simplex virus type 1 in normal and Alzheimer's disease brains. J. Med. Virol. *33*, 224–227.
Jamieson, G.A., Maitland, N.J., Wilcock, G.K., Yates, C.M., and Itzhaki, R.F. (1992). Herpes simplex virus type 1 DNA is present in specific regions of brain from aged people with and without senile dementia of the Alzheimer type. J. Pathol. *167*, 365–368.
Jensen, C.S., Hasselbalch, S.G., Waldemar, G.,

and Simonsen, A.H. (2015). Biochemical Markers of Physical Exercise on Mild Cognitive Impairment and Dementia: Systematic Review and Perspectives. Front. Neurol. *6*, 187.
Jeong, Y.H., Park, C.H., Yoo, J., Shin, K.Y., Ahn, S.-M., Kim, H.-S., Lee, S.H., Emson, P.C., and Suh, Y.-H. (2006). Chronic stress accelerates learning and memory impairments and increases amyloid deposition in APPV717I-CT100 transgenic mice, an Alzheimer's disease model. FASEB J. Off. Publ. Fed. Am. Soc. Exp. Biol. *20*, 729–731.
Ji, K., Akgul, G., Wollmuth, L.P., and Tsirka, S.E. (2013). Microglia actively regulate the number of functional synapses. PloS One *8*, e56293.
Johansson, L., Guo, X., Duberstein, P.R., Hällström, T., Waern, M., Ostling, S., and Skoog, I. (2014). Midlife personality and risk of Alzheimer disease and distress: a 38-year follow-up. Neurology *83*, 1538–1544.
Johnson, V.E., Stewart, W., and Smith, D.H. (2012). Widespread τ and amyloid-β pathology many years after a single traumatic brain injury in humans. Brain Pathol. Zurich Switz. *22*, 142–149.
Kandimalla, R., Thirumala, V., and Reddy, P.H. (2017). Is Alzheimer's disease a Type 3 Diabetes? A critical appraisal. Biochim. Biophys. Acta *1863*, 1078–1089.
Kane, M.J., Angoa-Pérez, M., Briggs, D.I., Viano, D.C., Kreipke, C.W., and Kuhn, D.M. (2012). A mouse model of human repetitive mild traumatic brain injury. J. Neurosci. Methods *203*, 41–49.
Kaushal, V., and Schlichter, L.C. (2008). Mechanisms of microglia-mediated neurotoxicity in a new model of the stroke penumbra. J. Neurosci. Off. J. Soc. Neurosci. *28*, 2221–2230.
Kenche, H., Baty, C.J., Vedagiri, K., Shapiro, S.D., and Blumental-Perry, A. (2013). Cigarette smoking affects oxidative protein folding in endoplasmic reticulum by modifying protein disulfide isomerase. FASEB J. Off. Publ. Fed. Am. Soc. Exp. Biol. *27*, 965–977.
Kierdorf, K., Erny, D., Goldmann, T., Sander, V., Schulz, C., Perdiguero, E.G., Wieghofer, P., Heinrich, A., Riemke, P., Hölscher, C., et al. (2013). Microglia emerge from erythromyeloid precursors via Pu.1- and Irf8-dependent pathways. Nat. Neurosci. *16*, 273–280.
Kim, B.-K., Shin, M.-S., Kim, C.-J., Baek, S.-B., Ko, Y.-C., and Kim, Y.-P. (2014). Treadmill exercise improves short-term memory by enhancing neurogenesis in amyloid beta-induced Alzheimer disease rats. J. Exerc. Rehabil. *10*, 2–8.
Kim, T.-S., Lim, H.-K., Lee, J.Y., Kim, D.-J., Park, S., Lee, C., and Lee, C.-U. (2008). Changes in the levels of plasma soluble fractalkine in patients with mild cognitive impairment and Alzheimer's disease. Neurosci. Lett. *436*, 196–200.
Kingham, P.J., Cuzner, M.L., and Pocock, J.M. (1999). Apoptotic pathways mobilized in microglia and neurones as a consequence of chromogranin A-induced microglial activation. J. Neurochem. *73*, 538–547.
Kiyota, T., Yamamoto, M., Xiong, H., Lambert, M.P., Klein, W.L., Gendelman, H.E., Ransohoff, R.M., and Ikezu, T. (2009). CCL2 accelerates microglia-mediated A?? oligomer formation and progression of neurocognitive dysfunction. PLoS ONE *4*.
Koenigsknecht-Talboo, J., and Landreth, G.E. (2005). Microglial phagocytosis induced by fibrillar beta-amyloid and IgGs are differentially regulated by proinflammatory cytokines. J. Neurosci. Off. J. Soc. Neurosci. *25*, 8240–8249.
Koo, J.W., and Duman, R.S. (2008). IL-1beta is an essential mediator of the antineurogenic and anhedonic effects of stress. Proc. Natl. Acad. Sci. U. S. A. *105*, 751–756.
Koronyo, Y., Salumbides, B.C., Sheyn, J., Pelissier, L., Li, S., Ljubimov, V., Moyseyev, M., Daley, D., Fuchs, D.-T., Pham, M., et al. (2015). Therapeutic effects of glatiramer acetate and grafted $CD115^{+}$ monocytes in a mouse model of Alzheimer's disease. Brain J. Neurol. *138*, 2399–2422.
Krabbe, G., Halle, A., Matyash, V., Rinnenthal, J.L., Eom, G.D., Bernhardt, U., Miller, K.R., Prokop, S., Kettenmann, H., and Heppner, F.L. (2013). Functional Impairment of Microglia Coincides with Beta-Amyloid Deposition in Mice with Alzheimer-Like Pathology. PLOS ONE *8*, e60921.
Kreisl, W.C., Lyoo, C.H., McGwier, M., Snow, J., Jenko, K.J., Kimura, N., Corona, W., Morse, C.L., Zoghbi, S.S., Pike, V.W., et al. (2013). In vivo radioligand binding to translocator protein correlates with severity of Alzheimer's disease. Brain J. Neurol. *136*, 2228–2238.
Kroner, Z. (2009). The relationship between Alzheimer's disease and diabetes: Type 3 diabetes? Altern. Med. Rev. J. Clin. Ther. *14*, 373–379.
Kukar, T., Prescott, S., Eriksen, J.L., Holloway, V., Murphy, M.P., Koo, E.H., Golde, T.E., and Nicolle, M.M. (2007). Chronic administration of R-flurbiprofen attenuates learning impairments in transgenic amyloid precursor protein mice. BMC Neurosci. *8*, 54.
Kummer, M.P., Hermes, M., Delekarte, A., Hammerschmidt, T., Kumar, S., Terwel, D., Walter, J., Pape, H.-C., König, S., Roeber, S., et al. (2011). Nitration of tyrosine 10 critically enhances amyloid β aggregation and plaque

formation. Neuron *71*, 833–844.
Kummer, M.P., Hammerschmidt, T., Martinez, A., Terwel, D., Eichele, G., Witten, A., Figura, S., Stoll, M., Schwartz, S., Pape, H.-C., et al. (2014). Ear2 deletion causes early memory and learning deficits in APP/PS1 mice. J. Neurosci. Off. J. Soc. Neurosci. *34*, 8845–8854.
Landreth, G.E., and Heneka, M.T. (2001). Anti-inflammatory actions of peroxisome proliferator-activated receptor gamma agonists in Alzheimer's disease. Neurobiol. Aging *22*, 937–944.
Lavisse, S., Guillermier, M., Hérard, A.-S., Petit, F., Delahaye, M., Van Camp, N., Ben Haim, L., Lebon, V., Remy, P., Dollé, F., et al. (2012). Reactive astrocytes overexpress TSPO and are detected by TSPO positron emission tomography imaging. J. Neurosci. Off. J. Soc. Neurosci. *32*, 10809–10818.
Lee, D.C., Rizer, J., Selenica, M.-L.B., Reid, P., Kraft, C., Johnson, A., Blair, L., Gordon, M.N., Dickey, C.A., and Morgan, D. (2010). LPS-induced inflammation exacerbates phospho-tau pathology in rTg4510 mice. J. Neuroinflammation *7*, 56.
Leem, Y.-H., Lim, H.-J., Shim, S.-B., Cho, J.-Y., Kim, B.-S., and Han, P.-L. (2009). Repression of tau hyperphosphorylation by chronic endurance exercise in aged transgenic mouse model of tauopathies. J. Neurosci. Res. *87*, 2561–2570.
Li, Y., Du, X.-F., Liu, C.-S., Wen, Z.-L., and Du, J.-L. (2012). Reciprocal regulation between resting microglial dynamics and neuronal activity in vivo. Dev. Cell *23*, 1189–1202.
Lim, G.P., Yang, F., Chu, T., Gahtan, E., Ubeda, O., Beech, W., Overmier, J.B., Hsiao-Ashec, K., Frautschy, S.A., and Cole, G.M. (2001). Ibuprofen effects on Alzheimer pathology and open field activity in APPsw transgenic mice. Neurobiol. Aging *22*, 983–991.
Liu, G.-J., Middleton, R.J., Hatty, C.R., Kam, W.W.-Y., Chan, R., Pham, T., Harrison-Brown, M., Dodson, E., Veale, K., and Banati, R.B. (2014). The 18 kDa translocator protein, microglia and neuroinflammation. Brain Pathol. Zurich Switz. *24*, 631–653.
Liu, S., Liu, Y., Hao, W., Wolf, L., Kiliaan, A.J., Penke, B., Rübe, C.E., Walter, J., Heneka, M.T., Hartmann, T., et al. (2012). TLR2 is a primary receptor for Alzheimer's amyloid β peptide to trigger neuroinflammatory activation. J. Immunol. Baltim. Md 1950 *188*, 1098–1107.
Lizcano, J.M., and Alessi, D.R. (2002). The insulin signalling pathway. Curr. Biol. CB *12*, R236-238.
Luchsinger, J.A., Tang, M.-X., Shea, S., Mayeux, R., DJ, S., W, W., PD, A., HC, H., DA, E., DS, G., et al. (2003). Antioxidant Vitamin Intake and Risk of Alzheimer Disease. Arch. Neurol. *60*, 203.
Lui, H., Zhang, J., Makinson, S.R., Cahill, M.K., Kelley, K.W., Huang, H.-Y., Shang, Y., Oldham, M.C., Martens, L.H., Gao, F., et al. (2016). Progranulin Deficiency Promotes Circuit-Specific Synaptic Pruning by Microglia via Complement Activation. Cell *165*, 921–935.
Luong, M., Zhang, Y., Chamberlain, T., Zhou, T., Wright, J.F., Dower, K., and Hall, J.P. (2012). Stimulation of TLR4 by recombinant HSP70 requires structural integrity of the HSP70 protein itself. J. Inflamm. Lond. Engl. *9*, 11.
Maezawa, I., Zimin, P.I., Wulff, H., and Jin, L.-W. (2011). Amyloid-beta protein oligomer at low nanomolar concentrations activates microglia and induces microglial neurotoxicity. J. Biol. Chem. *286*, 3693–3706.
Magaki, S., Yong, W.H., Khanlou, N., Tung, S., and Vinters, H.V. (2014). Comorbidity in dementia: update of an ongoing autopsy study. J. Am. Geriatr. Soc. *62*, 1722–1728.
Maggi, L., Scianni, M., Branchi, I., D'Andrea, I., Lauro, C., and Limatola, C. (2011). CX(3)CR1 deficiency alters hippocampal-dependent plasticity phenomena blunting the effects of enriched environment. Front. Cell. Neurosci. *5*, 22.
Mandrekar-Colucci, S., and Landreth, G.E. (2011). Nuclear receptors as therapeutic targets for Alzheimer's disease. Expert Opin. Ther. Targets *15*, 1085–1097.
Mao, P., Manczak, M., Calkins, M.J., Truong, Q., Reddy, T.P., Reddy, A.P., Shirendeb, U., Lo, H.-H., Rabinovitch, P.S., and Reddy, P.H. (2012). Mitochondria-targeted catalase reduces abnormal APP processing, amyloid β production and BACE1 in a mouse model of Alzheimer's disease: implications for neuroprotection and lifespan extension. Hum. Mol. Genet. *21*, 2973–2990.
Marosi, K., Bori, Z., Hart, N., Sárga, L., Koltai, E., Radák, Z., and Nyakas, C. (2012). Long-term exercise treatment reduces oxidative stress in the hippocampus of aging rats. Neuroscience *226*, 21–28.
Masliah, E., Alford, M., DeTeresa, R., Mallory, M., and Hansen, L. (1996). Deficient glutamate transport is associated with neurodegeneration in Alzheimer's disease. Ann. Neurol. *40*, 759–766.
Mathieu, M.-C., Sawyer, N., Greig, G.M., Hamel, M., Kargman, S., Ducharme, Y., Lau, C.K., Friesen, R.W., O'Neill, G.P., Gervais, F.G., et al. (2005). The C3a receptor antagonist SB 290157 has agonist activity. Immunol. Lett. *100*, 139–145.
McAteer, K.M., Corrigan, F., Thornton, E., Turner, R.J., and Vink, R. (2016). Short and Long Term Behavioral and Pathological Changes in a Novel Rodent Model of Repetitive Mild

Traumatic Brain Injury. PLOS ONE *11*, e0160220.
McKee, A.C., Carreras, I., Hossain, L., Ryu, H., Klein, W.L., Oddo, S., LaFerla, F.M., Jenkins, B.G., Kowall, N.W., and Dedeoglu, A. (2008). Ibuprofen reduces Abeta, hyperphosphorylated tau and memory deficits in Alzheimer mice. Brain Res. *1207*, 225–236.
McManus, R.M., and Heneka, M.T. (2017). Role of neuroinflammation in neurodegeneration: new insights. Alzheimers Res. Ther. *9*, 14.
Meinert, C.L., and Breitner, J.C.S. (2008). Chronic disease long-term drug prevention trials: lessons from the Alzheimer's Disease Anti-inflammatory Prevention Trial (ADAPT). Alzheimers Dement. J. Alzheimers Assoc. *4*, S7–S14.
Miguel-Hidalgo, J.J., Alvarez, X.A., Cacabelos, R., and Quack, G. (2002). Neuroprotection by memantine against neurodegeneration induced by beta-amyloid(1-40). Brain Res. *958*, 210–221.
Mitew, S., Kirkcaldie, M.T.K., Halliday, G.M., Shepherd, C.E., Vickers, J.C., and Dickson, T.C. (2010). Focal demyelination in Alzheimer's disease and transgenic mouse models. Acta Neuropathol. (Berl.) *119*, 567–577.
Moran, C., Phan, T.G., Chen, J., Blizzard, L., Beare, R., Venn, A., Münch, G., Wood, A.G., Forbes, J., Greenaway, T.M., et al. (2013). Brain atrophy in type 2 diabetes: regional distribution and influence on cognition. Diabetes Care *36*, 4036–4042.
Moran, O., Conti, F., and Tammaro, P. (2003). Sodium channel heterologous expression in mammalian cells and the role of the endogenous beta1-subunits. Neurosci. Lett. *336*, 175–179.
Moreira, P.I., Carvalho, C., Zhu, X., Smith, M.A., and Perry, G. (2010). Mitochondrial dysfunction is a trigger of Alzheimer's disease pathophysiology. Biochim. Biophys. Acta *1802*, 2–10.
Moreno-Gonzalez, I., Estrada, L.D., Sanchez-Mejias, E., and Soto, C. (2013). Smoking exacerbates amyloid pathology in a mouse model of Alzheimer's disease. Nat. Commun. *4*, 1495.
Mori, T., Koyama, N., Arendash, G.W., Horikoshi-Sakuraba, Y., Tan, J., and Town, T. (2010). Overexpression of human S100B exacerbates cerebral amyloidosis and gliosis in the Tg2576 mouse model of Alzheimer's disease. Glia *58*, 300–314.
Morris, M.C. (2012). Nutritional determinants of cognitive aging and dementia. Proc. Nutr. Soc. *71*, 1–13.
Morris, M.C., Tangney, C.C., Wang, Y., Sacks, F.M., Barnes, L.L., Bennett, D.A., and Aggarwal, N.T. (2015a). MIND diet slows cognitive decline with aging. Alzheimers Dement. J. Alzheimers Assoc. *11*, 1015–1022.
Morris, M.C., Tangney, C.C., Wang, Y., Sacks, F.M., Bennett, D.A., and Aggarwal, N.T. (2015b). MIND diet associated with reduced incidence of Alzheimer's disease. Alzheimers Dement. J. Alzheimers Assoc. *11*, 1007–1014.
Morris, M.C., Tangney, C.C., Wang, Y., Sacks, F.M., Barnes, L.L., Bennett, D.A., and Aggarwal, N.T. (2015c). MIND diet slows cognitive decline with aging. Alzheimers Dement. J. Alzheimers Assoc. *11*, 1015–1022.
Mortimer, J.A., van Duijn, C.M., Chandra, V., Fratiglioni, L., Graves, A.B., Heyman, A., Jorm, A.F., Kokmen, E., Kondo, K., and Rocca, W.A. (1991). Head trauma as a risk factor for Alzheimer's disease: a collaborative re-analysis of case-control studies. EURODEM Risk Factors Research Group. Int. J. Epidemiol. *20 Suppl 2*, S28-35.
Nagele, R.G., D'Andrea, M.R., Lee, H., Venkataraman, V., and Wang, H.-Y. (2003). Astrocytes accumulate A beta 42 and give rise to astrocytic amyloid plaques in Alzheimer disease brains. Brain Res. *971*, 197–209.
Nascimento, C.M.C., Pereira, J.R., de Andrade, L.P., Garuffi, M., Talib, L.L., Forlenza, O.V., Cancela, J.M., Cominetti, M.R., and Stella, F. (2014). Physical exercise in MCI elderly promotes reduction of pro-inflammatory cytokines and improvements on cognition and BDNF peripheral levels. Curr. Alzheimer Res. *11*, 799–805.
Nash, K.R., Lee, D.C., Hunt, J.B., Morganti, J.M., Selenica, M.L., Moran, P., Reid, P., Brownlow, M., Guang-Yu Yang, C., Savalia, M., et al. (2013). Fractalkine overexpression suppresses tau pathology in a mouse model of tauopathy. Neurobiol. Aging *34*, 1540–1548.
Natalwala, A., Potluri, R., Uppal, H., and Heun, R. (2008). Reasons for hospital admissions in dementia patients in Birmingham, UK, during 2002-2007. Dement. Geriatr. Cogn. Disord. *26*, 499–505.
Niraula, A., Sheridan, J.F., and Godbout, J.P. (2017). Microglia Priming with Aging and Stress. Neuropsychopharmacol. Off. Publ. Am. Coll. Neuropsychopharmacol. *42*, 318–333.
Okello, A., Edison, P., Archer, H.A., Turkheimer, F.E., Kennedy, J., Bullock, R., Walker, Z., Kennedy, A., Fox, N., Rossor, M., et al. (2009). Microglial activation and amyloid deposition in mild cognitive impairment: a PET study. Neurology *72*, 56–62.
Orre, M., Kamphuis, W., Osborn, L.M., Jansen, A.H.P., Kooijman, L., Bossers, K., and Hol, E.M. (2014). Isolation of glia from Alzheimer's mice reveals inflammation and dysfunction. Neurobiol.

Aging *35*, 2746–2760.
Owen, D.R., Yeo, A.J., Gunn, R.N., Song, K., Wadsworth, G., Lewis, A., Rhodes, C., Pulford, D.J., Bennacef, I., Parker, C.A., et al. (2012). An 18-kDa translocator protein (TSPO) polymorphism explains differences in binding affinity of the PET radioligand PBR28. J. Cereb. Blood Flow Metab. Off. J. Int. Soc. Cereb. Blood Flow Metab. *32*, 1–5.
Payão, S.L.M., Gonçalves, G.M., de Labio, R.W., Horiguchi, L., Mizumoto, I., Rasmussen, L.T., de Souza Pinhel, M.A., Silva Souza, D.R., Bechara, M.D., Chen, E., et al. (2012). Association of interleukin 1β polymorphisms and haplotypes with Alzheimer's disease. J. Neuroimmunol. *247*, 59–62.
Perez Nievas, B.G., Hammerschmidt, T., Kummer, M.P., Terwel, D., Leza, J.C., and Heneka, M.T. (2011). Restraint stress increases neuroinflammation independently of amyloid β levels in amyloid precursor protein/PS1 transgenic mice. J. Neurochem. *116*, 43–52.
Perry, V.H. (2010). Contribution of systemic inflammation to chronic neurodegeneration. Acta Neuropathol. (Berl.) *120*, 277–286.
Petraglia, A.L., Plog, B.A., Dayawansa, S., Dashnaw, M.L., Czerniecka, K., Walker, C.T., Chen, M., Hyrien, O., Iliff, J.J., Deane, R., et al. (2014). The pathophysiology underlying repetitive mild traumatic brain injury in a novel mouse model of chronic traumatic encephalopathy. Surg. Neurol. Int. *5*, 184.
Pisa, D., Alonso, R., Rábano, A., Rodal, I., and Carrasco, L. (2015a). Different Brain Regions are Infected with Fungi in Alzheimer's Disease. Sci. Rep. *5*, 15015.
Pisa, D., Alonso, R., Juarranz, A., Rábano, A., and Carrasco, L. (2015b). Direct visualization of fungal infection in brains from patients with Alzheimer's disease. J. Alzheimers Dis. JAD *43*, 613–624.
Pocock, J.M., and Kettenmann, H. (2007). Neurotransmitter receptors on microglia. Trends Neurosci. *30*, 527–535.
Podewils, L.J., Guallar, E., Kuller, L.H., Fried, L.P., Lopez, O.L., Carlson, M., and Lyketsos, C.G. (2005). Physical activity, APOE genotype, and dementia risk: findings from the Cardiovascular Health Cognition Study. Am. J. Epidemiol. *161*, 639–651.
Popoli, M., Yan, Z., McEwen, B.S., and Sanacora, G. (2011). The stressed synapse: the impact of stress and glucocorticoids on glutamate transmission. Nat. Rev. Neurosci. *13*, 22–37.
Porrini, V., Lanzillotta, A., Branca, C., Benarese, M., Parrella, E., Lorenzini, L., Calzà, L., Flaibani, R., Spano, P.F., Imbimbo, B.P., et al. (2015). CHF5074 (CSP-1103) induces microglia alternative activation in plaque-free Tg2576 mice and primary glial cultures exposed to beta-amyloid. Neuroscience *302*, 112–120.
Prinz, M., and Priller, J. (2014). Microglia and brain macrophages in the molecular age: from origin to neuropsychiatric disease. Nat. Rev. Neurosci. *15*, 300–312.
Prokop, S., Miller, K.R., Drost, N., Handrick, S., Mathur, V., Luo, J., Wegner, A., Wyss-Coray, T., and Heppner, F.L. (2015). Impact of peripheral myeloid cells on amyloid-β pathology in Alzheimer's disease-like mice. J. Exp. Med. *212*, 1811–1818.
Qiu, W.Q., and Folstein, M.F. (2006). Insulin, insulin-degrading enzyme and amyloid-beta peptide in Alzheimer's disease: review and hypothesis. Neurobiol. Aging *27*, 190–198.
Radak, Z., Hart, N., Sarga, L., Koltai, E., Atalay, M., Ohno, H., and Boldogh, I. (2010). Exercise plays a preventive role against Alzheimer's disease. J. Alzheimers Dis. JAD *20*, 777–783.
Raj, D.D.A., Jaarsma, D., Holtman, I.R., Olah, M., Ferreira, F.M., Schaafsma, W., Brouwer, N., Meijer, M.M., de Waard, M.C., van der Pluijm, I., et al. (2014). Priming of microglia in a DNA-repair deficient model of accelerated aging. Neurobiol. Aging *35*, 2147–2160.
Ramos-Rodriguez, J.J., Molina-Gil, S., Ortiz-Barajas, O., Jimenez-Palomares, M., Perdomo, G., Cozar-Castellano, I., Lechuga-Sancho, A.M., and Garcia-Alloza, M. (2014). Central Proliferation and Neurogenesis Is Impaired in Type 2 Diabetes and Prediabetes Animal Models. PLOS ONE *9*, e89229.
Reed-Geaghan, E.G., Savage, J.C., Hise, A.G., and Landreth, G.E. (2009). CD14 and toll-like receptors 2 and 4 are required for fibrillar A{beta}-stimulated microglial activation. J. Neurosci. Off. J. Soc. Neurosci. *29*, 11982–11992.
Reshef, R., Kreisel, T., Beroukhim Kay, D., and Yirmiya, R. (2014). Microglia and their CX3CR1 signaling are involved in hippocampal- but not olfactory bulb-related memory and neurogenesis. Brain. Behav. Immun. *41*, 239–250.
Riazi, K., Galic, M.A., Kuzmiski, J.B., Ho, W., Sharkey, K.A., and Pittman, Q.J. (2008). Microglial activation and TNFalpha production mediate altered CNS excitability following peripheral inflammation. Proc. Natl. Acad. Sci. U. S. A. *105*, 17151–17156.
Ries, M., and Sastre, M. (2016). Mechanisms of Aβ Clearance and Degradation by Glial Cells. Front. Aging Neurosci. *8*.
Risner, M.E., Saunders, A.M., Altman, J.F.B., Ormandy, G.C., Craft, S., Foley, I.M., Zvartau-Hind, M.E., Hosford, D.A., Roses, A.D., and

Rosiglitazone in Alzheimer's Disease Study Group (2006). Efficacy of rosiglitazone in a genetically defined population with mild-to-moderate Alzheimer's disease. Pharmacogenomics J. *6*, 246–254.
Rodriguez-Vieitez, E., Saint-Aubert, L., Carter, S.F., Almkvist, O., Farid, K., Schöll, M., Chiotis, K., Thordardottir, S., Graff, C., Wall, A., et al. (2016). Diverging longitudinal changes in astrocytosis and amyloid PET in autosomal dominant Alzheimer's disease. Brain J. Neurol. *139*, 922–936.
Rogers, J., Kirby, L.C., Hempelman, S.R., Berry, D.L., McGeer, P.L., Kaszniak, A.W., Zalinski, J., Cofield, M., Mansukhani, L., and Willson, P. (1993). Clinical trial of indomethacin in Alzheimer's disease. Neurology *43*, 1609–1611.
Rogers, J.T., Morganti, J.M., Bachstetter, A.D., Hudson, C.E., Peters, M.M., Grimmig, B.A., Weeber, E.J., Bickford, P.C., and Gemma, C. (2011). CX3CR1 deficiency leads to impairment of hippocampal cognitive function and synaptic plasticity. J. Neurosci. Off. J. Soc. Neurosci. *31*, 16241–16250.
Rothman, S.M., Herdener, N., Camandola, S., Texel, S.J., Mughal, M.R., Cong, W.-N., Martin, B., and Mattson, M.P. (2012). 3xTgAD mice exhibit altered behavior and elevated Aβ after chronic mild social stress. Neurobiol. Aging *33*, 830.e1-12.
Rovio, S., Kåreholt, I., Helkala, E.-L., Viitanen, M., Winblad, B., Tuomilehto, J., Soininen, H., Nissinen, A., and Kivipelto, M. (2005). Leisure-time physical activity at midlife and the risk of dementia and Alzheimer's disease. Lancet Neurol. *4*, 705–711.
Salminen, A., Ojala, J., Kauppinen, A., Kaarniranta, K., and Suuronen, T. (2009). Inflammation in Alzheimer's disease: amyloid-beta oligomers trigger innate immunity defence via pattern recognition receptors. Prog. Neurobiol. *87*, 181–194.
Santillo, A.F., Gambini, J.P., Lannfelt, L., Långström, B., Ulla-Marja, L., Kilander, L., and Engler, H. (2011). In vivo imaging of astrocytosis in Alzheimer's disease: an ^{11}C-L-deuteriodeprenyl and PIB PET study. Eur. J. Nucl. Med. Mol. Imaging *38*, 2202–2208.
Sato, T., Hanyu, H., Hirao, K., Kanetaka, H., Sakurai, H., and Iwamoto, T. (2011). Efficacy of PPAR-γ agonist pioglitazone in mild Alzheimer disease. Neurobiol. Aging *32*, 1626–1633.
Scarmeas, N., Stern, Y., Mayeux, R., and Luchsinger, J.A. (2006a). Mediterranean diet, Alzheimer disease, and vascular mediation. Arch. Neurol. *63*, 1709–1717.
Scarmeas, N., Stern, Y., Tang, M.-X., Mayeux, R., and Luchsinger, J.A. (2006b). Mediterranean diet and risk for Alzheimer's disease. Ann. Neurol. *59*, 912–921.
Scarmeas, N., Luchsinger, J.A., Schupf, N., Brickman, A.M., Cosentino, S., Tang, M.X., and Stern, Y. (2009). Physical activity, diet, and risk of Alzheimer disease. JAMA *302*, 627–637.
Schmidt, F.M., Weschenfelder, J., Sander, C., Minkwitz, J., Thormann, J., Chittka, T., Mergl, R., Kirkby, K.C., Faßhauer, M., Stumvoll, M., et al. (2015). Inflammatory cytokines in general and central obesity and modulating effects of physical activity. PloS One *10*, e0121971.
Schuit, A.J., Feskens, E.J., Launer, L.J., and Kromhout, D. (2001). Physical activity and cognitive decline, the role of the apolipoprotein e4 allele. Med. Sci. Sports Exerc. *33*, 772–777.
Sciacca, F.L., Ferri, C., Licastro, F., Veglia, F., Biunno, I., Gavazzi, A., Calabrese, E., Martinelli Boneschi, F., Sorbi, S., Mariani, C., et al. (2003). Interleukin-1B polymorphism is associated with age at onset of Alzheimer's disease. Neurobiol. Aging *24*, 927–931.
Scimemi, A., Meabon, J.S., Woltjer, R.L., Sullivan, J.M., Diamond, J.S., and Cook, D.G. (2013). Amyloid-β1-42 slows clearance of synaptically released glutamate by mislocalizing astrocytic GLT-1. J. Neurosci. Off. J. Soc. Neurosci. *33*, 5312–5318.
Scott, H.A., Gebhardt, F.M., Mitrovic, A.D., Vandenberg, R.J., and Dodd, P.R. (2011). Glutamate transporter variants reduce glutamate uptake in Alzheimer's disease. Neurobiol. Aging *32*, 553.e1-11.
Seet, R.C.S., Lee, C.-Y.J., Loke, W.M., Huang, S.H., Huang, H., Looi, W.F., Chew, E.S., Quek, A.M.L., Lim, E.C.H., and Halliwell, B. (2011). Biomarkers of oxidative damage in cigarette smokers: which biomarkers might reflect acute versus chronic oxidative stress? Free Radic. Biol. Med. *50*, 1787–1793.
Sellner, S., Paricio-Montesinos, R., Spieß, A., Masuch, A., Erny, D., Harsan, L.A., Elverfeldt, D.V., Schwabenland, M., Biber, K., Staszewski, O., et al. (2016). Microglial CX3CR1 promotes adult neurogenesis by inhibiting Sirt 1/p65 signaling independent of CX3CL1. Acta Neuropathol. Commun. *4*, 102.
Shadfar, S., Hwang, C.J., Lim, M.-S., Choi, D.-Y., and Hong, J.T. (2015). Involvement of inflammation in Alzheimer's disease pathogenesis and therapeutic potential of anti-inflammatory agents. Arch. Pharm. Res. *38*, 2106–2119.
Shen, C., Chen, Y., Liu, H., Zhang, K., Zhang, T., Lin, A., and Jing, N. (2008). Hydrogen Peroxide Promotes Aβ Production through JNK-dependent Activation of γ-Secretase. J. Biol. Chem. *283*,

17721–17730.
Shi, J.-Q., Shen, W., Chen, J., Wang, B.-R., Zhong, L.-L., Zhu, Y.-W., Zhu, H.-Q., Zhang, Q.-Q., Zhang, Y.-D., and Xu, J. (2011a). Anti-TNF-α reduces amyloid plaques and tau phosphorylation and induces CD11c-positive dendritic-like cell in the APP/PS1 transgenic mouse brains. Brain Res. *1368*, 239–247.
Shi, J.-Q., Wang, B.-R., Jiang, W.-W., Chen, J., Zhu, Y.-W., Zhong, L.-L., Zhang, Y.-D., and Xu, J. (2011b). Cognitive improvement with intrathecal administration of infliximab in a woman with Alzheimer's disease. J. Am. Geriatr. Soc. *59*, 1142–1144.
Shishido, H., Kishimoto, Y., Kawai, N., Toyota, Y., Ueno, M., Kubota, T., Kirino, Y., and Tamiya, T. (2016). Traumatic brain injury accelerates amyloid-β deposition and impairs spatial learning in the triple-transgenic mouse model of Alzheimer's disease. Neurosci. Lett. *629*, 62–67.
Shoelson, S.E., Lee, J., and Goldfine, A.B. (2006). Inflammation and insulin resistance. J. Clin. Invest. *116*, 1793–1801.
Sierra, A., Gottfried-Blackmore, A., Milner, T.A., McEwen, B.S., and Bulloch, K. (2008). Steroid hormone receptor expression and function in microglia. Glia *56*, 659–674.
Sierra, A., Encinas, J.M., Deudero, J.J.P., Chancey, J.H., Enikolopov, G., Overstreet-Wadiche, L.S., Tsirka, S.E., and Maletic-Savatic, M. (2010). Microglia shape adult hippocampal neurogenesis through apoptosis-coupled phagocytosis. Cell Stem Cell *7*, 483–495.
Simard, A.R., Soulet, D., Gowing, G., Julien, J.-P., and Rivest, S. (2006). Bone marrow-derived microglia play a critical role in restricting senile plaque formation in Alzheimer's disease. Neuron *49*, 489–502.
Simons, M., Schwärzler, F., Lütjohann, D., von Bergmann, K., Beyreuther, K., Dichgans, J., Wormstall, H., Hartmann, T., and Schulz, J.B. (2002). Treatment with simvastatin in normocholesterolemic patients with Alzheimer's disease: A 26-week randomized, placebo-controlled, double-blind trial. Ann. Neurol. *52*, 346–350.
Smith, D.H., Chen, X.H., Nonaka, M., Trojanowski, J.Q., Lee, V.M., Saatman, K.E., Leoni, M.J., Xu, B.N., Wolf, J.A., and Meaney, D.F. (1999). Accumulation of amyloid beta and tau and the formation of neurofilament inclusions following diffuse brain injury in the pig. J. Neuropathol. Exp. Neurol. *58*, 982–992.
Smith, D.H., Johnson, V.E., and Stewart, W. (2013a). Chronic neuropathologies of single and repetitive TBI: substrates of dementia? Nat. Rev. Neurol. *9*, 211–221.
Smith, J.C., Nielson, K.A., Woodard, J.L., Seidenberg, M., and Rao, S.M. (2013b). Physical Activity and Brain Function in Older Adults at Increased Risk for Alzheimer's Disease. Brain Sci. *3*, 54–83.
Sokolova, A., Hill, M.D., Rahimi, F., Warden, L.A., Halliday, G.M., and Shepherd, C.E. (2009). Monocyte chemoattractant protein-1 plays a dominant role in the chronic inflammation observed in Alzheimer's disease. Brain Pathol *19*, 392–398.
Sondag, C.M., Dhawan, G., and Combs, C.K. (2009). Beta amyloid oligomers and fibrils stimulate differential activation of primary microglia. J. Neuroinflammation *6*, 1.
Sparks, D.L., Sabbagh, M.N., Connor, D.J., Lopez, J., Launer, L.J., Browne, P., Wasser, D., Johnson-Traver, S., Lochhead, J., and Ziolwolski, C. (2005). Atorvastatin for the treatment of mild to moderate Alzheimer disease: preliminary results. Arch. Neurol. *62*, 753–757.
Stefaniak, J., and O'Brien, J. (2016). Imaging of neuroinflammation in dementia: a review. J. Neurol. Neurosurg. Psychiatry *87*, 21–28.
Stellwagen, D., and Malenka, R.C. (2006). Synaptic scaling mediated by glial TNF-alpha. Nature *440*, 1054–1059.
Stewart, W.F., Kawas, C., Corrada, M., and Metter, E.J. (1997). Risk of Alzheimer's disease and duration of NSAID use. Neurology *48*, 626–632.
Su, F., Bai, F., and Zhang, Z. (2016). Inflammatory Cytokines and Alzheimer's Disease: A Review from the Perspective of Genetic Polymorphisms. Neurosci. Bull. *32*, 469–480.
Suridjan, I., Pollock, B.G., Verhoeff, N.P.L.G., Voineskos, A.N., Chow, T., Rusjan, P.M., Lobaugh, N.J., Houle, S., Mulsant, B.H., and Mizrahi, R. (2015). In-vivo imaging of grey and white matter neuroinflammation in Alzheimer's disease: a positron emission tomography study with a novel radioligand, [18F]-FEPPA. Mol. Psychiatry *20*, 1579–1587.
Tahara, K., Kim, H.-D., Jin, J.-J., Maxwell, J.A., Li, L., and Fukuchi, K. (2006). Role of toll-like receptor signalling in Abeta uptake and clearance. Brain J. Neurol. *129*, 3006–3019.
Takata, K., Kitamura, Y., Kakimura, J., Shibagaki, K., Tsuchiya, D., Taniguchi, T., Smith, M.A., Perry, G., and Shimohama, S. (2003). Role of high mobility group protein-1 (HMG1) in amyloid-beta homeostasis. Biochem. Biophys. Res. Commun. *301*, 699–703.
Tan, Z.S., Beiser, A.S., Vasan, R.S., Roubenoff, R., Dinarello, C.A., Harris, T.B., Benjamin, E.J., Au, R., Kiel, D.P., Wolf, P.A., et al. (2007).

Inflammatory markers and the risk of Alzheimer disease The Framingham Study. Neurology *68*, 1902–1908.
Tanaka, K.F., Kashima, H., Suzuki, H., Ono, K., and Sawada, M. (2002). Existence of functional beta1- and beta2-adrenergic receptors on microglia. J. Neurosci. Res. *70*, 232–237.
Tangney, C.C., Kwasny, M.J., Li, H., Wilson, R.S., Evans, D.A., and Morris, M.C. (2011). Adherence to a Mediterranean-type dietary pattern and cognitive decline in a community population. Am. J. Clin. Nutr. *93*, 601–607.
Tangney, C.C., Li, H., Wang, Y., Barnes, L., Schneider, J.A., Bennett, D.A., and Morris, M.C. (2014). Relation of DASH- and Mediterranean-like dietary patterns to cognitive decline in older persons. Neurology *83*, 1410–1416.
Taupenot, L., Remacle, J.E., Helle, K.B., Aunis, D., and Bader, M.F. (1995). Recombinant human chromogranin A: expression, purification and characterization of the N-terminal derived peptides. Regul. Pept. *56*, 71–88.
Tay, T.L., Hagemeyer, N., and Prinz, M. (2016). The force awakens: insights into the origin and formation of microglia. Curr. Opin. Neurobiol. *39*, 30–37.
Teng, M.W.L., Bowman, E.P., McElwee, J.J., Smyth, M.J., Casanova, J.-L., Cooper, A.M., and Cua, D.J. (2015). IL-12 and IL-23 cytokines: from discovery to targeted therapies for immune-mediated inflammatory diseases. Nat. Med. *21*, 719–729.
Terada, K., Yamada, J., Hayashi, Y., Wu, Z., Uchiyama, Y., Peters, C., and Nakanishi, H. (2010). Involvement of cathepsin B in the processing and secretion of interleukin-1beta in chromogranin A-stimulated microglia. Glia *58*, 114–124.
Thériault, P., ElAli, A., and Rivest, S. (2015). The dynamics of monocytes and microglia in Alzheimer's disease. Alzheimers Res. Ther. *7*, 41.
Le Thuc, O., Blondeau, N., Nahon, J.L., and Rovère, C. (2015). The complex contribution of chemokines to neuroinflammation: Switching from beneficial to detrimental effects. Ann. N. Y. Acad. Sci. *1351*, 127–140.
Thundyil, J., and Lim, K.-L. (2015). DAMPs and neurodegeneration. Ageing Res. Rev. *24*, 17–28.
Tobinick, E.L., and Gross, H. (2008). Rapid cognitive improvement in Alzheimer's disease following perispinal etanercept administration. J. Neuroinflammation *5*, 2.
Tobinick, E., Gross, H., Weinberger, A., and Cohen, H. (2006). TNF-alpha modulation for treatment of Alzheimer's disease: a 6-month pilot study. MedGenMed Medscape Gen. Med. *8*, 25.
Town, T., Laouar, Y., Pittenger, C., Mori, T., Szekely, C.A., Tan, J., Duman, R.S., and Flavell, R.A. (2008). Blocking TGF-beta-Smad2/3 innate immune signaling mitigates Alzheimer-like pathology. Nat. Med. *14*, 681–687.
Trinchieri, G., Pflanz, S., and Kastelein, R.A. (2003). The IL-12 family of heterodimeric cytokines: new players in the regulation of T cell responses. Immunity *19*, 641–644.
Tsivgoulis, G., Judd, S., Letter, A.J., Alexandrov, A.V., Howard, G., Nahab, F., Unverzagt, F.W., Moy, C., Howard, V.J., Kissela, B., et al. (2013). Adherence to a Mediterranean diet and risk of incident cognitive impairment. Neurology *80*, 1684–1692.
Turkheimer, F.E., Rizzo, G., Bloomfield, P.S., Howes, O., Zanotti-Fregonara, P., Bertoldo, A., and Veronese, M. (2015). The methodology of TSPO imaging with positron emission tomography. Biochem. Soc. Trans. *43*, 586–592.
Turrigiano, G.G. (2008). The self-tuning neuron: synaptic scaling of excitatory synapses. Cell *135*, 422–435.
Tyas, S.L., Manfreda, J., Strain, L.A., and Montgomery, P.R. (2001). Risk factors for Alzheimer's disease: a population-based, longitudinal study in Manitoba, Canada. Int. J. Epidemiol. *30*, 590–597.
Um, H.S., Kang, E.B., Leem, Y.H., Cho, I.H., Yang, C.H., Chae, K.R., Hwang, D.Y., and Cho, J.Y. (2008). Exercise training acts as a therapeutic strategy for reduction of the pathogenic phenotypes for Alzheimer's disease in an NSE/APPsw-transgenic model. Int. J. Mol. Med. *22*, 529–539.
Van Gool, W.A., Weinstein, H.C., Scheltens, P., Walstra, G.J., and Scheltens, P.K. (2001). Effect of hydroxychloroquine on progression of dementia in early Alzheimer's disease: an 18-month randomised, double-blind, placebo-controlled study. Lancet Lond. Engl. *358*, 455–460.
Vance, R.E., Isberg, R.R., and Portnoy, D.A. (2009). Patterns of pathogenesis: discrimination of pathogenic and nonpathogenic microbes by the innate immune system. Cell Host Microbe *6*, 10–21.
Varley, J., Brooks, D.J., and Edison, P. (2015). Imaging neuroinflammation in Alzheimer's disease and other dementias: Recent advances and future directions. Alzheimers Dement. J. Alzheimers Assoc. *11*, 1110–1120.
Varrone, A., Oikonen, V., Forsberg, A., Joutsa, J., Takano, A., Solin, O., Haaparanta-Solin, M., Nag, S., Nakao, R., Al-Tawil, N., et al. (2015). Positron emission tomography imaging of the 18-kDa translocator protein (TSPO) with [18F]FEMPA in Alzheimer's disease patients and control subjects.

Eur. J. Nucl. Med. Mol. Imaging *42*, 438–446.
Varvel, N.H., Grathwohl, S. a., Degenhardt, K., Resch, C., Bosch, a., Jucker, M., and Neher, J.J. (2015). Replacement of brain-resident myeloid cells does not alter cerebral amyloid- deposition in mouse models of Alzheimer's disease. J. Exp. Med. *212*, jem.20150478-.
Vasek, M.J., Garber, C., Dorsey, D., Durrant, D.M., Bollman, B., Soung, A., Yu, J., Perez-Torres, C., Frouin, A., Wilton, D.K., et al. (2016). A complement-microglial axis drives synapse loss during virus-induced memory impairment. Nature *534*, 538–543.
Venneti, S., Lopresti, B.J., and Wiley, C.A. (2006). The peripheral benzodiazepine receptor (Translocator protein 18kDa) in microglia: from pathology to imaging. Prog. Neurobiol. *80*, 308–322.
Verdile, G., Fuller, S.J., and Martins, R.N. (2015). The role of type 2 diabetes in neurodegeneration. Neurobiol. Dis. *84*, 22–38.
Verreault, R., Laurin, D., Lindsay, J., and Serres, G.D. (2001). Past exposure to vaccines and subsequent risk of Alzheimer's disease. CMAJ Can. Med. Assoc. J. *165*, 1495–1498.
Vincent, A.J., Gasperini, R., Foa, L., and Small, D.H. (2010). Astrocytes in Alzheimer's disease: emerging roles in calcium dysregulation and synaptic plasticity. J. Alzheimers Dis. JAD *22*, 699–714.
Vodovotz, Y., Lucia, M.S., Flanders, K.C., Chesler, L., Xie, Q.W., Smith, T.W., Weidner, J., Mumford, R., Webber, R., Nathan, C., et al. (1996). Inducible nitric oxide synthase in tangle-bearing neurons of patients with Alzheimer's disease. J. Exp. Med. *184*, 1425–1433.
Vom Berg, J., Prokop, S., Miller, K.R., Obst, J., Kälin, R.E., Lopategui-Cabezas, I., Wegner, A., Mair, F., Schipke, C.G., Peters, O., et al. (2012). Inhibition of IL-12/IL-23 signaling reduces Alzheimer's disease-like pathology and cognitive decline. Nat. Med. *18*, 1812–1819.
van der Wal, E.A., Gómez-Pinilla, F., and Cotman, C.W. (1993). Transforming growth factor-beta 1 is in plaques in Alzheimer and Down pathologies. Neuroreport *4*, 69–72.
Waldstein, S.R., and Katzel, L.I. (2006). Interactive relations of central versus total obesity and blood pressure to cognitive function. Int. J. Obes. 2005 *30*, 201–207.
Walker, F.R., Nilsson, M., and Jones, K. (2013). Acute and chronic stress-induced disturbances of microglial plasticity, phenotype and function. Curr. Drug Targets *14*, 1262–1276.
Wang, H.X., Wahlin, A., Basun, H., Fastbom, J., Winblad, B., and Fratiglioni, L. (2001). Vitamin B(12) and folate in relation to the development of Alzheimer's disease. Neurology *56*, 1188–1194.
Wang, Y., Ulland, T.K., Ulrich, J.D., Song, W., Tzaferis, J.A., Hole, J.T., Yuan, P., Mahan, T.E., Shi, Y., Gilfillan, S., et al. (2016). TREM2-mediated early microglial response limits diffusion and toxicity of amyloid plaques. J. Exp. Med. *213*, 667–675.
Washington, P.M., Villapol, S., and Burns, M.P. (2016). Polypathology and dementia after brain trauma: Does brain injury trigger distinct neurodegenerative diseases, or should they be classified together as traumatic encephalopathy? Exp. Neurol. *275 Pt 3*, 381–388.
Watson, G.S., Cholerton, B.A., Reger, M.A., Baker, L.D., Plymate, S.R., Asthana, S., Fishel, M.A., Kulstad, J.J., Green, P.S., Cook, D.G., et al. (2005). Preserved cognition in patients with early Alzheimer disease and amnestic mild cognitive impairment during treatment with rosiglitazone: a preliminary study. Am. J. Geriatr. Psychiatry Off. J. Am. Assoc. Geriatr. Psychiatry *13*, 950–958.
Weggen, S., Eriksen, J.L., Das, P., Sagi, S.A., Wang, R., Pietrzik, C.U., Findlay, K.A., Smith, T.E., Murphy, M.P., Bulter, T., et al. (2001). A subset of NSAIDs lower amyloidogenic Abeta42 independently of cyclooxygenase activity. Nature *414*, 212–216.
Weiler, R., Lassmann, H., Fischer, P., Jellinger, K., and Winkler, H. (1990). A high ratio of chromogranin A to synaptin/synaptophysin is a common feature of brains in Alzheimer and Pick disease. FEBS Lett. *263*, 337–339.
Weiner, H.L., and Frenkel, D. (2006). Immunology and immunotherapy of Alzheimer's disease. Nat. Rev. Immunol. *6*, 404–416.
Wenk, G.L., Parsons, C.G., and Danysz, W. (2006). Potential role of N-methyl-D-aspartate receptors as executors of neurodegeneration resulting from diverse insults: focus on memantine. Behav. Pharmacol. *17*, 411–424.
Westin, K., Buchhave, P., Nielsen, H., Minthon, L., Janciauskiene, S., and Hansson, O. (2012). CCL2 is associated with a faster rate of cognitive decline during early stages of Alzheimer's disease. PLoS ONE *7*, 1–6.
Whitmer, R.A., Gustafson, D.R., Barrett-Connor, E., Haan, M.N., Gunderson, E.P., and Yaffe, K. (2008). Central obesity and increased risk of dementia more than three decades later. Neurology *71*, 1057–1064.
Wilkinson, K., and El Khoury, J. (2012). Microglial scavenger receptors and their roles in the pathogenesis of Alzheimer's disease. Int. J. Alzheimers Dis. *2012*, 489456.
Willett, W.C., Sacks, F., Trichopoulou, A., Drescher, G., Ferro-Luzzi, A., Helsing, E., and Trichopoulos, D. (1995). Mediterranean diet

pyramid: a cultural model for healthy eating. Am. J. Clin. Nutr. *61*, 1402S–1406S.
Wilson, R.S., Evans, D.A., Bienias, J.L., Mendes de Leon, C.F., Schneider, J.A., and Bennett, D.A. (2003). Proneness to psychological distress is associated with risk of Alzheimer's disease. Neurology *61*, 1479–1485.
Wilson, R.S., Schneider, J.A., Boyle, P.A., Arnold, S.E., Tang, Y., and Bennett, D.A. (2007). Chronic distress and incidence of mild cognitive impairment. Neurology *68*, 2085–2092.
Wong, W.T. (2013). Microglial aging in the healthy CNS: phenotypes, drivers, and rejuvenation. Front. Cell. Neurosci. *7*, 22.
World Health Organization (2008). The global burden of disease: 2004 update.
Wozniak, M.A., Shipley, S.J., Combrinck, M., Wilcock, G.K., and Itzhaki, R.F. (2005). Productive herpes simplex virus in brain of elderly normal subjects and Alzheimer's disease patients. J. Med. Virol. *75*, 300–306.
Wu, M.D., Montgomery, S.L., Rivera-Escalera, F., Olschowka, J.A., and O'Banion, M.K. (2013). Sustained IL-1β expression impairs adult hippocampal neurogenesis independent of IL-1 signaling in nestin+ neural precursor cells. Brain. Behav. Immun. *32*, 9–18.
Wyss-Coray, T., and Rogers, J. (2012). Inflammation in Alzheimer disease-a brief review of the basic science and clinical literature. Cold Spring Harb. Perspect. Med. *2*, a006346.
Wyss-Coray, T., Lin, C., Yan, F., Yu, G.Q., Rohde, M., McConlogue, L., Masliah, E., and Mucke, L. (2001). TGF-beta1 promotes microglial amyloid-beta clearance and reduces plaque burden in transgenic mice. Nat. Med. *7*, 612–618.
Wyss-Coray, T., Loike, J.D., Brionne, T.C., Lu, E., Anankov, R., Yan, F., Silverstein, S.C., and Husemann, J. (2003). Adult mouse astrocytes degrade amyloid-beta in vitro and in situ. Nat. Med. *9*, 453–457.
Yang, Y., Turner, R.S., and Gaut, J.R. (1998). The chaperone BiP/GRP78 binds to amyloid precursor protein and decreases Abeta40 and Abeta42 secretion. J. Biol. Chem. *273*, 25552–25555.
Yasuno, F., Kosaka, J., Ota, M., Higuchi, M., Ito, H., Fujimura, Y., Nozaki, S., Takahashi, S., Mizukami, K., Asada, T., et al. (2012). Increased binding of peripheral benzodiazepine receptor in mild cognitive impairment-dementia converters measured by positron emission tomography with [^{11}C]DAA1106. Psychiatry Res. *203*, 67–74.
Yin, F., Banerjee, R., Thomas, B., Zhou, P., Qian, L., Jia, T., Ma, X., Ma, Y., Iadecola, C., Beal, M.F., et al. (2010). Exaggerated inflammation, impaired host defense, and neuropathology in progranulin-deficient mice. J. Exp. Med. *207*, 117–128.
Yin, Y., Liu, Y., Pan, X., Chen, R., Li, P., Wu, H.-J., Zhao, Z.-Q., Li, Y.-P., Huang, L.-Q., Zhuang, J.-H., et al. (2016). Interleukin-1β Promoter Polymorphism Enhances the Risk of Sleep Disturbance in Alzheimer's Disease. PloS One *11*, e0149945.
Yirmiya, R., and Goshen, I. (2011). Immune modulation of learning, memory, neural plasticity and neurogenesis. Brain. Behav. Immun. *25*, 181–213.
Yokokura, M., Mori, N., Yagi, S., Yoshikawa, E., Kikuchi, M., Yoshihara, Y., Wakuda, T., Sugihara, G., Takebayashi, K., Suda, S., et al. (2011). In vivo changes in microglial activation and amyloid deposits in brain regions with hypometabolism in Alzheimer's disease. Eur. J. Nucl. Med. Mol. Imaging *38*, 343–351.
Yuan, H., Xia, Q., Ge, P., and Wu, S. (2013). Genetic polymorphism of interleukin 1β -511C/T and susceptibility to sporadic Alzheimer's disease: a meta-analysis. Mol. Biol. Rep. *40*, 1827–1834.
Zetterberg, H., Andreasen, N., and Blennow, K. (2004). Increased cerebrospinal fluid levels of transforming growth factor-beta1 in Alzheimer's disease. Neurosci. Lett. *367*, 194–196.
Zhang, J., Malik, A., Choi, H.B., Ko, R.W.Y., Dissing-Olesen, L., and MacVicar, B.A. (2014). Microglial CR3 activation triggers long-term synaptic depression in the hippocampus via NADPH oxidase. Neuron *82*, 195–207.
Zhang, K., Xu, H., Cao, L., Li, K., and Huang, Q. (2013). Interleukin-1β inhibits the differentiation of hippocampal neural precursor cells into serotonergic neurons. Brain Res. *1490*, 193–201.
Zhu, X.-C., Tan, L., Jiang, T., Tan, M.-S., Zhang, W., and Yu, J.-T. (2014). Association of IL-12A and IL-12B polymorphisms with Alzheimer's disease susceptibility in a Han Chinese population. J. Neuroimmunol. *274*, 180–184.
Zunszain, P.A., Anacker, C., Cattaneo, A., Choudhury, S., Musaelyan, K., Myint, A.M., Thuret, S., Price, J., and Pariante, C.M. (2012). Interleukin-1β: a new regulator of the kynurenine pathway affecting human hippocampal neurogenesis. Neuropsychopharmacol. Off. Publ. Am. Coll. Neuropsychopharmacol. *37*, 939–949.

Références

Références

Abramov, A.Y., Canevari, L., and Duchen, M.R. (2004). Beta-amyloid peptides induce mitochondrial dysfunction and oxidative stress in astrocytes and death of neurons through activation of NADPH oxidase. J. Neurosci. Off. J. Soc. Neurosci. 24, 565–575.

Aisen, P.S. (2002). The potential of anti-inflammatory drugs for the treatment of Alzheimer's disease. Lancet Neurol. 1, 279–284.

Allaman, I., Gavillet, M., Belanger, M., Laroche, T., Viertl, D., Lashuel, H.A., and Magistretti, P.J. (2010). Amyloid-beta aggregates cause alterations of astrocytic metabolic phenotype: impact on neuronal viability. J Neurosci 30, 3326–3338.

Allaman, I., Belanger, M., and Magistretti, P.J. (2011). Astrocyte-neuron metabolic relationships: for better and for worse. Trends Neurosci 34, 76–87.

Alonso, A.C., Zaidi, T., Grundke-Iqbal, I., and Iqbal, K. (1994). Role of abnormally phosphorylated tau in the breakdown of microtubules in Alzheimer disease. Proc. Natl. Acad. Sci. U. S. A. 91, 5562–5566.

Alonso, A.C., Grundke-Iqbal, I., and Iqbal, K. (1996). Alzheimer's disease hyperphosphorylated tau sequesters normal tau into tangles of filaments and disassembles microtubules. Nat. Med. 2, 783–787.

Alonso, A.D., Grundke-Iqbal, I., Barra, H.S., and Iqbal, K. (1997). Abnormal phosphorylation of tau and the mechanism of Alzheimer neurofibrillary degeneration: sequestration of microtubule-associated proteins 1 and 2 and the disassembly of microtubules by the abnormal tau. Proc. Natl. Acad. Sci. U. S. A. 94, 298–303.

Alvarez, J.I., Katayama, T., and Prat, A. (2013). Glial influence on the blood brain barrier. Glia 61, 1939–1958.

Alzheimer, A., Stelzmann, R.A., Schnitzlein, H.N., and Murtagh, F.R. (1995). An English translation of Alzheimer's 1907 paper, "Uber eine eigenartige Erkankung der Hirnrinde." Clin. Anat. N. Y. N 8, 429–431.

Anderson, M.A., Burda, J.E., Ren, Y., Ao, Y., O'Shea, T.M., Kawaguchi, R., Coppola, G., Khakh, B.S., Deming, T.J., and Sofroniew, M.V. (2016). Astrocyte scar formation aids central nervous system axon regeneration. Nature 532, 195–200.

Andreadis, A. (2012). Tau splicing and the intricacies of dementia. J. Cell. Physiol. 227, 1220–1225.

Andriezen, W.L. (1893). The Neuroglia Elements in the Human Brain. Br. Med. J. 2, 227–230.

Angulo, M.C., Kozlov, A.S., Charpak, S., and Audinat, E. (2004). Glutamate released from glial cells synchronizes neuronal activity in the hippocampus. J. Neurosci. Off. J. Soc. Neurosci. 24, 6920–6927.

Aramburu, J., Yaffe, M.B., López-Rodríguez, C., Cantley, L.C., Hogan, P.G., and Rao, A. (1999). Affinity-driven peptide selection of an NFAT inhibitor more selective than cyclosporin A. Science 285, 2129–2133.

Araque, A., Parpura, V., Sanzgiri, R.P., and Haydon, P.G. (1999). Tripartite synapses: glia, the unacknowledged partner. Trends Neurosci 22, 208–215.

Araque, A., Carmignoto, G., Haydon, P.G., Oliet, S.H., Robitaille, R., and Volterra, A. (2014). Gliotransmitters travel in time and space. Neuron 81, 728–739.

Babon, J.J., Varghese, L.N., and Nicola, N.A. (2014). Inhibition of IL-6 family cytokines by SOCS3. Semin Immunol 26, 13–19.

Bagyinszky, E., Giau, V.V., Shim, K., Suk, K., An, S.S.A., and Kim, S. (2017). Role of inflammatory molecules in the Alzheimer's disease progression and diagnosis. J. Neurol. Sci. 376, 242–254.

Bao, F., Wicklund, L., Lacor, P.N., Klein, W.L., Nordberg, A., and Marutle, A. (2012). Different β-amyloid oligomer assemblies in Alzheimer brains correlate with age of disease onset and impaired cholinergic activity. Neurobiol. Aging 33, 825.e1-13.

Bard, F., Cannon, C., Barbour, R., Burke, R.L., Games, D., Grajeda, H., Guido, T., Hu, K., Huang, J., Johnson-Wood, K., et al. (2000). Peripherally administered antibodies against amyloid beta-peptide enter the central nervous system and reduce pathology in a mouse model of Alzheimer disease. Nat. Med. 6, 916–919.

Bardehle, S., Kruger, M., Buggenthin, F., Schwausch, J., Ninkovic, J., Clevers, H., Snippert, H.J., Theis, F.J., Meyer-Luehmann, M., Bechmann, I., et al. (2013). Live imaging of astrocyte responses to acute injury reveals selective juxtavascular proliferation. Nat Neurosci 16, 580–586.

Barnum, S.R. (1995). Complement biosynthesis in the central nervous system. Crit. Rev. Oral Biol. Med. Off. Publ. Am. Assoc. Oral Biol. 6, 132–146.

von Bartheld, C.S., Bahney, J., and Herculano-Houzel, S. (2016). The search for true numbers of neurons and glial cells in the human brain: A review of 150 years of cell counting. J. Comp. Neurol. 524, 3865–3895.

Baumgärtel, K., and Mansuy, I.M. (2012). Neural functions of calcineurin in synaptic plasticity and memory. Learn. Mem. 19, 375–384.

Belanger, M., Allaman, I., and Magistretti, P.J. (2011). Brain energy metabolism: focus on astrocyte-neuron metabolic cooperation. Cell Metab 14, 724–738.

Ben Haim, L., Ceyzeriat, K., Carrillo-de Sauvage, M.A., Aubry, F., Auregan, G., Guillermier, M., Ruiz, M., Petit, F., Houitte, D., Faivre, E., et al. (2015). The JAK/STAT3 Pathway Is a Common Inducer of Astrocyte Reactivity in Alzheimer's and Huntington's Diseases. J Neurosci 35, 2817–2829.

Bernardinelli, Y., Randall, J., Janett, E., Nikonenko, I., Konig, S., Jones, E.V., Flores, C.E., Murai, K.K., Bochet, C.G., Holtmaat, A., et al. (2014). Activity-dependent structural plasticity of perisynaptic astrocytic domains promotes excitatory synapse stability. Curr Biol 24, 1679–1688.

Bialas, A.R., and Stevens, B. (2013). TGF-β signaling regulates neuronal C1q expression and developmental synaptic refinement. Nat. Neurosci. 16, 1773–1782.

Bignami, A., and Dahl, D. (1976). The astroglial response to stabbing. Immunofluorescence studies with antibodies to astrocyte-specific protein (GFA) in mammalian and submammalian vertebrates. Neuropathol Appl Neuro 2, 99–110.

Billings, L.M., Oddo, S., Green, K.N., McGaugh, J.L., and LaFerla, F.M. (2005). Intraneuronal Abeta causes the onset of early Alzheimer's disease-related cognitive deficits in transgenic mice. Neuron 45, 675–688.

Bindocci, E., Savtchouk, I., Liaudet, N., Becker, D., Carriero, G., and Volterra, A. (2017). Three-dimensional Ca(2+) imaging advances understanding of astrocyte biology. Science 356.

Blasko, I., Veerhuis, R., Stampfer-Kountchev, M., Saurwein-Teissl, M., Eikelenboom, P., and Grubeck-Loebenstein, B. (2000). Costimulatory effects of interferon-gamma and interleukin-1beta or tumor necrosis factor alpha on the synthesis of Abeta1-40 and Abeta1-42 by human astrocytes. Neurobiol. Dis. 7, 682–689.

Blazquez-Llorca, L., Valero-Freitag, S., Rodrigues, E.F., Merchán-Pérez, Á., Rodríguez, J.R., Dorostkar, M.M., DeFelipe, J., and Herms, J. (2017). High plasticity of axonal pathology in Alzheimer's disease mouse models. Acta Neuropathol. Commun. 5, 14.

Blennow, K., de Leon, M.J., and Zetterberg, H. (2006). Alzheimer's disease. Lancet Lond. Engl. 368, 387–403.

Bloom, O. (2014). Non-mammalian model systems for studying neuro-immune interactions after spinal cord injury. Exp Neurol 258, 130–140.

Bouvier, D.S., Jones, E.V., Quesseveur, G., Davoli, M.A., T, A.F., Quirion, R., Mechawar, N., and Murai, K.K. (2016). High Resolution Dissection of Reactive Glial Nets in Alzheimer's Disease. Sci Rep 6, 24544.

Bowman, G.L., Kaye, J.A., Moore, M., Waichunas, D., Carlson, N.E., and Quinn, J.F. (2007). Blood-brain barrier impairment in Alzheimer disease: stability and functional significance. Neurology 68, 1809–1814.

Braak, H., and Braak, E. (1991). Neuropathological stageing of Alzheimer-related changes. Acta Neuropathol. (Berl.) 82, 239–259.

Brookes, A.J., and St Clair, D. (1994). Synuclein proteins and Alzheimer's disease. Trends Neurosci. 17, 404–405.

Brooks, A.J., Dai, W., O'Mara, M.L., Abankwa, D., Chhabra, Y., Pelekanos, R.A., Gardon, O., Tunny, K.A., Blucher, K.M., Morton, C.J., et al. (2014). Mechanism of activation of protein kinase JAK2 by the growth hormone receptor. Science 344, 1249783.

Bu, G. (2009). Apolipoprotein E and its receptors in Alzheimer's disease: pathways, pathogenesis and therapy. Nat. Rev. Neurosci. 10, 333–344.

Burda, J.E., and Sofroniew, M.V. (2014). Reactive gliosis and the multicellular response to CNS damage and disease. Neuron 81, 229–248.

Burda, J.E., Bernstein, A.M., and Sofroniew, M.V. (2016). Astrocyte roles in traumatic brain injury. Exp Neurol 275 Pt 3, 305–315.

Bushong, E.A., Martone, M.E., Jones, Y.Z., and Ellisman, M.H. (2002). Protoplasmic astrocytes in CA1 stratum radiatum occupy separate anatomical domains. J Neurosci 22, 183–192.

Carter, S.F., Scholl, M., Almkvist, O., Wall, A., Engler, H., Langstrom, B., and Nordberg, A. (2012). Evidence for astrocytosis in prodromal Alzheimer disease provided by 11C-deuterium-L-deprenyl: a

multitracer PET paradigm combining 11C-Pittsburgh compound B and 18F-FDG. J Nucl Med 53, 37–46.

Castellano, J.M., Deane, R., Gottesdiener, A.J., Verghese, P.B., Stewart, F.R., West, T., Paoletti, A.C., Kasper, T.R., DeMattos, R.B., Zlokovic, B.V., et al. (2012). Low-density lipoprotein receptor overexpression enhances the rate of brain-to-blood Aβ clearance in a mouse model of β-amyloidosis. Proc. Natl. Acad. Sci. U. S. A. 109, 15502–15507.

Ceyzeriat, K., Abjean, L., Carrillo-de Sauvage, M.A., Ben Haim, L., and Escartin, C. (2016). The complex STATes of astrocyte reactivity: How are they controlled by the JAK-STAT3 pathway? Neuroscience 330, 205–218.

Chakrabarty, P., Jansen-West, K., Beccard, A., Ceballos-Diaz, C., Levites, Y., Verbeeck, C., Zubair, A.C., Dickson, D., Golde, T.E., and Das, P. (2010a). Massive gliosis induced by interleukin-6 suppresses Abeta deposition in vivo: evidence against inflammation as a driving force for amyloid deposition. FASEB J. Off. Publ. Fed. Am. Soc. Exp. Biol. 24, 548–559.

Chakrabarty, P., Ceballos-Diaz, C., Beccard, A., Janus, C., Dickson, D., Golde, T.E., and Das, P. (2010b). IFN-gamma promotes complement expression and attenuates amyloid plaque deposition in amyloid beta precursor protein transgenic mice. J. Immunol. Baltim. Md 1950 184, 5333–5343.

Chakrabarty, P., Herring, A., Ceballos-Diaz, C., Das, P., and Golde, T.E. (2011). Hippocampal expression of murine TNFα results in attenuation of amyloid deposition in vivo. Mol. Neurodegener. 6, 16.

Chakrabarty, P., Li, A., Ceballos-Diaz, C., Eddy, J.A., Funk, C.C., Moore, B., DiNunno, N., Rosario, A.M., Cruz, P.E., Verbeeck, C., et al. (2015). IL-10 alters immunoproteostasis in APP mice, increasing plaque burden and worsening cognitive behavior. Neuron 85, 519–533.

Cho, M.-H., Cho, K., Kang, H.-J., Jeon, E.-Y., Kim, H.-S., Kwon, H.-J., Kim, H.-M., Kim, D.-H., and Yoon, S.-Y. (2014). Autophagy in microglia degrades extracellular β-amyloid fibrils and regulates the NLRP3 inflammasome. Autophagy 10, 1761–1775.

Christopherson, K.S., Ullian, E.M., Stokes, C.C., Mullowney, C.E., Hell, J.W., Agah, A., Lawler, J., Mosher, D.F., Bornstein, P., and Barres, B.A. (2005). Thrombospondins are astrocyte-secreted proteins that promote CNS synaptogenesis. Cell 120, 421–433.

Chung, W.S., Clarke, L.E., Wang, G.X., Stafford, B.K., Sher, A., Chakraborty, C., Joung, J., Foo, L.C., Thompson, A., Chen, C., et al. (2013). Astrocytes mediate synapse elimination through MEGF10 and MERTK pathways. Nature 504, 394–400.

Chung, W.-S., Allen, N.J., and Eroglu, C. (2015). Astrocytes Control Synapse Formation, Function, and Elimination. Cold Spring Harb. Perspect. Biol. 7.

Clark, J.K., Furgerson, M., Crystal, J.D., Fechheimer, M., Furukawa, R., and Wagner, J.J. (2015). Alterations in synaptic plasticity coincide with deficits in spatial working memory in presymptomatic 3xTg-AD mice. Neurobiol. Learn. Mem. 125, 152–162.

Clinton, L.K., Billings, L.M., Green, K.N., Caccamo, A., Ngo, J., Oddo, S., McGaugh, J.L., and LaFerla, F.M. (2007). Age-dependent sexual dimorphism in cognition and stress response in the 3xTg-AD mice. Neurobiol. Dis. 28, 76–82.

Combs, C.K., Karlo, J.C., Kao, S.C., and Landreth, G.E. (2001). beta-Amyloid stimulation of microglia and monocytes results in TNFalpha-dependent expression of inducible nitric oxide synthase and neuronal apoptosis. J. Neurosci. Off. J. Soc. Neurosci. 21, 1179–1188.

Corder, E.H., Saunders, A.M., Strittmatter, W.J., Schmechel, D.E., Gaskell, P.C., Small, G.W., Roses, A.D., Haines, J.L., and Pericak-Vance, M.A. (1993). Gene dose of apolipoprotein E type 4 allele and the risk of Alzheimer's disease in late onset families. Science 261, 921–923.

Covelo, A., and Araque, A. (2016). Lateral regulation of synaptic transmission by astrocytes. Neuroscience 323, 62–66.

Crowe, A., James, M.J., Lee, V.M.-Y., Smith, A.B., Trojanowski, J.Q., Ballatore, C., and Brunden, K.R. (2013). Aminothienopyridazines and methylene blue affect Tau fibrillization via cysteine oxidation. J. Biol. Chem. 288, 11024–11037.

Dabir, D.V., Robinson, M.B., Swanson, E., Zhang, B., Trojanowski, J.Q., Lee, V.M., and Forman, M.S. (2006). Impaired glutamate transport in a mouse model of tau pathology in astrocytes. J Neurosci 26, 644–654.

Daneman, R., and Prat, A. (2015). The Blood–Brain Barrier. Cold Spring Harb. Perspect. Biol. 7, a020412.

Dani, J.W., Chernjavsky, A., and Smith, S.J. (1992). Neuronal activity triggers calcium waves in hippocampal astrocyte networks. Neuron 8, 429–440.

Dansokho, C., Ait Ahmed, D., Aid, S., Toly-Ndour, C., Chaigneau, T., Calle, V., Cagnard, N., Holzenberger, M., Piaggio, E., Aucouturier, P., et al. (2016). Regulatory T cells delay disease progression in Alzheimer-like pathology. Brain J. Neurol. 139, 1237–1251.

Darnell, J.E., Jr. (1997). STATs and gene regulation. Science 277, 1630–1635.

De Strooper, B., and Karran, E. (2016). The Cellular Phase of Alzheimer's Disease. Cell 164, 603–615.

Deng, W., Aimone, J.B., and Gage, F.H. (2010). New neurons and new memories: how does adult hippocampal neurogenesis affect learning and memory? Nat. Rev. Neurosci. 11, 339–350.

Derby, C.A., Burns, L.C., Wang, C., Katz, M.J., Zimmerman, M.E., L'italien, G., Guo, Z., Berman, R.M., and Lipton, R.B. (2013). Screening for predementia AD: time-dependent operating characteristics of episodic memory tests. Neurology 80, 1307–1314.

Desai, T.R., Leeper, N.J., Hynes, K.L., and Gewertz, B.L. (2002). Interleukin-6 causes endothelial barrier dysfunction via the protein kinase C pathway. J. Surg. Res. 104, 118–123.

Dobin, A., Davis, C.A., Schlesinger, F., Drenkow, J., Zaleski, C., Jha, S., Batut, P., Chaisson, M., and Gingeras, T.R. (2013). STAR: ultrafast universal RNA-seq aligner. Bioinforma. Oxf. Engl. 29, 15–21.

Doherty, J., Sheehan, A.E., Bradshaw, R., Fox, A.N., Lu, T.Y., and Freeman, M.R. (2014). PI3K signaling and Stat92E converge to modulate glial responsiveness to axonal injury. PLoS Biol 12, e1001985.

Dubois, B., Feldman, H.H., Jacova, C., Hampel, H., Molinuevo, J.L., Blennow, K., DeKosky, S.T., Gauthier, S., Selkoe, D., Bateman, R., et al. (2014). Advancing research diagnostic criteria for Alzheimer's disease: the IWG-2 criteria. Lancet Neurol. 13, 614–629.

Duyckaerts, C., Potier, M.C., and Delatour, B. (2008). Alzheimer disease models and human neuropathology: similarities and differences. Acta Neuropathol 115, 5–38.

Eckman, E.A., Reed, D.K., and Eckman, C.B. (2001). Degradation of the Alzheimer's amyloid beta peptide by endothelin-converting enzyme. J. Biol. Chem. 276, 24540–24548.

Eisele, Y.S., and Duyckaerts, C. (2016). Propagation of Aß pathology: hypotheses, discoveries, and yet unresolved questions from experimental and human brain studies. Acta Neuropathol. (Berl.) 131, 5–25.

Emmerling, M.R., Watson, M.D., Raby, C.A., and Spiegel, K. (2000). The role of complement in Alzheimer's disease pathology. Biochim. Biophys. Acta 1502, 158–171.

Eng, L.F., Vanderhaeghen, J.J., Bignami, A., and Gerstl, B. (1971). An acidic protein isolated from fibrous astrocytes. Brain Res 28, 351–354.

Eriksen, J.L., Sagi, S.A., Smith, T.E., Weggen, S., Das, P., McLendon, D.C., Ozols, V.V., Jessing, K.W., Zavitz, K.H., Koo, E.H., et al. (2003). NSAIDs and enantiomers of flurbiprofen target gamma-secretase and lower Abeta 42 in vivo. J. Clin. Invest. 112, 440–449.

Escartin, C., Pierre, K., Colin, A., Brouillet, E., Delzescaux, T., Guillermier, M., Dhenain, M., Deglon, N., Hantraye, P., Pellerin, L., et al. (2007). Activation of astrocytes by CNTF induces metabolic plasticity and increases resistance to metabolic insults. J Neurosci 27, 7094–7104.

Etcheberrigaray, R., Tan, M., Dewachter, I., Kuipéri, C., Van der Auwera, I., Wera, S., Qiao, L., Bank, B., Nelson, T.J., Kozikowski, A.P., et al. (2004). Therapeutic effects of PKC activators in Alzheimer's disease transgenic mice. Proc. Natl. Acad. Sci. U. S. A. 101, 11141–11146.

Fedorff, S. (2012). Astrocytes Pt 1: Development, Morphology, and Regional Specialization of Astrocytes (Elsevier).

Fellin, T., Pascual, O., Gobbo, S., Pozzan, T., Haydon, P.G., and Carmignoto, G. (2004). Neuronal synchrony mediated by astrocytic glutamate through activation of extrasynaptic NMDA receptors. Neuron 43, 729–743.

Fernandez, A.M., Jimenez, S., Mecha, M., Davila, D., Guaza, C., Vitorica, J., and Torres-Aleman, I. (2012). Regulation of the phosphatase calcineurin by insulin-like growth factor I unveils a key role of astrocytes in Alzheimer's pathology. Mol Psychiatry 17, 705–718.

Flaten, T.P. (2001). Aluminium as a risk factor in Alzheimer's disease, with emphasis on drinking water. Brain Res. Bull. 55, 187–196.

Fonseca, M.I., Zhou, J., Botto, M., and Tenner, A.J. (2004). Absence of C1q leads to less neuropathology in transgenic mouse models of Alzheimer's disease. J. Neurosci. Off. J. Soc. Neurosci. 24, 6457–6465.

Freeman, M.R. (2015). Drosophila Central Nervous System Glia. Cold Spring Harb. Perspect. Biol. 7.

Fukuyama, H., Ogawa, M., Yamauchi, H., Yamaguchi, S., Kimura, J., Yonekura, Y., and Konishi, J. (1994). Altered cerebral energy metabolism in Alzheimer's disease: a PET study. J Nucl Med 35, 1–6.

Furman, J.L., Sama, D.M., Gant, J.C., Beckett, T.L., Murphy, M.P., Bachstetter, A.D., Van Eldik, L.J., and Norris, C.M. (2012). Targeting astrocytes ameliorates neurologic changes in a mouse model of Alzheimer's disease. J Neurosci 32, 16129–16140.

Galimberti, D., Fenoglio, C., Lovati, C., Venturelli, E., Guidi, I., Corrà, B., Scalabrini, D., Clerici, F., Mariani, C., Bresolin, N., et al. (2006). Serum MCP-1 levels are increased in mild cognitive impairment and mild Alzheimer's disease. Neurobiol. Aging 27, 1763–1768.

Gao, S., Hendrie, H.C., Hall, K.S., and Hui, S. (1998). The relationships between age, sex, and the incidence of dementia and Alzheimer disease: a meta-analysis. Arch. Gen. Psychiatry 55, 809–815.

Garcia-Alloza, M., Robbins, E.M., Zhang-Nunes, S.X., Purcell, S.M., Betensky, R.A., Raju, S., Prada, C., Greenberg, S.M., Bacskai, B.J., and Frosch, M.P. (2006). Characterization of amyloid deposition in the APPswe/PS1dE9 mouse model of Alzheimer disease. Neurobiol Dis 24, 516–524.

Garcia-Marin, V., Garcia-Lopez, P., and Freire, M. (2007). Cajal's contributions to glia research. Trends Neurosci 30, 479–487.

Gauthier, S., Loft, H., and Cummings, J. (2008). Improvement in behavioural symptoms in patients with moderate to severe Alzheimer's disease by memantine: a pooled data analysis. Int. J. Geriatr. Psychiatry 23, 537–545.

Ghosh, S., Wu, M.D., Shaftel, S.S., Kyrkanides, S., LaFerla, F.M., Olschowka, J.A., and O'Banion, M.K. (2013). Sustained interleukin-1β overexpression exacerbates tau pathology despite reduced amyloid burden in an Alzheimer's mouse model. J. Neurosci. Off. J. Soc. Neurosci. 33, 5053–5064.

Gilman, S., Koller, M., Black, R.S., Jenkins, L., Griffith, S.G., Fox, N.C., Eisner, L., Kirby, L., Rovira, M.B., Forette, F., et al. (2005). Clinical effects of Abeta immunization (AN1792) in patients with AD in an interrupted trial. Neurology 64, 1553–1562.

Ginhoux, F., Greter, M., Leboeuf, M., Nandi, S., See, P., Gokhan, S., Mehler, M.F., Conway, S.J., Ng, L.G., Stanley, E.R., et al. (2010). Fate mapping analysis reveals that adult microglia derive from primitive macrophages. Science 330, 841–845.

Goate, A., Chartier-Harlin, M.C., Mullan, M., Brown, J., Crawford, F., Fidani, L., Giuffra, L., Haynes, A., Irving, N., and James, L. (1991). Segregation of a missense mutation in the amyloid precursor protein gene with familial Alzheimer's disease. Nature 349, 704–706.

Goedert, M. (2015). NEURODEGENERATION. Alzheimer's and Parkinson's diseases: The prion concept in relation to assembled Aβ, tau, and α-synuclein. Science 349, 1255555.

Griffin, J.L., Bollard, M., Nicholson, J.K., and Bhakoo, K. (2002). Spectral profiles of cultured neuronal and glial cells derived from HRMAS (1)H NMR spectroscopy. NMR Biomed. 15, 375–384.

van Groen, T., Kiliaan, A.J., and Kadish, I. (2006). Deposition of mouse amyloid beta in human APP/PS1 double and single AD model transgenic mice. Neurobiol. Dis. 23, 653–662.

Guerreiro, R., Wojtas, A., Bras, J., Carrasquillo, M., Rogaeva, E., Majounie, E., Cruchaga, C., Sassi, C., Kauwe, J.S., Younkin, S., et al. (2013). TREM2 variants in Alzheimer's disease. N Engl J Med 368, 117–127.

Guillot-Sestier, M.V., Doty, K.R., Gate, D., Rodriguez, J., Jr., Leung, B.P., Rezai-Zadeh, K., and Town, T. (2015). Il10 deficiency rebalances innate immunity to mitigate Alzheimer-like pathology. Neuron 85, 534–548.

Haan, S., Wüller, S., Kaczor, J., Rolvering, C., Nöcker, T., Behrmann, I., and Haan, C. (2009). SOCS-mediated downregulation of mutant Jak2 (V617F, T875N and K539L) counteracts cytokine-independent signaling. Oncogene 28, 3069–3080.

Halassa, M.M., Fellin, T., Takano, H., Dong, J.H., and Haydon, P.G. (2007). Synaptic islands defined by the territory of a single astrocyte. J Neurosci 27, 6473–6477.

Halle, A., Hornung, V., Petzold, G.C., Stewart, C.R., Monks, B.G., Reinheckel, T., Fitzgerald, K.A., Latz, E., Moore, K.J., and Golenbock, D.T. (2008). The NALP3 inflammasome is involved in the innate immune response to amyloid-beta. Nat Immunol 9, 857–865.

Hardy, J.A., and Higgins, G.A. (1992). Alzheimer's disease: the amyloid cascade hypothesis. Science 256, 184–185.

Heinrich, P.C., Behrmann, I., Haan, S., Hermanns, H.M., Muller-Newen, G., and Schaper, F. (2003). Principles of interleukin (IL)-6-type cytokine signalling and its regulation. Biochem J 374, 1–20.

Heneka, M.T., Sastre, M., Dumitrescu-Ozimek, L., Dewachter, I., Walter, J., Klockgether, T., and Van Leuven, F. (2005). Focal glial activation coincides with increased BACE1 activation and precedes amyloid plaque deposition in APP[V717I] transgenic mice. J. Neuroinflammation 2.

Heneka, M.T., Kummer, M.P., and Latz, E. (2014). Innate immune activation in neurodegenerative disease. Nat Rev Immunol 14, 463–477.

Heneka, M.T., Carson, M.J., El Khoury, J., Landreth, G.E., Brosseron, F., Feinstein, D.L., Jacobs, A.H., Wyss-Coray, T., Vitorica, J., Ransohoff, R.M., et al. (2015). Neuroinflammation in Alzheimer's disease. Lancet Neurol. 14, 388–405.

Hickman, S.E., and El Khoury, J. (2014). TREM2 and the neuroimmunology of Alzheimer's disease. Biochem Pharmacol 88, 495–498.

Hickman, S.E., Allison, E.K., and El Khoury, J. (2008). Microglial dysfunction and defective beta-amyloid clearance pathways in aging Alzheimer's disease mice. J Neurosci 28, 8354–8360.

Hoglund, K., Thelen, K.M., Syversen, S., Sjogren, M., von Bergmann, K., Wallin, A., Vanmechelen, E., Vanderstichele, H., Lutjohann, D., and Blennow, K. (2005). The effect of simvastatin treatment on the amyloid precursor protein and brain cholesterol metabolism in patients with Alzheimer's disease. Dement. Geriatr. Cogn. Disord. 19, 256–265.

Hol, E.M., and Pekny, M. (2015). Glial fibrillary acidic protein (GFAP) and the astrocyte intermediate filament system in diseases of the central nervous system. Curr Opin Cell Biol 32, 121–130.

Hong, L., Huang, H.-C., and Jiang, Z.-F. (2014). Relationship between amyloid-beta and the ubiquitin-proteasome system in Alzheimer's disease. Neurol. Res. 36, 276–282.

Hong, S., Beja-Glasser, V.F., Nfonoyim, B.M., Frouin, A., Li, S., Ramakrishnan, S., Merry, K.M., Shi, Q., Rosenthal, A., Barres, B.A., et al. (2016). Complement and microglia mediate early synapse loss in Alzheimer mouse models. Science 352, 712–716.

Huang, D.W., Sherman, B.T., and Lempicki, R.A. (2009). Systematic and integrative analysis of large gene lists using DAVID bioinformatics resources. Nat. Protoc. 4, 44–57.

Huang, Y.-W.A., Zhou, B., Wernig, M., and Südhof, T.C. (2017). ApoE2, ApoE3, and ApoE4 Differentially Stimulate APP Transcription and Aβ Secretion. Cell 168, 427–441.e21.

Hutchins, A.P., Diez, D., Takahashi, Y., Ahmad, S., Jauch, R., Tremblay, M.L., and Miranda-Saavedra, D. (2013). Distinct transcriptional regulatory modules underlie STAT3's cell type-independent and cell type-specific functions. Nucleic Acids Res 41, 2155–2170.

Ikonomovic, M.D., Klunk, W.E., Abrahamson, E.E., Mathis, C.A., Price, J.C., Tsopelas, N.D., Lopresti, B.J., Ziolko, S., Bi, W., Paljug, W.R., et al. (2008). Post-mortem correlates of in vivo PiB-PET amyloid imaging in a typical case of Alzheimer's disease. Brain J. Neurol. 131, 1630–1645.

Iram, T., Trudler, D., Kain, D., Kanner, S., Galron, R., Vassar, R., Barzilai, A., Blinder, P., Fishelson, Z., and Frenkel, D. (2016). Astrocytes from old Alzheimer's disease mice are impaired in Aβ uptake and in neuroprotection. Neurobiol. Dis. 96, 84–94.

Jack, C.R., Barkhof, F., Bernstein, M.A., Cantillon, M., Cole, P.E., Decarli, C., Dubois, B., Duchesne, S., Fox, N.C., Frisoni, G.B., et al. (2011). Steps to standardization and validation of hippocampal volumetry as a biomarker in clinical trials and diagnostic criterion for Alzheimer's disease. Alzheimers Dement. J. Alzheimers Assoc. 7, 474–485.e4.

Jankowsky, J.L., Fadale, D.J., Anderson, J., Xu, G.M., Gonzales, V., Jenkins, N.A., Copeland, N.G., Lee, M.K., Younkin, L.H., Wagner, S.L., et al. (2004). Mutant presenilins specifically elevate the levels of the 42 residue beta-amyloid peptide in vivo: evidence for augmentation of a 42-specific gamma secretase. Hum Mol Genet 13, 159–170.

Jansen, A.H., Reits, E.A., and Hol, E.M. (2014). The ubiquitin proteasome system in glia and its role in neurodegenerative diseases. Front Mol Neurosci 7, 73.

Janus, C., Flores, A.Y., Xu, G., and Borchelt, D.R. (2015). Behavioral abnormalities in APPSwe/PS1dE9 mouse model of AD-like pathology: comparative analysis across multiple behavioral domains. Neurobiol. Aging 36, 2519–2532.

Jaunmuktane, Z., Mead, S., Ellis, M., Wadsworth, J.D.F., Nicoll, A.J., Kenny, J., Launchbury, F., Linehan, J., Richard-Loendt, A., Walker, A.S., et al. (2015). Evidence for human transmission of amyloid-β pathology and cerebral amyloid angiopathy. Nature 525, 247–250.

Jay, T.R., Miller, C.M., Cheng, P.J., Graham, L.C., Bemiller, S., Broihier, M.L., Xu, G., Margevicius, D., Karlo, J.C., Sousa, G.L., et al. (2015). TREM2 deficiency eliminates TREM2+ inflammatory macrophages and ameliorates pathology in Alzheimer's disease mouse models. J. Exp. Med. 212, 287–295.

Jo, S., Yarishkin, O., Hwang, Y.J., Chun, Y.E., Park, M., Woo, D.H., Bae, J.Y., Kim, T., Lee, J., Chun, H., et al. (2014). GABA from reactive astrocytes impairs memory in mouse models of Alzheimer's disease. Nat Med 20, 886–896.

John Lin, C.C., Yu, K., Hatcher, A., Huang, T.W., Lee, H.K., Carlson, J., Weston, M.C., Chen, F., Zhang, Y., Zhu, W., et al. (2017). Identification of diverse astrocyte populations and their malignant analogs. Nat Neurosci.

Jonsson, T., Stefansson, H., Steinberg, S., Jonsdottir, I., Jonsson, P.V., Snaedal, J., Bjornsson, S., Huttenlocher, J., Levey, A.I., Lah, J.J., et al. (2013). Variant of TREM2 associated with the risk of Alzheimer's disease. N Engl J Med 368, 107–116.

Jorm, A.F. (2001). History of depression as a risk factor for dementia: an updated review. Aust. N. Z. J. Psychiatry 35, 776–781.

Kamphuis, W., Kooijman, L., Orre, M., Stassen, O., Pekny, M., and Hol, E.M. (2015). GFAP and vimentin deficiency alters gene expression in astrocytes and microglia in wild-type mice and changes the transcriptional response of reactive glia in mouse model for Alzheimer's disease. Glia 63, 1036–1056.

Kantor, B., Bailey, R.M., Wimberly, K., Kalburgi, S.N., and Gray, S.J. (2014). Methods for Gene Transfer to the Central Nervous System. Adv. Genet. 87, 125–197.

Keren-Shaul, H., Spinrad, A., Weiner, A., Matcovitch-Natan, O., Dvir-Szternfeld, R., Ulland, T.K., David, E., Baruch, K., Lara-Astaiso, D., Toth, B., et al. (2017). A Unique Microglia Type Associated with Restricting Development of Alzheimer's Disease. Cell 169, 1276–1290.e17.

Kershaw, N.J., Murphy, J.M., Liau, N.P., Varghese, L.N., Laktyushin, A., Whitlock, E.L., Lucet, I.S., Nicola, N.A., and Babon, J.J. (2013). SOCS3 binds specific receptor-JAK complexes to control cytokine signaling by direct kinase inhibition. Nat Struct Mol Biol 20, 469–476.

Kilgore, M., Miller, C.A., Fass, D.M., Hennig, K.M., Haggarty, S.J., Sweatt, J.D., and Rumbaugh, G. (2010). Inhibitors of class 1 histone deacetylases reverse contextual memory deficits in a mouse model of Alzheimer's disease. Neuropsychopharmacol. Off. Publ. Am. Coll. Neuropsychopharmacol. 35, 870–880.

Kiyota, T., Okuyama, S., Swan, R.J., Jacobsen, M.T., Gendelman, H.E., and Ikezu, T. (2010). CNS expression of anti-inflammatory cytokine interleukin-4 attenuates Alzheimer's disease-like pathogenesis in APP+PS1 bigenic mice. FASEB J 24, 3093–3102.

Kiyota, T., Ingraham, K.L., Swan, R.J., Jacobsen, M.T., Andrews, S.J., and Ikezu, T. (2012). AAV serotype 2/1-mediated gene delivery of anti-inflammatory interleukin-10 enhances neurogenesis and cognitive function in APP+PS1 mice. Gene Ther. 19, 724–733.

Kleinberger, G., Yamanishi, Y., Suarez-Calvet, M., Czirr, E., Lohmann, E., Cuyvers, E., Struyfs, H., Pettkus, N., Wenninger-Weinzierl, A., Mazaheri, F., et al. (2014). TREM2 mutations implicated in neurodegeneration impair cell surface transport and phagocytosis. Sci Transl Med 6, 243ra86.

Klunk, W.E., Engler, H., Nordberg, A., Wang, Y., Blomqvist, G., Holt, D.P., Bergström, M., Savitcheva, I., Huang, G., Estrada, S., et al. (2004). Imaging brain amyloid in Alzheimer's disease with Pittsburgh Compound-B. Ann. Neurol. 55, 306–319.

Koistinaho, M., Lin, S., Wu, X., Esterman, M., Koger, D., Hanson, J., Higgs, R., Liu, F., Malkani, S., Bales, K.R., et al. (2004). Apolipoprotein E promotes astrocyte colocalization and degradation of deposited amyloid-beta peptides. Nat Med 10, 719–726.

Kontsekova, E., Zilka, N., Kovacech, B., Novak, P., and Novak, M. (2014). First-in-man tau vaccine targeting structural determinants essential for pathological tau-tau interaction reduces tau oligomerisation and neurofibrillary degeneration in an Alzheimer's disease model. Alzheimers Res. Ther. 6, 44.

Kootstra, N.A., and Verma, I.M. (2003). Gene therapy with viral vectors. Annu. Rev. Pharmacol. Toxicol. 43, 413–439.

Kraft, A.W., Hu, X., Yoon, H., Yan, P., Xiao, Q., Wang, Y., Gil, S.C., Brown, J., Wilhelmsson, U., Restivo, J.L., et al. (2013). Attenuating astrocyte activation accelerates plaque pathogenesis in APP/PS1 mice. FASEB J 27, 187–198.

Krauthausen, M., Kummer, M.P., Zimmermann, J., Reyes-Irisarri, E., Terwel, D., Bulic, B., Heneka, M.T., and Müller, M. (2015). CXCR3 promotes plaque formation and behavioral deficits in an Alzheimer's disease model. J. Clin. Invest. 125, 365–378.

Laurent, C., Dorothée, G., Hunot, S., Martin, E., Monnet, Y., Duchamp, M., Dong, Y., Légeron, F.-P., Leboucher, A., Burnouf, S., et al. (2017). Hippocampal T cell infiltration promotes neuroinflammation and cognitive decline in a mouse model of tauopathy. Brain J. Neurol. 140, 184–200.

Lee, C.Y.D., and Landreth, G.E. (2010). The role of microglia in amyloid clearance from the AD brain. J. Neural Transm. Vienna Austria 1996 117, 949–960.

Lee, Y., Messing, A., Su, M., and Brenner, M. (2008). GFAP promoter elements required for region-specific and astrocyte-specific expression. Glia 56, 481–493.

Levy, D.E., and Darnell, J.E., Jr. (2002). Stats: transcriptional control and biological impact. Nat Rev Mol Cell Biol 3, 651–662.

Levy-Lahad, E., Wasco, W., Poorkaj, P., Romano, D.M., Oshima, J., Pettingell, W.H., Yu, C.E., Jondro, P.D., Schmidt, S.D., and Wang, K. (1995). Candidate gene for the chromosome 1 familial Alzheimer's disease locus. Science 269, 973–977.

Li, B., Chohan, M.O., Grundke-Iqbal, I., and Iqbal, K. (2007). Disruption of microtubule network by Alzheimer abnormally hyperphosphorylated tau. Acta Neuropathol. (Berl.) 113, 501–511.

Li, H., Rao, A., and Hogan, P.G. (2011). Interaction of calcineurin with substrates and targeting proteins. Trends Cell Biol. 21, 91–103.

Li, Y., Du, X.F., Liu, C.S., Wen, Z.L., and Du, J.L. (2012). Reciprocal regulation between resting microglial dynamics and neuronal activity in vivo. Dev Cell 23, 1189–1202.

Lian, H., Yang, L., Cole, A., Sun, L., Chiang, A.C.-A., Fowler, S.W., Shim, D.J., Rodriguez-Rivera, J., Taglialatela, G., Jankowsky, J.L., et al. (2015). NFκB-activated astroglial release of complement C3 compromises neuronal morphology and function associated with Alzheimer's disease. Neuron 85, 101–115.

Lian, H., Litvinchuk, A., Chiang, A.C.-A., Aithmitti, N., Jankowsky, J.L., and Zheng, H. (2016). Astrocyte-Microglia Cross Talk through Complement Activation Modulates Amyloid Pathology in Mouse Models of Alzheimer's Disease. J. Neurosci. Off. J. Soc. Neurosci. 36, 577–589.

Liddelow, S.A., Guttenplan, K.A., Clarke, L.E., Bennett, F.C., Bohlen, C.J., Schirmer, L., Bennett, M.L., Munch, A.E., Chung, W.S., Peterson, T.C., et al. (2017). Neurotoxic reactive astrocytes are induced by activated microglia. Nature 541, 481–487.

Lim, C.P., and Cao, X. (2006). Structure, function, and regulation of STAT proteins. Mol Biosyst 2, 536–550.

Lin, M.T., and Beal, M.F. (2006). Mitochondrial dysfunction and oxidative stress in neurodegenerative diseases. Nature 443, 787–795.

Lindsten, K., de Vrij, F.M.S., Verhoef, L.G.G.C., Fischer, D.F., van Leeuwen, F.W., Hol, E.M., Masucci, M.G., and Dantuma, N.P. (2002). Mutant ubiquitin found in neurodegenerative disorders is a ubiquitin fusion degradation substrate that blocks proteasomal degradation. J. Cell Biol. 157, 417–427.

Liu, L., Drouet, V., Wu, J.W., Witter, M.P., Small, S.A., Clelland, C., and Duff, K. (2012). Trans-synaptic spread of tau pathology in vivo. PloS One 7, e31302.

Liu, Q.Y., Schaffner, A.E., Chang, Y.H., Maric, D., and Barker, J.L. (2000). Persistent activation of GABA(A) receptor/Cl(-) channels by astrocyte-derived GABA in cultured embryonic rat hippocampal neurons. J. Neurophysiol. 84, 1392–1403.

Liu, Y., Walter, S., Stagi, M., Cherny, D., Letiembre, M., Schulz-Schaeffer, W., Heine, H., Penke, B., Neumann, H., and Fassbender, K. (2005). LPS receptor (CD14): a receptor for phagocytosis of Alzheimer's amyloid peptide. Brain 128, 1778–1789.

Lively, S., and Schlichter, L.C. (2013). The microglial activation state regulates migration and roles of matrix-dissolving enzymes for invasion. J. Neuroinflammation 10, 75.

López González, I., Garcia-Esparcia, P., Llorens, F., and Ferrer, I. (2016). Genetic and Transcriptomic Profiles of Inflammation in Neurodegenerative Diseases: Alzheimer, Parkinson, Creutzfeldt-Jakob and Tauopathies. Int. J. Mol. Sci. 17, 206.

Love, M.I., Huber, W., and Anders, S. (2014). Moderated estimation of fold change and dispersion for RNA-seq data with DESeq2. Genome Biol. 15, 550.

Lovestone, S., Boada, M., Dubois, B., Hüll, M., Rinne, J.O., Huppertz, H.-J., Calero, M., Andrés, M.V., Gómez-Carrillo, B., León, T., et al. (2015). A phase II trial of tideglusib in Alzheimer's disease. J. Alzheimers Dis. JAD 45, 75–88.

Lucin, K.M., O'Brien, C.E., Bieri, G., Czirr, E., Mosher, K.I., Abbey, R.J., Mastroeni, D.F., Rogers, J., Spencer, B., Masliah, E., et al. (2013). Microglial beclin 1 regulates retromer trafficking and phagocytosis and is impaired in Alzheimer's disease. Neuron 79, 873–886.

Luna-Muñoz, J., Harrington, C.R., Wischik, C.M., Flores-Rodríguez, P., Avila, J., Zamudio, S.R., Cruz, F.D. la, Mena, R., Meraz-Ríos, M.A., and Floran-Garduño, B. (2013). Phosphorylation of Tau Protein Associated as a Protective Mechanism in the Presence of Toxic, C-Terminally Truncated Tau in Alzheimer's Disease.

Lundgaard, I., Li, B., Xie, L., Kang, H., Sanggaard, S., Haswell, J.D.R., Sun, W., Goldman, S., Blekot, S., Nielsen, M., et al. (2015). Direct neuronal glucose uptake heralds activity-dependent increases in cerebral metabolism. Nat. Commun. 6, 6807.

Luo, Y., Bolon, B., Kahn, S., Bennett, B.D., Babu-Khan, S., Denis, P., Fan, W., Kha, H., Zhang, J., Gong, Y., et al. (2001). Mice deficient in BACE1, the Alzheimer's beta-secretase, have normal phenotype and abolished beta-amyloid generation. Nat. Neurosci. 4, 231–232.

Ma, J.-F., Huang, Y., Chen, S.-D., and Halliday, G. (2010). Immunohistochemical evidence for macroautophagy in neurones and endothelial cells in Alzheimer's disease. Neuropathol. Appl. Neurobiol. 36, 312–319.

Ma, T., Du, X., Pick, J.E., Sui, G., Brownlee, M., and Klann, E. (2012). Glucagon-like peptide-1 cleavage product GLP-1(9-36) amide rescues synaptic plasticity and memory deficits in Alzheimer's disease model mice. J. Neurosci. Off. J. Soc. Neurosci. 32, 13701–13708.

Magistretti, P.J. (2006). Neuron-glia metabolic coupling and plasticity. J Exp Biol 209, 2304–2311.

Makar, T.K., Nedergaard, M., Preuss, A., Gelbard, A.S., Perumal, A.S., and Cooper, A.J. (1994). Vitamin E, ascorbate, glutathione, glutathione disulfide, and enzymes of glutathione metabolism in cultures of chick astrocytes and neurons: evidence that astrocytes play an important role in antioxidative processes in the brain. J Neurochem 62, 45–53.

Malenka, R.C., and Bear, M.F. (2004). LTP and LTD: an embarrassment of riches. Neuron 44, 5–21.

Malm, T., Koistinaho, J., and Kanninen, K. (2011). Utilization of APPswe/PS1dE9 Transgenic Mice in Research of Alzheimer's Disease: Focus on Gene Therapy and Cell-Based Therapy Applications. Int. J. Alzheimers Dis. 2011, 517160.

Maragakis, N.J., and Rothstein, J.D. (2004). Glutamate transporters: animal models to neurologic disease. Neurobiol. Dis. 15, 461–473.

Martin, E., Boucher, C., Fontaine, B., and Delarasse, C. (2017). Distinct inflammatory phenotypes of microglia and monocyte-derived macrophages in Alzheimer's disease models: effects of aging and amyloid pathology. Aging Cell 16, 27–38.

Masliah, E., Alford, M., DeTeresa, R., Mallory, M., and Hansen, L. (1996). Deficient glutamate transport is associated with neurodegeneration in Alzheimer's disease. Ann Neurol 40, 759–766.

Masliah, E., Alford, M., Mallory, M., Rockenstein, E., Moechars, D., and Van Leuven, F. (2000). Abnormal glutamate transport function in mutant amyloid precursor protein transgenic mice. Exp Neurol 163, 381–387.

Masters, C.L., Bateman, R., Blennow, K., Rowe, C.C., Sperling, R.A., and Cummings, J.L. (2015). Alzheimer's disease. Nat. Rev. Dis. Primer 1, 15056.

Mathys, H., Adaikkan, C., Gao, F., Young, J.Z., Manet, E., Hemberg, M., De Jager, P.L., Ransohoff, R.M., Regev, A., and Tsai, L.-H. (2017). Temporal Tracking of Microglia Activation in Neurodegeneration at Single-Cell Resolution. Cell Rep. 21, 366–380.

McGeer, P.L., Itagaki, S., Tago, H., and McGeer, E.G. (1988). Occurrence of HLA-DR reactive microglia in Alzheimer's disease. Ann N Acad Sci 540, 319–323.

Medina, D.X., Caccamo, A., and Oddo, S. (2011). Methylene blue reduces aβ levels and rescues early cognitive deficit by increasing proteasome activity. Brain Pathol. Zurich Switz. 21, 140–149.

Merlini, M., Meyer, E.P., Ulmann-Schuler, A., and Nitsch, R.M. (2011). Vascular β-amyloid and early astrocyte alterations impair cerebrovascular function and cerebral metabolism in transgenic arcAβ mice. Acta Neuropathol. (Berl.) 122, 293–311.

Métais, C., Brennan, K., Mably, A.J., Scott, M., Walsh, D.M., and Herron, C.E. (2014). Simvastatin treatment preserves synaptic plasticity in AβPPswe/PS1dE9 mice. J. Alzheimers Dis. JAD 39, 315–329.

Michaud, J.-P., Bellavance, M.-A., Préfontaine, P., and Rivest, S. (2013). Real-time in vivo imaging reveals the ability of monocytes to clear vascular amyloid beta. Cell Rep. 5, 646–653.

Mildner, A., Schlevogt, B., Kierdorf, K., Böttcher, C., Erny, D., Kummer, M.P., Quinn, M., Brück, W., Bechmann, I., Heneka, M.T., et al. (2011). Distinct and non-redundant roles of microglia and myeloid subsets in mouse models of Alzheimer's disease. J. Neurosci. Off. J. Soc. Neurosci. 31, 11159–11171.

Miller, R.H., and Raff, M.C. (1984). Fibrous and protoplasmic astrocytes are biochemically and developmentally distinct. J. Neurosci. Off. J. Soc. Neurosci. 4, 585–592.

Miners, J.S., Baig, S., Tayler, H., Kehoe, P.G., and Love, S. (2009). Neprilysin and insulin-degrading enzyme levels are increased in Alzheimer disease in relation to disease severity. J. Neuropathol. Exp. Neurol. 68, 902–914.

Minkiewicz, J., de Rivero Vaccari, J.P., and Keane, R.W. (2013). Human astrocytes express a novel NLRP2 inflammasome. Glia 61, 1113–1121.

Mintun, M.A., Larossa, G.N., Sheline, Y.I., Dence, C.S., Lee, S.Y., Mach, R.H., Klunk, W.E., Mathis, C.A., DeKosky, S.T., and Morris, J.C. (2006). [11C]PIB in a nondemented population: potential antecedent marker of Alzheimer disease. Neurology 67, 446–452.

Mirra, S.S., Heyman, A., McKeel, D., Sumi, S.M., Crain, B.J., Brownlee, L.M., Vogel, F.S., Hughes, J.P., van Belle, G., and Berg, L. (1991). The Consortium to Establish a Registry for Alzheimer's Disease (CERAD). Part II. Standardization of the neuropathologic assessment of Alzheimer's disease. Neurology 41, 479–486.

Montine, T.J., Phelps, C.H., Beach, T.G., Bigio, E.H., Cairns, N.J., Dickson, D.W., Duyckaerts, C., Frosch, M.P., Masliah, E., Mirra, S.S., et al. (2012). National Institute on Aging-Alzheimer's Association guidelines for the neuropathologic assessment of Alzheimer's disease: a practical approach. Acta Neuropathol. (Berl.) 123, 1–11.

Mulder, S.D., Veerhuis, R., Blankenstein, M.A., and Nielsen, H.M. (2012). The effect of amyloid associated proteins on the expression of genes involved in amyloid-β clearance by adult human astrocytes. Exp. Neurol. 233, 373–379.

Nakanishi, H. (2003). Microglial functions and proteases. Mol. Neurobiol. 27, 163–176.

Namba, Y., Tomonaga, M., Kawasaki, H., Otomo, E., and Ikeda, K. (1991). Apolipoprotein E immunoreactivity in cerebral amyloid deposits and neurofibrillary tangles in Alzheimer's disease and kuru plaque amyloid in Creutzfeldt-Jakob disease. Brain Res. 541, 163–166.

Nelson, L.H., and Lenz, K.M. (2017). The immune system as a novel regulator of sex differences in brain and behavioral development. J. Neurosci. Res. 95, 447–461.

Nelson, T.J., Sun, M.-K., Lim, C., Sen, A., Khan, T., Chirila, F.V., and Alkon, D.L. (2017). Bryostatin Effects on Cognitive Function and PKCε in Alzheimer's Disease Phase IIa and Expanded Access Trials. J. Alzheimers Dis. JAD 58, 521–535.

Nestor, P.J., Fryer, T.D., and Hodges, J.R. (2006). Declarative memory impairments in Alzheimer's disease and semantic dementia. NeuroImage 30, 1010–1020.

Neve, R.L., Harris, P., Kosik, K.S., Kurnit, D.M., and Donlon, T.A. (1986). Identification of cDNA clones for the human microtubule-associated protein tau and chromosomal localization of the genes for tau and microtubule-associated protein 2. Brain Res. 387, 271–280.

Neves, G., Cooke, S.F., and Bliss, T.V.P. (2008). Synaptic plasticity, memory and the hippocampus: a neural network approach to causality. Nat. Rev. Neurosci. 9, 65–75.

Nielsen, H.M., Veerhuis, R., Holmqvist, B., and Janciauskiene, S. (2009). Binding and uptake of A beta1-42 by primary human astrocytes in vitro. Glia 57, 978–988.

Nixon, R.A., Wegiel, J., Kumar, A., Yu, W.H., Peterhoff, C., Cataldo, A., and Cuervo, A.M. (2005). Extensive involvement of autophagy in Alzheimer disease: an immuno-electron microscopy study. J. Neuropathol. Exp. Neurol. 64, 113–122.

Noli, L., Capalbo, A., Ogilvie, C., Khalaf, Y., and Ilic, D. (2015). Discordant Growth of Monozygotic Twins Starts at the Blastocyst Stage: A Case Study. Stem Cell Rep. 5, 946–953.

Nyakas, C., Granic, I., Halmy, L.G., Banerjee, P., and Luiten, P.G.M. (2011). The basal forebrain cholinergic system in aging and dementia. Rescuing cholinergic neurons from neurotoxic amyloid-β42 with memantine. Behav. Brain Res. 221, 594–603.

Oddo, S., Caccamo, A., Shepherd, J.D., Murphy, M.P., Golde, T.E., Kayed, R., Metherate, R., Mattson, M.P., Akbari, Y., and LaFerla, F.M. (2003a). Triple-transgenic model of Alzheimer's disease with plaques and tangles: intracellular Abeta and synaptic dysfunction. Neuron 39, 409–421.

Oddo, S., Caccamo, A., Kitazawa, M., Tseng, B.P., and LaFerla, F.M. (2003b). Amyloid deposition precedes tangle formation in a triple transgenic model of Alzheimer's disease. Neurobiol Aging 24, 1063–1070.

Oh, K.-J., Perez, S.E., Lagalwar, S., Vana, L., Binder, L., and Mufson, E.J. (2010). Staging of Alzheimer's Pathology in Triple Transgenic Mice: A Light and Electron Microscopic Analysis. Int. J. Alzheimers Dis. 2010.

Olabarria, M., Noristani, H.N., Verkhratsky, A., and Rodriguez, J.J. (2010). Concomitant astroglial atrophy and astrogliosis in a triple transgenic animal model of Alzheimer's disease. Glia 58, 831–838.

Oliet, S.H., Piet, R., and Poulain, D.A. (2001). Control of glutamate clearance and synaptic efficacy by glial coverage of neurons. Science 292, 923–926.

Olmos, G., and Lladó, J. (2014). Tumor necrosis factor alpha: a link between neuroinflammation and excitotoxicity. Mediators Inflamm. 2014, 861231.

Orre, M., Kamphuis, W., Dooves, S., Kooijman, L., Chan, E.T., Kirk, C.J., Dimayuga Smith, V., Koot, S., Mamber, C., Jansen, A.H., et al. (2013). Reactive glia show increased immunoproteasome activity in Alzheimer's disease. Brain 136, 1415–1431.

Orre, M., Kamphuis, W., Osborn, L.M., Jansen, A.H.P., Kooijman, L., Bossers, K., and Hol, E.M. (2014). Isolation of glia from Alzheimer's mice reveals inflammation and dysfunction. Neurobiol. Aging 35, 2746–2760.

Ortinski, P.I., Dong, J., Mungenast, A., Yue, C., Takano, H., Watson, D.J., Haydon, P.G., and Coulter, D.A. (2010). Selective induction of astrocytic gliosis generates deficits in neuronal inhibition. Nat Neurosci 13, 584–591.

Panatier, A., Theodosis, D.T., Mothet, J.P., Touquet, B., Pollegioni, L., Poulain, D.A., and Oliet, S.H. (2006). Glia-derived D-serine controls NMDA receptor activity and synaptic memory. Cell 125, 775–784.

Panatier, A., Vallee, J., Haber, M., Murai, K.K., Lacaille, J.C., and Robitaille, R. (2011). Astrocytes are endogenous regulators of basal transmission at central synapses. Cell 146, 785–798.

Panza, F., Solfrizzi, V., Seripa, D., Imbimbo, B.P., Lozupone, M., Santamato, A., Zecca, C., Barulli, M.R., Bellomo, A., Pilotto, A., et al. (2016). Tau-Centric Targets and Drugs in Clinical Development for the Treatment of Alzheimer's Disease. BioMed Res. Int. 2016, 3245935.

Perea, G., Navarrete, M., and Araque, A. (2009). Tripartite synapses: astrocytes process and control synaptic information. Trends Neurosci 32, 421–431.

Perry, G., Friedman, R., Shaw, G., and Chau, V. (1987). Ubiquitin is detected in neurofibrillary tangles and senile plaque neurites of Alzheimer disease brains. Proc. Natl. Acad. Sci. U. S. A. 84, 3033–3036.

Persidsky, Y., Ramirez, S.H., Haorah, J., and Kanmogne, G.D. (2006). Blood-brain barrier: structural components and function under physiologic and pathologic conditions. J. Neuroimmune Pharmacol. Off. J. Soc. NeuroImmune Pharmacol. 1, 223–236.

Pfaff, D., Fiedler, U., and Augustin, H.G. (2006). Emerging roles of the Angiopoietin-Tie and the ephrin-Eph systems as regulators of cell trafficking. J. Leukoc. Biol. 80, 719–726.

Pickford, F., Masliah, E., Britschgi, M., Lucin, K., Narasimhan, R., Jaeger, P.A., Small, S., Spencer, B., Rockenstein, E., Levine, B., et al. (2008). The autophagy-related protein beclin 1 shows reduced expression in early Alzheimer disease and regulates amyloid beta accumulation in mice. J. Clin. Invest. 118, 2190–2199.

Pini, L., Pievani, M., Bocchetta, M., Altomare, D., Bosco, P., Cavedo, E., Galluzzi, S., Marizzoni, M., and Frisoni, G.B. (2016). Brain atrophy in Alzheimer's Disease and aging. Ageing Res. Rev. 30, 25–48.

Pomilio, C., Pavia, P., Gorojod, R.M., Vinuesa, A., Alaimo, A., Galvan, V., Kotler, M.L., Beauquis, J., and Saravia, F. (2016). Glial alterations from early to late stages in a model of Alzheimer's disease: Evidence of autophagy involvement in Aβ internalization. Hippocampus 26, 194–210.

Porter, J.T., and McCarthy, K.D. (1997). Astrocytic neurotransmitter receptors in situ and in vivo. Prog Neurobiol 51, 439–455.

Pottier, C., Ravenscroft, T.A., Brown, P.H., Finch, N.A., Baker, M., Parsons, M., Asmann, Y.W., Ren, Y., Christopher, E., Levitch, D., et al. (2016). TYROBP genetic variants in early-onset Alzheimer's disease. Neurobiol. Aging 48, 222.e9-222.e15.

Prinz, M., and Priller, J. (2017). The role of peripheral immune cells in the CNS in steady state and disease. Nat. Neurosci. 20, 136–144.

Raina, P., Santaguida, P., Ismaila, A., Patterson, C., Cowan, D., Levine, M., Booker, L., and Oremus, M. (2008). Effectiveness of cholinesterase inhibitors and memantine for treating dementia: evidence review for a clinical practice guideline. Ann. Intern. Med. 148, 379–397.

Ransohoff, R.M. (2016). A polarizing question: do M1 and M2 microglia exist? Nat Neurosci 19, 987–991.

Refolo, L.M., Pappolla, M.A., LaFrancois, J., Malester, B., Schmidt, S.D., Thomas-Bryant, T., Tint, G.S., Wang, R., Mercken, M., Petanceska, S.S., et al. (2001). A cholesterol-lowering drug reduces beta-amyloid pathology in a transgenic mouse model of Alzheimer's disease. Neurobiol. Dis. 8, 890–899.

Reisberg, B., Doody, R., Stöffler, A., Schmitt, F., Ferris, S., Möbius, H.J., and Memantine Study Group (2003). Memantine in moderate-to-severe Alzheimer's disease. N. Engl. J. Med. 348, 1333–1341.

Ries, M., and Sastre, M. (2016). Mechanisms of Abeta Clearance and Degradation by Glial Cells. Front Aging Neurosci 8, 160.

Rodríguez, J.J., Jones, V.C., Tabuchi, M., Allan, S.M., Knight, E.M., LaFerla, F.M., Oddo, S., and Verkhratsky, A. (2008). Impaired adult neurogenesis in the dentate gyrus of a triple transgenic mouse model of Alzheimer's disease. PloS One 3, e2935.

Rodriguez, J.J., Olabarria, M., Chvatal, A., and Verkhratsky, A. (2009). Astroglia in dementia and Alzheimer's disease. Cell Death Differ 16, 378–385.

Rodriguez-Vieitez, E., Saint-Aubert, L., Carter, S.F., Almkvist, O., Farid, K., Scholl, M., Chiotis, K., Thordardottir, S., Graff, C., Wall, A., et al. (2016). Diverging longitudinal changes in astrocytosis and amyloid PET in autosomal dominant Alzheimer's disease. Brain 139, 922–936.

Roher, A.E., Lowenson, J.D., Clarke, S., Woods, A.S., Cotter, R.J., Gowing, E., and Ball, M.J. (1993). beta-Amyloid-(1-42) is a major component of cerebrovascular amyloid deposits: implications for the pathology of Alzheimer disease. Proc. Natl. Acad. Sci. U. S. A. 90, 10836–10840.

Rossner, S., Lange-Dohna, C., Zeitschel, U., and Perez-Polo, J.R. (2005). Alzheimer's disease beta-secretase BACE1 is not a neuron-specific enzyme. J. Neurochem. 92, 226–234.

Rudy, C.C., Hunsberger, H.C., Weitzner, D.S., and Reed, M.N. (2015). The role of the tripartite glutamatergic synapse in the pathophysiology of Alzheimer's disease. Aging Dis. 6, 131–148.

Saint-Aubert, L., Lemoine, L., Chiotis, K., Leuzy, A., Rodriguez-Vieitez, E., and Nordberg, A. (2017). Tau PET imaging: present and future directions. Mol. Neurodegener. 12, 19.

Sarazin, M., Chauviré, V., Gerardin, E., Colliot, O., Kinkingnéhun, S., de Souza, L.C., Hugonot-Diener, L., Garnero, L., Lehéricy, S., Chupin, M., et al. (2010). The amnestic syndrome of hippocampal type in Alzheimer's disease: an MRI study. J. Alzheimers Dis. JAD 22, 285–294.

Savarin-Vuaillat, C., and Ransohoff, R.M. (2007). Chemokines and chemokine receptors in neurological disease: raise, retain, or reduce? Neurother. J. Am. Soc. Exp. Neurother. 4, 590–601.

Schellenberg, G.D., Bird, T.D., Wijsman, E.M., Orr, H.T., Anderson, L., Nemens, E., White, J.A., Bonnycastle, L., Weber, J.L., and Alonso, M.E. (1992). Genetic linkage evidence for a familial Alzheimer's disease locus on chromosome 14. Science 258, 668–671.

Schliebs, R., and Arendt, T. (2006). The significance of the cholinergic system in the brain during aging and in Alzheimer's disease. J. Neural Transm. Vienna Austria 1996 113, 1625–1644.

Schmechel, D.E., Saunders, A.M., Strittmatter, W.J., Crain, B.J., Hulette, C.M., Joo, S.H., Pericak-Vance, M.A., Goldgaber, D., and Roses, A.D. (1993). Increased amyloid beta-peptide deposition in cerebral cortex as a consequence of apolipoprotein E genotype in late-onset Alzheimer disease. Proc. Natl. Acad. Sci. U. S. A. 90, 9649–9653.

Schöll, M., Lockhart, S.N., Schonhaut, D.R., O'Neil, J.P., Janabi, M., Ossenkoppele, R., Baker, S.L., Vogel, J.W., Faria, J., Schwimmer, H.D., et al. (2016). PET Imaging of Tau Deposition in the Aging Human Brain. Neuron 89, 971–982.

Schwarz, J.M., and Bilbo, S.D. (2012). Sex, glia, and development: interactions in health and disease. Horm. Behav. 62, 243–253.

Sedgwick, J.D., Schwender, S., Imrich, H., Dörries, R., Butcher, G.W., and ter Meulen, V. (1991). Isolation and direct characterization of resident microglial cells from the normal and inflamed central nervous system. Proc. Natl. Acad. Sci. U. S. A. 88, 7438–7442.

del Ser, T., Steinwachs, K.C., Gertz, H.J., Andrés, M.V., Gómez-Carrillo, B., Medina, M., Vericat, J.A., Redondo, P., Fleet, D., and León, T. (2013). Treatment of Alzheimer's disease with the GSK-3 inhibitor tideglusib: a pilot study. J. Alzheimers Dis. JAD 33, 205–215.

Serguera, C., and Bemelmans, A.-P. (2014). Gene therapy of the central nervous system: general considerations on viral vectors for gene transfer into the brain. Rev. Neurol. (Paris) 170, 727–738.

Shaffer, L.M., Dority, M.D., Gupta-Bansal, R., Frederickson, R.C., Younkin, S.G., and Brunden, K.R. (1995). Amyloid beta protein (A beta) removal by neuroglial cells in culture. Neurobiol. Aging 16, 737–745.

Shaftel, S.S., Griffin, W.S.T., and O'Banion, M.K. (2008). The role of interleukin-1 in neuroinflammation and Alzheimer disease: an evolving perspective. J. Neuroinflammation 5, 7.

Shen, Y., Lue, L., Yang, L., Roher, A., Kuo, Y., Strohmeyer, R., Goux, W.J., Lee, V., Johnson, G.V., Webster, S.D., et al. (2001). Complement activation by neurofibrillary tangles in Alzheimer's disease. Neurosci. Lett. 305, 165–168.

Shen, Y., Yang, L., and Li, R. (2013). What does complement do in Alzheimer's disease? Old molecules with new insights. Transl. Neurodegener. 2, 21.

Shi, Q., Chowdhury, S., Ma, R., Le, K.X., Hong, S., Caldarone, B.J., Stevens, B., and Lemere, C.A. (2017). Complement C3 deficiency protects against neurodegeneration in aged plaque-rich APP/PS1 mice. Sci. Transl. Med. 9 (392).

Shibuki, K., Gomi, H., Chen, L., Bao, S., Kim, J.J., Wakatsuki, H., Fujisaki, T., Fujimoto, K., Katoh, A., Ikeda, T., et al. (1996). Deficient cerebellar long-term depression, impaired eyeblink conditioning, and normal motor coordination in GFAP mutant mice. Neuron 16, 587–599.

Shuai, K., Horvath, C.M., Huang, L.H., Qureshi, S.A., Cowburn, D., and Darnell, J.E., Jr. (1994). Interferon activation of the transcription factor Stat91 involves dimerization through SH2-phosphotyrosyl peptide interactions. Cell 76, 821–828.

Sigurdsson, T., Doyère, V., Cain, C.K., and LeDoux, J.E. (2007). Long-term potentiation in the amygdala: a cellular mechanism of fear learning and memory. Neuropharmacology 52, 215–227.

Simmons, M.L., Frondoza, C.G., and Coyle, J.T. (1991). Immunocytochemical localization of N-acetyl-aspartate with monoclonal antibodies. Neuroscience 45, 37–45.

Simpson, J.E., Ince, P.G., Lace, G., Forster, G., Shaw, P.J., Matthews, F., Savva, G., Brayne, C., Wharton, S.B., Function, M.R.C.C., et al. (2010). Astrocyte phenotype in relation to Alzheimer-type pathology in the ageing brain. Neurobiol Aging 31, 578–590.

Sofroniew, M.V. (2009). Molecular dissection of reactive astrogliosis and glial scar formation. Trends Neurosci 32, 638–647.

Sompol, P., Furman, J.L., Pleiss, M.M., Kraner, S.D., Artiushin, I.A., Batten, S.R., Quintero, J.E., Simmerman, L.A., Beckett, T.L., Lovell, M.A., et al. (2017). Calcineurin/NFAT Signaling in Activated Astrocytes Drives Network Hyperexcitability in Aβ-Bearing Mice. J. Neurosci. Off. J. Soc. Neurosci. 37, 6132–6148.

Song, S., Kim, S.-Y., Hong, Y.-M., Jo, D.-G., Lee, J.-Y., Shim, S.M., Chung, C.-W., Seo, S.J., Yoo, Y.J., Koh, J.-Y., et al. (2003). Essential role of E2-25K/Hip-2 in mediating amyloid-beta neurotoxicity. Mol. Cell 12, 553–563.

Suzuki, A., Stern, S.A., Bozdagi, O., Huntley, G.W., Walker, R.H., Magistretti, P.J., and Alberini, C.M. (2011). Astrocyte-neuron lactate transport is required for long-term memory formation. Cell 144, 810–823.

Takeshita, Y., and Ransohoff, R.M. (2012). Inflammatory cell trafficking across the blood-brain barrier: chemokine regulation and in vitro models. Immunol. Rev. 248, 228–239.

Tanaka, J., Toku, K., Zhang, B., Ishihara, K., Sakanaka, M., and Maeda, N. (1999). Astrocytes prevent neuronal death induced by reactive oxygen and nitrogen species. Glia 28, 85–96.

Tateno, F., Sakakibara, R., Kawai, T., Kishi, M., and Murano, T. (2012). Alpha-synuclein in the cerebrospinal fluid differentiates synucleinopathies (Parkinson Disease, dementia with Lewy bodies, multiple system atrophy) from Alzheimer disease. Alzheimer Dis. Assoc. Disord. 26, 213–216.

Thal, D.R., Rüb, U., Orantes, M., and Braak, H. (2002). Phases of A beta-deposition in the human brain and its relevance for the development of AD. Neurology 58, 1791–1800.

Thal, D.R., Griffin, W.S.T., de Vos, R.A.I., and Ghebremedhin, E. (2008). Cerebral amyloid angiopathy and its relationship to Alzheimer's disease. Acta Neuropathol. (Berl.) 115, 599–609.

Theis, M., and Giaume, C. (2012). Connexin-based intercellular communication and astrocyte heterogeneity. Brain Res 1487, 88–98.

Theunis, C., Crespo-Biel, N., Gafner, V., Pihlgren, M., López-Deber, M.P., Reis, P., Hickman, D.T., Adolfsson, O., Chuard, N., Ndao, D.M., et al. (2013). Efficacy and safety of a liposome-based vaccine against protein Tau, assessed in tau.P301L mice that model tauopathy. PloS One 8, e72301.

Tweedie, D., Ferguson, R.A., Fishman, K., Frankola, K.A., Van Praag, H., Holloway, H.W., Luo, W., Li, Y., Caracciolo, L., Russo, I., et al. (2012). Tumor necrosis factor-α synthesis inhibitor 3,6'-dithiothalidomide attenuates markers of inflammation, Alzheimer pathology and behavioral deficits in animal models of neuroinflammation and Alzheimer's disease. J. Neuroinflammation 9, 106.

Uchoa, M.F., Moser, V.A., and Pike, C.J. (2016). Interactions between inflammation, sex steroids, and Alzheimer's disease risk factors. Front. Neuroendocrinol. 43, 60–82.

Ulrich, J.D., Finn, M.B., Wang, Y., Shen, A., Mahan, T.E., Jiang, H., Stewart, F.R., Piccio, L., Colonna, M., and Holtzman, D.M. (2014). Altered microglial response to Abeta plaques in APPPS1-21 mice heterozygous for TREM2. Mol Neurodegener 9, 20.

Ulrich, J.D., Ulland, T.K., Colonna, M., and Holtzman, D.M. (2017). Elucidating the Role of TREM2 in Alzheimer's Disease. Neuron 94, 237–248.

Vandesompele, J., De Preter, K., Pattyn, F., Poppe, B., Van Roy, N., De Paepe, A., and Speleman, F. (2002). Accurate normalization of real-time quantitative RT-PCR data by geometric averaging of multiple internal control genes. Genome Biol. 3, RESEARCH0034.

Vargas-Alarcon, G., Juarez-Cedillo, E., Martinez-Rodriguez, N., Fragoso, J.M., Garcia-Hernandez, N., and Juarez-Cedillo, T. (2016). Association of interleukin-10 polymorphisms with risk factors of Alzheimer's disease and other dementias (SADEM study). Immunol Lett 177, 47–52.

Varnum, M.M., and Ikezu, T. (2012). The classification of microglial activation phenotypes on neurodegeneration and regeneration in Alzheimer's disease brain. Arch. Immunol. Ther. Exp. (Warsz.) 60, 251–266.

Végh, M.J., Heldring, C.M., Kamphuis, W., Hijazi, S., Timmerman, A.J., Li, K.W., van Nierop, P., Mansvelder, H.D., Hol, E.M., Smit, A.B., et al. (2014). Reducing hippocampal extracellular matrix reverses early memory deficits in a mouse model of Alzheimer's disease. Acta Neuropathol. Commun. 2, 76.

Venegas, C., and Heneka, M.T. (2017). Danger-associated molecular patterns in Alzheimer's disease. J. Leukoc. Biol. 101, 87–98.

Verret, L., Jankowsky, J.L., Xu, G.M., Borchelt, D.R., and Rampon, C. (2007). Alzheimer's-type amyloidosis in transgenic mice impairs survival of newborn neurons derived from adult hippocampal neurogenesis. J. Neurosci. Off. J. Soc. Neurosci. 27, 6771–6780.

Viana da Silva, S., Haberl, M.G., Zhang, P., Bethge, P., Lemos, C., Gonçalves, N., Gorlewicz, A., Malezieux, M., Gonçalves, F.Q., Grosjean, N., et al. (2016). Early synaptic deficits in the APP/PS1 mouse model of Alzheimer's disease involve neuronal adenosine A2A receptors. Nat. Commun. 7, 11915.

Virchow, R. (1856). Gesammelte Abhandlungen zur wissenschaftlichen Medizin.

Volianskis, A., Køstner, R., Mølgaard, M., Hass, S., and Jensen, M.S. (2010). Episodic memory deficits are not related to altered glutamatergic synaptic transmission and plasticity in the CA1 hippocampus of the APPswe/PS1δE9-deleted transgenic mice model of ß-amyloidosis. Neurobiol. Aging 31, 1173–1187.

Vom Berg, J., Prokop, S., Miller, K.R., Obst, J., Kälin, R.E., Lopategui-Cabezas, I., Wegner, A., Mair, F., Schipke, C.G., Peters, O., et al. (2012). Inhibition of IL-12/IL-23 signaling reduces Alzheimer's disease-like pathology and cognitive decline. Nat. Med. 18, 1812–1819.

Walsh, D.M., and Selkoe, D.J. (2007). A beta oligomers - a decade of discovery. J. Neurochem. 101, 1172–1184.

Wang, Y., and Mandelkow, E. (2016). Tau in physiology and pathology. Nat. Rev. Neurosci. 17, 5–21.

Wang, W.-Y., Tan, M.-S., Yu, J.-T., and Tan, L. (2015a). Role of pro-inflammatory cytokines released from microglia in Alzheimer's disease. Ann. Transl. Med. 3, 136.

Wang, Y., Cella, M., Mallinson, K., Ulrich, J.D., Young, K.L., Robinette, M.L., Gilfillan, S., Krishnan, G.M., Sudhakar, S., Zinselmeyer, B.H., et al. (2015b). TREM2 lipid sensing sustains the microglial response in an Alzheimer's disease model. Cell 160, 1061–1071.

Wang, Y., Ulland, T.K., Ulrich, J.D., Song, W., Tzaferis, J.A., Hole, J.T., Yuan, P., Mahan, T.E., Shi, Y., Gilfillan, S., et al. (2016). TREM2-mediated early microglial response limits diffusion and toxicity of amyloid plaques. J. Exp. Med. 213, 667–675.

Wang, Y., Balaji, V., Kaniyappan, S., Krüger, L., Irsen, S., Tepper, K., Chandupatla, R., Maetzler, W., Schneider, A., Mandelkow, E., et al. (2017). The release and trans-synaptic transmission of Tau via exosomes. Mol. Neurodegener. 12, 5.

Webster, S., and Rogers, J. (1996). Relative efficacies of amyloid beta peptide (A beta) binding proteins in A beta aggregation. J. Neurosci. Res. 46, 58–66.

Webster, S.J., Bachstetter, A.D., and Van Eldik, L.J. (2013). Comprehensive behavioral characterization of an APP/PS-1 double knock-in mouse model of Alzheimer's disease. Alzheimers Res. Ther. 5, 28.

Weigert, C. (1895). Beiträge zur Kenntnis der normalen menschlichen Neuroglia. In Zeitschrift Für Psychologie Und Physiologie Der Sinnesorgane, Liepmann, ed. (Frankfurt).

Wilhelmsson, U., Bushong, E.A., Price, D.L., Smarr, B.L., Phung, V., Terada, M., Ellisman, M.H., and Pekny, M. (2006). Redefining the concept of reactive astrocytes as cells that remain within their unique domains upon reaction to injury. Proc Natl Acad Sci U A 103, 17513–17518.

Wirths, O., and Bayer, T.A. (2003). Alpha-synuclein, Abeta and Alzheimer's disease. Prog. Neuropsychopharmacol. Biol. Psychiatry 27, 103–108.

Wolozin, B., Kellman, W., Ruosseau, P., Celesia, G.G., and Siegel, G. (2000). Decreased prevalence of Alzheimer disease associated with 3-hydroxy-3-methyglutaryl coenzyme A reductase inhibitors. Arch. Neurol. 57, 1439–1443.

Wu, Z., Guo, Z., Gearing, M., and Chen, G. (2014). Tonic inhibition in dentate gyrus impairs long-term potentiation and memory in an Alzhiemer's disease model. Nat Commun 5, 4159.

Wyss-Coray, T., Lin, C., Yan, F., Yu, G.Q., Rohde, M., McConlogue, L., Masliah, E., and Mucke, L. (2001). TGF-beta1 promotes microglial amyloid-beta clearance and reduces plaque burden in transgenic mice. Nat Med 7, 612–618.

Wyss-Coray, T., Loike, J.D., Brionne, T.C., Lu, E., Anankov, R., Yan, F., Silverstein, S.C., and Husemann, J. (2003). Adult mouse astrocytes degrade amyloid-beta in vitro and in situ. Nat Med 9, 453–457.

Xia, M.Q., Qin, S.X., Wu, L.J., Mackay, C.R., and Hyman, B.T. (1998). Immunohistochemical study of the beta-chemokine receptors CCR3 and CCR5 and their ligands in normal and Alzheimer's disease brains. Am. J. Pathol. 153, 31–37.

Xia, M.Q., Bacskai, B.J., Knowles, R.B., Qin, S.X., and Hyman, B.T. (2000). Expression of the chemokine receptor CXCR3 on neurons and the elevated expression of its ligand IP-10 in reactive astrocytes: in vitro ERK1/2 activation and role in Alzheimer's disease. J. Neuroimmunol. 108, 227–235.

Xia, W., Yang, T., Shankar, G., Smith, I.M., Shen, Y., Walsh, D.M., and Selkoe, D.J. (2009). A specific enzyme-linked immunosorbent assay for measuring beta-amyloid protein oligomers in human plasma and brain tissue of patients with Alzheimer disease. Arch. Neurol. 66, 190–199.

Xiong, H., Callaghan, D., Wodzinska, J., Xu, J., Premyslova, M., Liu, Q.-Y., Connelly, J., and Zhang, W. (2011). Biochemical and behavioral characterization of the double transgenic mouse model (APPswe/PS1dE9) of Alzheimer's disease. Neurosci. Bull. 27, 221–232.

Xu, W., Marseglia, A., Ferrari, C., and Wang, H.-X. (2013). Alzheimer's Disease: A Clinical Perspective, Neurodegenerative Diseases, Dr. Uday Kishore (Ed.), InTech, DOI: 10.5772/54539. Available from: https://www.intechopen.com/books/neurodegenerative-diseases/alzheimer-s-disease-a-clinical-perspective.

Yamamoto, N., Tanida, M., Ono, Y., Kasahara, R., Fujii, Y., Ohora, K., Suzuki, K., and Sobue, K. (2014). Leptin inhibits amyloid β-protein degradation through decrease of neprilysin expression in primary cultured astrocytes. Biochem. Biophys. Res. Commun. 445, 214–217.

Yan, R. (2016). Stepping closer to treating Alzheimer's disease patients with BACE1 inhibitor drugs. Transl. Neurodegener. 5, 13.

Yan, P., Hu, X., Song, H., Yin, K., Bateman, R.J., Cirrito, J.R., Xiao, Q., Hsu, F.F., Turk, J.W., Xu, J., et al. (2006). Matrix metalloproteinase-9 degrades amyloid-beta fibrils in vitro and compact plaques in situ. J Biol Chem 281, 24566–24574.

Yanamandra, K., Kfoury, N., Jiang, H., Mahan, T.E., Ma, S., Maloney, S.E., Wozniak, D.F., Diamond, M.I., and Holtzman, D.M. (2013). Anti-tau antibodies that block tau aggregate seeding in vitro markedly decrease pathology and improve cognition in vivo. Neuron 80, 402–414.

Yanamandra, K., Jiang, H., Mahan, T.E., Maloney, S.E., Wozniak, D.F., Diamond, M.I., and Holtzman, D.M. (2015). Anti-tau antibody reduces insoluble tau and decreases brain atrophy. Ann. Clin. Transl. Neurol. 2, 278–288.

Yang, Y.-M., Shang, D.-S., Zhao, W.-D., Fang, W.-G., and Chen, Y.-H. (2013). Microglial TNF-α-dependent elevation of MHC class I expression on brain endothelium induced by amyloid-beta promotes T cell transendothelial migration. Neurochem. Res. 38, 2295–2304.

Yasojima, K., Schwab, C., McGeer, E.G., and McGeer, P.L. (1999). Up-regulated production and activation of the complement system in Alzheimer's disease brain. Am. J. Pathol. 154, 927–936.

Yu, W.H., Kumar, A., Peterhoff, C., Shapiro Kulnane, L., Uchiyama, Y., Lamb, B.T., Cuervo, A.M., and Nixon, R.A. (2004). Autophagic vacuoles are enriched in amyloid precursor protein-secretase activities: implications for beta-amyloid peptide over-production and localization in Alzheimer's disease. Int. J. Biochem. Cell Biol. 36, 2531–2540.

Yu, W.H., Cuervo, A.M., Kumar, A., Peterhoff, C.M., Schmidt, S.D., Lee, J.-H., Mohan, P.S., Mercken, M., Farmery, M.R., Tjernberg, L.O., et al. (2005). Macroautophagy--a novel Beta-amyloid peptide-generating pathway activated in Alzheimer's disease. J. Cell Biol. 171, 87–98.

Yuan, X.-Z., Sun, S., Tan, C.-C., Yu, J.-T., and Tan, L. (2017). The Role of ADAM10 in Alzheimer's Disease. J. Alzheimers Dis. JAD 58, 303–322.

Zamanian, J.L., Xu, L., Foo, L.C., Nouri, N., Zhou, L., Giffard, R.G., and Barres, B.A. (2012). Genomic analysis of reactive astrogliosis. J Neurosci 32, 6391–6410.

Zeis, T., Allaman, I., Gentner, M., Schroder, K., Tschopp, J., Magistretti, P.J., and Schaeren-Wiemers, N. (2015). Metabolic gene expression changes in astrocytes in Multiple Sclerosis cerebral cortex are indicative of immune-mediated signaling. Brain. Behav. Immun. 48, 313–325.

Zhang, B., Gaiteri, C., Bodea, L.G., Wang, Z., McElwee, J., Podtelezhnikov, A.A., Zhang, C., Xie, T., Tran, L., Dobrin, R., et al. (2013). Integrated systems approach identifies genetic nodes and networks in late-onset Alzheimer's disease. Cell 153, 707–720.

Titre : Modulation de la réactivité astrocytaire par ciblage de la voie JAK2-STAT3 : Conséquences dans des modèles murins de la maladie d'Alzheimer.

Mots clés : Astrocytes réactifs – Maladies neurodégénératives – Virus adéno-associés – Neuroinflammation – SOCS3

Résumé : Les astrocytes sont des éléments clés de la physiologie cérébrale. Dans les maladies neurodégénératives comme la maladie d'Alzheimer (MA), les astrocytes deviennent réactifs. Cette réactivité astrocytaire (RA) est essentiellement caractérisée par des changements morphologiques. En revanche, les effets de la réactivité sur les fonctions de support des astrocytes sont mal connus. De plus, les cascades de signalisation qui conduisent à la RA restent à déterminer. Les objectifs de ce projet étaient de : 1/ démontrer que la voie JAK2-STAT3 (Janus Kinase 2 - Signal Transducer and Activator of Transcription 3) joue un rôle central dans le contrôle de la RA au cours des maladies neurodégénératives ; 2/ comprendre quelle est l'implication de la RA dans les altérations moléculaires, cellulaires et fonctionnelles observées dans la MA. Nous avons montré que la voie JAK2-STAT3 est une cascade de signalisation centrale dans la RA (Ben Haim et al., 2015). Dans ce projet, nous démontrons en utilisant de nouveaux outils moléculaires basés sur des vecteurs viraux, que cette voie est nécessaire et suffisante à la RA.
Nos résultats montrent également que la modulation de la RA dans deux modèles murins de la MA (souris APP/PS1dE9 et 3xTg-AD) influence certains index pathologiques, mais de façon contexte-dépendante.
L'ensemble de ce travail a permis de valider de nouveaux outils pour étudier les astrocytes réactifs *in situ* et souligne l'importance et la complexité de leur fonctions au cours des maladies neurodégénératives.

Title: Modulation of astrocyte reactivity by targeting the JAK2-STAT3 pathway: Consequences in Alzheimer's disease mouse models.

Keywords: Astrocyte reactivity – Neurodegenerative diseases – Adeno-associated viruses – Neuroinflammation – SOCS3

Abstract: Astrocytes are emerging as key players in brain physiology. In Alzheimer's disease (AD), astrocytes become reactive. Astrocyte reactivity (AR) is essentially characterized by morphological changes. But how the normal supportive functions of astrocytes are changed by their reactive state is unclear. Moreover, signaling cascades leading to AR are not yet determined. In this study, we aim to: 1/ demonstrate the JAK2-STAT3 pathway (Janus Kinase 2 - Signal Transducer and Activator of Transcription 3) is responsible for AR in neurodegenerative diseases ; 2/ understand the contribution of reactive astrocytes to molecular, cellular and functional alterations in AD. We already reported that the JAK2- STAT3 pathway is a central cascade for AR (Ben Haim et al., 2015). Here, we demonstrate, with new molecular tools based on viral vectors, that this pathway is necessary and sufficient to AR.
Our results also show that the modulation of AR in two AD mouse models (APP/PS1dE9 and 3xTg-AD mice) influence several pathological hallmarks, but in a context-dependent manner.
Overall, this work has generated new original tools to study reactive astrocytes *in situ* and it underlines the importance and complexity of their functions in neurodegenerative diseases.